UNIVERSITY OF LATVIA
FACULTY OF MEDICINE AND LIFE SCIENCES

Toms Kalniņš

STUDIES ON TOTAL SYNTHESIS OF DIAZONAMIDE A AND ITS STRUCTURAL ANALOGS

Doctoral Thesis

Submitted for the PhD degree in Natural Science
Field of chemistry
Subfield of organic chemistry

Supervisor: Prof., Dr. chem. Edgars Sūna

RIGA, 2024

The development of the doctoral thesis was carried out at the Latvian Institute of Organic Synthesis from 2013 to 2024.

The thesis comprises the following sections: Introduction, 3 Chapters, Conclusions, References and 4 Appendices. Form of the thesis: dissertation in chemistry, organic chemistry.

Supervisor: Prof., Dr. chem. Edgars Sūna.

Reviewers:

1) Dr. chem. Janis Veliks (Latvian Institute of Organic synthesis);
2) Dr. chem. Gints Šmits (Riga Technical university);
3) Dr. Edvinas Orentas (Vilnius University, Lithuania);

The thesis will be defended at the public session of the Doctoral Committee of chemistry, University of Latvia, at 16:00 on November 15, 2024 at the Academic Center of Natural Science of the University of Latvia, Riga, Jelgavas street 1.

The thesis is available at the Library of the University of Latvia, Raiņa blvd. 19.

Chairman of the Doctoral Committee_____/*Vadims Bartkevičs/*

Secretary of the Doctoral Committee_____/*Vita Rudoviča/*

ANNOTATION

Studies on total synthesis of diazonamide A and its structural analogs. Kalniņš T., supervisor: Prof., Dr. chem. Sūna E. Doctoral thesis. Consists of 139 pages, 80 figures, 5 tables, 127 literature references and 5 appendices. Written in English.

Synthesis of natural diazonamide A and its structural analogs with altered core scaffold and macrocycle size was studied. Synthesis of chiral, enantiopure macrocyclic ketone by atropodiastereoselective *Dieckmann*-type cyclization was developed. The obtained macrocyclic ketone contains the following key structural elements of diazonamide A: 12-membered heterocyclic ring, tetracyclic hemiaminal moiety and the all-carbon quaternary stereocenter. Introduction of bioxazole moiety in the macrocycle was studied which resulted in synthesis of novel macrocyclic diazoketone. Next, preparation of previously unreported carba-analog of highly active anticancer agent DZ-2384 was explored. Investigation of three distinctive synthesis routes indicated the intrinsic challenges associated with formation of analogs of DZ-2384 (macrocyclization, introduction of quaternary stereocenter) and yielded three previously unreported dihydroindenoindole-core containing macrocycles. Finally, diastereoselective synthesis of 12- and 13-membered 2-indolinone-core containing analogs of DZ-2384 was shown. Dependence of the diastereoselectivity of macrocyclization on the size of the macrocycle to be formed was demonstrated. The antiproliferative activity of the obtained macrocyles reached nanomolar level against multiple cancer cell lines. SAR in the 2-indolinone-core containing series was explored.

Keywords: SYNTHESIS, DIAZONAMIDE A, ANALOGS, MACROCYCLE, CYCLIZATION

TABLE OF CONTENTS

ABBREVIATIONS

Ac – acetyl-
acac – acetylacetone
Alloc – allyloxycarbonyl -
Ar – aryl-
9-BBN – 9-borabicyclo(3.3.1)nonane
Bn – benzyl-
Boc – *tert*-butyloxycarbonyl-
Bu – butyl-
Cbz – benzyloxycarbonyl
Cy – cyclohexyl
COSY – correlation spectroscopy
DAST – diethylaminosulfur trifluoride
dba – dibenzylideneacetone
DBU – 1,8-diazabicyclo(5.4.0)undec-7-ene
DCE – 1,2-dichloroethane
DCM – dichloromethane
DDQ – 2,3-dichloro-5,6-dicyano-1,4-benzoquinone
DeoxoFluor – bis(2-methoxyethyl)aminosulfur trifluoride
DFT – density functional theory
DIAD – diisopropylazodicarboxylate
DIBAL-H – diisobutylaluminum hydride
DIC – diisopropylcarbodiimide
(+)-DIP-Cl – (+)-*B*-chlorodiisopinocampheylborane
DIPEA – *N*,*N*-diisopropylethylamine
DMA – dimethylacetamide
DMAP – 4-dimethylaminopyridine
DMDO – dimethyldioxirane
DMF – dimethylformamide
DMI – 1,3-dimethyl-2-imidazolidinone
DMP – Dess–Martin periodinane
DMSO – dimethylsulfoxide
DPEPhos – bis[(2-diphenylphosphino)phenyl]ether
DPM – (Z)-5-hydroxy-2,2,6,6-tetramethylhept-4-en-3-one
dppe – 1,2-bis(diphenylphosphino)ethane
dppf – 1,1'-bis(diphenylphosphino)ferrocene
dr – diastereomeric ratio
EDC – 1-ethyl-3-(3-dimethylamino-propyl)carbodiimide
equiv. – equivalents
Et – ethyl
Fmoc – fluorenylmethyloxycarbonyl-
Glu – glutamic acid
Glyme - dimethoxyethane
GTP – guanosine-5'-diphosphate disodium salt
HATU – azabenzotriazoletetramethyluronium hexafluorophosphate
HFIP – hexafluoro-2-propanol
HMPA – hexamethylphosphoramide
HOBt – hydroxybenzotriazole
HRMS – high resolution mass spectrometer
IBX – 2-iodoxybenzoic acid
TMS – trimethylsilyl-
IC_{50} – inhibitory concentration
*i*Pr – isopropyl
KHMDS – potassium bis(trimethylsilyl)amide
LAH – lithium aluminum hydride

LDA – lithium diisopropylamide

m-CPBA – *meta*-chloroperoxybenzoic acid

Me – methyl-

MOM – methoxymethyl-

Ms – methanesulfonyl-

MTT – 3-(4,5-dimethylthiazol-2-yl)-2,5-diphenyltetrazolium bromide

MW – microwaves

NBS – *N*-bromoscuccinimide

n-Bu – butyl-

NCS – *N*-chlorosuccinimide

NIS – *N*-iodosuccinimide

NMR – nuclear magnetic resonance spectroscopy

NOE – nuclear Overhauser effect

Oxone® – potassium peroxymonosulfate

*p*ABSA – *para*-acetamidobenzenesulfonyl azide

Ph – phenyl-

Pin – pinacol

PMB – *para*-methoxybenzyl-

ppm – parts per million

r.t. – room temperature

rac – racemate

SAR – structure-activity relationship

Ser – serine

S_NAr – nucleophilic aromatic substitution

SPhos – dicyclohexyl(2′,6′-dimethoxy[1,1′-biphenyl]-2-yl)phosphane

TAS-F – tris (dimethylamino)sulfonium difluorotrimethylsilicate

TBAF – tetra-*n*-butylammonium fluoride

TBDPS – *tert*-butyldiphenylsilyl-

TBS – *tert*-butyldimethylsilyl-

t-Bu – *terc*-butyl-

TCA – trichloroacetic acid

TEA – triethylamine

Teoc – 2-(trimethylsilyl)ethoxycarbonyl-

Tf – trifluoromethanesulfonyl-

TFA – trifluoroacetic acid

TFE – 2,2,2-trifluoroethanol

THF – tetrahydrofurane

TIPS – triisopropylsilyl-

Tyr – tyrosine

TLC – thin layer chromatography

Ts – toluenesulfonyl

UPLC-MS – ultra-high performance liquid chromatography–mass spectrometry

Val – valine

XantPhos – (9,9-dimethyl-9*H*-xanthene-4,5-diyl)bis(diphenylphosphane)

INTRODUCTION

The US National Cancer Institute defines cancer as a disease in which some of the body's cells grow uncontrollably and spread to other parts of the body.[1] Cancer poses a significant global health challenge with over 19 million new cases diagnosed and almost 10 million fatalities reported in 2022.[2] By 2040 the incidence is projected to increase by 47%, reaching an annual total of 28.4 million cases.[3] The rising occurrence of cancer, coupled with the significant mortality rates and the emergence of multidrug resistance[4] to standard-of-care antitumor treatments, underscores the urgent need for the development of novel and effective anticancer therapies.

Throughout history, a significant proportion of anticancer medicines have been derived from natural sources - around one third of small molecule anticancer drugs approved for clinical use from 1981 to 2019 were natural products or natural product derivatives.[5] Some of these, like the microtubule-targeting vinca alkaloids (vinorelbine, vincristine) and taxanes (paclitaxel, docetaxel), are now considered part of standard-of-care treatments.

Another naturally sourced microtubule-targeting agent is diazonamide A – marine metabolite with high antiproliferative activity against several cancer cell lines.[6] It possesses complex structure that includes two 12-membered macrocyclic rings as well as rigid, tetracyclic hemiaminal core and quaternary stereocenter. Even though four total syntheses of diazonamide A had been successful, few analogs of it had been prepared and little is known about its structure-activity relationship (SAR). Therefore, the design of modular, robust, and high yielding synthesis of diazonamide A could facilitate preparation of its analogs for SAR studies and development of novel anticancer medicines.

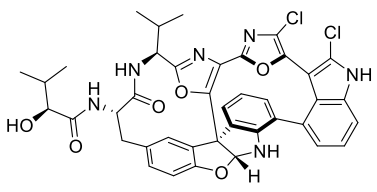

Diazonamide A

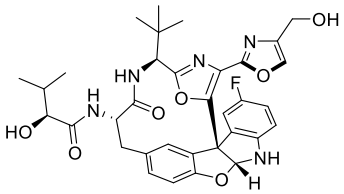

DZ-2384

Notwithstanding the four successful approaches, the total synthesis of diazonamide A is challenging and not always fruitful. Therefore, the development of novel analogs and study of SAR could be based on known simplified derivatives of natural diazonamide A, such as DZ-2384 that has been developed by Harran and possesses low nanomolar antiproliferative activity.[7] However, DZ-2384 still is highly complex and alteration of the most hard-to-

synthesize motifs (tetracyclic hemiaminal, quaternary stereocenter, 12-member macrocyclic ring) of the molecule could lead to easier-to-access analogs with retained biological activity and potential for further elaboration into more efficacious anticancer medicines.

The objective of the doctoral thesis is to contribute to the development of robust and modular synthesis of marine metabolite diazonamide A and explore the synthesis of its simplified analogs.

Tasks of the doctoral thesis:

1. To study synthesis of intermediate macrocyclic ketone that contains the following key structural elements of diazonamide A: the 12-membered heterocyclic ring, the tetracyclic hemiaminal moiety and the all-carbon quaternary stereocenter,

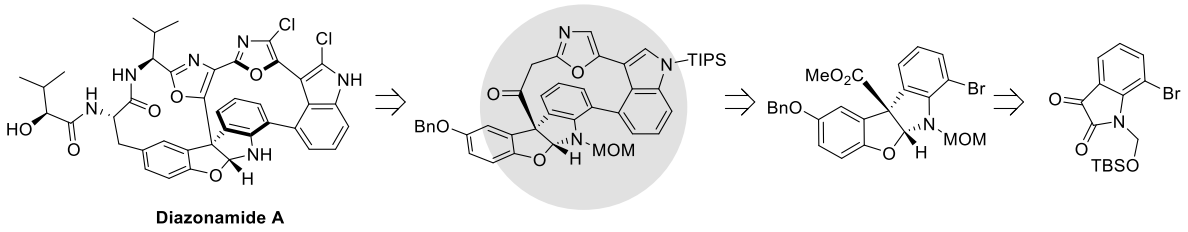

2. To investigate formation of bioxazole moiety towards synthesis of diazonamide A,

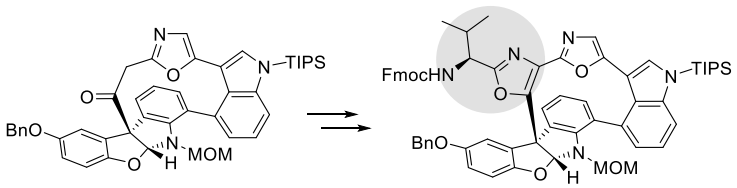

3. To study synthesis of analogs of DZ-2384 with altered core scaffold and macrocycle size,

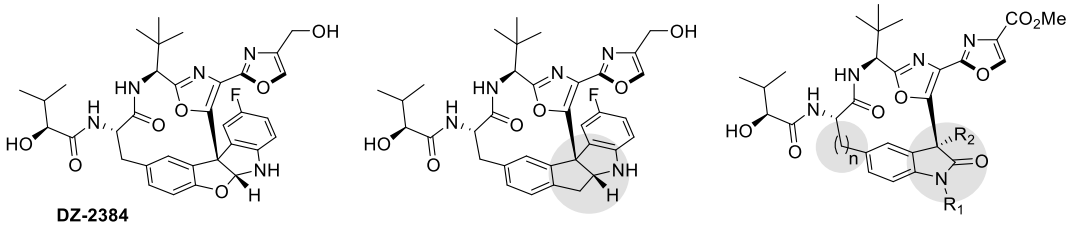

4. To assess impact of core scaffold and ring size changes on antiproliferative activity and to explore SAR.

The scientific novelty of the work:

1. An intermediate that contains the macrocyclic core of diazonamide A has been synthesized in enantiomerically pure form by atropodiastereoselective *Dieckmann*-type cyclization. The *Dieckmann*-type cyclization was shown to proceed below the threshold for interconversion of atropisomers, therefore, only the *M*-atropisomer underwent the ring closure, whereas the *P*-atropisomer did not react and equilibrated back to the starting 3:2 M/P mixture during the workup.

2. Stability of carbonyl-substituted dihydrobenzofuro[2,3-*b*]indoles was investigated indicating routes and mechanisms of cyclic hemiaminal ring opening under both acidic and basic conditions.

3. Preparation of previously unreported carba-analog of highly active anticancer agent DZ-2384 was explored. Investigation of three distinctive synthesis routes indicated the intrinsic challenges associated with formation of analogs of DZ-2384 and yielded three undesired, but previously unknown dihydroindenoindole-core containing macrocycles.

4. Evaluation of the antiproliferative activity of the obtained macrocycles illustrated the importance of the right bond connectivity between the core tetracycle and the rest of the molecule in the analog series.

5. Diastereoselective synthesis of 12- and 13-membered 2-indolinone-core containing analogs of DZ-2384 was shown for the first time. Dependence of the diastereoselectivity of macrocyclization on the size of the macrocycle to be formed was also demonstrated. SAR in the 2-indolinone-core containing series has been explored.

Practical significance of the doctoral thesis:

1. The doctoral work provides an important insight into SAR of natural diazonamide A and its synthetic analog DZ-2384. The SAR findings have been instrumental in the design of simplified analog series.

2. Previously unreported 13-membered macrocycles possessing nanomolar antiproliferative activity against a range of cancer cell lines have been synthesized.

3. Study of diazonamide synthesis provided knowledge for the development of efficient approaches to analog series.

Research of the doctoral thesis has been published in the following articles and patent applications:

1. Mutule, I.; Joo, B.; Medne, Z.; **Kalnins, T.**; Vedejs, E.; Suna, E. Stereoselective Synthesis of the Diazonamide A Macrocyclic Core. *J. Org. Chem.* **2015**, *80* (6), 3058–3066. https://doi.org/10.1021/jo5029419. Author contribution: 30%.

2. Mutule, I.; **Kalnins, T.**; Vedejs, E.; Suna, E. Diazonamide Synthetic Studies. Reactivity of N-Unsubstituted Benzofuro[2,3-b]Indolines. *Chem. Heterocycl. Compd.* **2015**, *51* (7), 613–620. https://doi.org/10.1007/s10593-015-1749-7. Author contribution: 40%.

3. Suna, E.; **Kalnins, T.**; Kazak, M.; Vitkovska, V.; Narvaiss, N.; Zelencova, D.; Jaudzems, K. Structurally Simplified Diazonamide Analogs as Antimitotic Agents. WO2021130515A1, July 1, 2021. Author contribution: 35%.

4. **Kalnins, T.**; Vitkovska, V.; Kazak, M.; Zelencova-Gopejenko, D.; Ozola, M.; Narvaiss, N.; Makrecka-Kuka, M.; Domračeva, I.; Kinens, A.; Gukalova, B.; Konrad, N.; Aav, R.; Bonato, F.; Lucena-Agell, D.; Díaz, J. F.; Liepinsh, E.; Suna, E. Development of Potent Microtubule Targeting Agent by Structural Simplification of Natural Diazonamide. *J. Med. Chem.* **2024**, *67* (11), 9227–9259. https://doi.org/10.1021/acs.jmedchem.4c00388. Author contribution: 35%.

Poster presentations at conferences:

1. Mutule, I.; Medne, Z.; **Kalniņš, T.**; Vedejs, E.; Suna, E. Stereoselective synthesis of the Diazonamide A macrocyclic core. Organometallic Chemistry Directed Towards Organic Synthesis OMCOS18, 2015, Sitges, Spain. Program and abstract book, P-577.

2. Mutule, I.; Medne, Z.; **Kalniņš, T.** Stereoselective synthesis of the Diazonamide A macrocyclic core. 9th Paul Walden Symposium on Organic Chemistry, Riga, Latvia, May 21 – 22, 2015. Abstract published in Material Science and Applied Chemistry, 2015, vol. 31, p. 66.

3. **Kalniņš, T.**, Suna, E. Studies towards the synthesis of novel anticancer agents based on Diazonamide A. 11th Paul Walden Symposium on Organic Chemistry 2019, Riga, Latvia, September 19 – 20. Program and abstract book, D-6.

Funding

The author is thankful for funding to ESF grant No. 1DP/1.1.1.2.0/13/APIA/VIAA/006, ERAF grant No. 1.1.1.1/16/A/281 and ERAF grant No. KC-PI-2020/16. Financial support from Latvian Institute of Organic Synthesis (Internal grant for PhD research No. IG-2015-06) is also acknowledged.

Acknowledgments

I would like to express my deep gratitude to Prof., Dr.Chem. Edgars Sūna, my research supervisor. Without his guidance and encouragement this work would not have been done and I would not be the chemist I am today. I also want to thank to Dr. Artis Kinens for computational studies, Dr. Ilona Domracheva for biological evaluation of compounds and my LIOS colleagues Linda K, Linda S, Olesja and Anete for the valuable everyday conversations. Finally, I cannot thank enough to my wife Zane, my family, and my friends (especially Martins and Karola) for the continuous support during these turbulent times.

1. LITERATURE REVIEW

1.1. Diazonamide A

Diazonamide A is a marine natural product that was first isolated in 1991 from colonial ascidian *Diazona angulata* found on the ceilings on several small caves along the coast of Siquijor islands, Philippines (54 mg of diazonamide A were obtained from 256 grams of lyophilized ascidian).[6] The initial structural assignment using single crystal X-ray spectroscopy, HRMS and NMR techniques described it as a highly complex compound bearing two 12-member macrocyclic rings, all-carbon quaternary stereocenter, tetracyclic acetal moiety and a valine sidechain (Figure 1.1, compound **1.1**). The compound also showed intriguing biological properties: low nanomolar *in vitro* antiproliferative activity against HCT-116 (human colon carcinoma) and B-16 (murine melanoma) cancer cell lines. Additionally, analysis of the diazonamide A in US National Cancer Institute 60 tumor cell line panel not only confirmed it as highly potent anticancer agent (mean GI_{50} value = 11 nM), but also suggested that the diazonamide A **1.1** was tubulin targeting agent (as indicated by COMPARE algorhytm).[8] Tubulin-targeting mechanism of action for natural product **1.1** was further confirmed using cell cycle and immunofluorescence microscopic analysis, where cells treated with diazonamide A showed a thinning of microtubules (MT) and disorganization of the overall MT network leading to cell cycle arrest at G_2/M phase.[9]

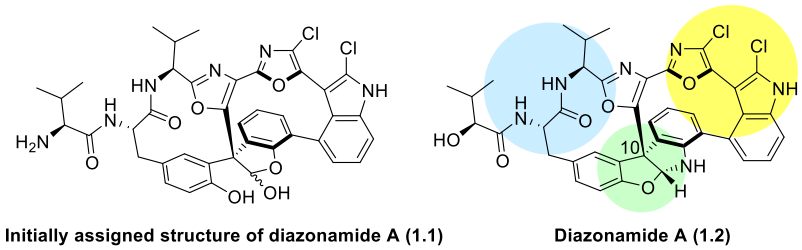

Figure 1.1 **Initially assigned (left) and revised (right) structure of diazonamide A**

The highly unusual macrocyclic structure of diazonamide A along with the biological activity sparked a high interest in the synthetic organic community and led to multiple synthesis attempts.[10,11] However, it was only through a total synthesis by group of Prof. Harran that it was found that the spectral data and biological activity of acetal **1.1** does not match those of the originally isolated natural product.[12] Revision of the data ensued, which resulted in designation of macrocyclic hemiaminal **1.2** as the actual structure of the diazonamide A.[13]

As noted, the structure of diazonamide A **1.2** contains several synthetically challenging features. The overall strained and rigid double-macrocyclic structure involving one 12-member ring with peptide backbone (Figure 1.1, compound **1.2**, blue circle) and other 12-member heterocycle based macrocycle (Figure 1.1, compound **1.2**, yellow circle) pose a difficult question on design of synthesis as construction of one ring will definitely affect the formation of other. Yet the single most challenging-to-synthesize motif of the **1.2** is the tetracyclic aminal core with tertiary all-carbon stereocenter at C10 (Figure 1.1, compound **1.2,** green circle) at the heart of the compound. The assembly of this structural subunit would call for multiple C-C bond formations in stereocontrolled manner. Not surprisingly, multiple groups embarked on tackling these synthetic challenges and considerable synthetic efforts culminated in four completed total syntheses of diazonamide A **1.2** by groups of Nicolaou[14,15], Harran[16] and MacMillan[17]. The syntheses are discussed in the next chapters.

1.1.1. First total synthesis by Nicolaou

The first two total syntheses of the revised diazonamide A **1.2** were accomplished in the laboratory of Nicolaou and were published in 2002 and 2003[14,15], and later described in more detail in 2004.[18,19] Previously the same group participated in the race for the first total synthesis of the originally proposed structure **1.1**, and although they did not reach the goal, the gained insight into the disconnection strategies and building block synthesis turned out to be useful in the total synthesis of diazonamide A **1.2**.[10]

In the first total synthesis of diazonamide A **1.2**, Nicolaou chose to employ strategy that relied on an initial assembly of the left side 12-member ring with peptide backbone under classic macrolactamization conditions (Figure 1.2). The more unconventional heterocycle-based macrocycle would be formed at later stage of the synthesis using *Witkop*-style reaction leading to atroposelective formation of the right side 12-member ring. The elements of C10 stereocenter were planned to introduce through electrophilic aromatic substitution and nucleophilic addition.

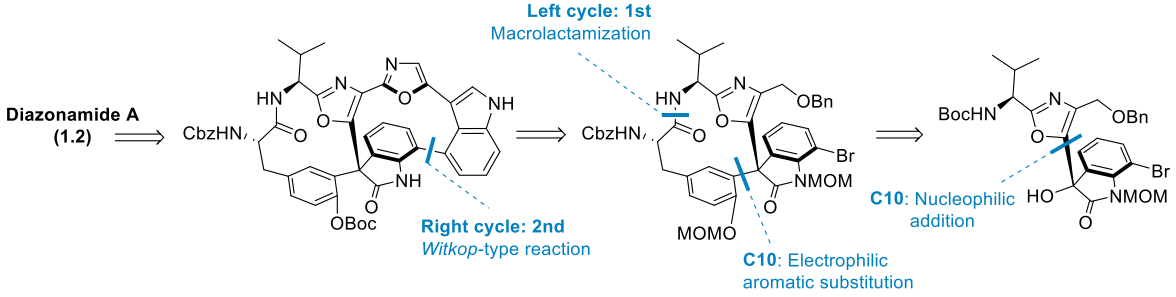

Figure 1.2 **General strategy for the first total synthesis of diazonamide A by Nicolaou**

The synthesis commenced by condensation of Ser-OMe (**1.3**) and *L*-Boc-Val-OH (**1.4**) into the oxazoline **1.5** using amide coupling followed by dehydration with *Burgess* reagent (Figure 1.3). Next, oxazoline ring was dehydrogenated to oxazole using $BrCl_3$/DBU. This cyclization/dehydrogenation sequence provided higher yield and less by-products than classic *Robinson-Gabriel* cyclodehydration conditions (heating with Lewis or Brønsted acid). Subsequent reduction of methyl ester and introduction of benzyl group provided compound **1.6**. Double deprotonation of **1.6** using *n*BuLi formed dianion **I**, and its subsequent nucleophilic addition to *N*-MOM protected bromo isatin **1.7** cleanly afforded tertiary alcohol **1.8** (73% yield) and completed the formation of the first part of the central tetracyclic hemiaminal core. Next, authors anticipated that reaction of the newly formed tertiary alcohol **1.8** with acid could generate cationic species which could be trapped with protected tyrosine **1.9** in electrophilic aromatic substitution manner thus generating compound **1.10**. Luckily, intensive screening of conditions indicated that substitution of the alcohol in compound **1.8** with **1.9** in the presence of *p*TsOH (4 equiv., DCE, 60 °C, 25 min.) affords macrocycle precursor **1.10** as mixture of epimers (1:1) in 33% yield. And as such the final substituent at the central C10 all-carbon quaternary stereocenter was introduced. The assessment of absolute configuration using NMR techniques proved to be impossible so both epimers of compound **1.10** (after chromatographical separation) were processed through the ensuing synthetic steps. Protecting group manipulations preceded the next key event - formation of the left hand-side 12-member macrocyclic ring. Fortunately, use of HATU and 2,4,6-collidine in DMF/DCM (1:2) facilitated formation of the macrocycle **1.11** from the corresponding amino acid with 36% yield. The use of high dilution (3.0×10^{-4} M final concentration) was required to minimize formation of dimeric and oligomeric side products. Notably, only the needed (*S*)-epimer could be cyclized into macrocycle **1.11**, while (*R*)-epimer formed dimeric and higher oligomeric structures. This unexpected feature allowed for retrospective identification and assignment of diastereomers of previously prepared compound **1.10**.

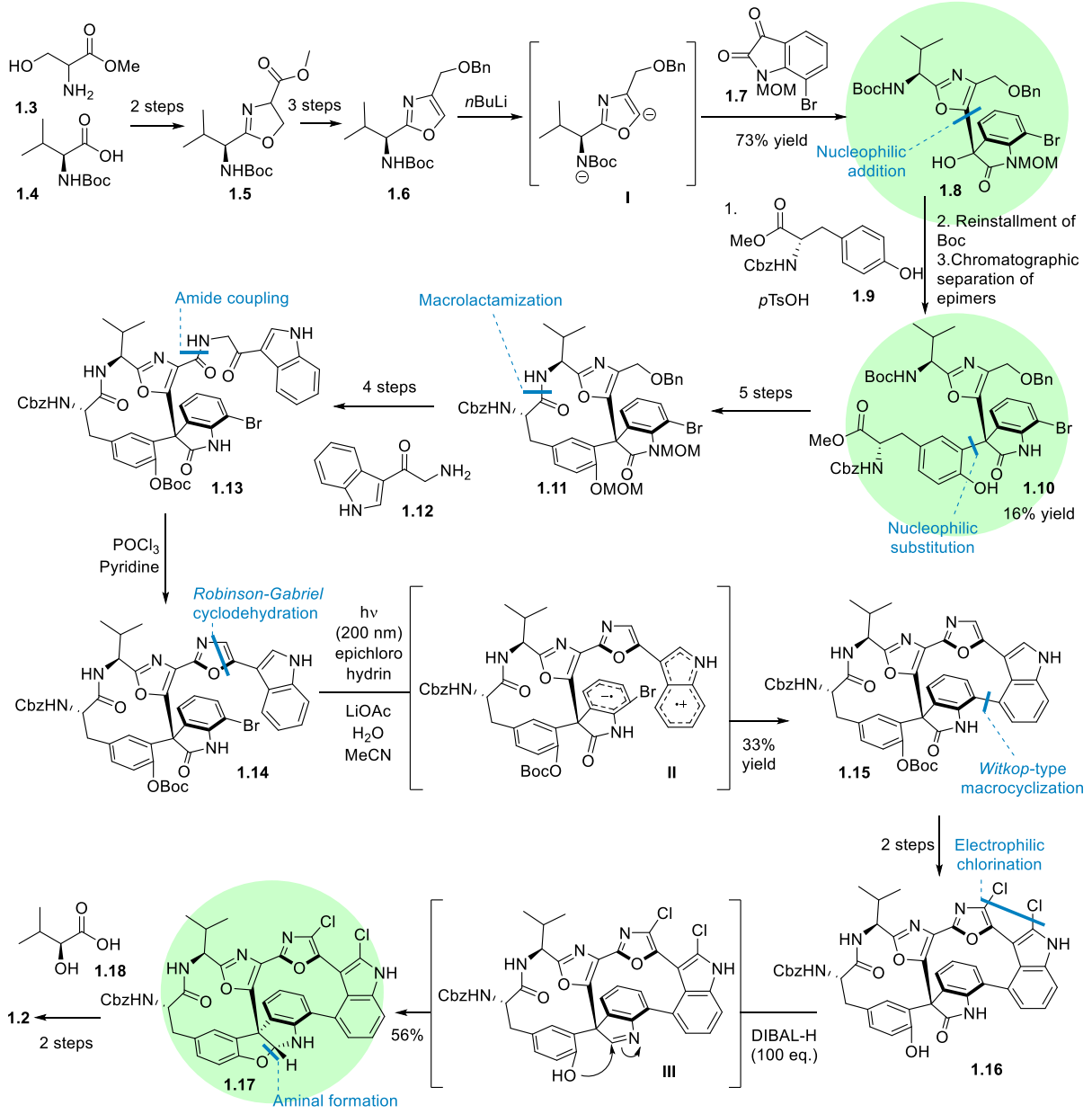

Figure 1.3 **First total synthesis of diazonamide A 1.2 by Nicolaou. Green circles indicate the steps for the formation of the tetracyclic core structure.**

Next, protective group manipulations, oxidation of hydroxymethyl moiety to carboxylic acid and introduction of indole-amide sidechain using aminoketone **1.12** led to compound **1.13** – precursor of the synthesis of bioxazole motif. Formation of the bioxazole **1.14** was achieved using *Robinson-Gabriel* cyclodehydration reaction in pyridine-buffered $POCl_3$ (52% yield). This set the stage for the key *Witkop*-type photolytic reaction which would form the biaryl bond between oxindole and indole moieties and close the right hand-side macrocycle. This transformation presumably involved generation of diradical species **II** along with expulsion of HBr and subsequent recombination of radicals. Indeed, the reaction conditions (LiOAc, 200 nm UV light and excess of epichlorohydrin as acid scavenger; appropriated from

[12]) promoted formation of the biaryl **1.15** as single atropisomer in 33% yield. The final stages of the total synthesis of diazonamide A **1.2** involved installment of chloro substituents in heterocycles using NCS, closure of the tetracyclic aminal and introduction of (*S*)-hydroxyisovaleric acid (*S*-H*i*VA) sidechain. After the Boc-deprotection of the phenolic hydroxyl group, authors subjected phenol **1.16** to a number of different conditions to close the tetracyclic hemiaminal core, which proved to be surprisingly challenging. The transformation was finally achieved using portion wise addition of 100 equivalents of DIBAL-H and several cooling and warming cycles. This reaction allegedly formed the substituted *3H*-indole **III**, which, after reaction with the nearby phenolic hydroxyl group, formed the hemiaminal **1.17** with 56% yield. Installment of the *S*-H*i*VA (**1.18**) side chain concluded the synthesis and provided diazonamide A **1.2**. Analytical data of compound **1.2** were in agreement with that reported for the natural extract. The synthesis required 21 steps in the longest linear sequence with an overall yield of 0.040%.

The first successful synthesis of diazonamide A **1.2** allowed Nicolaou to establish unambiguously the true structure of the marine natural product. Nicolaou also demonstrated that the initial assembly of the left-hand macrocycle, followed by construction of the right-hand macrocycle is a viable retrosynthetic strategy. It was also shown that the central tetracyclic hemiaminal core can be assembled at a late stage of the synthesis by the addition of phenolic OH onto adjacent iminium ion. Nicolaou also made good use of previously developed conditions for challenging transformations, *Robinson-Gabriel* cyclodehydration[10], *Witkop*-type macrocyclization[12] and nucleophilic substitution for synthesis of C10 quaternary stereocenter.[20]

Overall, the first total synthesis was lengthy and poor yielding. The non-stereoselective formation of the C10 quaternary stereocenter from **1.8** and **1.9** was an important flaw of the developed synthesis because it generated undesired diastereomer waste that, luckily, could be separated by chromatography, leading to poor yields (16%) of the desired macrocyclization precursor **1.10**. An additional drawback of the total synthesis was the late-stage assembly of the core tetracyclic hemiaminal that turned out to be a challenging task that required considerable efforts and could be only achieved under relatively harsh conditions (large excess of DIBAL-H). The above-mentioned shortcomings later spurred the design of alternative retrosynthetic strategies where the challenging tetracycle formation takes place at earlier stages of the total synthesis (see syntheses by Harran and MacMillan in chapters 1.1.3 and 1.1.4).

1.1.2. Second total synthesis by Nicolaou

To maximize chances of the success in their total synthesis endeavor, Nicolaou group pursued an alternative strategy for the preparation of diazonamide A **1.2** simultaneously with the total synthesis approach discussed above (chapter 1.1.1).[15] In the alternative strategy, the right hand-side heterocyclic macrocycle was formed before the peptide backbone-containing left hand-side ring, utilizing SmI_2-promoted hetero-pinacol coupling / oxime cleavage sequence (Figure 1.4). The other key feature of diazonamide A - quaternary all-carbon stereocenter at C10 – would be formed through series of nucleophilic additions.

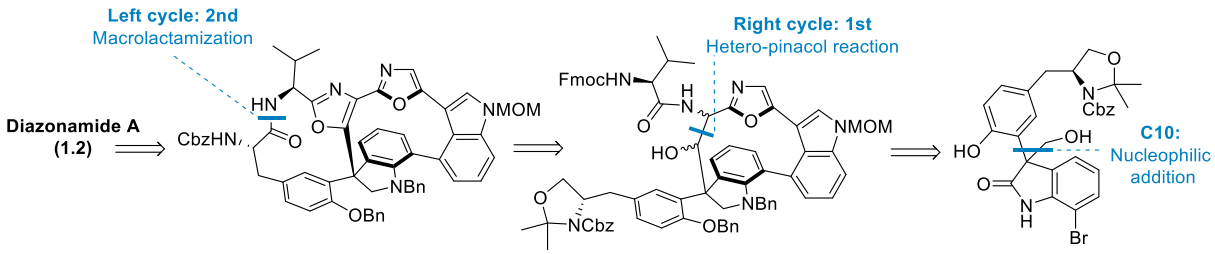

Figure 1.4 **General strategy for synthesis of diazonamide A by Nicolaou**

Synthesis was initiated by preparation of oxazolyl indole **1.22** as this building block later allowed for fast and modular introduction of the right hand-side macrocycle (Figure 1.5). The indole derivative **1.22** was made previously in the Nicolaou group for the use in the synthesis of initially assigned structure of diazonamide A **1.1**.[21] As such, commercially available 4-bromoindole (**1.19**) was transformed into amide **1.20** in three steps (*Michael* addition, reduction, amide coupling) in 74% overall yield. To install the oxazole moiety in the indole using *Robinson-Gabriel* cyclodehydration, oxidation of benzylic CH_2 to ketone was necessary. This transformation was effected by reaction with DDQ followed by further oxidation of the formed alcohol with IBX. Next, reaction under *Wipf's* conditions (Cl_3CCCl_3, PPh_3, TEA, DCM, r.t.) smoothly afforded the oxazole **1.21** in 75% yield over three steps. Protection of indole nitrogen with MOM group followed by Pd-catalyzed *Miyaura* borylation (B_2Pin_2, $Pd(dppf)_2Cl_2$, KOAc, 1,4-dioxane, 95 °C) afforded the building block **1.22**.

Synthesis of the remaining parts of the molecule **1.2** started by the $TiCl_4$-catalyzed nucleophilic addition of Cbz-Tyr-OMe (**1.9**) to 7-bromoisatin **1.23** thus furnishing tertiary alcohol **1.24** in 58% yield. This set in place three out of four substituents at the C10 central all-carbon quaternary stereocenter. Deoxygenation of the tertiary alcohol through the intermediacy of a chloride ($SOCl_2$, then $NaCNBH_3$) and transformation of the tyrosine domain into an acetonide afforded phenol **1.25**.

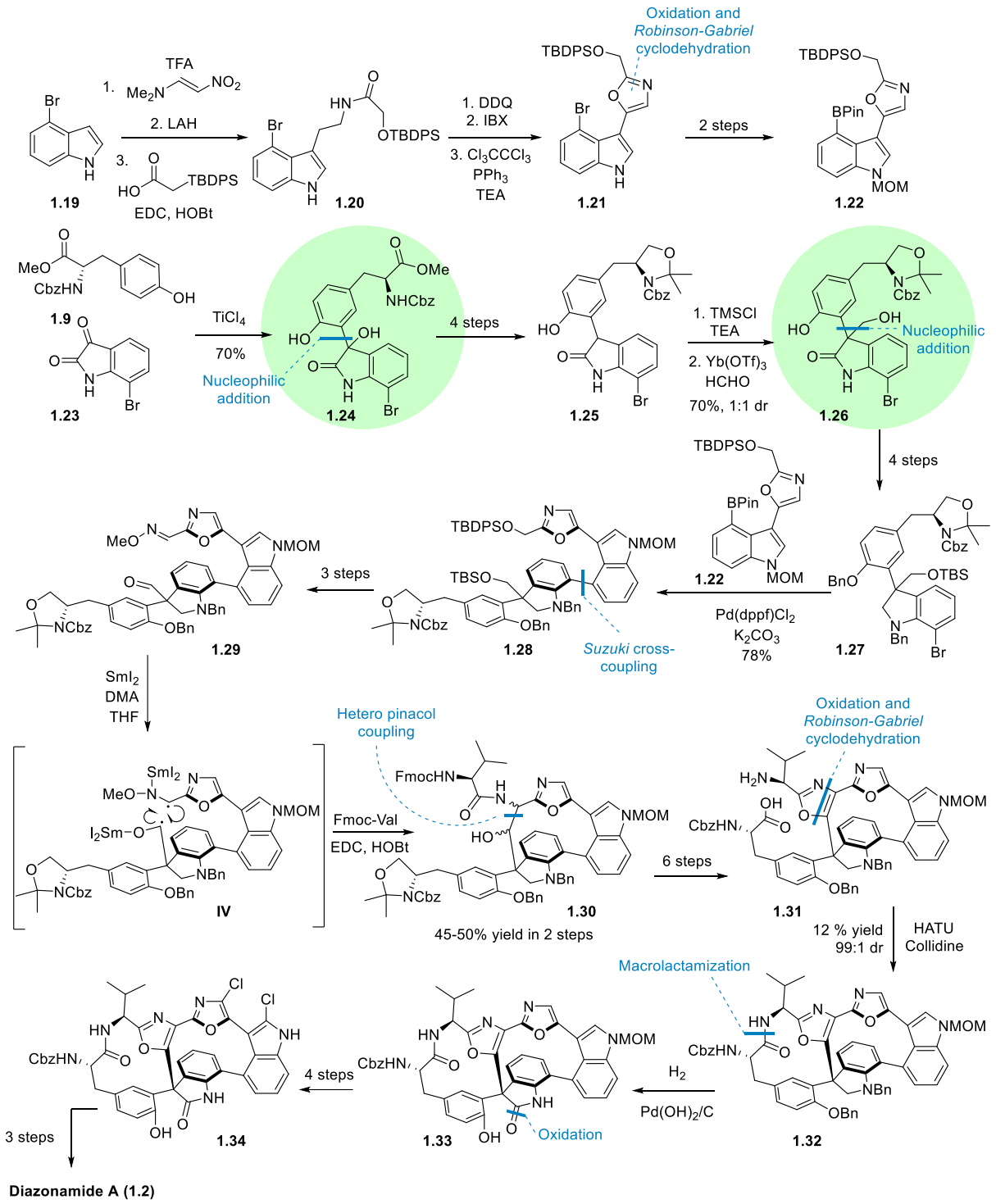

Figure 1.5 **Second total synthesis of diazonamide A by Nicolaou. Green circles indicate the steps for the formation of the tetracyclic core structure.**

Next, authors performed $Yb(OTf)_3$-catalyzed hydroxymethylation of silyl enol ether (derived from indolinone **1.25**) with formaldehyde to introduce a handle for the closing of the right hand-side macrocycle and construction of the C10 all-carbon quaternary stereocenter. The hydroxymethylation yielded alcohol **1.26** as 1:1 mixture of chromatographically inseparable diastereomers with total yield of 70%. Both diastereomers were carried forward in

the hopes that installment of additional functional groups will allow for better separation and structural assignment. Protecting group manipulations along with the reduction of the indolinone to indoline by 9-BBN in refluxing THF (to avoid base-promoted undesired de-formylation upon subsequent *O*-TBS removal) furnished the aryl bromide **1.27**. In contrast to the previous total synthesis where *Witkop*-type reaction was used (Figure 1.3), the biaryl bond connecting the tetracyclic core and the right-hand side indole fragment was assembled using *Suzuki* coupling between bromide **1.27** and pinacolyl boronate **1.22** ($Pd(dppf)_2$, K_2CO_3, DME, 85 °C, 78 %). Afterwards the obtained biaryl **1.28** was converted into aldoxime **1.29** through deprotection, oxidation and selective formation of oxime (selectivity was governed by the better steric accessibility and reactivity of oxazole-aldehyde over the C10 aldehyde). The key step of the synthesis was samarium(II) iodide facilitated hetero pinacol coupling between aldoxime and aldehyde under conditions developed during synthesis of the incorrectly assigned diazonamide A structure **1.1**.[21] Subsequent cleavage of N-O bond was performed using excess of SmI_2 (9 equiv.) and DMA (36 equiv.), and the reaction presumably involves an initial formation of diradical species **IV**. Aqueous work-up of the reaction and subsequent addition of valine fragment onto the newly formed amine furnished the macrocycle **1.30** as 1:1 mixture of diastereomers in 79% combined yield. Oxidation of the newly formed hydroxyl group, *Robinson-Gabriel* cyclodehydration ($POCl_3$, pyridine) and follow-up side chain manipulations (removal of acetonide and Fmoc groups and oxidation of hydroxymethyl group to acid) allowed for preparation of the macrocyclization precursor **1.31**. With **1.31** in hand, the installment of all the required (het)aryl fragments at the C10 quaternary stereocenter was completed and the right hand-side macrocycle assembled. Although the target **1.2** now looked to be within the reach, the macrolactamization of amino acid **1.31** turned out to be the most challenging synthetical step: stirring for seven days in the presence of HATU and 2,4,6-collidine afforded the macrocycle **1.32** in only 10-15% yield with the majority of the material degraded or dimerized. Luckily, it was finally possible to resolve the mixture of C10 epimers (formed in the synthesis of **1.26** and previously inseparable) as only the (*S*)-isomer cyclized into the lactam **1.32** while (*R*)-isomer was unreactive. The cleavage of both *N*- and *O*-benzyl protection as well as *N*-Cbz group with super stoichiometric amounts of $Pd(OH)_2/C$ under hydrogen atmosphere set the stage for the re-oxidation of the indoline subunit to oxindole that was necessary for the formation of the tetracyclic aminal. However, along with the desired removal of protecting groups, the formation of oxindole **1.33** was also observed under the hydrogenation conditions. Authors postulate that the formation of **1.33** might have involved coordination of indoline nitrogen to palladium leading to double β-hydride elimination and formation of 3*H*-indole that would subsequently undergo the addition of

hydroxide anion. The removal of remaining protecting groups, electrophilic aromatic chlorination (NCS, THF, CCl_4) and aminal formation (DIBAL-H; identical to previous synthesis by Nicolaou[14]) furnished diazonamide A **1.2**. Overall, the second total synthesis (31 steps in the longest linear sequence and 0.00014% total yield) proved to be less efficient as compared to the first one but afforded completely unique solutions to its many intricate problems.

With the successfully accomplished two total syntheses of diazonamide A, Nicolaou showed that the initial assembly of any of the two macrocycles (peptidic backbone-containing left-hand macrocycle or right-hand macrocycle) is a viable approach. However, the closure of the left-hand macrocycle with the right-side macrocycle already in place is challenging (at least as long as the rigid core tetracyclic aminal is not formed). Authors also displayed great ingenuity in the development of heteropinacol coupling and oxime cleavage sequence that furnished the left side macrocycle. The unexpected $Pd(OH)_2$-catalyzed oxidation of indoline **1.32** to to oxindole **1.33** is also noteworthy.

Overall, the 2nd synthesis of diazonamide A by Nicolaou was more modular than the 1st one, however it was longer (31 vs. 21 steps) and less efficient with only 0.00014% total yield. One of the main shortcomings of the synthesis was the non-stereoselective formation of C10 stereogenic center during the *Mukaiyama* aldol reaction between oxindole **1.25** and formaldehyde. Although suitable for the introduction of the necessary handle for up-coming reaction steps (70% yield), the reaction provided inseparable mixture of diastereomers of oxindole **1.26** that could be resolved only upon formation of the left side macrocycle downstream the synthesis. This, obviously, led to diminished overall yield of the second total synthesis. The synthesis was additionally complicated by the unexpected instability of the alcohol **1.26** which led to unplanned reduction of oxindole **1.26** to indoline **1.27** and late-stage re-oxidation (25% combined yield). In the meantime, the second total synthesis stands out among the other approaches in that the right-hand macrocycle is constructed before the peptide backbone-containing left-hand macrocycle. The tetracyclic hemiaminal core is assembled during the endgame of the total synthesis.

1.1.3. Total synthesis by Harran

Soon after Nicolaou's publications, a significantly different total synthesis of diazonamide A **1.2** was published by Harran's group.[16] Having prepared the initially incorrectly assigned structure of diazonamide A **1.1**[12] that triggered the structural reassignment, Harran was well-positioned to use the acquired knowledge towards the total

synthesis of the revised diazonamide A structure **1.2**. Authors envisioned assembly of the right-hand side macrocycle by the formation of biaryl bond between indole and indoline subunits after the left hand-side macrocyclic ring is in place (Figure 1.6). The macrocyclization via biaryl bond formation could be effected by the *Witkop*-type reaction. For closing of the peptide backbone-containing left hand-side macrocycle and formation of the C10 stereocenter, authors chose to utilize intramolecular oxidative addition between tyrosine phenol moiety and unprotected indole - method that would mimic the biosynthetic pathway of diazonamide A **1.2** and simultaneously deliver two key structural features.

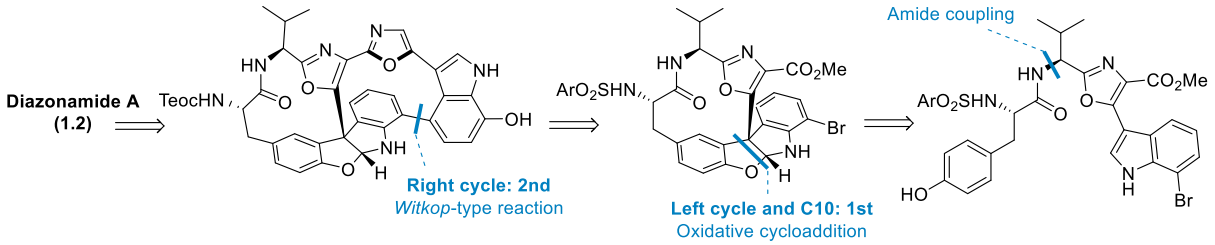

Figure 1.6 **General strategy for synthesis of diazonamide A by Harran**

The synthesis started with *in situ* preparation of acyl chloride from *N*-Z-(*L*)-Val-OH **1.35** using *Ghosez* reagent, and followed by reaction with racemic tryptophan derivative **1.36** to form the dipeptide **1.37** (Figure 1.7). Next, *Yonemitsu* benzylic oxidation (DDQ, THF, 70 ^{o}C) and subsequent HBr-mediated *Robinson-Gabriel* cyclodehydration formed the oxazole moiety, cleaved off the *N*-Cbz protection and delivered the indolyl-oxazole **1.38** in 85% yield after two steps. Condensation of the free amine with *N*-protected *L*-tyrosine furnished amide **1.39** that already contained all the necessary functionalities for the planned formation of the tetracyclic aminal core and closing of the left hand-side macrocyclic ring. Indeed, addition of **1.39** to cold solution of $PhI(OAc)_2$ and LiOAc in TFE (-20 °C, 10 min.) afforded macrocycle **1.40** in reproducible 20–25% yield along with 7-8% of its C10 epimer (both were chromatographically separable). The reaction mechanism involved oxidative formation of the phenoxonium ion **V** which was then captured by the tethered indole forming intermediate **VI**. Rearomatization of the phenol ring and attack of the oxygen on the nearby indolenium ion furnished the tetracyclic aminal **1.40**. This synthetic approach gave authors fast access (five steps) to highly elaborated macrocyclic compound **1.40** which contained almost all functionalities found in diazonamide A left hand-side macrocycle. Next, protective group manipulations and subsequent condensation of carboxylic acid with tryptamine yielded amide **1.41**, a precursor of bioxazole **1.42**. Subjection of **1.41** to benzylic oxidation (DDQ) and cyclodehydration under *Wipf's* conditions (PPh_3, $(CCl_3)_2$, TEA) swiftly yielded the elaborated

bis(oxazolyl)indole **1.42** and set the stage for the key *Witkop*-type photoinduced macrocyclization. Preparation of lithium phenoxide from **1.42** was followed by degassing and irradiation (300 nm) of the aqueous acetonitrile solution which delivered biaryl **1.43** as single atropisomer in 72% yield. The increased yield of the reaction as compared to earlier reports for very similar reactions by the same group (32-40% yield)[12] and Nicolaou (33% yield, see Figure 1.3)[14] was attributed to presence of hydroxyl substituent at indole ring (both Harran and Nicolaou previously used indole that was unsubstituted at the phenyl ring). Authors postulated that the increased electron density in the hydroxy indole chromophore facilitated the electron transfer reaction, and the formation of biradical species **VII**. Mesolytic elimination of bromide and internal collapse of the biradical formed indolenone **VIII** that tautomerized into the biaryl **1.43**. Deoxygenation of the indole ring (trough hydrogenolysis of the corresponding triflate), introduction of chlorine atoms and (*S*)-H*i*VA side chain comprised the endgame of the total synthesis and furnished the diazonamide A **1.2** in relatively short sequence (19 steps) and in 0.01% overall yield.

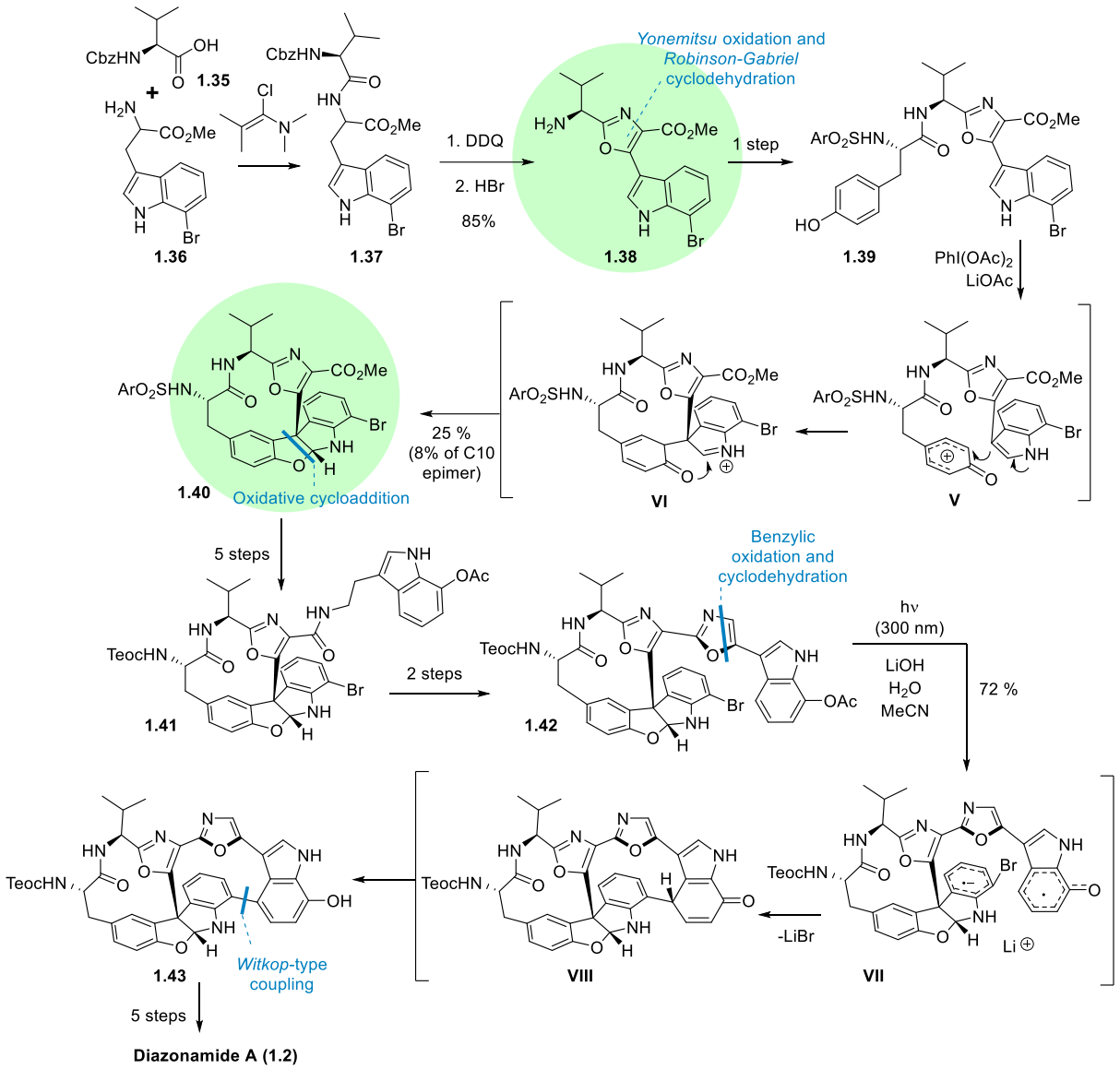

Figure 1.7 **Total synthesis of diazonamide A by Harran. Green circles indicate the steps for the formation of the tetracyclic core structure.**

Overall, Harran's total synthesis of diazonamide A **1.2** features a combination of biomimetic approach for the assembly of the left-hand macrocycle and tetracyclic hemiaminal subunit (oxidative cycloaddition between phenol and indole moieties) with proven transformations to furnish the right-hand macrocycle (*Robinson-Gabriel* cyclodehydration, *Witkop*-type coupling). The oxidative cycloaddition is particularly notable due to its ability to simultaneously form both the left-hand macrocycle and the tetracyclic hemiaminal, an approach that contrasts the stepwise methods developed by Nicolaou. The cycloaddition, however, suffered from the same shortcoming as the majority of other substrate-controlled formations of the C10 stereocenter that is the mediocre diastereoselectivity (compound **1.40** was formed with 2.7:1 dr). Noteworthy is also the improved *Witkop*-type macrocyclization between phenoxide and aryl bromide functionalities: introduction of the oxygen atom in the

indole chromophore allowed for two-fold increase in yield when compared to that for the unsubstituted indole.

1.1.4. Total synthesis by MacMillan

The fourth total synthesis of diazonamide A **1.2** was accomplished in the lab of David MacMillan and was published in 2011.[17] The synthesis comprised an initial stereoselective formation of the C10 quaternary stereocenter of the tetracyclic hemiaminal by organocatalytic *Michael* reaction. Subsequently, the left hand-side 12-membered macrocycle would be closed using *Lewis* acid-catalyzed macroaldolisation. Finally, the right hand-side ring would be constructed in Pd-catalyzed borylation-annulation sequence (Figure 1.8).

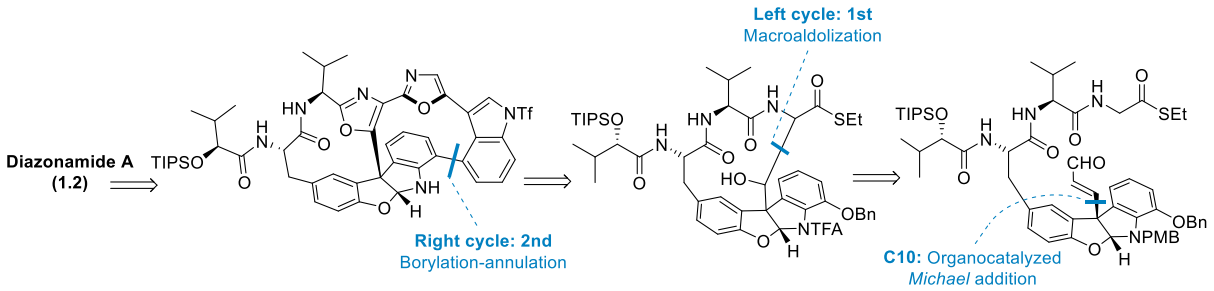

Figure 1.8 **General strategy for synthesis of diazonamide A by MacMillan**

The synthesis set off with Suzuki coupling between easily accessible building blocks, tyrosine derivative **1.44** and indole boronate **1.45**, and continued by saponification of methyl ester and coupling with amine **1.46** (Figure 1.9). This sequence delivered the highly decorated tetracycle precursor **1.47** in 78% yield after three steps. Its *Michael*-type addition to propynal in the presence of chiral imidazolidinone catalyst **1.48** was one of the key steps. Initially, relatively poor diastereoselectivity (4.2:1 dr) was observed for the tetracycle **1.49** when the reaction was performed in a 20:1 mixture of DCM:MeOH at -70 °C temperature using 30 mol% of catalyst **1.48** (as TFA salt) and 10 equivalents of propynal. Luckily, it was found that change of the counterion of the catalyst **1.48** from trifluoroacetate to trichloroacetate in combination with the use of ternary solvent mixture (10:10:1 $CHCl_3$:PhMe:MeOH) allowed for considerable improvement of the diastereocontrol to >20:1 dr, and afforded tetracycle **1.49** in 86% yield. Mechanistically, the tetracycle **1.49** formation involved diastereoselective nucleophilic conjugate addition of indole moiety to chiral iminium ion (formed *in situ* from imidazolidinone **1.48** and propynal) as in intermediate **IX.** Subsequent attack of phenolic hydroxyl onto the formed indolenium ion closed the tetracycle. The diastereocontrol was

exerted through the sterically large *tert*-butyl and benzyl substituents on the catalyst that fixed the geometry of the iminium ion and ensured enantiofacial discrimination (attack of indole was possible only from the *Si* face of iminium as *Re* was shielded). Importantly, when racemic organocatalyst **1.48** was used, the tetracyclic aldehyde **1.49** was delivered as 1:1 mixture of diastereomers evidencing that the diastereoselectivity of the *Michael* addition was fully catalyst controlled.

The successful diastereoselective assembly of tetracyclic aldehyde core **1.49** set the stage for the construction of the left-hand macrocycle by intramolecular macroaldolisation of aldehyde **1.50**. The latter was prepared from **1.49** by swap of protecting groups on indoline and ozonolysis of the double bond. Screening of the macroaldolisation reaction conditions resulted in $MgBr_2$-facilitated aldol reaction ($MgBr_2 \times Et_2O$ (10 equiv.), TMSCl, TEA, THF, r.t.) that delivered macrocyclic alcohol **1.51** in 67% yield. Addition of TMSCl was essential for avoiding the undesired retro-aldol reaction. Next, the newly formed alcohol was easily oxidized with DMP to form ketone. Subsequent cyclodehydration, however, turned out to be challenging and only reaction with DAST (PhH, r.t.) afforded the oxazole **1.52** (65% yield after two steps).

Even though macrocycle **1.52** shared structural similarity to total synthesis intermediates prepared by Nicolaou and Harran (e.g., compounds **1.11** and **1.40** respectively), instead of relying on *Witkop*-style electrocyclization, MacMillan chose to develop his own approach for the construction of the right-hand side 12-member macrocycle. Accordingly, the new approach comprised AgTFA-facilitated amide coupling between thioester of **1.52** and tryptamine derivative, subsequent cyclodehydration under *Wipf's* conditions (PPh_3, $(CCl_3)_2$, TEA, DCM), and protecting group manipulations to install the second oxazole fragment and to furnish the highly complex intermediate **1.53**, a precursor of palladium-catalyzed intramolecular borylation-annulation sequence. After an extensive experimentation, the borylation-annulation tandem transformation using $(BPin)_2$, KF and $Pd(PPh_3)_4$ at 120 °C temperature under microwave irradiation allowed authors to assemble the right-hand macrocycle (50% yield of **1.54**). Protective bromination of the tetracycle C15 position in **1.54** (NBS, THF, r.t.) was required for subsequent selective chlorination of indole and oxazole moieties (NCS, THF, 40 °C). Finally, hydrogenolysis of the aryl bromide and removal of *O*-TIPS group (TASF, DMF, r.t.) completed the synthesis of diazonamide A **1.2** (Figure 1.9).

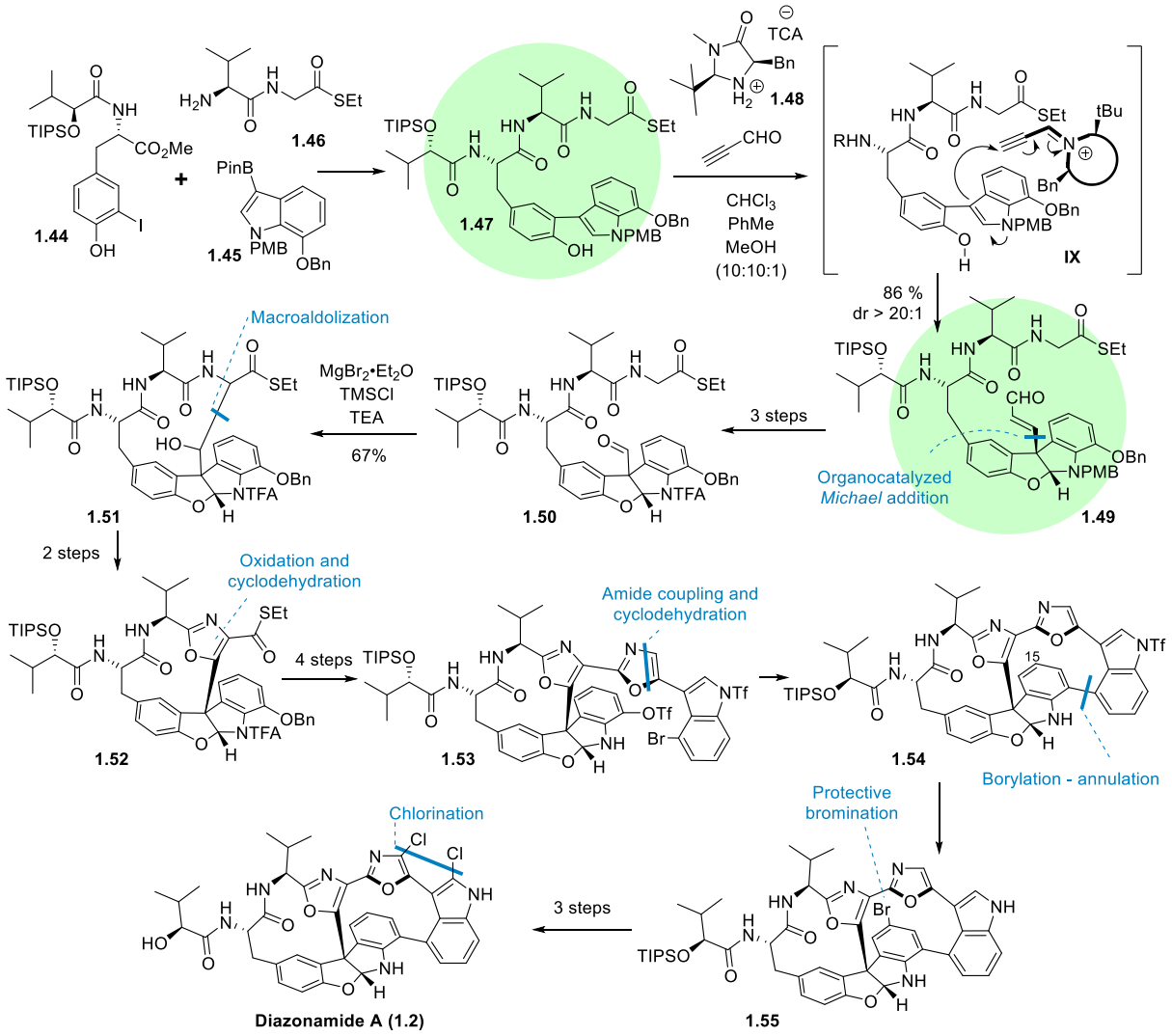

Figure 1.9 **Total synthesis of diazonamide A by MacMillan. Green circles indicate the steps for the formation of the tetracyclic core structure.**

Overall, the synthesis of diazonamide A **1.2** by MacMillan appears to be the 2nd shortest (20 steps vs. Harran's 19 steps) and most efficient (1.8 % overall yield) of the four reported total syntheses. Here authors employed powerful combination of organo- and transition metal catalysis to assemble the complex natural product. The chiral imidazolidinone-catalyzed highly diastereoselective (>20:1 dr) formation of the C10 quaternary stereocenter and simultaneous closing of the tetracyclic hemiaminal core represent a significant improvement over the previous syntheses as this led to simpler purification, less wasted material, greater overall yield, and higher throughput of material. Similarly, the initial preparation of 13-membered left side macrocycle (**1.51**) with subsequent ring contraction (**1.52**) proved to be great strategy for highly efficient formation of left-hand side macrocycle.

1.1.5. Formal total synthesis by Magnus

Even though the hard-to-reach goal of total synthesis of diazonamide A **1.2** had been successfully achieved by Nicolaou, Harran and MacMillan, other groups kept pushing for their own versions of the total synthesis. The most notable in this field were labs of Magnus, Sammakia and Moody, all of whom reported formal total synthesis - preparation of elaborated precursors to diazonamide A **1.2** which could be converted into the natural product using previously disclosed strategies.

The formal total synthesis of diazonamide A **1.2** published by Magnus in 2007 was based on a strategy initially devised for the synthesis of the incorrectly assigned "acetal" structure of diazonamide A **1.1**.[22]. The formal synthesis featured the construction of the tetracyclic hemiaminal and all-carbon quaternary stereocenter by nucleophilic addition and *Fries*-type rearrangement. The synthesis was commenced by preparation of valine-derived oxazole ester **1.5** that has been previously prepared by Nicolaou (Figure 1.10).[10] Saponification of the ester and deprotonation of the resulting carboxylic acid **1.56** with 3.4 equivalents of *t*BuLi (HMPA (3.4 equiv.), THF, -78 °C) led to the formation of trianion **X** that was *in situ* reacted with 7-bromoisatin **1.7** and, after methylation of the free carboxylic acid with TMS-diazomethane, produced a racemic mixture of the tertiary alcohol **1.57** in 35-50% yield. Deprotection of the *N*-Boc group (TFA, DCM, r.t.), formation of the amide bond with *O*,*N*-protected tyrosine derivative **1.58** under standard reaction conditions (EDC, HOBt, DMF, r.t.) and chlorination of the C10 tertiary alcohol ($SOCl_2$, 2,4,6-collidine) afforded the chloride **1.59** as a 1:1 mixture of diastereomers in 35% yield after three steps. Luckily, exposure of the chloride **1.59** to TBAF in THF brought on the *O*-TIPS cleavage and clean formation of ether **1.60** as 1:1 mixture of diastereomers. Next, it was found that heating of **1.60** in $CHCl_3$ at 61 °C for six hours facilitated the *Fries*-type *O*-to-*C* rearrangement with 99% yield but mediocre stereoselectivity (70:30 dr) in favor of the desired diastereomer (*S*)-**1.61**. In more polar solvents (HFIP, DMSO, MeCN, EtOH) macrocycle **1.61** was formed with lower diastereoselectivity (49:51 to 67:33). Mechanistically, the thermal *O*-to-*C* rearrangement involved C-O bond dissociation and the formation of ion-pair **XI**. Subsequent nucleophilic addition of phenolate to the carbocation furnished the new C-C bond in **1.61** and established the quaternary stereocenter. The formal synthesis was continued by protection of phenolic hydroxyl group (MOM-Cl, DIPEA), reduction of the methyl ester ($LiBH_4$, THF) and benzylation of the newly formed primary alcohol (BnBr, NaH, TBAI, DMF, THF) to obtain macrocycle **1.11** with 58% yield over three steps. Macrocycle **1.11** was an advanced intermediate in the first total synthesis by Nicolaou[14] and all analytical data of the newly

prepared **1.11** was in agreement with the reported values. This constituted a formal total synthesis of diazonamide A **1.2** as compound **1.11** could be transformed into diazonamide A **1.2** using methods described earlier.

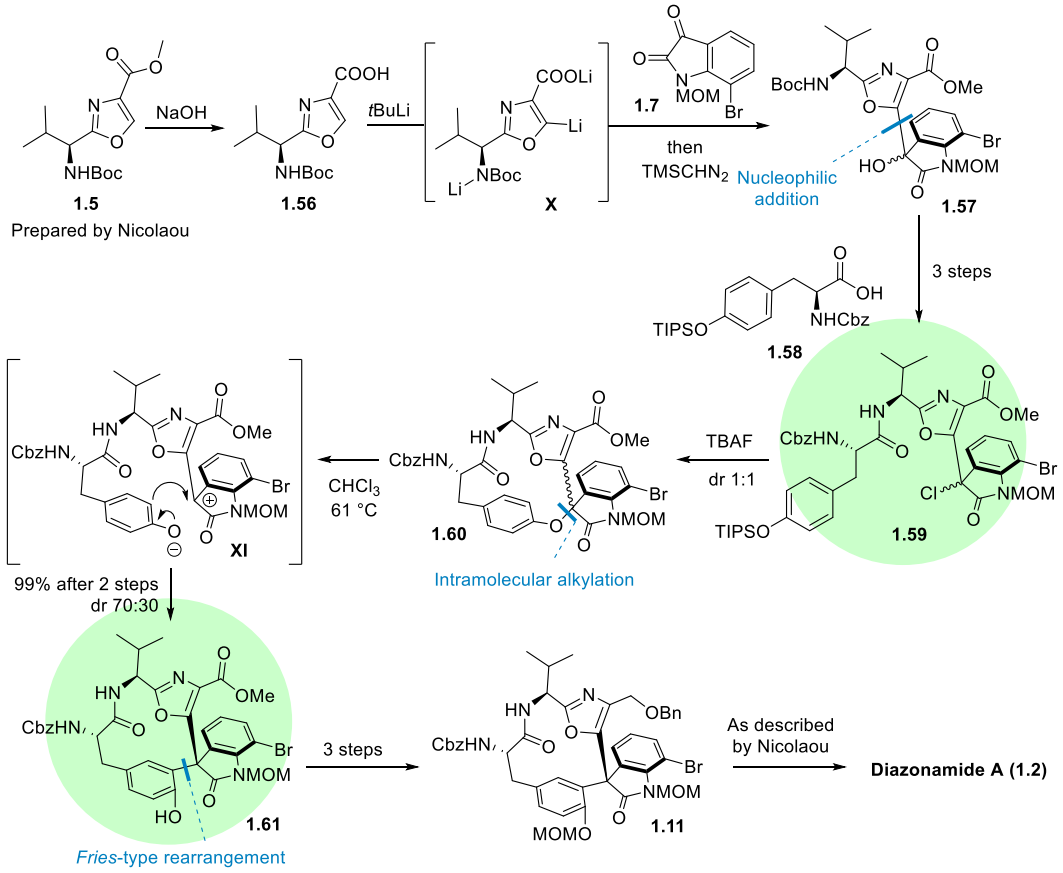

Figure 1.10 **Formal total synthesis of diazonamide A by Magnus. Green circles indicate the steps for the formation of the tetracyclic core structure.**

Overall, Magnus had disclosed an elegant synthesis of advanced intermediate **1.11** using intramolecular *Fries*-type *O*-to-*C* migration for the preparation of the all-carbon quaternary stereocenter. The developed method for synthesis of quaternary stereogenic center proved to be high yielding (99% from **1.59** to **1.61**), however it was plagued by the same mediocre diastereoselectivity (70:30 dr) as was observed in the majority of other substrate-controlled constructions of the quaternary stereogenic center. Importantly, the formal total synthesis made use of well-known and easily accessible building blocks, namely oxazole **1.5**, isatin **1.7** and tyrosine derivative **1.58**.

1.1.6. Formal total synthesis by Sammakia

Few years after Magnus, Sammakia published the synthesis of another advanced intermediate **1.66** from the Nicolaou's total synthesis of diazonamide A **1.2.**[23] In the Sammakia's formal total synthesis, preparation of quaternary stereogenic center and tetracyclic hemiaminal capitalized on an intramolecular diastereoselective S_NAr-type arylation (Figure 1.11). The synthesis commenced by addition of tyrosine-derived magnesium phenolate **1.9** to 7-bromoisatin **1.23** which produced indolinone **1.62** as a 1:1 mixture of diastereomers in 74% yield. Deoxygenation of the tertiary alcohol through intermediacy of chloride ($SOCl_2$, then $NaBH_3CN$), saponification of methyl ester (LiOH, THF, H_2O) and introduction of cianooxazole moiety in the molecule using amide coupling with amine **1.63** (EDC, HOBt, TEA) led to the macrocyclization precursor **1.64**. When it was subjected to basic reaction conditions at elevated temperature (Na_2CO_3, DMF, 65 °C), the intramolecular S_NAr-type arylation of oxindole sodium enolate with bromo oxazole resulted in the formation of macrocycle **1.65** as single diastereomer with 56% yield. Hydrolysis of the nitrile functional group and subsequent reduction of the amide with SmI_2 led to published macrocycle **1.66** that could be elaborated into diazonamide A **1.2** in several steps following method devised by Nicolaou. As such, this scheme constituted another formal total synthesis diazonamide A.

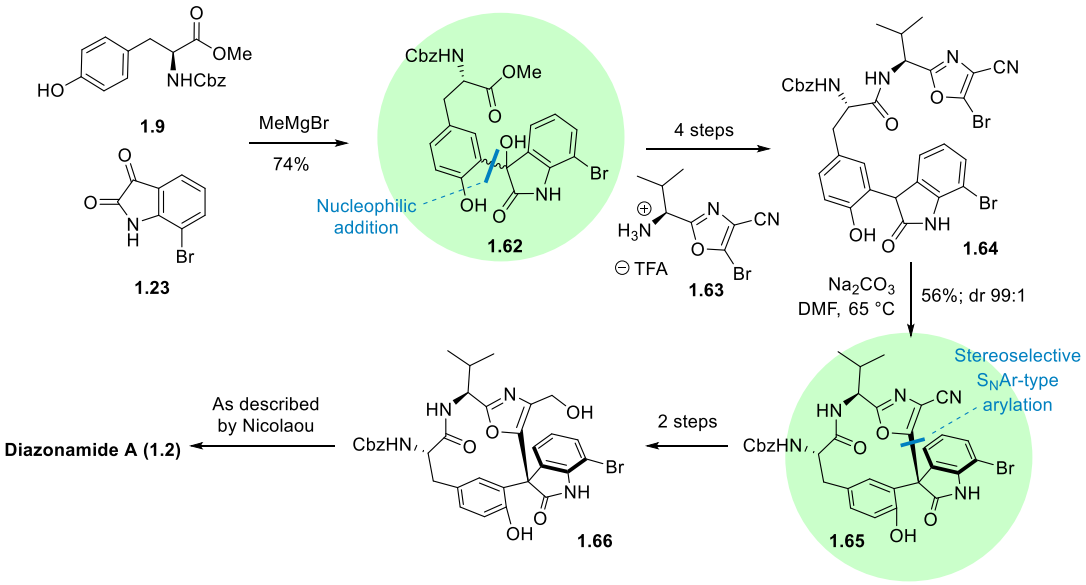

Figure 1.11 **Formal total synthesis of diazonamide A by Sammakia. Green circles indicate the steps for the formation of the tetracyclic core structure.**

Overall, Sammakia did show fundamentally original approach for the construction of quaternary stereogenic center and assembly of the left-hand macrocycle. The intramolecular

S_NAr-type reaction between enolate of oxindole and the tethered bromo oxazole turned out to be remarkably diastereoselective (99:1 dr) when compared to the other substrate-controlled approaches for the quaternary stereogenic center formation.[14,16,22] Notable is also the use of simple and easily accessible building blocks for the construction of cyclization precursor **1.64** (namely tyrosine **1.9**, isatin **1.23** and bromooxazole **1.63**). The Sammakia's approach provides the most efficient solution for the construction of quaternary stereogenic center and peptide backbone-containing 12-membered macrocycle.

1.1.7. Formal total synthesis by Moody

Like Sammakia, Moody also aimed at the synthesis of Nicolaou's advanced intermediate **1.11**, and his synthesis of closely related structural analog **1.75** (*O*-Bn instead of *O*-MOM as in **1.11**) was published in 2016.[24] Moody's approach to the quaternary stereocenter formation relied on an oxidative rearrangement of 2,3-disubstituted indole (Figure 1.12). At first, a highly complex indole derivative **1.69** was prepared in 75% yield through *ipso*-borodesylilation - *Suzuki* coupling sequence (BCl_3, DCM, then $Pd(PPh_3)_4$, Na_2CO_3, DME, MW, 100 °C) from 2-silylindole **1.67** (prepared in two steps from 7-bromoindole) and iodo oxazole **1.68** (prepared in three steps from oxazole carboxylate **1.6**[14]). The *ipso*-borodesylilation - *Suzuki* coupling method had been developed by Snieckus[25] and involves reaction with BCl_3 for *in situ* preparation of dichloroborane species that participate in the coupling reaction. Next, iodination of the indole **1.69** (NIS, DMF) and *Suzuki* coupling with trypthophan derivative **1.70** ($Pd(dppf)Cl_2$, K_2CO_3, MeCN, H_2O, 60 °C) delivered the elaborated intermediate **1.71**. Removal of protective groups (LiOH, then TFA) and macrolactamization (HATU, DIPEA, DCM) furnished macrolactam **1.72**. Oxidation of the indole (*via* epoxide **XII**) by *in situ* generated DMDO (Oxone®, $NaHCO_3$, acetone, H_2O) resulted in the formation of the hydroxyindole **1.73** in 21 % yield (along with its epimer in 54% yield). Finally, $Sc(OTf)_3$-promoted migratory rearrangement of oxazole moiety from C2 to C3 position of indole afforded the desired macrocycle **1.75**, however, reaction was compromised by poor yields (10%), and the formation of the isomeric C3 to C2 phenol migration product **1.74** (22% yield). The migratory rearrangement of **1.73** presumably involved initial coordination of the indolic nitrogen with the $Sc(OTf)_3$ (Lewis acid; LA) to form the intermediate **XIII**. Next, intramolecular attack of the hydroxylic oxygen onto the iminium ion formed epoxide **XIV**. Migration of the oxazole moiety from C2 to C3 along with rearrangement of epoxide and subsequent aqueous work-up formed the 2-indolinone **1.75**.

Comparison of analytical data of the obtained **1.75** (after removal of benzyl groups) with those reported by Nicolaou and Sammakia confirmed the identity of the macrocycle.

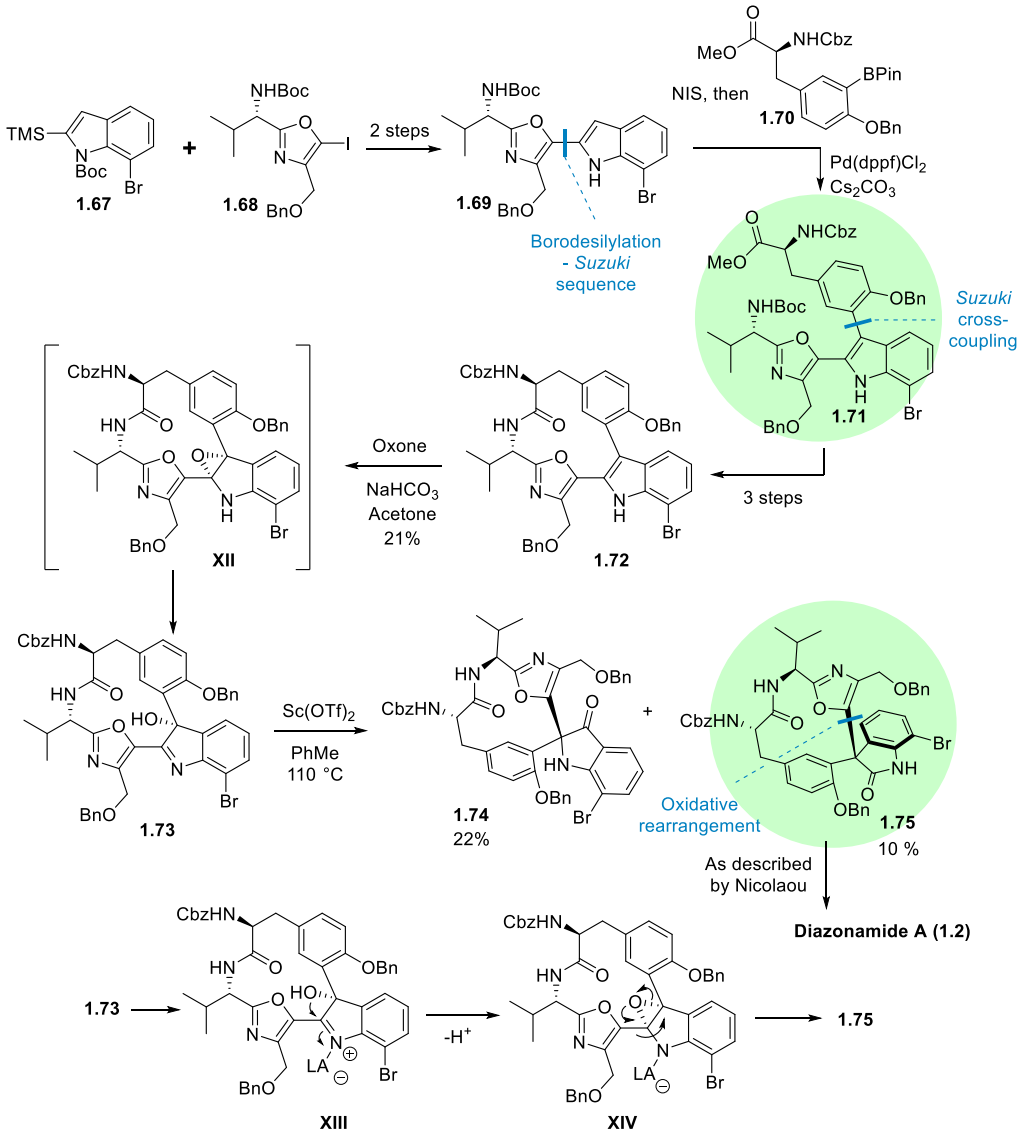

Figure 1.12 **Formal total synthesis of diazonamide A by Moody. Green circles indicate the steps for the formation of the tetracyclic core structure.**

Overall, Moody had disclosed unusual and unprecedented strategy for the synthesis of the complex macrocycle **1.75** that capitalized on intramolecular oxidative rearrangement as the key step for quaternary stereogenic center formation. In the meantime, important drawback of the Moody's approach is the extremely poor overall yield (2%) for the two-step transformation of indole **1.72** into compound **1.75** that could be attributed to the predominant formation of the undesired diastereomeric alcohol during oxidation of the indole as well as competing migration of phenol group instead of oxazole during the rearrangement process.

To conclude, the complex architecture of diazonamide A **1.2** had presented a significant challenge for the total synthesis community. In the end it was tackled in several ingenious ways, each presenting a new answer to the diazonamide A key challenges – synthesis of two fused 12-membered macrocycles, quaternary all-carbon stereocenter and tetracyclic hemiaminal core. Assembly of the peptide backbone-derived left hand macrocycle before the construction of the right hand polyaromatic macrocycle had been used more frequently because it helped to control atroposelectivity in the formation of the latter.[16] Furthermore, in the right-to-left strategy, macrolactamization on the left side cycle can be complicated by strain induced from the right side ring.[15] Substrate controlled formation of quaternary stereogenic center generally afforded mediocre diastereoselectivity[14,16,22] with the only exception being method used by Sammakia (intramolecular S_NAr-type cyclization).[23] Chiral catalyst-controlled reaction, however, could alleviate this problem, leading to higher stereocontrol as evidenced in synthesis by MacMillan.[17] Late stage formation of the tetracyclic hemiaminal core can be challenging[14] and is generally easier to accomplish at the early stage of the total synthesis.[16,17]

1.2. Compound DZ-2384

Although the high biological activity and the unique, highly complex structure makes diazonamide A **1.2** an attractive target for total synthesis community, the very difficult access to it (either through isolation from natural sources or total synthesis) complicates its development into marketable drug. As such, search for analogues of diazonamide A **1.2** with less complex, easier-to-synthesize structure but maintained biological activity might be of high interest.

Having successfully completed the total synthesis of diazonamide A **1.2** (chapter 1.1.3)[16], Harran embarked on drug discovery program aimed at the development of anticancer agents based on the highly toxic marine metabolite **1.2.** Building upon the experience gained during the total synhtesis endeavour, Harran's group has synthesized more than 200 analogues of **1.2**.[26–28] This effort culminated in the development of structurally simplified diazonamide A analog DZ-2384 **1.76** that retained or even surpassed the antiproliferative activitiy of the parent marine metabolite (Figure 1.13).

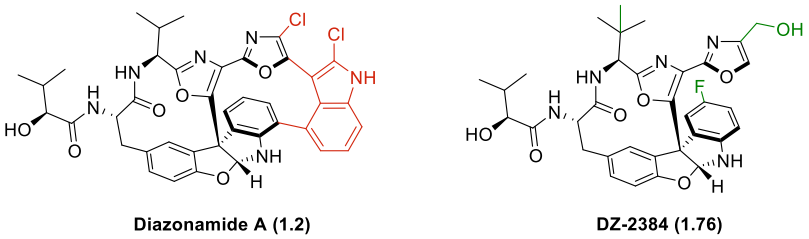

Figure 1.13 **Diazonamide A (left) and DZ-2384 (right)**

Macrocycle **1.76** retained the left hand peptide backbone-derived 12-membered macrocycle, tetracyclic aminal core, bioxazole moiety and (*S*)-hydroxyisovalerate fragments from the parent **1.2**, but it was lacking the right hand polyarometic macrocycle. Additionally, the isopropyl group was replaced by *tert*-butyl and fluorine substituent was installed in the indoline moiety of the tetracyclic heminaminal. These changes allowed for sharp increase in the antiproliferative activity (IC_{50}) against melanoma cell line A2058 rose from 57 nM to 0.47 nM and lymphoma cell line U937 from 86 nM to 0.74 nM when compared to diazonamide A **1.2**.[26–28] Similarly to the parent natural product **1.2**, the so-called "synthetic diazonamide" DZ-2384 **1.76** was shown to be an antimitotic agent. A genome-wide RNA interference screen indicated the cell cycle, mitosis and microtubules as the main interaction pathways for DZ-2384 **1.76**, and cells treated with **1.76** accumulated in the G_2/M phase of the cell cycle.[7] Notably, in addition to being highly efficacious, the "synthetic diazonamide" **1.76** had a significantly higher safety margin when compared to established microtubule-targeting anti-cancer drugs such as vinorelbine, paclitaxel and docetaxel, caused less and more reversible damage to peripheral neurons at maximum tolerated dose when compared to docetaxel.[7] The preclinical development required large amount of the material, so multigram-scale synthesis of **1.76** was developed in 2015[29] as shown below.

1.2.1. Synthesis of DZ-2384

Synthesis of macrocycle **1.76** commenced from the dipeptide Cbz-*tert*-Leu-Ser-OH **1.77** (prepared in three steps from *L*-*tert*-Leu) and 5-fluoroindole **1.78**, which, after condensation in the presence of Ac_2O (AcOH, 65 °C), gave the tryptophan derivative **1.79** (Figure 1.14). The reaction presumably involved initial formation of intermediate **XV** which then participated in Michael addtion reaction with indole **1.78**. The coupling of tryptophan derivative **1.79** with *L*-serine methyl ester (EDC, HOBt, DIPEA, DMF, r.t.) resulted in tripeptide that was then oxidized using DDQ (THF, 85 °C) to yield a single isomer of 3-(5-oxazolyl)indole **1.80** in 73% yield over two steps. After dehydration of crude **1.80** with

Deoxo-Fluor (DCM, -20 °C) the resulting oxazoline underwent further oxidation using a combination of $BrCCl_3$ and DBU (Na_2CO_3, Galvinoxyl, DCM, r.t.) and cleavage of *N*-Cbz group (HBr in AcOH, iPr_2O, r.t.) to deliver the bioxazole **1.81** in 52% yield over three steps. Although not essential to the reaction, addition of Na_2CO_3 and galvinoxyl radical during the oxidation with $BrCCl_3$ and DBU suppressed formation of several byproducts and increased the yield of the synthetic step from 31% to 64%. Next, amine **1.81** underwent coupling with Z-Tyr-OH. The methyl ester of the resulting product was subsequently reduced by $LiBH_4$ into alcohol **1.82**. The reduction step posed challenges due to the limited solubility of the substrate in ether solvents. These problems were alleviated by the addition of trifluoroethanol (1 equiv. relative to $LiBH_4$) which created a strongly reducing system and a homogeneous solution.

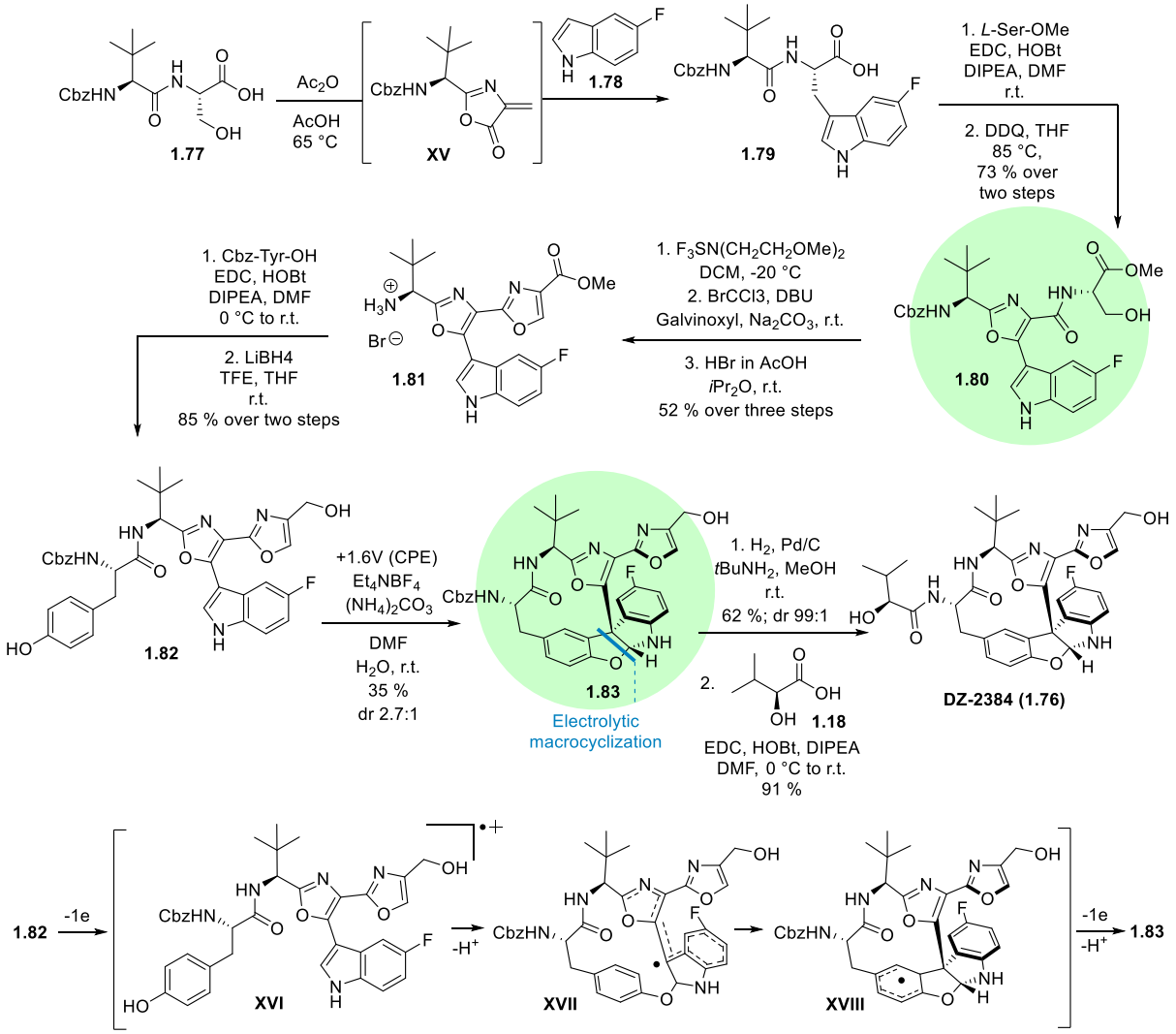

Figure 1.14 **Synthesis of compound DZ-2384 (1.76). Green circles indicate the steps for the formation of the tetracyclic core structure.**

Amide **1.82** was then subjected to electrolysis at +1.6 V potential (potentiostatic mode, graphite anode vs. Ag/AgCl, undivided cell open to air, Et_4NBF_4 and $(NH_4)_2CO_3$ as the

supporting electrolytes, in wet DMF (1.8% H_2O) at 25 °C) that afforded macrocycle **1.83** in 35% yield with modest diastereoselectivity (2.7:1 dr). In contrast to the method used by Harran for the cyclization step during total synthesis of diazonamide A **1.2** ($PhI(OAc)_2$, LiOAc, TFE, -20 °C, Figure 1.7), where the tetracycle formation was initiated by PIDA oxidation of the phenol moiety, in the electrooxidation approach the indole heterocycle in amide **1.82** was proposed to be the one that underwent single electron oxidation into cation radical **XVI**. The latter underwent an attack by phenolic oxygen to form intermediate **XVII**. Subseuent radical cyclization formed intermediate **XVIII** that after another one electron oxidation/deprotonation sequence afforded macrocycle **1.83**. The switching from hypervalent iodine(III) oxidant to anodic oxidation helped to diminish the amount of undesired byproducts compared to the $PhI(OAc)_2$-mediated oxidation. Chromatographic separation of the diastereomers, removal of *N*-Cbz moiety (H_2, Pd/C (10 mol%), *t*$BuNH_2$, MeOH, r.t.) and installation of the (*S*)-HiVA functionality (EDC, HOBt, DIPEA, DMF, 0 °C) afforded the "synthetic diazonamide" DZ-2384 **1.76**.

The synthesis of DZ-2384 **1.76** was remarkably short and highly efficient with the yield reaching respectable 5.7% over 13 steps. As it was developed for multigram preparation of **1.76** for drug development program, the synthesis made use of relatively cheap and accesssible reagents (e.g. aminoacids) and conditions (electrooxidation) as well as avoided homogenous transition metal-catalyzed reactions. Similarly to the Harran's total synthesis of diazonamide A **1.2**, the core tetracyclic aminal and quaternary stereocenter were generated in a single step. The developed method is also a notable example of biomimetic approach in synthesis of complex molecules: similarly to the proposed biosynthesis of the natural diazonamide A[16], all the main building blocks *en route* to **1.76** are amino acid-based.

The key step in the synthesis of **1.76** is electrochemical oxidative macrocyclization. Being an attractive method for preparative scale, the anodic oxidation was performed on a purpose-built electrochemical cell that might cause reproducibility issues when performed in a different lab (See SI of [29]). Additionally, although the electrochemical oxidative macrocyclization allows for simulatenous formation of C10 stereocenter and closing of the macrocycle, it suffers from the same mediocre diastereoselectivity (2.7:1 dr) as majority of the substrate controlled diazonamide A synthesis.[14–16,22,24]

Overall, the discovery of DZ-2384 **1.76** represents an example of highly successful structural simplification of natural diazonamide A **1.2** without affecting its biological activity. Removal of the right hand-side heterocyclic 12-membered, replacement of *i*-Pr by *t*-Bu group and and introduction of an additional fluorine substituent in the tetracyclic heminaminal subunit not only rendered the synthesis shorter but also significantly improved the

antiproliferative activity of DZ-2384 **1.76** when compared to the parent compound **1.2**. However, the DZ-2384 **1.76** still incorporates the relatively hard-to-synthesize tetracyclic hemiaminal core and quaternary all-carbon stereocenter. This leaves room for further structural simplification of diazonamide A scaffold to prepare compounds with improved drug-like properties.

1.3. Microtubule targeting agents

Microtubules (MT) are hollow, polarized, and cylindrical biopolymers that are present in all eukaryotic cells and, together with microfilaments and intermediate filaments, form the cytoskeleton. They play essential role in maintaining the shape of the cell, in positioning of organelles inside the cell, in signaling, movement and internal transport as well as in cell division and reproduction.[30]

Microtubule targeting agents (MTAs) are a large and diverse family of chemical compounds that can bind tubulin and interfere with the dynamic behavior of MTs. The majority of MTAs are natural products or synthetic derivatives thereof that originate from natural sources such as marine sponges, plants, or bacteria.[31] MTAs have been used as a first-line therapy for cancer treatment since the mid-1960s[30] and currently there are ten U.S. Food and Drug Administration (FDA) approved MTAs for anticancer therapy.[32] MTAs are effective for treatment of head, breast, ovarian, lung, bladder, prostate, skin, esophageal, lymphatic and testicular cancers as standalone therapies or in combination with other agents.[32] For long time it was generally accepted that the anticancer activity of MTAs arises from the disruption of MT dynamics in the mitotic spindle, eliciting the mitotic checkpoint, arresting cells in metaphase, and triggering cell death.[30] However, there is gathering evidence that along the action on actively dividing cells, MTAs also affect the tumor cells during the interphase.[30]

Like all other classes of antineoplastic drugs, use of MTAs has met with several challenges. The first is drug resistance - multiple MTAs (e.g., clinically important Vinca alkaloids) are good substrates for P-glycoprotein (Pgp) efflux pumps, which ensure that the drug does not reside in the cells long enough to have the desired effect. Similarly, in response to MTAs, cells might upregulate antiapoptotic protein expression, which might lead to a diminished efficacy of the drug.[33] However, the most severe problem associated with clinical use of microtubule-targeting agents is neurotoxicity.[34] Due to the high content and important role of MT in neural cells (tracks for transport of nutrients, organelles, proteins, and RNA within the cell)[35], especially the long peripheral sensory neurons, they are the first and most

severely affected of the healthy cells. Chemotherapy-induced peripheral neuropathy is a debilitating and dose-limiting side effect that is manifested by a sensory, length-dependent process resulting from a drug cumulative dose. Symptoms can be sufficiently severe to require a reduction in drug dosage or discontinuation of treatment.[36]

In summary, MTAs are critical components in modern treatment of cancer. They are effective against a wide variety of cancers and have been used for almost 60 years. However, there still are further details emerging about the mechanism of action of this wide class of compounds.

2. RESULTS

2.1. Attempted total synthesis of diazonamide A

This section is based on *JOC* and *Chem. Heterocycl. Comp.* featured articles published in 2015.[37,38]

2.1.1. Introduction and retrosynthesis

Even though four total syntheses and several formal total syntheses of diazonamide A (**1.2**) have been successfully accomplished over the last two decades[14–17] its complex macrocyclic structure and remarkable antiproliferative activity continues to captivate synthetic organic chemists even today. This is in part because the design of robust, modular, and high yielding synthesis of such complex and bioactive molecule can pave road to elaborate structures, which ideally would be even more potent than the natural compound. Hence, a total synthesis of diazonamide A has been an initial focus of dissertation work that was performed in collaboration with Prof. Edwin Vedejs.

Our approach toward diazonamide A was based on an initial construction of a so-called right hand polyaromatic macrocycle with subsequent assembly of the second, left-hand ring. In that our strategy differed from the majority of published total syntheses that typically started by the construction of the left-hand peptidic macrocycle.[14,16,17] As such, we envisioned that diazonamide A (**1.2**) could be accessed from macrocycle (*R*,*R*)-**2.1**. It's macrolactamization, chlorination of oxazole and indole moieties, and side chain modifications would afford **1.2**. Introduction of alanine moiety through Pd-catalyzed *Negishi* cross-coupling and removal of protective groups would lead to elaborate macrocycle (*R*,*R*)-**2.1** from the fused bioxazole (*R*,*R*)-**2.2**, which itself could be prepared from the macrocyclic ketone (*R*,*R*)-**2.3** using ketone α-amination, acylation and cyclodehydration. The stereoselective assembly of the right-hand heteroaromatic macrocycle (*R*,*R*)-**2.3** could be achieved by *Suzuki* cross-coupling of enantiomerically pure hemiaminal bromide (*R*,*R*)–**2.5** with indolyl boronate **2.6**, followed by atropo-diastereoselective *Dieckmann*-type cyclization of biaryl (*R*,*R*)–**2.4** (Figure 2.1).

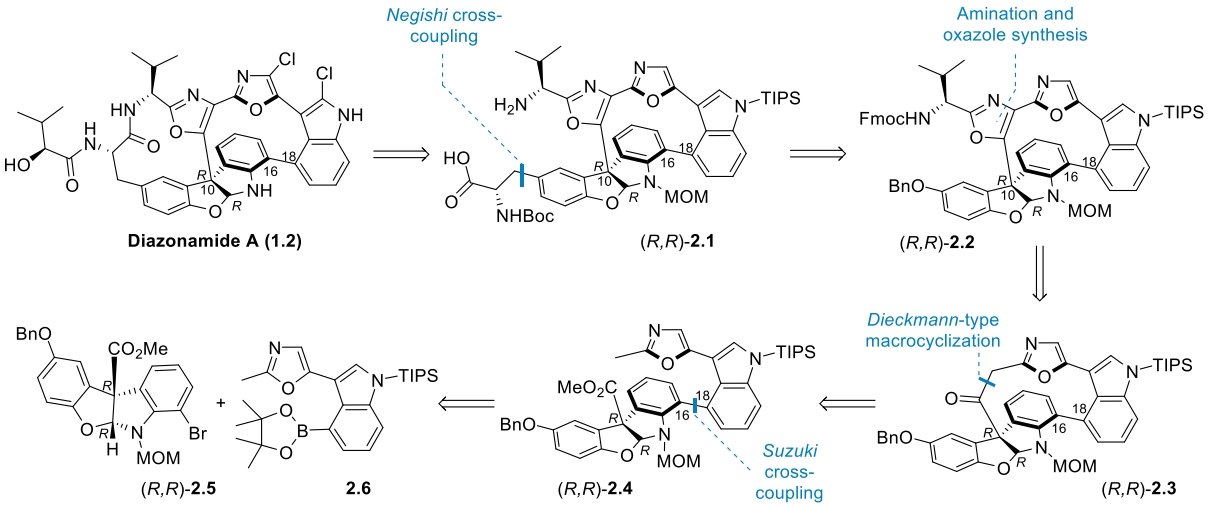

Figure 2.1 **Retrosynthetic analysis of diazonamide A (1.2)**

The *Suzuki* approach to C16–C18 bond formation in biaryl (*R*,*R*)-**2.4** would be superior to *Stille* methodology reported earlier by Vedejs[39], because the latter would require transformation of the expensive enantiomerically pure hemiaminal bromide (*R*,*R*)–**2.5** into the corresponding stannate. Furthermore, the *Stille* coupling had used an excess of the stannate for stoichiometric coupling with an isolable palladium derivative related to **2.6** (palladium in place of boron).

2.1.2. Synthesis of building block (*R*,*R*)-2.5

The C16–C18 biaryl bond formation via *Suzuki* coupling required preparation of the enantiomerically pure bromide (*R*,*R*)–**2.5**. We chose to rely on chiral auxiliary-based synthesis for closely related enantiomerically pure bromide (*R*,*R*)–**2.7** that was developed by Vedejs and Peris (Figure 2.2).[40]

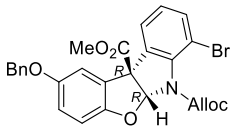

Figure 2.2 **Compound (*R*,*R*)–2.7**

The synthesis of bromide (*R*,*R*)–**2.7** commenced by preparation of 7-bromoisatin (**2.11**) in two steps from 2-bromo aniline (**2.8**), chloral hydrate (**2.9**) and hydroxylamine (Figure 2.3).[41] The reaction was performed multiple times with highest loading of eight grams of 2-bromo aniline (**2.8**) in a batch. Protection of nitrogen atom in isatin **2.11** by freshly prepared *tert*-butyl(chloromethoxy)dimethylsilane (**2.14**) (obtained in three steps from ethanesulfide

2.12[42]) afforded the building block **2.15** in 58% yield. The *N*-protection reaction was carried out multiple times using up to 28 grams of isatin **2.11** in single batch.

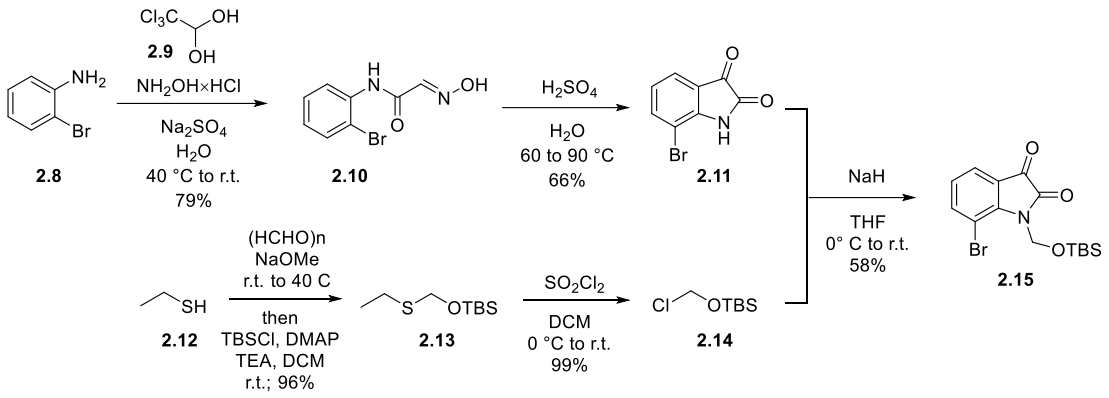

Figure 2.3 **Synthesis of isatin 2.15**

The reported synthesis of enantiopure bromide (*R,R*)–**2.7** relied on the presence of chiral auxiliary to control the diastereoselective formation of the C10 quaternary stereocenter. Vedejs found that chiral benzyl ether allowed for the best diastereocontrol (5.2:1 dr) in the acylation of deprotonated oxindole (*S*)-**2.16** with *Mander's* reagent (NC-CO_2Me) (Figure 2.4). The stereo induction model possibly involved chiral auxiliary-promoted formation of single atropisomer (*M*-isomer) around the indole-benzene bond thus leading to blockage of the *Si*-face of enolate (*S*)-**2.16** by the sterically large naphthyl moiety which forced the acylating reagent to approach from the *Re*-face of the molecule resulting in (*R,S*)-**2.17**. The chiral auxiliary not only facilitated stereoselective introduction of C10 quaternary center during the acylation but also enabled chromatographic separation of diastereomers during purification which resulted in highly diastereoenriched (98:2 dr) product (*R,S*)-**2.17**.

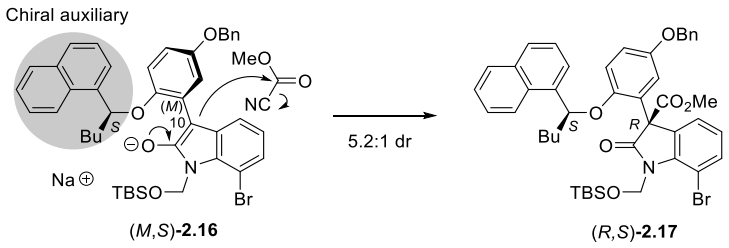

Figure 2.4 **Use of chiral auxiliary for stereoselective synthesis of (*R,S*)-2.17**

The chiral auxiliary-containing indolinone (*S*)-**2.16** was obtained from isatin **2.15** and enantiopure ether (*S*)-**2.22**. The later was synthesized from phenol **2.21** and enantiomerically pure alcohol (*R*)-**2.20** (Figure 2.5). Ether (*S*)-**2.22** was accessible in three step sequence involving the addition of *n*BuLi to aldehyde **2.18**, followed by oxidation of the resulting

alcohol with Jone's reagent, and enantioselective reduction of ketone **2.19** by (+)-DIP-Cl at -42 °C temperature within three days.[43] Alcohol (*R*)-**2.20** was obtained with excellent enantioselectivity (97% ee, analytical HPLC on chiral stationary phase), and stereo induction level matched that reported in the literature.[40] Next, the chiral alcohol (*R*)-**2.20** was reacted with phenol **2.21** under Mitsunobu conditions (*n*Bu_3P, DIAD, PhMe, -45 °C, 130 h). The ether synthesis proceeded with clean *Walden* inversion at stereogenic center (97% ee). Notably, optical purity of ether (*S*)-**2.22** turned out to be slightly higher than that in the original publication (94% ee). The slight enhancement can be attributed to lower reaction temperature (-42 °C) as compared to that in the published procedure (-23 °C) which leads to even less rotation around the biaryl bond and better separation of atropisomer (see Figure 2.4).

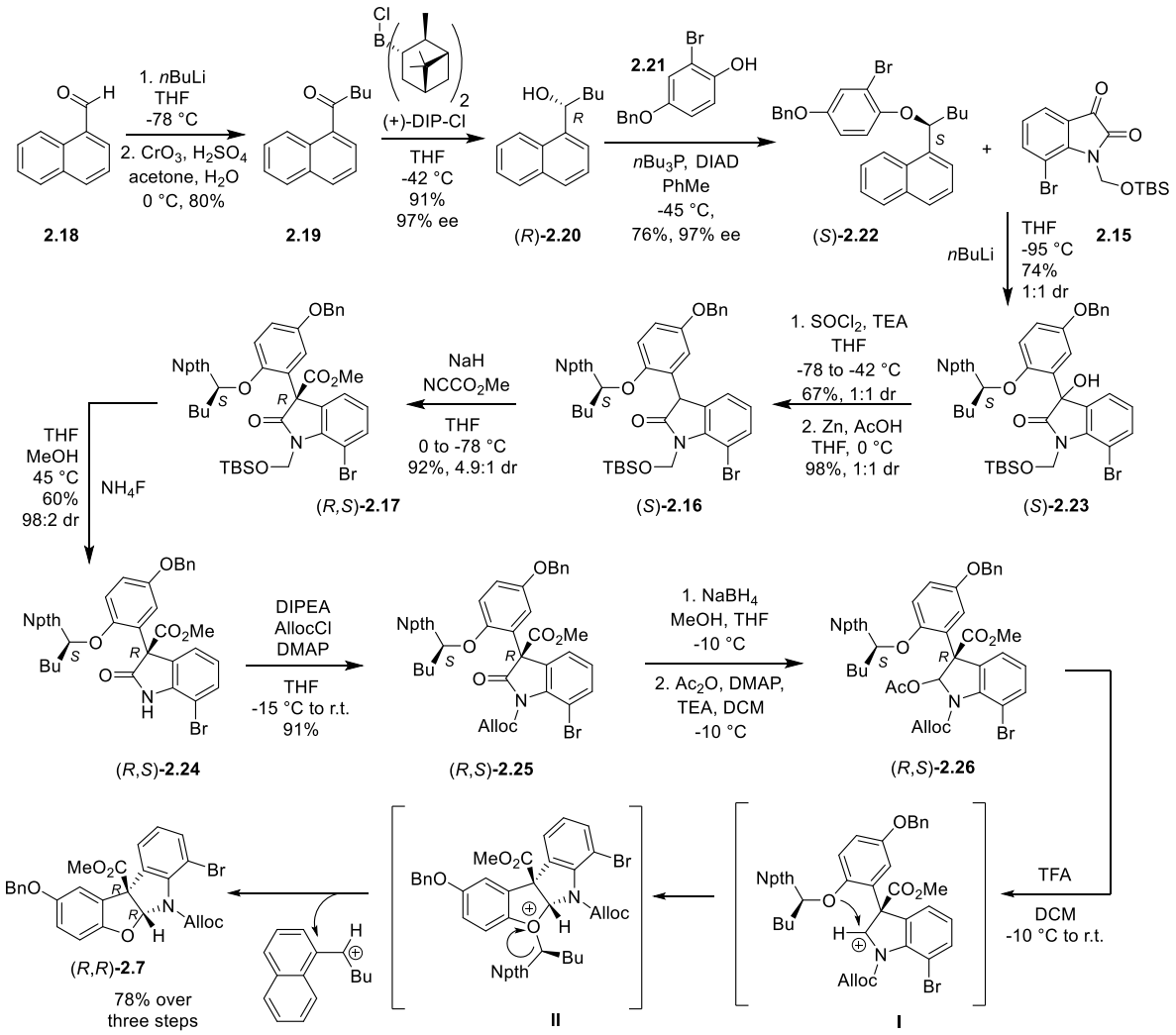

Figure 2.5 **Preparation of enantiopure bromide (*R,R*)-2.7**

With supply of (*S*)-**2.22** secured, we proceeded to reaction with previously prepared isatin **2.15**. Lithium-halogen exchange in bromide (*S*)-**2.22** (*n*BuLi, THF, -95 °C), followed

by instant addition of isatin **2.15** (keeping less than one minute timespan between the addition of *n*BuLi and isatin was critical to diminish degradation of transient aryl lithium) allowed for the formation of indolinone (*S*)-**2.23** as 1:1 mixture of diastereomers in 74% yield. Conversion of the tertiary alcohol into chloride ($SOCl_2$, TEA, THF, -78 to -42 °C) and subsequent reduction with Zn/AcOH (THF, 0 °C) furnished oxindole (*S*)-**2.16** as a oxidation-prone yellow solid, which was used in the next step without additional purification by chromatography. Thus, low temperature deprotonation of indolinone (*S*)-**2.16** with NaH (THF, -78 °C) and reaction with *Mander's* reagent (NC-CO_2Me) at -78 °C effected the formation of ester (*R,S*)-**2.17** as a 4.9:1 mixture of diastereomers in 92% yield (5.2:1 d.r. was reported in the original procedure[40]). Purification of the desired major diastereomer (*R,S*)-**2.17** was not performed at this stage. Instead, CH_2OTBS protecting group was removed by NH_4F at 45 °C to provide indolinone (*R,S*)-**2.24** as a stable solid. Diastereomerically pure material (98:2 d.r.) was obtained by separation of diastereomers using column chromatography on silica gel. Following the published procedure, indolinone (*R,S*)-**2.24** was converted into *N*-Alloc protected analog (*R,S*)-**2.25** (Alloc-Cl, DMAP, DIPEA, THF, -15 °C to r.t., 91% yield) and subjected to the two-step cyclization sequence into tetracyclic hemiaminal (*R,R*)-**2.7**.

Accordingly, the two-step process comprised the reduction of amide in (*R,S*)-**2.25** with $NaBH_4$ in MeOH at -10 °C to transient hemiaminal was trapped by the acetylation with Ac_2O in the presence of DMAP. Subsequent addition of TFA (30 equiv.) to the *O*-acetylated aminal (*R,S*)-**2.26** generated cation **I**. Nucleophilic attack of the nearby phenolic oxygen closed the core tetracyclic aminal (intermediate **II**) and heterolysis of the benzylic C-O bond yielded the compound (*R,R*)–**2.7** as single diastereomer with 78% yield after purification (reaction was done in two gram scale). The diastereoselectivity of the cyclization was governed by the already present quaternary stereogenic center which allowed the attack of the phenolic oxygen only from the *Re*-face of the carbocation. Notably, the presence of *N*-Alloc protective group made the tetracycle (*R,R*)-**2.7** highly crystalline and effected its purification through crystallization. Overall, enantiomerically pure tetracyclic hemiaminal (*R,R*)-**2.7** was prepared in 15 linear steps starting from 2-bromoaniline **2.8**. The synthesis developed by Vedejs[40] proved to be well reproducible and scalable, allowing the preparation of more than two grams in total of enantiomerically pure hemiaminal (*R,R*)-**2.7**.

So far, we relied on method developed by Vedejs, but further synthesis was not known in literature and demanded design of the appropriate synthetic steps. We started with addressing the necessary change of the nitrogen-protecting group in tetracyclic bromide (*R,R*)–**2.7** to avoid undesired cleavage of *N*-Alloc group during the planned Pd-catalyzed *Suzuki* cross-coupling and *Dieckmann* reaction steps (Figure 2.1). We decided to introduce the

base and transition metal-compatible *N*-MOM protective group which had seen widespread use in total synthesis of diazonamide A (**1.2**).[14,23,39] Unfortunately, *N*-MOM group could not be introduced earlier because of its incompatibility with the acidic reaction conditions used in the cyclization step (TFA in DCM) (see Figure 2.5). The *N*-MOM tetracycle (*R,R*)–**2.5** was made from *N*-Alloc protected enantiomerically pure bicyclic hemiaminal (*R,R*)–**2.7** in a two-step sequence comprising a cleavage of the *N*-Alloc protecting group using $Pd(PPh_3)_4$ and 1,3-dimethylbarbituric acid (as described previously[39]) and installation of an *N*-MOM protecting group in the TMS-Cl mediated reaction of (*R,R*)–**2.27** with paraformaldehyde and MeOH (Figure 2.6).[44] Introduction of *N*-MOM protection using base mediated reaction between unprotected indoline (*R,R*)-**2.27** and MOM-Cl was not possible due to instability of (*R,R*)-**2.27** under basic conditions (see chapter 2.1.3).

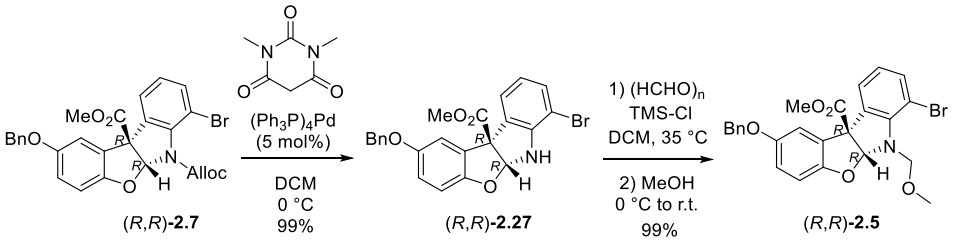

Figure 2.6 **Preparation of hemiaminal (*R,R*)-2.5**

Although the above-mentioned synthetic route allowed us to prepare the enantiomerically pure hemiaminal (*R,R*)-**2.5** in reasonable quantities for the planned total synthesis of diazonamide A (**1.2**), we realized that the use of the precious enantiomerically pure material in the optimization of reaction conditions for multistep total synthesis would rapidly consume all available amount and, hence, is impractical. Therefore, the synthesis of racemic hemiaminal was also performed since the synthesis of *rac*-**2.5** does not require chiral auxiliary as well as separation of diastereomers, and hence would save time and resources.

The racemic hemiaminal *rac*-**2.5** was synthesized following procedure developed by Vedejs and Zajac.[39] The synthesis started by adding of magnesium 4-benzyloxyphenolate to *N*-protected isatin **2.15** and was followed by PMB protection of the phenolic oxygen to afford alcohol **2.28** in 80% yield (Figure 2.7). The quality of PMB-Cl reagent proved to be critical to achieve high yields in the protection step, so only freshly opened batches were used. Conversion of the tertiary alcohol **2.28** into chloride ($SOCl_2$, DIPEA, DCM, 0 °C), followed by reduction with zinc dust in glacial acetic afforded indolinone **2.29** in 83% yield over two steps. By analogy, to the preparation of enantiopure material, methoxycarbonyl group was introduced in indolinone **2.29** by NaH deprotonation and acetylation with *Mander's* reagent

(92% yield of **2.30**). The latter synthesis step could be easily upscaled to four grams of **2.29** in a batch.

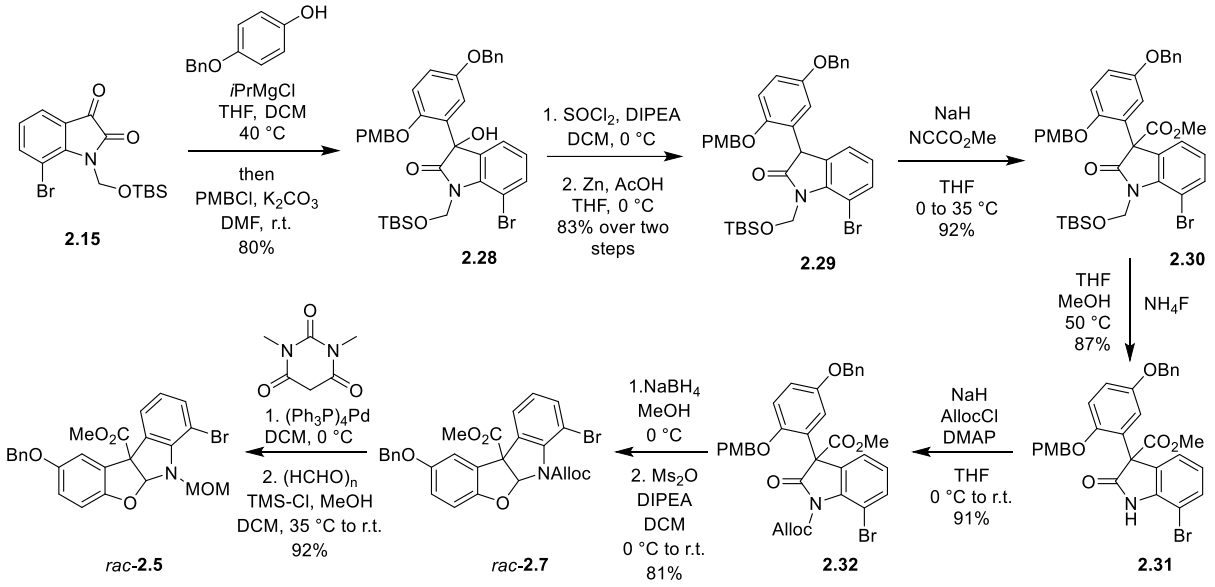

Figure 2.7 **Preparation of hemiaminal *rac*-2.5**

Removal of the CH_2OTBS group with NH_4F and introduction of *N*-Alloc protection (NaH, Alloc-Cl, DMAP, THF, 0 °C to r.t.) delivered indolinone **2.32**. Next, reduction of carbonyl group with $NaBH_4$ (MeOH, 0 °C) and mesylating of the resulting alcohol with Ms_2O (DIPEA, DCM, 0 °C to r.t.) provided the tetracyclic hemiaminal *rac*-**2.7** in 81% yield (for mechanism of similar transformation, see Figure 2.5). The swap of *N*-Alloc protection for *N*-MOM as in enantiomerically pure tetracycle (*R,R*)-**2.5** afforded the racemic hemiaminal *rac*-**2.5** in 92% yield. The synthesis of racemic hemiaminal *rac*-**2.5** comprised 10 linear steps (starting from isatin **2.15**) and it was used to produce more than three grams of target compound *rac*-**2.5** in total.

2.1.3. Instability of tetracyclic aminal

During the studies that involved removal of *N*-Alloc protecting group from compounds (*R,R*)-**2.7** and *rac*-**2.7** (see Figure 2.6 and Figure 2.7), it was found that *N*-unprotected tetracyclic hemiaminal is not compatible with basic reaction conditions.[38] Thus, very slow formation of 3-arylindole *rac*-**2.33** was observed after the addition of TEA (2 equiv.) to a solution of the hemiaminal *rac*-**2.27** in $CDCl_3$ at room temperature. After 24 h at room temperature only trace amounts (<5%) of compound *rac*-**2.33** were formed and complete conversion of the hemiaminal *rac*-**2.27** to indole *rac*-**2.33** required 57 days at room

temperature. We hypothesized that the formation of 3-arylindole *rac*-**2.33** would proceed through an initial formation of 3*H*-indole intermediate *rac*-**2.34**.

Unfortunately, we could not observe the formation of ring-opening intermediates such as compound *rac*-**2.34** by NMR spectroscopy in the base-facilitated fragmentation of hemiaminal *rac*-**2.27** to indole *rac*-**2.33**. Possibly, the lifetime of putative intermediate *rac*-**2.34** was too short on the timescale of the NMR experiment. Therefore, an electrophilic reagent was sought to trap the intermediate *rac*-**2.34**. Boc_2O was chosen as the trapping reagent because it did not react with the starting hemiaminal *rac*-**2.27** in the absence of base (Boc_2O in DCM, rt, 24 h or neat Boc_2O, rt, 24 h, or Boc_2O, $ZrCl_4$, MeCN, rt, 24 h).

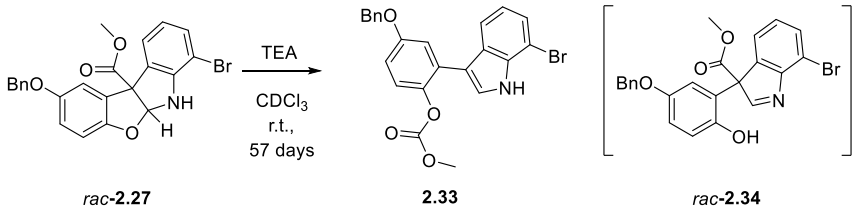

Figure 2.8 **Formation of compound 2.33**

Disappointingly, addition of Boc_2O (2 equiv.) to the hemiaminal *rac*-**2.27** in the presence of TEA (2 equiv.) in $CDCl_3$ returned no detectable amounts of *O*-Boc-protected phenol **2.35** or any other intermediates derived from the ring opening of the tetracycle *rac*-**2.27**. The unreacted hemiaminal *rac*-**2.27** (<5% conversion) was the only species observed after 24 h at room temperature. However, we were pleased to see that addition of catalytic amounts (10 mol%) of DMAP to the mixture of hemiaminal *rac*-**2.27**, Boc_2O, and TEA brought about a rapid conversion of *rac*-**2.27** (more than 95% after 30 min at room temperature) and formation of *O*-Boc phenol *rac*-**2.35** as a major product (66%) together with *N*-Boc indole **2.36** (18%) (Figure 2.9).

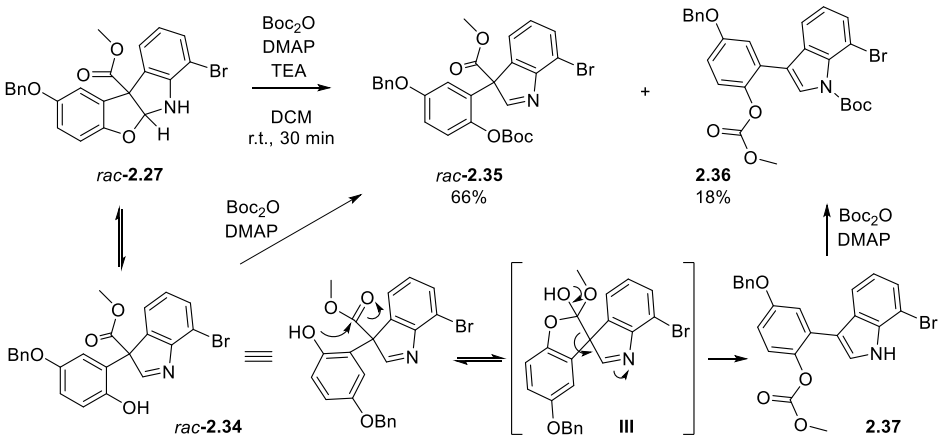

Figure 2.9 **Formation of indoles *rac*-2.35 and 2.36**

Importantly, a control experiment without added Boc_2O (*rac*-**2.27**, 5 equiv. of TEA, and 0.5 equiv. of DMAP in $CDCl_3$ at room temperature) showed only unreacted tetracycle *rac*-**2.27** after 24 h (<5% conversion). Evidently, DMAP-catalyzes trapping of the equilibrating ring-opened intermediate *rac*-**2.34** with Boc_2O to form *O*-Boc phenol *rac*-**2.35,** thus facilitating fragmentation of hemiaminal *rac*-**2.27** by shifting the equilibrium between compounds *rac*-**2.27** and *rac*-**2.34** toward the latter.

The isolation of *O*-Boc phenol *rac*-**2.35** provided evidence that the ring opening of hemiaminal *rac*-**2.27** was the first step of the multistep rearrangement process. In the absence of external electrophile such as Boc_2O phenol *rac*-**2.27** may undergo an intramolecular acyl transfer via tetrahedral intermediate **III** with indole acting as a good leaving group to form the *N*-unsubstituted indole **2.37**. Notably, for phenol *rac*-**2.27**, the intramolecular acyl transfer from carbon to oxygen to afford compound **2.36** was a competing side reaction (yield 18%) to DMAP-catalyzed intermolecular *O*-acylation with the excess of Boc_2O (2 equiv.). It should be noted that in the presence of DMAP/Boc_2O anionic versions of intermediates *rac*-**2.34** and **III** could also be involved, but they are not illustrated here for simplicity (Figure 2.9).

2.1.4. Synthesis of biaryl (*R*,*R*)-2.4

With tetracyclic hemiaminal (*R,R*)-**2.5** in hand we now only needed the indolyl boronate **2.6** to address the preparation of biaryl (*R,R*)-**2.4**. Triflate **2.43** was the key intermediate *en route* to indolyl boronate **2.6** (Figure 2.10). The synthesis of triflate **2.43** has been reported previously, but involved the use of methylisocyanide for the oxazole formation.[45,46] Methylisocyanide is extremely foul-smelling and explosive, properties that are poorly compatible with preparative scale synthesis. Therefore, we developed an alternative procedure that avoided the use of methylisocyanide (Figure 2.10). Accordingly, ethyl acetamidoacetate was converted into *Weinreb* amide **2.39** using Me_2AlCl and *N,O*-dimethylhydroxylamine hydrochloride. Next, the relatively acidic amide moiety in **2.39** was deprotonated by *i*-PrMgCl to avoid quenching of the indolyl lithium nucleophile **IV** in the following step. The resulting magnesium amide intermediate was reacted with lithiated indole **IV**, which was prepared from 3-bromoindole **2.38**[45] by low-temperature lithium-halogen exchange with *t*-BuLi. The resulting ketoamide **2.40** was transformed into the oxazole **2.41** using *Wipf's* cyclodehydration conditions (PPh_3, I_2, NEt_3).[47] Subsequent reductive cleavage of the benzyl ether (Pd/C, H_2) and treatment of the resulting phenol **2.42** with NaH and $PhN(SO_2CF_3)_2$ afforded the triflate **2.43** in 95% yield.

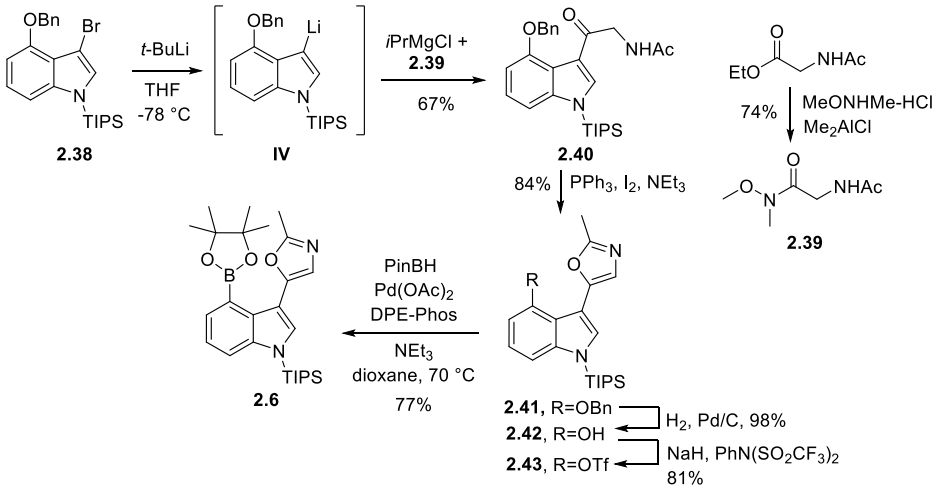

Figure 2.10 **Synthesis of boronate 2.6**

Next, the conversion of triflate **2.43** to boronate **2.6** was addressed. The use of bis(pinacolato)diboron $(BPin)_2$ under various conditions ($PdCl_2$(dppf)/KOAc/DMSO,[48] $Pd(Ph_3P)_4$/KOAc/NMP[49] and $Pd(OAc)_2$/S-Phos/K_3PO_4/dioxane[50]) resulted in poor conversion and different decomposition products such as those derived from the cleavage of *N*–TIPS, hydrolysis of the triflate **2.43** or protonolysis of the boronate **2.6**. We also found that the yield of the desired boronate **2.6** depended on the quality of the $(BPin)_2$: even 5 – 10 mol% content of pinacol in the $(BPin)_2$ reagent was sufficient to decrease the conversion of the triflate **2.43** by 40-60%. In contrast, the use of pinacol borane (PinBH) as a boron source and $Pd(OAc)_2$/DPE-Phos as a catalyst[51] allowed for the conversion of the indolyl triflate **2.43** into the boronate **2.6** in reproducible 77% yield.

With both tetracyclic hemiaminal (*R*,*R*)-**2.5** and indolyl boronate **2.6** in hand, the synthesis of biaryl (*R*,*R*)-**2.4** was accomplished under the *Suzuki*-Miyaura cross-coupling conditions that were developed by Dr. Ilga Mutule and M.Sc. Zane Medne (Figure 2.11).[37]

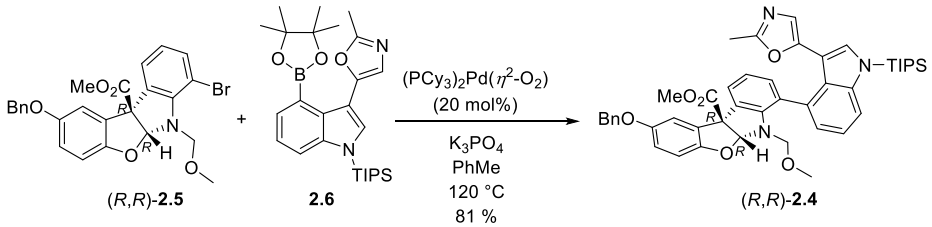

Figure 2.11 **Synthesis of biaryl (*R*,*R*)-2.4**

Thus, biaryl (*R*,*R*)-**2.4** was obtained in 81% yield from (*R*,*R*)-**2.5** and **2.6** in the presence of custom-made palladium oxo-complex $(PCy_3)_2Pd(\eta^2\text{-}O_2)$ (20 mol%) and K_3PO_4 as a base in toluene at 120 °C. Under the same reaction conditions, use of racemic hemiaminal *rac*-**2.5**

allowed us to obtain racemic *Suzuki-Miyaura* cross-coupling product *rac*-**2.4** in comparable and well reproducible 76% yield.

2.1.5. Synthesis of macrocyclic ketone (*R,R*)-2.3 by atroposelective *Dieckmann* condensation

The ^{1}H-NMR spectrum of the biaryl (*R,R*)–**2.4** in C_6D_6 at 20 °C displayed two sets of signals in a 3:2 ratio corresponding to a mixture of two atropisomers. The ratio was measured by integration of signals corresponding to the C(27) oxazole proton (δ 6.53 and 6.04 ppm), C(30) ester protons (δ 3.44 and 3.13 ppm) and C(29) methyl group (δ 2.02 and 1.76 ppm). The structures of the atropisomers were assigned based on NOE experiment. Thus, a medium intensity NOE cross peak was observed between the C(29) methyl group and the C(30) ester protons of the major atropisomer, whereas weak intensity NOE interactions between C(29) methyl group and aromatic C(5) and C(6) protons were observed for the minor atropisomer (see Figure 2.12 and SI of [37]). Consequently, the major and minor atropisomers of the biaryl (*R,R*)–**2.4** were assigned (*M*) and (*P*) configurations around the C16–C18 bond, respectively. The two atropisomers underwent interconversion at room temperature, and the free energy of activation and rate constants for the atropisomerization of (*R,R*)–**2.4** were determined at 25 °C in benzene-d_6 by NMR methods. The barrier to rotation around the C16–C18 bond was measured to be 20.0 kcal/mol, which corresponds to a half-life of ca. 58 s for atropisomerization. However, at temperatures below –20 °C, the interconversion between (*M*) and (*P*) atropisomers of (*R,R*)–**2.4** in THF–d_8 was slow on the NMR timescale.

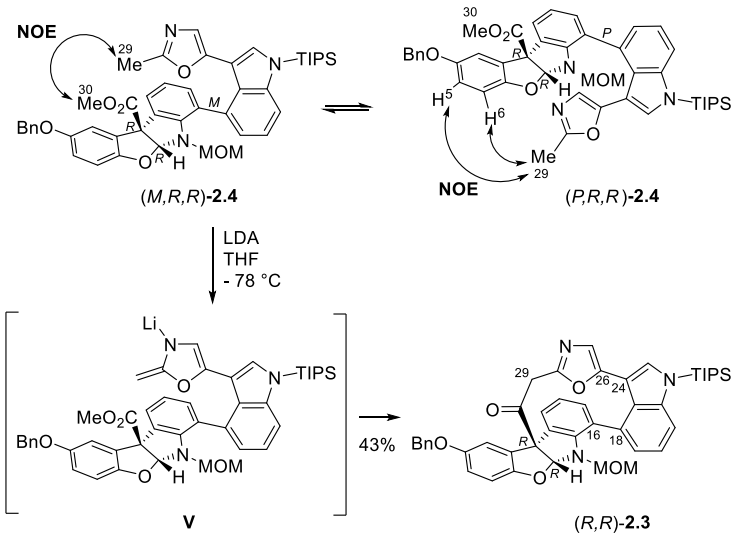

Figure 2.12 **Atropisomerization of (*R,R*)-2.4 and synthesis of (*R,R*)-2.3**

Next, we subjected the equilibrium mixture of atropisomers ((*M*):(*P*)=3:2) to the *Dieckmann*-type macrocyclization with LDA as base at –78 °C (Figure 2.12). The low temperature was critical for the success of the macrocyclization because at higher temperatures (–40 °C) the decomposition of the lithiated (*R*,*R*)-**2.4** became a major reaction. Importantly, the macrocyclization at –78 °C apparently proceeded below the threshold for atropisomer interconversion, meaning that only the major atropisomer (*M*,*R*,*R*)-**2.4** could be transformed into the macrocycle (*R*,*R*)-**2.3** in ca. 60% theoretical yield. In fact, the target macrocycle (*R*,*R*)-**2.3** was formed in 43% (71% brsm) yield already within 10 minutes, and prolonged reaction time (30 min) did not improve the outcome. The unreacted biaryl (*R*,*R*)-**2.4** was recovered as a 3:2 *M*:*P* mixture of atropisomers (40% yield, 83% material balance). Evidently, the unreacted atropisomer (*P*,*R*,*R*)-**2.4** did re-equilibrate to the 3:2 *M*:*P* equilibrium mixture during workup and this allowed for the reuse of the recovered material in the macrocyclization reaction. Comparable results (up to 40% yield of *rac*-**2.3** and 80% mass balance) were obtained when racemic biaryl compound *rac*-**2.4** was used.

2.1.6. Attempted construction of bioxazole subunit

With both enantiomerically pure and racemic forms of macrocyclic ketone **2.3** in hand, the next step in the synthesis of diazonamide A (**1.2**) was the construction of the bioxazole subunit and macrocycle (*R*,*R*)-**2.2** (Figure 2.13). To this end we planned to follow the well-known α-amidoketone cyclodehydration route (including *Wipf's* conditions that were successfully employed in the synthesis of boronate **2.6**, Figure 2.10), which has been frequently used in the synthesis of diazonamide A.[14,16] Introduction of the requisite amide functionality in the α-position of the ketone and formation of (*R*,*R*)-**2.44** was envisioned via acylation of α-aminoketone (*R*,*R*)-**2.45** (route **A**), which itself could be prepared from ketone (*R*,*R*)-**2.3** either through direct electrophilic ketone amination[39,52,53] or in a three-step sequence involving α-halogenation, halide-to-azide exchange and azide reduction. Alternatively,(*R*,*R*)-**2.44** could be also obtained by transition metal-catalyzed direct amidation of α-diazoketone (*R*,*R*)-**2.46** (route **B**).[54,55] Finally, the diazo group in (*R*,*R*)-**2.46** could be also reductively transformed into α-aminoketone (*R*,*R*)-**2.45**.[56,57]

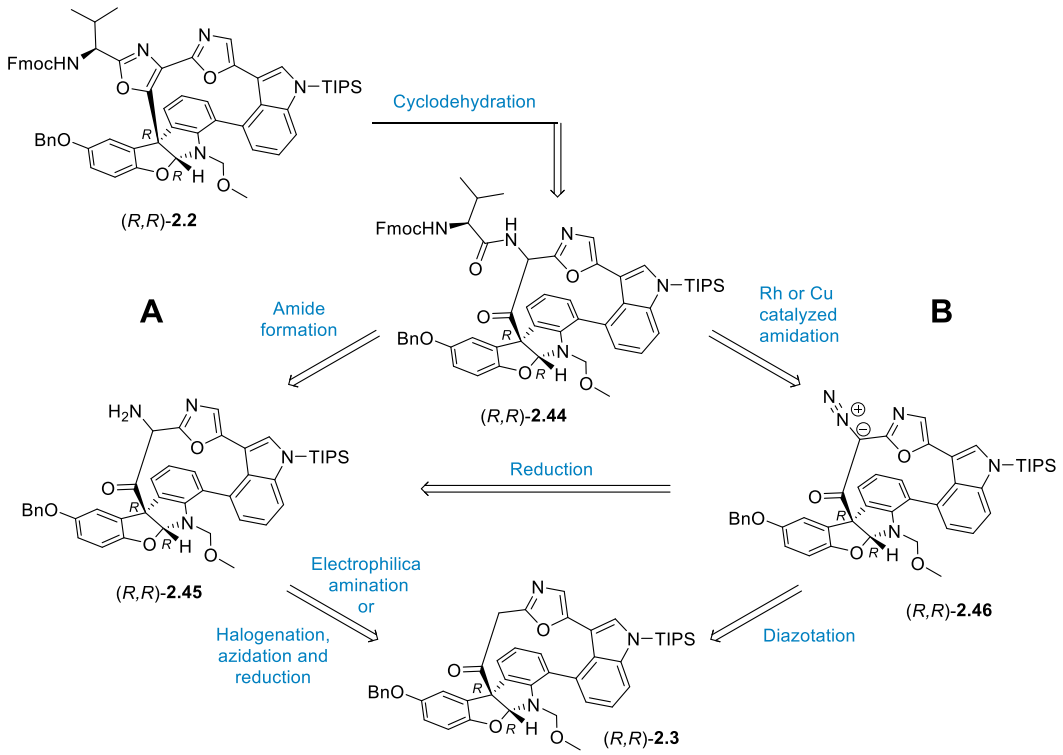

Figure 2.13 **Retrosynthetic analysis of macrocycle (*R,R*)-2.2**

For the bioxazole synthesis studies, we chose to use the easier-to-obtain racemic macrocyclic ketone *rac*-**2.3** as the starting material. Initially, the formation α-aminoketone *rac*-**2.45** was attempted by electrophilic amination procedure that was developed by Vedejs for *N*-Boc (instead of *N*-TIPS) protected analog of ketone **2.3**.[39] In the published precedent, the authors reported partially successful amination (14% yield, 10 mg reaction scale, 55% mass balance) of ketone enolate using di(4-*N*-butoxyphenyl)phosphinyl hydroxylamine (**2.47**) whose preparation was not disclosed (Figure 2.14). In light of this, we opted to start with the preparation of similar, albeit better described compound - di(4-methoxyphenyl)phosphinyl hydroxylamine (**2.48**), which was also reported by Vedejs.[52]

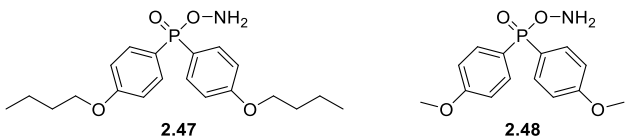

Figure 2.14 **Diarylphosphinates 2.47 and 2.48**

The electrophilic aminating agent **2.48** was synthesized from diarylphosphinate **2.52** using TFA-promoted deprotection (DCM, r.t., 52%) and subsequent basic aqueous work-up, followed by precipitation of solid **2.48** from DCM solution by addition of hexanes (Figure 2.15). Diarylphosphinate **2.52** itself was synthesized from diethylphosphite (**2.49**) that was

reacted with freshly prepared 4-methoxyphenylmagnesium bromide reagent to afford diarylphosphinic acid **2.50** in 20% yield. Chlorination by $SOCl_2$ (PhH, 80 °C) and subsequent reaction with *N*-Boc protected hydroxylamine (TEA, DCM, 0 °C to r.t.) furnished phosphinate **2.52**.

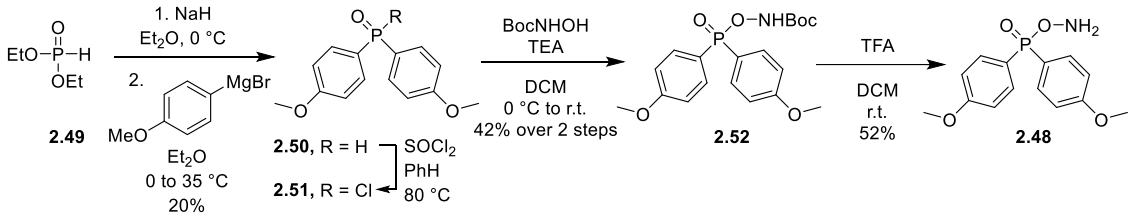

Figure 2.15 **Synthesis of diarylphosphinyl hydroxylamine 2.48**

Despite much effort, all attempts to employ the above-mentioned synthesis approach for preparation of di(4-*N*-butoxyphenyl)phosphinyl hydroxylamine (**2.47)** did not allow us to obtain the *n*-butyl analog of compound **2.48**. The higher solubility of compound **2.47** in nonpolar solvents (DCM, Et_2O, hexanes) and apparent chemical instability (the hydrolysis of **2.47** into diarylphosphinic acid during the aqueous work-up (necessary for removal of the $NaHCO_3$ used for neutralizing of remaining TFA)) left us without means of purification of the final compound.

O-(2,4-Dinitrophenyl)hydroxylamine (**2.56**) is another frequently used reagent for electrophilic amination of carbonyl compounds that was also prepared in our lab (Figure 2.16).[53] This was achieved by S_NAr-type reaction between *N*-hydroxyphtalimide (**2.53**) and 2,4-dinitrochlorobenzene (**2.54**) (TEA, acetone, r.t., 94%) with subsequent phthalimide cleavage in **2.55** with hydrazine hydrate. Notably, the desired hydroxylamine **2.56** was obtained in sufficient purity (>90%) and yield (57%) by simple filtration and extraction.

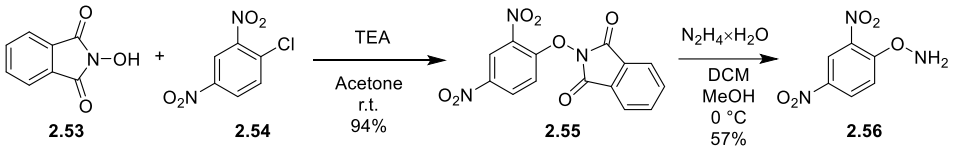

Figure 2.16 **Synthesis of *O*-(2,4-dinitrophenyl)hydroxylamine (2.56)**

With hydroxylamine derivatives **2.48** and **2.56** in hand, the electrophilic amination of ketone *rac*-**2.3** was investigated (Figure 2.17). The ketone was converted into enolate by KHMDS (conditions A-B) or LDA (conditions C) at -78 °C, and then aminating reagent **2.48** was added at -78 °C with gradual warming to room temperature, followed by Ac_2O quench. Unfortunately, the formation of acetamide *rac*-**2.57** was not detected (by UPLC-MS) in any of

the tested conditions and only starting ketone *rac*-**2.3** or unknown degradation products could be observed. We observed incomplete dissolution of the aminating agent **2.48** under reaction conditions and realized that this issue could be at least partially responsible for the poor formation of acetamide *rac*-**2.57**. To address the observed incomplete dissolution of **2.48** in THF at -78 °C, anhydrous glyme (dimethoxyethane) was added in several experiments under conditions B and C. However, this did not affect the reaction conversion and no formation of acetamide *rac*-**2.57** was detected by UPLC-MS. The use of *O*-(2,4-dinitrophenyl)hydroxylamine (**2.56**) (Figure 2.17, conditions D**)** as an alternative electrophilic amination also did not lead to the formation of the desired macrocycle *rac*-**2.57**, and ketone *rac*-**2.3** was recovered together with unidentified degradation products. The unsuccessful synthesis of the amination product **2.57** could be attributed to lesser solubility of amination reagent **2.48** as compared to the published *O*-butyl analog **2.47**. It should be noted, however, that even the use of apparently better soluble *O*-butyl analog allowed Vedejs and Zajac to obtain the desired amination product **2.57** in only 14% yield (at 55% mass balance), so the enolate amination procedure evidently is not well suited for the synthesis of α-amino ketone **2.57**.

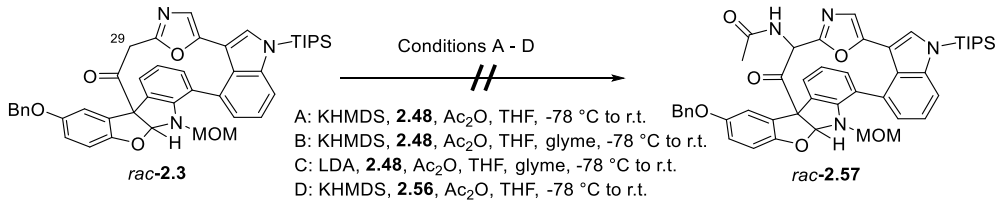

Figure 2.17 **Attempted introduction of acetamide moiety in ketone *rac*-2.3**

Next, the preparation of α-haloketone and its subsequent S_N2 reaction with a sodium azide was attempted. Accordingly, an initial deprotonation of the ketone *rac*-**2.3** by KHMDS or LDA and subsequent reaction of the formed potassium or lithium enolate with either Br_2 or I_2 (Figure 2.18, conditions A and B, respectively) was followed by exchange with NaN_3. Under both conditions poor conversion of the starting ketone *rac*-**2.3** was observed with no detectable formation (UPLC-MS assay) of either α-halo or α-azido ketone.

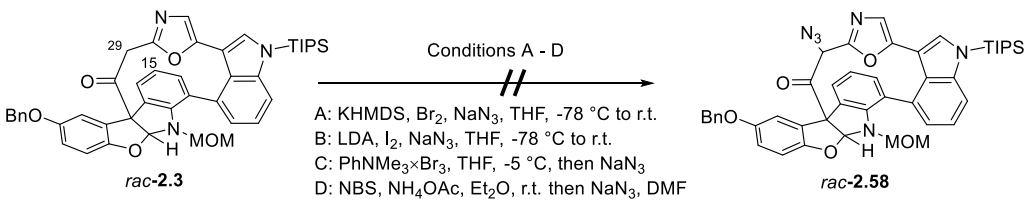

Figure 2.18 **Attempted introduction of azide moiety in ketone *rac*-2.3**

In contrast, an electrophilic bromination reaction using $PhNMe_3 \times Br_3$ (Figure 2.178, conditions C) brought about full consumption of the ketone *rac*-**2.3** and formation of complex mixture of unidentified products. Similarly, bromination using NBS (NH_4OAc, Et_2O, r.t.) facilitated slow conversion of ketone *rac*-**2.3** to several mono- and dibrominated products (indicated by UPLC-MS) that degraded after addition of NaN_3 solution in DMF (conditions D). It is known that diazonamide A (**1.2**) can be brominated with NBS at position C15 of the tetracyclic aminal moiety, which together with halogenations at position C29, could explain the rise of multibrominated products.[17] Unfortunately, the formation of multiple decomposition products complicated their isolation, purification and characterization.

The unsuccessful attempts to obtain α-functionalized ketone led us to investigate the reactivity of ketone **2.3**-derived enolate by deuterium quench. To this end, potassium enolate was prepared by KHMDS deprotonation of ketone *rac*-**2.3**, and then transferred *via cannula* to the excess of AcOH-d_4 in THF at -78 °C (Figure 2.19).

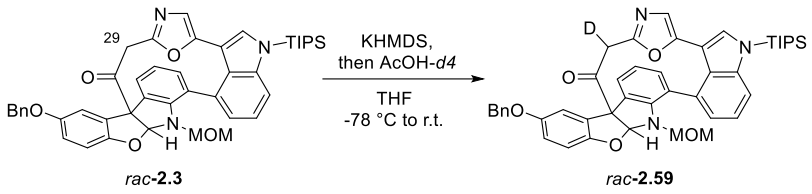

Figure 2.19 **Introduction of deuterium in ketone *rac*-2.3**

After solvent evaporation, ^{1}H-NMR spectra of the crude residue in C_6D_6 showed a diminished integral values for both methylene protons in the α-position to the ketone (0.49 H or 51% D incorporation for signal at δ=3.83 ppm and 0.39 H or 61% deuterium incorporation for signal at 3.45 ppm; see Figure 2.20). The observed deuterium incorporation provided evidence for the enolate formation from ketone *rac*-**2.3**, and >100% deuterium incorporation (111% in total) pointed at partial acid-catalyzed ketone enolization after the AcOH-d_4 quench.

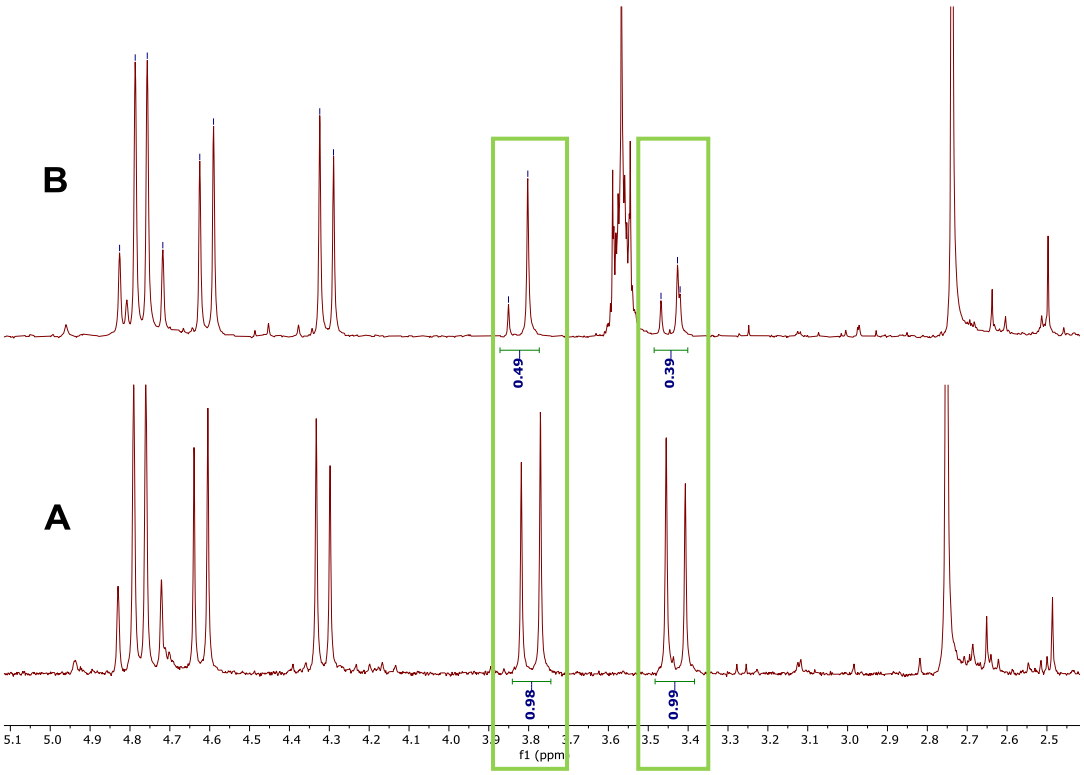

Figure 2.20 **1H-NMR spectra of *rac*-2.3 (spectrum A) and *rac*-2.59 (spectrum B). The methylene signals at C(29) are encircled with green**

With the base-mediated formation of enolate from ketone *rac*-**2.3** confirmed, a search for methods to introduce nitrogen functionality α to the ketone was continued. We were delighted to find that diazo moiety could be introduced with ca. 70% yield (unpurified sample) by *Regitz* diazo transfer reaction using *para*-acetamido benzosulfonylazide (*p*ABSA, **2.60**) in the presence of DBU as a base (Figure 2.21).[58]

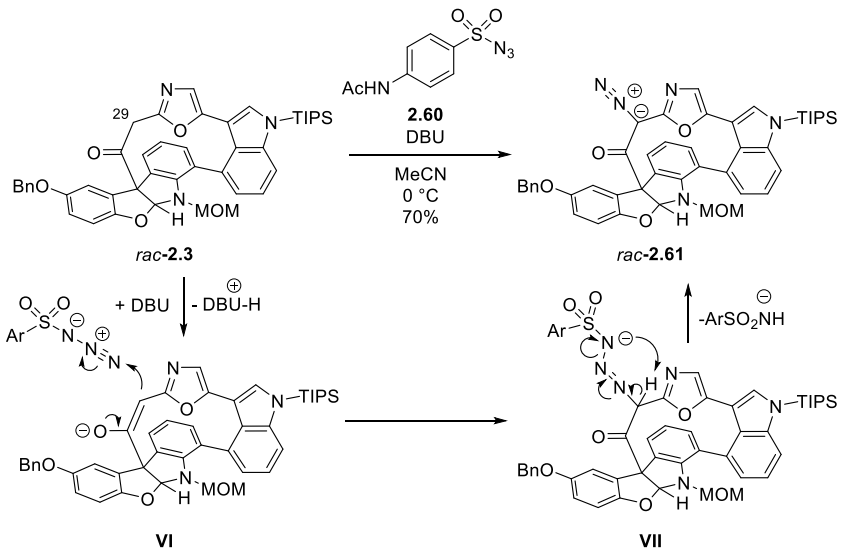

Figure 2.21 **Synthesis of α-diazoketone *rac*-2.61**

In the diazotransfer process, ketone-derived enolate **VI** reacted with sulfonyl azide **2.60** forming adduct **VII**, which then rearranged into diazoketone *rac*-**2.61** with expulsion of sulfonamide anion. The diazo transfer proceeded well in both MeCN and DCM, however about one hour was required to reach full conversion in DCM, whereas 10 minutes was sufficient time in MeCN. Evidence for the formation of diazoketone *rac*-**2.61** was obtained by UPLC-MS assay (strong signal with 750 m/z corresponding to $[M\text{-}Me+H]^+$; the loss of methyl group is signature fragmentation of MOM group) and ^{1}H-NMR analysis (disappearance of C(29) methylene protons with rest of the signals being intact although somewhat shifted (see Figure 2.22.). Unfortunately, diazoketone *rac*-**2.61** was unstable in solution and it decomposed at ambient temperature, thus making isolation, purification, and further analysis impossible.

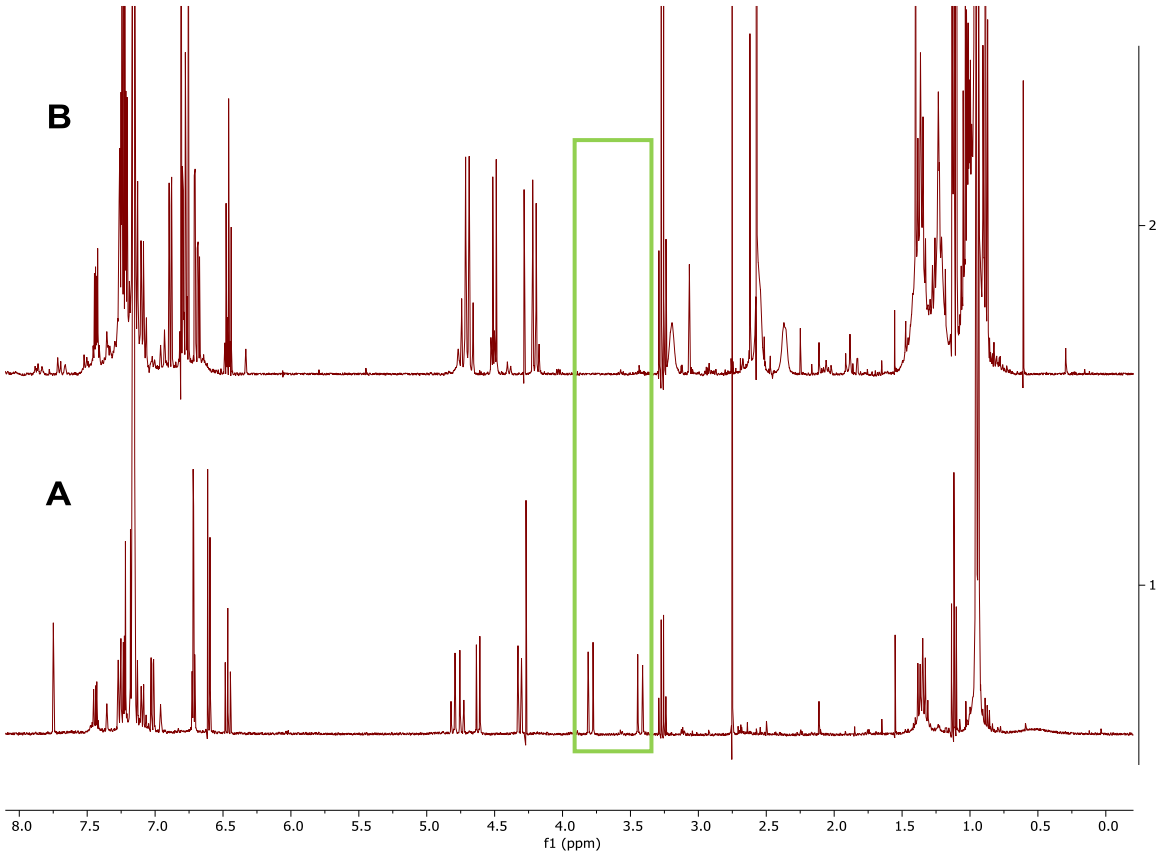

Figure 2.22 **^{1}H-NMR spectra of *rac*-2.3 (spectrum A) and *rac*-2.61 (spectrum B). The methylene signals at C(29) are encircled with green.**

With α-diazoketone *rac*-**2.61** in hand, the synthesis of bioxazole fragment was addressed. Our initial attempts concentrated on the direct, rhodium-catalyzed reaction between the α-diazocarbonyl compound and primary alkyl- or arylamides (Figure 2.13).[59] This reaction presumably involves an initial formation of electrophilic rhodium alkylidene

complex **IX** from diazoketone **VIII** and dirhodium carboxylate catalyst (usually $Rh_2(OAc)_4$) (Figure 2.23).[60] Complex **IX** in turn reacts with primary amide to form rhodium-associated ylide **X**. Dissociation of rhodium catalyst generates the free ylide **XI**, which after 1,2-proton shift yields the secondary amide **XII**. Unfortunately, the Rh(II)-catalyzed reaction between diazoketone *rac*-**2.61** and acetamide under conditions developed by Moody ($Rh_2(OAc)_4$, DCM, 40 °C, slow addition of diazoketone to catalyst using syringe pump)[55] led to complete degradation of starting material and no signals of acetamide *rac*-**2.57** were observed (UPLC-MS data) (Figure 2.23, conditions A). Likewise, only trace levels of the desired ketoamide *rac*-**2.62** were detected in the reaction with 4-fluorobenzamide (conditions B).

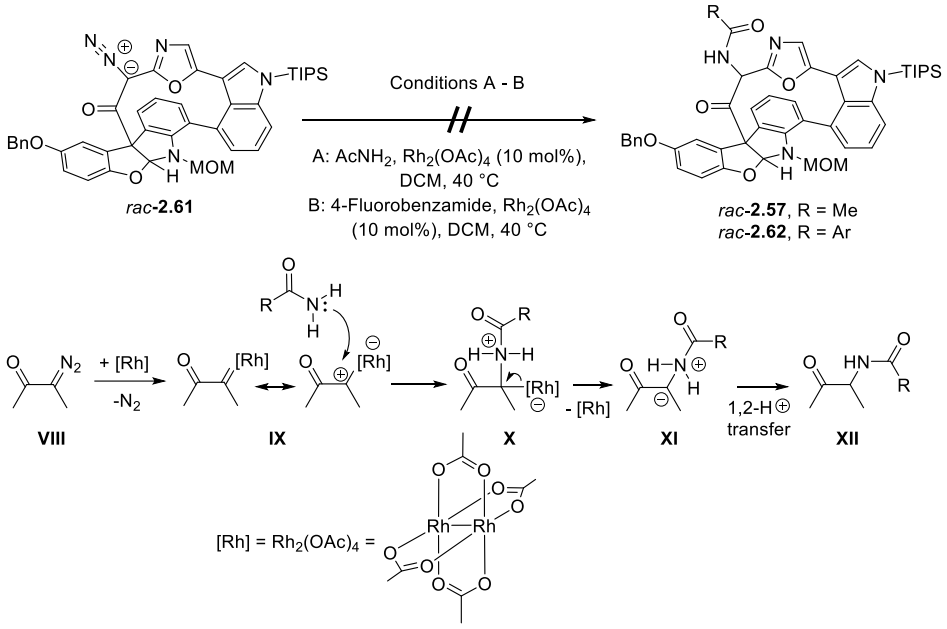

Figure 2.23 **Attempted Rh-catalyzed reaction between diazoketone *rac*-2.61 and primary amides and its mechanism[60]**

Next, we explored the possibility to convert diazoketone *rac*-**2.61** into the bioxazole *rac*-**2.63** by transition metal (Rh, Cu) or *Lewis* acid-catalyzed reaction with acetonitrile. In the transition metal-catalyzed approach, acetonitrile adds to the rhodium alkylidene **IX** and forms rhodium-associated ylide **XIII**. Dissociation of Rh(II) catalyst produces ylide **XIV** that undergoes cyclization into oxazole **XV** (Figure 2.24).[61,62]When *Lewis* acid (most frequently $BF_3 \times Et_2O$) is used as the promoter, it coordinates to oxygen of the diazoketone and forms intermediate betaine **XVI**. The latter then reacts with MeCN with expulsion of N_2 and produces nitrilium betaine **XVII** which cyclizes to the oxazole **XV**.[63,64]

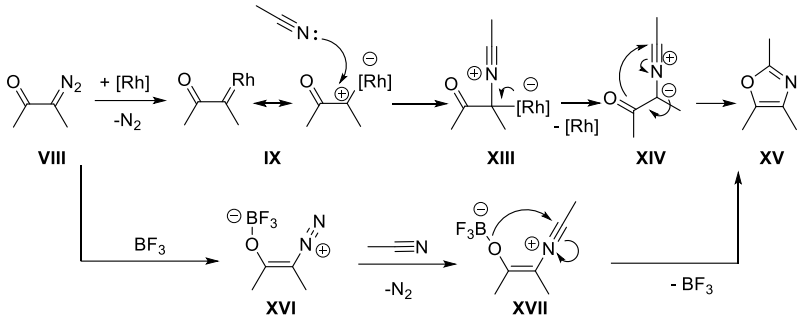

Figure 2.24 **Mechanism of reaction between diazoketone and acetonitrile[62,63]**

However, the desired transformation using acetonitrile proved to be incompatible with macrocycle *rac*-**2.61**. Extensive degradation of *rac*-**2.61** and no formation of the bioxazole *rac*-**2.63** was observed in the reaction with MeCN in the presence of Lewis acid ($BF_3 \times OEt_2$; Figure 2.25, conditions A) or catalytic transition metal complexes (($Rh_2(OAc)_4$, conditions B or $Cu(acac)_2$, conditions C)

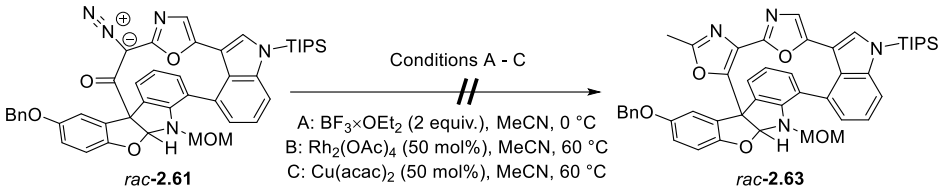

Figure 2.25 **Attempted synthesis of bioxazole *rac*-2.63**

We speculated that the observed degradation of *rac*-**2.61** in the presence of $BF_3 \times OEt_2$ and Lewis acidic transition metal complexes such as $Rh_2(OAc)_4$ and $Cu(acac)_2$ could be attributed to the poor stability of the core tetracyclic hemiaminal under the reaction conditions. For example, the *N*-MOM protected tetracyclic aminal *rac*-**2.3** undergoes ring-opening in the presence of Brønsted acid and nucleophile (HCl in MeOH) (Figure 2.26). In this transformation, attack of methanol on protonated ketone **XVIII** leads to the formation tetrahedral intermediate **XIX** that collapses in a *Grob*-type fragmentation reaction into 3-arylindole **2.64**. The possible driving force of the reaction is the restoration of the aromaticity of the indole ring.

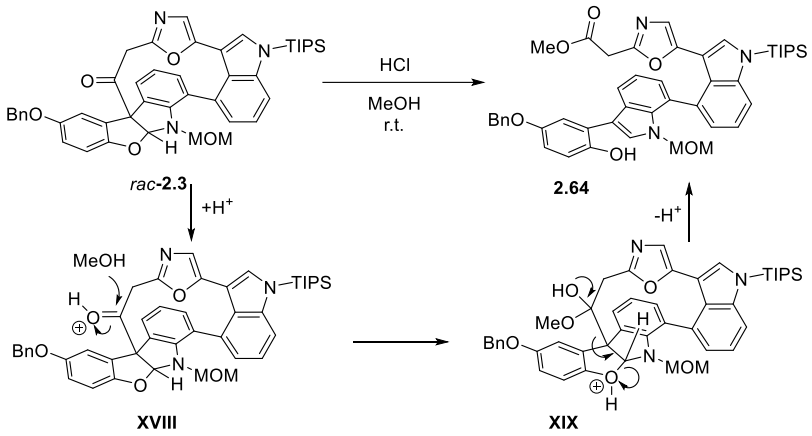

Figure 2.26 **Observed Grob-type fragmentation of *rac*-2.3**

Finally, the reduction of the diazo group in compound *rac*-**2.61** to primary amine *rac*-**2.65** was explored under Pd-catalyzed hydrogenation conditions[56] or using samarium(II) iodide.[65] In addition, the reduction of diazo moiety to hydrazone *rac*-**2.66** was also attempted by $LiBHEt_3$[66] or triphenylphosphine[67].

Unfortunately, our attempts to reduce the diazo moiety in macrocycle *rac*-**2.61** were met with limited success. Palladium-catalyzed hydrogenolysis in MeOH did not deliver the aminoketone *rac*-**2.65**. Instead, cleavage of the diazo moiety and formation of the ketone *rac*-**2.3** already within one hour took place (as evidenced by UPLC-MS) (Figure 2.27A, conditions A). Although undesired in our case, such transformation is well known.[68] On the other hand, the reaction with freshly prepared samarium(II) iodide solution in anhydrous *i*PrOH delivered trace amounts of the desired amine *rac*-**2.65** (UPLC-MS data) (Figure 2.27A, conditions B). Regrettably, the SmI_2-mediated reduction of diazoketone *rac*-**2.61** also facilitated formation of side-products *rac*-**2.67** and *rac*-**2.68** (UPLC-MS data) which putative structures are depicted in Figure 2.24B. While compound *rac*-**2.67** arises from the reduction of ketone moiety[69], compound *rac*-**2.68** would form through addition of *i*PrOH to the ketone. Both reactions would involve opening of macrocycle like sequence depicted Figure 2.26. The concomitant formation of inseparable byproducts and poor reproducibility rendered the SmI_2-mediated reduction unsuitable.

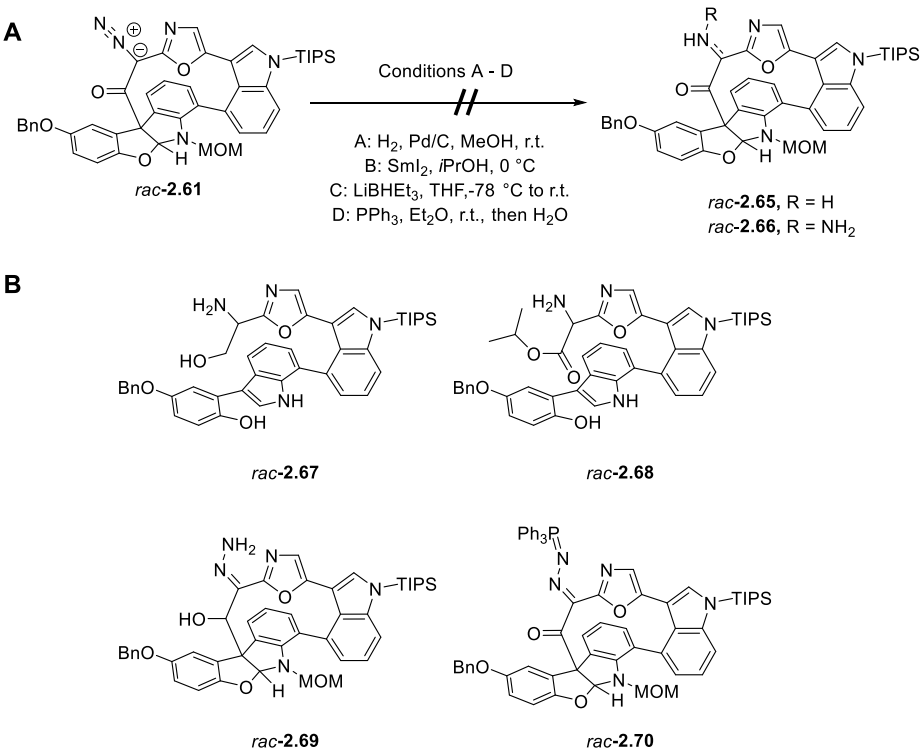

Figure 2.27 **Attempted reduction of diazo moiety in *rac*-2.61**

In contrast to the attempted reductions into primary amine, methods for the reduction of diazo group into the corresponding hydrazone **2.66** delivered better results (as evidenced by UPLC-MS). Specifically, the use of $LiBHEt_3$ (THF, -78 °C to r.t.) produced about 30% of the target hydrazone *rac*-**2.66** together putative double-reduction product – alcohol *rac*-**2.69** (Figure 2.27A, conditions C). However, attempts to isolate and purify hydrazone *rac*-**2.66** by preparative TLC procedure resulted in degradation. Finally, when the diazoketone *rac*-**2.61** was subjected to reaction with triphenylphosphine (Et_2O, r.t.), formation of the expected triphenylphosphoranylidene hydrazone *rac*-**2.70** was recorded by UPLC-MS assay (Figure 2.27A, conditions D). However, hydrolysis of *rac*-**2.70** to hydrazone *rac*-**2.6** and attempted purification of the crude material with preparative TLC method led to complete decomposition.

The multiple unsuccessful attempts toward the construction of the second oxazole ring consumed all of the precious ketone *rac*-**2.3**. Furthermore, the limited amount of the available ketone *rac*-**2.3** reduced our ability to perform extensive optimization of reactions such as the reduction of the diazo moiety. Because the re-synthesis of *rac*-**2.3** would require considerable synthetic resources, the total synthesis project was discontinued.

2.1.7. Summary

In summary, our contribution to the total synthesis of diazonamide A (**1.2**) involved a development of synthesis of enantiomerically pure macrocyclic ketone (*R*,*R*)–**2.3** which incorporates the right hand-side heteroaromatic 12-membered macrocycle of diazonamide A as well as the core tetracyclic hemiaminal moiety and all-carbon stereogenic center. Synthesis was done by atropodiastereoselective *Dieckmann*-type cyclization of biaryl (*R*,*R*)–**2.4** and **t**he diastereoselectivity of the cyclization was controlled by the (*R*)-stereogenic center at C10 of the rigid tetracyclic hemiaminal moiety. Biaryl (*R*,*R*)–**2.4** existed as 3:2 mixture of atropoisomers in solution at room temperature, but only (*M*)-isomer participated in the macrocyclization while (*P*)-isomer was recovered after work-up. Synthesis of (*R*,*R*)–**2.3** was made possible by preparation of both racemic and enantiopure tetracyclic hemiaminal bromide **2.5** on multi-gram scale by previously reported methods.

We studied the stability of carbonyl-substituted tetracyclic hemiaminal moiety and indicated the decomposition pathway of *N*-unprotected tetracycle *rac*-**2.27** under basic conditions. We also discovered that *N*-MOM protected tetracyclic hemiaminal-containing ketone *rac*-**2.3** is not stable under acidic conditions in presence of nucleophile and might not be compatible with *Lewis* or *Broensted* acid-mediated ketone α-amination reaction conditions.

We studied the α-amination/oxazole introduction of ketone *rac*-**2.3** and indicated that this is not viable path to the total synthesis of diazonamide A **1.2**. However, we did obtain the elaborate diazoketone *rac*-**2.61** as the only α-nitrogen-containing derivative of ketone **2.3**, which leaves options for the introduction of the necessary bioxazole moiety after additional optimization of reaction conditions. Although we had to discontinue the total synthesis of diazonamide A **1.2** due to the lack of material to work with, the gained experience was helpful in the synthesis of other diazonamide A (**1.2**) analogs as described below.

2.2. Attempted synthesis of macrocycle 2.71

2.2.1. Introduction

Our main motivation to accomplish the total synthesis of diazonamide A (**1.2**) was the exploration of SAR around this highly cytotoxic microtubule targeting agent that would allow us to develop its structurally simplified analogs. Having exhausted all possibilities and material for synthesis of diazonamide A (**1.2**) (see chapter 2.1) we had to reevaluate our approach to design of new anticancer medicines. From the obtained results it became evident

that 1) design of simpler and easier to synthesize analogs of diazonamide A (**1.2**) would allow for much faster preparation and biological evaluation of new potential drug compounds and 2) utilization of other core structures, less labile than the tetracyclic hemiaminal, would enable use of more diverse synthetic approaches and conditions for the preparation of the designed compounds. Consequently, we elected to rely on DZ-2384 **2.71**, a highly potent diazonamide A **1.2** analog, as the starting platform for design of new compounds that would allow us to fulfill both abovementioned suggestions. We also realized that structural modifications of challenging-to-synthesize and relatively unstable tetracyclic hemiaminal subunit is a key to the successful development of potent analogs. Accordingly, we envisaged that change of benzofuran to indane moiety in the tetracyclic core structure could help address the instability of the hemiaminal. Hence compound **2.71** emerged as potential molecule of interest (Figure 2.28).

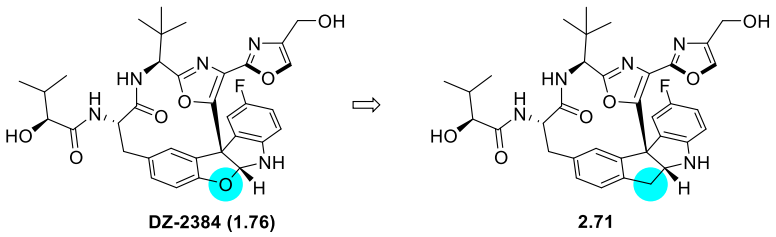

Figure 2.28 **DZ-2384 (1.76) and macrocycle 2.71**

Macrocycle **2.71** maintains all the essential functional groups of DZ-2384 (**1.76**) – hydroxymethyl-substituted bioxazole moiety, *tert*-butyl group, left hand-side (*S*)-hydroxyisovaleric acid side chain as well as rigid, hydrophobic tetracyclic core structure bearing quaternary stereocenter with *S*-configuration. The only structural change would be substitution of oxygen atom with carbon atom in the core tetracyclic ring system. We envisioned that substituting the oxygen with methylene group would not alter target binding and the compound's overall three-dimensional structure which is necessary for the biological effect. As a result, we anticipated macrocycle **2.71** to possess comparable biological activity to DZ-2384 (**1.76**). Furthermore, synthesis and biological evaluation of macrocycle **2.71** would also add a significant data point on the structure-activity relationship map of diazonamide A (**1.2**) analogs.

2.2.2. First generation synthesis

Although the structures of macrocycles **1.76** and **2.71** are highly similar, the absence of the oxygen atom in the tetracyclic moiety of **2.71** changes the retrosynthetic disconnections, rendering methods for preparation of DZ-2384 (**1.76**) unsuitable. Therefore, we performed a retrosynthetic analysis of macrocycle **2.71** as shown in Figure 2.29.

We envisioned that macrocycle **2.71** could be prepared from ciano oxazole **2.72**, which in turn could be accessed from enantiopure ketone **2.73** under *Fischer* indole synthesis conditions. Synthesis of **2.73** could be accomplished using intramolecular Pd-catalyzed ketone α-arylation of indanone **2.74**, which could be prepared from the building blocks **2.75** and **2.76** through amide coupling.

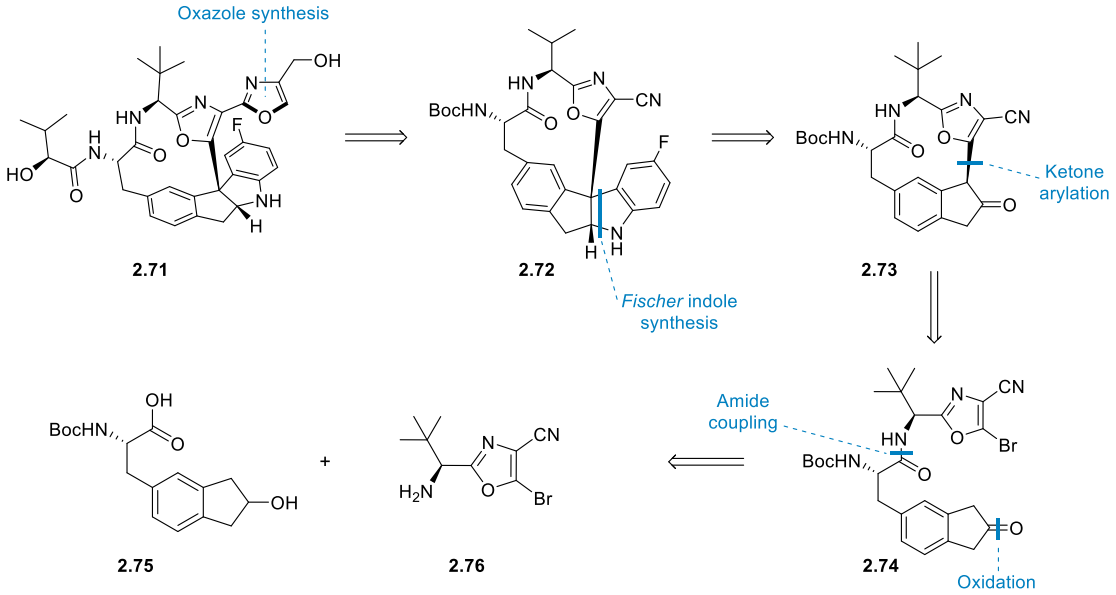

Figure 2.29 **Retrosynthesis of macrocycle 2.71**

The synthesis of macrocycle **2.71** commenced with the preparation of building block **2.75** from the commercially available 2-indanol (**2.77**) (Figure 2.30).[70,71] Thus, acetylation of the hydroxy group and subsequent electrophilic bromination with NBS in the dark for five days gave aryl bromide **2.79** in 45% yield after two steps. Although the bromination is well-precedented in the literature, in our hands it turned out to be poorly reproducible with poor conversion of starting material and product yields ranging from 0% to 45%. Next, the amino ester moiety was introduced by *Negishi* cross-coupling reaction ($Pd_2(dba)_3$, SPhos, DMF, 55 °C) between the aryl bromide **2.79** and freshly prepared alkyl zincate **2.81**.[72] Phenylalanine derivative **2.82** was obtained in 74% yield as 1:1 mixture of diastereomers. Finally,

simultaneous hydrolysis of methyl ester and acetate under basic conditions (LiOH, MeOH, H_2O, 0 °C) afforded carboxylic acid **2.75** in 63% yield.

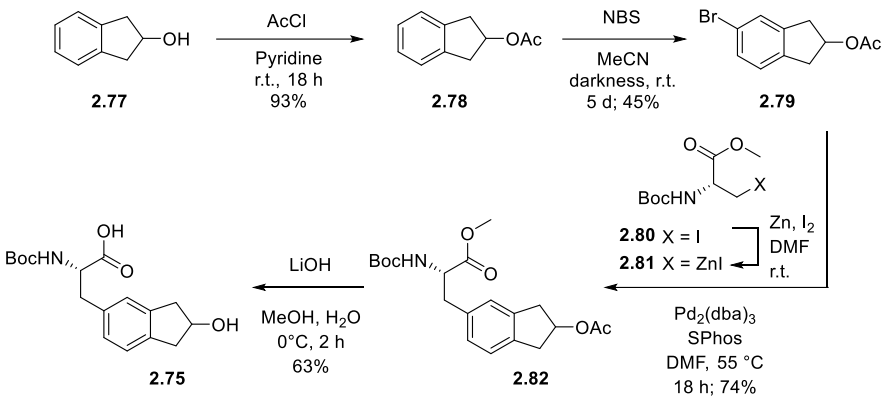

Figure 2.30 **Synthesis of carboxylic acid 2.75**

Aminomethyl oxazole **2.76** was accessed from the bromooxazole **2.83** (Figure 2.31), which has been prepared previously in our laboratory.[73] Hydrogenative cleavage of the *N*-Cbz-group in the presence of catalytic amount of Pd/C (20 mol%) could not be employed due to predominant proto-debromination of **2.83** (as detected by UPLC-MS). Therefore, *N*-Cbz protecting group was removed with HBr solution in a mixture of AcOH and 1,4-dioxane. Although the acidic cleavage of the Cbz-group allowed us to obtain the amine **2.76**, concomitant hydrolysis of nitrile group to primary amide and *N*-benzylation of the unprotected amino group during work-up (with BnBr resulting from the reaction of Cbz-group with HBr) led to moderate yield (48%). Nevertheless, amide bond formation between amine **2.76** and acid **2.75** in the presence of EDC×HCl in pyridine gave amide **2.84** with 80% yield. Finally, DMP oxidation of alcohol furnished ketone **2.74** in 74% yield.

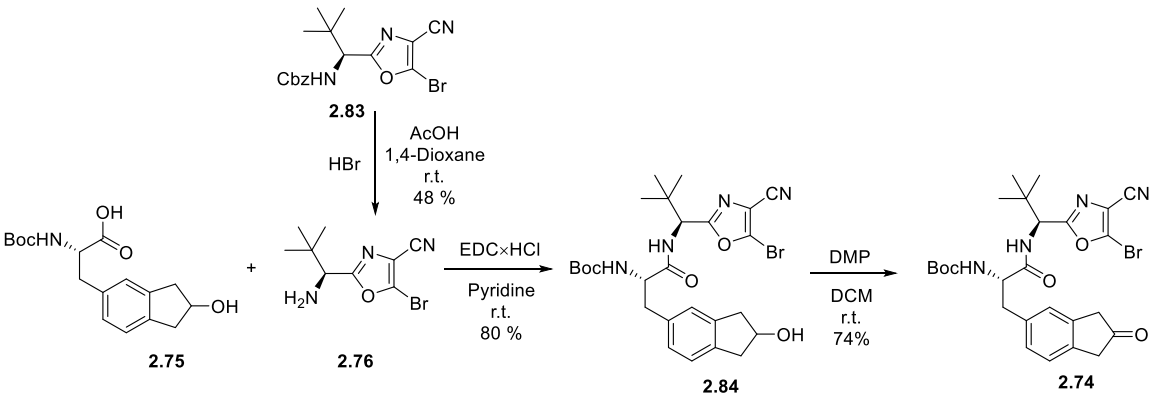

Figure 2.31 **Synthesis of ketone 2.74**

With ketone **2.74** in hand, the formation of 12-member macrocycle **2.73** was addressed. We envisioned that the macrocyclization could be accomplished by intramolecular Pd-catalyzed ketone α-arylation and so we ran a short screening of the reaction conditions on small scale (15 mg (0,027 mmol) of ketone **2.74** (Figure 2.32). We found that multiple commonly used ketone arylation conditions ($Pd_2(dba)_3$ (4 mol%), XantPhos (12 mol%), K_3PO_4 (3 equiv.), PhMe, 80 °C, conditions A[74]; $Pd_2(dba)_3$ (4 mol%), XantPhos (12 mol%), Cs_2CO_3 (3 equiv.), 1,4-dioxane, 80 °C, conditions B[75]; $Pd(PPh_3)Cl_2$ (4 mol%), dppe (12 mol%), Cs_2CO_3 (3 equiv.), 1,4-dioxane, 80 °C, conditions C[76]) caused degradation of the ketone **2.74** with no formation of the macrocycle **2.73** (as indicated by UPLC-MS).

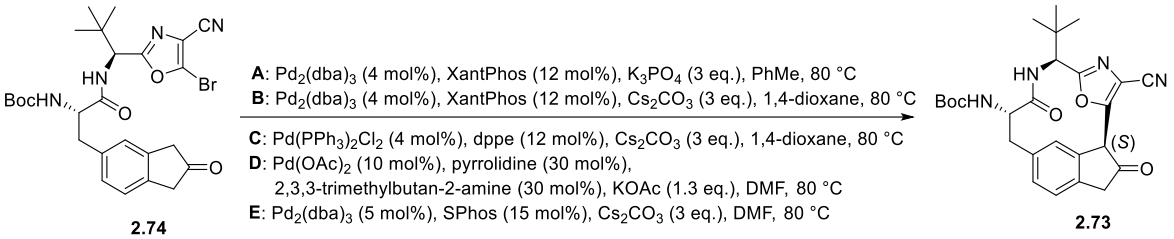

Figure 2.32 **Investigation of macrocyclization conditions**

Luckily, conditions developed by Dong specifically for α-arylation of cyclopentanones ($Pd(OAc)_2$ (10 mol%), pyrrolidine (30 mol%), 2,3,3-trimethylbutan-2-amine (30 mol%), KOAc (1.3 equiv.), DMF, 80 °C, 21 h, Figure 2.32. conditions D) provided 90% conversion of ketone **2.74** and formation of macrocycle **2.73** along with several unidentified byproducts after 21 h at 80 °C temperature.[77] However, the fastest and the most selective conversion of ketone **2.74** into macrocycle **2.73** was achieved when we employed conditions previously used for *Negishi* cross coupling ($Pd_2(dba)_3$ (5 mol%), SPhos (15 mol%), Cs_2CO_3 (3 equiv.), DMF, 80 °C, Figure 2.32. conditions E): full conversion of ketone **2.74** and formation of macrocycle **2.73** was detected already after four hours. When the reaction was run on 100 mg (0.19 mmol) scale, we were able to obtain the macrocycle **2.73** in 46% yield. However, further increase in ketone **2.74** loading (500 mg – 1.4 g; 0.9 – 2.5 mmol) consistently afforded reduced (28 – 29%) yields of macrocycle **2.73** with the rest being unidentified byproducts (Figure 2.33).

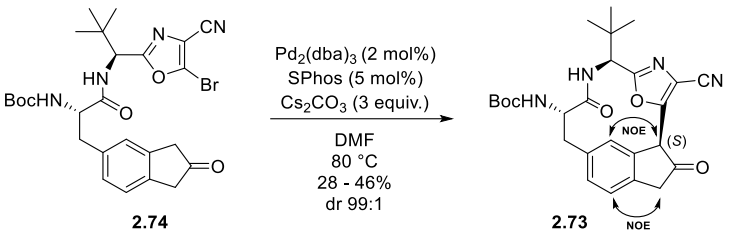

Figure 2.33 **Synthesis of macrocycle 2.73**

Notably, the macrocyclization proceeded with excellent regio- and stereoselectivity (99:1 dr) favoring the formation of 12-membered macrocycle vs. 13-membered analog. The structure of macrocycle **2.73** was established based on the observed NOE cross peaks between protons of the cyclopentanone and benzene rings. The absolute configuration of the newly formed stereocenter, however, could not be determined using NMR techniques because of the lack of useful correlations. Furthermore, macrocycle **2.73** was obtained as an amorphous material and attempts to grow single crystal suitable for X-ray crystallographic analysis were unsuccessful. However, the stereogenic center was later assigned *S* absolute configuration based on analogy with oxindole-containing macrocycles **2.153b,c** (see Section 2.3.2).

Although the Pd-catalyzed macrocyclization conditions described above ($Pd_2(dba)_3$, SPhos, Cs_2CO_3 in DMF) allowed us to obtain macrocycle **2.73**, a review of work done by Sammakia[23] on structurally similar substrates prompted us to investigate whether the macrocycle **2.73** could be delivered under Pd-free and base-promoted S_NAr-type reaction conditions. Indeed, small scale (5 mg of ketone **2.74**) reaction using only Cs_2CO_3 in DMF gave complete conversion of the ketone **2.74** to the macrocycle **2.73** (UPLC-MS assay). Obviously, the bromine substituent in the ciano oxazole is sufficiently activated toward S_NAr-type displacement by enolate, and presence of transition metal catalyst is not required for successful macrocyclization. Notably, diastereoselectivity was not affected by the change of the macrocyclization conditions as the cyclization product **2.73** was formed with 99:1 dr.

Successful macrocyclization did set the stage for the elaboration of the macrocyclic ketone **2.73** into the tetracyclic subunit-containing target molecule **2.72** under the *Fischer* indole synthesis conditions (see retrosynthesis in Figure 2.29). As such, reaction with 4-fluorophenylhydrazine hydrochloride **2.85** was carried out in *i*PrOH at 75 °C temperature[78] (Figure 2.34) and a product possessing the desired mass spectrum was obtained in 68% yield. However, NMR spectra in $CDCl_3$ showed presence of singlet of one aliphatic proton with 5.26 ppm chemical shift which was attached to tertiary carbon (as evidenced by HSQC spectrum) with 40.1 ppm chemical shift. This meant that the undesired regioisomer **2.86** has been formed exclusively without traces of the target **2.87**. Macrocycle **2.86** was isolated as single stereoisomer (dr 99:1).

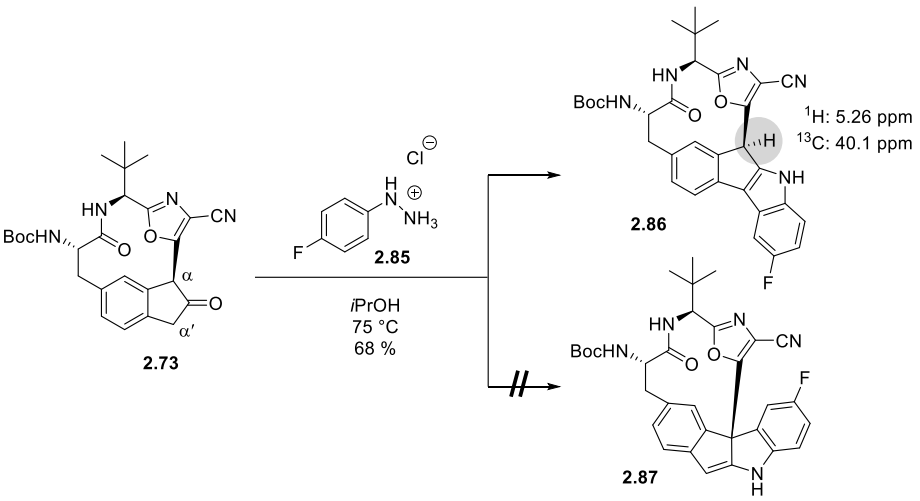

Figure 2.34 **Synthesis of macrocycle 2.86**

The selectivity of the reaction between ketone **2.73** and hydrazine **2.85** towards the formation of indole **2.86** can be explained by preference for the "kinetic" ene-hydrazine intermediate **XXI** over the "thermodynamic" ene-hydrazine **XXII** during the *Fischer* reaction (Figure 2.35). Although the use of weakly acidic conditions and electronically poor hydrazine favors the formation of the more substituted "thermodynamic" ene-hydrazine **XXII**[79], the sterically bulky ciano oxazole substituent at the α-position of ketone **2.73** , apparently, shifts the equilibrium towards the less substituted and more accessible "kinetic" ene-hydrazine intermediate **XXI**. The subsequent ene-reaction and rearomatization of benzene ring forms the aminoimine **XXIV**, which, after cyclization and elimination of ammonia, provides the indole **2.86**.

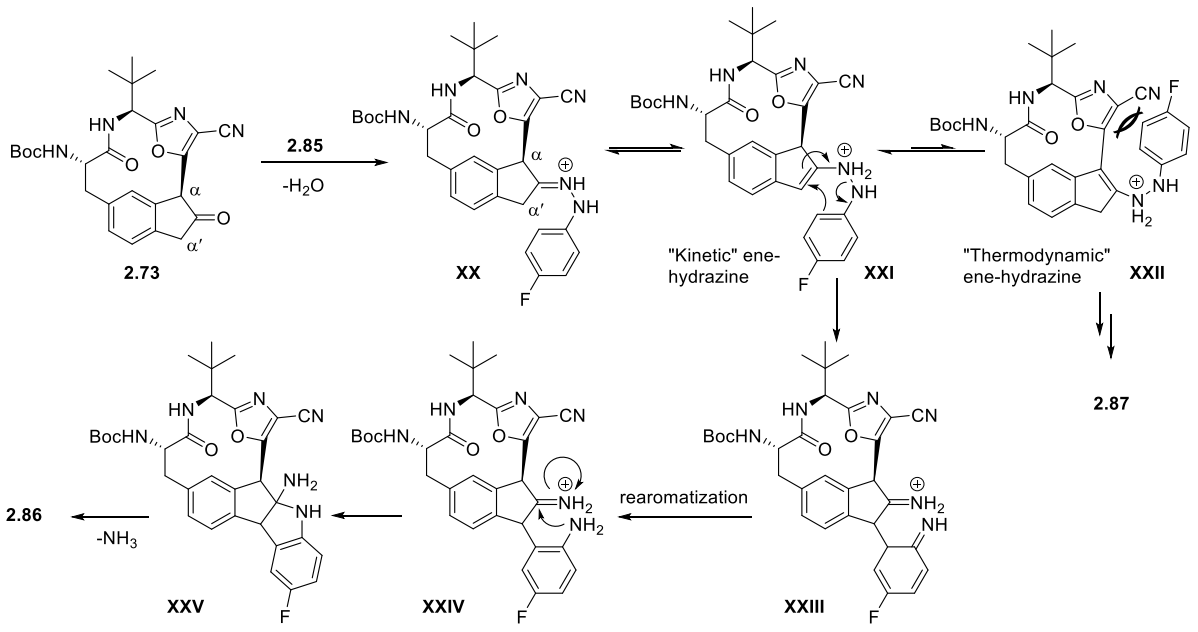

Figure 2.35 **Mechanism of *Fischer* indole synthesis**

The undesired macrocycle **2.86** was further elaborated into compound **2.89** to assess its antiproliferative properties for better understanding of structure-activity relationship. Luckily, the indolic double bond was easily reduced by $NaCNBH_3$ in the presence of TFA[80], which also facilitated a concomitant *N*-Boc cleavage (Figure 2.36). As a result, the indoline core-containing amine (*S,R*)-**2.88** was obtained with good diastereoselectivity (90:10 dr). The absolute configuration of the newly created stereogenic centers in macrocycle **2.88** was established to be *S,R* using DFT calculations as NMR spectroscopy could not give a definitive answer (see discussion below). Finally, amide coupling with (*S*)-hydroxyisovaleric acid ((*S*)-H*i*VA) under standard conditions (EDC, HOBt, DIPEA, DMF, r.t.) furnished the macrocycle **2.89** in 14% yield over two steps. Diastereomeric purity of the amide **2.89** reached 99:1 dr after chromatographic purification.

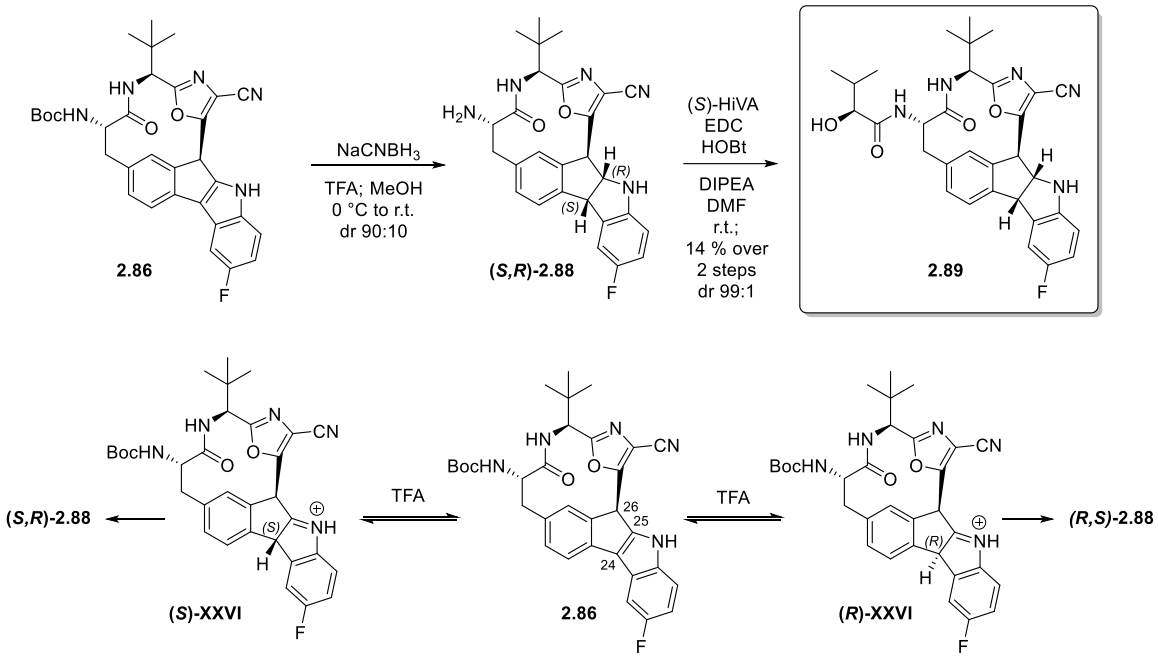

Figure 2.36 **Synthesis of compound 2.89**

To understand the rationale behind the formation of the (*S,R*)-**2.88**, a closer look at the mechanism of the reduction of indole in the presence of TFA is required (Figure 2.36). The initial step of the reduction of the fused indole **2.86** presumably involves protonation of the cyclic enamine at position C24[81] thus forming two diastereomerically distinct indolenium ions (*S*)-**XXVI** and (*R*)-**XXVI**. Under the reaction conditions these compounds are in equilibrium with the indole **2.86**. DFT calculations done by Dr. Artis Kinens (m062x level of theory, Def2SVP basis set), however, indicated that the indolenium ion (*R*)-**XXVI** is thermodynamically less stable than (*S*)-**XXVI** by 2.0 kcal due to the steric clash of fluor indole and cianooxazole moieties. This leads to predominant (calculated dr 97:3) formation of

indolenium ion (*S*)-**XXVI** which is then reduced with $NaCNBH_3$ leading to the *cis*-bridged indoline core of macrocycle (*S,R*)-**2.88**. Finaly, macrocycle **2.89** was assayed for antiproliferative potency on multiple cancer cell lines. Unfortunately, it possessed very low levels of activity (see section 2.4) so further elaboration of oxazolyl nitrile subunit into bioxazole moiety was not attempted.

At this point it became evident that the enantiomerically pure macrocyclic ketone **2.73** is not a viable substrate for synthesis of macrocycle **2.71** and we prepared to redesign the synthesis avoiding the late-stage formation of the tetracyclic indoline core.

2.2.3. Second generation synthesis

The unsuccessful attempts to construct the tetracycle subunit at the end of the multistep synthesis of macrocycle **2.71** prompted us to re-design the synthesis scheme (Figure 2.37). Accordingly, we envisioned that the tetracyclic moiety **2.92** could be prepared early on by the *Fischer* indole synthesis and then tethered to amino bioxazole building block **2.93** through the amide bond. The resulting amide **2.91** could be regarded as precursor to macrocycle **2.90**, deprotonated tetracycle subunit in compounds **2.91** could serve as a nucleophile in the S_NAr-type reaction with bromo-oxazole by analogy to the related macrocyclization of ketone enolate as shown in section 2.2.2 (Figure 2.33). We realized that the tetracycle has two positions of comparable acidity: indole N-H ($pKa_{(DMSO)}$ = 21.0)[82] and C-H of indene ($pKa_{(DMSO)}$ = 20.1).[83] Because of comparable thermodynamic acidity of the competing positions, the two deprotonated forms **XVII** and **XVIII** would likely exist in equilibrium (Figure 2.37, bottom). Furthermore, three nucleophilic centers will be generated due to the resonance stabilization in the deprotonated tetracycle. We speculated that each of them may undergo intramolecular S_NAr-type reaction with bromo-oxazole leading to macrocycles of distinct size: the desired 12-membered macrocycle in the cyclization involving trisubstituted carbon anion, 13-membered cycle from benzylic anion and 14-membered macrocycle for nitrogen nucleophile. We also hypothesized that the cyclization will occur under *Curtin-Hammett* conditions, where conformational preferences of macrocycle will control the cyclization of rapidly equilibrating anions **XVII** and **XVIII**. After the cyclization of **2.91** into **2.90**, the synthesis endgame would involve diastereoselective reduction of the double bond and side-chain manipulations.

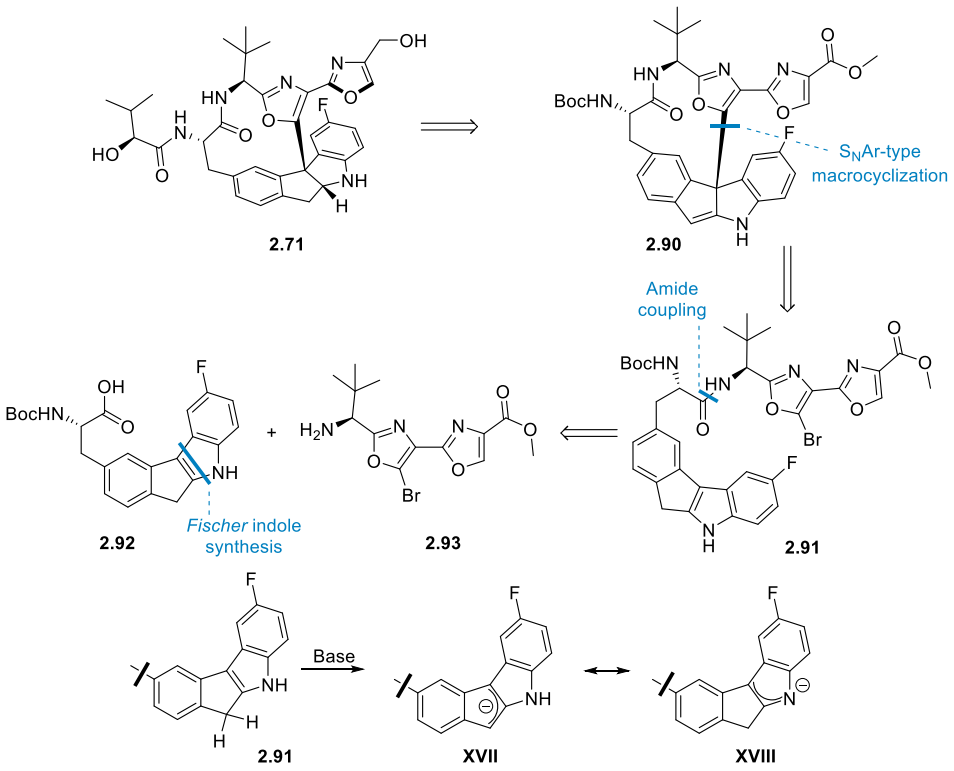

Figure 2.37 **Second generation retrosynthetic analysis of compound 2.71**

The synthesis of the building block **2.92** was commenced from the commercially available 6-bromo-1-indanone (**2.94**) by following the literature procedure (Figure 2.38).[84] Accordingly, the reduction of the ketone ($NaBH_4$ in MeOH) and the dehydration of the formed alcohol **2.95** afforded the 5-bromoindene (**2.96**) in a 59% yield over two steps. Subsequent epoxidation of the double bond with *m*CPBA and $BF_3{\times}Et_2O$-promoted 1,2-proton shift furnished the 5-bromo-2-indanone (**2.98**) with 64% yield.

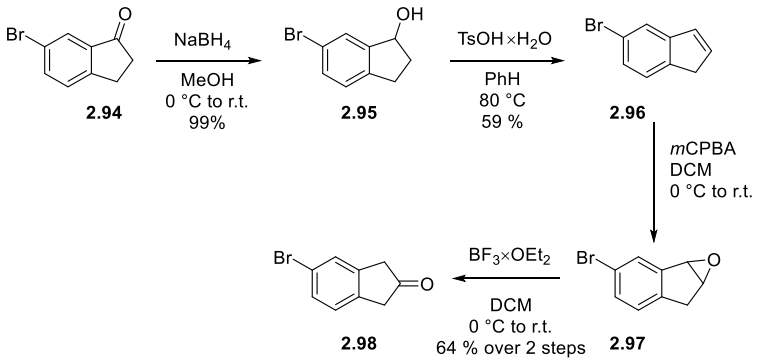

Figure 2.38 **Synthesis of ketone 2.98**

Next, the prepared ketone **2.98** was subjected to the *Fischer* indole synthesis conditions (hydrazine **2.85** in *i*PrOH at 75 °C) that produced two regioisomeric dihydroindeno[2,1-*b*]indoles **2.99** and **2.100** in 2:1 ratio (Figure 2.39). The separation of the isomers proved

challenging, and multiple column chromatography purifications were needed to obtain individual isomers with satisfactory purity (>95%). Identification of structures for tetracyclic isomers **2.99** and **2.100** was possible by 2D-NMR analysis of downstream compound **2.101** that was obtained from **2.100**. Accordingly, COSY experiment for **2.101** indicated clear ^{1}H-^{1}H cross peak between methylene protons at C7 and aryl proton at C3. The preferential formation of undesired regioisomer **2.99** was unexpected and prompted us to work on a larger scale to prepare sufficient amounts of the desired aryl bromide **2.100**. After enough tetracyclic bromide **2.100** was prepared, the Pd-catalyzed *Negishi* cross-coupling ($Pd_2(dba)_3$ / SPhos) with freshly prepared alkyl zincate **2.81** delivered ester **2.101** in 68% yield. Saponification of methyl ester with LiOH afforded carboxylic acid **2.92** that was subjected to amide bond formation with amino bromooxazole **2.93** (prepared from previously reported *N*-Boc bioxazole[85]) in the presence of EDC×HCl in pyridine. The desired amide **2.91** was obtained in 40% yield, setting the stage for the key macrocyclization step.

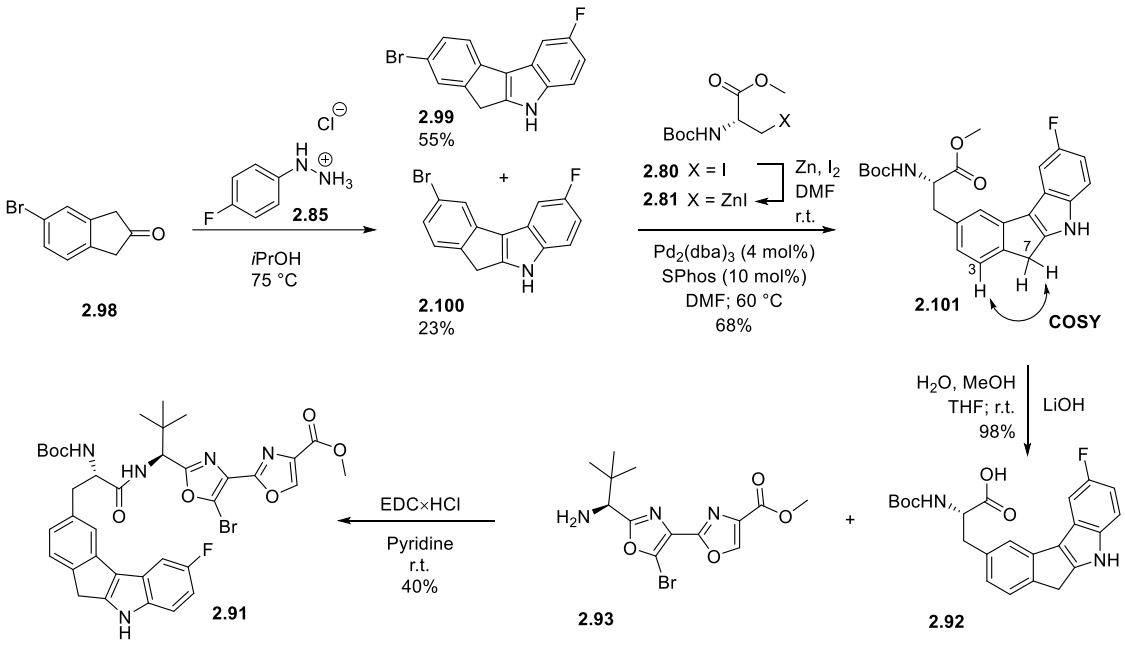

Figure 2.39 **Synthesis of amide 2.91**

The macrocyclization of amide **2.91** in the presence of Cs_2CO_3 in DMF generated a single product whose mass spectral signature (m/z 670.3 $[M+H]^+$) corresponded to the target compound **2.90** (Figure 2.40). However, NMR analysis of purified material revealed presence of singlet of one aliphatic proton at 5.86 ppm connected to tertiary carbon atom (as evidenced by HSQC spectrum) with chemical shift of 42.7 ppm. The NMR data pointed to the formation of the undesired 13-membered macrocycle **2.102** (formed from the anion **XVII**)**.** We later confirmed the NMR-based structural assignment by X-ray crystallographic analysis. The

undesired macrocycle **2.102** was formed with excellent diastereoselectivity (99:1 dr). The absolute configuration of the newly created stereogenic center was established as S by X-ray crystallographic analysis. Unfortunately, formation of compounds **2.90** and **2.103** (both rising from anion **XVIII**) was not detected.

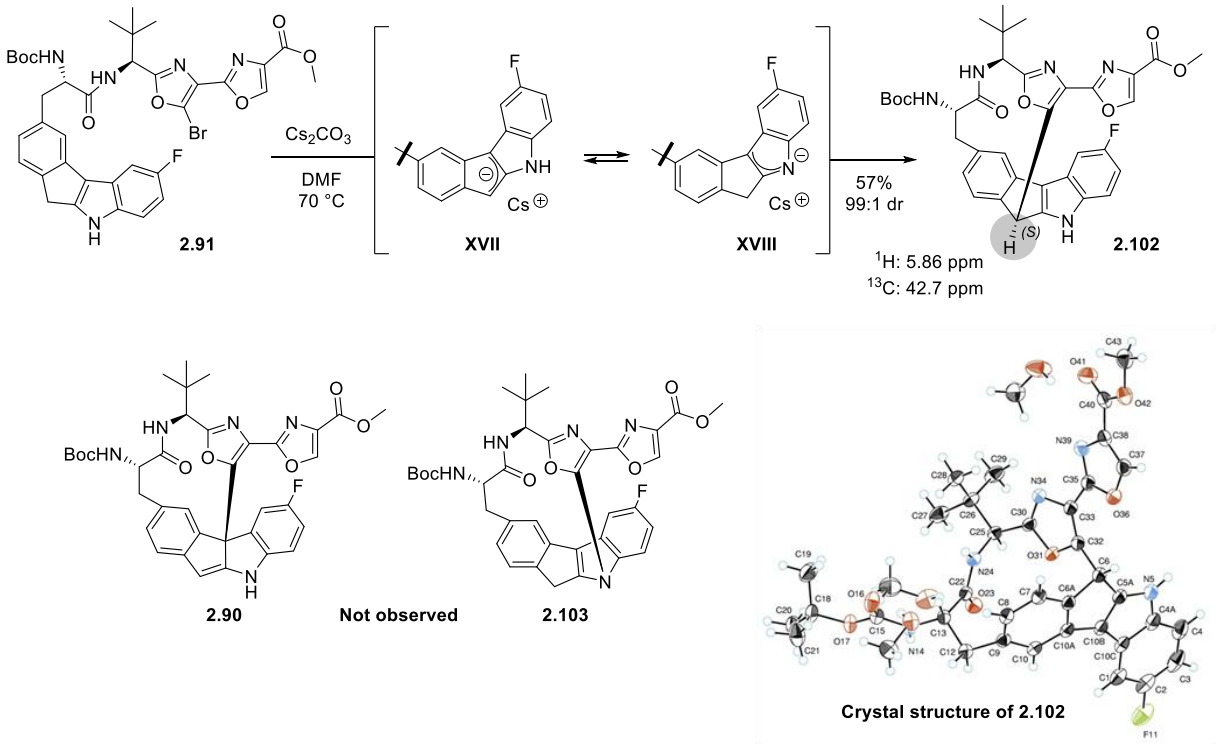

Figure 2.40 **Macrocyclization of compound 2.91**

DFT calculations done by Dr. A.Kinens (b3lyp level of theory and 6-31+g(d) basis set) indicated that energies for transition states involved in formation of 12- and 14-membered macrocycles **2.90** and **2.103** were 18.4 and 23.1 kcal/mol, respectively, which is 9.3 and 14.0 kcal/mol higher in energy than for 13-membered macrocycle **2.102** (9.1 kcal/mol). The energy difference ensured that the formation of macrocycle **2.102** was favored over regioisomers **2.90** and **2.103** with ratio >99:1, which agrees with experimental results. We speculated that the high energetic cost of dearomatization of the highly conjugated dihydroindenoindole system as well as the low nucleophilicity of 5-fluoroindole moiety has rendered the formation of macrocycle **2.90** unfavorable. In the meantime, the formation of **2.103** is also unfavorable due to the incorporation of the rigid and planar dihydroindenoindole moiety in the 14-membered macrocyclic ring system which makes it highly strained and energetically costly. It should be noted that DFT calculations could not be performed in our lab at the time when the synthesis was done.

To explore SAR around DZ-2384 analogs, the macrocycle **2.102** was elaborated into tetracycle **2.104** by *N*-Boc cleavage using TFA and subsequent amide bond formation with

(*S*)-H*i*VA, EDC×HCl and HOBt (Figure 2.41). Additionally, reduction of the double bond in compound **2.102** with $NaCNBH_3$ in TFA (3:1 dr) furnished diastereomeric macrocycles (*S,R*)-**2.105** and (*R,S*)-**2.105** that were chromatographically separated yielding 56% of (*S,R*)-**2.105** and miniscule amount of (*R,S*)-**2.105**. Relative configuration of (*S,R*)-**2.105** and (*R,S*)-**2.105** was established by comparing measured ^{1}H-NMR coupling constants with those calculated using *Karplus* equation.[86] For compound (*S,R*)-**2.105** the calculated dihedral angle between protons H_a and H_b and corresponding coupling constant was -100° and 1 Hz respectively, and those for compound (*R,S*)-**2.105** were 12° and 8 Hz, respectively. For the double bond reduction product the measured coupling constant between H_a and H_b was less than 1 Hz, indicating the predominant formation of (*S,R*) isomer. Additional evidence for this assumption was provided by DFT calculations done by A.Kinens using b3lyp level of theory and 6-31+g(d) basis set. Similarly to reduction of indole **2.86** (Figure 2.36), the conversion of indolenium ion into (*S,R*)-**2.105** was found to be 1.6 kcal/mol more favorable than formation of (*R,S*)-**2.105**, and the calculated energy difference matched the observed 3:1 diastereomeric ratio. Finally, amidation of the amine (*S,R*)-**2.105** with (*S*)-H*i*VA using EDC×HCl and HOBt furnished compound **2.106** in 69% yield. Antiproliferative activity against multiple cancer cell lines was measured for both macrocycles and results are discussed in section 2.4.

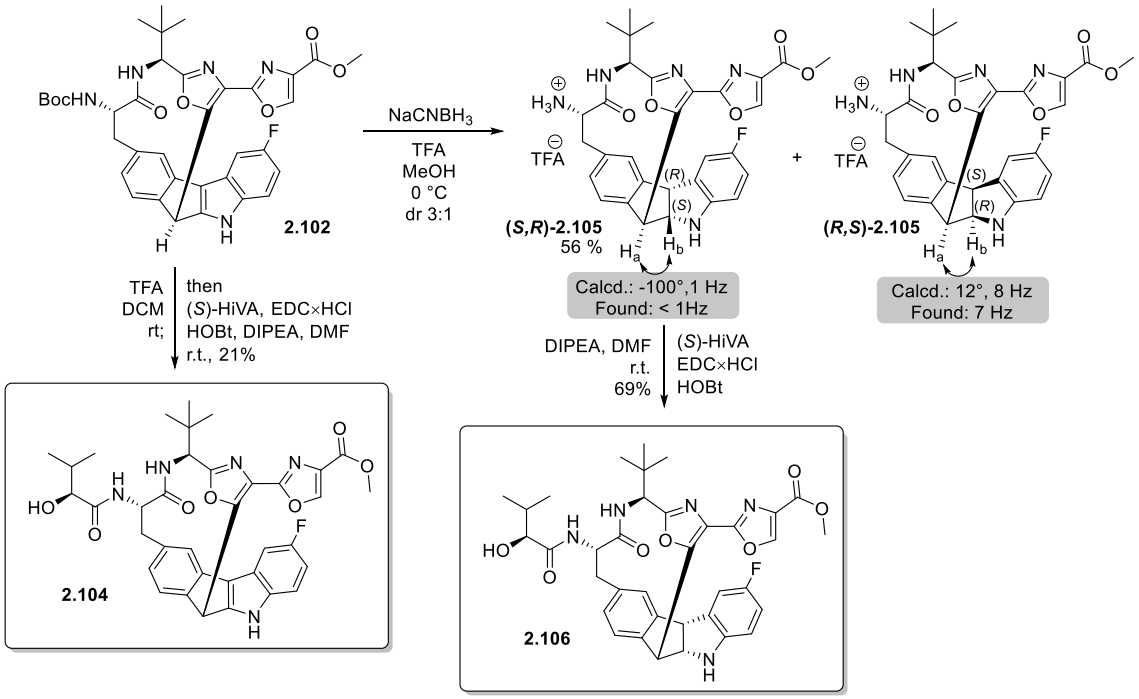

Figure 2.41 **Synthesis of macrocycles 2.104 and 2.106**

The undesired regioselectivity in the macrocyclization involving nucleophilic S_NAr-type reaction of indene-derived carbanion with bromo bioxazole that led to 13-membered

macrocycle **2.102** (Figure 2.40) prompted us to attempt blocking of the most reactive nucleophilic position and move the reaction center to the 3rd position of the indole. To achieve this, we chose to introduce dithiolane group which can be easily converted to methylene moiety under mild conditions using nickel, tin or organic agents.[87–90]

The new disconnection approach is depicted in Figure 2.42. The requisite starting material **2.108** for the macrocyclization leading to macrocycle **2.107** can accessed by amide coupling of tetracyclic building block **2.109** and bioxazole **2.93**. Tetracycle **2.109** is accessible by the proven *Fischer* indole synthesis and *Negishi* cross-coupling sequence.

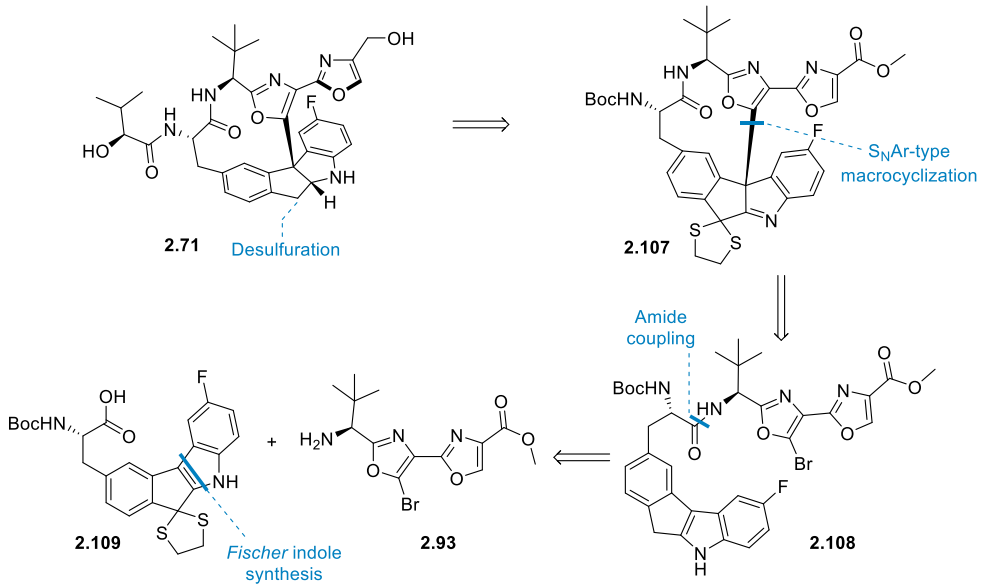

Figure 2.42 **Retrosynthetic analysis of compound 2.71**

The synthesis commenced with the preparation of suitably substituted tetracycle **2.114** from indanedione **2.112** using the *Fischer* indole synthesis conditions (Figure 2.43). The dione **2.112** was accessible by published route from the commercially available 5-bromo-1-indanone (**2.110**).[91] Accordingly, oxidation of indanone of **2.110** with *i*BuONO in the presence of concentrated HCl afforded oxime **2.111**, which was hydrolyzed to the corresponding 5-bromo-1,2-indanedione (**2.112**). The corresponding monodithiolane **2.113** was prepared from diketone **2.112** in the reaction with ethane disulfide and $BF_3 \times Et_2O$ according to a known method.[92] The workup of the reaction required special caution because of the extremely foul odor of ethane disulfide.

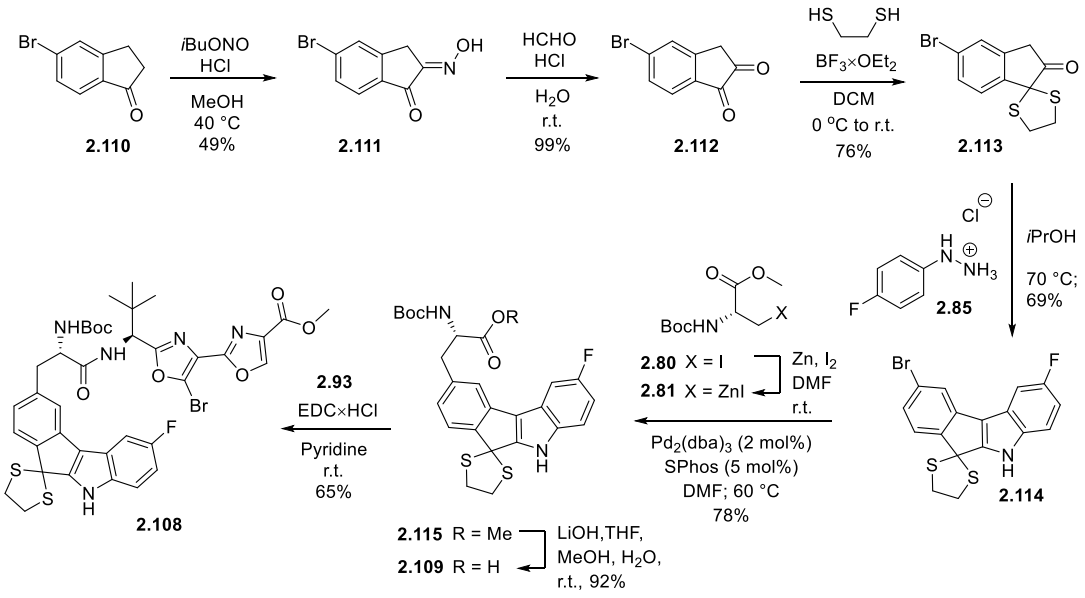

Figure 2.43 **Synthesis of macrocyclic precursor 2.108**

Gratifyingly, the previously used *Fischer* indole synthesis conditions (hydrazine **2.85,** *i*PrOH, 70 °C) delivered indole **2.114** in 69% yield that was further elaborated into amino acid **2.109** in a two-step sequence. The first step involved *Negishi* cross-coupling with freshly prepared alkyl zincate **2.81** ($Pd_2(dba)_3$ and SPhos in DMF). Despite the presence of two potentially coordinating sulfur atoms in indole **2.114**, no slow-down or reduction of yield was observed (78% for **2.114** after purification vs. 68% for CH_2 analog **2.101**). In the second step, saponification of the methyl ester with LiOH in THF/MeOH/H_2O solution at room temperature furnished tetracycle **2.109** in 92% yield. The latter was reacted with amine **2.93** under standard amidation conditions (EDC×HCl, pyridine) to give macrocyclization precursor **2.108** in 65% yield.

The prepared compound **2.108** was subjected to previously utilized S_NAr-type reaction conditions (Cs_2CO_3, DMF) (Figure 2.44). Unfortunately, no formation of macrocycle **2.107** was detected by UPLC-MS even at temperatures as high as 110 °C. Instead, prolonged heating caused compound **2.108** to decompose into several unknown byproducts.

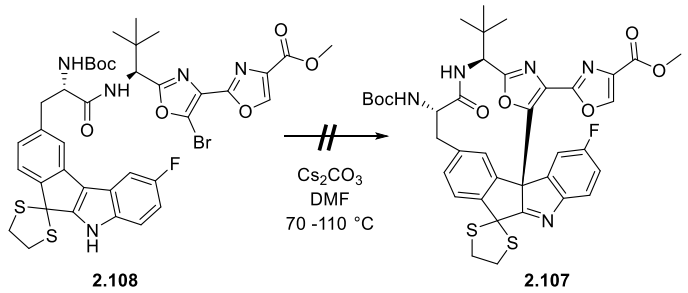

Figure 2.44 **Attempted macrocyclization of 2.108**

The lack of reactivity for indole **2.108** under S_NAr-type reaction conditions, as in the case of macrocycle **2.90** (see Figure 2.40), may be attributed to the high energetic cost of dearomatization of the highly conjugated dihydroindenoindole system as well as the low nucleophilicity of 5-fluoroindole moiety. Although the introduction of the dithiane group has helped to avoid the formation of the undesired 13-membered macrocycle **2.102**, it did not alter the overall electronic properties of the tetracyclic dihydroindenoindole core.

Overall, the second-generation synthesis of carba-analog of DZ-2384 (**2.71**) via macrocyclization of pre-assembled tetracycle subunit tethered to bromo-bioxazole moiety was not successful. The macrocyclization either occurred with undesired regioselectivity and delivered 13-membered macrocycle **2.102** (for precursor **2.91**) or it did not proceed at all (precursor **2.108**). The unsuccessful attempt at synthesis of carba-DZ-2384 (**2.71**) prompted us to evaluate alternative disconnections as shown in section 2.2.4.

2.2.4. Third generation synthesis of macrocycle 2.71

The unsuccessful synthesis of carba-DZ-2384 (**2.71**) by the assembly of the dihydroindenoindole subunit in the pre-formed macrocycle (chapter 2.2.2) and by the macrocyclization of pre-formed tetracycle tethered to bioxazole subunit (chapter 2.2.3) prompted us to consider alternative retrosynthetic strategy. It has become evident that early preparation of the dihydroindenoindole core would be beneficial, especially since we learned that the tetracyclic indoline could be prepared relatively easily using *Fischer* indole synthesis (chapter 2.2.2). Hence, the main challenge to be solved is the C-C connection of the bioxazole moiety and the quaternary center of the tetracyclic indoline subunit. We envisaged that the recent advances in decarboxylative coupling between redox-active esters and (hetero)aryl species could render the crucial C-C bond formation possible.[93] Accordingly, the revised retrosynthetic disconnections towards macrocycle **2.71** (Figure 2.45) involved closure of the macrocycle by amide bond formation, followed by the addition of the (*S*)-H*i*VA sidechain. Ester **2.116** could be prepared from the aryl bromide **2.117** using the proven *Negishi* coupling conditions (zincate **2.81**, $Pd_2(dba)_3$, SPhos, DMF, 60 °C) (see chapter 2.2.2). The key C-C bond formation step would rely on transition metal-catalyzed decarboxylative cross-coupling of the redox-active ester (*R*,*S*)-**2.118** (synthesis described below) and metalated bioxazole **2.119**.

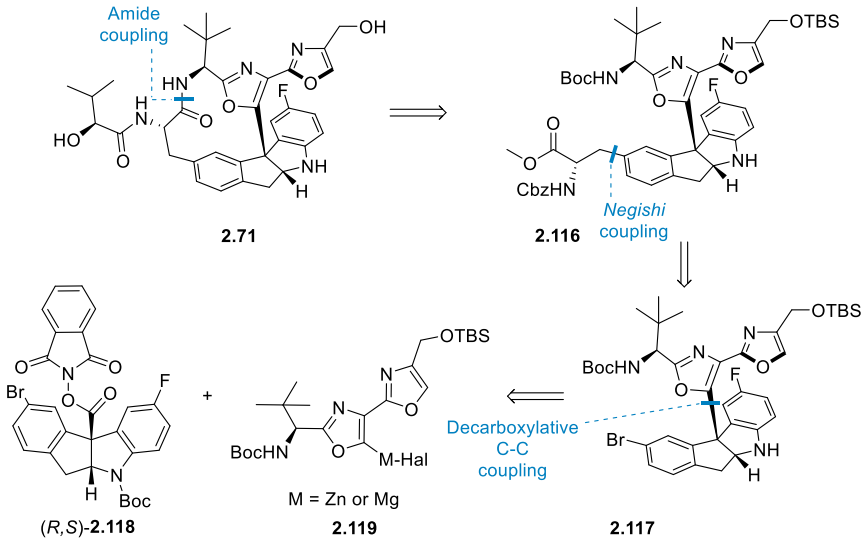

Figure 2.45 **Retrosynthetic analysis of compound 2.71**

We realized that the redox-active ester **2.118** could be prepared from the carboxylic acid **2.120** using conditions reported by Baran (*N*-hydroxyphtalimide, DIC, DMAP, DCM) (Figure 2.46).[93] The acid **2.120** could be accessible either through arylation of β-ketoester **2.121** with *ortho*-azido phenyllead triacetate **2.122**, followed by cyclization via the reduction of transient imine (a method reported by Driver[94]), or by allylation of indole **2.124** followed by isomerization of the double bond, ozonolysis and oxidation. Both methods (starting from **2.121** or **2.124**) would afford racemic compound **2.118**, which could be separated into enantiomers using column chromatography on chiral stationary phase. Crystallization of diastereomeric salts of acid **2.120** could also be attempted.

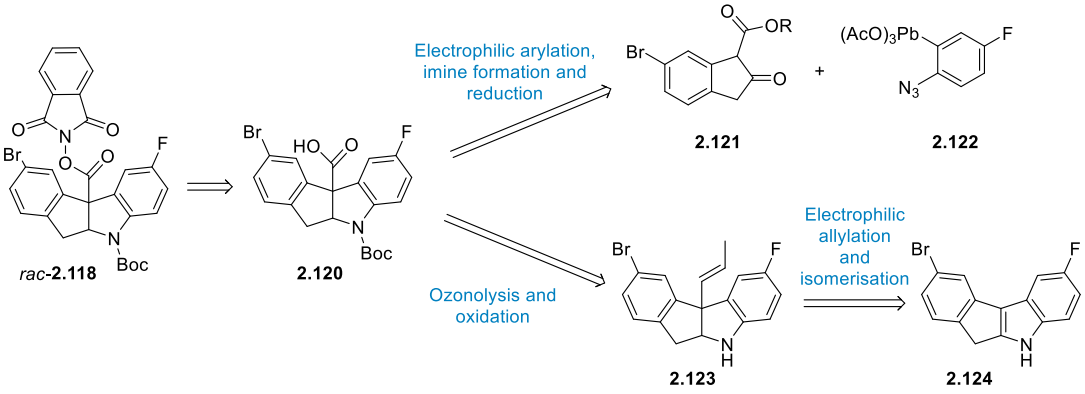

Figure 2.46 **Retrosynthetic analysis of tetracycle *rac*-2.118**

First, we addressed the synthesis of the *β*-ketoester **2.121**. Although it could be prepared by direct acylation of 5-bromo-2-indanone-derived enolate[95], a mixture of regioisomers would likely form, requiring their separation and leading to a drop in yield. For this reason we chose to follow longer, albeit easier-to-control procedure for the synthesis of *β*-ketoester **2.121**

(Figure 2.47). Accordingly, the commercially available phenylacetic acid **2.125** was converted into acid chloride **2.126** ($(COCl)_2$, DMF (2 mol%), PhMe, r.t. to 55 °C) and then reacted with *Meldrum's* acid (**2.127**) (pyridine, DCM, 0 °C to r.t.) to furnish the tricarbonyl compound **2.128**. Heating of the latter in toluene at 85 °C temperature facilitated thermal decomposition of the 1,3-dioxane-4,6-dione moiety and formation of transient ketene **XIX** along with acetone and carbon dioxide. Trapping of the intermediate ketene with methanol furnished the *β*-ketoester **2.129 (**65% yield after three steps). Subsequent *Regitz* diazo transfer reaction using *para*-acetamido benzene sulfonyl azide (**2.60**) in presence of TEA furnished diazoketoester **2.130** in 75% yield.

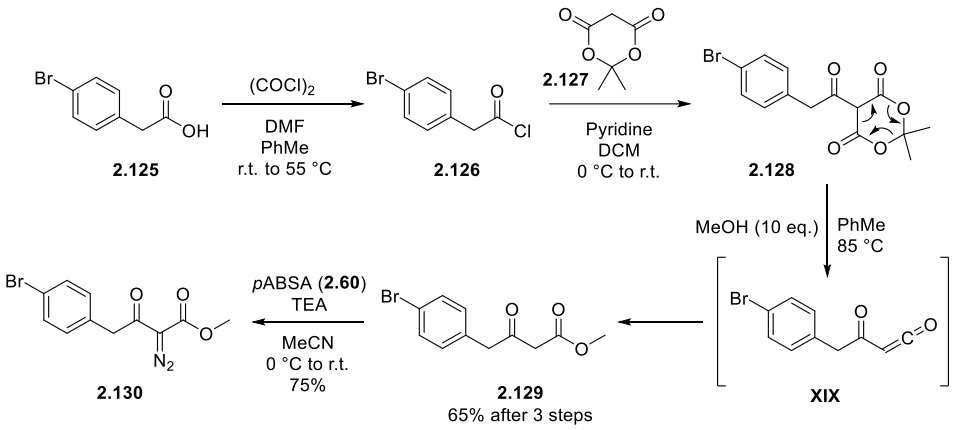

Figure 2.47 **Synthesis of diazoketoester 2.130**

Next, diazoketoester **2.130** was subjected to dirhodium(II)-catalyzed cyclization to indanone **2.131** via formal aromatic C−H insertion ($[(TFA)_2Rh]_2$ (2 mol%), DCM, r.t. slow addition of **2.130** to catalyst solution in one hour[96]), which proceeded with 90% yield (Figure 2.48). The mechanism of the dirhodium(II)-catalyzed C−C bond formation involves an initial formation of rhodium carbenoid **XX**, which undergoes attack by the phenyl moiety forming a new C-C bond in **XXI**.[97,98] Subsequent intramolecular proton transfer (through transition state **XXII**) and departure of a rhodium complex yielded the product **2.131** with the regeneration of the catalyst. Finally, BF_3-catalyzed reaction of methyl ester **2.131** with benzyl alcohol afforded benzyl analog **2.132** (72% yield).[99]

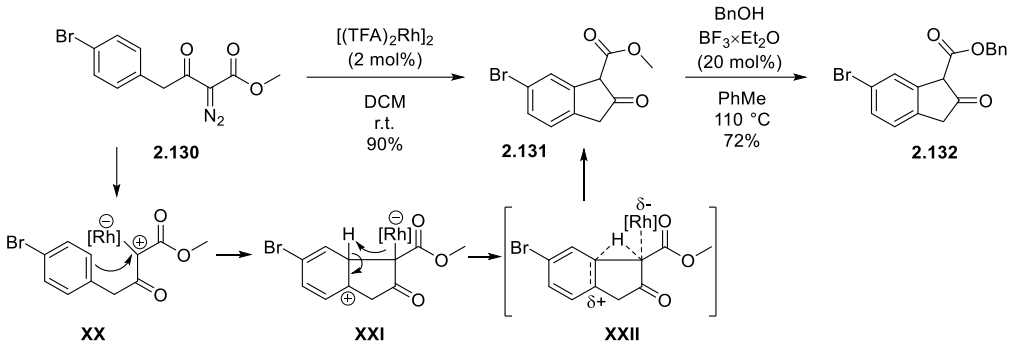

Figure 2.48 **Synthesis of esters 2.131 and 2.132**

Prior to the preparation of the known-in-literature, yet complex *ortho*-azido phenyllead building block **2.122** for the multistep reaction sequence toward tetracycle **2.120**, we elected to evaluate the feasibility of quaternary center formation by the arylation of indanone **2.132** with *ortho*-tolyllead triacetate **2.134**. The latter is easier-to-synthesize and sterically similar analog of compound **2.122**. The model reagent **2.134** was obtained in 48% yield from *ortho*-tolylboronic acid (**2.133**) in $Hg(OAc)_2$-mediated transmetallation reaction ($CHCl_3$, 50 °C) as described by Pinhey (Figure 2.49).[100] Fortunately, the arylation of ketoester **2.132** with the model *ortho*-tolyllead triacetate **2.134** (pyridine, $CHCl_3$, 50 °C) furnished quaternary carbon-containing product **2.135** in 74% yield.[100] From the mechanistic viewpoint, the arylation of **2.132** with aryl lead reagent **2.134** requires an initial deprotonation of *β*-ketoester with pyridine to form enolate **XXIII** (Figure 2.49). Next, the formed enolate replaces one of the acetate ligands on the lead to furnish intermediate **XXIV**, which undergoes intramolecular arylation of lead enolate to yield the arylated ester **2.135** and $Pb(OAc)_2$.[101] It should be noted that such a reductive coupling is typical not only for lead derivatives, but also for aryl bismuth derivatives,[102] diaryl-λ^3-iodanes[103] and several other main group elements such as thallium, tellurium and selenium.[104]

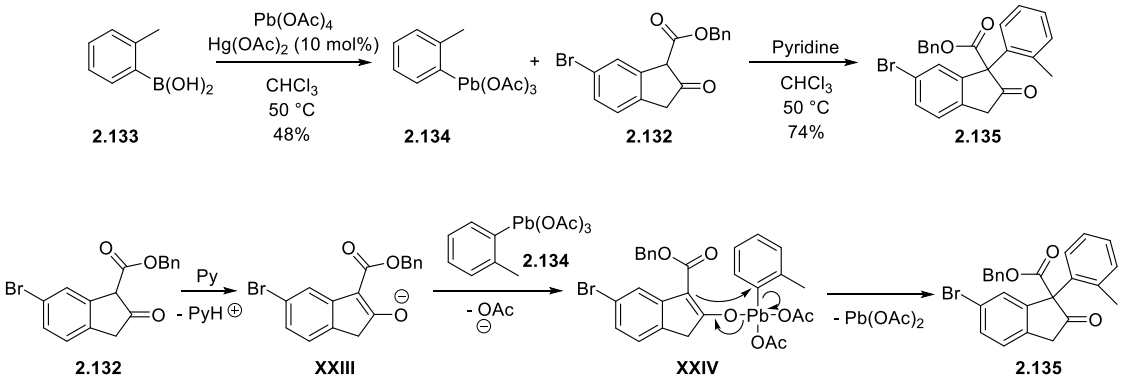

Figure 2.49 **Synthesis of compound 2.135**

Encouraged by the successful arylation of ketoester **2.132** with *ortho*-tolyllead triacetate **2.134**, we set out to prepare 2-azido-4-fluorophenyllead triacetate **2.122** for the synthesis of tetracycle **2.120**. The synthesis of **2.122** was conducted as described by Driver (Figure 2.50).[94] Accordingly, 2-bromo-4-fluoroaniline **2.136** was subjected to Pd-catalyzed borylation (PinBH, $Pd(dppf)Cl_2$ (10 mol%), TEA, 1,4-dioxane, 120 °C) to afford boronate **2.137** in 66% yield. Diazotation of the aniline with *t*BuONO followed by treatment with TMS-azide (MeCN; 0 °C to r.t.)[105] led to aryl azide **2.138** in 42% yield, which represented a slight increase over the reported outcome (34%). The last step of the synthesis, the Hg-catalyzed transmetallation proved to be challenging. Although Driver had reported successful preparation of the aryl lead triacetate **2.122** in 34% yield, we were unable to reproduce this result. Multiple attempts did not produce material, which ^{1}H-NMR spectra (in $CDCl_3$) would correspond to the literature data. Although the obtained spectra varied across the many attempted reactions, they suggested formation of unidentified degradation and / or dimerization products of compound **2.138**. As the factors leading to the poor reproducibility of the transmetallation reaction could not be identified, this synthesis route to tetracycle **2.120** through arylation of *β*-ketoester **2.135** was put on hold, and further efforts were directed at the alternative route starting from indenoindole **2.124** (Figure 2.46).

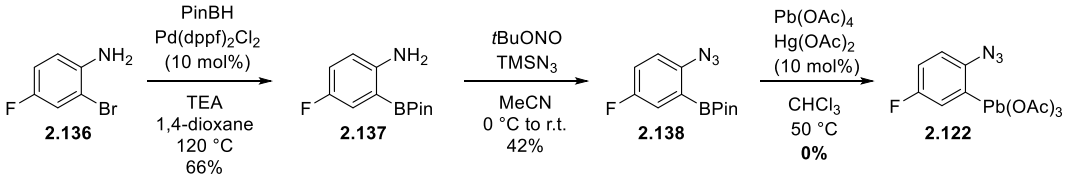

Figure 2.50 **Attempted synthesis of aryl lead triacetate 2.122**

In order to assess the feasibility of tetracycle **2.120** synthesis from indenoindole **2.124** (Figure 2.46), we elected to perform initial model studies using an easier-to-prepare des-bromo indole **2.140** that was prepared from 4-fluorophenylhydrazine hydrochloride (**2.85**) and 2-indanone (**2.139**) in 82% yield using *Fischer* indole synthesis conditions (*i*PrOH; 75 °C) (Figure 2.51). For the planned selective C3 allylation of indole **2.140** we chose to follow the method developed by Hashim and co-workers,[106] who demonstrated that selective C3 alkylation of 2,3-disubstituted indoles could be achieved in high yields (45 – 95%) without the formation of undesired *N*- and C2 alkylation products by initial preparation of *N*-indolyl triethyl boronate complex **XXV**. The high C3 selectivity of the alkylation was attributed to the increased nucleophilicity of indole and also the relatively strong N–B bond in boronate **XXV**, which prevents not only the competing *N*-alkylation but also the C2-alkylation pathway.[107] The prerequisite *N*-indolyl trialkyl boronate **XXV** was prepared by indole N-H deprotonation

with NaO*t*Bu and reaction with triethylborane. As anticipated, the alkylation with allyl bromide proceeded with excellent C3 selectivity to furnish imine **XXVI** that was subsequently reduced *in situ* by $NaBH_3CN$ into indoline **2.141** as single diastereomer (99:1 dr) with 68% overall yield.

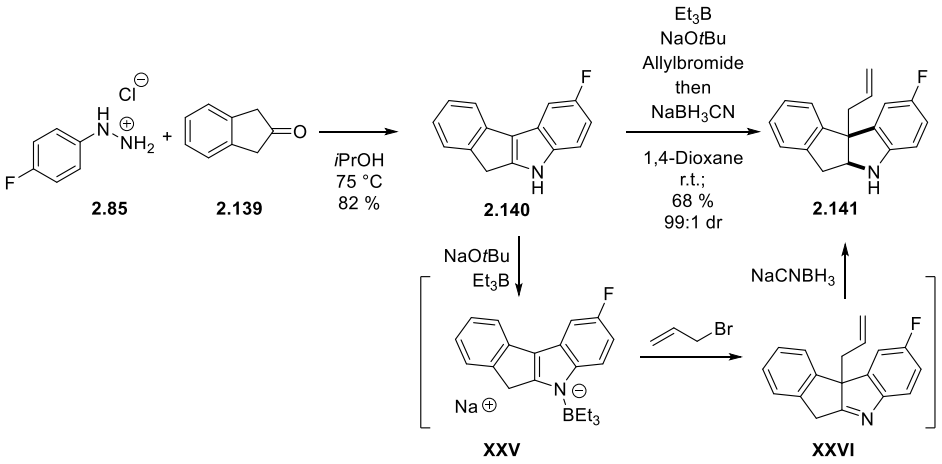

Figure 2.51 **Synthesis of indoline 2.141**

Next, transition metal-catalyzed isomerization of the double bond in the allyl moiety was addressed. Screening of various transition metal catalysts (A: $PdCl_2(MeCN)_2$ (10 mol%), PhMe, 60 °C; B: $RhCl_3{\times}H_2O$ (10 mol%), K_2CO_3, EtOH, 60 °C; C: *Grubb's* 2nd generation catalyst (10 mol%), MeOH, 60 °C)[108–110] helped to identify rhodium chloride hydrate as the catalyst of choice that effected complete conversion of **2.141** into **2.142** within 16 hours. *Grubb's* 2nd generation catalyst also facilitated isomerization albeit with concomitant formation of unidentified side products, whereas $PdCl_2(MeCN)_2$ was completely inactive. At larger scale (3.4 g of **2.141** instead of 20 mg), $RhCl_3$-catalyzed isomerization turned out to be sluggish and afforded **2.142** with incomplete conversion even after 40 hours (Figure 2.52). In addition, the formation of unidentified byproducts was also observed. Nevertheless, the isomerization product **2.143** could be obtained after *N*-Boc protection (KHMDS, Boc_2O, THF, 0 °C to r.t.) in 21% over two steps.

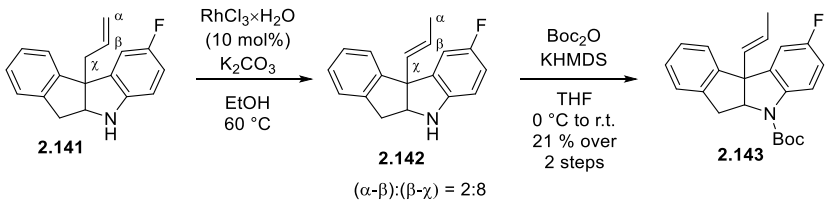

Figure 2.52 **Synthesis of alkene 2.143**

The mechanism of Rh-catalyzed double bond isomerization presumably involves initial reaction of terminal alkene **2.141** with in situ generated Rh(III) hydride to form the rhodium hydride complex **XXVII** (Figure 2.53).[111] Subsequent hydrometallation of alkene leads to a pair of regioisomers (shown is only alkyl rhodium complex **XXVIII**) that undergo β-hydride elimination to afford alkene-rhodium complex **XXIX** and, finally, alkene **2.142**. All the reaction steps are reversible and formation of the internal alkene **2.142** was governed by the thermodynamic preference for more substituted double bond.

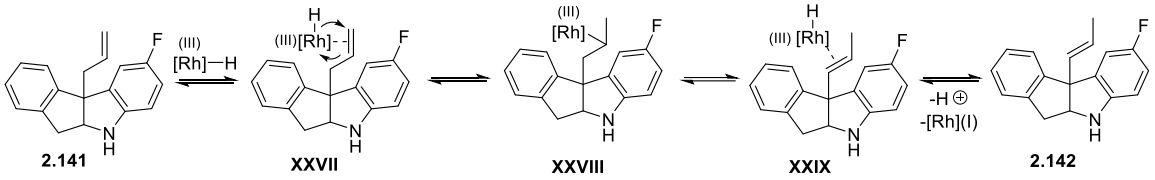

Figure 2.53 **Mechanism of the Rh-catalyzed double bond isomerization**

Endgame of the model synthesis involved ozonolysis of double bond, oxidation of the formed aldehyde to carboxylic acid and DIC-mediated preparation of the ester **2.146** (Figure 2.54). Ozonolysis of the alkene **2.143** and quenching of the reaction with dimethyl sulfide cleanly furnished the aldehyde **2.144** which, after subjection to *Pinnick* oxidation conditions ($NaClO_4$, NaH_2PO_4, resorcinol, DMSO, 5 °C to r.t.), afforded carboxylic acid **2.145** in 55% yield over two steps. Notably, *N*-Boc protection of tetracycle **2.143** was crucial as ozonolysis of unprotected indoline **2.142** caused degradation and no formation of aldehyde. Use of triphenylphosphine instead of dimethyl sulfide was also possible but produced large amount of triphenylphosphine oxide, which complicated the purification procedure. Finally, synthesis of *N*-hydroxyphtalimide (NHPI) ester **2.146** was accomplished using conditions reported by Baran (DMAP, DIC, DCM, r.t.).[93]

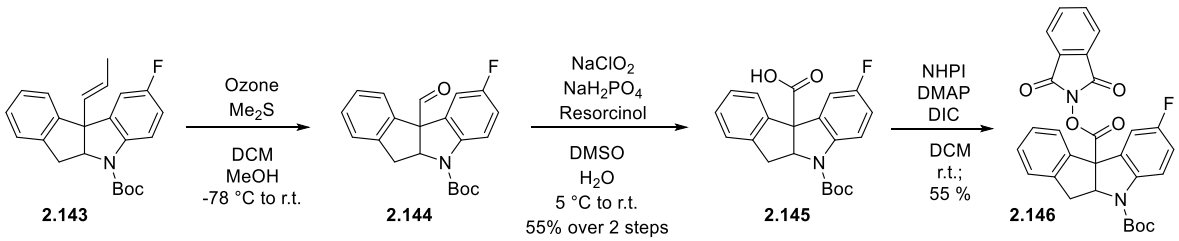

Figure 2.54 **Synthesis of compound 2.146**

Next, we turned our attention to the key transition metal-catalyzed decarboxylative coupling of the redox-active ester **2.146** and metalated bioxazole **2.119** (Figure 2.45). Baran had demonstrated that some cyclic tertiary carboxylic acid-derived NHPI esters can

participate in Fe-catalyzed cross-coupling with aryl zinc or aryl magnesium species.[93] Unfortunately, when the cyclic tertiary NHPI ester **2.146** was reacted with PhMgBr×LiCl as the model *Grignard* reagent under Baran's conditions ($Fe(acac)_3$ (100 mol%); THF; DMP; r.t.), the formation of the desired coupling product **2.147** was not observed (by UPLC-MS assay) even though complete consumption of the redox-active ester **2.146** was noted (Figure 2.55). Analysis of the UPLC-MS data indicated that the indoline **XXXII** was the main product of the reaction. Formation of tetracycle **XXXII** presumably involved single electron transfer from Fe-catalyst to phthalimide moiety in **2.146** and generation of the anion radical **XXX**, followed by its decomposition to tertiary radical **XXXI**.[93] However, due to not fully understood reasons, the reaction of radical **XXXI** with *Grignard* reagent was obviously sluggish. Instead, H-atom abstraction took place to generate **XXXII** (H-abstraction is known competing side process in coupling reactions that involve alkyl radicals.[112]

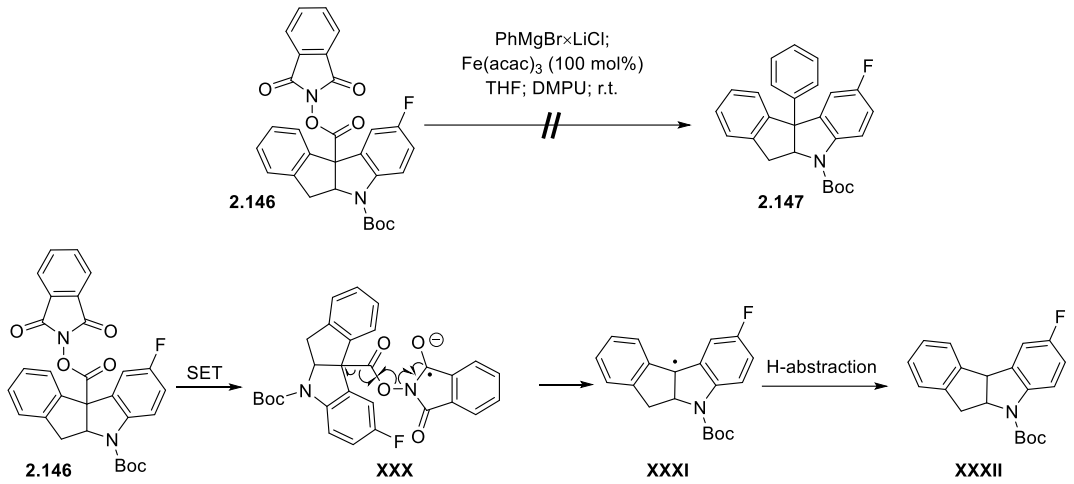

Figure 2.55 **Attempted synthesis of 2.147**

Shortly after our unsuccessful Fe-catalyzed cross-coupling attempts, Baran disclosed a method for nickel-catalyzed coupling of tertiary *N*-hydroxy tetrachlorophthalimide (TCNHPI) esters with diary zinc species.[113] The requisite TCNHPI ester **2.148** was readily prepared from acid **2.145** and subjected to a model reaction with freshly prepared di(4-methoxyphenyl)zinc under the reported conditions ($Ni(DPM)_2 \times H_2O$ (20 mol%); $ZnBr_2$ (100 mol%); THF; DMI, r.t.) (Figure 2.56). Despite the fact, that Ni-catalyzed coupling method was specifically designed for the use with tertiary carboxylic acid derivatives, it failed to produce the coupling product **2.149** (as detected by UPLC-MS). Similarly to the previously described Fe-catalyzed coupling, the redox-active ester **2.148** was fully consumed and the undesired indoline **XXXII** was the main reaction product (Figure 2.55). Additionally, formation of di(4-methoxyphenyl)zinc-derived biaryl compound was detected.

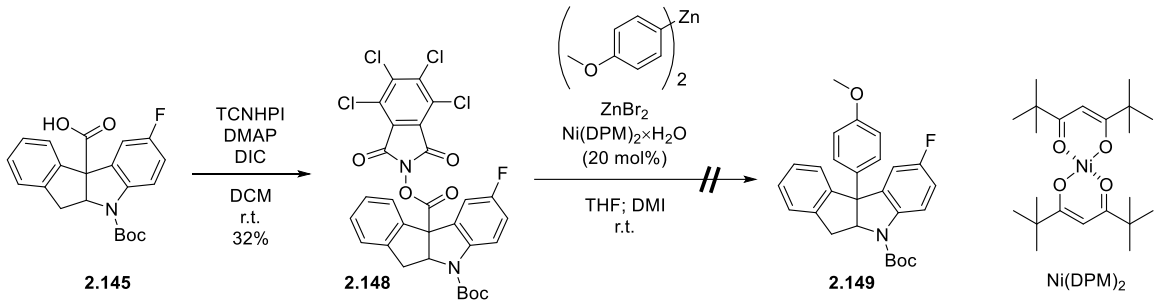

Figure 2.56 **Attempted synthesis of tetracycle 2.149**

The experienced setback prompted us to investigate the reproducibility of the reported Ni-catalyzed cross coupling. To this end, we prepared the known TCNHPI ester **2.151** from 1-methylcyclohexyl carboxylic acid (**2.150**) and subjected it to reaction with freshly prepared di(4-methoxyphenyl)zinc under the reported conditions ($Ni(DPM)_2 \times xH_2O$ (20 mol%); $ZnBr_2$ (100 mol%); THF; DMI, r.t.) (Figure 2.57).[113] This time, however, the cross coupling product **2.152** was produced in 64% yield after purification which is in good agreement with the yield reported in literature (60%).

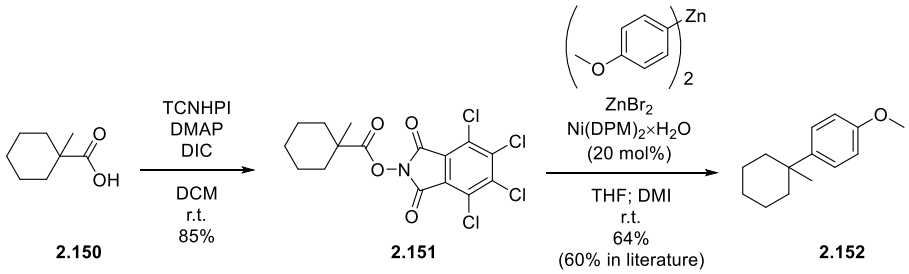

Figure 2.57 **Synthesis of compound 2.152**

The mechanism of $Ni(DPM)_2$ catalyzed cross coupling between TCNHPI ester **2.151** and di(4-methoxyphenyl)zinc involves single electron transfer from nickel catalyst to phthalimide moiety and formation of anion radical **XXXIII** with simultaneous oxidation of Ni(II) to Ni(III) (Figure 2.58).[114] The anion radical then undergoes fragmentation into tertiary radical **XXXIV**, phthalimide anion and CO_2. Interestingly, Molander has shown that tertiary alkyl radicals in $Ni(DPM)_2$-catalyzed coupling reactions undergo outer sphere radical coupling with the aryl moiety of *in situ* generated Ni(III)-aryl complex **XXXV** (transition state **XXXVI)** that leads to formation of the product **2.152.**[115] The mechanistic requirement for a direct attack of the tertiary radical onto the aryl moiety in the Ni-complex might be responsible for the failure of reaction involving ester **2.148**: the formed tertiary radical is sterically too hindered to approach the Ni-complex and furnish the product **2.149**. Such

assumption is corroborated by fact that Baran has reported the successful coupling of only those tertiary redox-esters that possess at least one sterically small methyl substituent.[113]

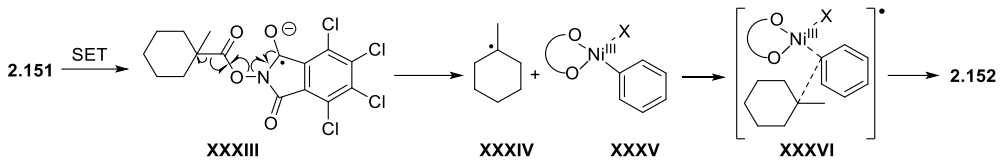

Figure 2.58 **Mechanism for the formation of compound 2.152**

To sum up, three different strategies toward synthesis of dihydroindenoindole core-containing macrocycle **2.71** – carba analog of DZ-2384 (**1.76**) – have been examined (Figure 2.59). First, *Fischer* indole synthesis and late-stage construction of the dihydroindenoindole core-based approach from the macrocyclic ketone **2.73** was explored (path A). Then, macrocyclization of **2.91** in base promoted S_NAr-type reaction was evaluated (path B) and, finally, formation of the key oxazole-tetracycle C-C bond by transition metal-catalyzed decarboxylative coupling of **2.148** was looked into (path C).

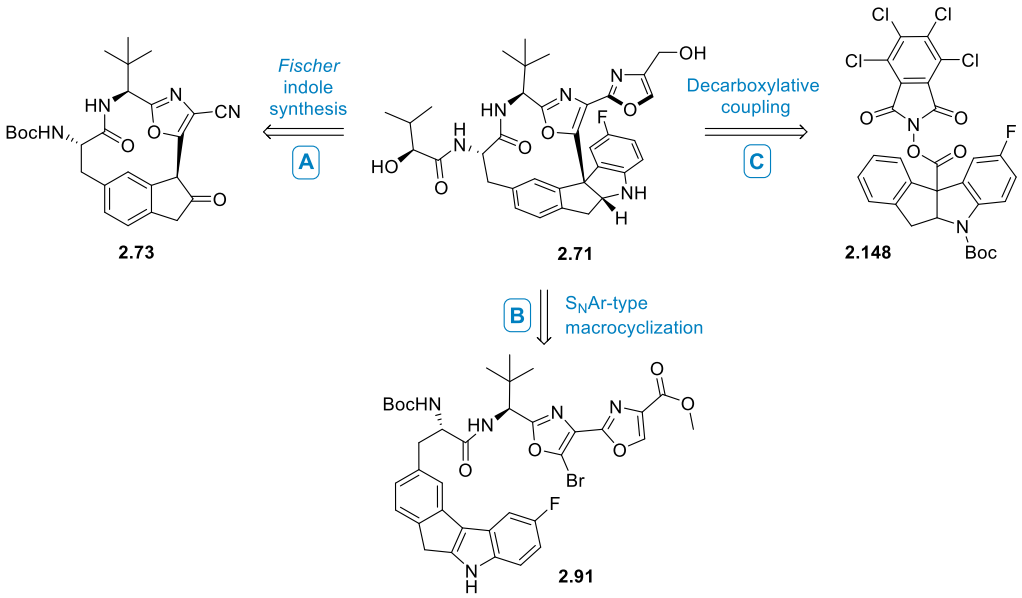

Figure 2.59 **Strategies toward synthesis of macrocycle 2.71**

Even though the syntheses did not reach their goal, the multiple synthetical approaches examined during the attempted preparation of macrocycle **2.71** provided access to unique and previously unreported macrocycles **2.89**, **2.104** and **2.106**. Each of them incorporates macrocyclic structure, α-hydroxy amide sidechain and chiral tetracyclic moiety. Macrocycles **2.89**, **2.104** and **2.106** were subjected to *in vitro* antiproliferative activity assay against multiple cancer cell lines and the results are discussed in chapter 2.4.

2.3. Simplified analogs of DZ-2384

Chapter based on PCT patent published in 2021[116] **and *J.Med.Chem.* featured article published in 2024.**[117]

2.3.1. Introduction

Challenges encountered during the attempted synthesis of both diazonamide A (**1.2**) and carba-analog of DZ-2384 (**2.71**) clearly indicated that reduction of structural complexity of the tetracyclic core would facilitate the development of new antiproliferative agents based on the highly cytotoxic macrocycles **1.2** and DZ-2384 (**1.76**). Consequently, a re-scaffolding approach was considered in the design of less complex analogs of diazonamide A (**1.2**) with improved drug-like properties. Specifically, we envisioned the replacement of the entire tetracyclic core with chiral quaternary center-containing indolin-2-one subunit, while retaining both the bioxazole moiety and the peptide-based macrocycle. This approach would enable us to explore structure-activity relationships and prepare potent analogs of the natural diazonamide A (**1.2**) and its synthetic analog DZ-2384 (**1.76**). The corresponding design is illustrated by the macrocycle series **2.153** and **2.154** (Figure 2.60).

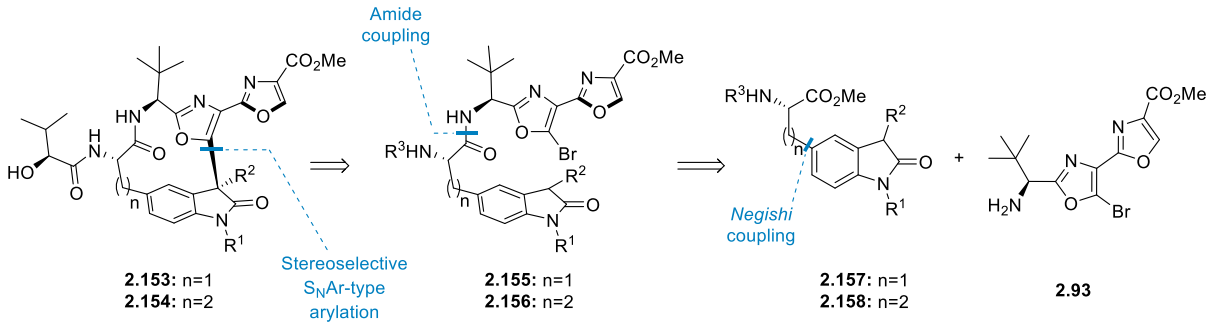

Figure 2.60 **Retrosynthesis of compounds 2.153 and 2.154**

We envisaged that macrocycles **2.153** and **2.154** could be prepared using similar approach to that developed by Sammakia and co-workers in their formal total synthesis of diazonamide A (**1.2**) (see chapter 1.1.6),[23] where the key macrocyclization step and the formation of quaternary stereogenic center was accomplished under S_NAr-type arylation conditions (Na_2CO_3, DMF, 65 °C). The cyclization precursors **2.155** and **2.156** could be prepared from indolin-2-ones **2.157** and **2.158** and the bromo oxazole **2.93**. Finally, indolin-2-ones **2.157** and **2.158** are accessible from the commercially available 5-iodoisatin (**2.159**).

The retrosynthetic strategy (Figure 2.60) has been verified by coworkers V. Vitkovska[118] and M. Kazak in their synthesis of 12-memebered macrocycles. However, 13-membered macrocyclic homologs were also required for SAR studies. We realized that the macrocyclization of 13-membered cycles may differ from that of the 12-membered analogs in terms of yields and diastereoselectivity. Besides, the synthesis of amino acid esters **2.158** (n=2) from 5-iodoisatin would require C-C bond formation chemistry different from that of amino acid derivatives **2.157** (n=1). With this in mind we embarked on the synthesis of 13-membered macrocycle series **2.154a-d** (Figure 2.61).

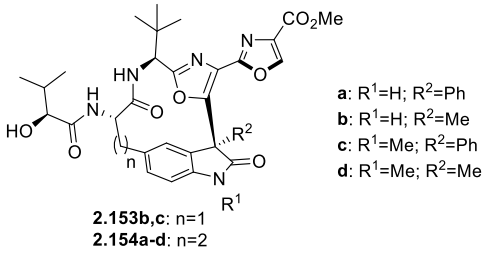

Figure 2.61 **Target 12- and 13-membered macrocycles 2.153 and 2.154**

In addition, we synthesized 12-membered analogs **2.153b** (described in [118]) and **2.153c** to study the ease of the macrocycle formation depending on the ring size. Finally, biological evaluation of compounds **2.153** and **2.154** would offer valuable contribution to the understanding of SAR.

2.3.2. Synthesis

The synthesis of macrocycles **2.513** and **2.154** began by preparation of the aryl bromides **2.161a-d** from the commercially available 5-iodoisatin (**2.159**) (Figure 2.62). Addition of phenyl- or methyl magnesium halides to the carbonyl group of isatin **2.159** (with or without a prior methylation of the nitrogen of the isatin) furnished alcohols **2.160a-d**. Subsequent reductive cleavage of the hydroxyl group using $SnCl_2$ in AcOH at elevated temperature (involving protonation of hydroxyl moiety, elimination of water molecule and reduction of the formed tertiary carbocation) afforded iodo-indolin-2-ones **2.161a-d** in 33% to 44% yield over two steps.[119]

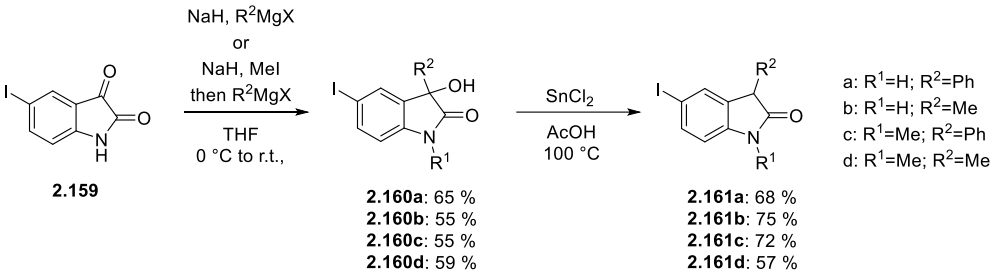

Figure 2.62 **Synthesis of oxindoles 2.161a-d**

12-Memebered macrocycle precursors **2.155b,c** were then prepared by Pd-catalyzed *Negishi* cross-coupling of heteroaryl iodides **2.161b,c** with freshly prepared alkyl zinc iodide **2.81**,[72] followed by saponification of the methyl ester and EDC-mediated amide coupling with amine **2.93** (Figure 2.63). The sequence afforded bioxazoles **2.155b** and **2.155c** in 42% and 63% yield over three steps.

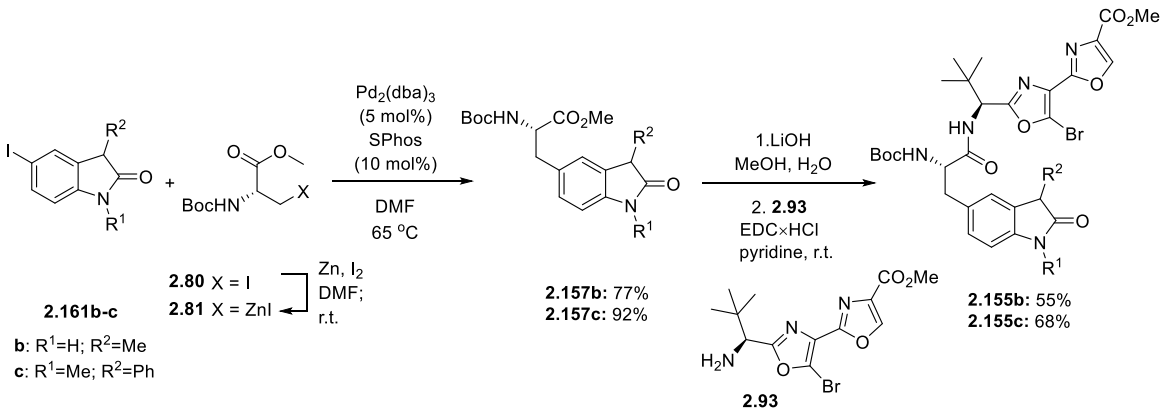

Figure 2.63 **Preparation of compounds 2.155b,c**

In the meantime, due to the low stability and complicated preparation of homoalanine-derived alkyl zincate (homolog of **2.81**),[120] different approach was utilized to access precursors for 13-membered macrocycle **2.156**. Thus, nickel catalyzed decarboxylative coupling[121] between iodides **2.161a-d** and the redox-active NHPI-ester **2.162** (prepared from *N*-Boc-*L*-Glu-OBn and *N*-hydroxyphtalimide[93] allowed us to obtain amino acid derivatives **2.163a,b** and **d** in 23–52% yield (Figure 2.64). Unexpectedly, the reaction between 5-iodo-1-methyl-3-phenylindolin-2-one (**2.161c**) and NHPI-ester **2.162** failed to give any coupling product and led to extensive degradation of both reaction partners. Finally, hydrogenative cleavage of benzyl ester moiety in **2.163a,b** and **d** was followed by amide bond formation with amine **2.93** leading to the macrocycle precursors **2.156a,b,d** (15-38% yields over three steps).

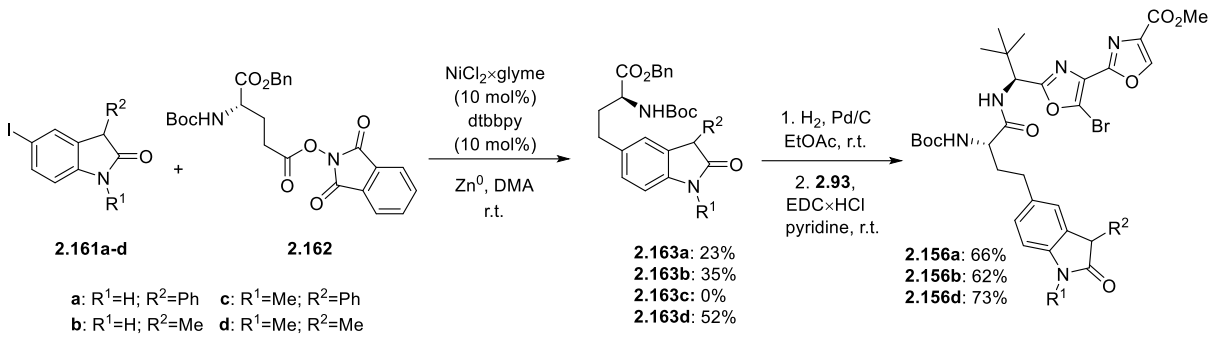

Figure 2.64 **Preparation of amides 2.156a,b,d**

An alternative approach was employed to prepare amino acid derivative **2.158c** that could not be obtained through a decarboxylative coupling between compounds **2.161c** and **2.162**. Thus, aryl-alkyl *Suzuki* cross-coupling reaction between aryl iodide **2.161c** and alkylboronate **2.165** (prepared in-situ from *N*-Cbz-vinylglicine methyl ester **2.164**) afforded the Cbz-protected amino acid derivative **2.158c** in 29% yield (Figure 2.65).[122] Saponification of the methyl ester and condensation of the resulting carboxylic acid with amine **2.93** gave the macrocycle precursor **2.156c** with the overall yield of 10% over three steps.

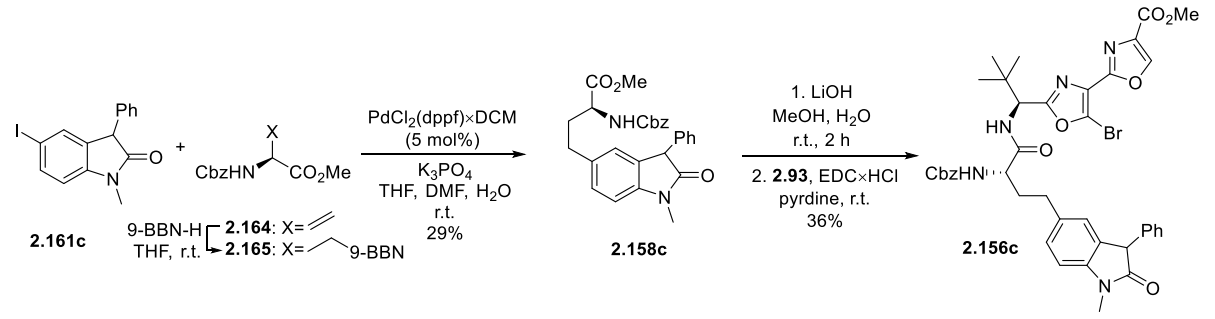

Figure 2.65 **Synthesis of amide 2.156c**

Having obtained amides **2.155b,c** and **2.156a-d**, the key macrocyclization reaction was addressed. We were delighted to observe that when both phenylalanine analogs **2.155b** and **2.155c** were exposed to the Sammakia's cyclization conditions (Na_2CO_3, DMF, 65 °C), the respective 12-membered macrocycles **2.166b,c** were formed with excellent diastereoselectivity (dr 99:1 and 95:5, Figure 2.66). Chromatographic purification enabled us to isolate both macrocycles **2.166b,c** as individual diastereomers in good yield (37% - 75%), The absolute configuration of the newly formed quaternary stereocenter was assigned *S* based on an analogy with previously prepared 12-membered macrocycles.[118] Additional evidence for the formation of (*S*)-stereogenic center was gained using DFT calculations (b3lyp level of theory and 6-311++g(2d,p) basis set, performed by Dr. A.Kinens) – the formation of (*S*)-

macrocycle was showed to be 5 kcal/mol more favorable than formation of macrocycle bearing (*R*)-stereocenter, which corresponds to >99:1 dr and is in good agreement with the measured value (99:1 dr).

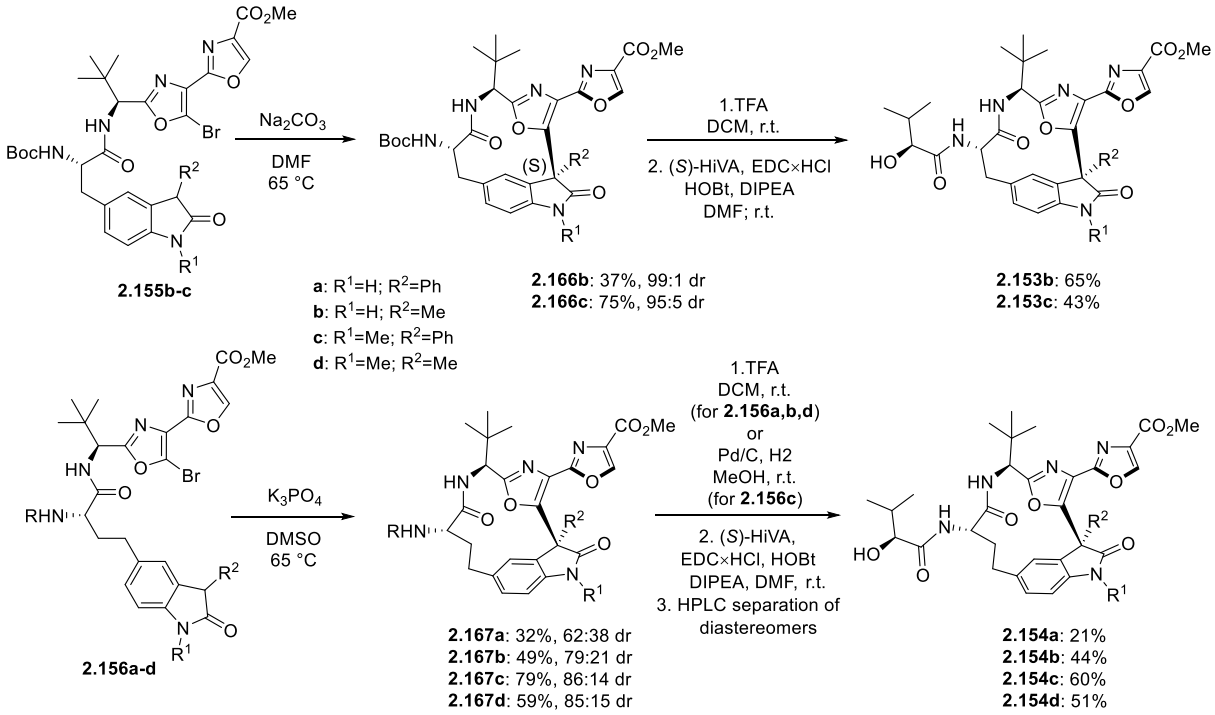

Figure 2.66 **Synthesis of macrocycles 2.153b,c and 2.154a-d**

We then shifted our focus to the synthesis of larger, 13-membered macrocycles from homo phenylalanine analogs **2.156a-d** (Figure 2.66). The target macrocycles **2.167a-d** were obtained with yields like those of the 12-membered macrocycles **2.166b** and **c** (ranging from 32% to 79% after purification). However, the diastereoselectivity was noticeably lower, ranging from 62:38 to 86:14 dr. In the meantime, these values are in good agreement with ones gained from DFT calculations (b3lyp level of theory and 6-311++g(2d,p) basis set, performed by Dr. A.Kinens) which indicated that in 13-membered macrocycle series formation of ring possessing (*S*)-stereogenic center is only 1.3 kcal/mol more favorable than generation of (*R*)-center which corresponds to 90:10 dr. At this stage, the diastereomers of the 13-membered macrocycles **2.167a,b** and **d** were inseparable and they were carried forward as mixtures, albeit slightly diastereomerically enriched compared to the crude mixture. An exception was the compound **2.167c**, for which a single diastereomer (97:3 dr) could be obtained by chromatographical purification.

Reliable determination of the relative configuration of the newly created quaternary stereogenic center in macrocycles **2.167a-d** posed a challenge. NMR methods were not helpful due to the absence of useful H-H or C-H interactions near the relevant stereogenic

center. In addition, all attempts to grow single crystals for X-ray crystallography were unsuccessful. Eventually, the absolute configuration of the quaternary stereogenic center was established in both diastereomers by comparing the experimental electronic circular dichroism (ECD) spectra with those calculated using DFT methods for the downstream compounds **2.154d** and *epi*-**2.154d**. Based on this, *S* configuration was assigned to all major diastereomers of the 13-membered macrocycles **2.167a-d**. We thank Prof. Riina Aav and Nele Konrad (Tallinn University of Technology, Tallinn, Estonia) for ECD measurements and Dr. Artis Kinens for DFT calculations.

To finalize the synthesis, all prepared macrocycles were decorated with (*S*)-hydroxy *iso*-valeric acid ((*S*)-H*i*VA) sidechain. Thus, *N*-Boc groups were cleaved with TFA (compounds **2.166b,c** and **2.167a,b,d**) while *N*-Cbz group (compound **2.167c**) was removed by Pd/C catalyzed hydrogenolysis. The resulting amines were coupled with (*S*)-H*i*VA in the presence of EDC×HCl and HOBt. The 12-membered macrocycles **2.153b** and **c** were furnished in good yield (65% and 43% respectively) while the yield for 13-membered macrocycles **2.154a-d** was somewhat lower (21% to 60%) because of the need for chromatographic separation of diastereomers. In the case of compound **2.174d** we were able to separate and purify also the minor epimer – compound *epi*-**2.174d** (4% yield; 99:1 dr).

Overall, structurally simplified analogs of highly complex natural product diazonamide A (**1.2**) were developed by the replacement of the challenging-to-synthesize tetracyclic subunit with 2-indolinone motif. It was shown that intramolecular S_NAr-type reaction between deprotonated oxindole and bromooxazole fragments is suitable for the formation of both 12- (**2.153b,c**) and 13-membered (**2.154a-d**) macrocycles. In all cases, the yields after purification ranged from acceptable to very good (32% – 79%). However, diastereoselectivity varied significantly. The 12-membered macrocycles **2.153b,c** were formed exclusively as single diastereomers regardless of the substitution pattern at the oxindole moiety. In contrast, the diastereoselectivity of the more flexible 13-membered macrocycles ranged from poor (62:38 dr; **2.154a**) to good (86:14 dr; **2.154c**) thus complicating purification and lowering the overall yield. All prepared macrocycles were subjected to *in vitro* antiproliferative activity assay.

2.4. Antiproliferative activity

Macrocycles synthesized in chapters 2.2 and 2.3 were evaluated for their *in vitro* antiproliferative activity against four cancer cell lines (epithelial pancreatic carcinoma PANC-1, pancreatic carcinoma MiaPaCa-2, estrogen positive breast adenocarcinoma MCF-7 and

estrogen negative breast adenocarcinoma MDA-MB-231) by the MTT assay with vinorelbine as the positive control. We kindly thank Dr. Ilona Domračeva (LIOS, Riga, Latvia) for running the assay.

The *in vitro* antiproliferative activities (as measured by GI_{50} – concentration of compound needed to inhibit cell growth by 50%) of macrocycles **2.89**, **2.104**, **2.106** (synthesis described in chapter 2.2) are depicted in Table 2.1. Antiproliferative activities of DZ-2384 (**1.76**) are added for comparison.

Table 2.1

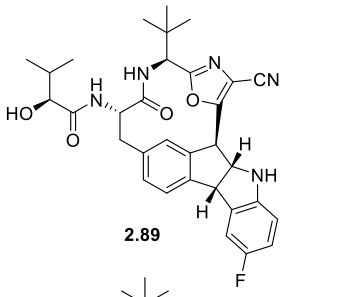

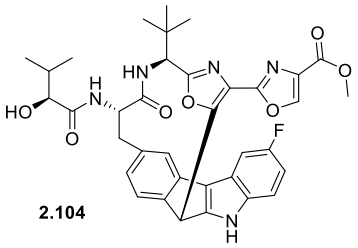

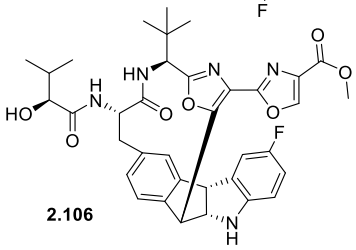

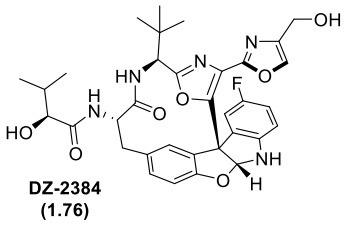

***In vitro* antiproliferative activity of compounds 2.89, 2.104, 2.106 and 1.76**

Entry	Compound	GI_{50}, μM			
		PANC-1	MiaPaCa-2	MCF-7	MDA-MB-231
1	**2.89**	100±15	-	>100	No effect
2	**2.104**	56±2	33±2	73±5	40±3
3	**2.106**	>100	11±2	17±2	85±3
4	**1.76**	0.0030 ±0.0006	0.000022 ±0.000006	0.0012 ±0.0004	0.0075 ±0.002

The macrocycles **2.89**, **2.104** and **2.106** featured low antiproliferative activity with only macrocycle **2.106** reaching 10 μM activity level on a single cell line (MiaPaCa-2) (Table 2.1, entry 3). The poor antiproliferative effects of compounds **2.89**, **2.104** and **2.106** illustrate the importance of the spatial structure at the tetracyclic indoline core. Despite containing the same bioxazole motif, peptide-based macrocycle and (*S*)-hydroxyisovaleric acid side chain as in DZ-2384 (**1.76**), the tested compounds **2.104** and **2.106** were at least four orders of magnitude less biologically active and the cianooxazole-containing macrocycle **2.89** was virtually inactive.

Gratifyingly, antiproliferative activities of indolinone core-containing 12- and 13-membered macrocycles **2.153b,c** and **2.154a-d** as well as *epi*-**2.154d** (synthesis described in chapter 2.3) were considerably higher (Table 2.2).

Table 2.2

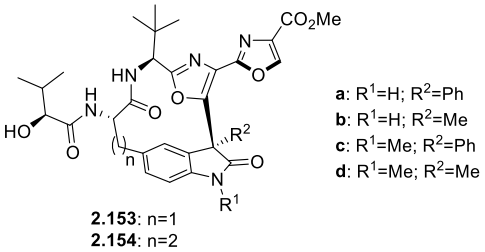

***In vitro* antiproliferative activities of compounds 2.153a-d and 2.154a-d**

Entry	Compound	n	R^1	R^2	GI_{50}, μM			
					PANC-1	MiaPaCa-2	MCF-7	MDA-MB-231
1	**2.153a**[a]	1	H	Ph	12±2	0.67±0.005	1.2±0.3	8±2
2	**2.153b**	1	H	Me	11±2	0.68±0.09	0.53±0.09	1.4±0.3
3	**2.153c**	1	Me	Ph	1.2±0.2	0.42±0.07	0.39±0.08	0.36±0.02
4	**2.153d**[a]	1	Me	Me	4.5±1	0.50±0.02	0.75±0.07	2.5±0.1
5	**2.154a**	2	H	Ph	1.2±0.3	0.46±0.04	7.7±0.3	0.26±0.03
6	**2.154b**	2	H	Me	>100	17±2	12±3	21±3
7	**2.154c**	2	Me	Ph	7.10±1	3.4±0.5	1.8±0.4	4.9±2
8	**2.154d**	2	Me	Me	>100	>100	15±2	4.8±1
9	*epi*-**2.154d**	2	Me	Me	>100	>100	79±6	75±8

[a]Macrocycle was prepared by V.Vitkovska and synthesis is described in[117]

We were delighted to see that macrocycle **2.153b** (Table 2.2, entry 2), **2.153c** (entry 3) and **2.154a** (entry 5) showed cancer cell growth inhibition at low micromolar or high nanomolar concentrations. In the 12-membered (n=1) macrocycle series, both compounds **2.153b** (R^2 = Me, entry 2) and **2.153c** (R^2 = Ph, entry 3) showed comparable nanomolar activity against MiaPaCa-2 and MCF-7 cancer cell lines, while in PANC-1 and MDA-MB-231 cell lines phenyl-substituted analog **2.153c** (R^2=Ph, entry 3) was up to order of magnitude more active. Notably, the SAR pattern in the 13-member macrocycle series was different. In both *N*-Me and *N*-H series, the phenyl group-bearing compounds were clearly more active than their Me-containing analogs and the highest activities were measured for macrocycle **2.154a** (R^1=H, R^2=Ph; entry 5). In contrast to the 12-membered macrocycles, the *N*-methylation seemed to have a detrimental effect in 13-membered homologs: compounds

2.154c,d displayed lower activity than their N-H analogs **2.154a,b**. Importantly, ring enlargement to 13-membered homologue **2.154a** (R^1 = H, R^2 = Ph, entry 5) helped to increase activity against MDA-MB-231 and PANC-1, while keeping comparable efficacy against MCF-7and MiaPaCa-2 cancer cell lines as compared to the 12-membered congener **2.153a** (entry 1). In contrast, considerable drop in the antiproliferative activity against all cell lines was observed when going from 12- to13-membered macrocycles, possessing methyl group either at the quaternary center (**2.153b** vs **2.154b**, entry 2 vs entry 6 and **2.153d** vs **2.154d**, entry 4 vs entry 8) or, less pronounced, at indolinone nitrogen (**2.153c** vs **2.154c**, entry 3 vs entry 7). Hence, the phenyl at quaternary center is superior substituent to the methyl group in the 13-membered macrocycle series. Finally, comparison of compounds **2.154d** (entry 6) and *epi*-**2.154d** (entry 7) shows the importance of having the right (*S*) configuration of the key quaternary stereogenic center: the *epi*-**2.154d** (*R* isomer) had a significantly lower activity in the MCF-7 and MDA-MB-231 cancer cell lines.

The efficacy of the best-performing macrocycles **2.153b,c** and **2.154a** was further evaluated in a series of additional cancer cell lines (histiocytic lymphoma U-937, melanoma A-2058 and lung adenocarcinoma HCC-44) by the MTT assay with vinorelbine as the positive control (Table 2.3). All three compounds exerted nanomolar activity on U-937 and A2058 cell lines, with **2.154a** (entry 3) being the most effective. It also inhibited the proliferation of HCC-44 cancer cell line at low nanomolar concentration.

Table 2.3

Additional *in vitro* antiproliferative activities of compounds 2.153b,c and 2.154a

Entry	Compound	GI_{50}, μM		
		U-937	A2058	HCC-44
1	**2.153b**	0.084±0.007	0.35±0.01	2.4±0.07
2	**2.153c**	0.043±0.001	0.31±0.03	1.3±0.1
3	**2.154a**	0.0087±0.001	0.049±0.001	0.26±0.02

We also evaluated the selectivity of antiproliferative activity of macrocycles **2.153b,c** and **2.154a** using non-cancerous cell lines HEK-293 (human embryonic kidney cells) and GM08402 (human dermal fibroblasts) (Table 2.4). Surprisingly, *N*-methyl indoline derivative **2.153c** (Table 2.4, entry 2) showed poor selectivity with antiproliferative activity against HEK-293 cells comparable to that in cancer cell lines (PANC-1 and HCC-44; Table 2.2 and Table 2.3). In contrast, *N*-H indolines **2.153b** and **2.154a** (entries 1 and 3) featured one to three orders of magnitude lower activity against non-cancerous cells as compared to cancer

cell lines. Similarly, high selectivity was also observed for all macrocycles when human dermal fibroblast cells (GM08402 cell line) were used.

Table 2.4

***In vitro* antiproliferative activities of compounds 2.153b,c and 2.154a against non-cancerous cell lines**

Entry	Compound	GI_{50}, μM	
		Hek293	GM08402
1	**2.153b**	44±8	53±9
2	**2.153c**	1.2±0.3	>100
3	**2.154a**	10±1	17±3

Additionally, 12-membered macrocycle **2.153b** and 13-membered homolog **2.154a** were submitted to dose-response screening assay against 60 human tumor cell line panel NCI-60 (US National Cancer Institute) at five concentrations (ranging from 0.01 to 100 μM).[123] In the assay macrocycle **2.154a** displayed sub micromolar average GI_{50} values, whereas **2.153b** exhibited mean inhibitory activity at the micromolar range (Table 2.5, entries 1-2). It was evident that, despite considerable structural alteration, macrocycle **2.154a** was only ca. 20-fold less active than the natural diazonamide **1a** as well as marketed MTA vinorelbine and paclitaxel as evidenced by their mean GI_{50} values in NCI-60 panel (entry 2 vs. entries 3-6). Significantly, compounds **2.153b** and **2.154a** showed low acute toxicity towards the tested cancer cell lines as evidenced by the mean LC_{50} (concentration of compound needed to kill 50% of cells) values above 100 μM assay threshold. However, low TGI (total growth inhibition) values for macrocycles **2.153b** and **2.154a** did not allow for assessment of cytostatic vs. cytotoxic properties. Overall, the results in dose-response screening assay against NCI-60 panel cell lines (Table 2.5) are in line with our data (Table 2.2 and Table 2.3) and point to the good antiproliferative potency of macrocycle **2.154a**.

It should be also noted that macrocycles **2.153b** and **2.154a** demonstrated differential cytotoxicity pattern highly similar to that of marketed microtubule-targeting agents paclitaxel and vinblastine (correlation coefficients 0.71 and 0.68 for **2.153b** and 0.79 and 0.76 for **2.154a**, respectively as indicated by COMPARE algorithm).[123] The overall activity pattern of compounds **2.153b** and **2.154a** and its similarity to the marketed MTA paclitaxel and vinblastine suggests that the observed antiproliferative activity of macrocyclic series is associated with their effect on microtubule dynamics.

Table 2.5

Results from NCI-60 cancer cell line screen

Entry	Compound	NSC ID	Mean GI_{50}, uM	Mean TGI, uM	Mean LC_{50}, uM
1	**2.153b**	830922	4.1	>100[a]	>100[a]
2	**2.154a**	830921	0.38	>100[a]	>100[a]
4	vinorelbine[b]	608210	0.018	4.2	52
5	paclitaxel[b]	125973	0.025	3.9	75
6	diazonamide A (**1.2**)[c]	700089	0.011	>10[c]	>10[c]

[a] TGI and LC_{50} values exceeded the upper concentration limit (100 μM) for more than half of NCI-60 cell lines; [b]Data from ref. [124]; [c] Data from ref. [125]; [c] TGI values exceeded the upper concentration limit (10 μM) for more than half and LC_{50} for 90% of cell lines in NCI-60 panel.

The measured antiproliferative activities of macrocycles **2.89**, **2.104**, **2.106**, **2.153b,c** and **2.154a-d** provide important insight into SAR of diazonamide A that is critical for successful development of its less complex analogs. Thus, the tetracyclic hemiaminal core apparently secures the bioactive conformation of both the highly cytotoxic natural diazonamide A (**1.2**) and its synthetic analog DZ-2384 (**1.76**). Variation of the bond connectivity between the core tetracycle and the rest of the molecule does not allow the (dihydro)indenoindole-core containing macrocyles **2.89**, **2.104** and **2.106** to adapt the bioactive conformation, leading to drop in antiproliferative activity compared to DZ-2384 (**1.76**).

However, the hard-to-synthesize tetracyclic core structure of diazonamide A and DZ-2384 can be replaced by much simpler 2-indolinone (as in compounds **2.153c,b** and **2.154 a-d**) without critical loss of antiproliferative activity against cancer cells. Additionally, change of the macrocyclic ring size from the 12- (simplified analogs **2.153b,c** as well as natural diazonamide A (**1.2**) and DZ-2384 (**1.76**)) to 13-membered ring (**2.154a-d**) is generally well tolerated and can have beneficial effect (as with macrocycle **2.154a**). However, change in absolute configuration at the quaternary stereogenic center of the 2-indolinone core is not tolerated and needs to adopt *S*-configuration (as illustrated with macrocycles **2.154d** and *epi*-**2.154d**). This further illustrates the high impact of spatial arrangement of core structure onto the biological activity of diazonamide A analogs. The obtained SAR insights will be used in further development of the simplified analogs of diazonamide A.

3. EXPERIMENTAL PART

General. Unless otherwise noted, all chemicals were used as obtained from commercial sources and all reactions were performed under argon atmosphere in oven-dried (120 °C) glassware. Anhydrous MeOH, pyridine, DMF, DMA and DMSO were purchased from Acros. Anhydrous PhMe, Et_2O, THF and DCM were obtained by passing commercially available solvent through activated alumina columns. Reactions were monitored by analytical TLC (precoated silica gel F-254 plates, Merck) or by UPLC-MS assay (Waters Acquity column: Acquity UPLC BEH-C18 (2.1 mm × 50 mm, 1.7 μm, (30.0 ± 5.0) °C); gradient, 0.01% TFA in water/CH_3CN 90:10 to 0.01% TFA in water/CH_3CN 5:95; flow rate, 0.5 mL/min; run time, 8 min; detector, PDA (photodiode matrix), 220−320 nm, SQ detector with an electrospray ion source (APCI). Purification by preparative reverse phase chromatography was performed using Waters Xbridge BEH C18 OBD column (5 μm, 10 × 150 mm) or Waters Atlantis Prep OBD T3 column (30 mm × 100 mm, 5 μm). All NMR spectra were recorded at 600, 400 or 300 MHz for ^{1}H-NMR, 151 or 101 MHz for ^{13}C-NMR and 376 MHz for ^{19}F-NMR. Chemical shifts are reported in parts per million (ppm) relative to TMS or with the residual solvent peak as an internal reference. High-resolution mass spectra (HRMS) were recorded on a Waters Synapt G2-Si TOF MS instrument using the ESI technique. Specific rotation was recorded on a Kruss P3000 instrument.

Synthesis of macrocyclic ketone (*R,R*)-**2.3** is described in: Mutule, I.; Joo, B.; Medne, Z.; Kalnins, T.; Vedejs, E.; Suna, E. Stereoselective Synthesis of the Diazonamide A Macrocyclic Core. *J. Org. Chem*. **2015**, *80* (6), 3058–3066 (see appendix I).

Synthesis of compounds **2.33 – 2.36** is described in: Mutule, I.; Kalnins, T.; Vedejs, E.; Suna, E. Diazonamide Synthetic Studies. Reactivity of *N*-Unsubstituted Benzofuro[2,3-*b*]Indolines. *Chem. Heterocycl. Compd.* **2015**, *51* (7), 613–620 (see appendix II).

Synthesis of compounds **2.153b,c** and **2.154a-d** as well as supporting information of the experiments are described in: Kalnins, T.; Vitkovska, V.; Kazak, M.; Zelencova-Gopejenko, D.; Ozola, M.; Narvaiss, N.; Makrecka-Kuka, M.; Domračeva, I.; Kinens, A.; Gukalova, B.; Konrad, N.; Aav, R.; Bonato, F.; Lucena-Agell, D.; Díaz, J. F.; Liepinsh, E.; Suna, E. Development of Potent Microtubule Targeting Agent by Structural Simplification of Natural Diazonamide. *J. Med. Chem.* **2024**, *67* (11), 9227–9259 (see appendix IV).

Tetracycle (*R,R*)-**2.7** was prepared as described by Peris and Vedejs.[40] Tetracycle *rac*-**2.7** was prepared as described by Zajac and Vedejs.[39] Di(4-methoxyphenyl)phosphinyl hydroxylamine (**2.48**) was prepared as described by Smulik and Vedejs.[52] *O*-(2,4-dinitrophenyl)hydroxylamine (**2.58**) was prepared as described by Miller.[53] Compounds **2.151**

and **2.152** were prepared as described by Baran.[113] Indane derivative **2.78** was prepared as described by Dalton.[70] Aniline **2.137** and aryl azide **2.138** were prepared as described by Driver.[94]

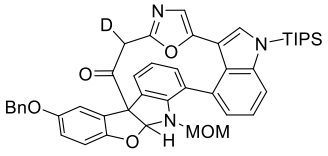

rac-**2.59**

Macrocyclic ketone *rac*-2.59. To solution of macrocyclic ketone *rac*-**2.3** (10 mg; 0.0136 mmol) in anhydrous THF (0.20 mL) was slowly added 0.34 M KHMDS solution in THF (80 µL; 0.027 mmol; 2 equiv.) at -78 °C. After stirring for two minutes the orange solution was cannulated through cooled (dry ice) cannula to AcOH-d_4 (12 µL; 0.20 mmol; 15 equiv.) solution in anhydrous THF (0.10 mL) at -78 °C. After stirring for five minutes the vial was allowed to warm up to room temperature and solvent was evaporated by stream of argon. The orange residue was additionally dried at high vacuum which yielded 10 mg (99%) of compound *rac*-**2.59** as light-yellow film. ^{1}H NMR (300 MHz, C_6D_6): δ 7.76 – 7.71 (m, 1H), 7.44 (dd, *J* = 6.4, 3.0 Hz, 1H), 7.29 – 7.24 (m, 2H), 7.24 – 7.20 (m, 2H), 7.19 – 7.16 (m, 1H), 7.14 – 7.07 (m, 2H), 7.03 (dd, *J* = 7.5, 1.3 Hz, 1H), 6.74 – 6.68 (m, 3H), 6.61 (s, 1H), 6.61 – 6.58 (m, 1H), 6.47 (t, *J* = 7.5 Hz, 1H), 4.81, 4.75 (ABq, *J* = 11.5 Hz, 2H), 4.61, 4.31 (ABq, *J* = 10.5 Hz, 2H), 3.83, 3.45 (ABq, *J* = 14.0 Hz, 1H), 2.74 (s, 3H), 1.41 – 1.28 (m, 3H), 0.95 (d, *J* = 7.1 Hz, 18H). ^{13}C NMR (101 MHz, C_6D_6): δ 197.2, 156.2, 154.5, 153.0, 146.2, 145.5, 140.9, 138.0, 133.4, 133.0, 133.0, 132.0, 128.6, 128.4, 128.2, 128.1, 128.0, 127.9, 123.1, 122.9, 122.5, 121.4, 119.3, 116.4, 114.0, 113.8, 110.1, 107.2, 102.3, 77.8, 71.0, 54.7, 40.7, 18.1, 12.9. LRMS-ESI (*m/z*) calcd. for $C_{44}H_{43}DN_5O_5Si$ $[M\text{-}Me+2H]^+$ 725.7; found 725.3.

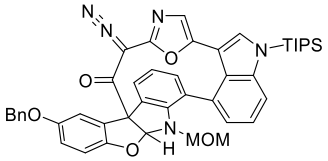

rac-**2.61**

Diazoketone *rac*-2.61. Solution of macrocyclic ketone *rac*-**2.3** (20 mg; 0.027 mmol) and *p*-acetamidobenzenesulfonyl azide (**2.60**) (6.9 mg; 0.029 mmol; 1.05 equiv.) in anhydrous MeCN (1.5 mL) was cooled to 0 °C. DBU (4.2 µL; 0.028 mmol; 1.05 equiv.) was added and the orange solution was stirred at 0 °C for one hour. Solvent was evaporated under reduced pressure at room temperature and the orange residue was suspended in Et_2O and filtered through a plug of cotton. Filtrate was evaporated under reduced pressure to yield 15 mg

(72%) of compound *rac*-**2.61** as air and moisture sensitive yellow oil. ^{1}H NMR (400 MHz, C_6D_6): δ 7.46 – 7.41 (m, 1H), 7.27 – 7.25 (m, 1H), 7.25 – 7.24 (m, 2H), 7.24 – 7.22 (m, 3H), 7.22 – 7.20 (m, 1H), 7.14 – 7.08 (m, 2H), 6.91 – 6.86 (m, 1H), 6.80 – 6.79 (m, 1H), 6.78 – 6.77 (m, 1H), 6.76 (s, 1H), 6.72 – 6.70 (m, 1H), 6.70 – 6.67 (m, 1H), 6.50 – 6.42 (m, 1H), 4.77, 4.68 (ABq, *J* = 12.0 Hz, 2H), 4.50, 4.21 (ABq, *J* = 10.5 Hz, 2H), 2.57 (s, 3H), 1.40 – 1.32 (m, 3H), 0.95 (d, *J* = 7.5 Hz, 18H). LRMS-ESI (*m/z*) calcd. for $C_{44}H_{44}N_5O_5Si$ [M-Me+2H]$^+$ 750.3; found 750.5.

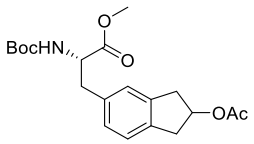

2.82

Methyl (2*S*)-3-(2-acetoxy-2,3-dihydro-1*H*-inden-5-yl)-2-((*tert*-butoxycarbonyl)amino)propanoate (2.82). To solution of aryl bromide **2.79** (prepared following procedure described in[71]) (832 mg; 3.26 mmol), $Pd_2(dba)_3$ (29 mg; 0.032 mmol; 0.01 equiv.) and SPhos (40 mg; 0.098 mmol; 0.03 equiv.) in anhydrous DMF (28 mL) was added freshly prepared alkyl zincate **2.81** (prepared following procedure described in[72]) (0.5 M in DMF; 6.85 mL; 3.42 mmol; 1.05 equiv.). The flask was placed in preheated oil bath at 55 °C and the orange solution was stirred for 18 hours. Solution was then cooled to room temperature, quenched with aqueous saturated NH_4Cl solution and extracted with Et_2O. Combined organic extracts were washed with water and brine, dried over $MgSO_4$ and evaporated to dryness under reduced pressure. The residue was purified by flash chromatography on silica (100% hexanes to 80% EtOAc in hexanes) to afford 910 mg (74 %) of compound **2.82** (1:1 dr) as orange oil. ^{1}H NMR (400 MHz, $CDCl_3$): δ 7.15 (d, *J* = 7.6 Hz, 1H), 6.99 (s, 1H), 6.93 (d, *J* = 7.6 Hz, 1H), 5.55 – 5.45 (m, 1H), 4.96 (d, *J* = 8.3 Hz, 1H), 4.60 – 4.51 (m, 1H), 3.73 (s, 1.5H), 3.72 (s, 1.5H), 3.32 – 3.23 (m, 2H), 3.13 – 2.99 (m, 2H), 2.96 (dd, *J* = 17.0, 3.0 Hz, 2H), 2.02 (s, 1.5H), 2.02 (s, 1.5H), 1.42 (s, 9H). ^{13}C NMR (101 MHz, $CDCl_3$): δ 172.5, 171.2, 155.2, 141.0, 139.4, 134.7, 128.0, 128.0, 125.7, 125.6, 124.8, 80.0, 75.5, 54.7, 52.3, 39.6, 39.6, 39.4, 39.4, 38.3, 28.4, 28.4, 21.4. HRMS (ESI) m/z calcd for $C_{20}H_{27}NO_6Na$ [M+Na]$^+$: 400.1736, found: 400.1751.

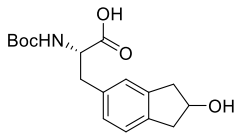

2.75

(2*S*)-2-((*tert*-Butoxycarbonyl)amino)-3-(2-hydroxy-2,3-dihydro-1*H*-inden-5-yl)propanoic acid (2.75). To ice cold solution of methyl ester **2.82** (5.20 g; 13.8 mmol) in MeOH and water mixture (1:1 v/v; 120 mL) was added solid LiOH (1.32 g; 55.1 mmol; 4 equiv.) and the clear yellow solution was stirred at 0 °C for two hours Then the solution was acidified to pH 4 with 4 M aqueous HCl solution and the MeOH was evaporated. The resulting suspension was extracted with DCM and the combined organic layers were washed with brine, dried over Na_2SO_4 and evaporated under reduced pressure. Residue purified with flash chromatography on silica (100% DCM to 22% MeOH in DCM) to yield 2.80 g (63%) of carboxylic acid **2.75** as yellow amorphous solid. ^{1}H NMR (400 MHz, MeOH-d_4): δ 7.16 – 7.06 (m, 2H), 7.03 – 6.98 (m, 1H), 4.60 (tt, J = 6.1, 3.6 Hz, 1H), 4.34 – 4.19 (m, 1H), 3.18 – 3.06 (m, 3H), 2.92 – 2.77 (m, 3H), 1.39 (m, 9H). ^{13}C NMR (101 MHz, MeOH-d4): δ 175.5, 157.8, 142.6, 140.9, 136.8, 128.7, 126.6, 125.6, 80.5, 73.8, 56.5, 43.0, 42.7, 38.6, 28.7. HRMS (ESI) m/z calcd. for $C_{17}H_{23}NO_5Na$ $[M+Na]^+$: 344.1474, found: 344.1488.

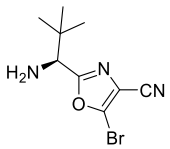

2.76

(*S*)-2-(1-Amino-2,2-dimethylpropyl)-5-bromooxazole-4-carbonitrile (2.76). To the solution of oxazole **2.83** (prepared according to procedure described in[85]) (150 mg; 0.38 mmol) in anhydrous 1,4-dioxane (1.0 mL) was added HBr in AcOH (33 %; 2.64 mL; 15.30 mmol; 40 equiv.). The yellow solution was stirred at room temperature for 10 minutes after which it was poured into an ice-cold aqueous saturated Na_2CO_3 and extracted with EtOAc. The combined organic extracts were washed with 1 M aqueous HCl. The combined water layers were basified with aqueous NH_3 to pH 9 and extracted with EtOAc. Organic layers were combined, dried over $MgSO_4$, evaporated to dryness under reduced pressure and purified by flash chromatography on silica (100% hexanes to 100% EtOAc) to yield 47 mg (48%) of compound **2.76** as yellow oil. ^{1}H NMR (400 MHz, $CDCl_3$): δ 3.78 (s, 1H), 2.24 – 1.89 (br s, 2H), 0.99 (s, 9H). ^{13}C NMR (101 MHz, $CDCl_3$): δ 169.2, 130.6, 115.8, 111.1, 59.7, 35.6, 26.3. HRMS (ESI) m/z calcd. for $C_9H_{13}N_3OBr$ $[M+H]^+$: 258.0242, found: 258.0239. $[\alpha]^{20}_D$ +10 (*c* 1.0, $CHCl_3$).

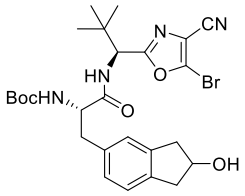

2.84

***tert*-Butyl ((2*S*)-1-(((*S*)-1-(5-bromo-4-cyanooxazol-2-yl)-2,2-dimethylpropyl)amino)-3-(2-hydroxy-2,3-dihydro-1*H*-inden-5-yl)-1-oxopropan-2-yl)carbamate (2.84)**. Carboxylic acid **2.75** (1.36 g; 4.23 mmol), amine **2.76** (1.31 g; 5.08 mmol; 1.2 equiv.) and EDC×HCl (811 mg; 4.23 mmol; 1 equiv.) were dissolved in anhydrous pyridine (50 mL) and the resulting yellow suspension was stirred at room temperature for 16 hours. Then solvent was evaporated to dryness under reduced pressure and the orange residue was dissolved in EtOAc, washed with 1 M aqueous HCl solution and brine, dried over $MgSO_4$ and evaporated under reduced pressure. The residual material was purified by flash chromatography on silica (100% DCM to 60% Et_2O in DCM) to yield 1.90 g (80%) of amide **2.84** (1:1 dr) as light-yellow foam. ^{1}H NMR (400 MHz, MeOH-d_4): δ 7.13 – 6.83 (m, 3H), 4.96 (d, J = 3.1 Hz, 1H), 4.64 – 4.56 (m, 1H), 4.39 – 4.29 (m, 1H), 3.18 – 3.01 (m, 2H), 2.98 – 2.88 (m, 1H), 2.86 – 2.73 (m, 3H), 1.40 (s, 9H), 0.98 (s, 9H). ^{13}C NMR (101 MHz, MeOH-d4): δ 174.5, 166.8, 166.7, 157.6, 142.6, 142.5, 140.8, 140.7, 136.3, 133.1, 133.0, 128.6, 126.8, 125.5, 125.3, 116.6, 116.5, 112.0, 80.6, 73.7, 73.7, 57.4, 57.1, 57.1, 43.0, 43.0, 42.8, 38.8, 36.5, 28.7, 26.5. HRMS (ESI) m/z calcd. for $C_{26}H_{33}N_4O_5NaBr$ $[M+Na]^+$: 583.1532, found: 583.1530.

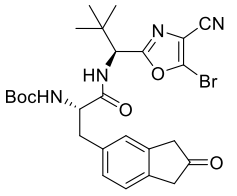

2.74

***tert*-Butyl ((*S*)-1-(((*S*)-1-(5-bromo-4-cyanooxazol-2-yl)-2,2-dimethylpropyl)amino)-1-oxo-3-(2-oxo-2,3-dihydro-1*H*-inden-5-yl)propan-2-yl)carbamate (2.74).** To the solution of alcohol **2.84** (1.93 g; 3.44 mmol) in anhydrous DCM (50 mL) was added solid DMP (1.46 g; 3.43 mmol; 1 equiv.). The colorless suspension was stirred at room temperature two hours after which it was diluted with Et_2O and washed with aqueous saturated $Na_2S_2O_3$ solution, aqueous saturated $NaHCO_3$ solution and brine. The organic layer was dried over $MgSO_4$ and evaporated under reduced pressure. The residue was purified by flash chromatography on silica (100% DCM to 60% EtOAc in DCM) to yield 1.42 g (74%) of ketone **2.74** as light-yellow foam. ^{1}H NMR (400 MHz, MeOH-d_4): δ 7.18 – 7.11 (m, 2H), 7.05 (d, J = 7.8 Hz, 1H), 4.96 (s, 1H), 4.38 (t, J = 7.8 Hz, 1H), 3.51 (s, 2H), 3.49 (d, J = 5.4 Hz, 2H), 3.00 – 2.91 (m,

1H), 2.88 – 2.80 (m, 1H), 1.40 (s, 9H), 0.99 (s, 9H). ^{13}C NMR (101 MHz, MeOH-*d*4): δ 217.1, 174.4, 166.8, 157.6, 139.3, 137.6, 137.3, 133.1, 129.5, 127.0, 125.7, 116.5, 111.9, 80.7, 57.2, 57.2, 44.8, 44.6, 38.9, 36.5, 28.7, 26.5. HRMS (ESI) m/z calcd. for $C_{26}H_{31}N_4O_5NaBr$ $[M+Na]^+$: 581.1376, found: 581.1373. $[\alpha]^{20}_D$ +4 (*c* 1.0, MeOH).

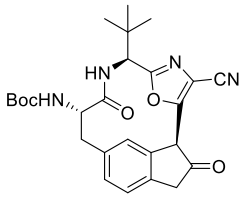

2.73

***tert*-Butyl ((21*S*,4*S*,7*S*)-7-(*tert*-butyl)-14-cyano-22,5-dioxo-22,23-dihydro-21*H*-6-aza-1(5,2)-oxazole-2(1,6)-indenacycloheptaphane-4-yl)carbamate (2.73).** To ketone **2.74** (105 mg; 0.19 mmol), $Pd_2(dba)_3$ (8.6 mg; 0.005 mmol; 0.05 equiv.), SPhos (11.6 mg; 0.028 mmol; 0.15 equiv.) and oven dried Cs_2CO_3 (183 mg; 0.56 mmol; 3 equiv.) was added anhydrous DMF (7 mL) and argon was passed through the mixture for 20 minutes. The orange suspension was stirred at 80 °C for three hours after which it was cooled to room temperature. The dark orange suspension was diluted with Et_2O and washed with aqueous saturated NH_4Cl solution, water, and brine. The organic layer was dried over MgSO4 and evaporated under reduced pressure. The residue was purified by flash chromatography on silica (100% DCM to 60% Et_2O in DCM) to yield 41 mg (46%) of macrocycle **2.73** (99:1 dr) as a yellow oil. ^{1}H NMR (400 MHz, $CDCl_3$): δ 7.30 (d, *J* = 7.9 Hz, 1H), 7.26 – 7.23 (m, 1H), 6.70 (s, 1H), 5.86 (d, *J* = 6.7 Hz, 1H), 5.14 (d, *J* = 9.3 Hz, 1H), 5.07 (s, 1H), 4.59 (d, *J* = 6.7 Hz, 1H), 3.90 – 3.84 (m, 1H), 3.88, 3.56 (ABq, J_{AB} = 22.0 Hz, 2H), 3.21 (dd, *J* = 12.2, 12.1 Hz, 1H), 2.78 (dd, *J* = 12.2, 3.2 Hz, 1H), 1.42 (s, 9H), 0.94 (s, 9H). ^{13}C NMR (101 MHz, $CDCl_3$): δ 206.6, 171.9, 163.5, 156.8, 155.3, 139.2, 136.6, 136.0, 129.9, 129.6, 125.7, 115.2, 111.9, 80.7, 59.0, 58.0, 51.8, 43.8, 37.6, 33.3, 28.4, 26.5. RMS (ESI) m/z calcd. for $C_{26}H_{30}N_4O_5Na$ $[M+Na]^+$: 501.2114, found: 501.2111. $[\alpha]^{20}_D$ -113 (*c* 0.2, MeOH).

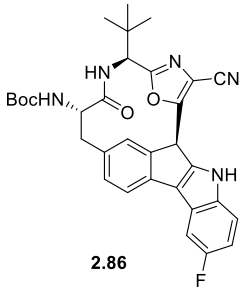

2.86

***tert*-Butyl ((26*R*,4*S*,7*S*)-7-(*tert*-butyl)-14-cyano-22-fluoro-5-oxo-25,26-dihydro-6-aza-1(5,2)-oxazola-2(6,8)-indeno[2,1-*b*]indolacycloheptaphane-4-yl)carbamate (2.86).**

Solution of the ketone **2.73** (80 mg; 0.17 mmol) and 4-fluorophenylhydrazine hydrochloride **2.85** (41 mg; 0.25 mmol; 1.5 equiv.) in *i*PrOH (4 mL) was stirred at 75 °C for six hours. Then the dark orange suspension was cooled to room temperature and the solvent was evaporated under reduced pressure. The residue was purified by reverse phase flash chromatography (10% MeCN in water to 100% MeCN) to yield 65 mg (68%; 99:1 dr) of compound **2.86** as yellow amorphous solid. ^{1}H NMR (400 MHz, MeOH-d_4): δ 7.53 – 7.43 (m, 2H), 7.43 (dd, *J* = 8.9, 4.4 Hz, 1H), 7.28 – 7.18 (m, 2H), 6.97 (td, *J* = 9.2, 2.6 Hz, 1H), 5.44 (s, 1H), 4.97 (s, 1H), 4.01 (dd, *J* = 11.8, 3.5 Hz, 1H), 3.16 (dd, *J* = 12.3, 12.3 Hz, 1H), 2.76 (dd, *J* = 12.3, 3.5 Hz, 1H), 1.44 (s, 9H), 1.01 (s, 9H). ^{13}C NMR (101 MHz, MeOH-d_4): δ 175.1, 166.0, 161.4, 159.6 (d, *J* = 234.1 Hz), 157.1, 146.4, 145.0, 139.1, 138.8, 133.7, 130.4, 129.3, 123.3 (d, *J* = 4.8 Hz), 122.7 (d, *J* = 10.3 Hz), 120.0, 114.5 (d, *J* = 9.6 Hz), 112.6, 111.1 (d, *J* = 26.4 Hz), 105.1 (d, *J* = 24.1 Hz), 80.5, 58.8, 58.4, 41.9, 38.9, 33.9, 28.7, 26.6. ^{19}F NMR (376 MHz, MeOH-*d*4): δ -125.75. HRMS (ESI) m/z calcd. for $C_{32}H_{32}N_5O_4FNa$ $[M+Na]^+$: 592.2336, found: 592.2333. $[\alpha]^{20}_D$ -180 (*c* 0.4, MeOH).

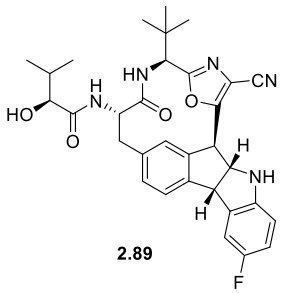

2.89

(*S*)-*N*-((25a*R*,26*R*,210b*S*,4*S*,7*S*)-7-(*tert*-Butyl)-14-cyano-22-fluoro-5-oxo-25,25a,26,210b-tetrahydro-6-aza-1(5,2)-oxazola-2(6,8)-indeno[2,1-b]indolacycloheptaphane-4-yl)-2-hydroxy-3-methylbutanamide (2.89). To ice cold solution of indole **2.86** (60 mg; 0.11 mmol) in TFA (3 mL) was added $NaCNBH_3$ (26 mg; 0.42 mmol; 4 equiv.) in MeOH (1 mL). The dark orange solution was stirred 30 minutes at 0 °C and one hour at room temperature. Then the solution was basified with aqueous saturated Na_2CO_3 solution to pH 9 and extracted with EtOAc. The organic layers were combined, washed with brine, dried over $MgSO_4$ and evaporated under reduced pressure. Residue was purified with flash chromatography on silica (100% DCM to 15% MeOH in DCM) to yield 32 mg (64%; 90:10 dr) of amine (*S*,*R*)-**2.88** as a yellow amorphous solid. To the solution of amine (*S*,*R*)-**2.88** (30 mg; 0.064 mmol), (*S*)-2-hydroxy-3-methylbutanoic acid (9.0 mg; 0.076 mmol; 1.2 equiv.), EDC×HCl (18 mg; 0.096 mmol; 1.5 equiv.) and HOBt (13 mg; 0.096 mmol; 1.5 equiv.) in anhydrous DMF (1 mL) was added DIPEA (55 μL; 0.32 mmol; 5.0 equiv.) and the yellow solution was stirred at room temperature for four hours. Then the solution was diluted with EtOAc and washed with 0.5 M

aqueous HCl solution and brine. The organic layer was dried over $MgSO_4$ and evaporated under reduced pressure. The resulting orange oil was purified by flash chromatography on silica (100% DCM to 15 % MeOH in DCM). The title compound was additionally purified by reverse phase HPLC (20% to 60% MeCN in 0.1% aqueous TFA) to yield 8 mg (22%; 99:1 dr) of the compound **2.89** as an off-white amorphous solid. ^{1}H NMR (400 MHz, $CDCl_3$): δ 7.36 (d, *J* = 7.8 Hz, 1H), 7.26 – 7.13 (m, 3H), 7.08 (dd, *J* = 8.2, 2.6 Hz, 1H), 6.67 (td, *J* = 8.8, 2.6 Hz, 1H), 6.50 (s, 1H), 6.38 – 6.32 (m, 1H), 5.84 (d, *J* = 6.4 Hz, 1H), 5.25 (m, 1H), 5.11 (d, *J* = 7.3 Hz, 1H), 5.06 (d, *J* = 8.5 Hz, 1H), 4.39 (d, *J* = 6.4 Hz, 1H), 4.21 (m, 1H), 3.98 (d, *J* = 3.0 Hz, 1H), 3.16 (t, *J* = 12.2 Hz, 1H), 2.77 (dd, *J* = 12.2, 3.4 Hz, 1H), 2.21 – 2.10 (m, 1H), 1.02 (d, *J* = 6.9 Hz, 3H), 0.85 (d, *J* = 6.9 Hz, 3H), 0.76 (s, 9H). ^{13}C NMR (101 MHz, $CDCl_3$): δ 173.1, 171.6, 163.4, 160.0 (d, *J* = 306.0 Hz), 142.8, 142.6, 135.9, 129.7 (d, *J* = 10.4 Hz), 129.2, 128.4, 125.4, 124.9, 114.6 (d, *J* = 23.2 Hz), 112.7, 111.4 (d, *J* = 24.0 Hz), 76.3, 66.6, 58.9, 56.0, 54.3, 49.4, 38.0, 33.3, 32.0, 26.3, 19.3, 15.6. ^{19}F NMR (376 MHz, MeOH-d_4): δ -76.06. HRMS (ESI) m/z calcd. for $C_{32}H_{35}N_5O_4F$ $[M+H]^+$: 572.2673, found: 572.2682. $[\alpha]^{20}_D$ -121 (*c* 0.2, MeOH).

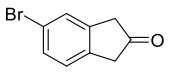

2.98

5-Bromo-1,3-dihydro-2*H*-inden-2-one (2.98). To ice cold solution of indene **2.96** (prepared according to method escribed in[84]) (2.70 g; 13.84 mmol) in anhydrous DCM (60 mL) solid *m*CPBA (72%; 3.65 g; 15.22 mmol; 1.1 equiv.) was added portion wise. The turbid colorless solution was stirred at 0 °C for 30 minutes, warmed to room temperature and stirred for one hour. Then the solvent was evaporated, and the residue dissolved in EtOAc, washed with aqueous saturated $Na_2S_2O_3$ solution, aqueous saturated $NaHCO_3$ solution and brine. The organic layer was dried over $MgSO_4$ and evaporated under reduced pressure to give a light yellow amorphous solid. The obtained material was dissolved in anhydrous DCM (60 mL) under argon atmosphere and cooled to 0 °C. $BF_3{\times}OEt_2$ (2.14 mL; 17.00 mmol; 1.2 equiv.) was added dropwise. The orange solution was stirred at 0 °C for 20 minutes and at room temperature for one hour. Reaction was quenched with saturated aqueous NH_4Cl solution. Layers were separated and the water layer was extracted with DCM. The organic layers were combined, washed with brine, dried over $MgSO_4$ and evaporated under reduced pressure. The residue was purified by flash chromatography on silica (100% hexanes to 20% EtOAc in hexanes) to give 1.92 g (64%) of ketone **2.98** as off-white amorphous solid. ^{1}H NMR (400 MHz, $CDCl_3$): δ 7.45 (s, 1H), 7.40 (d, *J* = 8.1 Hz, 1H), 7.18 (d, *J* = 8.1 Hz, 1H), 3.56 (s, 2H),

3.50 (s, 2H). ^{13}C NMR (101 MHz, $CDCl_3$): δ 213.7, 140.0, 136.7, 130.7, 128.3, 126.7, 121.2, 44.1, 43.8. LRMS (EI) m/z calcd. for C_9H_7BrO [M]: 210.0; 212.0, found: 210.1; 212.1.

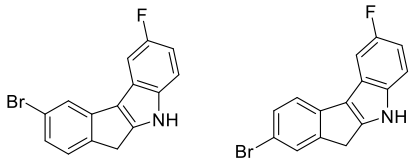

2.100 **2.99**

9-Bromo-2-fluoro-5,6-dihydroindeno[2,1-*b*]indole (2.100) and 8-bromo-2-fluoro-5,6-dihydroindeno[2,1-*b*]indole (2.99). Solution of the ketone **2.98** (1.90 g; 9.00 mmol) and 4-fluorophenylhydrazine hydrochloride **2.85** (2.20 g; 13.50 mmol; 1.5 equiv.) in *i*PrOH (50 mL) was stirred at 75 °C for two hours. Then the brown solution was cooled to room temperature and evaporated to dryness under reduced pressure. The solid residue was dissolved in EtOAc, filtered through a sintered glass filter and washed on filter with EtOAc. The filtrate was evaporated, and the remaining material was purified by three consecutive direct phase flash chromatography procedures (100% hexanes to 40% EtOAc in hexanes; isocratic 20% EtOAc in hexanes; 10% to 80% Et_2O in hexanes) to yield compounds **2.100** and **2.99**. **9-Bromo-2-fluoro-5,6-dihydroindeno[2,1-*b*]indole (2.100).** Deep brown amorphous solid, 614 mg (23%). ^{1}H NMR (400 MHz, MeOH-d_4): δ 7.59 (d, J = 1.9 Hz, 1H), 7.42 – 7.29 (m, 2H), 7.25 (d, J = 7.9 Hz, 1H), 7.13 (dd, J = 7.9, 1.9 Hz, 1H), 6.89 (td, J = 9.2, 2.5 Hz, 1H), 3.64 (s, 2H). ^{13}C NMR (101 MHz, MeOH-d_4): δ 159.5 (d, J = 233.4 Hz), 151.1, 143.3, 142.7, 139.0, 127.0, 125.8, 123.0 (d, J = 10.4 Hz), 121.8, 121.0 (d, J = 4.3 Hz), 113.6 (d, J = 9.8 Hz), 109.9 (d, J = 26.3 Hz), 104.7 (d, J = 24.1 Hz), 31.4. ^{19}F NMR (376 MHz, MeOH-d_4): δ -126.15. HRMS (ESI) m/z calcd. for $C_{15}H_9NFBr$ $[M]^+$: 300.9903, found: 300.9884. **8-Bromo-2-fluoro-5,6-dihydroindeno[2,1-b]indole (2.99).** Deep brown amorphous solid, 1.51 g (55%). ^{1}H NMR (400 MHz, $CDCl_3$): δ 8.30 (s, 1H), 7.55 – 7.51 (m, 1H), 7.50 – 7.40 (m, 3H), 7.32 (dd, J = 8.9, 4.3 Hz, 1H), 6.97 (td, J = 9.1, 2.5 Hz, 1H), 3.74 (s, 2H). ^{13}C NMR (101 MHz, MeOH-d_4): δ 162.0 (d, J = 278.8 Hz), 150.2, 146.2, 140.3, 139.0, 130.8, 128.9, 120.1, 116.3, 113.7 (d, J = 9.9 Hz), 109.9 (d, J = 26.1 Hz), 104.7 (d, J = 24.3 Hz), 31.7. ^{19}F NMR (376 MHz, MeOH-d_4): δ -126.41. HRMS (ESI) m/z calcd. for $C_{15}H_9NFBr$ $[M]^+$: 300.9903, found: 300.9895.

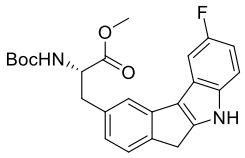

2.101

Methyl (*S*)-2-((*tert*-butoxycarbonyl)amino)-3-(2-fluoro-5,6-dihydroindeno[2,1-*b*]indol-9-yl)propanoate (2.101). To the solution of aryl bromide **2.100** (600 mg; 1.99 mmol), $Pd_2(dba)_3$ (73 mg; 0.079 mmol; 0.04 equiv.) and SPhos (82 mg; 0.199 mmol; 0.1 equiv.) in anhydrous DMF (14 mL) was added freshly prepared solution of alkyl zincate **2.81** (0.5 M in DMF; 4.37 mL; 2.18 mmol; 1.1 equiv.) and the brown solution was stirred at 60 °C for 23 hours. The solution was cooled to room temperature, quenched with aqueous saturated NH_4Cl solution, and extracted with EtOAc. The organic layers were combined and washed with water and brine, dried over $MgSO_4$ and evaporated under reduced pressure. The residue was purified by flash chromatography on silica (100% hexanes to 60% EtOAc in hexanes) to give 570 mg (68%) of compound **2.101** as an off-white amorphous solid. ^{1}H NMR (400 MHz, MeOH-d_4): δ 7.44 (dd, *J* = 9.7, 2.5 Hz, 1H), 7.39 (d, *J* = 1.6 Hz, 1H), 7.34 (dd, *J* = 8.8, 4.5 Hz, 1H), 7.29 (d, *J* = 7.5 Hz, 1H), 6.91 – 6.83 (m, 2H), 4.44 (dd, *J* = 8.8, 5.5 Hz, 1H), 3.71 (s, 3H), 3.66 (s, 2H), 3.16 (dd, *J* = 13.7, 5.5 Hz, 1H), 2.98 (dd, *J* = 13.7, 8.8 Hz, 1H), 1.40 – 1.27 (m, 9H). ^{13}C NMR (101 MHz, MeOH-d_4): δ 174.4, 159.4 (d, *J* = 232.8 Hz), 157.8, 150.5, 142.4, 141.4, 138.9, 136.9, 125.6, 124.2, 123.2 (d, *J* = 10.4 Hz), 122.0 (d, *J* = 4.4 Hz), 119.9, 113.5 (d, *J* = 9.9 Hz), 109.5 (d, *J* = 26.3 Hz), 104.6 (d, *J* = 23.9 Hz), 80.7, 56.8, 52.6, 39.0, 31.4, 28.6. ^{19}F NMR (376 MHz, MeOH-d_4): δ -126.74. HRMS (ESI) m/z calcd. for $C_{24}H_{25}N_2O_4FNa$ $[M+Na]^+$: 447.1696, found: 447.1697. $[\alpha]^{20}_D$ +20 (*c* 1.1, MeOH).

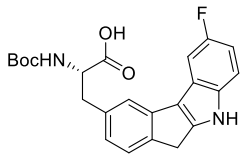

2.92

(*S*)-2-((*tert*-Butoxycarbonyl)amino)-3-(2-fluoro-5,6-dihydroindeno[2,1-b]indol-9-yl)propanoic acid (2.92). To solution of ester **2.101** (550 mg; 1.30 mmol) in MeOH and THF mixture (1:1 v/v; 20 mL) was added a LiOH (62 mg; 2.59 mmol; 2 equiv.) solution in water (10 mL). The orange solution was stirred at room temperature for one hour after which the organic solvents were evaporated. The remaining water solution was acidified to pH 4 with 1 M aqueous HCl solution and extracted with EtOAc. The combined organic layers were washed with brine, dried over $MgSO_4$ and evaporated under reduced pressure. The light brown oil was dissolved in DCM and left to stand at rt. Light yellow powder slowly

precipitated which was filtered and washed on filter with DCM yielding 540 mg (98%) of acid **2.92**. ^{1}H NMR (400 MHz, MeOH-d_4): δ 7.48 – 7.42 (m, 2H), 7.38 – 7.30 (m, 2H), 6.92 (dd, *J* = 7.6, 1.7 Hz, 1H), 6.88 (td, *J* = 9.2, 2.6 Hz, 1H), 5.49 (s, 1H), 4.42 (dd, *J* = 8.8, 5.0 Hz, 1H), 3.71 (s, 2H), 3.23 (dd, *J* = 13.8, 5.0 Hz, 1H), 3.00 (dd, *J* = 13.8, 8.8 Hz, 1H), 1.40 – 1.28 (m, 9H). ^{13}C NMR (101 MHz, MeOH-d_4): δ 175.6, 159.4 (d, *J* = 232.8 Hz), 157.8, 150.5, 142.3, 141.4, 139.0, 137.1, 125.5, 124.4, 123.3 (d, *J* = 10.2 Hz), 122.0 (d, *J* = 4.2 Hz), 120.0, 113.5 (d, *J* = 9.8 Hz), 109.5 (d, *J* = 26.2 Hz), 104.7 (d, *J* = 23.9 Hz), 80.6, 56.6, 38.9, 31.5, 28.7. ^{19}F NMR (376 MHz, $CDCl_3$): δ -126.9. HRMS (ESI) m/z calcd. for $C_{23}H_{23}N_2O_4F$ $[M]^+$: 410.1642, found: 410.1642. $[\alpha]^{20}_D$ +38 (*c* 0.8, MeOH).

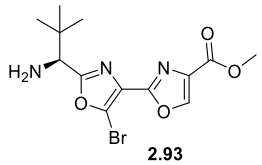

2.93

Methyl (*S*)-2'-(1-amino-2,2-dimethylpropyl)-5'-bromo-[2,4'-bioxazole]-4-carboxylate (2.93). Methyl (*S*)-2'-(1-amino-2,2-dimethylpropyl)-5'-bromo-[2,4'-bioxazole]-4-carboxylate (prepared according to method described in[85]) (124 mg; 0.27 mmol) was dissolved in anhydrous DCM (2 mL) and TFA (207 µL; 2.70 mmol; 10 equiv.) was added. The yellow solution was stirred at room temperature for three hours. The reaction was poured into aqueous saturated $NaHCO_3$ solution and extracted with EtOAc. The combined organic layers were washed with aqueous saturated $NaHCO_3$ solution and brine, dried over $MgSO_4$ and evaporated to yield 95 mg (98%) of amine **2.93** as a yellow oil. ^{1}H NMR (400 MHz, MeOH-d_4): δ 8.73 (s, 1H), 4.57 (s, 1H), 3.93 (s, 3H), 1.15 (s, 9H). ^{13}C NMR (101 MHz, MeOH-d_4): δ 162.6, 162.5, 156.0, 146.5, 135.3, 129.6, 126.6, 58.6, 52.7, 35.7, 26.2. HRMS (ESI) m/z calcd. for $C_{13}H_{17}N_3O_4Br$ $[M+H]^+$: 358.0402, found: 358.0400. $[\alpha]^{20}_D$ -18 (*c* 0.5, MeOH).

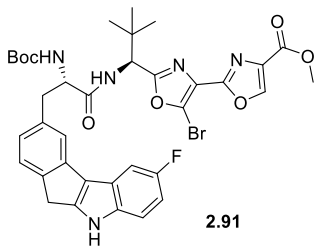

2.91

Methyl 5'-bromo-2'-((*S*)-1-((*S*)-2-((*tert*-butoxycarbonyl)amino)-3-(2-fluoro-5,6-dihydroindeno[2,1-b]indol-9-yl)propanamido)-2,2-dimethylpropyl)-[2,4'-bioxazole]-4-carboxylate (2.91). Solution of acid **2.92** (157 mg; 0.38 mmol), amine **2.93** (136 mg; 0.38 mmol; 1 equiv.) and EDC×HCl (73 mg; 0.38 mmol; 1 equiv.) in anhydrous pyridine (12 mL) was stirred at room temperature for five hours. The pyridine was evaporated under reduced

pressure and the remaining red material dissolved in EtOAc and washed with 0.5 M aqueous HCl solution and brine. The organic layer was dried over $MgSO_4$ and evaporated under reduced pressure. The resultant solid was purified by flash chromatography on silica (100% hexanes to 100% EtOAc) after which the material was additionally purified by reverse phase flash chromatography (10% MeCN in H_2O to 100% MeCN) to yield 114 mg (40%) of the compound **2.91** as yellow amorphous solid. ^{1}H NMR (400 MHz, $CDCl_3$): δ 8.48 (s, 1H), 8.01 (s, 1H), 7.39 (dd, *J* = 9.4, 2.5 Hz, 1H), 7.32 (s, 1H), 7.21 (dd, *J* = 8.8, 4.3 Hz, 1H), 7.15 (d, *J* = 7.6 Hz, 1H), 6.89 (td, *J* = 9.0, 2.5 Hz, 1H), 6.86 – 6.83 (m, 1H), 6.56 (d, *J* = 8.6 Hz, 1H), 5.21 (d, *J* = 7.1 Hz, 1H), 5.02 (d, *J* = 9.3 Hz, 1H), 4.44 – 4.32 (m, 1H), 3.93 (s, 3H), 3.51 (d, *J* = 2.8 Hz, 2H), 3.15 (dd, *J* = 13.4, 6.4 Hz, 1H), 3.02 (dd, *J* = 13.4, 8.7 Hz, 1H), 1.45 (s, 9H), 0.91 (s, 9H). ^{13}C NMR (101 MHz, $CDCl_3$): δ 171.4, 164.5, 161.6, 158.3 (d, *J* = 235.7 Hz), 155.6, 154.4, 148.4, 143.8, 140.9, 140.0, 137.1, 135.3, 134.3, 127.6, 124.6, 123.7, 122.7, 122.1 (d, *J* = 10.3 Hz), 121.7 (d, *J* = 4.4 Hz), 119.1, 112.2 (d, *J* = 9.9 Hz), 109.5 (d, *J* = 25.9 Hz), 104.6 (d, *J* = 23.9 Hz), 80.4, 57.0, 55.7, 52.4, 38.8, 36.2, 31.0, 28.5, 26.3. ^{19}F NMR (376 MHz, $CDCl_3$): δ -123.59. HRMS (ESI) m/z calcd. for $C_{36}H_{37}N_5O_7FNaBr$ $[M+Na]^+$: 772.1758, found: 772.1757. $[\alpha]^{20}_D$ -19 (*c* 3.8, MeOH).

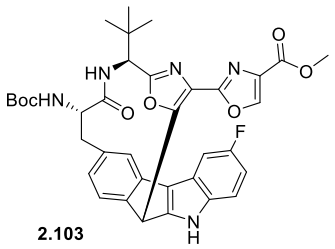

2.103

Methyl 2-((29*R*,4*S*,7*S*)-4-((*tert*-butoxycarbonyl)amino)-7-(*tert*-butyl)-23-fluoro-5-oxo-24*b*,29-dihydro-6-aza-1(5,2)-oxazola-2(9,6)-indeno[1,2-a]indenacycloheptaphane-14-yl)oxazole-4-carboxylate (2.103). To amide **2.91** (88 mg; 0.12 mmol) and anhydrous Cs_2CO_3 (115 mg; 0.35 mmol; 3 equiv.) was added anhydrous DMF (12 mL) and the yellow turbid solution was stirred at 70 °C for two hours. Then the solution was cooled to room temperature, quenched with aqueous saturated NH_4Cl solution and extracted with Et_2O. The combined organic layers were washed with water and brine, dried over $MgSO_4$ and evaporated under reduced pressure. The residue was purified by flash chromatography on silica (100% DCM to 40% Et_2O in DCM) to afford 45 mg (57%; 99:1 dr) of macrocycle **2.103** as light yellow amorphous solid. ^{1}H NMR (400 MHz, $CDCl_3$): δ 9.61 (s, 1H), 8.32 (s, 1H), 7.48 (dd, *J* = 9.4, 2.5 Hz, 2H), 7.39 – 7.34 (m, 1H), 7.31 (dd, *J* = 9.0, 4.2 Hz, 1H), 7.00 – 6.88 (m, 2H), 6.79 (d, *J* = 8.0 Hz, 1H), 5.86 (s, 1H), 5.27 (d, *J* = 10.2 Hz, 1H), 5.13 (d, *J* = 9.2 Hz, 1H), 4.46 (d, *J* = 10.2 Hz, 1H), 4.07 – 3.98 (m, 1H), 3.98 (s, 3H), 3.35 (dd, *J* = 12.5, 5.9

Hz, 1H), 2.82 (t, *J* = 12.0 Hz, 1H), 1.41 (s, 9H), 0.88 (s, 9H). ^{13}C NMR (101 MHz, $CDCl_3$): δ 170.3, 162.1, 161.5, 158.5 (d, *J* = 236.1 Hz), 156.7, 155.5, 154.0, 147.0, 145.3, 143.7, 142.4, 137.4, 137.3, 134.2, 125.3, 124.7, 124.3, 124.1, 123.4 (d, *J* = 4.4 Hz), 122.2 (d, *J* = 10.5 Hz), 113.1 (d, *J* = 9.8 Hz), 110.5 (d, *J* = 26.4 Hz), 105.2 (d, *J* = 23.6 Hz), 80.3, 58.1, 54.8, 52.6, 42.7, 38.9, 33.6, 28.4, 25.9. ^{19}F NMR (376 MHz, $CDCl_3$): δ -123.24. HRMS (ESI) m/z calcd. for $C_{36}H_{36}N_5O_7FNa$ $[M+Na]^+$: 692.2496, found: 692.2495. $[\alpha]^{20}_D$ -126 (*c* 0.6, MeOH).

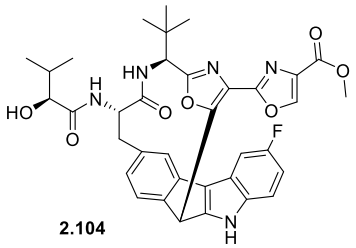

2.104

Methyl 2-((26*S*,4*S*,7*S*)-7-(*tert*-butyl)-22-fluoro-4-((*S*)-2-hydroxy-3-methylbutanamido)-5-oxo-25,26-dihydro-6-aza-1(5,2)-oxazola-2(6,9)-indeno[2,1-*b*]indolacycloheptaphane-14-yl)oxazole-4-carboxylate (2.104). To solution of **2.103** (60 mg; 0.089 mmol) in anhydrous DCM (1 mL) was added TFA (105 µL; 1.37 mmol; 40 equiv.). The green solution was stirred at room temperature for 18 hours, after which the solution was diluted with EtOAc and washed with saturated aqueous $NaHCO_3$ solution and brine, dried over $MgSO_4$ and evaporated under reduced pressure. To the resulting brown amorphous solid was added (*S*)-H*i*VA (6.2 mg; 0.053 mmol; 1.5 equiv.), EDC×HCl (13 mg; 0.070 mmol; 2 equiv.) and HOBt (9.5 mg; 0.070 mmol; 2 equiv.) and the solids were dissolved in anhydrous DMF (2 mL). DIPEA (18 µL; 0.11 mmol; 3 equiv.) was added and the brown solution was stirred at room temperature for two hours. The solution was then diluted with EtOAc and washed with 0.5 M aqueous HCl solution, water and brine, dried over $MgSO_4$ and evaporated under reduced pressure. The residue was purified by flash chromatography on silica (100% DCM to 15% MeOH in DCM). Additional purification by reverse phase flash chromatography (10% MeCN in water to 100% MeCN) yielded 5 mg (21%) of compound **2.104** as a light yellow amorphous solid. ^{1}H NMR (400 MHz, MeOH-d_4): δ 8.71 (s, 1H), 7.50 (dd, *J* = 9.6, 2.4 Hz, 1H), 7.41 – 7.33 (m, 2H), 7.06 (dd, *J* = 8.0, 1.1 Hz, 1H), 6.94 (td, *J* = 9.2, 2.6 Hz, 1H), 6.88 (d, *J* = 7.9 Hz, 1H), 6.00 (s, 1H), 4.58 (dd, *J* = 11.4, 6.2 Hz, 1H), 4.45 (s, 1H), 3.97 (s, 3H), 3.85 (d, *J* = 3.8 Hz, 1H), 3.37 – 3.33 (m, 1H), 2.94 – 2.86 (m, 1H), 2.12 – 2.03 (m, 1H), 1.00 (d, *J* = 6.9 Hz, 3H), 0.97 (s, 9H), 0.89 (d, *J* = 6.9 Hz, 3H). ^{13}C NMR (101 MHz, MeOH-d_4): δ 176.0, 172.6, 163.4, 163.0, 155.6, 149.0, 148.8, 148.6, 147.1, 145.9, 139.1, 138.0, 135.1, 126.8, 126.5, 125.5, 124.3, 114.2 (d, *J* = 10.5 Hz), 76.8, 56.2, 56.0, 52.7, 43.7, 39.9, 34.6,

33.1, 26.5, 19.6, 16.3. ^{19}F NMR (376 MHz, MeOH-d_4): δ -125.97. HRMS (ESI) m/z calcd. for $C_{36}H_{37}N_5O_7F$ $[M+H]^+$: 670.2677, found: 670.2684. $[\alpha]^{20}_D$ -113 (*c* 0.2, DMSO).

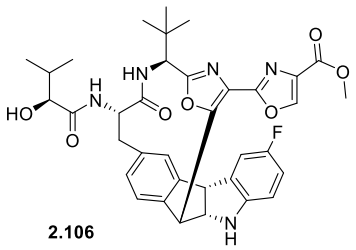

2.106

Methyl 2-((25a*S*,26*S*,210b*R*,4*S*,7*S*)-7-(*tert*-butyl)-22-fluoro-4-((*S*)-2-hydroxy-3-methylbutanamido)-5-oxo-25,25a,26,210b-tetrahydro-6-aza-1(5,2)-oxazola-2(6,9)-indeno[2,1-*b*]indolacycloheptaphane-14-yl)oxazole-4-carboxylate (2.106). To ice cold solution of compound **2.103** (60 mg; 0.089 mmol) in TFA (4 mL) was added $NaCNBH_3$ (17 mg; 0.27 mmol; 3 equiv.) solution in MeOH (1 mL). The yellow solution was stirred at 0 °C for 40 minutes after which it was neutralized with 2 M aqueous Na_2CO_3 solution and extracted with EtOAc. The combined organic layers were dried over $MgSO_4$ and evaporated under reduced pressure. The residue was purified by flash chromatography on silica (100% DCM to 15% MeOH in DCM). Additional purification by reverse phase HPLC (isocratic 40% MeCN in 0.4% aqueous TFA) yielded 34 mg (56%; dr 99:1) of trifluoroacetate salt of (*S*,*R*)-**2.105** as an off-white powder. The salt was dissolved in EtOAc and washed with aqueous saturated $NaHCO_3$ solution, dried over $MgSO_4$ and evaporated to dryness under reduced pressure. The prepared amine (28 mg; 0.050 mmol), (*S*)-H*i*VA (7.0 mg; 0.060 mmol; 1.2 equiv.), EDC×HCl (14 mg; 0.074 mmol; 1.5 equiv.) and HOBt (10 mg; 0.074 mmol; 1.5 equiv.) were dissolved in anhydrous DMF (2 mL) and DIPEA (43 µL; 0.25 mmol; 5 equiv.) was added. The colorless solution was stirred at room temperature for 18 hours after which it was diluted with EtOAc and washed with 0.5 M aqueous HCl solution. The combined water layers were extracted with EtOAc. The combined organic extracts were washed with 0.5 M aqueous HCl solution, water, and brine, dried over $MgSO_4$ and evaporated under reduced pressure. The residue was purified by flash chromatography on silica (100% hexanes to 80% EtOAc in hexanes) to yield 23 mg (69%; 99:1 dr) of compound **2.106** as a light yellow amorphous solid. ^{1}H NMR (600 MHz, MeOH-d_4): δ 8.65 (s, 1H), 8.08 (d, *J* = 9.8 Hz, 1H), 7.26 (s, 1H), 7.16 (d, *J* = 8.0 Hz, 1H), 7.13 (dd, *J* = 8.4, 2.5 Hz, 1H), 6.99 (d, *J* = 8.0 Hz, 1H), 6.70 (td, *J* = 8.9, 2.6 Hz, 1H), 6.53 (dd, *J* = 8.4, 4.2 Hz, 1H), 5.23 (s, 1H), 4.98 (d, *J* = 7.5 Hz, 1H), 4.78 (d, *J* = 7.5 Hz, 1H), 4.69 – 4.64 (m, 1H), 4.50 (dd, *J* = 11.4, 5.9 Hz, 1H), 3.95 (s, 3H), 3.86 (d, *J* = 3.9 Hz, 1H), 3.24 (dd, *J* = 12.2, 5.9 Hz, 1H), 2.92 (t, *J* = 11.8 Hz, 1H), 2.11 – 2.03 (m, 1H), 1.06 (s, 9H), 1.00 (d, *J* = 6.9 Hz, 3H), 0.89 (d, *J* = 6.9 Hz, 3H). ^{13}C NMR (101

MHz, MeOH-d_4): δ 176.0, 172.7, 163.1, 163.0, 158.3 (d, J = 233.9 Hz), 158.1, 157.4, 148.0, 147.3, 145.7, 144.3, 138.7, 135.0, 133.0 (d, J = 7.8 Hz), 130.3, 129.2, 128.1, 124.0, 114.7 (d, J = 23.3 Hz), 112.0 (d, J = 24.3 Hz), 110.3 (d, J = 8.2 Hz), 76.8, 68.1, 56.3 (d, J = 7.1 Hz), 54.8, 53.5, 52.7, 39.8, 34.7, 33.1, 26.6, 19.6, 16.3. ^{19}F NMR (376 MHz, MeOH-*d*4): δ -128.84. HRMS (ESI) m/z calcd. for $C_{36}H_{39}N_5O_7F$ $[M+H]^+$: 672.2834, found: 672.2864. $[\alpha]^{20}_D$ -11 (*c* 0.3, DMSO).

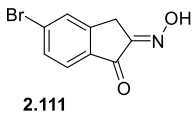

2.111

5-Bromo-2-(hydroxyimino)-2,3-dihydro-1*H*-inden-1-one (2.111). Suspension of 5-bromo-1-indanone **2.110** (4.00 g; 18.95 mmol) in MeOH (50 mL) was heated to 40 °C. Isoamyl nitrite (2.79 mL; 20.85 mmol; 1.1 equiv.) was added followed by addition of conc. HCl (1.60 mL; 18.95 mmol; 1 equiv.). The suspension turned into a clear solution but later developed large amount of white precipitate. The suspension was kept at 40 °C for one hour and then cooled to room temperature. The white solid was filtered off, washed on filter with MeOH and dried at high vacuum to yield 2.22 g (49%) of oxime **2.111** as white amorphous solid. ^{1}H NMR (400 MHz, MeOH-d_4): δ 7.84 (s, 1H), 7.79 – 7.56 (m, 2H), 3.84 (s, 2H). ^{13}C NMR (101 MHz, MeOH-d_4): δ 190.8, 155.2, 150.7, 137.9, 132.6, 132.0, 131.5, 126.4, 29.0. HRMS (ESI) m/z calcd. for $C_9H_7NO_2Br$ $[M+H]^+$: 239.9660, found: 239.9657.

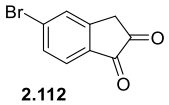

2.112

5-Bromo-1*H*-indene-1,2(3*H*)-dione (2.112). Oxime **2.111** (2.73 g; 11.37 mmol) was suspended in 37% aqueous formaldehyde (31.53 mL; 1.14 mol; 100 equiv.) and conc. HCl (28.80 mL; 0.34 mol; 30 equiv.) and the yellow suspension was stirred at room temperature for 18 hours. The solution was diluted with water and extracted with DCM. The combined organic layers were washed with water and brine, dried over $MgSO_4$ and evaporated to yield 2.63 g (99%) of the diketone **2.112** as yellow amorphous solid. ^{1}H NMR (300 MHz, $CDCl_3$): δ 7.81 – 7.75 (m, 2H), 7.68 – 7.63 (m, 1H), 3.63 (s, 2H). ^{13}C NMR (101 MHz, $CDCl_3$): δ 198.7, 186.2, 147.9, 135.6, 133.4, 132.6, 130.9, 127.1, 36.4. HRMS (ESI) m/z calcd. for $C_9H_4O_2Br$ $[M-H]^-$: 222.9395, found: 222.9397.

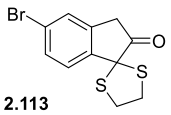

2.113

5-Bromospiro[indene-1,2'-[1,3]dithiolan]-2(3*H*)-one (2.113). To ice cold solution of diketone **2.112** (2.60 g; 11.55 mmol) in anhydrous DCM (60 mL) was added ethanedithiol (1.07 mL; 12.71 mmol; 1.1 equiv.) followed by dropwise addition of $BF_3 \times Et_2O$ (1.45 mL; 11.55 mmol; 1 equiv.). The orange solution was warmed to room temperature and stirred for 16 hours. The solution was diluted with DCM and washed with water, 0.5 M aqueous $Cu(NO_3)_2$ solution and brine. The organic layer was dried over $MgSO_4$, evaporated under reduced pressure and purified by flash chromatography on silica (100% hexanes to 40% EtOAc in hexanes) to afford 2.64 g (76%) of ketone **2.113** as yellow amorphous solid. ^{1}H NMR (400 MHz, MeOH-d_4): δ 7.84 (s, 1H), 7.79 – 7.56 (m, 2H), 3.84 (s, 2H). ^{13}C NMR (101 MHz, MeOH-d_4): δ 190.8, 155.2, 150.7, 137.9, 132.6, 132.0, 131.5, 126.4, 29.0. HRMS (ESI) m/z calcd. for $C_{11}H_{10}OS_2Br$ $[M+H]^+$: 300.9356, found: 300.9355.

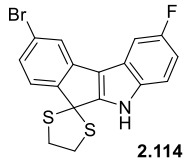

2.114

9-Bromo-2-fluoro-5*H*-spiro[indeno[2,1-b]indole-6,2'-[1,3]dithiolane] (2.114). Solution of ketone **2.113** (600 mg; 1.99 mmol) and 4-fluorophenylhydrazine hydrochloride **2.85** (389 mg; 2.39 mmol; 1.2 equiv.) in *i*PrOH (20 mL) was stirred at 70 °C for 18 hours. The orange solution was cooled to room temperature and filtered through sintered glass filter. The filtrate was evaporated under reduced pressure and the residue was purified by flash chromatography on silica (100% hexanes to 60% EtOAc in hexanes) to yield 537 mg (69%) of indole **2.114** as yellow amorphous solid. ^{1}H NMR (400 MHz, $CDCl_3$): δ 8.33 (s, 1H), 7.56 (d, *J* = 1.8 Hz, 1H), 7.45 – 7.35 (m, 2H), 7.32 (dd, *J* = 8.9, 4.3 Hz, 1H), 7.26 (dd, *J* = 8.1, 1.9 Hz, 1H), 6.99 (td, *J* = 9.1, 2.5 Hz, 1H), 3.83 – 3.65 (m, 4H). ^{13}C NMR (101 MHz, $CDCl_3$): δ 158.8 (d, *J* = 237.3 Hz), 152.0, 150.6, 138.8, 137.6, 127.2, 126.0, 122.9, 122.2, 122.0 (d, *J* = 10.3 Hz), 118.3 (d, *J* = 4.5 Hz), 113.2 (d, *J* = 9.7 Hz), 111.4 (d, *J* = 26.2 Hz), 105.2 (d, *J* = 24.0 Hz), 62.3, 42.3. ^{19}F NMR (376 MHz, $CDCl_3$): δ -122.02. HRMS (ESI) m/z calcd. for $C_{17}H_{11}NFS_2Br$ $[M]^+$: 390.9500, found: 390.9500.

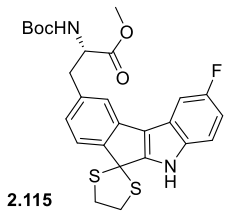

2.115

Methyl (*S*)-2-((*tert*-butoxycarbonyl)amino)-3-(2-fluoro-5*H*-spiro[indeno[2,1-*b*]indole-6,2'-[1,3]dithiolan]-9-yl)propanoate (2.115). The aryl bromide **2.114** (500 mg; 1.27 mmol), $Pd_2(dba)_3$ (23 mg; 0.026 mmol; 0.02 equiv.) and SPhos (26 mg; 0.064 mmol; 0.05 equiv.) were dissolved in anhydrous DMF (40 mL) under argon atmosphere. Alkyl zincate **2.81** (0.5 M in DMF; 3.06 mL; 1.53 mmol; 1.2 equiv.) was added and the yellow solution was stirred at 60 °C for three hours. Then the mixture was cooled to 0 °C, quenched with saturated aqueous NH_4Cl solution and extracted with EtOAc. The combined organic extracts were washed with water and brine, dried over $MgSO_4$ and evaporated under reduced pressure. The residue was purified by flash chromatography on silica (100% hexanes to 60% EtOAc in hexanes) to yield 510 mg (78%) of the ester **2.115** as yellow amorphous solid. ^{1}H NMR (400 MHz, $CDCl_3$): δ 8.85 – 8.64 (m, 1H), 7.46 (d, *J* = 7.6 Hz, 1H), 7.36 (d, *J* = 8.6 Hz, 1H), 7.28 (dd, *J* = 8.9, 4.3 Hz, 1H), 7.19 (s, 1H), 6.95 (td, *J* = 9.1, 2.5 Hz, 1H), 6.87 (d, *J* = 7.6 Hz, 1H), 5.16 – 4.97 (m, 1H), 4.66 (q, *J* = 6.6 Hz, 1H), 3.79 – 3.62 (m, 7H), 3.14 (qd, *J* = 13.9, 5.9 Hz, 2H), 1.44 (s, 9H). ^{13}C NMR (101 MHz, $CDCl_3$): δ 172.4, 158.4 (d, *J* = 236.3 Hz), 155.2, 152.0, 150.0, 137.6, 137.3, 136.6, 125.2, 124.6, 121.9 (d, *J* = 10.2 Hz), 119.8, 118.7 (d, *J* = 3.4 Hz), 113.1 (d, *J* = 9.9 Hz), 110.7 (d, *J* = 26.1 Hz), 104.8 (d, *J* = 24.0 Hz), 80.1, 62.3, 54.5, 52.3, 41.9, 41.9, 38.3, 28.3. ^{19}F NMR (376 MHz, $CDCl_3$): δ -122.66. HRMS (ESI) m/z calcd. for $C_{26}H_{27}N_2O_4FNaS_2$ $[M+Na]^+$: 537.1294, found: 537.1293. $[\alpha]^{20}_D$ +54 (*c* 2.0, MeOH).

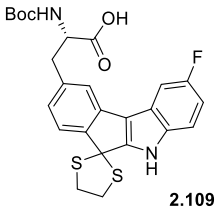

2.109

(*S*)-2-((*tert*-Butoxycarbonyl)amino)-3-(2-fluoro-5*H*-spiro[indeno[2,1-*b*]indole-6,2'-[1,3]dithiolan]-9-yl)propanoic acid (2.109). To a solution of ester **2.115** (500 mg; 0.97 mmol) in MeOH and THF mixture (1:1 v/v; 20 mL) was added LiOH (47 mg; 1.94 mmol; 2 equiv.) solution in water (10 mL). The brown solution was stirred at room temperature for one hour. The organic solvents were evaporated under reduced pressure and the remaining water solution was acidified with 1 M aqueous HCl solution to pH 4 and extracted with EtOAc. The combined organic extracts were dried over $MgSO_4$ and evaporated under reduced pressure to yield 446 mg (92%) of the carboxylic acid **2.109** as light yellow amorphous solid. ^{1}H NMR

(400 MHz, MeOH-d_4): δ 7.49 – 7.39 (m, 2H), 7.38 – 7.32 (m, 2H), 6.97 – 6.88 (m, 2H), 4.44 (dd, *J* = 9.0, 4.9 Hz, 1H), 3.75 (dtd, *J* = 14.2, 7.4, 2.5 Hz, 4H), 3.23 (dd, *J* = 13.8, 4.9 Hz, 1H), 2.98 (dd, *J* = 13.8, 9.0 Hz, 1H), 1.37 – 1.26 (m, 9H). ^{13}C NMR (101 MHz, MeOH-d_4): δ 175.5, 159.6 (d, *J* = 233.9 Hz), 157.8, 155.5, 149.7, 139.4, 139.2, 139.1, 125.9, 125.8, 122.8 (d, *J* = 10.4 Hz), 120.5, 118.1 (d, *J* = 4.5 Hz), 114.2 (d, *J* = 9.9 Hz), 110.8 (d, *J* = 26.3 Hz), 105.2 (d, *J* = 24.1 Hz), 80.6, 63.6, 56.3, 42.5, 38.9, 28.7. ^{19}F NMR (376 MHz, $CDCl_3$): δ -122.47. HRMS (ESI) m/z calcd. for $C_{25}H_{25}N_2O_4FS_2$ $[M]^+$: 500.1240, found: 500.1264. $[\alpha]^{20}_D$ +34 (*c* 1.4, MeOH).

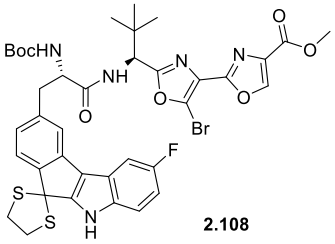

2.108

Methyl 5'-bromo-2'-((*S*)-1-((*S*)-2-((*tert*-butoxycarbonyl)amino)-3-(2-fluoro-5*H*-spiro[indeno[2,1-*b*]indole-6,2'-[1,3]dithiolan]-9-yl)propanamido)-2,2-dimethylpropyl)-[2,4'-bioxazole]-4-carboxylate (2.108). Amine **2.93** (34 mg; 0.095 mmol; 1.1 equiv.), carboxylic acid **2.109** (43 mg; 0.086 mmol; 1.5 equiv.) and EDC×HCl (33 mg; 0.17 mmol; 2 equiv.) were dissolved in anhydrous pyridine (1.3 mL) and the orange solution was stirred at room temperature for three hours. The solvent was evaporated under reduced pressure and the orange residue was purified by reverse phase flash chromatography (10% MeCN in 0.1% aq. AcOH to 100% MeCN) to yield 47 mg (65%) of the amide **2.108** as a yellow amorphous solid. ^{1}H NMR (600 MHz, $CDCl_3$): δ 8.37 (s, 1H), 8.23 (s, 1H), 7.44 (d, *J* = 7.7 Hz, 1H), 7.39 (dd, *J* = 9.2, 2.4 Hz, 1H), 7.30 (d, *J* = 1.6 Hz, 1H), 7.28 (dd, *J* = 8.9, 4.3 Hz, 1H), 6.97 (dd, *J* = 7.7, 1.6 Hz, 1H), 6.94 (td, *J* = 8.9, 2.4 Hz, 1H), 6.91 – 6.82 (m, 1H), 5.09 (d, *J* = 9.2 Hz, 1H), 5.07 (d, *J* = 8.5 Hz, 1H), 4.39 (q, *J* = 7.5 Hz, 1H), 3.93 (s, 3H), 3.77 – 3.72 (m, 2H), 3.71 – 3.65 (m, 2H), 3.17 – 3.07 (m, 2H), 1.43 (s, 9H), 0.95 (s, 9H). ^{13}C NMR (151 MHz, $CDCl_3$): δ 171.2, 164.8, 161.5, 158.6 (d, *J* = 236.6 Hz), 155.8, 154.8, 151.7, 150.3, 144.0, 137.6, 137.5, 134.6, 128.0, 125.6, 124.8, 123.2, 122.1 (d, *J* = 10.2 Hz), 119.9, 119.1, 113.1 (d, *J* = 9.8 Hz), 111.0 (d, *J* = 26.2 Hz), 105.2 (d, *J* = 24.0 Hz), 80.7, 62.3, 56.2, 55.9, 52.4, 42.1, 42.1, 37.5, 35.9, 28.4, 26.4. ^{19}F NMR (376 MHz, $CDCl_3$): δ -122.38. HRMS (ESI) m/z calcd. for $C_{38}H_{39}N_5O_7FNaS_2Br$ $[M+Na]^+$: 862.1356, found: 862.1359. $[\alpha]^{20}_D$ +14 (*c* 0.8, $CDCl_3$).

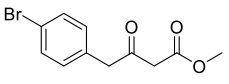

2.129

Methyl 4-(4-bromophenyl)-3-oxobutanoate (2.129). To a solution of 2-(4-bromophenyl)acetic acid (**2.125**) (5.00 g; 23.3 mmol) and anhydrous DMF (0.09 mL; 1.2 mmol; 0.05 equiv.) in anhydrous toluene (50 mL) was slowly added oxalyl chloride (2.6 mL; 30.2 mmol; 1.3 equiv.). The clear yellow solution was stirred at room temperature for 30 minutes and 2.5 hours at 55 °C. The solution was then cooled to ambient temperature and solvents were evaporated under reduced pressure. The residual yellow oil was dissolved in anhydrous DCM (20 mL) and slowly added to solution of Meldrum's acid (3.35 g; 23.2 mmol; 1.0 equiv.) and pyridine (3.70 mL; 46.4 mmol; 2.0 equiv.) in anhydrous DCM (30 mL) at 0 °C. The red solution was slowly warmed to room temperature and stirred for 18 hours. The solution was diluted with DCM and washed with 0.1 M aqueous HCl solution. The organic layer was dried over $MgSO_4$, filtered and evaporated under reduced pressure. The red amorphous solid was dissolved in anhydrous toluene (50 mL) and MeOH (4.70 mL; 116.1 mmol; 10 equiv.) was added. The red solution was refluxed for three hours after which the solvents were evaporated under reduced pressure and the residue was purified by column chromatography on silica (100% hexanes to 30% EtOAc in hexanes). Ketoester **2.129** was obtained as a yellow oil (2.04 g, 65%) that solidified upon standing in room temperature. ^{1}H NMR (400 MHz, $CDCl_3$): δ 7.39 (m, 2H), 7.01 (m, 2H), 3.72 (s, 2H), 3.65 (s, 3H), 3.40 (s, 2H). ^{13}C KMR (101 MHz, $CDCl_3$): δ 199.4, 167.4, 132.0, 131.9, 131.2, 121.4, 52.4, 49.1, 48.1. HRMS-ESI (*m/z*) calcd. for $C_{11}H_{10}O_3Br$ $[M-H]^-$ 268.9813; found 268.9812.

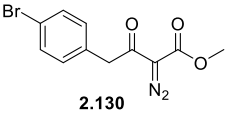

2.130

Methyl 4-(4-bromophenyl)-2-diazo-3-oxobutanoate (2.130). To ice cold solution of ketoester **2.129** (2.04 g; 7.5 mmol) in anhydrous MeCN (25 mL) was added TEA (1.05 mL; 7.5 mmol; 1 equiv.) followed by dropwise addition of *p*-acetamidobenzenesulfonylazide **2.60** (1.90 g; 7.9 mmol; 1.0 equiv.) solution in anhydrous MeCN (15 mL). The clear orange solution was stirred at room temperature for 24 hours after which the solvent was evaporated under reduced pressure. The residue was suspended in Et_2O, filtered, and evaporated under reduced pressure. Purification by column chromatography on silica (100% hexanes to 40% EtOAc in hexanes) yielded 1.68 g (75%) of compound **2.130** as light yellow amorphous solid. ^{1}H NMR (400 MHz, $CDCl_3$): δ 7.43 (d, J = 8.4 Hz, 2H), 7.17 (d, J = 8.4 Hz, 2H), 4.07 (s,

2H), 3.78 (s, 3H). ^{13}C NMR (101 MHz, $CDCl_3$): δ 188.5, 161.5, 132.8, 131.6, 131.4, 121.1, 52.3, 45.1. HRMS (ESI) m/z calcd. for $C_{11}H_9N_2O_3Br$ [M-H]$^-$ 294.9718; found 294.9709.

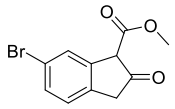

2.131

Methyl 6-bromo-2-oxo-2,3-dihydro-1*H*-indene-1-carboxylate (**2.131**). To a solution of $Rh_2(TFA)_4$ (44.3 mg; 0.067 mmol; 0.02 equiv.) in anhydrous DCM (25 mL) was added solution of diazoketone **2.130** (1.00 g; 3.37 mmol) in anhydrous DCM (25 ml) at room temperature over period of 30 minutes. The solvent was then evaporated under reduced pressure and the green residue was suspended in hexanes (5 mL), filtered, and washed on filter with MeCN (1 mL). Filtrate was evaporated under reduced pressure and the solid material was suspended in hexanes (5 mL), filtered, and washed on filter with MeCN (1 mL). The residual solids were combined to yield 815 mg (90%) of compound **2.131** as white amorphous solid. ^{1}H NMR (400 MHz, $CDCl_3$): δ 11.05 (s, 1H), 7.70 (d, *J* = 1.8 Hz, 1H), 7.23 (dd, *J* = 7.9, 1.8 Hz, 1H), 7.14 (d, J = 7.9 Hz, 1H), 3.97 (s, 3H), 3.53 (s, 2H). ^{13}C NMR (101 MHz, $CDCl_3$): δ 181.4, 141.5, 131.7, 126.5, 124.9, 123.2, 121.2, 104.6, 51.7, 37.3. HRMS (ESI) m/z calcd. for $C_{11}H_8O_3Br$ [M-H]$^-$ 266.9657; found 266.9660.

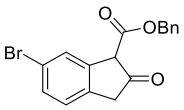

2.132

Benzyl 6-bromo-2-oxo-2,3-dihydro-1*H*-indene-1-carboxylate (**2.132**). To a solution of **2.131** (120 mg; 0.45 mmol) in anhydrous toluene (15 mL) was added benzyl alcohol (0.19 mL; 1.80 mmol; 4.0 equiv.) and BF_3×OEt_2 (11 µL; 0.089 mmol; 0.20 equiv.). The solution was heated at 110 °C for 18 hours. Then the flask was cooled to room temperature and the solvent was evaporated under reduced pressure. The light brown residue was suspended in hexanes (2 mL), filtered, and washed on filter with MeCN (1 mL). Filtrate was evaporated and the solid material was suspended in hexanes (2 mL), filtered, and washed on filter with MeCN (1 mL). The residual solids were combined to yield 111 mg (72%) of compound **2.132** as white amorphous solid. ^{1}H NMR (400 MHz, $CDCl_3$): δ 11.01 (s, 1H), 7.71 (d, *J* = 1.8 Hz, 1H), 7.47-7.34 (m, 5H), 7.21 (dd, *J* = 7.9, 1.8 Hz, 1H), 7.14 – 7.09 (m, 1H), 5.41 (s, 2H), 3.51 (s, 2H). ^{13}C NMR (101 MHz, $CDCl_3$): δ 181.7, 141.5, 135.5, 131.7, 128.7, 128.4, 128.1, 126.5, 124.9, 123.4, 121.2, 104.6, 66.4, 37.3. HRMS (ESI) m/z calcd. for $C_{17}H_{12}O_3Br$ [M-H]$^-$ 342.9970; found 342.9964.

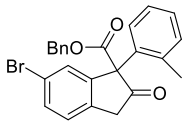

2.135

Benzyl 6-bromo-2-oxo-1-(*o*-tolyl)-2,3-dihydro-1*H*-indene-1-carboxylate (2.135). Ketoester **2.132** (62 mg; 0.18 mmol) and freshly re-crystalized *o*-tolyllead triacetate (**2.134**) (prepared according to method described by[126]) (128 mg; 0.27 mmol; 1.5 equiv.) were dissolved in $CHCl_3$ (2.5 mL) at room temperature. To the red solution was added anhydrous pyridine (65 µL; 0.81 mmol; 4.5 equiv.) and the solution was stirred at 50 °C for five hours. The orange suspension was cooled to room temperature and poured into aqueous saturated NH_4Cl solution and extracted with DCM. Organic extracts were combined, washed with brine, dried over $MgSO_4$ and evaporated under reduced pressure. The orange oil was purified by reverse phase flash chromatography (10% MeCN in H_2O to 100% MeCN) to yield 58 mg (74%) of compound **2.135** as light-yellow oil. ^{1}H NMR (400 MHz, $CDCl_3$): δ 7.54 – 7.49 (m, 2H), 7.34 – 7.27 (m, 4H), 7.24 – 7.18 (m, 4H), 7.08 – 7.02 (m, 1H), 6.76 – 6.72 (m, 1H), 5.26, 5.14 (ABq, *J* = 12.0 Hz, 2H), 3.74, 3.56 (ABq, *J* = 22.5 Hz, 2H), 2.26 (s, 3H). ^{13}C NMR (101 MHz, $CDCl_3$): δ 206.8, 169.6, 142.5, 138.2, 136.3, 135.2, 134.8, 132.6, 132.4, 130.2, 128.7, 128.6, 128.6, 128.4, 128.4, 126.7, 125.8, 121.9, 70.5, 68.0, 42.4, 21.2. HRMS (ESI) m/z calcd. for $C_{24}H_{18}O_3Br$ $[M-H]^-$ 433.0439; found 433.0450.

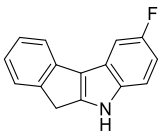

2.140

2-Fluoro-5,6-dihydroindeno[2,1-*b*]indole (2.140). 2-Indanone **2.139** (2.00 g; 15.13 mmol) and 4-fluorophenylhydrazine hydrochloride (**2.85**) (2.95 g; 18.16 mmol; 1.2 equiv.) were suspended in *i*PrOH (40 mL) and the brown mixture was stirred at 75 °C for 18 hours The suspension was cooled to room temperature, filtered through sintered glass filter and washed with *i*PrOH. The filtrate was evaporated under reduced pressure and purified by flash chromatography on silica (100% hexanes to 60% EtOAc in hexanes) to afford 2.77 g (82%) of the compound **2.140** as green amorphous solid. ^{1}H NMR (400 MHz, $CDCl_3$): δ 8.27 (s, 1H), 7.60 (d, *J* = 7.5 Hz, 1H), 7.50 (dd, *J* = 9.4, 2.3 Hz, 1H), 7.47 – 7.40 (m, 1H), 7.38 – 7.33 (m, 1H), 7.33 – 7.27 (m, 1H), 7.12 (t, *J* = 7.4 Hz, 1H), 6.95 (td, *J* = 9.1, 2.5 Hz, 1H), 3.76 (s, 2H). ^{13}C NMR (101 MHz, $CDCl_3$): δ 158.4 (d, *J* = 235.0 Hz), 147.9, 142.3, 139.6, 137.1, 127.3, 124.9, 123.0, 122.5, 118.5, 112.3 (d, *J* = 9.9 Hz), 109.6 (d, *J* = 26.1 Hz), 104.7 (d, *J* =

24.0 Hz), 31.4. ^{19}F NMR (376 MHz, $CDCl_3$): δ -123.59. HRMS (ESI) m/z calcd. for $C_{15}H_{10}NF$ $[M]^+$: 223.0797, found: 223.0802.

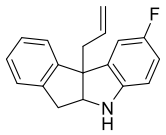

2.141

10*b*-Allyl-2-fluoro-5,5*a*,6,10*b*-tetrahydroindeno[2,1-*b*]indole (2.141). Indole **2.140** (4.25 g; 19.04 mmol) was dissolved in anhydrous 1,4-dioxane (105 mL) and solid NaO*t*Bu (1.92 g; 20.00 mmol; 1.05 equiv.) was added in one portion. The dark red suspension was stirred at room temperature for 20 minutes after which Et_3B (1 M in THF; 20.00 mL; 20.00 mmol; 1.05 equiv.) was added dropwise. The red-brown suspension was stirred at room temperature for 30 minutes after which allyl bromide (2.25 mL; 26.65 mmol; 1.4 equiv.) was added and the stirring was continued for three hours. Then the reaction was quenched with aqueous saturated NH_4Cl solution and extracted with EtOAc. The combined extracts were washed with brine, dried over $MgSO_4$ and evaporated under reduced pressure. The resulting orange oil was dissolved in AcOH (105 mL) and $NaCNBH_3$ (3.59 g; 57.11 mmol; 3 equiv.) was added in one portion. The orange solution was stirred at room temperature for one hour after which the solvent was evaporated under reduced pressure, the residue was dissolved in EtOAc and washed with aqueous saturated $NaHCO_3$ solution and brine. The organic extract was dried over $MgSO_4$ and evaporated under reduced pressure and the resulting material was purified by flash chromatography on silica (100% hexanes to 40% EtOAc in hexanes) to yield 3.44 g (68%) alkene **2.141** as yellow amorphous solid. ^{1}H NMR (400 MHz, $CDCl_3$): δ 7.33 – 7.25 (m, 1H), 7.26 – 7.13 (m, 3H), 7.02 (dd, *J* = 8.4, 2.6 Hz, 1H), 6.71 (ddd, *J* = 9.2, 8.5, 2.6 Hz, 1H), 6.49 (dd, *J* = 8.5, 4.3 Hz, 1H), 5.56 (ddt, *J* = 17.1, 10.1, 7.2 Hz, 1H), 5.13 – 5.03 (m, 1H), 5.06 – 4.98 (m, 1H), 4.53 (dd, *J* = 6.4, 2.1 Hz, 1H), 3.29 (dd, *J* = 16.6, 6.4 Hz, 1H), 3.01 (dd, *J* = 16.6, 1.8 Hz, 1H), 2.82 – 2.65 (m, 2H). ^{13}C NMR (101 MHz, $CDCl_3$): δ 157.4 (d, *J* = 235.7 Hz), 146.0, 145.7, 141.5, 135.3 (d, *J* = 7.3 Hz), 134.1, 127.5, 127.3, 125.3, 123.4, 118.3, 114.0 (d, *J* = 23.3 Hz), 110.4 (d, *J* = 23.8 Hz), 110.0 (d, *J* = 8.2 Hz), 68.6, 62.9 (d, *J* = 1.9 Hz), 43.2, 40.4. ^{19}F NMR (376 MHz, $CDCl_3$): δ -125.80. HRMS (ESI) m/z calcd. for $C_{18}H_{17}NF$ $[M+H]^+$: 266.1345, found: 266.1353.

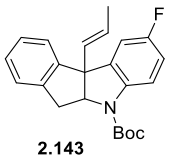

2.143

***tert*-Butyl (*E*)-2-fluoro-10*b*-(prop-1-en-1-yl)-6,10*b*-dihydroindeno[2,1-*b*]indole-5(5a*H*)-carboxylate (2.143).** Alkene **2.141** (3.42 g; 12.89 mmol) was dissolved in absolute EtOH (150 mL) and $RhCl_3 \times H_2O$ (293 mg; 1.29 mmol; 0.1 equiv.) and anhydrous K_2CO_3 (1.78 g; 12.89 mmol; 1 equiv.) were added. The deep brown suspension was stirred at 65 °C for 40 hours. The solvent was evaporated under reduced pressure and the black residue was partitioned between aqueous saturated NH_4Cl solution and EtOAC. The water layer was extracted with EtOAc and the combined organic extracts were washed with water and brine, dried over $MgSO_4$ and evaporated under reduced pressure. The residue was purified by flash chromatography on silica (10% DCM in hexanes to 100% DCM) to yield 1.32 g (39%) of a mixture of alkenes (8 : 2 internal : terminal) as brown amorphous solid. The prepared mixture of the alkenes (1.20 g; 4.53 mmol) was dissolved in anhydrous THF and cooled to 0 °C. KHMDS (1 M in THF; 5.43 mL; 5.43 mmol; 1.2 equiv.) was added dropwise and the dark red solution was stirred at 0 °C for 15 minutes after which the Boc_2O (1.28 g; 5.88 mmol; 1.3 equiv.) was added as a solid in one portion. The solution was warmed to r.t and stirred for three hours. The reaction was quenched with aqueous saturated NH_4Cl solution and EtOAc was added. The layers were separated, and the organic layer was washed with water and brine, dried over $MgSO_4$ and evaporated under reduced pressure. The residue was purified by flash chromatography on silica (100% hexanes to 40% EtOAc in hexanes) to yield 910 mg (55%) of the alkene **2.143** as yellow amorphous solid. ^{1}H NMR (400 MHz, MeOH-d_4): δ 7.34 (d, J = 7.4 Hz, 1H), 7.27 – 7.16 (m, 4H), 7.02 (dd, J = 8.3, 2.7 Hz, 1H), 6.89 (td, J = 8.9, 2.7 Hz, 1H), 5.81 (dq, J = 15.4, 1.6 Hz, 1H), 5.33 (dq, J = 15.4, 6.5 Hz, 1H), 4.83 (dd, J = 7.9, 4.1 Hz, 1H), 3.59 (dd, J = 17.4, 7.9 Hz, 1H), 3.05 (dd, J = 17.4, 4.1 Hz, 1H), 1.71 (dd, J = 6.5, 1.6 Hz, 3H), 1.59 (s, 9H). ^{13}C NMR (101 MHz, MeOH-d_4): δ 160.3 (d, J = 240.1 Hz), 148.4, 146.0, 142.1, 135.9, 134.6, 128.8, 128.4, 127.9, 125.9, 125.7, 124.3, 119.2, 116.9, 115.1 (d, J = 23.2 Hz), 112.6 (d, J = 24.1 Hz), 86.4, 73.2, 28.7, 27.6, 17.9. ^{19}F NMR (376 MHz, MeOH-d_4): δ -122.72. LRMS (ESI) m/z calcd. for $C_{23}H_{25}FNO_2$ $[M+H]^+$: 366.2, found: 366.1.

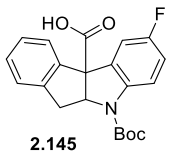

2.145

5-(*tert*-Butoxycarbonyl)-2-fluoro-5*a*,6-dihydroindeno[2,1-*b*]indole-10*b*(5*H*)-carboxylic acid (2.145). Alkene **2.143** (595 mg; 1.63 mmol) was dissolved in mixture of anhydrous DCM and MeOH (10:1 v/v; 33 mL) and cooled to -78 °C. A stream of ozone in oxygen was passed through the yellow solution for 15 minutes while maintaining the temperature of the solution below -70 °C. The remaining ozone was sparged from the solution by stream of argon. Me_2S (598 µL; 8.14 mmol; 5 equiv.) was added after which the solution was warmed to room temperature and stirred for 18 hours. The remaining Me_2S was sparged from the solution by stream of argon and the solvent was evaporated under reduced pressure. The residue was purified by flash chromatography on silica (100% hexanes to 40% EtOAc in hexanes) to yield 475 mg (83%) of the aldehyde **2.144** as yellow amorphous solid. The freshly prepared aldehyde **2.144** (475 mg; 1.34 mmol) was dissolved in DMSO (12 mL) and resorcinol (296 mg; 2.68 mmol; 2 equiv.) was added followed by NaH_2PO_4 (371 mg; 2.68 mmol; 2 equiv.) solution in water (2 mL). The solution became warm and was cooled to 5 °C. Then $NaClO_2$ (243 mg; 2.68 mmol; 2 equiv.) solution in water (2 mL) was added and the bright purple solution was stirred at room temperature for two hours. The reaction was quenched with aqueous saturated NH_4Cl solution, acidified with 1 M aqueous HCl solutionto pH 3 and extracted with EtOAc. The combined organic extracts were dried over $MgSO_4$ and evaporated under reduced pressure. The residue was purified by reverse phase flash chromatography (10% MeCN in water to 100% MeCN) to afford 330 mg (67%) of carboxylic acid **2.145** as colorless amorphous solid. ^{1}H NMR (400 MHz, MeOH-d_4): δ 7.76 – 7.65 (m, 1H), 7.43 (dd, *J* = 8.5, 2.7 Hz, 1H), 7.32 – 7.13 (m, 4H), 6.94 (td, *J* = 8.9, 2.7 Hz, 1H), 5.57 (dd, *J* = 8.2, 3.6 Hz, 1H), 3.73 (dd, *J* = 17.7, 8.2 Hz, 1H), 3.13 (dd, *J* = 17.7, 3.6 Hz, 1H), 1.61 (s, 9H). ^{13}C NMR (101 MHz, MeOH-*d4*): δ 174.0, 160.2 (d, *J* = 239.8 Hz), 143.0, 142.2, 129.6, 128.8 (d, *J* = 2.3 Hz), 128.5, 126.0, 125.5, 124.2, 116.7, 116.0 (d, *J* = 23.2 Hz), 113.2 (d, *J* = 25.2 Hz), 70.5, 68.9, 41.8, 28.7, 28.7. ^{19}F NMR (376 MHz, MeOH-*d4*): δ -122.71. LRMS (ESI) m/z calcd. for $C_{21}H_{20}FNO_4$ $[M]^+$: 369.1, found: 369.0.

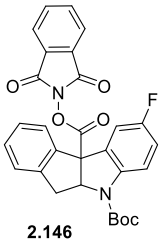

2.146

5-(*tert*-Butyl) 10*b*-(1,3-dioxoisoindolin-2-yl) 2-fluoro-5*a*,6-dihydroindeno[2,1-*b*]indole-5,10*b*-dicarboxylate (2.146). To suspension of carboxylic acid **2.145** (300 mg; 0.81 mmol), *N*-hydroxyphtalimide (132 mg; 0.81 mg; 1 equiv.) and DMAP (9.9 mg; 0.081 mmol; 0.1 equiv.) in anhydrous DCM (10 mL) was added DIC (139 µL; 0.89 mmol; 1.1 equiv.). The yellow suspension was stirred at room temperature for three hours after which it was filtered through a short plug of silica. The filtrate was evaporated under reduced pressure and the residue was purified by flash chromatography on silica (100% hexanes to 40% EtOAc in hexanes) to yield 230 mg (55%) of compound **2.146** as colorless amorphous solid. ^{1}H NMR (400 MHz, $CDCl_3$): δ 7.83 – 7.76 (m, 5H), 7.72 – 7.69 (m, 1H), 7.43 (dd, *J* = 8.5, 2.8 Hz, 1H), 7.28 – 7.21 (m, 3H), 6.94 (td, *J* = 8.9, 2.8 Hz, 1H), 5.56 (dd, *J* = 8.2, 3.7 Hz, 1H), 3.72 (dd, *J* = 17.7, 8.2 Hz, 1H), 3.13 (dd, *J* = 17.7, 3.7 Hz, 1H), 1.61 (s, 9H). ^{13}C NMR (101 MHz, $CDCl_3$): δ 173.9, 165.8, 160.1 (d, *J* = 239.7 Hz), 153.5, 142.9, 142.1, 139.1, 135.5, 134.4, 130.5, 129.6, 128.5, 126.0, 125.5, 124.0, 116.7, 116.0 (d, *J* = 23.3 Hz), 113.1 (d, *J* = 25.1 Hz), 68.9, 67.6, 41.8, 28.7. ^{19}F NMR (376 MHz, $CDCl_3$): δ -122.66. LRMS (ESI) m/z calcd. for $C_{25}H_{16}FN_2O_6$ [M-*t*Bu+2H]$^+$: 459.1, found: 459.0.

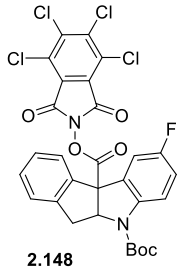

2.148

5-(*tert*-Butyl) 10*b*-(4,5,6,7-tetrachloro-1,3-dioxoisoindolin-2-yl) 2-fluoro-5*a*,6-dihydroindeno[2,1-*b*]indole-5,10*b*-dicarboxylate (2.148). To suspension of carboxylic acid **2.145** (190 mg; 0.51 mmol), *N*-hydroxy tetrachlorophthalimide (155 mg; 0.51 mg; 1 equiv.) and DMAP (6.3 mg; 0.051 mmol; 0.1 equiv.) in anhydrous DCM (5 mL) was added DIC (88 µL; 0.57 mmol; 1.1 equiv.). The yellow suspension was stirred at room temperature for 18 hours after which it was filtered through a short plug of silica. Filtrate was evaporated to dryness under reduced pressure. Residue was purified by flash chromatography on silica (100% hexanes to 40% EtOAc in hexanes) to yield 107 mg (32%) of compound **2.148** as yellow amorphous solid. ^{1}H NMR

(400 MHz, $CDCl_3$): δ 7.75 – 7.70 (m, 1H), 7.41 – 7.29 (m, 3H), 7.28 – 7.19 (m, 2H), 6.97 (m, 1H), 5.71 (s, 1H), 3.85 (dd, *J* = 17.7, 8.1 Hz, 1H), 3.30 (d, *J* = 17.7 Hz, 1H), 1.63 (s, 9H). ^{13}C NMR (101 MHz, $CDCl_3$): δ 171.3, 165.8, 158.9 (d, *J* = 242.0 Hz), 151.7, 141.4, 139.5, 138.3, 130.7, 130.5, 129.5, 128.5, 128.2, 125.4, 124.7, 124.6, 116.5 (d, *J* = 23.0 Hz), 116.2 (d, *J* = 7.6 Hz), 112.3 (d, *J* = 25.1 Hz), 82.0, 68.2, 65.1, 41.7, 28.6. ^{19}F NMR (376 MHz, $CDCl_3$): δ -119.62. LRMS (ESI) m/z calcd. for $C_{25}H_{12}Cl_4FN_2O_6$ $[M\text{-}tBu+2H]^+$: 596.9, found: 596.8.

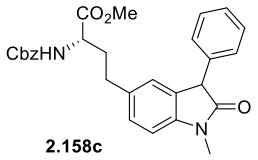

2.158c

Methyl (2*S*)-2-(((benzyloxy)carbonyl)amino)-4-(1-methyl-2-oxo-3-phenylindolin-5-yl)butanoate (2.158c). To a solution of methyl (*S*)-2-(((benzyloxy)carbonyl)amino)but-3-enoate **2.164** (prepared according to method described in[127]) (55 mg; 0.22 mmol) in THF (1 mL) was added 9-BBN (1.1 mL; 0.44 mmol; 0.5 M solution in THF; 2 equiv.) at 0 °C. After stirring for three hours at room temperature, K_3PO_4 (3 M solution in water; 0.22 mL; 0.66 mmol; 3 equiv.) was added dropwise. After stirring at room temperature for 30 min, the solution of $Pd(dppf)Cl_2$×DCM (1 mg; 0.1 mmol; 0.05 equiv.) and aryl iodide **2.161c** (synthesis described in[117]) (77 mg: 0.22 mmol; 1 equiv.) in degassed DMF (1 mL) was added. After stirring for 20 h at room temperature, the reaction was quenched with saturated aqueous NH_4Cl solution and EtOAc was added. Layers were separated and the water layer was extracted with EtOAc. Combined organic phases were washed with saturated $NaHCO_3$ solution and brine, dried over $MgSO_4$ and evaporated under reduced pressure. Product **2.158c** was purified by reverse phase flash chromatography (10% to 70% MeCN in water) to afford 30 mg (29%; 1:1 dr) as a yellow amorphous solid. ^1H NMR (400 MHz, $CDCl_3$): δ 7.40 – 7.27 (m, 8H), 7.22 – 7.15 (m, 2H), 7.12 (d, *J* = 8.0 Hz, 1H), 6.97 (s, 1H), 6.80 (d, *J* = 8.0 Hz, 1H), 5.39 – 5.30 (m, 1H), 5.13 – 5.09 (m, 2H), 4.57 (s, 1H), 4.44 – 4.35 (m, 1H), 3.71 (s, 3H), 3.23 (s, 3H), 2.67 – 2.57 (m, 2H), 2.19 – 2.07 (m, 1H), 1.98 – 1.87 (m, 1H). ^{13}C NMR (101 MHz, $CDCl_3$): δ 176.0, 172.8, 155.9, 142.9, 136.8, 136.3, 135.2, 129.3, 129.3, 129.0, 128.7, 128.6, 128.6, 128.4, 128.3, 128.2, 127.7, 125.3, 125.2, 108.2, 67.2, 53.6, 52.6, 52.5, 52.2, 34.7, 31.3, 31.3, 26.6. HRMS (ESI) *m/z* calcd. for $C_{28}H_{29}N_2O_5$ $[M+H]^+$: 473.2076, found: 473.2079.

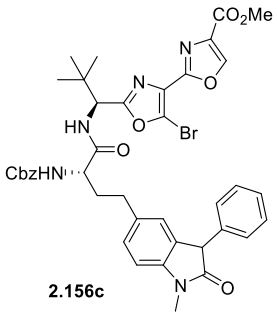

2.156c

Methyl 2'-((1*S*)-1-((2*S*)-2-(((benzyloxy)carbonyl)amino)-4-(1-methyl-2-oxo-3-phenylindolin-5-yl)butanamido)-2,2-dimethylpropyl)-5'-bromo-[2,4'-bioxazole]-4-carboxylate (2.156c). Methyl ester **2.158c** (50 mg; 0.11 mmol) was dissolved in MeOH/water mixture (3:2 v/v; 3.5 mL) and stream of argon was passed through the solution for 20 minutes. Solid LiOH (8 mg; 0.33 mmol; 3 equiv.) was added and the clear solution was stirred at room temperature for two hours. Solution was then acidified with 1 M aqueous HCl solution to pH 4 and MeOH was evaporated under reduced pressure. The resulting suspension was extracted with EtOAc, combined organic layers were washed with brine, dried over Na_2SO_4 and evaporated to dryness under reduced pressure. To the resulting crude carboxylic acid was added amine **2.93** (38 mg; 0.11 mmol; 1 equiv.), EDC×HCl (27 mg; 0.14 mmol; 1.3 equiv.) and anhydrous pyridine (1 mL). The resulting suspension was stirred at room temperature for one hour. The orange solution was then evaporated to dryness under reduced pressure and the solid residue was dissolved in EtOAc, washed with 1 M aqueous HCl aolution and brine, dried over Na_2SO_4 and evaporated under reduced pressure. Purification by reverse phase chromatography (30% to 95% MeCN in water) afforded 31 mg (36%, 1:1 dr) of amide **2.156c** as a yellow oil. ^{1}H NMR (400 MHz, $CDCl_3$): δ 8.27 (s, 0.5H), 8.24 (s, 0.5H), 7.38 – 7.23 (m, 7H), 7.18 – 7.13 (m, 2H), 7.09 (d, *J* = 7.9 Hz, 1H), 6.96 (s, 1H), 6.78 (d, *J* = 7.9 Hz, 1H), 6.77 (d, *J* = 7.9 Hz, 1H), 5.22 (dd, *J* = 7.9, 2.7 Hz, 1H), 5.13 – 5.10 (m, 2H), 5.07 (d, *J* = 2.0 Hz, 1H), 5.05 (d, *J* = 2.0 Hz, 1H), 4.57 (s, 0.5H), 4.53 (s, 0.5H), 4.18 – 4.09 (m, 1H), 3.94 (s, 3H), 3.218 (s, 1.5H), 3.215 (s, 1.5H), 2.64 – 2.55 (m, 2H), 2.16 – 2.04 (m, 1H), 1.97 – 1.81 (m, 1H), 0.95 (s, 9H). ^{13}C NMR (101 MHz, $CDCl_3$): δ 176.1, 176.1, 171.2, 171.2, 165.0, 161.3, 156.4, 154.8, 154.8, 144.1, 143.0, 136.8, 136.8, 136.1, 135.2, 134.7, 134.7, 129.4, 129.4, 129.0, 128.7, 128.6, 128.5, 128.4, 128.3, 128.1, 127.7, 125.2, 123.3, 108.3, 108.3, 67.4, 55.9, 54.4, 52.5, 52.3, 52.2, 35.9, 33.6, 33.5, 31.4, 26.6, 26.3. HRMS (ESI) *m/z* calcd. for $C_{40}H_{41}N_5O_8Br$ $[M+H]^+$: 798.2139, found: 798.2137

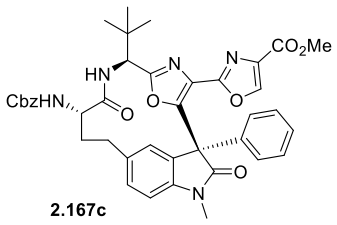

2.167c

Methyl 2-((23*S*,5*S*,8*S*)-5-(((benzyloxy)carbonyl)amino)-8-(*tert*-butyl)-2^1-methyl-2^2,6-dioxo-2^3-phenyl-7-aza-1(5,2)-oxazola-2(3,5)-indolinacyclooctaphane-1^4-yl)oxazole-4-carboxylate (2.167c). Amide **2.156c** (31 mg; 0.04 mmol) and oven dried K_3PO_4 (25 mg; 0.12 mmol; 3 equiv.) were suspended in anhydrous degassed DMF (2 mL) and stream of argon was passed through the suspension for 10 minutes. The suspension was stirred at 65 °C for five hours during which macrocycle **2.167c** was formed with 86:14 dr. After cooling to room temperature, the reaction was quenched with saturated aqueous NH_4Cl solution and extracted with EtOAc. Combined organic layers were washed with brine, dried over Na_2SO_4 and evaporated under reduced pressure. Chromatographical purification on silica (0% to 40% EtOAc in DCM) afforded 22 mg (79%; 97:3 dr) of macrocycle **2.167c** as white amorphous solid. ^{1}H NMR (400 MHz, $CDCl_3$): δ 7.91 (s, 1H), 7.38 – 7.29 (m, 7H), 7.25 – 7.20 (m, 3H), 7.15 (dd, *J* = 8.0, 1.7 Hz, 1H), 7.10 (d, *J* = 1.7 Hz, 1H), 6.83 (d, *J* = 8.0 Hz, 1H), 6.60 (d, *J* = 8.0 Hz, 1H), 5.15 (d, *J* = 8.7 Hz, 1H), 5.13 – 5.01 (m, 2H), 4.75 (d, *J* = 8.0 Hz, 1H), 3.88 (s, 3H), 3.62 (td, *J* = 8.5, 3.7 Hz, 1H), 3.30 (s, 3H), 3.07 – 2.98 (m, 1H), 2.88 –2.79 (m, 1H), 2.70 – 2.59 (m, 1H), 1.82 – 1.72 (m, 1H), 0.96 (s, 9H). ^{13}C NMR (101 MHz, $CDCl_3$): δ 173.4, 171.3, 161.9, 161.6, 156.9, 155.4, 149.8, 144.3, 141.1, 137.1, 136.0, 134.3, 134.1, 131.4, 129.7, 128.9, 128.8, 128.6, 128.3, 128.1, 127.6, 127.5, 127.2, 109.1, 67.6, 58.1, 57.5, 52.8, 52.1, 33.7, 31.6, 30.0, 29.8, 27.1, 26.5. HRMS (ESI) *m/z* calcd. for $C_{40}H_{40}N_5O_8$ $[M+H]^+$: 718.2877, found: 718.2874. $[\alpha]^{20}_D$ -24 (*c* 0.8, $CHCl_3$).

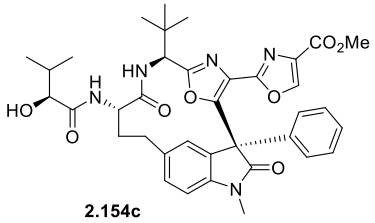

2.154c

Methyl 2-((2^3*S*,5*S*,8*S*)-8-(*tert*-butyl)-5-((*S*)-2-hydroxy-3-methylbutanamido)-2^1-methyl-2^2,6-dioxo-2^3-phenyl-7-aza-1(5,2)-oxazola-2(3,5)-indolinacyclooctaphane-1^4-yl)oxazole-4-carboxylate (2.154c). Macrocycle **2.167c** (22 mg; 0.31 mmol) and 10% Pd/C (3 mg; 0.0031 mmol; 0.1 equiv.) were suspended in MeOH and stream of H_2 was passed through the suspension for six hours at room temperature. Then the mixture was filtered through a plug of Celite, washed on filter with MeOH and evaporated to dryness under reduced pressure. The

white amorphous residue was dissolved in anhydrous DMF (1 mL) and (*S*)-HiVA (5 mg; 0.044 mmol; 1.5 equiv.), EDC×HCl (11 mg; 0.058 mmol; 2 equiv.) and HOBt (12 mg; 0.087 mmol; 3 equiv.) were added followed by DIPEA (30 µL; 0.17 mmol; 6 equiv.). The yellow solution was stirred at room temperature for one hour. The solution was diluted with saturated aqueous NH_4Cl solution and EtOAc. Layers were separated and the organic phase was washed with water and brine, dried over Na_2SO_4 and evaporated under reduced pressure. Purification by reverse phase flash chromatography (5% to 60% MeCN in water) afforded 12 mg (60%; dr 99:1) of macrocycle **2.154c** as white amorphous solid. ^{1}H NMR (400 MHz, MeOH-d_4): δ 8.36 (s, 1H), 7.32 – 7.29 (m, 5H), 7.25 (dd, *J* = 8.0, 1.8 Hz, 1H), 7.23 (d, *J* = 1.8 Hz, 1H), 7.04 (d, *J* = 8.0 Hz, 1H), 4.14 – 4.09 (m, 1H), 3.88 (s, 3H), 3.84 (d, *J* = 3.9 Hz, 1H), 3.28 (s, 3H), 3.02 – 2.94 (m, 1H), 2.83 – 2.76 (m, 1H), 2.76 – 2.68 (m, 1H), 2.06 (sept d, *J* = 6.9, 3.9 Hz, 1H), 1.76 – 1.67 (m, 1H), 1.09 – 1.02 (m, 10H), 0.99 (d, *J* = 6.9 Hz, 3H), 0.87 (d, *J* = 6.9 Hz, 3H). ^{13}C NMR (101 MHz, MeOH-d_4): δ 176.4, 174.8, 173.8, 164.0, 162.6, 156.6, 151.6, 146.5, 142.4, 138.3, 137.5, 134.8, 132.0, 131.2, 129.9, 129.3, 128.4, 127.4, 127.1, 110.6, 76.9, 59.4, 58.2, 52.8, 52.5, 34.5, 33.1, 31.9, 31.8, 27.3, 26.7, 19.6, 16.4. HRMS (ESI) *m/z* calcd. for $C_{37}H_{42}N_5O_8$ $[M+H]^+$: 684.3033, found: 684.3034. $[\alpha]^{20}_D$ -178 (*c* 1.0, MeOH).

CONCLUSIONS

1.Atropodiastereoselective *Dieckmann*-type cyclization provides a previously unreported route to ketone (*R*,*R*)-**2.3** and the macrocyclic core of diazonamide A (**1.2**) in enantiomerically pure form. Ketone (*R*,*R*)-**2.3** contains the following key structural elements of diazonamide A: right side 12-membered heterocyclic ring, enantiopure chiral tetracyclic hemiaminal and all-carbon quaternary stereogenic center. Approach toward synthesis of diazonamide A (**1.2**) through preparation of ketone (*R*,*R*)-**2.3** and initial assembly of right side polyaromatic macrocycle differs from the majority of previously disclosed total synthesis that typically started by the construction of the left-hand peptidic macrocycle.

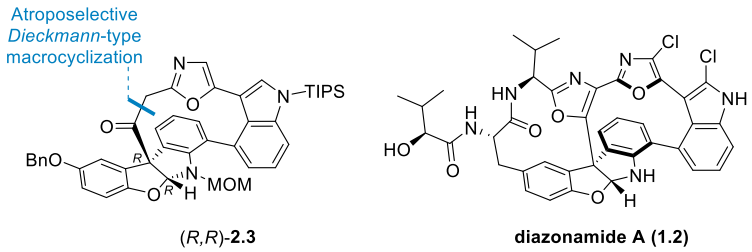

2. The diastereoselectivity of the macrocyclization of biaryl (*R*,*R*)-**2.4** was controlled by the (*R*)-stereogenic center at C10 of the rigid tetracyclic hemiaminal moiety. Notably, *M*-configuration around both C16–C18 and C24–C26 biaryl bonds of the macrocycle (*R*,*R*)-**2.3** was simultaneously established in the cyclization step. The *Dieckmann*-type cyclization proceeded below the threshold for interconversion of atropisomers around the C16–C18 biaryl bond in the starting biaryl (*R*,*R*)-**2.4**. Therefore, only the *M*-atropisomer underwent the ring closure, whereas the *P*-atropisomer did not react. However, the unreacted *P*-atropisomer equilibrated back to the starting 3:2 *M*/*P* mixture during the workup, and hence, the recovered biaryl (*R*,*R*)-**2.4** could be reused in the macrocyclization.

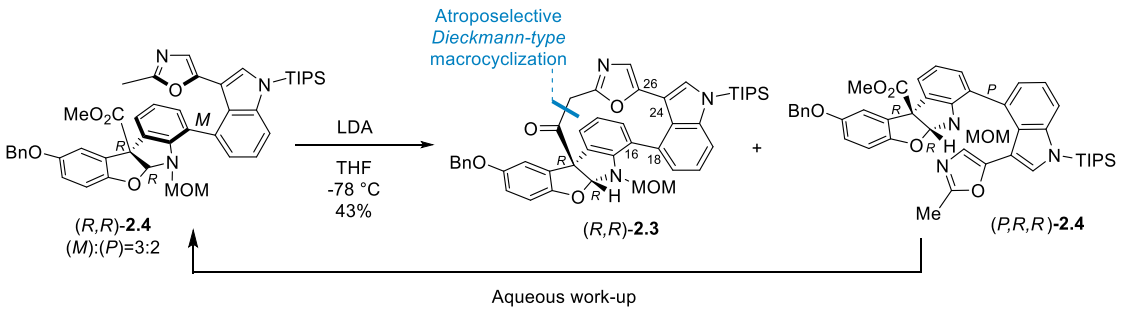

3. Construction of the bioxazole moiety in the pre-formed 12-membered macrocyclic ketone *rac*-**2.3** by direct α-amination/oxazole synthesis is not a viable strategy due to poor reactivity and stability of macrocycle *rac*-**2.3**. However, diazotation of ketone *rac*-**2.3** with *p*ABSA/DBU was successful and provided α-diazoketone *rac*-**2.61** as potential handle for introduction of bioxazole moiety after additional optimization of reaction conditions.

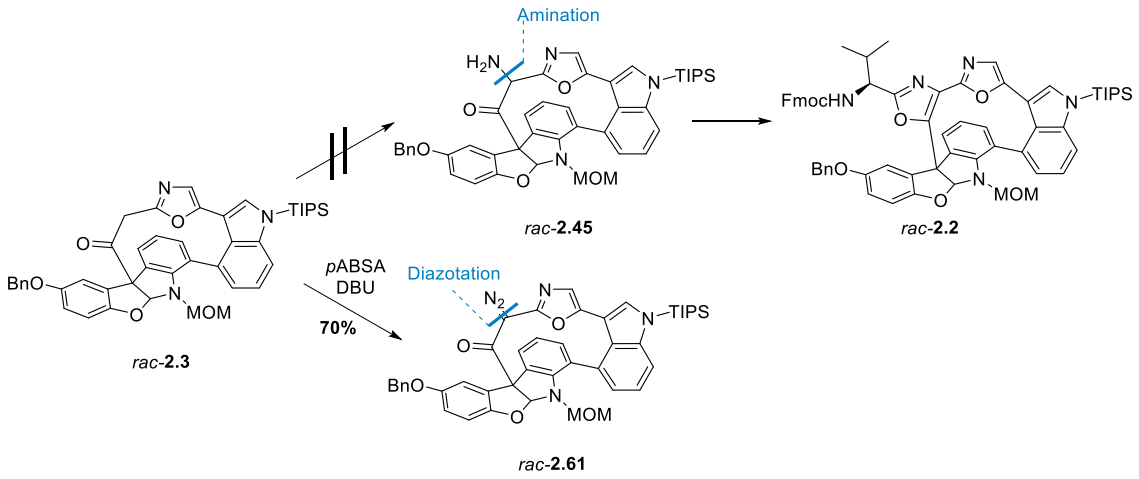

4. Dihydrobenzofuro[2,3-*b*]indole that contains carbonyl substituent at the quaternary stereocenter is relatively unstable: it is prone to ring opening under both acidic and basic conditions. *N*-Unprotected tetracyclic hemiaminal *rac*-**2.27** in presence of TEA exists in equilibrium with indole *rac*-**2.34**, which can be trapped with Boc_2O to give compound *rac*-**2.35**, but macrocyclic ketone *rac*-**2.3** in the presence HCl and MeOH forms intermediate **XIX** which leads to macrocycle opening and formation of indole **2.64**. Driving force in both cases is rearomatization of the indole ring.

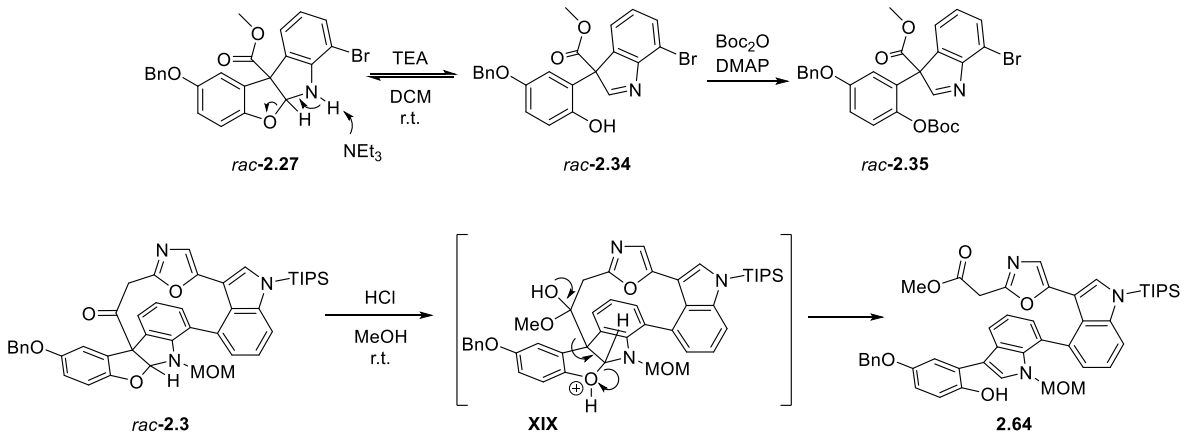

5. The explored synthesis strategies are not suitable for the preparation of the carba-analog of DZ-2384, the dihydroindenoindole-core containing macrocycle **2.71**.

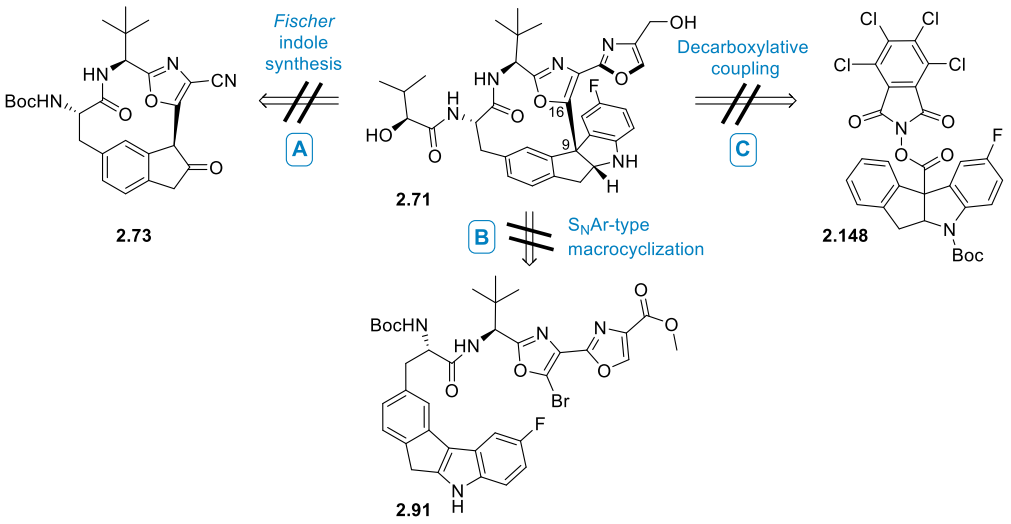

5.1. Synthesis of macrocycle **2.71** by late-stage construction of dihydroindenoindole core using *Fischer* indole synthesis between ketone **2.73** (prepared by diastereoselective intramolecular ketone arylation from amide **2.74**) and arylhydrazine **2.85** is not viable and produce the undesired indole regioisomer **2.86**. The regioselectivity of the indole synthesis is shifted towards the kinetic product **2.86** by steric crowding around the α-position of the ketone **2.73**.

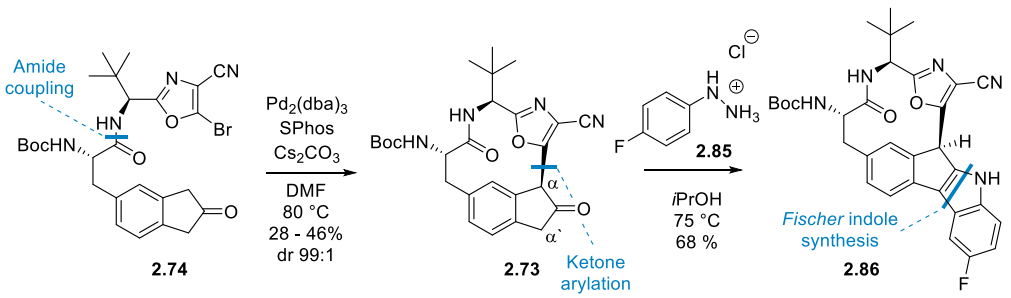

5.2. Synthesis of macrocycle **2.71** by intramolecular S_NAr-type macrocyclization of tethered indole-oxazole **2.91** (prepared from pre-formed bioxazole building block **2.93** and dihydroindenoindole **2.92**) produces undesired macrocycle **2.102** with good yield and high diastereoselectivity (99:1 dr). The selective formation of the undesired macrocycle **2.102** can be explained by the low nucleophilicity and prohibitive cost of dearomatization of indole moiety.

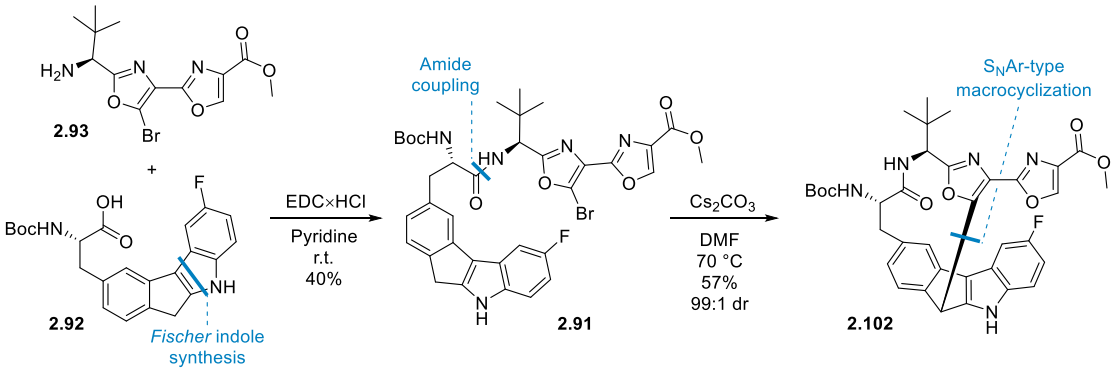

5.3. Synthesis of macrocycle **2.71** by decarboxylative coupling of preformed redox-active ester **2.148** (prepared from pre-formed dihydroindenoindole **2.140** by electrophilic allylation and subsequent double bond isomerization, oxidation, and ester synthesis) and aryl zinc species is not feasible. Model reaction between ester **2.148** and di(paramethoxyphenyl)zinc did not produce coupling product **2.149**. The poor coupling results can be attributed to the sterically crowded environment around the reaction site on dihydroindenoindole **2.148** which prevents the approach of the reactive species.

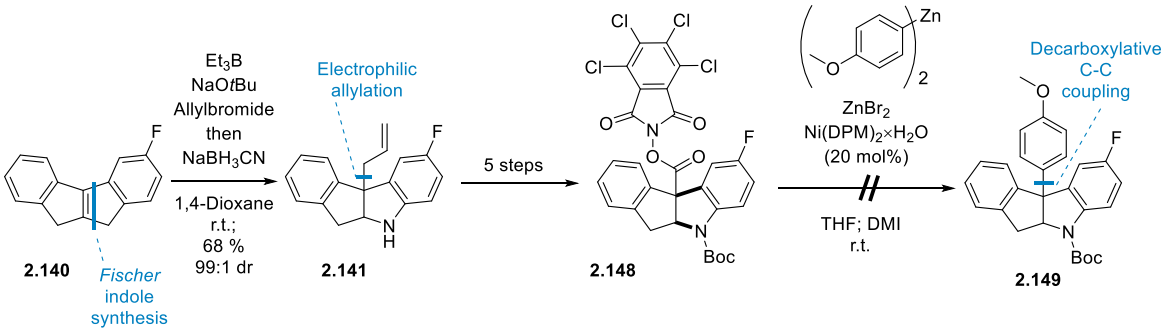

6. Variation of the bond connectivity between the core tetracycle and the rest of the molecule does not allow the (dihydro)indenoindole-core containing macrocycles **2.89**, **2.104** and **2.106** to adapt the bioactive conformation, leading to drop in antiproliferative activity compared to DZ-2384 (**1.76**).

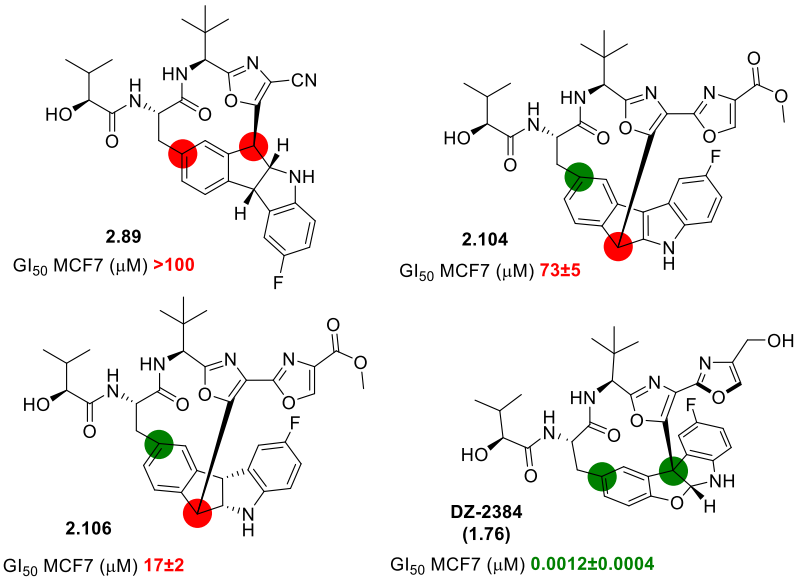

7. S_NAr-type macrocyclization of 2-indolinone-tethered bromooxazoles **2.155** and **2.156** is well suited for preparation of indolinone core-containing macrocycles **2.166** and **2.167**. The lower diastereoselectivity of macrocyclization of 13-membered analogs **2.167** (<86:14 dr) compared to 12-membered **2.166** (99:1 dr) is due to larger number of rotatable bonds in the oxindole-oxazole tether (7 vs 6 respectively) of precursor **2.156** and smaller energy difference between transition states leading to individual diastereomers of macrocycle **2.167**.

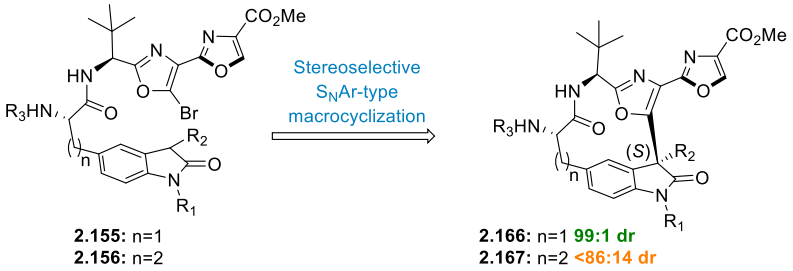

8. The phenyl moiety at quaternary center (**2.154a**) is superior substituent to the methyl group (**2.154b**) in the 13-membered macrocycle series. Additionally, ring enlargement from 12- to 13-membered macrocycle is beneficial to *N*-unsubstituted, 3-phenyloxindole-core containing compound and allows for 10-fold increase in antiproliferative activities against PANC-1 and MDA-MB-231 cancer cell lines (**2.153a** vs **2.154a**).

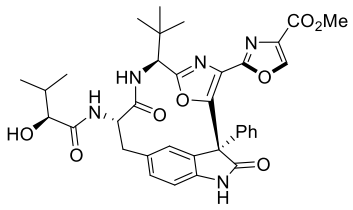

12-membered ring

2.153a*

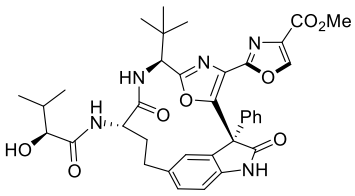

13-membered ring

2.154a

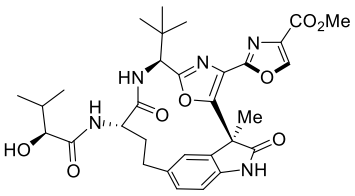

13-membered ring

2.154b

GI_{50} PANC-1 (μM)	**12±2**	**1.2±0.3**	**>100**
GI_{50} MiaPaCa-2 (μM)	**0.67±0.005**	**0.46±0.04**	**17±2**
GI_{50} MCF-7 (μM)	**1.2±0.3**	**7.7±0.3**	**12±3**
GI_{50} MDA-MB-231 (μM)	**8±2**	**0.26±0.03**	**21±3**

*Synthesized by V.Vitkovska

9. Change in absolute configuration from (*S*) to (*R*) at the quaternary stereogenic center of the 2-indolinone core-containing analogs of diazonamide A is not tolerated and leads to diminished antiproliferative activity.

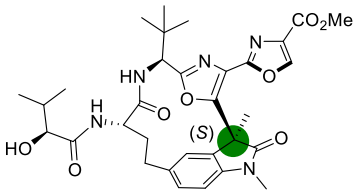

2.154d

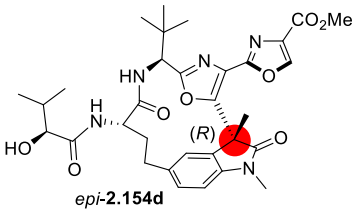

epi-**2.154d**

GI_{50} MCF7 (μM)	**15±2**	**79±6**
GI_{50} MDA-MB-231 (μM)	**4.8±1**	**75±8**

REFERENCES

(1) *What Is Cancer? - NCI*. https://www.cancer.gov/about-cancer/understanding/what-is-cancer (accessed 2024-06-19).

(2) *Cancer Today*. https://gco.iarc.who.int/today/ (accessed 2024-06-19).

(3) Sung, H.; Ferlay, J.; Siegel, R. L.; Laversanne, M.; Soerjomataram, I.; Jemal, A.; Bray, F. Global Cancer Statistics 2020: GLOBOCAN Estimates of Incidence and Mortality Worldwide for 36 Cancers in 185 Countries. *CA. Cancer J. Clin.* **2021**, *71* (3), 209–249. https://doi.org/10.3322/caac.21660.

(4) Vaidya, F. U.; Sufiyan Chhipa, A.; Mishra, V.; Gupta, V. K.; Rawat, S. G.; Kumar, A.; Pathak, C. Molecular and Cellular Paradigms of Multidrug Resistance in Cancer. *Cancer Rep.* **2022**, *5* (12), e1291. https://doi.org/10.1002/cnr2.1291.

(5) Newman, D. J.; Cragg, G. M. Natural Products as Sources of New Drugs over the Nearly Four Decades from 01/1981 to 09/2019. *J. Nat. Prod.* **2020**, *83* (3), 770–803. https://doi.org/10.1021/acs.jnatprod.9b01285.

(6) Lindquist, N.; Fenical, W.; Van Duyne, G. D.; Clardy, J. Isolation and Structure Determination of Diazonamides A and B, Unusual Cytotoxic Metabolites from the Marine Ascidian Diazona Chinensis. *J. Am. Chem. Soc.* **1991**, *113* (6), 2303–2304. https://doi.org/10.1021/ja00006a060.

(7) Wieczorek, M.; Tcherkezian, J.; Bernier, C.; Prota, A. E.; Chaaban, S.; Rolland, Y.; Godbout, C.; Hancock, M. A.; Arezzo, J. C.; Ocal, O.; Rocha, C.; Olieric, N.; Hall, A.; Ding, H.; Bramoulle, A.; Annis, M. G.; Zogopoulos, G.; Harran, P. G.; Wilkie, T. M.; Brekken, R. A.; Siegel, P. M.; Steinmetz, M. O.; Shore, G. C.; Brouhard, G. J.; Roulston, A. The Synthetic Diazonamide DZ-2384 Has Distinct Effects on Microtubule Curvature and Dynamics without Neurotoxicity. *Sci Transl Med* **2016**, *8* (365), 365ra159. https://doi.org/10.1126/scitranslmed.aag1093.

(8) Vervoort, H. C. Novel Anticancer Agents from Ascidiacea. **1999**.

(9) Cruz-Monserrate, Z.; Vervoort, H. C.; Bai, R.; Newman, D. J.; Howell, S. B.; Los, G.; Mullaney, J. T.; Williams, M. D.; Pettit, G. R.; Fenical, W.; Hamel, E. Diazonamide A and a Synthetic Structural Analog: Disruptive Effects on Mitosis and Cellular Microtubules and Analysis of Their Interactions with Tubulin. *Mol. Pharmacol.* **2003**, *63* (6), 1273–1280. https://doi.org/10.1124/mol.63.6.1273.

(10) Nicolaou, K. C.; Snyder, S. A.; Huang, X.; Simonsen, K. B.; Koumbis, A. E.; Bigot, A. Studies toward Diazonamide A: Initial Synthetic Forays Directed toward the Originally Proposed Structure. *J Am Chem Soc* **2004**, *126* (32), 10162–10173. https://doi.org/10.1021/ja040090y.

(11) Jeong, S.; Chen, X.; Harran, P. G. Macrocyclic Triarylethylenes via Heck Endocyclization: A System Relevant to Diazonamide Synthesis. *J. Org. Chem.* **1998**, *63* (24), 8640–8641. https://doi.org/10.1021/jo981791e.

(12) Li, J.; Jeong, S.; Esser, L.; Harran, P. G. Total Synthesis of Nominal Diazonamides—Part 1: Convergent Preparation of the Structure Proposed for (−)-Diazonamide A. *Angew. Chem. Int. Ed.* **2001**, *40* (24), 4765–4769. https://doi.org/10.1002/1521-3773(20011217)40:24<4765::AID-ANIE4765>3.0.CO;2-1.

(13) Li, J.; Burgett, A. W. G.; Esser, L.; Amezcua, C.; Harran, P. G. Total Synthesis of Nominal Diazonamides—Part 2: On the True Structure and Origin of Natural Isolates. *Angew. Chem. Int. Ed.* **2001**, *40* (24), 4770–4773. https://doi.org/10.1002/1521-3773(20011217)40:24<4770::AID-ANIE4770>3.0.CO;2-T.

(14) Nicolaou, K. C.; Bella, M.; Chen, D. Y.-K.; Huang, X.; Ling, T.; Snyder, S. A. Total Synthesis of Diazonamide A. *Angew. Chem. Int. Ed.* **2002**, *41* (18), 3495–3499. https://doi.org/10.1002/1521-3773(20020916)41:18<3495::AID-ANIE3495>3.0.CO;2-7.

(15) Nicolaou, K. C.; Bheema Rao, P.; Hao, J.; Reddy, M. V.; Rassias, G.; Huang, X.; Chen, D. Y.-K.; Snyder, S. A. The Second Total Synthesis of Diazonamide A. *Angew. Chem. Int. Ed.* **2003**, *42* (15), 1753–1758. https://doi.org/10.1002/anie.200351112.
(16) Burgett, A. W. G.; Li, Q.; Wei, Q.; Harran, P. G. A Concise and Flexible Total Synthesis of (−)-Diazonamide A. *Angew. Chem. Int. Ed.* **2003**, *42* (40), 4961–4966. https://doi.org/10.1002/anie.200352577.
(17) Knowles, R. R.; Carpenter, J.; Blakey, S. B.; Kayano, A.; Mangion, I. K.; Sinz, C. J.; MacMillan, D. W. C. Total Synthesis of Diazonamide A. *Chem Sci* **2011**, *2* (2), 308–311. https://doi.org/10.1039/C0SC00577K.
(18) Nicolaou, K. C.; Chen, D. Y.-K.; Huang, X.; Ling, T.; Bella, M.; Snyder, S. A. Chemistry and Biology of Diazonamide A: First Total Synthesis and Confirmation of the True Structure. *J. Am. Chem. Soc.* **2004**, *126* (40), 12888–12896. https://doi.org/10.1021/ja040092i.
(19) Nicolaou, K. C.; Hao, J.; Reddy, M. V.; Rao, P. B.; Rassias, G.; Snyder, S. A.; Huang, X.; Chen, D. Y.-K.; Brenzovich, W. E.; Giuseppone, N.; Giannakakou, P.; O'Brate, A. Chemistry and Biology of Diazonamide A: Second Total Synthesis and Biological Investigations. *J. Am. Chem. Soc.* **2004**, *126* (40), 12897–12906. https://doi.org/10.1021/ja040093a.
(20) Klumpp, D. A.; Yeung, K. Y.; Prakash, G. K. S.; Olah, G. A. Preparation of 3,3-Diaryloxindoles by Superacid-Induced Condensations of Isatins and Aromatics with a Combinatorial Approach. *J. Org. Chem.* **1998**, *63* (13), 4481–4484. https://doi.org/10.1021/jo980588g.
(21) Nicolaou, K. C.; Huang, X.; Giuseppone, N.; Bheema Rao, P.; Bella, M.; Reddy, M. V.; Snyder, S. A. Construction of the Complete Aromatic Core of Diazonamide A by a Novel Hetero Pinacol Macrocyclization Cascade Reaction. *Angew. Chem. Int. Ed.* **2001**, *40* (24), 4705–4709. https://doi.org/10.1002/1521-3773(20011217)40:24<4705::AID-ANIE4705>3.0.CO;2-D.
(22) Cheung, C.-M.; Goldberg, F. W.; Magnus, P.; Russell, C. J.; Turnbull, R.; Lynch, V. An Expedient Formal Total Synthesis of (−)-Diazonamide A via a Powerful, Stereoselective O-Aryl to C-Aryl Migration To Form the C10 Quaternary Center. *J. Am. Chem. Soc.* **2007**, *129* (40), 12320–12327. https://doi.org/10.1021/ja0744448.
(23) Mai, C.-K.; Sammons, M. F.; Sammakia, T. A Concise Formal Synthesis of Diazonamide A by the Stereoselective Construction of the C10 Quaternary Center. *Angew. Chem. Int. Ed.* **2010**, *49* (13), 2397–2400. https://doi.org/10.1002/anie.200906318.
(24) David, N.; Pasceri, R.; Kitson, R. R. A.; Pradal, A.; Moody, C. J. Formal Total Synthesis of Diazonamide A by Indole Oxidative Rearrangement. *Chem. – Eur. J.* **2016**, *22* (31), 10867–10876. https://doi.org/10.1002/chem.201601605.
(25) Zhao, Z.; Jaworski, A.; Piel, I.; Snieckus, V. Anionic Indole N-Carbamoyl N → C Translocation. A Directed Remote Metalation Route to 2-Aryl- and 2-Heteroarylindoles. Synthesis of Benz[a]Carbazoles and Indeno[1,2-b]Indoles. *Org. Lett.* **2008**, *10* (13), 2617–2620. https://doi.org/10.1021/ol800307g.
(26) Wei, Q.; Zhou, M.; Xu, X.; Caldwell, C.; Harran, S.; Wang, L. Diazonamide Analogs, October 26, 2012.
(27) Hanson, G. J.; Wei, Q.; Caldwell, C.; Zhou, M.; Wang, L.; Harran, S. Indoline Anti-Cancer Agents, October 18, 2012.
(28) Wei, Q.; Zhou, M.; Xu, X.; Caldwell, C.; Harran, S.; Wang, L. Diazonamide Analogs. US8846734B2, September 30, 2014. https://patents.google.com/patent/US8846734B2/en (accessed 2023-10-20).
(29) Ding, H.; DeRoy, P. L.; Perreault, C.; Larivée, A.; Siddiqui, A.; Caldwell, C. G.; Harran, S.; Harran, P. G. Electrolytic Macrocyclizations: Scalable Synthesis of a

Diazonamide-Based Drug Development Candidate. *Angew. Chem. Int. Ed.* **2015**, *54* (16), 4818–4822. https://doi.org/10.1002/anie.201411663.

(30) Wordeman, L.; Vicente, J. J. Microtubule Targeting Agents in Disease: Classic Drugs, Novel Roles. *Cancers* **2021**, *13* (22), 5650. https://doi.org/10.3390/cancers13225650.

(31) Steinmetz, M. O.; Prota, A. E. Microtubule-Targeting Agents: Strategies To Hijack the Cytoskeleton. *Trends Cell Biol.* **2018**, *28* (10), 776–792. https://doi.org/Pelletier.

(32) *Targets | DrugBank Online*. https://go.drugbank.com/targets?_gl=1*16u7r2n*_up*MQ..*_ga*NTYyODEzMDM0LjE3MTg4MDc4OTM.*_ga_DDLJ7EEV9M*MTcxODgwNzg5Mi4xLjAuMTcxODgwNzg5Mi4wLjAuMA.. (accessed 2024-06-19).

(33) Bates, D.; Eastman, A. Microtubule Destabilising Agents: Far More than Just Antimitotic Anticancer Drugs. *Br. J. Clin. Pharmacol.* **2017**, *83* (2), 255–268. https://doi.org/10.1111/bcp.13126.

(34) Inoue, M.; Matsumoto, K.; Tanaka, M.; Yoshida, Y.; Satake, R.; Goto, F.; Shimada, K.; Mukai, R.; Hasegawa, S.; Suzuki, T.; Ikesue, H.; Liao, J.; Hashida, T.; Nakamura, M. Analysis of Chemotherapy-Induced Peripheral Neuropathy Using the Japanese Adverse Drug Event Report Database. *Sci. Rep.* **2021**, *11* (1), 11324. https://doi.org/10.1038/s41598-021-90848-6.

(35) Brunden, K. R.; Trojanowski, J. Q.; Smith, A. B.; Lee, V. M.-Y.; Ballatore, C. Microtubule-Stabilizing Agents as Potential Therapeutics for Neurodegenerative Disease. *Bioorg. Med. Chem.* **2014**, *22* (18), 5040–5049. https://doi.org/10.1016/j.bmc.2013.12.046.

(36) Malacrida, A.; Meregalli, C.; Rodriguez-Menendez, V.; Nicolini, G. Chemotherapy-Induced Peripheral Neuropathy and Changes in Cytoskeleton. *Int. J. Mol. Sci.* **2019**, *20* (9), 2287. https://doi.org/10.3390/ijms20092287.

(37) Mutule, I.; Joo, B.; Medne, Z.; Kalnins, T.; Vedejs, E.; Suna, E. Stereoselective Synthesis of the Diazonamide A Macrocyclic Core. *J. Org. Chem.* **2015**, *80* (6), 3058–3066. https://doi.org/10.1021/jo5029419.

(38) Mutule, I.; Kalnins, T.; Vedejs, E.; Suna, E. Diazonamide Synthetic Studies. Reactivity of N-Unsubstituted Benzofuro[2,3-b]Indolines. *Chem. Heterocycl. Compd.* **2015**, *51* (7), 613–620. https://doi.org/10.1007/s10593-015-1749-7.

(39) Zajac, M. A.; Vedejs, E. A Synthesis of the Diazonamide Heteroaromatic Biaryl Macrocycle/Hemiaminal Core. *Org. Lett.* **2004**, *6* (2), 237–240. https://doi.org/10.1021/ol036179a.

(40) Peris, G.; Vedejs, E. Enantiocontrolled Synthesis of a Tetracyclic Aminal Corresponding to the Core Subunit of Diazonamide A. *J. Org. Chem.* **2015**, *80* (6), 3050–3057. https://doi.org/10.1021/jo502939a.

(41) Ma, D.; Wu, Q. Enantioselective Construction of the Oxidized Tryptophan Fragment of Proteasome Inhibitors TMC-95A and TMC-95B. *Tetrahedron Lett.* **2000**, *41* (47), 9089–9093. https://doi.org/10.1016/S0040-4039(00)01657-9.

(42) Benneche, T.; Gundersen, L.-L.; Undheim, K.; Norinder, U.; Wittman, G.; Gera, L.; Bartók, M.; Pelczer, I.; Dombi, G. (Tert-Butyldimethylsilyloxy)Methyl Chloride: Synthesis and Use as N-Protecting Group in Pyrimidinones. *Acta Chem. Scand.* **1988**, *42b*, 384–389. https://doi.org/10.3891/acta.chem.scand.42b-0384.

(43) Brown, H. C.; Chandrasekharan, J.; Ramachandran, P. V. Chiral Synthesis via Organoboranes. 14. Selective Reductions. 41. Diisopinocampheylchloroborane, an Exceptionally Efficient Chiral Reducing Agent. *J. Am. Chem. Soc.* **1988**, *110* (5), 1539–1546. https://doi.org/10.1021/ja00213a030.

(44) Quan, Z.-J.; Wang, X.-C.; Ren, R.-G.; Da, Y.-X.; Zhang, Z.; Jia, X.-D.; Yang, C.-X. One-Pot Two-Step Synthesis of N3-Functionalized 3,4-Dihydropyrimidinones in the Presence of TMSCl. *HETEROCYCLES* **2010**, *81* (8), 1827. https://doi.org/10.3987/COM-10-11968.

(45) Vedejs, E.; Barda, D. A. Progress toward Synthesis of Diazonamide A. Preparation of a 3-(Oxazol-5-Yl)-4-Trifluoromethylsulfonyloxyindole and Its Use in Biaryl Coupling Reactions. *Org Lett* **2000**, *2* (8), 1033–1035. https://doi.org/10.1021/ol005548p.
(46) Vedejs, E.; Zajac, M. A. Synthesis of the Diazonamide A Macrocyclic Core via a Dieckmann-Type Cyclization. *Org. Lett.* **2001**, *3* (16), 2451–2454. https://doi.org/10.1021/ol016097r.
(47) Wipf, P.; Miller, C. P. A New Synthesis of Highly Functionalized Oxazoles. *J Org Chem* **1993**, *58* (14), 3604–3606. https://doi.org/10.1021/jo00066a004.
(48) Ishiyama, T.; Murata, M.; Miyaura, N. Palladium(0)-Catalyzed Cross-Coupling Reaction of Alkoxydiboron with Haloarenes: A Direct Procedure for Arylboronic Esters. *J Org Chem* **1995**, *60* (23), 7508–7510. https://doi.org/10.1021/jo00128a024.
(49) Miyashita, K.; Sakai, T.; Imanishi, T. Total Synthesis of (±)-Spiroxin C. *Org Lett* **2003**, *5* (15), 2683–2686. https://doi.org/10.1021/ol034856v.
(50) Billingsley, K. L.; Buchwald, S. L. An Improved System for the Palladium-Catalyzed Borylation of Aryl Halides with Pinacol Borane. *J Org Chem* **2008**, *73* (14), 5589–5591. https://doi.org/10.1021/jo800727s.
(51) Broutin, P.-E.; Čerňa, I.; Campaniello, M.; Leroux, F.; Colobert, F. Palladium-Catalyzed Borylation of Phenyl Bromides and Application in One-Pot Suzuki−Miyaura Biphenyl Synthesis. *Org. Lett.* **2004**, *6* (24), 4419–4422. https://doi.org/10.1021/ol048303b.
(52) Smulik, J. A.; Vedejs, E. Improved Reagent for Electrophilic Amination of Stabilized Carbanions. *Org. Lett.* **2003**, *5* (22), 4187–4190. https://doi.org/10.1021/ol035629w.
(53) Radhakrishna, A. S.; Loudon, G. M.; Miller, M. J. Amination of Ester Enolates with O-(2,4-Dinitrophenyl)Hydroxylamine. *J. Org. Chem.* **1979**, *44* (26), 4836–4841. https://doi.org/10.1021/jo00394a020.
(54) Matsushita, H.; Lee, S.-H.; Yoshida, K.; Clapham, B.; Koch, G.; Zimmermann, J.; Janda, K. D. N−H Insertion Reactions of Boc-Amino Acid Amides: Solution- and Solid-Phase Synthesis of Pyrazinones and Pyrazines. *Org. Lett.* **2004**, *6* (24), 4627–4629. https://doi.org/10.1021/ol047933a.
(55) Davies, J. R.; Kane, P. D.; Moody, C. J.; Slawin, A. M. Z. Control of Competing N−H Insertion and Wolff Rearrangement in Dirhodium(II)-Catalyzed Reactions of 3-Indolyl Diazoketoesters. Synthesis of a Potential Precursor to the Marine 5-(3-Indolyl)Oxazole Martefragin A. *J. Org. Chem.* **2005**, *70* (15), 5840–5851. https://doi.org/10.1021/jo050303h.
(56) Pineiro, J. L. C.; Dinnell, K.; Elliott, J. M.; Hollingworth, G. J.; Shaw, D. E.; Swain, C. J.; Yang, L. Cyclohexyl Derivatives and Their Use as Therapeutic Agents. WO2001087866A1, November 22, 2001. https://patents.google.com/patent/WO2001087866A1/en?oq=WO+01%2f87866 (accessed 2024-01-22).
(57) Hashimoto, S.; Watanabe, N.; Ikegami, S. Highly Selective Insertion into Aromatic C–H Bonds in Rhodium(II) Triphenylacetate-Catalysed Decomposition of α-Diazocarbonyl Compounds. *J. Chem. Soc. Chem. Commun.* **1992**, No. 20, 1508–1510. https://doi.org/10.1039/C39920001508.
(58) Baum, J. S.; Shook, D. A.; Davies, H. M. L.; Smith, H. D. Diazotransfer Reactions with P-Acetamidobenzenesulfonyl Azide. *Synth. Commun.* **1987**, *17* (14), 1709–1716. https://doi.org/10.1080/00397918708063988.
(59) Doyle, K. J.; Moody, C. J. The Rhodium Carbenoid Route to Oxazoles. Synthesis of 4-Functionalised Oxazoles; Three Step Preparation of a Bis-Oxazole. *Tetrahedron* **1994**, *50* (12), 3761–3772. https://doi.org/10.1016/S0040-4020(01)90396-5.
(60) Zhu, S.-F.; Xu, B.; Wang, G.-P.; Zhou, Q.-L. Well-Defined Binuclear Chiral Spiro Copper Catalysts for Enantioselective N–H Insertion. *J. Am. Chem. Soc.* **2012**, *134* (1), 436–442. https://doi.org/10.1021/ja2084493.

(61) Budeev, A.; Kantin, G.; Dar'in, D.; Krasavin, M. Diazocarbonyl and Related Compounds in the Synthesis of Azoles. *Molecules* **2021**, *26* (9), 2530. https://doi.org/10.3390/molecules26092530.
(62) Moody, C. J.; Doyle, K. J. Chapter 1 The Synthesis of Oxazoles from Diazocarbonyl Compounds. In *Progress in Heterocyclic Chemistry*; Gribble, G. W., Gilchrist, T. L., Eds.; Elsevier, 1997; Vol. 9, pp 1–16. https://doi.org/10.1016/S0959-6380(97)80003-7.
(63) Doyle, M. P.; Buhro, W. E.; Davidson, J. G.; Elliott, R. C.; Hoekstra, J. W.; Oppenhuizen, M. Lewis Acid Promoted Reactions of Diazocarbonyl Compounds. 3. Synthesis of Oxazoles from Nitriles through Intermediate .Beta.-Imidatoalkenediazonium Salts. *J. Org. Chem.* **1980**, *45* (18), 3657–3664. https://doi.org/10.1021/jo01306a023.
(64) Ibata, T.; Sato, R. The Acid Catalyzed Decomposition of Diazo Compounds. I. Synthesis of Oxazoles in the BF3 Catalyzed Reaction of Diazo Carbonyl Compounds with Nitriles. *Bull. Chem. Soc. Jpn.* **1979**, *52* (12), 3597–3600. https://doi.org/10.1246/bcsj.52.3597.
(65) Hashimoto, T.; Kimura, H.; Kawamata, Y.; Maruoka, K. Generation and Exploitation of Acyclic Azomethine Imines in Chiral Brønsted Acid Catalysis. *Nat. Chem.* **2011**, *3* (8), 642–646. https://doi.org/10.1038/nchem.1096.
(66) Hasegawa, K.; Kimura, N.; Arai, S.; Nishida, A. Novel Synthesis of Cinnolines and 1-Aminoindolines via Cu-Catalyzed Intramolecular N-Arylation of Hydrazines and Hydrazones Prepared from 3-Haloaryl-3-Hydroxy-2-Diazopropanoates. *J. Org. Chem.* **2008**, *73* (16), 6363–6368. https://doi.org/10.1021/jo8010864.
(67) Bestmann, H. J.; Buckschewski, H.; Leube, H. Phosphazine, I. Über α-Keto-triphenylphosphazine und ihre Verwendung zur partiellen Reduktion der Diazoketone zu α-Ketoaldehyd-al-hydrazonen. *Chem. Ber.* **1959**, *92* (6), 1345–1354. https://doi.org/10.1002/cber.19590920617.
(68) Pellicciari, R.; Natalini, B.; Cecchetti, S.; Fringuelli, R. Reduction of α-Diazo-β-Hydroxy Esters to β-Hydroxy Esters: Application in One of Two Convergent Syntheses of a (22S)-22-Hydroxy Bile Acid from Fish Bile and Its (22R)-Epimer. *J Chem Soc Perkin Trans 1* **1985**, No. 0, 493–497. https://doi.org/10.1039/P19850000493.
(69) Fukuzawa, S.; Nakano, N.; Saitoh, T. Reduction of Carbonyl Compounds by Lanthanide Metal/2-Propanol: In-Situ Generation of Samarium Isopropyloxide for Stereoselective Meerwein−Ponndorf−Verley Reduction. *Eur. J. Org. Chem.* **2004**, *2004* (13), 2863–2867. https://doi.org/10.1002/ejoc.200400030.
(70) Bowers, N. I.; Boyd, D. R.; Sharma, N. D.; Goodrich, P. A.; Groocock, M. R.; Blacker, A. J.; Goode, P.; Dalton, H. Stereoselective Benzylic Hydroxylation of 2-Substituted Indanes Using Toluene Dioxygenase as Biocatalyst. *J. Chem. Soc. Perkin 1* **1999**, No. 11, 1453–1462. https://doi.org/10.1039/A901453E.
(71) Göksu, S.; Seçen, H. Concise Syntheses of 2-Aminoindans via Indan-2-Ol. *Tetrahedron* **2005**, *61* (28), 6801–6807. https://doi.org/almog.
(72) Ross, A. J.; Lang, H. L.; Jackson, R. F. W. Much Improved Conditions for the Negishi Cross-Coupling of Iodoalanine Derived Zinc Reagents with Aryl Halides. *J. Org. Chem.* **2010**, *75* (1), 245–248. https://doi.org/10.1021/jo902238n.
(73) Vitkovska, V.; Zogota, R.; Kalnins, T.; Zelencova, D.; Suna, E. Aliphatic Chain-Containing Macrocycles as Diazonamide A Analogs. *Chem. Heterocycl. Compd.* **2020**, *56* (5), 586–602. https://doi.org/10.1007/s10593-020-02704-6.
(74) Fox, J. M.; Huang, X.; Chieffi, A.; Buchwald, S. L. Highly Active and Selective Catalysts for the Formation of α-Aryl Ketones. *J. Am. Chem. Soc.* **2000**, *122* (7), 1360–1370. https://doi.org/10.1021/ja993912d.
(75) Willis, M. C.; Brace, G. N.; Holmes, I. P. Palladium-Catalyzed Tandem Alkenyl and Aryl C□N Bond Formation: A Cascade N-Annulation Route to 1-Functionalized

Indoles. *Angew. Chem. Int. Ed.* **2005**, *44* (3), 403–406. https://doi.org/10.1002/anie.200461598.

(76) Tietze, L. F.; Braun, H.; Steck, P. L.; El Bialy, S. A. A.; Tölle, N.; Düfert, A. Efficient Synthesis of Cephalotaxine- and Deoxyharringtonine Analogues by a Trimethylaluminium-Mediated Domino Reaction. *Tetrahedron* **2007**, *63* (28), 6437–6445. https://doi.org/10.1016/j.tet.2007.03.020.

(77) Xu, Y.; Su, T.; Huang, Z.; Dong, G. Practical Direct α-Arylation of Cyclopentanones by Palladium/Enamine Cooperative Catalysis. *Angew. Chem. Int. Ed.* **2016**, *55* (7), 2559–2563. https://doi.org/10.1002/anie.201510638.

(78) Grandini, C.; Camurati, I.; Guidotti, S.; Mascellani, N.; Resconi, L.; Nifant'ev, I. E.; Kashulin, I. A.; Ivchenko, P. V.; Mercandelli, P.; Sironi, A. Heterocycle-Fused Indenyl Silyl Amido Dimethyl Titanium Complexes as Catalysts for High Molecular Weight Syndiotactic Amorphous Polypropylene. *Organometallics* **2004**, *23* (3), 344–360. https://doi.org/10.1021/om030543s.

(79) Hughes, D. L. PROGRESS IN THE FISCHER INDOLE REACTION. A REVIEW. *Org. Prep. Proced. Int.* **1993**, *25* (6), 607–632. https://doi.org/10.1080/00304949309356257.

(80) Mirand, C.; Döé de Maindreville, M.; Cartier, D.; Lévy, J. N-Benzene-Sulfonyl-Indole as Terminator in a Biomimetic Polyene Cyclization: Synthesis of a Pentacyclic Indolosesquiterpene. *Tetrahedron Lett.* **1987**, *28* (31), 3565–3568. https://doi.org/10.1016/S0040-4039(00)95537-0.

(81) Xiao, Y.-C.; Wang, C.; Yao, Y.; Sun, J.; Chen, Y.-C. Direct Asymmetric Hydrosilylation of Indoles: Combined Lewis Base and Brønsted Acid Activation. *Angew. Chem. Int. Ed.* **2011**, *50* (45), 10661–10664. https://doi.org/10.1002/anie.201105341.

(82) Bordwell, F. G.; Drucker, G. E.; Fried, H. E. Acidities of Carbon and Nitrogen Acids: The Aromaticity of the Cyclopentadienyl Anion. *J. Org. Chem.* **1981**, *46* (3), 632–635. https://doi.org/10.1021/jo00316a032.

(83) Bordwell, F. G.; Drucker, G. E. Acidities of Indene and Phenyl-, Diphenyl-, and Triphenylindenes. *J. Org. Chem.* **1980**, *45* (16), 3325–3328. https://doi.org/10.1021/jo01304a037.

(84) Jo, J.; Jeong, M.; Ahn, J.-S.; Akter, J.; Kim, H.-S.; Suh, Y.-G.; Yun, H. Total Synthesis of Anmindenol A and Its Application to the Design, Synthesis, and Biological Evaluation of Derivatives Thereof. *J. Org. Chem.* **2019**, *84* (17), 10953–10961. https://doi.org/10.1021/acs.joc.9b01564.

(85) Kazak, M.; Vasilevska, A.; Suna, E. Preparative Scale Synthesis of Functionalized Bioxazole. *Chem. Heterocycl. Compd.* **2020**, *56* (3), 355–364. https://doi.org/10.1007/s10593-020-02667-8.

(86) Haasnoot, C. A. G.; de Leeuw, F. A. A. M.; Altona, C. The Relationship between Proton-Proton NMR Coupling Constants and Substituent Electronegativities—I: An Empirical Generalization of the Karplus Equation. *Tetrahedron* **1980**, *36* (19), 2783–2792. https://doi.org/10.1016/0040-4020(80)80155-4.

(87) Kuehm-Caubère, C.; Guilmart, A.; Adach-Becker, S.; Fort, Y.; Caubère, P. Dramatic Acceleration of the Desulfurization, with Ni Containing Complex Reducing Agents (NiCRA's). *Tetrahedron Lett.* **1998**, *39* (49), 8987–8990. https://doi.org/10.1016/S0040-4039(98)02034-6.

(88) Gualandi, A.; Emer, E.; Capdevila, M. G.; Cozzi, P. G. Highly Enantioselective α Alkylation of Aldehydes with 1,3-Benzodithiolylium Tetrafluoroborate: A Formal Organocatalytic α Alkylation of Aldehydes by the Carbenium Ion. *Angew. Chem. Int. Ed.* **2011**, *50* (34), 7842–7846. https://doi.org/10.1002/anie.201102562.

(89) McIntosh, J. M.; Schram, C. K. Reductive Desulfurization Using Tributyltin Hydride. *Can. J. Chem.* **1977**, *55* (21), 3755–3757. https://doi.org/10.1139/v77-529.

(90) Nozawa-Kumada, K.; Ito, S.; Noguchi, K.; Shigeno, M.; Kondo, Y. Super Electron Donor-Mediated Reductive Desulfurization Reactions. *Chem. Commun.* **2019**, *55* (86), 12968–12971. https://doi.org/10.1039/C9CC06775B.
(91) Gupta, S. K.; Marathe, S. A. Mild and Safe Procedure for Hydrolyzing Oximes: Improved Synthesis of 1,2-Indandione. *J. Pharm. Sci.* **1976**, *65* (1), 134–135. https://doi.org/10.1002/jps.2600650132.
(92) Almog, J.; Stepanov, N.; Dubnikova, F. Protection of the Carbonyl Groups in 1,2-Indanedione: Propellane versus Acetal Formation. *Tetrahedron Lett.* **2008**, *49* (11), 1870–1876. https://doi.org/10.1016/j.tetlet.2008.01.012.
(93) Toriyama, F.; Cornella, J.; Wimmer, L.; Chen, T.-G.; Dixon, D. D.; Creech, G.; Baran, P. S. Redox-Active Esters in Fe-Catalyzed C–C Coupling. *J. Am. Chem. Soc.* **2016**, *138* (35), 11132–11135. https://doi.org/10.1021/jacs.6b07172.
(94) Zhou, F.; Driver, T. G. Efficient Synthesis of 3H-Indoles Enabled by the Lead-Mediated α-Arylation of β-Ketoesters or γ-Lactams Using Aryl Azides. *Org. Lett.* **2014**, *16* (11), 2916–2919. https://doi.org/10.1021/ol5010615.
(95) Ros, A.; Magriz, A.; Dietrich, H.; Lassaletta, J. M.; Fernández, R. Stereoselective Synthesis of Syn β-Hydroxy Cycloalkane Carboxylates: Transfer Hydrogenation of Cyclic β-Keto Esters via Dynamic Kinetic Resolution. *Tetrahedron* **2007**, *63* (32), 7532–7537. https://doi.org/10.1016/j.tet.2007.05.058.
(96) Taber, D. F.; Ruckle, R. E. Cyclopentane Construction by Dirhodium Tetraacetate-Mediated Intramolecular C-H Insertion: Steric and Electronic Effects. *J. Am. Chem. Soc.* **1986**, *108* (24), 7686–7693. https://doi.org/10.1021/ja00284a037.
(97) Park, C. P.; Nagle, A.; Yoon, C. H.; Chen, C.; Jung, K. W. Formal Aromatic C−H Insertion for Stereoselective Isoquinolinone Synthesis and Studies on Mechanistic Insights into the C−C Bond Formation. *J. Org. Chem.* **2009**, *74* (16), 6231–6236. https://doi.org/10.1021/jo9011255.
(98) Kim, J.; Ohk, Y.; Park, S. H.; Jung, Y.; Chang, S. Intramolecular Aromatic Carbenoid Insertion of Biaryldiazoacetates for the Regioselective Synthesis of Fluorenes. *Chem. – Asian J.* **2011**, *6* (8), 2040–2047. https://doi.org/10.1002/asia.201100142.
(99) Yang, J.; Ji, C.; Zhao, Y.; Li, Y.; Jiang, S.; Zhang, Z.; Ji, Y.; Liu, W. BF3·OEt2: An Efficient Catalyst for Transesterification of β-Ketoesters. *Synth. Commun.* **2010**, *40* (7), 957–963. https://doi.org/10.1080/00397910903029842.
(100) Morgan, J.; Pinhey, J. T. Reaction of Arylboronic Acids and Their Derivatives with Lead Tetra-Acetate. The Generation of Aryl–Lead Triacetates, and Meta- and Para-Phenylenebis(Lead Triacetate), in Situ for Electrophilic Arylation. *J. Chem. Soc. Perkin 1* **1990**, *0* (3), 715–720. https://doi.org/10.1039/P19900000715.
(101) Ganina, O. G.; Zamotaeva, S. G.; Nosarev, M. A.; Kosenkova, O. V.; Naumov, M. I.; Shavyrin, A. S.; Finet, J.-P.; Fedorov, A. Yu. 2-(Azidomethyl)Phenylboronic Acid in the Synthesis of Isoquinoline Derivatives. *Russ. Chem. Bull.* **2005**, *54* (7), 1606–1611. https://doi.org/10.1007/s11172-006-0011-y.
(102) Elliott, G. I.; Konopelski, J. P. Arylation with Organolead and Organobismuth Reagents. *Tetrahedron* **2001**, *57* (27), 5683–5705. https://doi.org/10.1016/S0040-4020(01)00385-4.
(103) Yoshimura, A.; Zhdankin, V. V. Advances in Synthetic Applications of Hypervalent Iodine Compounds. *Chem. Rev.* **2016**, *116* (5), 3328–3435. https://doi.org/10.1021/acs.chemrev.5b00547.
(104) Chapter 8 Ligand Coupling Involving Other Heteroatoms. In *Tetrahedron Organic Chemistry Series*; Finet, J.-P., Ed.; Ligand Coupling Reactions with Heteroatomic Compounds; Elsevier, 1998; Vol. 18, pp 249–283. https://doi.org/10.1016/S1460-1567(98)80023-8.

(105) Barral, K.; Moorhouse, A. D.; Moses, J. E. Efficient Conversion of Aromatic Amines into Azides: A One-Pot Synthesis of Triazole Linkages. *Org. Lett.* **2007**, *9* (9), 1809–1811. https://doi.org/10.1021/ol070527h.
(106) Lin, A.; Yang, J.; Hashim, M. N-Indolyltriethylborate: A Useful Reagent for Synthesis of C3-Quaternary Indolenines. *Org. Lett.* **2013**, *15* (8), 1950–1953. https://doi.org/10.1021/ol4005992.
(107) Westermaier, M.; Mayr, H. Electrophilic Allylations and Benzylations of Indoles in Neutral Aqueous or Alcoholic Solutions. *Org. Lett.* **2006**, *8* (21), 4791–4794. https://doi.org/10.1021/ol0618555.
(108) Petrova, K. V.; Mohr, J. T.; Stoltz, B. M. Enantioselective Total Synthesis of (+)-Cassiol. *Org. Lett.* **2009**, *11* (2), 293–295. https://doi.org/10.1021/ol802410t.
(109) Bell, R. P. L.; Wijnberg, J. B. P. A.; de Groot, A. A Novel Route to the Marasmane Skeleton via a Tandem Rearrangement−Cyclopropanation Reaction. Total Synthesis of (+)-Isovelleral. *J. Org. Chem.* **2001**, *66* (7), 2350–2357. https://doi.org/10.1021/jo0015568.
(110) Hanessian, S.; Giroux, S.; Larsson, A. Efficient Allyl to Propenyl Isomerization in Functionally Diverse Compounds with a Thermally Modified Grubbs Second-Generation Catalyst. *Org. Lett.* **2006**, *8* (24), 5481–5484. https://doi.org/10.1021/ol062167o.
(111) Cramer, R. Olefin Coordination Compounds of Rhodium. III. The Mechanism of Olefin Isomerization. *J. Am. Chem. Soc.* **1966**, *88* (10), 2272–2282. https://doi.org/10.1021/ja00962a034.
(112) Primer, D. N.; Molander, G. A. Enabling the Cross-Coupling of Tertiary Organoboron Nucleophiles through Radical-Mediated Alkyl Transfer. *J. Am. Chem. Soc.* **2017**, *139* (29), 9847–9850. https://doi.org/10.1021/jacs.7b06288.
(113) Chen, T.-G.; Zhang, H.; Mykhailiuk, P. K.; Merchant, R. R.; Smith, C. A.; Qin, T.; Baran, P. S. Quaternary Centers by Nickel-Catalyzed Cross-Coupling of Tertiary Carboxylic Acids and (Hetero)Aryl Zinc Reagents. *Angew. Chem. Int. Ed.* **2019**, *58* (8), 2454–2458. https://doi.org/10.1002/anie.201814524.
(114) Parida, S. K.; Mandal, T.; Das, S.; Hota, S. K.; De Sarkar, S.; Murarka, S. Single Electron Transfer-Induced Redox Processes Involving N-(Acyloxy)Phthalimides. *ACS Catal.* **2021**, *11* (3), 1640–1683. https://doi.org/10.1021/acscatal.0c04756.
(115) Yuan, M.; Song, Z.; Badir, S. O.; Molander, G. A.; Gutierrez, O. On the Nature of C(Sp3)–C(Sp2) Bond Formation in Nickel-Catalyzed Tertiary Radical Cross-Couplings: A Case Study of Ni/Photoredox Catalytic Cross-Coupling of Alkyl Radicals and Aryl Halides. *J. Am. Chem. Soc.* **2020**, *142* (15), 7225–7234. https://doi.org/10.1021/jacs.0c02355.
(116) Suna, E.; Kalnins, T.; Kazak, M.; Vitkovska, V.; Narvaiss, N.; Zelencova, D.; Jaudzems, K. Structurally Simplified Diazonamide Analogs as Antimitotic Agents, July 1, 2021. https://patentscope.wipo.int/search/en/detail.jsf?docId=WO2021130515&_cid=P21-LXN428-17507-1 (accessed 2024-06-20).
(117) Kalnins, T.; Vitkovska, V.; Kazak, M.; Zelencova-Gopejenko, D.; Ozola, M.; Narvaiss, N.; Makrecka-Kuka, M.; Domračeva, I.; Kinens, A.; Gukalova, B.; Konrad, N.; Aav, R.; Bonato, F.; Lucena-Agell, D.; Díaz, J. F.; Liepinsh, E.; Suna, E. Development of Potent Microtubule Targeting Agent by Structural Simplification of Natural Diazonamide. *J. Med. Chem.* **2024**, *67* (11), 9227–9259. https://doi.org/10.1021/acs.jmedchem.4c00388.
(118) Vitkovska, V. Simplified Analogs of Diazonamide A as Anticancer Agents. Unpublished, University of Latvia, 2024.
(119) Trost, B. M.; Xie, J.; Sieber, J. D. The Palladium Catalyzed Asymmetric Addition of Oxindoles and Allenes: An Atom-Economical Versatile Method for the Construction of

Chiral Indole Alkaloids. *J. Am. Chem. Soc.* **2011**, *133* (50), 20611–20622. https://doi.org/10.1021/ja209244m.
(120) Jackson, R. F. W.; Moore, R. J.; Dexter, C. S.; Elliott, J.; Mowbray, C. E. Concise Synthesis of Enantiomerically Pure Phenylalanine, Homophenylalanine, and Bishomophenylalanine Derivatives Using Organozinc Chemistry: NMR Studies of Amino Acid-Derived Organozinc Reagents. *J. Org. Chem.* **1998**, *63* (22), 7875–7884. https://doi.org/10.1021/jo981133u.
(121) Huihui, K. M. M.; Caputo, J. A.; Melchor, Z.; Olivares, A. M.; Spiewak, A. M.; Johnson, K. A.; DiBenedetto, T. A.; Kim, S.; Ackerman, L. K. G.; Weix, D. J. Decarboxylative Cross-Electrophile Coupling of N-Hydroxyphthalimide Esters with Aryl Iodides. *J. Am. Chem. Soc.* **2016**, *138* (15), 5016–5019. https://doi.org/10.1021/jacs.6b01533.
(122) Umemiya, S.; Sakamoto, D.; Kawauchi, G.; Hayashi, Y. Enantioselective Total Synthesis of Beraprost Using Organocatalyst. *Org. Lett.* **2017**, *19* (5), 1112–1115. https://doi.org/10.1021/acs.orglett.7b00134.
(123) Shoemaker, R. H. The NCI60 Human Tumour Cell Line Anticancer Drug Screen. *Nat. Rev. Cancer* **2006**, *6* (10), 813–823. https://doi.org/10.1038/nrc1951.
(124) Holbeck, S. L.; Collins, J. M.; Doroshow, J. H. Analysis of Food and Drug Administration–Approved Anticancer Agents in the NCI60 Panel of Human Tumor Cell Lines. *Mol. Cancer Ther.* **2010**, *9* (5), 1451–1460. https://doi.org/10.1158/1535-7163.MCT-10-0106.
(125) *DTP COMPARE Search COMPARE Data*. https://dtp.cancer.gov/public_compare/ (accessed 2024-06-19).
(126) Saito, S.; Kano, T.; Muto, H.; Nakadai, M.; Yamamoto, H. Asymmetric Coupling of Phenols with Arylleads. *J. Am. Chem. Soc.* **1999**, *121* (38), 8943–8944. https://doi.org/10.1021/ja990646v.
(127) Afzali-Ardakani, A.; Rapoport, H. L-Vinylglycine. *J. Org. Chem.* **1980**, *45* (24), 4817–4820. https://doi.org/10.1021/jo01312a002.

APPENDICES

Appendix I – STEREOSELECTIVE SYNTHESIS OF THE DIAZONAMIDE A MACROCYCLIC CORE

Ilga Mutule, Beomjun Joo, Zane Medne, Toms Kalnins, Edwin Vedejs, and Edgars Suna

J. Org. Chem. **2015**, *80* (6), 3058–3066

JOC The Journal of Organic Chemistry

Article

pubs.acs.org/joc

Stereoselective Synthesis of the Diazonamide A Macrocyclic Core

Ilga Mutule,[†] Beomjun Joo,[‡] Zane Medne,[†] Toms Kalnins,[†] Edwin Vedejs,[‡] and Edgars Suna*[,†]

[†]Latvian Institute of Organic Synthesis, Aizkraukles 21, LV-1006, Riga, Latvia

[‡]Department of Chemistry, University of Michigan, Ann Arbor, Michigan 48109, United States

Supporting Information

ABSTRACT: Stereoselective synthesis of the right-hand heteroaromatic macrocycle of diazonamide A features C16–C18 bond formation in the Suzuki–Miyaura cross-coupling and atropodiastereoselective Dieckmann-type macrocyclization as key steps. The Suzuki–Miyaura cross-coupling gave the best yields when it was catalyzed by a palladium–dioxygen complex.

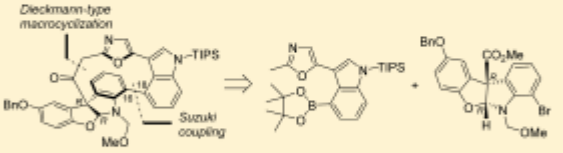

INTRODUCTION

Diazonamide A, a marine metabolite isolated from the colonial ascidian *Diazona angulata* exerts nanomolar cytotoxicity against human tumor cell lines.[1] The recent discovery of a novel mechanism of action of diazonamide A[2] has opened the door to a rational design of its simplified analogues as potential clinical agents. Not surprisingly, total synthesis of diazonamide A remains a focus of intense research efforts.

Diazonamide A contains many synthetically challenging structural elements such as a quaternary C10 stereocenter and two fused macrocycles: the left-hand 12-membered peptide ring and a right-hand heteroaromatic macrocycle possessing three axially chiral biaryl bonds (Scheme 1). Since 2002,[3] considerable synthetic efforts have resulted in four completed total syntheses[4−7] and several formal total syntheses[8] of diazonamide A. The synthetic strategy of the Harran,[4a] Nicolaou,[5] and MacMillan[7] total syntheses relied on the construction of the left-hand peptide ring prior to the formation of the right-hand heteroaromatic macrocycle. The right-hand heteroaromatic ring closure has been achieved by atropodiastereoselective formation of the C16–C18 biaryl bond using either photochemical Witkop-type cyclization (Harran, Nicolaou) or Pd-catalyzed Suzuki–Miyaura cross-coupling (MacMillan). In addition to the Suzuki–Miyaura cross-coupling,[9] other Pd-catalyzed methods such as Negishi[10] and Stille[11] reactions have also been used to establish the C16–C18 connection in a series of diazonamide A synthetic studies.

Our approach toward diazonamide A is based on an initial stereoselective assembly of the right-hand heteroaromatic macrocycle **2** by Suzuki cross-coupling of enantiomerically pure hemiaminal bromide (*R*,*R*)-**5** with indolyl boronate **4**, followed by atropodiastereoselective Dieckmann-type cyclization of biaryl **3** (Scheme 1). The Suzuki approach to C16–C18 bond formation is superior to Stille methodology reported earlier because the latter requires elaboration of the expensive enantiomerically pure hemiaminal bromide (*R*,*R*)-**5** to the corresponding stannate.[11] Furthermore, the Stille coupling had used an excess of the stannane for stoichiometric coupling with an isolable palladium intermediate related to **4** (Pd in place of B).

RESULTS AND DISCUSSION

The C16–C18 connection via Suzuki coupling required preparation of the chiral, nonracemic bromide (*R*,*R*)-**5** and N-protected indolyl boronate **4**. The bromide (*R*,*R*)-**5** was obtained from *N*-Alloc-protected enantiomerically pure bicyclic hemiaminal (*R*,*R*)-**6**[12] in a two-step sequence comprising a cleavage of the *N*-Alloc protecting group using Pd(0) catalyst and 1,3-dimethylbarbituric acid **7** as described previously,[11] followed by installation of an *N*-MOM protecting group in the TMS-Cl-mediated reaction of (*R*,*R*)-**8**[13] with paraformaldehyde and MeOH (Scheme 2).[14]

The indolyl boronate subunit **4** for the Suzuki cross-coupling was prepared from a known triflate **15** (Scheme 3). The synthesis of triflate **15** was reported earlier, but this procedure was difficult due to the need to handle methylisocyanide during the formation of the oxazole moiety.[9b] This sequence proved to be especially challenging on a large scale, so an alternative procedure has been developed. Thus, ethyl acetamidoacetate was converted into the Weinreb amide **11** using diethylaluminum activation of *N*,*O*-dimethylhydroxylamine hydrochloride. Next, the acidic proton in the amide functional group of **11** was deprotonated with *i*-PrMgCl to avoid quenching the basic intermediate in the next step. Thus, the resulting magnesiated amide intermediate was reacted with lithiated indole **10**, prepared from 3-bromoindole **9**[9b] by low-temperature lithium–halogen exchange with *t*-BuLi. The resulting ketoamide **12** was transformed into the oxazole **13** using Wipf's cyclodehydration conditions.[15] Subsequent cleavage of the benzyl ether (Pd/C, H_2) and treatment of the resulting phenol **14** with NaH and $PhN(SO_2CF_3)_2$ afforded the triflate **15** in 92% yield.

Next, conversion of triflate **15** to boronate **4** was addressed. The use of bis(pinacolato)diboron $(BPin)_2$ under various

Received: December 29, 2014
Published: February 23, 2015

DOI: 10.1021/jo5029419
J. Org. Chem. 2015, 80, 3058−3066

JOC The Journal of Organic Chemistry

Article

pubs.acs.org/joc

Stereoselective Synthesis of the Diazonamide A Macrocyclic Core

Ilga Mutule,[†] Beomjun Joo,[‡] Zane Medne,[†] Toms Kalnins,[†] Edwin Vedejs,[‡] and Edgars Suna*[,†]

[†]Latvian Institute of Organic Synthesis, Aizkraukles 21, LV-1006, Riga, Latvia

[‡]Department of Chemistry, University of Michigan, Ann Arbor, Michigan 48109, United States

Supporting Information

ABSTRACT: Stereoselective synthesis of the right-hand heteroaromatic macrocycle of diazonamide A features C16–C18 bond formation in the Suzuki–Miyaura cross-coupling and atropodiastereoselective Dieckmann-type macrocyclization as key steps. The Suzuki–Miyaura cross-coupling gave the best yields when it was catalyzed by a palladium–dioxygen complex.

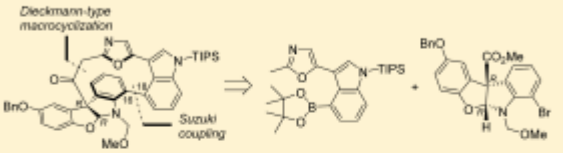

INTRODUCTION

Diazonamide A, a marine metabolite isolated from the colonial ascidian *Diazona angulata* exerts nanomolar cytotoxicity against human tumor cell lines.[1] The recent discovery of a novel mechanism of action of diazonamide A[2] has opened the door to a rational design of its simplified analogues as potential clinical agents. Not surprisingly, total synthesis of diazonamide A remains a focus of intense research efforts.

Diazonamide A contains many synthetically challenging structural elements such as a quaternary C10 stereocenter and two fused macrocycles: the left-hand 12-membered peptide ring and a right-hand heteroaromatic macrocycle possessing three axially chiral biaryl bonds (Scheme 1). Since 2002,[3] considerable synthetic efforts have resulted in four completed total syntheses[4−7] and several formal total syntheses[8] of diazonamide A. The synthetic strategy of the Harran,[4a] Nicolaou,[5] and MacMillan[7] total syntheses relied on the construction of the left-hand peptide ring prior to the formation of the right-hand heteroaromatic macrocycle. The right-hand heteroaromatic ring closure has been achieved by atropodiastereoselective formation of the C16–C18 biaryl bond using either photochemical Witkop-type cyclization (Harran, Nicolaou) or Pd-catalyzed Suzuki–Miyaura cross-coupling (MacMillan). In addition to the Suzuki–Miyaura cross-coupling,[9] other Pd-catalyzed methods such as Negishi[10] and Stille[11] reactions have also been used to establish the C16–C18 connection in a series of diazonamide A synthetic studies.

Our approach toward diazonamide A is based on an initial stereoselective assembly of the right-hand heteroaromatic macrocycle **2** by Suzuki cross-coupling of enantiomerically pure hemiaminal bromide (*R*,*R*)-**5** with indolyl boronate **4**, followed by atropodiastereoselective Dieckmann-type cyclization of biaryl **3** (Scheme 1). The Suzuki approach to C16–C18 bond formation is superior to Stille methodology reported earlier because the latter requires elaboration of the expensive enantiomerically pure hemiaminal bromide (*R*,*R*)-**5** to the corresponding stannate.[11] Furthermore, the Stille coupling had used an excess of the stannane for stoichiometric coupling with an isolable palladium intermediate related to **4** (Pd in place of B).

RESULTS AND DISCUSSION

The C16–C18 connection via Suzuki coupling required preparation of the chiral, nonracemic bromide (*R*,*R*)-**5** and N-protected indolyl boronate **4**. The bromide (*R*,*R*)-**5** was obtained from *N*-Alloc-protected enantiomerically pure bicyclic hemiaminal (*R*,*R*)-**6**[12] in a two-step sequence comprising a cleavage of the *N*-Alloc protecting group using Pd(0) catalyst and 1,3-dimethylbarbituric acid **7** as described previously,[11] followed by installation of an *N*-MOM protecting group in the TMS-Cl-mediated reaction of (*R*,*R*)-**8**[13] with paraformaldehyde and MeOH (Scheme 2).[14]

The indolyl boronate subunit **4** for the Suzuki cross-coupling was prepared from a known triflate **15** (Scheme 3). The synthesis of triflate **15** was reported earlier, but this procedure was difficult due to the need to handle methylisocyanide during the formation of the oxazole moiety.[9b] This sequence proved to be especially challenging on a large scale, so an alternative procedure has been developed. Thus, ethyl acetamidoacetate was converted into the Weinreb amide **11** using diethylaluminum activation of *N*,*O*-dimethylhydroxylamine hydrochloride. Next, the acidic proton in the amide functional group of **11** was deprotonated with *i*-PrMgCl to avoid quenching the basic intermediate in the next step. Thus, the resulting magnesiated amide intermediate was reacted with lithiated indole **10**, prepared from 3-bromoindole **9**[9b] by low-temperature lithium–halogen exchange with *t*-BuLi. The resulting ketoamide **12** was transformed into the oxazole **13** using Wipf's cyclodehydration conditions.[15] Subsequent cleavage of the benzyl ether (Pd/C, H_2) and treatment of the resulting phenol **14** with NaH and $PhN(SO_2CF_3)_2$ afforded the triflate **15** in 92% yield.

Next, conversion of triflate **15** to boronate **4** was addressed. The use of bis(pinacolato)diboron $(BPin)_2$ under various

Received: December 29, 2014
Published: February 23, 2015

DOI: 10.1021/jo5029419
J. Org. Chem. 2015, 80, 3058−3066

Scheme 1. Retrosynthetic Analysis of Diazonamide A

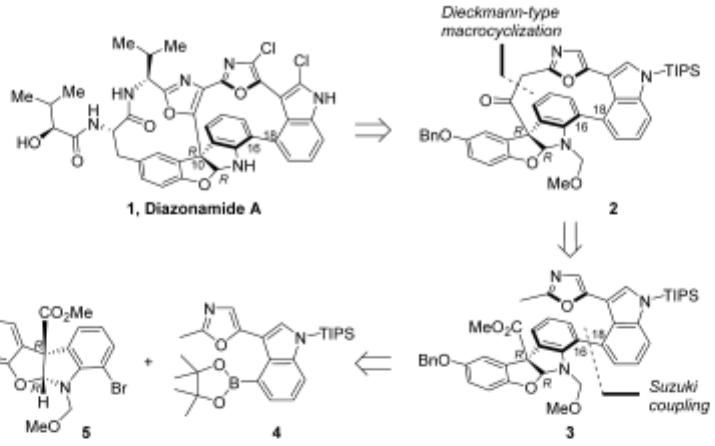

Scheme 2. Preparation of Hemiaminal (*R*,*R*)-5

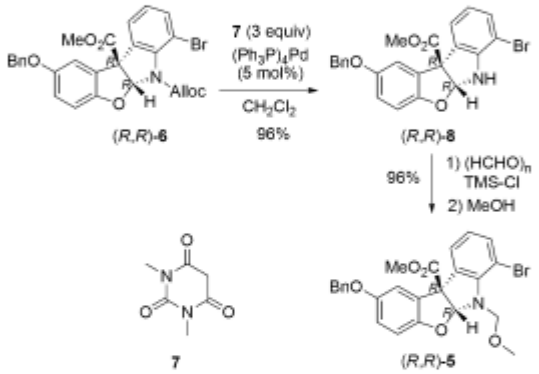

conditions ($PdCl_2$(dppf)/KOAc/DMSO,[16] $Pd(Ph_3P)_4$/KOAc/NMP,[17] and $Pd(OAc)_2$/S-Phos/K_3PO_4/dioxane[18]) resulted in poor conversion and different decomposition products such as those derived from the cleavage of *N*-TIPS, hydrolysis of the triflate **15**, or protonolysis of the boronate **4**. It was also found that the yield of the desired boronate **4** depended on the quality of the bis(pinacolato)diboron: even small amounts of the pinacol impurity (5–10 mol %) in the $(BPin)_2$ reagent was sufficient to decrease the conversion of the triflate **15** by 40–60%. In contrast, the use of pinacol borane (PinBH) as an alternative boron source and $Pd(OAc)_2$/DPE-Phos as a catalyst[19] allowed for the conversion of the indolyl triflate **15** into the boronate **4** in reproducible 91% yield.

With both subunits for the cross-coupling in hand, a preliminary screening of the Suzuki–Miyaura reaction conditions was performed using the boronate **4** and 7-bromindoline as a model bromide. 1,4-Dioxane was found to be the best solvent, and K_2CO_3 and K_3PO_4 were the most suitable bases which did not affect the *N*-TIPS protecting group in the boronate **4**. Importantly, rigorous removal of moisture and oxygen traces was found to be critical for the success of the cross-coupling.[20] After the best base was established, screening of Pd catalysts was performed using the hemiaminal bromide (*R*,*R*)-**5** and the boronate **4**. Among various Pd catalysts examined, those formed in situ from $Pd(dba)_2$ and biaryl phosphine ligands were least efficient, affording debrominated (*R*,*R*)-**5** and the protodeboronated derivative of **4** as major products (entries 1 and 2, Table 1). Substantial amounts of the debrominated (*R*,*R*)-**5** were also formed using $Pd(PPh_3)_4$ and

Scheme 3. Synthesis of Boronate 4

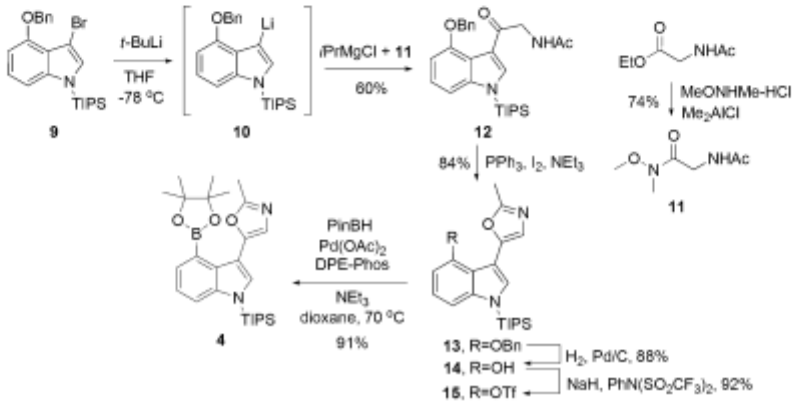

DOI: 10.1021/jo5029419
J. Org. Chem. 2015, 80, 3058–3066

Table 1. Catalyst Screening for Suzuki–Miyaura Cross-Coupling Reaction

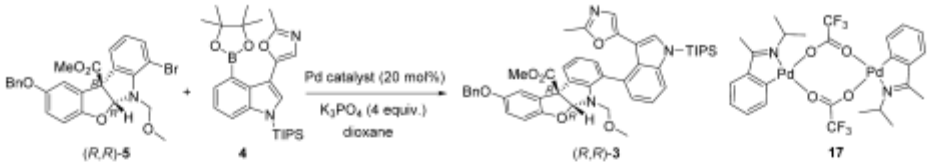

entry	catalyst, conditions[a]	conversion of (R,R)-5, %[b]	(R,R)-3, %[b]	major side product[c]
1	$Pd(dba)_2$, S-Phos (Pd/L = 1:2), 100 °C, 40 h	51	10	A, B
2	$Pd(dba)_2$, X-Phos (Pd/L = 1:2), 100 °C, 40 h	56	4	A, B
3	$Pd(PPh_3)_4$, 100 °C, 120 h	68	63	A
4	$Pd(dppf)Cl_2 x CH_2Cl_2$, 100 °C, 40 h	76	50	A
5	$(P\text{-}tBu_3)_2Pd$, 100 °C, 20 h	40	11	B
6	$Pd_2(dba)_3$, PCy_3 (Pd/L = 1:2), 100 °C, 40 h[d]	44	20	A
7	$(PCy_3)_2Pd$,[f] 120 °C, 20 h	96	81 (82)[e]	
8	$(PCy_3)_2Pd$,[g] 120 °C, 20 h	80	55 (47)[e]	
9	$(PCy_3)_2Pd$,[h] 120 °C, 20 h	42	20	A
10	$(PCy_3)_2Pd(\eta^2\text{-}O_2)$ (**16**), 120 °C, 20 h	99	83 (81)[i]	
11[j]	$(PCy_3)_2Pd(\eta^2\text{-}O_2)$ (**16**), 110 °C, 38 h	99	(76)[e]	
12[j]	palladacycle **17**, 110 °C, 20 h	58	57	
13[j]	$(PCy_3)_2Pd(\eta^2\text{-}O_2)$ (**16**), metallic Hg,[k] 110 °C, 18 h	60	21	

[a]With 20 mol % of palladium catalyst used in all experiments. [b]Determined by HPLC using three-point calibration and 4-methylbenzonitrile as an internal standard; reactions performed on 0.1 mmol scale. [c]A: debrominated (*R*,*R*)-**5**. B: Protodeboronated **4**. [d]Use of 1.2 equiv of PCy_3 per Pd afforded increased amounts (38%) of debrominated (*R*,*R*)-**5** (at 60% conversion). [e]In parentheses, isolated yield of >95% pure (*R*,*R*)-**3** (HPLC assay), 0.4 mmol scale. [f]Batch of the catalyst which was handled under air. [g]Fresh, unopened batch of catalyst as received from vendor. [h]Catalyst synthesized from $(COD)PdBr_2$ (see ref 22a) and handled in a glovebox. [i]In parentheses, isolated yields of >92% pure (*R*,*R*)-**3** (HPLC assay), 0.4 mmol scale. [j]Reaction was performed in toluene. [k]Metallic Hg was added 30 min after the beginning of the cross-coupling reaction.

$Pd(dppf)Cl_2 x CH_2Cl_2$ as catalysts (entries 3 and 4). $(P\text{-}tBu_3)_2Pd$[21] afforded poor conversion and delivered a considerable amount of the protodeboronated indole **4** (entry 5). In sharp contrast, $(PCy_3)_2Pd$ catalyzed the formation of the desired biaryl **3** in excellent yields (entry 7), but these results proved difficult to reproduce. A catalyst formed in situ from $Pd_2(dba)_3$ and PCy_3 (Pd/L = 1:2) was far less efficient (entry 6).

Importantly, inconsistent yields of the biaryl **3** were obtained using different batches of the $(PCy_3)_2Pd$ catalyst. Thus, a 2-fold decrease in yield was observed using a freshly opened batch of the commercial $(PCy_3)_2Pd$ catalyst compared to a batch that was handled under air (entry 8 vs entry 7). Comparison of ^{31}P NMR spectra (in C_6D_6) of the two $(PCy_3)_2Pd$ samples showed that both possessed two signals: one at 39.0 ppm (assigned to $(PCy_3)_2Pd$ species)[22] and another signal at 45.0 ppm. The latter signal was tentatively assigned to a dioxygen complex $(PCy_3)_2Pd(\eta^2\text{-}O_2)$ (**16**) that could form upon exposure of solid $(PCy_3)_2Pd$ to air.[23] The ratio of the ^{31}P NMR signals was different in all of the commercial $(PCy_3)_2Pd$ batches. Thus, the more active Pd catalyst (entry 7; $(PCy_3)_2Pd$, exposed to air) displayed a major signal at 45.0 ppm corresponding to the dioxygen complex $(PCy_3)_2Pd(\eta^2\text{-}O_2)$ (**16**), whereas the ^{31}P NMR spectrum of the less active Pd catalyst batch (entry 8) showed the major signal at 39.0 ppm, corresponding to the $(PCy_3)_2Pd$ species. To determine if the catalytic activity is associated with Pd–dioxygen complex **16**, pure $(PCy_3)_2Pd$ was synthesized from $(COD)PdBr_2$[22a] under oxygen-free conditions using the Schlenk technique. The ^{31}P NMR spectrum of the synthesized $(PCy_3)_2Pd$ catalyst did not contain the signal at 45.0 ppm, confirming the absence of $(PCy_3)_2Pd(\eta^2\text{-}O_2)$. This relatively pure catalyst turned out to be the least efficient among all tested $(PCy_3)_2Pd$ batches (entry 9), confirming that the Pd–dioxygen complex **16** apparently is an actual catalyst in the cross-coupling between the bromide (*R*,*R*)-**5** and the boronate **4**. Finally, pure $(PCy_3)_2Pd(\eta^2\text{-}O_2)$ (**16**) was synthesized by suspending the white crystalline $(PCy_3)_2Pd$ in precooled Et_2O (at −20 °C) and stirring for 10 min under air to afford an aquamarine solid which showed a single peak in the ^{31}P NMR spectrum at 45.0 ppm. The structure of the Pd–dioxygen complex **16** was confirmed by X-ray crystallographic analysis (Figure 1).[24,25]

As anticipated from the control studies described above, but contrary to our initial expectations and intuition, an experiment using $(PCy_3)_2Pd(\eta^2\text{-}O_2)$ (**16**) resulted in complete conversion of (*R*,*R*)-**5**, affording the biaryl (*R*,*R*)-**3** in 81% yield (entry 10).

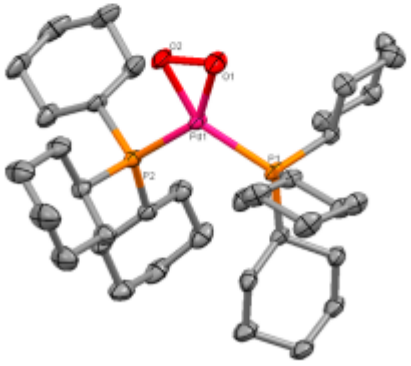

Figure 1. X-ray crystal structure of $(PCy_3)_2Pd(\eta^2\text{-}O_2)$ (**16**) (ellipsoids at 50% probability) with hydrogen atoms omitted for clarity. Selected bond distances (Å) and angles (deg): O1–O2, 1.443(6); Pd–O1, 2.015(4); Pd–O2, 2.021(4); Pd–P1, 2.301(1); Pd–P2, 2.295(1); P1–Pd–P2, 111.75(5). See the Supporting Information for details.

DOI: 10.1021/jo5029419
J. Org. Chem. 2015, 80, 3058–3066

Scheme 4. Synthesis of Macrocycle (*M*,*M*,*R*,*R*)-2

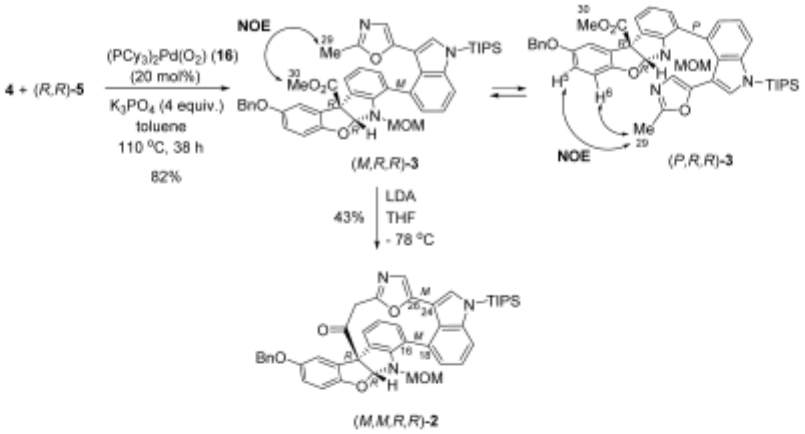

Dioxane and toluene were equally efficient as solvents (entries 10 and 11); however, better reproducibility of the cross-coupling yields was observed in toluene. Therefore, toluene was used as the solvent in all subsequent cross-coupling experiments. The Suzuki reaction in THF and DME delivered the *N*-TIPS-deprotected biaryl **3** as the major product (50−60%) together with the debrominated (*R*,*R*)-**5** (30%). To the best of our knowledge, this is the first example of the Suzuki−Miyaura cross-coupling that is catalyzed by a Pd−dioxygen complex.[26]

The superiority of $(PCy_3)_2Pd(\eta^2\text{-}O_2)$ (**16**) as the catalyst compared to $(PCy_3)_2Pd$ species is intriguing given a low thermal stability of the Pd−dioxygen complex **16**.[24a] Thus, 64% of $(PCy_3)_2Pd(\eta^2\text{-}O_2)$ (**16**) was decomposed to $Cy_3P{=}O$ (57%) and $(PCy_3)_2Pd$ species (7%) after 15 min at 60 °C in dioxane-d_8, as evidenced by ^{31}P spectroscopy. Furthermore, the solution turned brown, and formation of Pd black was also observed. Poor thermal stability of the Pd−dioxygen complex **16** puts in question its involvement in the catalytic cycle of the cross-coupling between (*R*,*R*)-**5** and **4**, as the latter requires prolonged heating at 110−120 °C to go to completion (entries 10 and 11). On the other hand, the observed formation of black colloidal palladium upon thermal degradation of **16** suggests an involvement of heterogeneous Pd species in the catalytic cycle of the Suzuki cross-coupling. It has been demonstrated that heterogeneous Pd species are true catalysts in the Suzuki−Miyaura reaction[27] and that certain palladacycles such as **17**[28] produce catalytically active heterogeneous Pd species at elevated temperatures used in cross-coupling reactions.[29] The imine-based palladacycle **17** was tested as the catalyst in the cross-coupling between (*R*,*R*)-**5** and **4** under the optimal conditions (entry 12, Table 1). The biaryl (*R*,*R*)-**3** was formed in 57% yield, so the Pd species formed from **17** can indeed catalyze the cross-coupling in the absence of stabilizing phosphine ligands. Further evidence for a possible involvement of heterogeneous Pd species was obtained in a "mercury drop" test.[30] Accordingly, 600 equiv of metallic Hg (with respect to the Pd−dioxygen complex **16**) was added to the cross-coupling reaction mixture 30 min after the reaction had been initiated (entry 13). Within the 30 min (before the mercury drop was added), the biaryl (*R*,*R*)-**3** had already been formed in 20% yield (39% conversion). After the Hg addition, the heating at 110 °C was continued for another 18 h. Importantly, the yield of the biaryl (*R*,*R*)-**3** remained virtually unchanged (21% at 60% conversion) after the prolonged heating. Apparently, the added mercury inhibited the cross-coupling catalyzed by Pd−dioxygen complex **16**, presumably by amalgamation of heterogeneous Pd species. Thus, we regard the catalysis by the heterogeneous Pd species formed in situ to be plausible;[31] however, operation of a homogeneous pathway leading to the formation of biaryl (*R*,*R*)-**3** cannot be ruled out.[32]

The ^1H NMR spectrum of the biaryl (*R*,*R*)-**3** in benzene-d_6 at 20 °C displayed two sets of signals in a 3:2 ratio corresponding to a mixture of two atropisomers. The ratio was measured by integration of signals corresponding to the C27 oxazole proton (δ 6.53 and 6.04 ppm), C30 ester protons (δ 3.44 and 3.13 ppm), and C29 methyl group (δ 2.02 and 1.76 ppm). The structures of the atropisomers were assigned on the basis of NOE experiment. Thus, a medium intensity NOE cross-peak was observed between the C29 methyl group and the C30 ester protons of the major atropisomer, whereas weak intensity NOE interactions between C29 methyl group and aromatic C5 and C6 protons were observed for the minor atropisomer (Scheme 4). Consequently, the major and minor atropisomers of the biaryl (*R*,*R*)-**3** were assigned *M*- and *P*-configurations around the C16−C18 bond, respectively. The two atropisomers underwent interconversion at room temperature, and the free energy of activation and rate constants for the atropisomerization of (*R*,*R*)-**3** were determined at 25 °C in benzene-d_6 by NMR methods.[33] The barrier to rotation around the C16−C18 bond was measured to be 20.0 kcal/mol, which corresponds to a half-life of ca. 58 s for atropisomerization. However, at temperatures below −20 °C, the interconversion between *M*- and *P*-atropisomers of (*R*,*R*)-**3** in THF-d_8 was slow on the NMR time scale.

The *M*/*P* = 3:2 equilibrium mixture of atropisomers was employed in the subsequent Dieckmann-type macrocyclization at −78 °C by using lithium diisopropylamide (LDA) as the base. The low temperature was critical for the success of the macrocyclization because at higher temperatures (such as −40 °C) the decomposition of the lithiated (*R*,*R*)-**3** became a major reaction. Importantly, the macrocyclization at −78 °C apparently proceeds below the threshold for atropisomer interconversion. This implies that only the major atropisomer (*M*,*R*,*R*)-**3** may be transformed into the macrocycle (*M*,*M*,*R*,*R*)-**2** with ca. 60% theoretical yield. In fact, the target macrocycle (*M*,*M*,*R*,*R*)-**2** was formed in 43% yield within 10 min, and

DOI: 10.1021/jo5029419
J. Org. Chem. 2015, 80, 3058−3066

prolonged reaction times (30 min) did not improve the yield. The unreacted biaryl (*R*,*R*)-**3** was also recovered as a *M*/*P* = 3:2 mixture of atropisomers (40% yield, 83% material balance). Evidently, the unreacted atropisomer (*P*,*R*,*R*)-**3** had re-equilibrated during workup to the *M*/*P* = 3:2 equilibrium mixture. This allows for the reuse of the recovered material in the macrocyclization.

■ CONCLUSIONS

Atropodiastereoselective Dieckmann-type cyclization provides an access to the macrocyclic core of diazonamide A in enantiomerically pure form. The diastereoselectivity of the macrocyclization was controlled by the (*R*)-stereogenic center at C10 of the rigid tetracyclic hemiaminal moiety. Notably, *M*-configuration around both C16−C18 and C24−C26 biaryl bonds of the macrocycle was simultaneously established in the cyclization step. The Dieckmann-type cyclization proceeded below the threshold for interconversion of atropisomers around the C16−C18 biaryl bond in the starting biaryl (*R*,*R*)-**3**. Therefore, only the *M*-atropisomer underwent the ring closure, whereas the *P*-atropisomer did not react. However, the unreacted *P*-atropisomer equilibrated back to the starting 3:2 *M*/*P* mixture during the workup, and hence, the recovered biaryl (*R*,*R*)-**3** can be reused in the macrocyclization. The biaryl (*R*,*R*)-**3** was prepared in the Suzuki−Miyaura cross-coupling between the chiral, nonracemic tetracyclic hemiaminal bromide and indolyl boronate. Unexpectedly, palladium−dioxygen complex $(PCy_3)_2Pd(\eta^2\text{-}O_2)$ (**16**) was found to be the most efficient catalyst in the Suzuki−Miyaura reaction. Suzuki−Miyaura coupling has been used in other diazonamide studies, but only the MacMillan synthesis included an intact unprotected aminal subunit having the correct functionality.[7] Further elaboration of the enantiomerically pure macrocyclic core of diazonamide A will be reported in due course.

■ EXPERIMENTAL SECTION

General Information. Unless otherwise noted, all chemicals were used as obtained from commercial sources and all reactions were performed under nitrogen or argon atmosphere in glassware dried in an oven (120 °C) and cooled under a stream of nitrogen or argon. Toluene, tetrahydrofuran (THF), and 1,4-dioxane were distilled from sodium/benzophenone prior the use. Dry CH_2Cl_2 and Et_2O were obtained by passing commercially available anhydrous solvents through activated alumina columns. Commercially available anhydrous K_3PO_4 was heated at 250 °C for 3 h and stored in a glovebox under argon atmosphere.

Analytical thin-layer chromatography (TLC) was performed on precoated silica gel F-254 plates. Flash chromatography was performed using Davisil LC60A 35−70 μm silica gel. High-resolution mass spectra were recorded on a mass spectrometer with a time-of-flight (TOF) mass analyzer. Nuclear magnetic resonance spectra were recorded on NMR spectrometers at the following frequencies: ^1H, 400 or 600 MHz; $^{13}C\{^1H\}$, 101 or 126 MHz; ^{31}P, 162 MHz. Chemical shifts were referenced to Me_4Si as an internal reference or to residual solvent peaks. Signals in ^{31}P were referenced to H_3PO_4 as an external standard.

2-Acetylamino-*N*-methoxy-*N*-methylacetamide (11). To a suspension of *N*,*O*-dimethylhydroxylamine hydrochloride (9.76 g, 100 mmol) in CH_2Cl_2 (400 mL) was added Me_2AlCl (1.0 M in hexanes, 100 mL, 100 mmol) at 0 °C.[34] After being stirred at room temperature for 30 min, ethyl acetamidoacetate (7.26 g, 50.0 mmol) was added, and stirring at room temperature was continued for 2 h. The reaction mixture was then treated with EtOAc (50 mL) and MeOH (50 mL) and stirred for 10 min. To this solution was added SiO_2 (50 g), and the suspension was concentrated under reduced pressure. The resulting crude solid was loaded onto SiO_2 and eluted with EtOAc, followed by 10% MeOH in EtOAc to afford **11** (5.90 g, 74% yield) as a white solid: analytical TLC on silica gel, EtOAc, R_f = 0.16; pure material was obtained by crystallization from CH_2Cl_2/hexanes; mp 96−97 °C; IR (film, cm^{-1}) 3278 (N−H), 1676 (C═O), 1654 (C═O); ^1H NMR (400 MHz, $CDCl_3$, ppm) δ 6.36 (1H, br s), 4.18 (2H, d, *J* = 4.0 Hz), 3.71 (3H, s), 3.21 (3H, s), 2.04 (3H, s); $^{13}C\{^1H\}$ NMR (101 MHz, $CDCl_3$, ppm) δ 170.3, 169.9, 61.7, 41.0, 32.5, 23.2. Anal. Calcd for $C_6H_{12}N_2O_3$: C, 44.99; H, 7.55; N, 17.49. Found: C, 45.00; H, 7.57; N, 17.50.

***N*-(2-(4-(Benzyloxy)-1-(triisopropylsilyl)-1*H*-indol-3-yl)-2-oxoethyl)acetamide (12).** A solution of 2-acetylamino-*N*-methyl-*N*-methoxyacetamide (**11**) (1.20 g, 7.50 mmol) in anhydrous THF (75 mL) was cooled to −15 °C under nitrogen atmosphere, and *i*-PrMgCl (2.0 M solution in THF, 5.60 mL, 11.2 mmol) was slowly added. The resulting light gray suspension was stirred for 30 min at −15 °C under nitrogen atmosphere.[35] In a separate flask, to a cooled solution of 4-benzyloxy-3-bromo-1-triisopropylsilylindole (**9**)[9b] (3.44 g, 7.5 mmol) in anhydrous THF (75 mL) was slowly added *t*-BuLi (1.6 M solution in pentane, 9.4 mL, 15 mmol) at −78 °C under nitrogen atmosphere at a rate to maintain the internal temperature below −70 °C. The resulting orange solution was stirred for 15 min at −78 °C, whereupon the color changed to carmine red. The solution of the lithiated indole was then transferred using a metal cannula to the light gray suspension of magnesium amide from above, which was cooled to −15 °C. The resulting pale yellow slurry was warmed to room temperature and left to stir for 20 h, whereupon a clear pale yellow solution was formed. The reaction was quenched with saturated aqueous NH_4Cl (100 mL) and extracted with EtOAc (3 × 50 mL). The organic layer was washed with saturated aqueous $NaHCO_3$ solution (100 mL) and brine (100 mL), and the combined aqueous layers were extracted with EtOAc (150 mL). The combined organic layers were dried over Na_2SO_4 and concentrated under reduced pressure. The crude residue was loaded on SiO_2, which had been pretreated with 0.1% triethylamine in hexanes. Elution with 50% EtOAc and 0.1% NEt_3 in hexanes afforded **12** (2.16 g, 60%) as a white solid: analytical TLC on silica gel, 1:1 hexanes/EtOAc, R_f = 0.60; pure material was obtained by crystallization from Et_2O; mp 137−138 °C; IR (film, cm^{-1}) 3364 (N−H), 1674 (C═O), 1650 (C═O); ^1H NMR (400 MHz, $CDCl_3$, ppm) δ 7.84 (1H, s), 7.54 (2H, d, *J* = 7.6 Hz), 7.37 (2H, t, *J* = 7.9 Hz), 7.32−7.27 (1H, m), 7.14−7.08 (2H, m), 6.73 (1H, dd, *J* = 6.4, 2.1 Hz), 6.46 (1H, br s), 5.27 (2H, s), 4.74 (2H, d, *J* = 4.4 Hz), 2.01 (3H, s), 1.69 (3H, septet), 1.13 (18H, d, *J* = 7.4 Hz); $^{13}C\{^1H\}$ NMR (101 MHz, $CDCl_3$, ppm) δ 191.4, 170.0, 152.6, 143.5, 137.8, 136.9, 128.5, 127.99, 127.95, 123.8, 118.8, 117.6, 107.8, 104.4, 70.5, 49.2, 23.0, 17.9, 12.6. Anal. Calcd for $C_{29}H_{38}N_2O_3Si$: C, 70.25; H, 8.00; N, 5.85. Found: C, 70.24; H, 8.00; N, 5.80.

5-(4-(Benzyloxy)-1-(triisopropylsilyl)-1*H*-indol-3-yl)-2-methyloxazole (13). To a stirred solution of ketone **12** (1.20 g, 2.51 mmol) in anhydrous CH_2Cl_2 (100 mL) under nitrogen atmosphere was added PPh_3 (3.17 g, 12.05 mmol), followed by I_2 (3.06 g, 12.05 mmol) and NEt_3 (3.50 mL, 25.10 mmol). The reaction mixture was stirred at room temperature for 2 h, diluted with EtOAc (100 mL), and washed with saturated aqueous $Na_2S_2O_3$ solution (2 × 100 mL) and saturated aqueous $NaHCO_3$ (100 mL). The aqueous washings were combined and extracted with EtOAc (100 mL). Organic extracts were combined and dried over Na_2SO_4. Column chromatography on silica gel using gradient elution from 6% EtOAc in hexanes to 20% EtOAc in hexanes afforded **13** as a yellow foam (972 mg, 84% yield): analytical TLC on silica gel, 2:5 EtOAc/hexanes, R_f = 0.33; ^1H NMR (400 MHz, $CDCl_3$, ppm) δ 7.43−7.29 (6H, m), 7.14−7.04 (3H, m), 6.64 (1H, d, *J* = 7.6 Hz), 5.17 (2H, s), 2.34 (3H, s), 1.70 (3H, septet), 1,15 (18H, d, *J* = 7.8); $^{13}C\{^1H\}$ NMR (101 MHz, $CDCl_3$) δ 159.4, 153.1, 147.6, 143.4, 136.8, 128.9, 128.7, 128.3, 128.2, 123.4, 123.1, 118.1, 107.9, 107.5, 102.2, 70.5, 18.3, 14.1, 12.9; HRMS-ESI (*m*/*z*) calcd for $C_{28}H_{37}N_2O_2Si$ $[M + H]^+$ 461.2619, found 461.2621.

3-(2-Methyloxazol-5-yl)-1-(triisopropylsilyl)-1*H*-indol-4-ol (14). To a solution of indole **13** (1.97 g, 4.28 mmol) in abs. EtOH (40 mL) was added 10% Pd−C (182 mg, 0.171 mmol, 4 mol %), and H_2 gas was passed through the resulting suspension at room temperature.

DOI: 10.1021/jo5029419
J. Org. Chem. 2015, 80, 3058−3066

Progress of the hydrogenation was followed by TLC (2:5 EtOAc/hexanes, starting indole **13** R_f = 0.33; product **14** R_f = 0.13). Usually, it required 4−6 h for the hydrogenation to go to completion. In case of incomplete conversion after 6 h, it is recommended to add an additional amount of 10% Pd−C (182 mg, 0.171 mmol, 4 mol %) and continue the hydrogenation. Once the reaction is completed, it was filtered through a plug of Celite. The filter cake was washed with EtOH (120 mL), EtOAc (200 mL), and Et_2O (120 mL). All filtrates were combined and solvents were concentrated (aspirator) to afford **14** as a grayish amorphous material (1.4 g, 88% yield): analytical TLC on silica gel, 1:1 EtOAc/hexanes, R_f = 0.41; IR (film, cm^{-1}) 3143 (O−H); ^1H NMR (400 MHz, $CDCl_3$, ppm) δ 7.38 (1H, s), 7.18 (1H, s), 7.07−7.05 (2H, m), 6.69 (1H, br s), 6.63 (1H, m), 2.54 (3H, s), 1.70 (3H, septet, J = 7.5 Hz), 1.15 (18H, d, J = 7.5 Hz); $^{13}C\{^1H\}$ NMR (101 MHz, $CDCl_3$, ppm) δ 159.3, 149.6, 147.4, 143.5, 128.6, 123.5, 121.3, 116.4, 106.9, 106.3, 105.4, 18.0, 14.1, 12.7; HRMS-ESI (m/z) calcd for $C_{21}H_{31}N_2O_2Si$ $[M + H]^+$ 371.2149, found 371.2153.

3-(2-Methyloxazol-5-yl)-1-(triisopropylsilyl)-1*H*-indol-4-yltrifluoromethanesulfonate (15). A dispersion of NaH in mineral oil (60%, 290 mg, 1.23 mmol) was added portionwise to a solution of 4-hydroxyindole **14** (1.30 g, 3.51 mmol) in anhydrous THF (40 mL) at 0 °C under atmosphere of nitrogen. The resulting suspension was stirred at ambient temperature for 2 h until gas evolution ceased. Then a solution of *N*-phenyl-bis(trifluoromethanesulfonimide) (2.19 g, 6.14 mmol) in anhydrous THF (10 mL) was added in one portion, and the reaction mixture was stirred for 1 h at room temperature, whereupon it was poured into aqueous $NaHCO_3$ solution (100 mL; aqueous saturated $NaHCO_3$ solution was diluted 1:1 with water). Aqueous layer was extracted with Et_2O (2 × 100 mL), and combined organic extracts were washed with H_2O (130 mL) and brine (150 mL) and dried over Na_2SO_4. Column chromatography (100 mL silica gel, column i.d. 30 mm) using gradient elution from 10% EtOAc in hexanes to 20% EtOAc in hexanes afforded **15** as a yellowish amorphous solid (1.61 g, 92% yield): analytical TLC on silica gel, 2:5 EtOAc/hexanes, R_f = 0.52; IR (film, cm^{-1}) 1221 (S═O), 1213 (S═O); ^1H NMR (400 MHz, $CDCl_3$, ppm) δ 7.51 (1H, d, J = 8.2 Hz), 7.43 (1H, s), 7.19 (1H, t, J = 8.1 Hz), 7.13 (1H, d, J = 8.1 Hz), 7.04 (1H, s), 2.52 (3H, s), 1.70 (3H, septet, J = 7.5 Hz), 1.15 (18 H, d, J = 7.5 Hz); $^{13}C\{^1H\}$ NMR (101 MHz, $CDCl_3$, ppm) δ 161.1, 145.0, 143.8, 142.7, 132.6, 123.9, 122.2, 121.0, 120.2, 114.3, 112.8, 105.4, 18.0, 14.0, 12.7; HRMS-ESI (m/z) calcd for $C_{22}H_{30}F_3N_2O_4SSi$ $[M + H]^+$ 503.1642, found 503.1651.

2-Methyl-5-(4-(4,4,5,5-tetramethyl-1,3,2-dioxaborolan-2-yl)-1-(triisopropylsilyl)-1*H*-indol-3-yl)oxazole (4). To a mixture of $Pd(OAc)_2$ (13.0 mg, 0.057 mmol, 1.5 mol %), DPE-Phos (61 mg, 0.114 mmol, 3 mol %), and triflate **15** (1.70 g, 3.38 mmol) in anhydrous dioxane (30 mL) under nitrogen atmosphere was added NEt_3 (1.6 mL, 11.43 mmol), followed by pinacolborane (830 μL, 5.72 mmol). The resulting yellow solution was heated at 80 °C for 1 h in a sealed vessel under nitrogen atmosphere, cooled to ambient temperature, poured into water (150 mL), and extracted with EtOAc (2 × 150 mL). The organic extracts were combined and washed with brine, dried on Na_2SO_4, filtered, and concentrated. Column chromatography (200 mL of silica gel, column i.d. 45 mm) using gradient elution from 10% EtOAc in hexanes to 50% EtOAc in hexanes afforded **4** as a yellowish oil (1.48 g, 91%) that crystallized upon standing: analytical TLC on silica gel, 1:1 Et_2O/hexanes, R_f = 0.20; pure material was obtained by crystallization from CH_2Cl_2/hexanes, mp 97−98 °C; IR (film, cm^{-1}) 1363 (B−O); ^1H NMR (400 MHz, $CDCl_3$, ppm) δ 7.61 (2H, dt, J = 8.5, 0.8 Hz), 7.34 (1H, s), 7.17 (1H, m), 6.92 (1H, s), 2.50 (3H, s), 1.68 (3H, septet, J = 7.6 Hz), 1.21 (12H, s), 1.13 (18H, d, J = 7.7 Hz); $^{13}C\{^1H\}$ NMR (101 MHz, $CDCl_3$, ppm) δ 160.1, 147.1, 140.7, 134.2, 133.1, 129.1, 124.3, 121.4, 116.8, 107.7, 83.3, 29.8, 24.7, 18.0, 14.5, 12.8. Anal. Calcd for $C_{27}H_{41}N_2O_3SiB$: C, 67.49; H, 8.60; N, 5.83. Found: C, 67.23; H, 8.79; N, 5.65.

Methyl (5a*R*,10b*R*)-2-(benzyloxy)-7-bromo-5a,6-dihydro-10b*H*-benzofuro[2,3-*b*]indole-10b-carboxylate (*R*,*R*-8). 1,3-Dimethylbarbituric acid (7) (437 mg, 2.80 mmol) and $Pd(PPh_3)_4$ (54 mg, 0.047 mmol, 5 mol %) were added to a cooled (0 °C) solution of bromide (*R*,*R*)-**6**[12] (500 mg, 0.932 mmol) in anhydrous CH_2Cl_2 (15 mL). The reaction mixture was stirred at 0 °C for 15−20 min, and the color of the solution turned bright yellow. The reaction was complete at that point. The solution was poured into a 1:1:2 mixture of water, saturated aqueous $NaHCO_3$, and saturated aqueous Na_2CO_3 (50 mL). Layers were separated, and the aqueous layer was extracted with Et_2O (3 × 80 mL). The organic extracts were combined, washed with water (100 mL) and brine, and dried over Na_2SO_4. Column chromatography (50 mL silica gel, column i.d. 30 mm) using gradient elution from 10% EtOAc in hexanes to 30% EtOAc in hexanes afforded (*R*,*R*)-**8** as colorless solid (405 mg, 96% yield): analytical TLC on silica gel, 2:5 EtOAc/hexanes, R_f = 0.58; pure material was obtained by crystallization from CH_2Cl_2/hexanes, mp 183−184 °C; IR (film, cm^{-1}) 1734 (C═O), 1487; ^1H NMR (400 MHz, $CDCl_3$, ppm) δ 7.44−7.30 (6H, m), 7.26 (1H, dd, J = 8.0, 1.0 Hz), 7.22 (1H, d, J = 2.7 Hz), 6.85 (1H, d, J = 2.7 Hz), 6.81 (1H, dd, J = 8.7, 2.7 Hz), 6.75 (1H, d, J = 8.7 Hz), 6.67 (1H, t, J = 7.8 Hz), 5.27 (1H, d, J = 2.4 Hz), 5.01 (2H, s), 3.82 (3H, s); $^{13}C\{^1H\}$ NMR (101 MHz, $CDCl_3$, ppm) δ 169.7, 154.0, 152.7, 146.2, 137.1, 132.0, 128.7, 128.1, 128.1, 127.8, 127.2, 123.3, 121.1, 116.1, 111.9, 110.5, 102.8, 99.2, 71.3, 67.3, 53.4; HRMS-ESI (m/z) calcd for $C_{23}H_{19}BrNO_4$ $[M + H]^+$ 452.0492, found 452.0495; optical rotation $[\alpha]_D^{20}$ −176 (*c* 0.1, benzene). Anal. Calcd for $C_{23}H_{18}BrNO_4$: C, 61.08; H, 4. 01; N, 3.10. Found: C, 60.61; H, 3.96; N, 2.99.

Methyl (5a*R*,10b*R*)-2-(Benzyloxy)-7-bromo-6-(methoxymethyl)-5a,6-dihydro-10b*H*-benzofuro[2,3-*b*]indole-10b-carboxylate (*R*,*R*-5). An oven-dried pressure tube was charged with hemiaminal bromide (*R*,*R*)-**8** (390 mg, 0.86 mmol) and paraformaldehyde (129 mg, 4.30 mmol) and flushed with nitrogen. Anhydrous DCM (25 mL) was added, and to the resulting suspension was added TMSCl (275 μL, 2.15 mmol). The pressure tube was closed, and the pale yellow suspension was heated for 24 h at 35 °C. After being cooled to ambient temperature, the suspension was transferred dropwise to precooled (0 °C) anhydrous MeOH (15 mL) using a metal cannula. Stirring was continued at room temperature for 15 min, then the reaction mixture was poured into saturated aqueous $NaHCO_3$ (50 mL) and extracted with Et_2O (3 × 50 mL). The organic extracts were combined, washed with brine, and dried on Na_2SO_4. Column chromatography on silica gel using 10% EtOAc in hexanes as a mobile phase afforded (*R*,*R*)-**5** as an amorphous colorless solid (410 mg, 96% yield): analytical TLC on silica gel, 2:5 EtOAc/hexanes, R_f = 0.50; IR ($CHCl_3$, cm^{-1}) 1738 (C═O), 1488; ^1H NMR (400 MHz, C_6D_6, ppm) δ 7.48 (1 H, dd, J = 7.5, 1.2 Hz), 7.43 (1 H, d, J = 2.7 Hz), 7.25−7.21 (2 H, m), 7.16−7.05 (4 H, m), 7.01 (1 H, s), 6.67 (1 H, d, J = 8.7 Hz), 6.57 (1 H, dd, J = 8.7, 2.7 Hz), 6.39 (1 H, t, J = 7.8 Hz), 5.42 (1 H, d, J = 10.6 Hz), 4.76 (1 H, d, J = 10.6 Hz), 4.65 (2 H, s), 3.13 (3 H, s), 3.11 (3 H, s); $^{13}C\{^1H\}$ NMR (101 MHz, C_6D_6, ppm) δ 169.4, 154.4, 153.1, 144.7, 137.7, 134.90, 132.7, 128.6, 128.2, 128.0, 127.8, 123.9, 122.5, 116.2, 112.5, 110.8, 105.1, 104.3, 79.4, 71.0, 64.5, 55.0, 52.6; HRMS-ESI (m/z) calcd for $C_{25}H_{23}BrNO_5$ $[M + H]^+$ 496.0754, found 496.0764; optical rotation $[\alpha]_D^{20}$ −235 (*c* 0.33, benzene).

General Procedure for Optimization of the Suzuki Cross-Coupling (Table 1). The hemiaminal bromide (*R*,*R*)-**5** (30 mg, 0.0604 mmol), the indolyl boronate **4** (29 mg, 0.0604 mmol), an oven-dried K_3PO_4 (51 mg, 0.242 mmol), Pd catalyst (20 mol %), and phosphine ligand (if indicated in Table 1) were weighted into an oven-dried pressure vial in a glovebox (argon atmosphere). A solution of 4-cyanotoluene as an internal standard (0.0604 mmol, 1 equiv with respect to the hemiaminal bromide (*R*,*R*)-**5**) in dry degassed dioxane or toluene (2 mL) was added, and the pressure vial was closed. The reaction mixture was heated in an oil bath (for appropriate time and temperature, see Table 1), and progress of the reaction was monitored by reversed-phase HPLC (an aliqot of the reaction mixture was diluted with MeCN, filtered trough a plug of Celite, and submitted to HPLC analysis). Conversion of the starting bromide (*R*,*R*)-**5** and yield of the biaryl product (*R*,*R*)-**3** were determined based on a calibration curve using the internal standard.

Preparation of $(PCy_3)_2Pd(\eta^2\text{-}O_2)$ (16). A freshly prepared solid $Pd(PCy_3)_2$ complex[22a] (294 mg, 0.44 mmol) was weighted into a

DOI: 10.1021/jo5029419
J. Org. Chem. 2015, 80, 3058−3066

round-bottom flask with stir-bar under an argon atmosphere (in a glovebox), closed with a septum, and immersed into an acetone/dry ice cooling bath (−30 °C). Then the flask was opened, and anhydrous precooled (−20 °C) diethyl ether (3 mL) was added. The resulting colorless suspension was stirred under air at −30 °C for 10 min, whereupon the color of the suspension changed to greenish blue. Stirring was stopped, and the supernatant solution was decanted. Another portion of cold Et_2O (1 mL) was added, and the suspension was stirred under air at −30 °C for 2 min, followed with decantation of the supernatant. The addition of Et_2O/stirring sequence was repeated once more, and after the decantation of the supernatant, the cold solid containing a residual diethyl ether was immediately transferred to a rotary evaporator (preventing the solid to warm to room temperature). Careful drying on rotary evaporator (without immersing of the flask into a bath) afforded **16** (279 mg, 91% yield) as aquamarine powder:[36] ^{1}H NMR (400 MHz, C_6D_6, ppm) δ 2.04 (12H, d, J = 12.3 Hz), 1.96−1.86 (6H, m), 1.78−1.58 (30H, m), 1.28−1.16 (18H, m); ^{13}C{^{1}H} NMR (101 MHz, C_6D_6, ppm) δ 35.7 (t, J_{C-P} = 7.8 Hz), 30.8, 28.0 (t, J_{C-P} = 5.3 Hz), 26.7; ^{31}P NMR (162 MHz, C_6D_6, ppm) δ 44.96; ^{31}P NMR (162 MHz, dioxane-d_8, ppm) δ 44.84.

Methyl (5a*R*,10b*R*)-2-(Benzyloxy)-6-(methoxymethyl)-7-(3-(2-methyloxazol-5-yl)-1-(triisopropylsilyl)-1*H*-indol-4-yl)-5a,6-dihydro-10b*H*-benzofuro[2,3-*b*]indole-10b-carboxylate (*R*,*R*-3). The hemiaminal bromide (*R*,*R*)-**5** (200 mg, 0.40 mmol), the indolyl boronate **4** (194 mg, 0.40 mmol), $Pd(PCy_3)_2O_2$ (**16**) (54 mg, 20 mol %), and an oven-dried K_3PO_4 (342 mg, 1.61 mmol) were weighted into an oven-dried pressure vial in a glovebox (argon atmosphere). Anhydrous toluene (13 mL; degassed by freeze−pump−thaw technique prior to use) was added, and the reaction mixture was heated in an oil bath at 110 °C for 38 h, then diluted with EtOAc (50 mL) and washed with water (50 mL). The aqueous layer was back-extracted with EtOAc (50 mL). Combined organic extracts were washed with brine, dried over Na_2SO_4, filtered, and concentrated (rotary evaporator). Column chromatography on silica gel using gradient elution from 10% acetone in hexanes to 30% acetone in hexanes afforded (*R*,*R*)-**3** as a colorless foam (253 mg, 82% yield, Figures 2 and 3): analytical TLC on silica gel, 2:5 EtOAc/hexanes, R_f

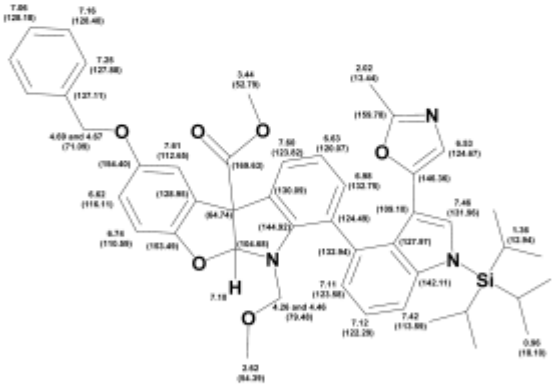

Figure 2. ^{1}H and ^{13}C NMR assignment for the major atropisomer (*M*,*R*,*R*)-**3**.

=0.1−0.50 (tailing); IR (film from $CHCl_3$, cm^{-1}) 1739 (C=O), 1487; ^{1}H NMR (400 MHz, C_6D_6, ppm) δ 7.70 (minor atropisomer, 0.65H, dd, J = 7.6, 1.3 Hz), 7.61 (major atropisomer, 1H, d, J = 2.7 Hz), 7.60 (major, 1H, dd, J = 7.6, 1.3 Hz), 7.59 (minor, 0.65H, d, J = 2.5 Hz), 7.48 (minor, 0.65H, s), 7.47 (minor, 0.65H, dd, J = 8.1, 1.2 Hz), 7.46 (major, 1H, s), 7.42 (major, 1H, dd, J = 6.9, 2.5 Hz), 7.40−7.36 (minor, 1.3H, m), 7.28−7.05 (10.9H, m), 7.10 (major, 1H, s), 7.01 (minor, 0.65H, s), 6.98 (major, 1H, dd, J = 7.6, 1.3 Hz), 6.80 (minor, 0.65H, t, J = 7.6 Hz), 6.76 (minor, 0.65H, dd, J = 8.8, 2.5 Hz), 6.74 (major, 1H, d, J = 8.8 Hz), 6.73 (minor, 0.65H, dd, J = 8.6, 0.5 Hz), 6.63 (major, 1H, t, J = 7.6 Hz), 6.62 (major, 1H, dd, J = 8.8, 2.7 Hz),

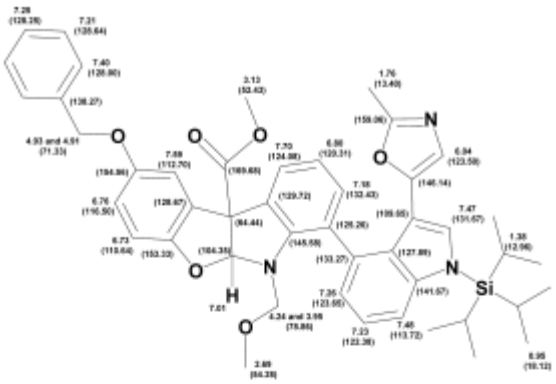

Figure 3. ^{1}H and ^{13}C NMR assignment for the minor atropisomer (*P*,*R*,*R*)-**3**.

6.53 (major, 1H, s), 6.04 (minor, 0.65H, s), 4.93, 4.91 (minor, 1.3H, ABq, J_{AB} = 12.2 Hz), 4.69, 4.67 (major, 2H, ABq, J_{AB} = 12.1 Hz) 4.46 (major, 1H, d, J = 9.9 Hz), 4.26 (major, 1H, d, J = 9.9 Hz), 4.24 (minor, 0.65H, d, J = 9.9 Hz), 3.95 (minor, 0.65H, d, J = 9.9 Hz), 3.44 (major, 3H, s), 3.13 (minor, 1.95H, s), 2.69 (minor, 1.95H, s), 2.62 (major, 3H, s), 2.02 (major, 3H, s), 1.76 (minor, 1.95H, s), 1.44−1.31 (4.95H, m), 0.99−0.93 (29.7H, m); ^{13}C{^{1}H} NMR (100.6 MHz, C_6D_6, ppm) δ 169.68, 169.63, 159.78, 159.06, 154.58, 154.40, 153.49, 153.33, 146.36, 146.14, 145.58, 144.92, 142.11, 141.67, 138.27, 137.11, 133.27, 132.94, 132.75, 132.43, 131.96, 131.67, 130.09, 129.72, 128.95, 128.67, 128.64, 128.40, 128.25 (overlapping with residual solvent signal), 128.18, 128.00 (overlapping with residual solvent signal), 127.97, 127.89, 127.88, 125.26, 124.67, 124.49, 124.08, 123.82, 123.65, 123.58, 123.50, 122.38, 122.29, 120.31, 120.07, 116.50, 116.11, 113.72, 113.59, 112.70, 112.65, 110.64, 110.59, 109.65, 109.10, 104.68, 104.35, 79.48, 78.86, 71.33, 71.09, 64.74, 64.44, 54.39, 54.28, 52.79, 52.43, 18.12, 18.10, 13.44, 13.40, 12.96, 12.94; HRMS-ESI (m/z) calcd for $C_{46}H_{52}N_3O_6Si$ [M + H]$^+$ 770.3620, found 770.3615; optical rotation $[\alpha]_D^{20}$ −130 (c 0.35, benzene).

Macrocycle (*M*,*M*,*R*,*R*)-2. A solution of the biaryl (*R*,*R*)-**3** (50 mg, 0.065 mmol) in anhydrous THF (13 mL) was cooled to −78 °C under argon atmosphere, and LDA (0.30 M solution in THF, 0.54 mL, 0.163 mmol) was added in one portion. The reaction mixture was stirred at −78 °C for 10 min, whereupon the clear colorless solution became yellow. At this point, glacial AcOH (0.125 mL) was added, and the resulting colorless solution was allowed to warm to room temperature. The reaction mixture was poured into aqueous 5% $NaHCO_3$ solution (30 mL) and extracted with Et_2O (3 × 30 mL). The combined organic extracts were dried on $MgSO_4$ and concentrated. Purification of the residue by preparative HPLC (Grom-Sil Si NP-2, 5 μM, 150 × 20 mm) using gradient elution from 0% EtOAc in hexanes to 60% EtOAc in hexanes provided 20 mg (40% recovery) of the starting biaryl (*R*,*R*)-**3** and macrocycle (*M*,*M*,*R*,*R*)-**2** (21 mg, 43% yield) as a pale yellow foam: analytical TLC on silica gel, 1:1 EtOAc/hexanes, R_f = 0.75; IR (film from $CHCl_3$, cm^{-1}) 1714 (C=O), 1485; ^{1}H NMR (600 MHz, C_6D_6, ppm) δ 7.76−7.74 (1H, m), 7.44 (1H, dd, J = 7.0, 2.3 Hz), 7.30−7.25 (2H, m), 7.25−7.21 (2H, m), 7.18 (1H, s), 7.15−7.13 (2H, m), 7.10−7.07 (1H, m), 7.04−7.01 (1H, m), 6.73−6.70 (3H, m), 6.60 (2H, d, J = 9.5 Hz), 6.46 (1H, t, J = 7.5 Hz), 4.80, 4.75 (2H, ABq, J = 11.7 Hz), 4.62 (1H, d, J = 10.3 Hz), 4.31 (1H, d, J = 10.3 Hz), 3.80 (1H, d, J = 14.4 Hz), 3.43 (1H, d, J = 14.4 Hz), 2.75 (3H, s), 1.38−1.29 (3H, m), 0.95 (18H, dd, J = 7.5, 1.0 Hz); ^{13}C{^{1}H} NMR (126 MHz, C_6D_6, ppm) δ 197.4, 156.0, 154.5, 153.0, 146.1, 145.5, 140.9, 138.0, 133.4, 133.1, 133.0, 132.0, 128.6, 128.5, 128.4, 128.2, 128.0, 127.4, 123.1, 122.9, 122.5, 121.4, 119.3, 116.3, 114.0, 113.8, 110.1, 107.3, 102.3, 77.9, 71.0, 54.7, 41.7, 18.0, 12.9; HRMS-ESI (m/z) calcd for $C_{45}H_{48}N_3O_5Si$ [M + H]$^+$ 738.3358, found 738.3346; optical rotation $[\alpha]_D^{20}$ −286 (c 1.30, EtOAc).

DOI: 10.1021/jo5029419
J. Org. Chem. 2015, 80, 3058−3066

■ ASSOCIATED CONTENT

Supporting Information

^{1}H, ^{13}C, and ^{31}P NMR spectra, X-ray crystallographic data for Pd complex **16** (CIF), Pd particle size measurements, and TEM images. This material is available free of charge via the Internet at http://pubs.acs.org.

■ AUTHOR INFORMATION

Corresponding Author

*E-mail: edgars@osi.lv.

Notes

The authors declare no competing financial interest.

■ ACKNOWLEDGMENTS

We are grateful to the European Social Fund (Project No. 1DP/1.1.1.2.0/13/APIA/VIAA/006) for financial support of this research. We thank Dr. S. Belyakov for X-ray crystallographic analysis, Dr. I. Nakurte for HRMS analyses, Dr. K. Pajuste for Pd particle size measurements, Dr. K. Smits and Dr. V. Ose-Klinklava for assistance with acquiring TEM images. We also thank E. Elksnis and Dr. J. Belani for preliminary borylation and coupling experiments involving the *N*-Boc analogue of **4**.

■ REFERENCES

(1) Cruz-Monserrate, Z.; Vervoort, H. C.; Bai, R.; Newman, D. J.; Howell, S. B.; Los, G.; Mullaney, J. T.; Williams, M. D.; Pettit, G. R.; Fenical, W.; Hamel, E. *Mol. Pharmacol.* **2003**, *63*, 1273.

(2) (a) Williams, N. S.; Burgett, A. W. G.; Atkins, A. S.; Wang, X.; Harran, P. G.; McKnight, S. L. *Proc. Natl. Acad. Sci. U.S.A.* **2007**, *104*, 2074. (b) Wang, G.; Shang, L.; Burgett, A. W. G.; Harran, P. G.; Wang, X. *Proc. Natl. Acad. Sci. U.S.A.* **2007**, *104*, 2068.

(3) For reviews on synthesis of diazonamide A, see: (a) Lachia, M.; Moody, C. *Nat. Prod. Rep.* **2008**, *25*, 227. (b) Ritter, T.; Carreira, E. M. *Angew. Chem., Int. Ed.* **2002**, *41*, 2489.

(4) (a) Burgett, A. W. G.; Li, Q.; Wei, Qi.; Harran, P. G. *Angew. Chem., Int. Ed.* **2003**, *42*, 4961. For total synthesis of originally proposed hemiacetal, see: (b) Li, J.; Jeong, S.; Esser, L.; Harran, P. G. *Angew. Chem., Int. Ed.* **2001**, *40*, 4765.

(5) Nicolaou first total synthesis: (a) Nicolaou, K. C.; Bella, M.; Chen, D. Y.-K.; Huang, X.; Ling, T.; Snyder, S. A. *Angew. Chem., Int. Ed.* **2002**, *41*, 3495. (b) Nicolaou, K. C.; Chen, D. Y. K.; Snyder, S. A.; Huang, X.; Ling, T.; Bella, M. *J. Am. Chem. Soc.* **2004**, *126*, 12888.

(6) Nicolaou second total synthesis: (a) Nicolaou, K. C.; Rao, P. B.; Hao, J.; Reddy, M. V.; Rassias, G.; Huang, X.; Chen, D. Y.-K.; Snyder, S. A. *Angew. Chem., Int. Ed.* **2003**, *42*, 1753. (b) Nicolaou, K. C.; Hao, J.; Reddy, M. V.; Rao, P. B.; Rassias, G.; Snyder, S. A.; Huang, X.; Chen, D. Y.-K.; Brenzovich, W. E.; Giuseppone, N.; Giannakakou, P.; O'Brate, A. *J. Am. Chem. Soc.* **2004**, *126*, 12897.

(7) Knowles, R. R.; Carpenter, J.; Blakey, S. B.; Kayano, A.; Mangion, I. K.; Sinz, C. J.; MacMillan, D. W. C. *Chem. Sci.* **2011**, *2*, 308.

(8) (a) Cheung, C.-M.; Goldberg, F. W.; Magnus, P.; Russell, C. J.; Turnbull, R.; Lynch, V. *J. Am. Chem. Soc.* **2007**, *129*, 12320. (b) Mai, C.-K.; Sammons, M. F.; Sammakia, T. *Angew. Chem., Int. Ed.* **2010**, *49*, 2397.

(9) For selected examples using Suzuki–Miyaura conditions, see: (a) Nicolaou, K. C.; Snyder, S. A.; Simonsen, K. B.; Koumbis, A. E. *Angew. Chem., Int. Ed.* **2000**, *39*, 3473. (b) Vedejs, E.; Barda, D. A. *Org. Lett.* **2000**, *2*, 1033. (c) Nicolaou, K. C.; Huang, X.; Giuseppone, N.; Bheema Rao, P.; Bella, M.; Reddy, M. V.; Snyder, S. A. *Angew. Chem., Int. Ed.* **2001**, *40*, 4705. (d) Vedejs, E.; Zajac, M. A. *Org. Lett.* **2001**, *3*, 2451. (e) Nicolaou, K. C.; Snyder, S. A.; Giuseppone, N.; Huang, X.; Bella, M.; Reddy, M. V.; Rao, P. B.; Koumbis, A. E.; Giannakakou, P.; O'Brate, A. *J. Am. Chem. Soc.* **2004**, *126*, 10174. (f) Davies, J. R.; Kane, P. D.; Moody, C. J. *J. Org. Chem.* **2005**, *70*, 7305. (g) Booker, J. E. M.; Boto, A.; Churchill, G. H.; Green, C. P.; Ling, M.; Meek, G.; Prabhakaran, J.; Sinclair, D.; Blake, A. J.; Pattenden, G. *Org. Biomol. Chem.* **2006**, *4*, 4193. (h) Lin, J.; Gerstenberger, B. S.; Stessman, N. Y. T.; Konopelski, J. P. *Org. Lett.* **2008**, *10*, 3969.

(10) Feldman, K. S.; Eastman, K. J.; Lessene, G. *Org. Lett.* **2002**, *4*, 3525.

(11) Zajac, M. A.; Vedejs, E. *Org. Lett.* **2004**, *6*, 237.

(12) Peris, G.; Vedejs, E. *J. Org. Chem.* **2015**, DOI: 10.1021/jo502939a.

(13) Under basic conditions,the N-unsubstituted cyclic aminal (*R*,*R*)-**8** exists in equilibrium with its ring-opened form, 3-(2-hydroxyphenyl)-3*H*-indole. Therefore, the use of MOM-Cl in the presence of a base (such as NEt_3) could result in the formation of the undesired *O*-MOM phenol.

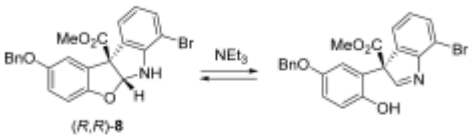

(*R*,*R*)-**8**

(14) (a) Quan, Z.-J.; Wang, X.-C.; Ren, R.-G.; Da, Y.-X.; Zhang, Z.; Jia, X.-D.; Yang, C.-X. *Heterocycles* **2010**, *81*, 1827. (b) It should be noted that *N*-MOM aminal (*R*,*R*)-**5** is unstable in $CDCl_3$ and DMSO-d_6.

(15) Wipf, P.; Miller, C. P. *J. Org. Chem.* **1993**, *58*, 3604.

(16) Ishiyama, T.; Murata, M.; Miyaura, N. *J. Org. Chem.* **1995**, *60*, 7508.

(17) Miyashita, K.; Sakai, T.; Imanishi, T. *Org. Lett.* **2003**, *5*, 2683.

(18) Billingsley, K. L.; Barder, T. E.; Buchwald, S. L. *Angew. Chem., Int. Ed.* **2007**, *46*, 5359.

(19) Broutin, P.-E.; Čerňa, I.; Campaniello, M.; Leroux, F.; Colobert, F. *Org. Lett.* **2004**, *6*, 4419.

(20) Anhydrous dioxane was distilled from sodium/benzophenone, degassed by multiple freeze–thaw cycles,and handled using Schlenk techniques

(21) Littke, A. F.; Dai, C.; Fu, G. C. *J. Am. Chem. Soc.* **2000**, *122*, 4020.

(22) (a) Li, H.; Grasa, G. A.; Colacot, T. J. *Org. Lett.* **2010**, *12*, 3332. (b) Norton, D. M.; Mitchell, E. A.; Botros, N. R.; Jessop, P. G.; Baird, M. C. *J. Org. Chem.* **2009**, *74*, 6674.

(23) (a) Yoshida, T.; Otsuka, S. *J. Am. Chem. Soc.* **1977**, *99*, 2134. (b) Sergeev, A. G.; Neumann, H.; Spannenberg, A.; Beller, M. *Organometallics* **2010**, *29*, 3368.

(24) Pd–dioxygen complex **16** has been reported: (a) Wilke, G.; Schott, H.; Heimbach, P. *Angew. Chem., Int. Ed. Engl.* **1967**, *6*, 92. (b) See ref 23a. However, to the best of our knowledge, the X-ray structure of complex **16** has never been reported in the literature.

(25) For recent reviews on Pd–dioxygen complexes, see: (a) Scheuermann, M. L.; Goldberg, K. I. *Chem.—Eur. J.* **2014**, *20*, 14556. (b) Muzart, J. *Chem.—Asian J.* **2006**, *1*, 508. (c) Stahl, S. S. *Angew. Chem., Int. Ed.* **2004**, *43*, 3400.

(26) Pd–peroxo complex catalyzed the homocoupling of arylboronic acids: Adamo, C.; Amatore, C.; Ciofini, I.; Jutand, A.; Lakmini, H. *J. Am. Chem. Soc.* **2006**, *128*, 6829.

(27) For selected recent reviews on Suzuki cross-coupling catalyzed by heterogeneous Pd catalysts, see: (a) Balanta, A.; Godard, C.; Claver, C. *Chem. Soc. Rev.* **2011**, *40*, 4973. (b) Fihri, A.; Bouhrara, M.; Nekoueishahraki, B.; Basset, J.-M.; Polshettiwar, V. *Chem. Soc. Rev.* **2011**, *40*, 5181. (c) Astruc, D. *Inorg. Chem.* **2007**, *46*, 1884. (d) Phan, N. T. S.; Van Der Sluys, M.; Jones, C. W. *Adv. Synth. Catal.* **2006**, *348*, 609.

(28) Palladacycle **17** was reported to be thermally unstable, and upon heating at 140 °C, it decomposes into metallic Pd species which are true catalysts of the Heck reaction between aryl iodide and olefin: Nowotny, M.; Hanefeld, U.; van Koningsveld, H.; Maschmeyer, T. *Chem. Commun.* **2000**, 1877.

(29) (a) Beletskaya, I. P.; Cheprakov, A. V. *J. Organomet. Chem.* **2004**, *689*, 4055 and references cited therein. (b) Rocaboy, C.; Gladysz, J. A. *Org. Lett.* **2002**, *4*, 1993.

DOI: 10.1021/jo5029419
J. Org. Chem. 2015, 80, 3058–3066

(30) (a) Anton, D. R.; Crabtree, R. H. *Organometallics* **1983**, *2*, 855. (b) Foley, P.; DiCosimo, R.; Whitesides, G. M. *J. Am. Chem. Soc.* **1980**, *102*, 6713.

(31) It should be noted that attempts to observe the formation of heterogeneous Pd species (Pd nanoparticles) from the Pd−dioxygen complex **16** under elevated temperatures by transmission electron microscopy and dynamic light scattering were unsuccessful; see Supporting Information (page S2) for details.

(32) Formation of reactive monophosphine Pd intermediates Cy_3P−Pd^0 or dinuclear Pd^{II}−Pd^I complexes during the thermal decomposition of the Pd−dioxygen complex **16** can also be envisioned. For relevant studies, see: (a) Wei, C. S.; Davies, G. H. M.; Soltani, O.; Albrecht, J.; Gao, Q.; Pathirana, C.; Hsiao, Y.; Tummala, S.; Eastgate, M. *Angew. Chem., Int. Ed.* **2013**, *52*, 5822 and references cited therein. (b) Proutiere, F.; Aufiero, M.; Schoenebeck, F. *J. Am. Chem. Soc.* **2012**, *134*, 606. (c) Proutiere, F.; Lyngvi, E.; Aufiero, M.; Sanhueza, I. A.; Schoenebeck, F. *Organometallics* **2014**, *33*, 6879.

(33) A series of 2D EXSY spectra were acquired by using the phase-sensitive NOESY pulse sequence to establish reasonable mixing times. A mixing time of 1 s at T = 258 K was subsequently chosen for all 2D EXSY experiments. The rate constants for chemical exchange were calculated from the ratio of diagonal and exchange cross-peaks as described in the following: (a) Perrin, C. L.; Dwyer, T. G. *Chem. Rev.* **1990**, *90*, 935. (b) Gibson, K. R.; Hitzel, L.; Mortishire-Smith, R. J.; Gerhard, U.; Jelley, R. A.; Reeve, A. J.; Rowley, M.; Nadin, A.; Owens, A. P. *J. Org. Chem.* **2002**, *67*, 9354. See also the Supporting Information (page S12) for details.

(34) For the use of Me_2AlCl in the preparation of Weinreb amide, see: Shimizu, T.; Osako, K.; Nakata, T. *Tetrahedron Lett.* **1997**, *38*, 2685.

(35) For the use of *i*-PrMgCl as a sacrificial base, see: Liu, J.; Ikemoto, N.; Petrillo, D.; Amstrong, J. D., III. *Tetrahedron Lett.* **2002**, *43*, 8223.

(36) The Pd−dioxygen complex **16** is stable and retains catalytic activity for several hours if stored at room temperature. At temperatures below −20 °C, it can be stored for 2 months without losing catalytic activity. In a solution, slow decomposition takes place at room temperature, whereupon the turquoise color of the complex changes to yellow.

DOI: 10.1021/jo5029419
J. Org. Chem. 2015, 80, 3058−3066

Appendix II – DIAZONAMIDE SYNTHETIC STUDIES. REACTIVITY OF *N*-UNSUBSTITUTED BENZOFURO[2,3-*b*]INDOLINES

Ilga Mutule, Toms Kalnins, Edwin Vedejs, and Edgars Suna

Chem. Heterocycl. Compd. **2015**, *51* (7), 613–620

DOI 10.1007/s10593-015-1749-7

Chemistry of Heterocyclic Compounds **2015**, *51*(7), 613–620

Diazonamide synthetic studies. Reactivity of *N*-unsubstituted benzofuro[2,3-*b*]indolines

Ilga Mutule[1], Toms Kalnins[1], Edwin Vedejs[1,2], Edgars Suna[1]*

[1] *Latvian Institute of Organic Synthesis, 21 Aizkraukles St., Riga LV-1006, Latvia; e-mail: edgars@osi.lv*

[2] *Department of Chemistry, University of Michigan, Ann Arbor, Michigan 48109, U. S. A.; e-mail: edved@umich.edu*

Published in Khimiya Geterotsiklicheskikh Soedinenii, 2015, *51*(7), 613–620

Submitted June 30, 2015
Accepted July 16, 2015

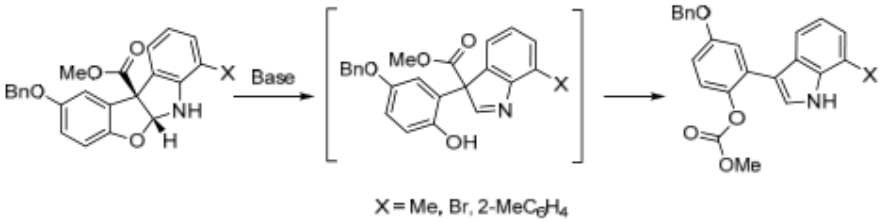

Benzofuro[2,3-*b*]indolines undergo ring opening in the presence of base to generate 3*H*-indolines. The latter can rearrange into 3-arylindoles through an intramolecular transfer of the methoxycarbonyl moiety from quaternary carbon to oxygen of phenol. The intermediate 3*H*-indolines can be isolated upon DMAP-catalyzed *O*-acylation of the phenol moiety with Boc_2O.

Keywords: diazonamide, DMAP, hemiaminal, indole, 3*H*-indoline.

Benzofuro[2,3-*b*]indoline is a core structure in a number of natural products such as the marine metabolite diazonamide A (**1**), azonazine (**2**), and voacalgine A (**3**), a representative of the pleiocarpamine family of alkaloids (Fig. 1). Among them, diazonamide A (**1**) is an especially important synthetic target[1] because it exerts nanomolar cytotoxicity against a broad panel of human tumor cell lines.[2] Not surprisingly, the development of methods for the assembly and further functionalization of benzofuro[2,3-*b*]indoline heterocyclic system has been a focus of research efforts.[3,4]

A majority of the natural products contains an *N*-substituted benzofuro[2,3-*b*]indoline scaffold and only diazonamide A (**1**) possesses the *N*-unsubstituted tetracyclic core. In the context of diazonamide A total synthesis, this structural feature imposes challenges associated with a potentially labile nature of the *N*-unsubstituted cyclic hemiaminal moiety. Thus, our group[5] and Moody[6] have observed fragmentation of the benzofuro[2,3-*b*]-indoline to indolic side products. For example, during attempted Suzuki cross coupling of the *N*-unsubstituted benzofuro[2,3-*b*]indoline **4a** with boronate **5a** in the presence of base, we obtained 3-arylindole **6a** as a major product (86% yield, Scheme 1, Conditions A). Installation of an *N*-MOM protecting group in the benzofuro[2,3-*b*]-indoline moiety helped to avoid the fragmentation of the cyclic hemiaminal in the Suzuki cross coupling and allowed for the desired biaryl **7a** to be isolated in 82% yield (Scheme 1, Conditions A).[7] The formation of the undesired 3-arylindole **6b** was encountered also in the Stille cross coupling involving the *N*-unsubstituted tetracyclic stannane **4b** under virtually neutral conditions

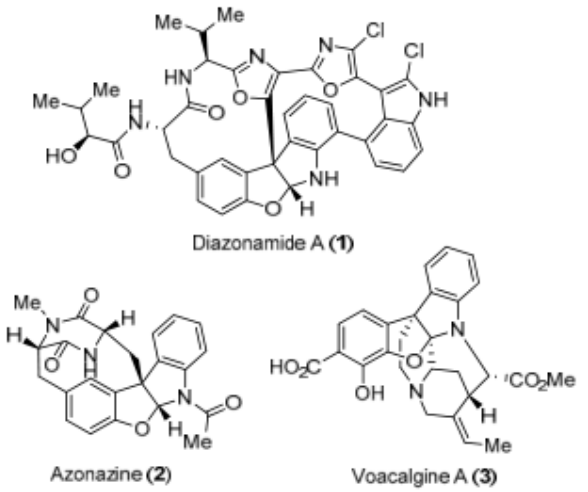

Figure 1. Benzofuro[2,3-*b*]indoline motif-containing representative natural products.

Scheme 1

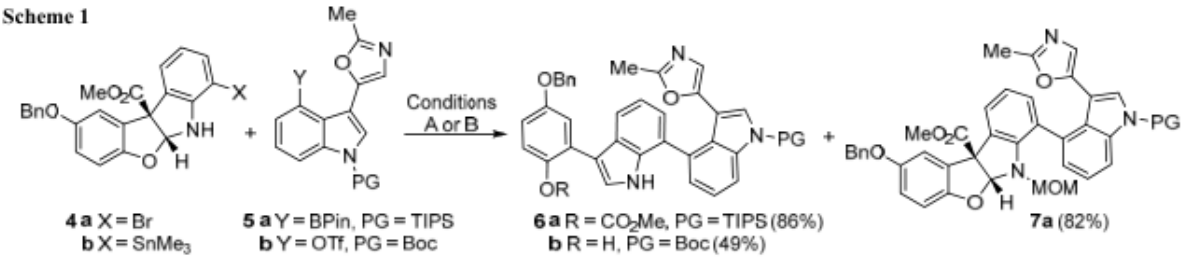

Fragmentation of *N*-unsubstituted benzofuro[2,3-*b*]indolines **4a**,**b**

Scheme 2

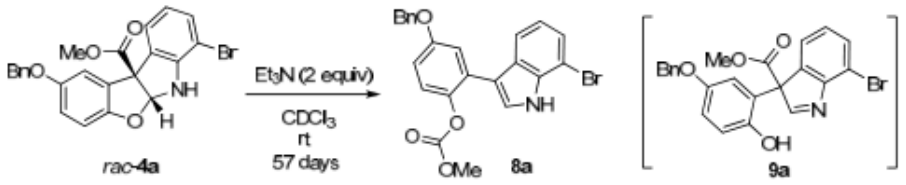

Base-mediated fragmentation of hemiaminal *rac*-**4a**

(49%, Scheme 1, Conditions B).[5a] The observed fragmentation of the cyclic hemiaminals to 3-arylindoles under basic or neutral cross-coupling conditions prompted us to investigate stability and reactivity of the *N*-unsubstituted benzofuro[2,3-*b*]indoline **4a**.

The hemiaminal *rac*-**4a** was found to be stable in $CDCl_3$ solution at room temperature, but addition of Et_3N (2 equiv) resulted in very slow formation of 3-arylindole **8a** (Scheme 2). After 24 h at room temperature only trace amounts (<5%) of compound **8a** were formed and complete conversion of the hemiaminal *rac*-**4a** to indole **8a** required 57 days at room temperature. We hypothesized that the formation of 3-arylindole **8a** would proceed through an initial formation of 3*H*-indoline intermediate **9a**.

Unfortunately, we could not observe the formation of ring-opening intermediates such as compound **9a** by NMR spectroscopy in the base-facilitated fragmentation of hemiaminal *rac*-**4a** to indole **8a**. Possibly, the lifetime of putative intermediate **9a** was too short on the timescale of the NMR experiment. Therefore, an electrophilic reagent was sought to trap the intermediate **9a**. Boc_2O was chosen as the trapping reagent because it did not react with the starting benzofuro[2,3-*b*]indoline *rac*-**4a** in the absence of base (Boc_2O in CH_2Cl_2, rt, 24 h or neat Boc_2O, rt, 24 h, or Boc_2O, $ZrCl_4$, MeCN, rt, 24 h). Disappointingly, addition of Boc_2O (2 equiv) to the hemiaminal *rac*-**4a** in the presence of Et_3N (2 equiv) in $CDCl_3$ returned no detectable amounts of *O*-Boc-protected phenol **9a** or any other intermediates derived from the ring opening of the hemiaminal *rac*-**4a**. The unreacted hemiaminal *rac*-**4a** (<5% conversion) was the only species observed after 24 h at room temperature. However, we were pleased to see that addition of catalytic amounts (10 mol %) of DMAP to the mixture of hemiaminal *rac*-**4a**, Boc_2O, and Et_3N brought about a rapid conversion of the starting hemiaminal *rac*-**4a** (>95% after 30 min at room temperature) and formation of *O*-Boc-phenol **10a** as a major product (66%) together with *N*-Boc-indole **11a*** (18%, Scheme 3).

Importantly, a control experiment without added Boc_2O (hemiaminal *rac*-**4a**, 5 equiv of Et_3N, and 0.5 equiv of DMAP in $CDCl_3$ at room temperature) showed only

* Isolated compound **11a** was converted to *N*-deprotected indole **8a** under thermal conditions (PhMe, 160°C, 30 min)[8] to confirm the structural assignment for compound **8a**, which was based on the NMR experiments.

Scheme 3

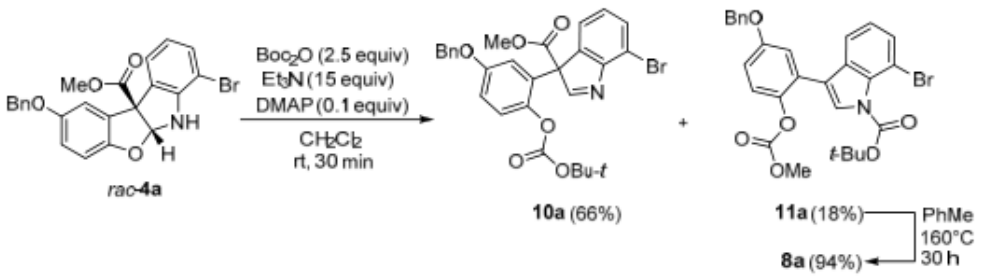

Ring opening of the hemiaminal *rac*-**4a** in the presence of Boc_2O

Table 1. Influence of substituents on the fragmentation of hemiaminals *rac*-**4a**,**c**–**e**

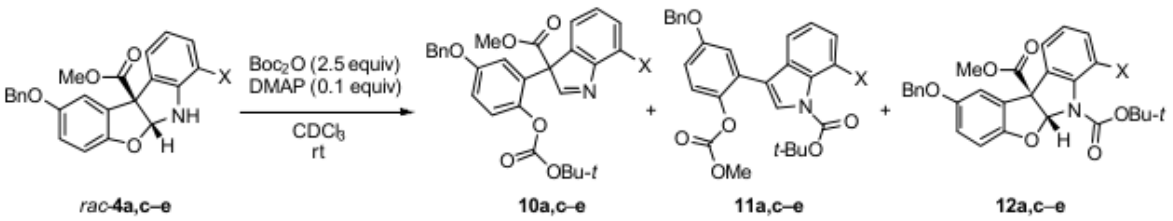

rac-**4a**,**c**–**e** **10a**,**c**–**e** **11a**,**c**–**e** **12a**,**c**–**e**

Entry	Hemiaminal*	X	Reaction time, h	Product yield**, %		
				10a,**c**–**e**	**11a**,**c**–**e**	**12a**,**c**–**e**
1	**4a**	Br	1.5	85***	15***	–
2	**4c**	Me	72	91	–	–
3	**4d**	2-MeC_6H_4	72	81	–	–
4	**4e**	CN	20	–	–	98

* Racemic, diastereomerically pure hemiaminals **4a**,**c**–**e** were used.
** Isolated yields.
*** Yields established by ^{1}H NMR spectroscopy.

unreacted hemiaminal *rac*-**4a** after 24 h (<5% conversion). Evidently, DMAP-catalyzed trapping of the equilibrating ring-opened intermediate **9a** with Boc_2O to form *O*-Boc-phenol **10a** facilitates fragmentation of the benzofuro[2,3-*b*]-indoline *rac*-**4a** by shifting the equilibrium between compounds **4a** and **9a** toward the latter.

Surprisingly, DMAP-catalyzed transformation of the hemiaminal *rac*-**4a** to *O*-Boc-phenol **10a** and indole **11a** proceeded even without the added triethylamine. Thus, 10 mol % of DMAP effected the complete conversion of the benzofuro[2,3-*b*]indoline *rac*-**4a** within 1.5 h (Table 1, entry 1). Apparently, the facile formation of *O*-Boc-phenol **10a** is achieved by *tert*-butoxide, the strong base formed *in situ* in the reaction of DMAP with Boc_2O.* Notably, electron-releasing substituents at position 7 of the benzofuro[2,3-*b*]-indoline (*rac*-**4c** X = Me and *rac*-**4d** X = 2-MeC_6H_4) considerably slowed down the rearrangement of the corresponding hemiaminals (from 1.5 to 72 h; entries 2, 3). Furthermore, the formation of 3-arylindoles **11c**,**d** was not observed for these substrates and 3*H*-indoles **10c**,**d** were the only products. In sharp contrast, 7-cyanobenzofuro[2,3-*b*]-indoline *rac*-**4e** did not undergo ring opening under standard conditions (entry 4). Instead, *N*-Boc-protected hemiaminal **12e** was isolated in almost quantitative yield (98%).

The isolation of *O*-Boc phenols **10a**,**c**,**d** provide evidence that the ring opening of the benzofuro[2,3-*b*]indolines **4a**,**c**–**e** is the first step of the multistep rearrangement process (Scheme 4). Presumably, electron-withdrawing substituents (X = CN) in the benzofuro[2,3-*b*]indoline *rac*-**4e** stabilize the tetracyclic system and prevent the ring opening to form compound **9e**. Hence, DMAP-catalyzed *N*-acylation of benzofuro[2,3-*b*]indoline *rac*-**4e** with Boc_2O affords the ring-closed *N*-Boc hemiaminal **12e**. Other benzofuro[2,3-*b*]indolines *rac*-**4a**,**c**,**d** apparently lack the stabilization by substituent and exist in the equilibrium with the corresponding phenols **9a**,**c**,**d**. For these substrates, *N*-acylation rates with Boc_2O are presumably slower compared to the competing *O*-acylation of the corresponding opened forms **9a**,**c**,**d**. Possibly, diminished *N*-acylation rates of the benzofuro[2,3-*b*]indolines *rac*-**4a**,**c**,**d** compared to *rac*-**4e** are the result of steric hindrance around the nitrogen atom introduced by *ortho* substituents X. Since a CN group is the smallest substituent in the series, increased steric hindrance imposed by other substituents (X = Me, 2-MeC_6H_4, Br) may account for reduced rates of the catalytic *N*-acylation of tetracycles *rac*-**4a**,**c**,**d** with Boc_2O. Hence, the competing DMAP-catalyzed *O*-acylation with Boc_2O facilitates the opening of the benzofuro[2,3-*b*]-indolines *rac*-**4a**,**c**,**d** to form 3*H*-indolines **10a**,**c**,**d**.

In the absence of external electrophile such as Boc_2O phenols **9** may undergo an intramolecular acyl transfer *via* tetrahedral intermediate **13** with indole acting as a good leaving group to form the *N*-unsubstituted indole **14**. Notably, for phenol **9a**, the intramolecular acyl transfer from carbon to oxygen to afford compound **14a** was a competing side reaction (yield 15%, Table 1, entry 1) to DMAP-catalyzed intermolecular *O*-acylation with the excess of Boc_2O (2 equiv). Possibly, the better leaving group ability of the 7-bromoindole moiety compared to 7-methyl- and 7-(2-methylphenyl)-substituted analogs ensures sufficiently rapid decomposition of the putative tetrahedral intermediate **13a** to form compound **14a** (Scheme 4). It should be noted that in the presence of DMAP/Boc_2O anionic versions of intermediates *rac*-**4a**,**c**–**e** and **9a**,**c**–**e** could also be involved,[9] but they are not illustrated in the Scheme 4 for simplicity.

In summary, the fragmentation reaction of benzofuro-[2,3-*b*]indolines *rac*-**4a**,**c**–**e** has been studied. They undergo ring opening to the corresponding phenols **9a**,**c**,**d** in the presence of a base such as Et_3N or DMAP/Boc_2O.[9] The intermediate phenols **9a**,**c**,**d** can be isolated upon DMAP-

* As has been demonstrated by Hassner,[9] the reaction of DMAP with Boc_2O produces ion pair: *N*-Boc-pyridinium *tert*-butoxycarboxylate. The *tert*-butoxycarboxylate decomposes to CO_2 and the strong base *tert*-butoxide.

Scheme 4

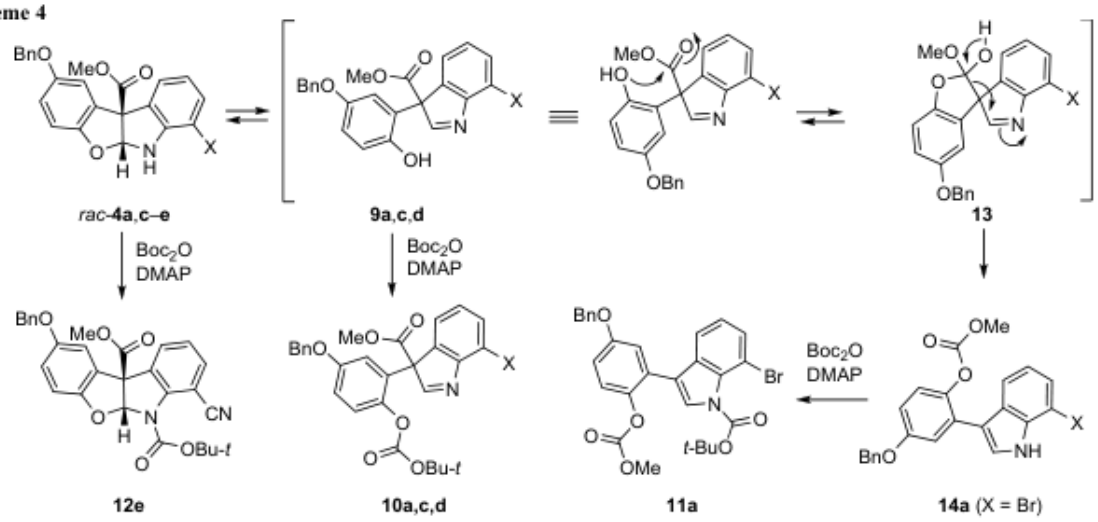

Working mechanism for DMAP-catalyzed fragmentation of benzofuro[2,3-b]indolines *rac*-**4a**,**c**–**e**

Scheme 5

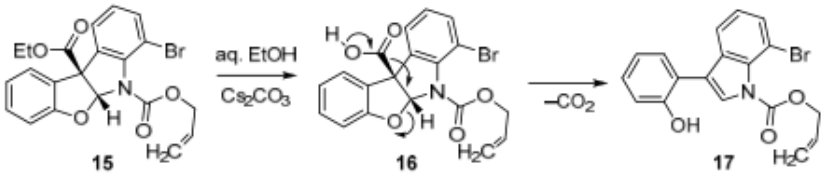

Mechanism suggested by Moody

catalyzed *O*-acylation with Boc_2O. Without the added Boc_2O, phenols **9** undergo an intramolecular transfer of the methoxycarbonyl group *via* the tetrahedral intermediate **13** with indole acting as a good leaving group to form *O*-methoxycarbonyl phenols **14**. The proposed mechanism differs from an alternative base-mediated pathway suggested by Moody for *N*-substituted benzofuro[2,3-*b*]-indolines,[6] which would involve an initial hydrolysis of ester **15** by aqueous base, followed by decarboxylation of the intermediate carboxylic acid **16** with concomitant formation of *N*-substituted aromatic indole **17** (Scheme 5).

According to the mechanism proposed by Moody, phenolate acts as a good leaving group resulting in the formation of *O*-unsubstituted *N*-protected phenol **17** as the fragmentation product. It should be noted, that we observed the formation of *N*-unsubstituted *O*-methoxycarbonyl-phenols **6a** and **14a** with the methoxycarbonyl moiety originating from the ester moiety at the quaternary carbon in the starting benzofuro[2,3-*b*]indolines, hence suggesting that our mechanism differs from that of Moody. Therefore, benzofuro[2,3-*b*]indolines may undergo fragmentation to 3-arylindoles by two alternative mechanisms, depending on the reaction conditions.

Experimental

IR spectra were recorded on a Shimadzu IR Prestige21 FTIR spectrometer in thin film. ^1H and ^{13}C NMR spectra were recorded at ambient temperature on a Varian Mercury NMR spectrometer (400 and 100 MHz, respectively) in $CDCl_3$ with TMS as internal standard. High-resolution mass spectra (ESI) were obtained on a Waters Tof Synapt GSi mass spectrometer. Preparative HPLC was performed on a Waters SunFire™ Prep Silica OBD™ 5μm, 30 × 100 mm, mobile phase 10% EtOAc in petroleum ether, flow rate 35 ml/min. Analytical thin-layer chromatography (TLC) was performed on precoated silica gel F-254 plates (Merck).

Unless otherwise noted, all chemicals were used as obtained from commercial sources and all reactions were performed under argon atmosphere in an oven-dried (120°C) glassware. Toluene was distilled from sodium/benzophenone prior the use. Anhydrous 1,4-dioxane (Acros), *N*,*N*-dimethylacetamide (Acros), and toluene were degassed by multiple freeze-pump-thaw cycles, and handled using Schlenk technique. Anhydrous CH_2Cl_2 was obtained by passing commercially available solvent through activated alumina columns. Commercially available anhydrous K_3PO_4 was heated at 250°C for 3 h and stored in a glove box under argon atmosphere.

Methyl 2-(benzyloxy)-7-methyl-6,10b-dihydro-5a*H*-benzofuro[2,3-*b*]indole-10b-carboxylate (4c). *N*-MOM-protected hemiaminal *rac*-**4a**[7] (25 mg, 0.055 mmol) and $PdCl_2$(dppf) (2.1 mg, 0.0025 mmol) were placed into a 5 ml pressure vial and suspended in anhydrous dioxane (1.0 ml)

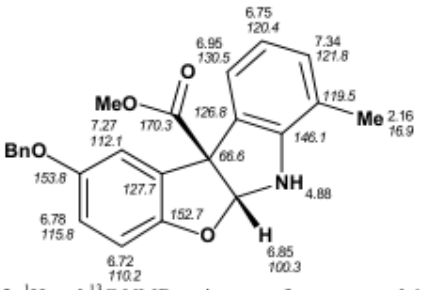

Figure 2. ^{1}H and ^{13}C NMR assignment for compound **4c**.

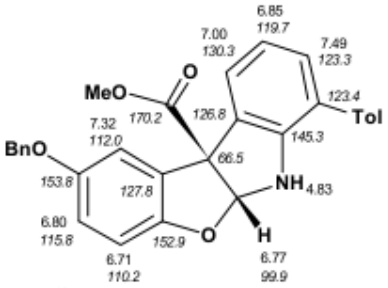

Figure 3. ^{1}H and ^{13}C NMR assignment for compound **4d**.

under nitrogen atmosphere. Then dimethylzinc (1.2 M solution in toluene, 83 μl, 0.10 mmol) was added and the resulting clear yellow solution was heated in an oil bath at 100°C for 1 h. The off-white precipitate was filtered through a pad of Celite and the pad was washed with EtOAc (25 ml). The filtrate was washed with water (10 ml) and the layers were separated. The aqueous layer was back-extracted with EtOAc (2×10 ml) and the combined organic extracts were washed with brine, dried over Na_2SO_4, and concentrated (rotary evaporator). The residue was purified on silica gel column using gradient elution from 2% EtOAc in petroleum ether to 25% EtOAc in petroleum ether to afford colorless oil (15 mg) comprising a mixture of MOM-protected and MOM-deprotected products. To achieve complete cleavage of the *N*-MOM protecting group in the product, the isolated mixture of products was dissolved in MeOH (2 ml) and aqueous concentrated HCl (50 μl) was added. The colorless solution was stirred at room temperature for 5 h, basified with aqueous sat. $NaHCO_3$ solution to pH 7 and extracted with CH_2Cl_2 (3×10 ml). The combined organic extracts were washed with brine, dried over Na_2SO_4, and concentrated (rotary evaporator). Column chromatography on silica gel using gradient elution from 2% EtOAc in petroleum ether to 25% EtOAc in petroleum ether afforded the product as colorless oil (9 mg, 47%, Fig. 2). R_f 0.43 (petroleum ether–EtOAc, 5:4). IR spectrum, ν, cm^{-1}: 3395 (NH), 1736 (C=O). ^{1}H NMR spectrum, δ, ppm (*J*, Hz): 7.45–7.30 (6H, m); 7.27 (1H, dd, *J* = 2.7, *J* = 0.4); 6.95 (1H, ddd, *J* = 7.5, *J* = 1.2, *J* = 0.7); 6.86 (1H, d, *J* = 3.5); 6.78 (1H, dd, *J* = 8.7, *J* = 2.7); 6.75 (1H, t, *J* = 7.5); 6.72 (1H, dd, *J* = 8.7, *J* = 0.4); 5.00 (2H, s); 4.88 (1H, d, *J* = 3.5); 3.80 (3H, s); 2.16 (3H, s). ^{13}C{^{1}H} NMR spectrum, δ, ppm: 170.3; 153.8; 152.7; 146.1; 137.3; 130.5; 128.7; 128.1; 127.8; 127.7; 126.8; 121.8; 120.4; 119.5; 115.8; 112.1; 110.2; 100.3; 71.3; 66.6; 53.2; 16.9. Found, *m*/*z*: 388.1542 [M+H]$^+$. $C_{24}H_{22}NO_4$. Calculated, *m*/*z*: 388.1549.

Methyl 2-(benzyloxy)-7-(*ortho*-tolyl)-6,10b-dihydro-5a*H*-benzofuro[2,3-*b*]indole-10b-carboxylate (4d). *N*-MOM-protected *rac*-**4a**[7] (50 mg, 0.11 mmol), *ortho*-tolylboronic acid pinacolyl ester (26 mg, 0.12 mmol), $(PCy_3)_2Pd(\eta^2\text{-}O_2)$[7] (14 mg, 20 mol %), and oven-dried K_3PO_4 (85 mg, 0.44 mmol) were weighed into a 5 ml pressure vial in a glove box (argon atmosphere). Anhydrous degassed toluene (2.5 ml) was added, and the reaction mixture was heated in an oil bath at 110°C for 18 h, then diluted with EtOAc (15 ml) and washed with water (15 ml). The aqueous layer was back-extracted with EtOAc (15 ml). Combined organic extracts were washed with brine, dried over Na_2SO_4, filtered, and concentrated (rotary evaporator). Column chromatography on silica gel using gradient elution from 2% EtOAc in petroleum ether to 25% EtOAc in petroleum ether afforded product as yellow oil (38 mg) comprising a mixture of MOM-protected and MOM-deprotected products according to ^{1}H NMR. To achieve complete cleavage of *N*-MOM protecting group in the product, the mixture of products was dissolved in MeOH (3 ml) and aqueous concentrated HCl (100 μl) was added. The reaction mixture was stirred at room temperature for 20 h, then basified to pH 7 using aqueous saturated $NaHCO_3$ solution and extracted with CH_2Cl_2 (3×15 ml). The combined organic extracts were washed with brine, dried over Na_2SO_4, and concentrated (rotary evaporator). Purification of the residue on the silica gel column using gradient elution from 2% EtOAc in petroleum ether to 25% EtOAc in petroleum ether afforded the biaryl **4d** as colorless oil (17 mg, 33%, Fig. 3). R_f 0.53 (petroleum ether–EtOAc, 5:2). IR spectrum, ν, cm^{-1}: 3394 (N–H), 1733 (C=O). ^{1}H NMR spectrum, δ, ppm: 7.49 (1H, d, *J* = 7.6); 7.47–7.33 (5H, m); 7.32 (1H, d, *J* = 2.7); 7.28–7.20 (4H, m); 7.00 (1H, dd, *J* = 7.6, *J* = 1.1); 6.85 (1H, t, *J* = 7.6); 6.80 (1H, dd, *J* = 8.7, *J* = 2.7); 6.77 (1H, d, *J* = 2.7); 6.71 (1H, d, *J* = 8.7); 5.03 (2H, s); 4.83 (1H, s); 3.84 (3H, s); 2.18 (3H, s). ^{13}C{^{1}H} NMR spectrum, δ, ppm: 170.2; 153.8; 152.9; 145.3; 137.6; 137.3; 136.6 (br. s); 130.6; 130.3; 129.9 (br. s); 128.7; 128.1; 128.0; 127.8; 126.7 (br. s); 126.2; 123.4 (br. s); 123.3; 119.7; 115.8; 112.0; 110.2; 99.9; 71.3; 66.5; 53.3; 20.1. Found, *m*/*z*: 464.1861 [M+H]$^+$. $C_{30}H_{26}NO_4$. Calculated, *m*/*z*: 464.1862.

Methyl 2-(benzyloxy)-7-cyano-6,10b-dihydro-5a*H*-benzofuro[2,3-*b*]indole-10b-carboxylate (4e). *N*-MOM-protected *rac*-**4a**[7] (100 mg, 0.20 mmol), $Pd_2(dba)_3$ (9.2 mg, 0.005 mmol), dppf (11.1 mg, 0.10 mmol), and $Zn(CN)_2$ (16.6 mg, 0.14 mmol) were weighed into a 5 ml pressure vial and anhydrous degassed DMA (2.5 ml) was added under nitrogen. The suspension was stirred at 110°C for 2 h, filtered through a pad of Celite, and the pad was washed with EtOAc (30 ml). The filtrate was washed with water (2×15 ml), brine, dried over Na_2SO_4, and concentrated (rotary evaporator). Purification of a brown oily residue on silica gel column using gradient elution from 7% EtOAc in petroleum ether to 56% EtOAc in petroleum ether was followed by additional purification on preparative TLC using 25% acetone in petroleum ether and

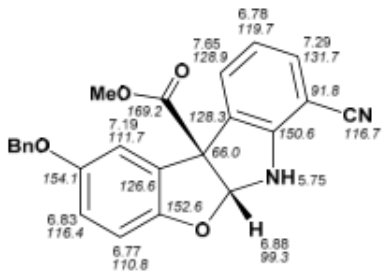

Figure 4. ^{1}H and ^{13}C NMR assignment for compound **4e**.

afforded **methyl 2-(benzyloxy)-7-cyano-6-(methoxymethyl)-6,10b-dihydro-5a*H*-benzofuro[2,3-*b*]indole-10b-carboxylate** as a brownish oil (46 mg, 53%). R_f 0.37 (petroleum ether–EtOAc, 5:2). IR spectrum, ν, cm^{-1}: 2222 (C≡N), 1738 (C=O). ^{1}H NMR spectrum, δ, ppm (*J*, Hz): 7.69 (1H, ddd, *J* = 7.5, *J* = 1.2, *J* = 0.5); 7.43–7.30 (6H, m); 7.17 (1H, d, *J* = 2.6); 6.86–6.76 (4H, m); 5.39 (1H, d, *J* = 10.9); 5.04 (1H, d, *J* = 10.9); 5.00 (2H, s); 3.82 (3H, s); 3.47 (3H, s). ^{13}C{^{1}H} NMR spectrum, δ, ppm: 169.0; 154.2; 152.3; 147.9; 137.0; 134.0; 130.3; 128.9; 128.7; 128.2; 127.7; 126.8; 120.2; 117.7; 116.5; 111.9; 110.9; 103.1; 92.1; 77.1; 71.3; 63.6; 55.3; 53.6. Found, *m/z*: 411.1344 [M–CH_3O]$^+$. $C_{25}H_{19}N_2O_4$. Calculated, *m/z*: 411.1345.

The *N*-MOM-protected hemiaminal from above (40 mg, 0.09 mmol) was dissolved in MeOH (2 ml), aqueous concentrated HCl (300 µl) was added, and the reaction mixture was stirred at room temperature for 36 h, then basified with aqueous saturated $NaHCO_3$ to pH 7 and extracted with CH_2Cl_2 (3×10 ml). The combined organic extracts were washed with brine, dried over Na_2SO_4, and concentrated (rotary evaporator). The residue was purified on silica gel column using gradient elution from 7% EtOAc in petroleum ether to 60% EtOAc in petroleum ether to afford compound **4e** as a colorless solid (18 mg, 56%, Fig. 4). R_f 0.38 (petroleum ether–EtOAc, 5:4). IR spectrum, ν, cm^{-1}: 3335 (N–H), 2224 (C≡N), 1728 (C=O). ^{1}H NMR spectrum, δ, ppm (*J*, Hz): 7.65 (1H, d, *J* = 7.5); 7.44–7.31 (5H, m); 7.29 (1H, dd, *J* = 7.9, *J* = 1.1); 7.19 (1H, d, *J* = 2.6); 6.88 (1H, d, *J* = 2.2); 6.83 (1H, dd, *J* = 8.8, *J* = 2.6); 6.78 (1H, t, *J* = 7.7); 6.77 (1H, d, *J* = 8.8); 5.75 (1H, s); 5.01 (2H, s); 3.83 (3H, s). ^{13}C{^{1}H} NMR spectrum, δ, ppm: 169.2; 154.1; 152. 6; 150.6; 137.0; 131.7; 128. 9; 128.7; 128.3; 128.2; 127.7; 126.6; 119.7; 116.7; 116.4; 111.7; 110.8; 99.3; 91.8; 71.3; 66.0; 53.6. Found, *m/z*: 399.1326 [M+H]$^+$. $C_{24}H_{19}N_2O_4$. Calculated, *m/z*: 399.1345.

4-(Benzyloxy)-2-[3-(2-methyloxazol-5-yl)-1-(triisopropylsilyl)-1*H*,1'*H*-[4,7'-biindol]-3'-yl]phenyl methyl carbonate (**6a**). A hemiaminal *rac*-**4a**[7] (100 mg, 0.22 mmol), *N*-TIPS indolyl boronate **5a**[7] (106 mg, 0.22 mmol), $(PCy_3)_2Pd(\eta^2\text{-}O_2)$[7] (30 mg, 20 mol %), and an oven-dried K_3PO_4 (188 mg, 0.88 mmol) were weighed into an oven-dried pressure vial in a glove box (argon atmosphere). Anhydrous degassed dioxane (4 ml) was added, and the reaction mixture was heated in an oil bath at 100°C for 20 h, then diluted with EtOAc (25 ml) and washed with water (25 ml). The aqueous layer was back-extracted with EtOAc (25 ml). Combined organic extracts were washed

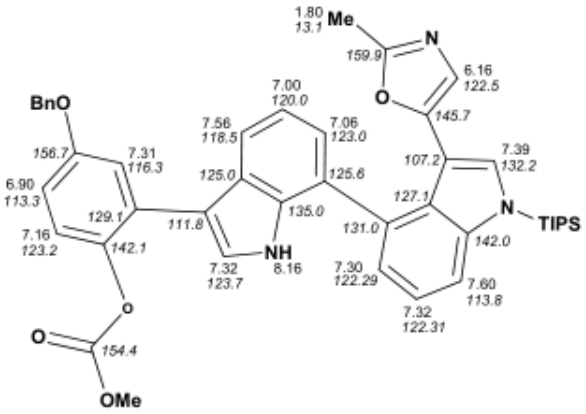

Figure 5. ^{1}H and ^{13}C NMR assignment for compound **6a**.

with brine, dried over Na_2SO_4, filtered, and concentrated (rotary evaporator). Column chromatography on silica gel using gradient elution from 5% acetone in hexanes to 25% acetone in hexanes afforded the product **6a** as off-white foam (130 mg, 86%, Fig. 5). R_f 0.19 (petroleum ether–EtOAc, 5:2). IR spectrum, ν, cm^{-1}: 3421 (N–H), 1763 (C=O). ^{1}H NMR spectrum, δ, ppm (*J*, Hz): 8.16 (1H, d, *J* = 1.5); 7.60 (1H, dd, *J* = 6.6, *J* = 2.7); 7.56 (1H, dd, *J* = 7.5, *J* = 1.5); 7.49–7.38 (5H, m); 7.38–7.29 (5H, m); 7.16 (1H, d, *J* = 8.9); 7.06–6.98 (2H, m); 6.90 (1H, dd, *J* = 8.9, *J* = 3.1); 6.16 (1H, s); 5.12 (2H, s); 3.70 (3H, s); 1.80 (3H, s); 1.75 (3H, septet, *J* = 7.5); 1.20 (18H, d, *J* = 7.5). ^{13}C{^{1}H}NMR spectrum, δ, ppm: 159.9; 156.7; 154.4; 145.7; 142.1; 142.0; 136.9; 135.0; 132.2; 131.0; 129.1; 128.7; 128.0; 127.4; 127.1; 125.6; 125.0; 123.7; 123.2; 122.9; 122.5; 122.3; 120.0; 118.5; 116.3; 113.8; 113.3; 111.8; 107.2; 70.4; 55.3; 18.2; 13.0; 12.8. Found, *m/z*: 726.3351 [M+H]$^+$. $C_{44}H_{48}N_3O_5Si$. Calculated, *m/z*: 726.3363.

4-(Benzyloxy)-2-(7-bromo-1*H*-indol-3-yl)phenyl methyl carbonate (**8a**). A solution of hemiaminal *rac*-**4a**[7] (10 mg, 0.022 mmol) in $CDCl_3$ (0.7 ml) was placed in NMR tube and Et_3N (6 µl, 0.044 mmol) was added. The solution was kept at room temperature and progress of the reaction was monitored by ^{1}H NMR. Full conversion to the starting hemiaminal bromide *rac*-**4a** was observed after 57 days.

For structure assignment and compound characterization purposes, the indole **8a** was synthesized from *N*-Boc-indole **11a**. Accordingly, a solution of *N*-Boc-indole **11a** (30 mg, 0.054 mmol) in toluene (2.0 ml) was heated at 160°C in a closed 5 ml pressure vial for 30 h, then the solvent was evaporated and the brownish solid residue was purified on silica gel column using gradient elution from 7% EtOAc in petroleum ether to 60% EtOAc in petroleum ether. Indole **8a** was obtained as colorless foam (23 mg, 94%, Fig. 6). R_f 0.38 (petroleum ether–EtOAc, 5:2). IR spectrum, ν, cm^{-1}: 3422 (N–H), 1761 (C=O). ^{1}H NMR spectrum, δ, ppm (*J*, Hz): 8.48 (1H, s); 7.55 (1H, d, *J* = 8.0); 7.47–7.32 (7H, m); 7.22 (1H, d, *J* = 3.0); 7.19 (1H, d, *J* = 8.9); 7.01 (1H, t, *J* = 7.8); 6.95 (1H, dd, *J* = 8.9, *J* = 3.0); 5.12 (2H, s); 3.70 (3H, s). ^{13}C {^{1}H} NMR spectrum, δ, ppm: 156.9; 154.4; 142.3; 137.0; 135.9; 128.8; 128.5; 128.2; 127.6; 127.5;

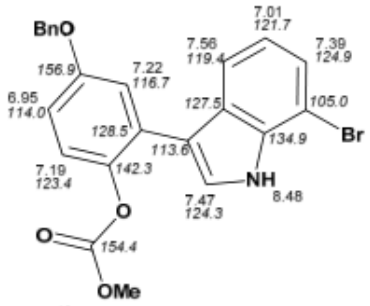

Figure 6. ^{1}H and ^{13}C NMR assignment for compound **8a**.

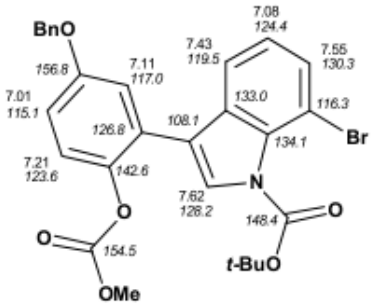

Figure 8. ^{1}H and ^{13}C NMR assignment for compound **11a**.

124.9; 124.3; 123.4; 121.7; 119.4; 116.7; 114.0; 113.6; 105.0; 70.6; 55.5. Found, *m*/*z*: 452.0479 $[M+H]^+$. $C_{23}H_{19}BrNO_4$. Calculated, *m*/*z*: 452.0497.

Ring opening of the hemiaminal *rac*-4a in the presence of Boc_2O. The hemiaminal *rac*-**4a**[7] (880 mg, 1.64 mmol) was dissolved in anhydrous CH_2Cl_2 (70 ml) under nitrogen atmosphere, and the resulting solution was cooled to 0°C. Then Et_3N (3.4 ml, 24.6 mmol) was added dropwise, followed by Boc_2O (892 mg, 4.10 mmol) and DMAP (50 mg, 0.40 mmol). The colorless solution was stirred at room temperature for 30 min, then the solvent was evaporated and the residue was purified on silica gel column (80 ml SiO_2, mobile phase 30% EtOAc in petroleum ether) to afford a mixture of *O*-Boc-phenol **10a** and *N*-Boc-indole **11a.** These two products were separated on the preparative HPLC.

Methyl 3-{5-(benzyloxy)-7-bromo-2-[(*tert*-butoxycarbonyl)oxy]phenyl}-3*H*-indole-3-carboxylate (10a) was obtained as a colorless foam (597 mg, 66%, Fig. 7). R_f 0.47 (petroleum ether–EtOAc, 5:2). IR spectrum, ν, cm^{-1}: 1761 (C=O), 1743 (C=O). ^{1}H NMR spectrum, δ, ppm (*J*, Hz): 8.27 (1H, s); 7.62 (1H, d, *J* = 8.0); 7.45 (1H, d, *J* = 7.5); 7.34–7.17 (7H, m); 6.93 (1H, dd, *J* = 9.0, *J* = 3.0); 6.32 (1H, d, *J* = 3.0); 4.87 (1H, ABq, J_{AB} = 12.0); 4.86 (1H, ABq, J_{AB} = 12.0); 3.70 (3H, s); 1.55 (9H, s). $^{13}C\{^{1}H\}$ NMR spectrum, δ, ppm: 170.3; 168.6; 156.3; 154.1; 151.2; 143.5; 136.7; 136.1; 133.1; 128.5; 128.0; 127.3; 126.1; 123.9; 115.5; 115.1; 113.9; 84.0; 71.5; 70.3; 53.0; 27.6. Found, *m*/*z*: 574.0834 $[M+Na]^+$. $C_{28}H_{26}BrNNaO_6$. Calculated, *m*/*z*: 574.0841.

***tert*-Butyl 3-{5-(benzyloxy)-7-bromo-2-[(methoxycarbonyl)oxy]phenyl}-1*H*-indole-1-carboxylate (11a)** was obtained as a colorless oil (167 mg, 18%, Fig. 8). R_f 0.53 (petroleum ether–EtOAc, 5:2). IR spectrum, ν, cm^{-1}: 1763 (C=O), 1738 (C=O). ^{1}H NMR spectrum, δ, ppm (*J*, Hz): 7.62 (1H, s); 7.55 (1H, dd, *J* = 7.8, *J* = 1.0); 7.46–7.32 (6H, m); 7.21 (1H, d, *J* = 8.9); 7.11 (1H, d, *J* = 3.0); 7.08 (1H, t, *J* = 7.8); 7.01 (1H, dd, *J* = 8.9, *J* = 3.0); 5.11 (2H, s); 3.71 (3H, s); 1.67 (9H, s). $^{13}C\{^{1}H\}$ NMR spectrum, δ, ppm: 156.8; 154.5; 148.4; 142.6; 136.8; 134.1; 133.0; 130.3; 128.9; 128.2 (2 peaks overlapping); 127.6; 126.8; 124.4; 123.6; 119.5; 117.0; 116.3; 115.1; 108.1; 84.7; 70.6; 55.5; 28.1. Found, *m*/*z*: 452.0484 $[M-(CH_3)_3COC(O)+2H]^+$. $C_{23}H_{19}BrNO_4$. Calculated, *m*/*z*: 452.0497.

Methyl 3-{5-(benzyloxy)-2-[(*tert*-butoxycarbonyl)oxy]-phenyl}-7-methyl-3*H*-indole-3-carboxylate (10c). A solution of hemiaminal **4c** (20 mg, 0.052 mmol, Fig. 9) in $CDCl_3$ (0.7 ml) was placed in NMR tube and DMAP (0.64 mg, 0.0052 mmol) was added, followed with Boc_2O (28 mg, 0.130 mmol). The clear colorless solution was kept at room temperature and progress of the reaction was monitored by ^{1}H NMR. Complete conversion of the starting hemiaminal **4c** was observed after 72 h. The solution was poured onto the silica gel column and purified using CH_2Cl_2 as a mobile phase to afford product **10c** (23 mg, 91%) as a yellowish oil. R_f 0.45 (petroleum ether – EtOAc, 5:2). IR spectrum, ν, cm^{-1}: 1761 (C=O), 1733 (C=O). ^{1}H NMR spectrum, δ, ppm (*J*, Hz): 8.20 (1H, s); 7.35 (1H, dd, *J* = 7.2, *J* = 1.0); 7.34–7.22 (7H, m); 7.22 (1H, d, *J* = 9.0); 6.92 (1H, dd, *J* = 9.0, *J* = 3.0); 6.37 (1H, d, *J* = 3.0); 4.86 (2H, s); 3.70 (3H, s); 2.61 (3H, s); 1.58 (9H, s). $^{13}C\{^{1}H\}$ NMR spectrum, δ, ppm: 169.6; 168.4; 156.5; 154.5; 151.6; 144.0; 134.5; 134.9; 131.8; 131.3; 128.7; 128.2; 127.7; 127.4; 127.2; 123.9; 122.5; 115.0; 114.2; 84.0; 70.5; 70.3; 53.1; 27.9; 17.0. Found, *m*/*z*: 510.1886 $[M+Na]^+$. $C_{29}H_{29}NNaO_6$. Calculated, *m*/*z*: 510.1892.

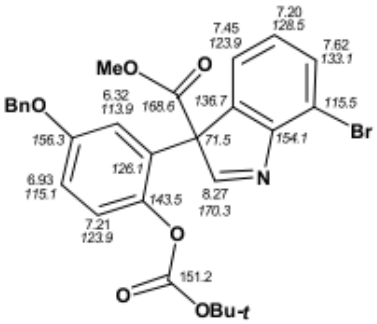

Figure 7. ^{1}H and ^{13}C NMR assignment for compound **10a**.

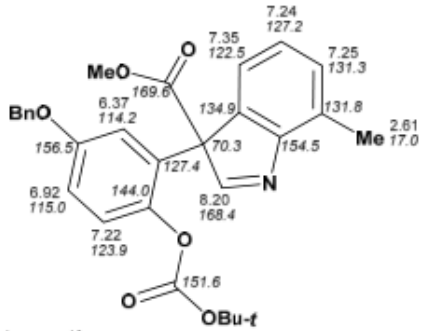

Figure 9. ^{1}H and ^{13}C NMR assignment for compound **10c**.

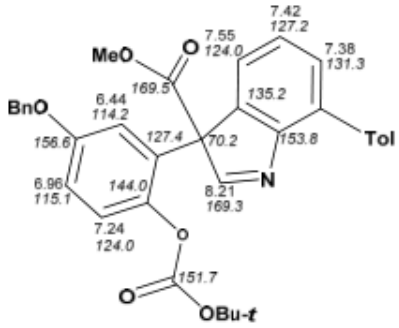

Figure 10. ^{1}H and ^{13}C NMR assignment for compound **10d**.

Methyl 3-{5-(benzyloxy)-2-[(*tert*-butoxycarbonyl)oxy]-phenyl}-7-(*ortho*-tolyl)-3*H*-indole-3-carboxylate (10d). To a solution of hemiaminal **4d** (30 mg, 0.065 mmol) in anhydrous CH_2Cl_2 (4 ml) under nitrogen atmosphere, DMAP (0.8 mg, 0.0065 mmol) and Boc_2O (36 mg, 0.16 mmol) were added. The clear colorless solution was stirred at room temperature for 72 h. The solvent was evaporated and the residue was purified on silica gel column using gradient elution from 2% EtOAc in petroleum ether to 25% EtOAc in petroleum ether to afford the product **10d** as yellow oil (30 mg, 82%, Fig. 10). R_f 0.49 (petroleum ether–EtOAc, 5:2). IR spectrum, ν, cm^{-1}: 1760 (C=O), 1742 (C=O). ^{1}H NMR spectrum, δ, ppm (*J*, Hz): 8.21 (1H, s); 7.55 (1H, dd, *J* = 6.4, *J* = 2.3); 7.43–7.27 (11H, m); 7.24 (1H, d, *J* = 9.0); 6.96 (1H, dd, *J* = 9.0, *J* = 3.0); 6.44 (1H, d, *J* = 3.0); 4.90, 4.88 (2H, ABq, *J* = 12.0); 3.73 (3H, s); 2.19 (3H, s); 1.57 (9H, s). ^{13}C{^{1}H} NMR spectrum, δ, ppm: 169.5; 169.3; 156.6; 154.3; 153.8; 151.7; 144.0; 138.1; 136.5; 136.4; 135.7; 135.2; 131.3; 130.3; 128.8; 128.3; 128.0; 127.7; 127.4; 127.2; 125.7; 124.0; 124.0; 115.1; 114.2; 70.6; 70.2; 53.1; 27.9; 20.6. Found, *m*/*z*: 586.2222 [M+Na]$^{+}$. $C_{35}H_{33}NO_6Na$. Calculated, *m*/*z*: 586.2206.

6-*tert*-Butyl 10b-methyl 2-(benzyloxy)-7-cyano-6*H*-[1]benzofuro[2,3-*b*]indole-6,10b(5a*H*)-dicarboxylate (*rac*-12e). A solution of hemiaminal *rac*-**4e** (15 mg, 0.038 mmol) in $CDCl_3$ (0.7 ml) was placed in NMR tube and DMAP (0.46 mg, 0.0038 mmol) was added, followed with Boc_2O (21 mg, 0.094 mmol). The clear colorless solution was kept at room temperature and progress of the reaction was monitored by ^{1}H NMR spectroscopy. Complete conversion of the starting hemiaminal **4e** was observed after 20 h. The solution was poured onto the silica gel column and purified using CH_2Cl_2 as a mobile phase to afford *rac*-**12e** as a yellowish oil (16 mg, 83%, Fig. 11). R_f 0.38 (petroleum ether–EtOAc, 5:2). IR spectrum, ν, cm^{-1}: 2231 (C≡N), 1811 (C=O), 1742 (C=O). ^{1}H NMR spectrum, δ, ppm (*J*, Hz): 7.72 (1H, d, *J* = 7.7); 7.55 (1H, d, *J* = 7.8); 7.44–7.30 (5H, m); 7.22 (1H, d, *J* = 2.5); 7.14 (1H, dd, *J* = 7.7, *J* = 7.8); 7.13 (1H, s); 6.82 (1H, dd, *J* = 8.8, *J* = 2.5); 6.77 (1H, d, *J* = 8.8);

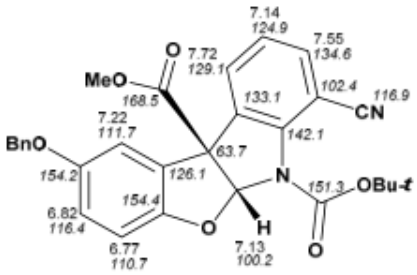

Figure 11. ^{1}H and ^{13}C NMR assignment for compound **12e**.

5.01 (2H, s); 3.84 (3H, s); 1.67 (9H, s). ^{13}C{^{1}H} NMR spectrum, δ, ppm: 168.5; 154.2; 152.4; 151.3; 142.2; 136.9; 134.6; 133.1; 129.1; 128.8; 128.2; 127.7; 126.1; 124.9; 116.9; 116.4; 111.7; 110.7; 102.4; 100.2; 85.1; 71.3; 63.7; 53.8; 28.2. Found, *m*/*z*: 499.1850 [M+H]$^{+}$. $C_{29}H_{27}N_2O_6Na$. Calculated, *m*/*z*: 499.1869.

We thank European Social Fund (project No. 1DP/1.1.1.2.0/13/APIA/VIAA/006) for financial support of this research. E. Vedejs thanks InnovaBalt project for funding.

References

1. For review on synthesis of diazonamide A, see: Lachia, M.; Moody, C. *Nat. Prod. Rep.* **2008**, *25*, 227.
2. Cruz-Monserrate, Z.; Vervoort, H. C.; Bai, R.; Newman, D. J.; Howell, S. B.; Los, G.; Mullaney, J. T.; Williams, M. D.; Pettit, G. R.; Fenical, W.; Hamel, E. *Mol. Pharmacol.* **2003**, *63*, 1273.
3. For review, see: Beaud, R.; Tomakinian, T.; Denizot, N.; Pouilhès, A.; Kouklovsky, C.; Vincent, G. *Synlett* **2015**, *26*, 432.
4. (a) Tomakinian, T.; Kouklovsky, C.; Vincent, G. *Synlett* **2015**, *26*, 1269. (b) Ding, H.; DeRoy, P. L.; Perreault, C.; Larivée, A.; Siddiqui, A.; Caldwell, C. G.; Harran, S.; Harran, P. G. *Angew. Chem., Int. Ed.* **2015**, *54*, 4818. (c) Tomakinian, T.; Guillot, R.; Kouklovsky, C.; Vincent, G. *Angew. Chem., Int. Ed.* **2014**, *53*, 11881. (d) Liao, L.; Shu, C.; Zhang, M.; Liao, Y.; Hu, X.; Zhang, Y.; Wu, Z.; Yuan, W.; Zhang, X. *Angew. Chem., Int. Ed.* **2014**, *53*, 10471. (e) Shu, C.; Liao L.-H.; Liao Y.-J.; Hu, X.-Y.; Zhang, Y.-H.; Yuan, W.-C.; Zhang, X.-M. *Eur. J. Org. Chem.* **2014**, 4467. (f) Denizot, N.; Pouilhès, A.; Cucca, M.; Beaud, R.; Guillot, R.; Kouklovsky, C.; Vincent, G. *Org. Lett.* **2014**, *16*, 5752. (g) Zhao, J.-C.; Yu, S.-M.; Liu, Y.; Yao, Z.-J. *Org. Lett.* **2013**, *15*, 4300. (h) Beaud, R.; Guillot, R.; Kouklovsky, C.; Vincent, G. *Angew. Chem., Int. Ed.* **2012**, *51*, 12546.
5. (a) Zajac, M. A.; Vedejs, E. *Org. Lett.* **2004**, *6*, 237. (b) Peris, G.; Vedejs, E. *J. Org. Chem.* **2015**, *80*, 3050.
6. Poriel, C.; Lachia, M.; Wilson, C.; Davies, J. R.; Moody, C. J. *J. Org. Chem.* **2007**, *72*, 2978.
7. Mutule, I.; Joo, B.; Medne, Z.; Kalnins, T.; Vedejs, E.; Suna, E. *J. Org. Chem.* **2015**, *80*, 3058.
8. Rawal, V. H.; Cava, M. P. *Tetrahedron Lett.* **1985**, *26*, 6141.
9. Basel, Y.; Hassner, A. *J. Org. Chem.* **2000**, *65*, 6368.

Appendix III – STRUCTURALLY SIMPLIFIED DIAZONAMIDE ANALOGS AS ANTIMITOTIC AGENTS

Edgars Suna, Toms Kalnins, Mihail Kazak, Viktorija Vitkovska, Nauris Narvaiss, Diana Zelencova-Gopejenko, Kristaps, Jaudzems

PCT patent Nr. WO2021130515, July 1, 2021.

(12) INTERNATIONAL APPLICATION PUBLISHED UNDER THE PATENT COOPERATION TREATY (PCT)

(19) World Intellectual Property Organization
International Bureau

(43) International Publication Date
01 July 2021 (01.07.2021)

WIPO | PCT

(10) International Publication Number
WO 2021/130515 A1

(51) International Patent Classification:
C07D 498/18 (2006.01) *A61K 31/424* (2006.01)
A61P 35/00 (2006.01)

(21) International Application Number:
PCT/IB2019/061264

(22) International Filing Date:
23 December 2019 (23.12.2019)

(25) Filing Language: English

(26) Publication Language: English

(71) Applicant: **LATVIAN INSTITUTE OF ORGANIC SYNTHESIS** [LV/LV]; Aizkraukles street 21, LV-1006 Riga (LV).

(72) Inventors: **SUNA, Edgars**; Alsungas 5a, LV-1004 Riga (LV). **KALNINS, Toms**; Jana Street 1, LV-4033 Salacgriva (LV). **KAZAK, Mihail**; A. Keldisa 2-68, LV-1082 Riga (LV). **VITKOVSKA, Viktorija**; Ruses Street 5-19, LV-1029 Riga (LV). **NARVAISS, Nauris**; Krasta Street 11-39, LV-3701 Dobele (LV). **ZELENCOVA, Diana**; Ozolciema Street 14-k1/22, LV-1058 Riga (LV). **JAUDZEMS, Kristaps**; Bikernieku Street 160 k2-17B, LV-1079 Riga (LV).

(81) Designated States *(unless otherwise indicated, for every kind of national protection available)*: AE, AG, AL, AM, AO, AT, AU, AZ, BA, BB, BG, BH, BN, BR, BW, BY, BZ, CA, CH, CL, CN, CO, CR, CU, CZ, DE, DJ, DK, DM, DO, DZ, EC, EE, EG, ES, FI, GB, GD, GE, GH, GM, GT, HN, HR, HU, ID, IL, IN, IR, IS, JO, JP, KE, KG, KH, KN, KP, KR, KW, KZ, LA, LC, LK, LR, LS, LU, LY, MA, MD, ME, MG, MK, MN, MW, MX, MY, MZ, NA, NG, NI, NO, NZ, OM, PA, PE, PG, PH, PL, PT, QA, RO, RS, RU, RW, SA, SC, SD, SE, SG, SK, SL, SM, ST, SV, SY, TH, TJ, TM, TN, TR, TT, TZ, UA, UG, US, UZ, VC, VN, ZA, ZM, ZW.

(84) Designated States *(unless otherwise indicated, for every kind of regional protection available)*: ARIPO (BW, GH, GM, KE, LR, LS, MW, MZ, NA, RW, SD, SL, ST, SZ, TZ, UG, ZM, ZW), Eurasian (AM, AZ, BY, KG, KZ, RU, TJ, TM), European (AL, AT, BE, BG, CH, CY, CZ, DE, DK, EE, ES, FI, FR, GB, GR, HR, HU, IE, IS, IT, LT, LU, LV, MC, MK, MT, NL, NO, PL, PT, RO, RS, SE, SI, SK, SM, TR), OAPI (BF, BJ, CF, CG, CI, CM, GA, GN, GQ, GW, KM, ML, MR, NE, SN, TD, TG).

Published:
— *with international search report (Art. 21(3))*

(54) Title: STRUCTURALLY SIMPLIFIED DIAZONAMIDE ANALOGS AS ANTIMITOTIC AGENTS

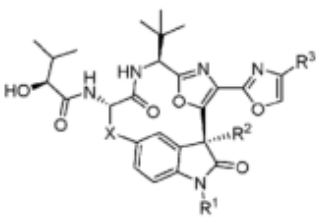

Formula I

(57) Abstract: The present invention relates to medicine and in particular to the treatment of metastatic tumors, more particularly to antimitotic agents and microtubule polymerization inhibitors. Even more particularly, the invention relates to novel analogs of natural antimitotic agent diazonamide A and pharmaceutical compositions thereof and the use of the novel analogs as inhibitors of microtubule polymerization. Formula (I):

WO 2021/130515 A1

Appendix IV – DEVELOPMENT OF POTENT MICROTUBULE TARGETING AGENT BY STRUCTURAL SIMPLIFICATION OF NATURAL DIAZONAMIDE

Toms Kalnins, Viktorija Vitkovska, Mihail Kazak, Diana Zelencova-Gopejenko, Melita Ozola, Nauris Narvaiss, Marina Makrecka-Kuka, Ilona Domraceva, Artis Kinens, Baiba Gukalova, Nele Konrad, Riina Aav, Francesca Bonato, Daniel Lucena-Agell, J. Fernando Díaz, Edgars Liepinsh, and Edgars Suna

J. Med. Chem. **2024**, *67* (11), 9227–9259

Journal of Medicinal Chemistry

pubs.acs.org/jmc

Article

Development of Potent Microtubule Targeting Agent by Structural Simplification of Natural Diazonamide

Toms Kalnins, Viktorija Vitkovska, Mihail Kazak, Diana Zelencova-Gopejenko, Melita Ozola, Nauris Narvaiss, Marina Makrecka-Kuka, Ilona Domračeva, Artis Kinens, Baiba Gukalova, Nele Konrad, Riina Aav, Francesca Bonato, Daniel Lucena-Agell, J. Fernando Díaz, Edgars Liepinsh,* and Edgars Suna*

Cite This: *J. Med. Chem.* 2024, 67, 9227−9259

Read Online

ACCESS | Metrics & More | Article Recommendations | Supporting Information

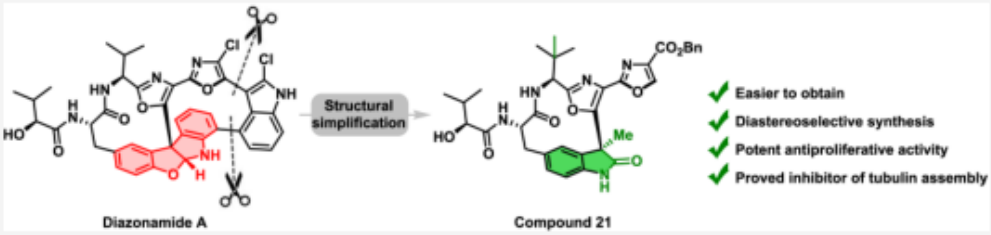

ABSTRACT: The marine metabolite diazonamide A exerts low nanomolar cytotoxicity against a range of tumor cell lines; however, its highly complex molecular architecture undermines the therapeutic potential of the natural product. We demonstrate that truncation of heteroaromatic macrocycle in natural diazonamide A, combined with the replacement of the challenging-to-synthesize tetracyclic hemiaminal subunit by oxindole moiety leads to considerably less complex analogues with improved drug-like properties and nanomolar antiproliferative potency. The structurally simplified macrocycles are accessible in 12 steps from readily available indolin-2-one and *tert*-leucine with excellent diastereoselectivity (99:1 dr) in the key macrocyclization step. The most potent macrocycle acts as a tubulin assembly inhibitor and exerts similar effects on A2058 cell cycle progression and induction of apoptosis as does marketed microtubule-targeting agent vinorelbine.

INTRODUCTION

Cancer is a major public health problem worldwide, with more than 19 million new cases diagnosed and 10 million lethal outcomes in 2020. By 2040, the increase of cancer incidence is expected to rise by 47% and reach 28.4 million cases annualy.[1] Growing incidence and high mortality, together with increasing multidrug resistance toward cancer therapeutics[2] put the development of new effective anticancer treatments among top priorities worldwide. Notably, a considerable number of anticancer medications currently used in clinics originated from natural sources. Thus, about one-third of small molecule anticancer drugs approved for clinical use from 1981 to 2019 are natural products and natural product derivatives.[3] Among them, microtubule-targeting agents (MTAs) such as vinca alkaloids (vinorelbine, vincristine) and taxanes (paclitaxel, docetaxel) have become a standard-of-care treatment in combination chemotherapy regimens.

MTAs of natural origin feature remarkable structural complexity and a high molecular weight that compromise their ADMET and physicochemical properties (leading to, e.g., poor oral bioavailability and solubility) and also limit compound availability due to highly challenging chemical synthesis and difficulties with large-scale isolation from rare source materials.[4] These shortcomings have been addressed by a structural simplification approach toward less complex and synthetically more accessible molecules with improved drug-likeness.[5] Even though the pharmacological potency of a simplified analogue may be reduced as compared to that of a parent natural product, this is compensated by improved ADMET properties and easier synthetic accessibility. Herein, we report a structural simplification of a highly cytotoxic marine metabolite diazonamide A (**1a**) that resulted in the development of analogues with reduced molecular complexity and cytotoxicity profile comparable to those of parent natural product **1a**.

First isolated in 1991 from rare colonial ascidian *Diazona angulata* (54 mg of **1a** was obtained from 256 g of the

Received: February 15, 2024
Revised: April 16, 2024
Accepted: May 24, 2024
Published: June 4, 2024

https://doi.org/10.1021/acs.jmedchem.4c00388
J. Med. Chem. 2024, 67, 9227−9259

lyophilized ascidian),[6] diazonamide A (**1a**) has attracted broad interest owing to its low nanomolar cytotoxicity against a range of tumor cell lines and highly complex molecular architecture. Indeed, diazonamide A contains many synthetically challenging structural elements such as a quaternary C10 stereocenter and two fused macrocycles: 12-membered ring and heteroaromatic macrocycle, possessing three axially chiral biaryl bonds (Figure 1). Considerable synthetic efforts have

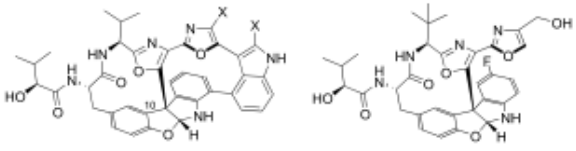

Figure 1. Diazonamide A 1a and its simplified analogues.

culminated in four completed total syntheses[7] and several formal total syntheses[8] of diazonamide A (**1a**). Unfortunately, these notable synthetic accomplishments did not solve the problem of the poor availability of **1a**. As a consequence, only a limited number of studies on the mechanism of diazonamide A antitumor activity were conducted, generating somewhat controversial data. Thus, it has been demonstrated that the low nanomolar cytotoxicity of diazonamide **1a** arises from the inhibition of mitotic spindle assembly during cell division. Hamel and coworkers proposed binding to tubulin and inhibition of tubulin polymerization as an underlying mechanism for antimitotic activity of **1a**.[9] However, a binding site on heterodimeric tubulin could not be established for diazonamide A. Wang, Harran, et al. suggested an alternative mechanism of action for **1a** that involved the inhibition of mitotic functions of ornithine δ-amino transferase.[10] Later, Harran et al. succeeded in obtaining structurally simplified diazonamide analogue **2** by removing the right-hand heteroaromatic macrocycle.[11] The diazonamide analogue **2** was shown to bind at the vinca domain of tubulin heterodimer and inhibit microtubule growth rate, leading to mitotic arrest and tumor cell apoptosis.[12] Importantly, diazonamide analogues **1b** and **2** featured high safety margins and reduced systemic toxicity in *in vivo* models as compared to other clinically used antimitotic agents such as vinca alkaloids and taxanes.[12,13]

Despite the notable example of successful structural simplification of diazonamide A **1a** by truncation of the right-hand polyaromatic macrocycle, the presence of difficult-to-synthesize tetracyclic hemiaminal subunit[14] with a chiral quaternary stereogenic center confers considerable molecular complexity to the simplified diazonamide A analogue **2**. We hypothesized that the replacement of the tetracycle by a chiral quaternary center-containing indolin-2-one core, while retaining both bioxazole subunit and peptide macrocycle, would allow easier synthesis of less complex analogues with improved drug-like properties. The respective design is exemplified by macrocycle series **3** and **4** (Scheme 1) that were used to explore SAR and eventually allowed for the development of potent analogues of cytotoxic natural diazonamide **1a** as shown below.

RESULTS AND DISCUSSION

Chemistry. The synthesis of macrocycle series **3** and **4** capitalized on an approach developed by Sammakia and coworkers in their formal total synthesis of diazonamide A, where diastereoselective intramolecular S_NAr-type arylation approach was employed to assemble the 12-membered macrocycle with quaternary center of *S* absolute configuration (Scheme 1).[8b] We realized that the base-mediated diastereoselective macrocyclization with concomitant quaternary center formation would be the most efficient strategy toward **3** and **4** provided that bromo-bioxazole subunit in **5** and **6** is sufficiently reactive under S_NAr conditions. We also hypothesized that the desired *S* configuration at the quaternary center could be secured by the stereogenic centers in the peptide backbone. The cyclization precursors **5** and **6** can be readily assembled from 3-substituted indolin-2-ones **7**, **8**, and bromo-bioxazole **9**[15] (Scheme 1).

The synthesis of the macrocyclization precursors **5a−h** commenced by Negishi cross-coupling[16] of known 3-alkyl- or 3-aryl-substituted 5-iodoindolin-2-ones **10a−h** with freshly prepared alkylzinc iodide **11** to afford amino acid esters **7a−h** in good to excellent yields (Scheme 2). Saponification of the ester was followed by EDC-mediated amide coupling with **9** to furnish amides **5a−h**. The synthesis of homologue series **6a,b,i** was accomplished by the decarboxylative coupling[17] between 5-iodoindolin-2-ones **10a,b,i** and *N*-hydroxyphthalimide ester **12** (prepared from *N*-Boc-L-Glu-OBzl and *N*-hydroxyphthalimide).[18] Subsequent hydrogenative cleavage of benzyl ester and amide bond formation with **9** yielded the macrocyclization precursors **6a,b,i** (Scheme 2).

With amides **5a−h** and **6a,b,i** in hand, the macrocyclization reaction was addressed. We were pleased to find that the bromo-bioxazole subunit in **5a−h** is sufficiently reactive to undergo S_NAr-type substitution of bromine by oxindole enolate (formed in situ upon the addition of Na_2CO_3 or K_3PO_4) at elevated temperatures. Under these conditions, macrocycles **3a−h** were obtained in 54−82% yield (Scheme 3A). Notably, the macrocyclization proceeded with excellent diastereoselectivities (from 93:7 dr to 99:1 dr; determined by

Scheme 1. Retrosynthesis of Macrocycles 3 and 4

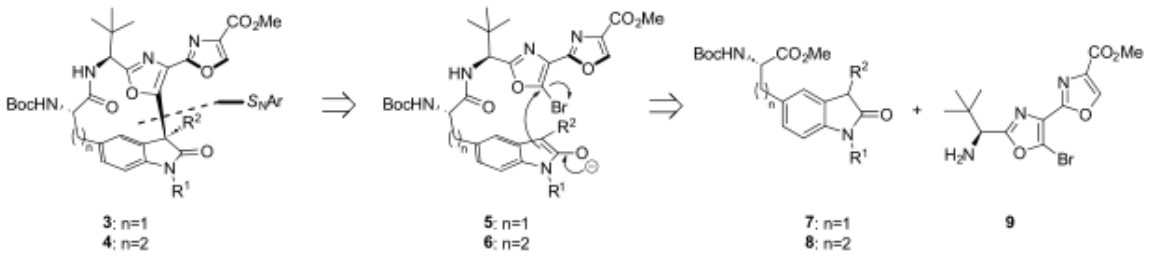

https://doi.org/10.1021/acs.jmedchem.4c00388
J. Med. Chem. 2024, 67, 9227−9259

Scheme 2. Synthesis of Macrocyclization Precursors 5a−h and 6a,b,i

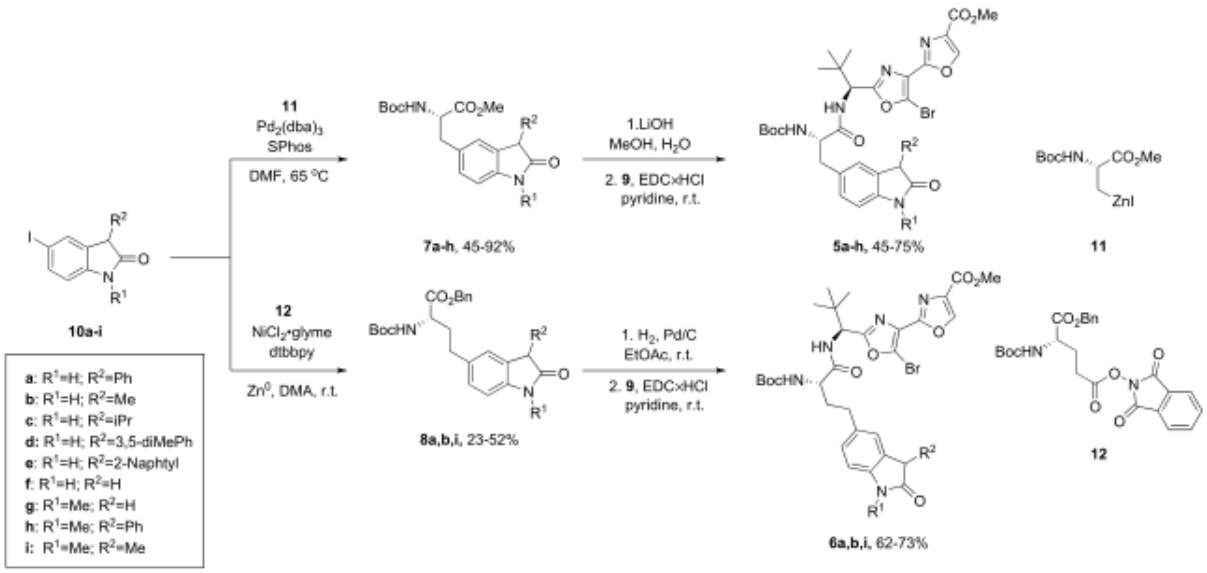

HPLC-UV/MS assay for the crude reaction mixture) for all substrates **5a−h**, and the corresponding 12-membered macrocycles **3a−h** were obtained as single diastereomers after purification by flash column chromatography (Scheme 3A). The desired *S* configuration at the quaternary stereogenic center was confirmed for the downstream macrocycle **14d** by single crystal X-ray analysis.[19] Hence, *S* configuration was assigned by analogy for all macrocycles **3a−h** in a series (Scheme 3A).

Disappointingly, the macrocyclization of homologue series **6a,b,i** proceeded with markedly reduced diastereoselectivities (62:38 dr for **4a**, 79:21 dr for **4b** and 85:15 dr for **4i**) and lower yields (32−59%, see Scheme 3B). Diastereomers of 13-membered macrocycles **4a,b,i** were not separated at this stage, and individual diastereomers were obtained for the downstream products **15a,b,i** after column chromatography. The assignment of relative configuration at the quaternary stereogenic center in macrocycles **15a,b,i** turned out to be a nontrivial task. NMR methods were not helpful due to the lack of useful H−H or C−H interactions near the stereogenic center in question. All attempts to grow single crystals for X-ray crystallography were also unsuccessful. Finally, the relative configuration at the stereogenic quaternary center in both diastereomers of **15i** was established by comparing experimental electronic circular dichroism (ECD) spectra with those calculated by DFT methods (see Supporting Information, page S19). The major diastereomer of **15i** was formed with *S* absolute configuration. By analogy, *S* configuration was assigned to all major diastereomers of 13-membered macrocycles **15a,b,i**.

Macrocycles **3a−h** and **4a,b,i** were converted into target structures **14a−h** and **15a,b,i**, respectively, in a two-step sequence comprising *N*-Boc cleavage and amide bond formation with (*S*)-hydroxyisovaleric acid (**13**). The methyl ester moiety in the bioxazole subunit of **14** was well-suited for further synthetic transformations, aimed at the increase of structural diversity for SAR studies. Accordingly, the saponification of the ester in **14a** afforded carboxylic acid **16** that was further converted into amide **17**. In the meantime, direct aminolysis of ester **14a** afforded amides **18**,**19**. Bioxazole esters **20** and **21** were also obtained from **14b** by titanium isopropoxide-mediated transesterification (Scheme 3A). Aminolysis/amide dehydratation sequence allowed for the synthesis of cyanobioxazole **22** from ester **3a**. Subsequent TFA-mediated *N*-Boc cleavage and amide bond formation with (*S*)-hydroxyisovaleric acid (**13**) yielded cyanobioxazole **23** (Scheme 3C). Benzyl ester **24** was synthesized by Ti(O*i*Pr)$_4$-mediated transeterification, followed by *N*-Boc deprotection and amide coupling with (*S*)-hydroxyisovaleric acid. Finally, hydroxymethyl bioxazole **25** was obtained in a three-step sequence involving the reduction of methyl ester, *N*-Boc cleavage, and amide coupling.

The excellent macrocyclization diastereoselectivities observed for 12-membered series **3a−h** suggest a large energy difference between the two diastereomeric transition states for the S$_N$Ar-type cyclization. Indeed, DFT calculations using b3lyp/6-311++g(2d,p)//b3lyp/6-31+g(d) basis set demonstrated that energy of the TS leading to (*S*)-**3a** is 5 kcal/mol lower than that for the formation of diastereomeric (*R*)-**3a** (see Figure S5, page S23). Importantly, the formation of *S* isomers was also favored by 1 kcal/mol in homologue series **4a,b,i**. Of note, the calculated energy differences for diastereomeric TS of the S$_N$Ar-type cyclization matched perfectly the observed ratios of diastereomers for both macrocycles **3a−h** and **4a,b,i**. Hence, DFT calculation provided additional support for the *S* configuration at the quaternary center for both **3a−h** and **4a,b,i** series.

The highly diastereoselective intramolecular S$_N$Ar-type arylation of oxindoles **5a−h** prompted us to examine the C-alkylation of macrocycle (*S*)-**3g** as a convenient approach to the late-stage formation of quaternary stereogenic center. Gratifyingly, the alkylation of **3g** sodium enolate with a series of alkylating agents proceeded with high diastereoselectivity (from 86:14 dr to 92:8 dr; see Scheme 4). The observed diastereoselectivity matched the calculated energy difference of 1 kcal/mol between diastereomeric TS for the alkylation, with *S* isomer being the favored. The formation of the *S* isomer was later confirmed by the counter-synthesis of **14i** from (*S*)-**3b**

https://doi.org/10.1021/acs.jmedchem.4c00388
J. Med. Chem. 2024, 67, 9227−9259

Scheme 3. Synthesis of Tubulin Binding Agents using Macrocyclization as the Key Step[a,b]

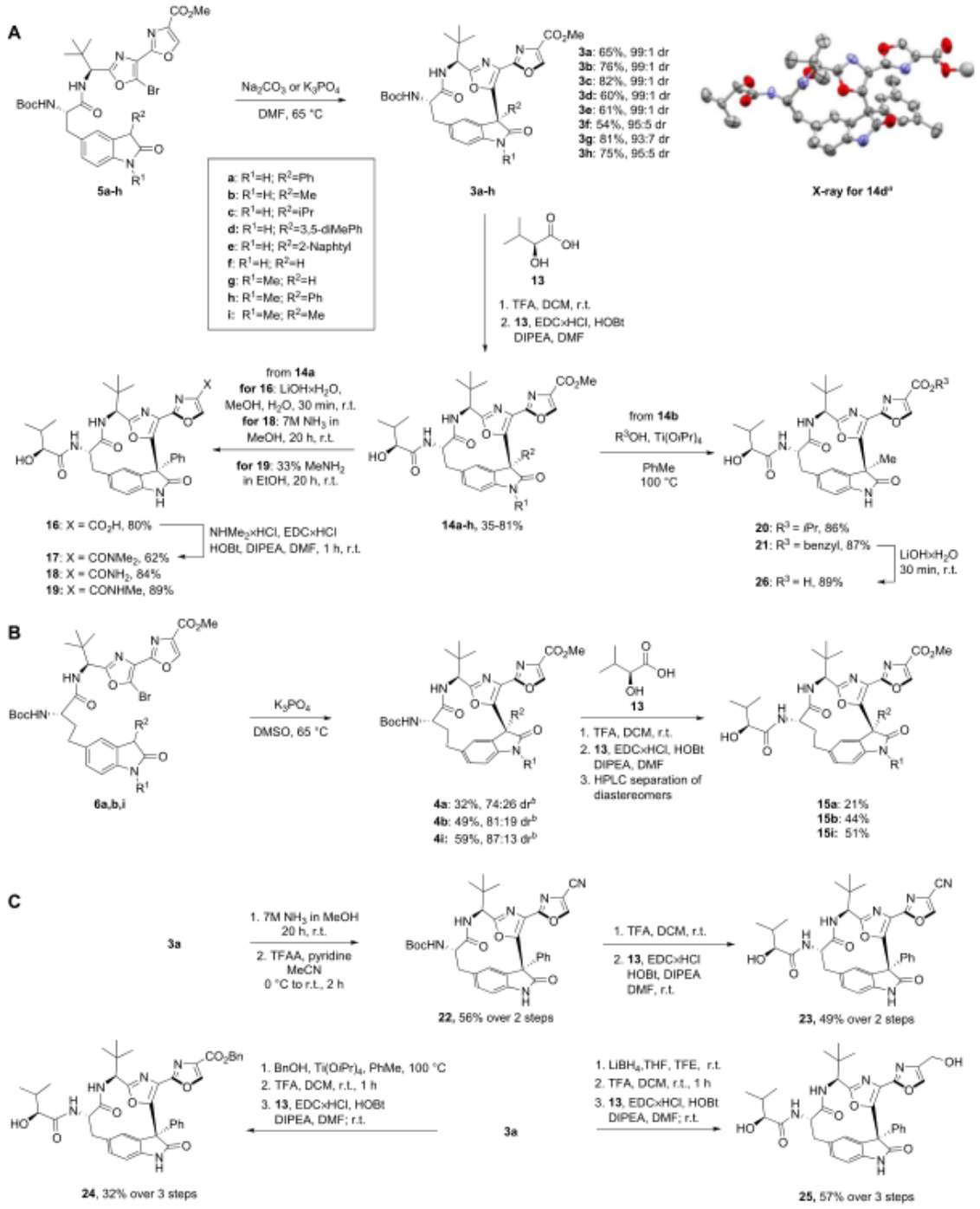

[a]Ellipsoids are shown at 50 probability, with hydrogen atoms omitted for clarity. [b]Diastereomeric purity of isolated product.

involving N-methylation, *N*-Boc deprotection, and amide bond formation with **13**. Identical NMR spectra for **14i** prepared by the C-alkylation route (from (*S*)-**3g**) and by the macrocyclization of **5b** provided compelling evidence for the formation of *S* isomers in the diastereoselective alkylation of **3g** sodium enolate.

Finally, macrocycle **27** with differently disconnected tetracycle was also synthesized for SAR studies using Sammakia's approach (Scheme 5).[8b] Accordingly, magnesium phenoxide

https://doi.org/10.1021/acs.jmedchem.4c00388
J. Med. Chem. 2024, 67, 9227−9259

Scheme 4. Alkylation of 3g Sodium Enolate[a]

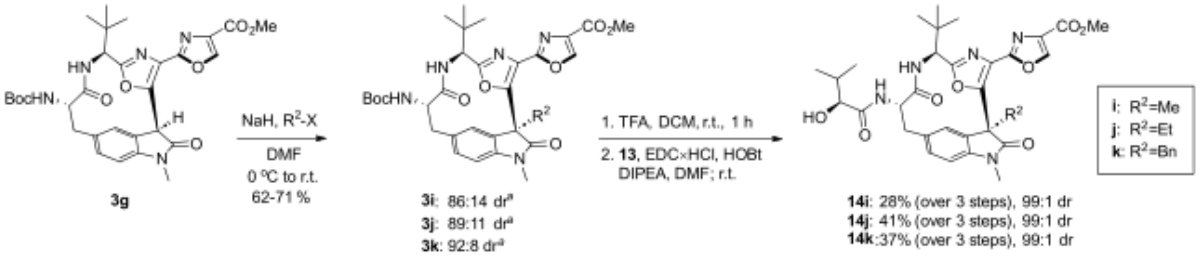

[a]Diastereoselectivity of the alkylation.

Scheme 5. Synthesis of Macrocycle 27

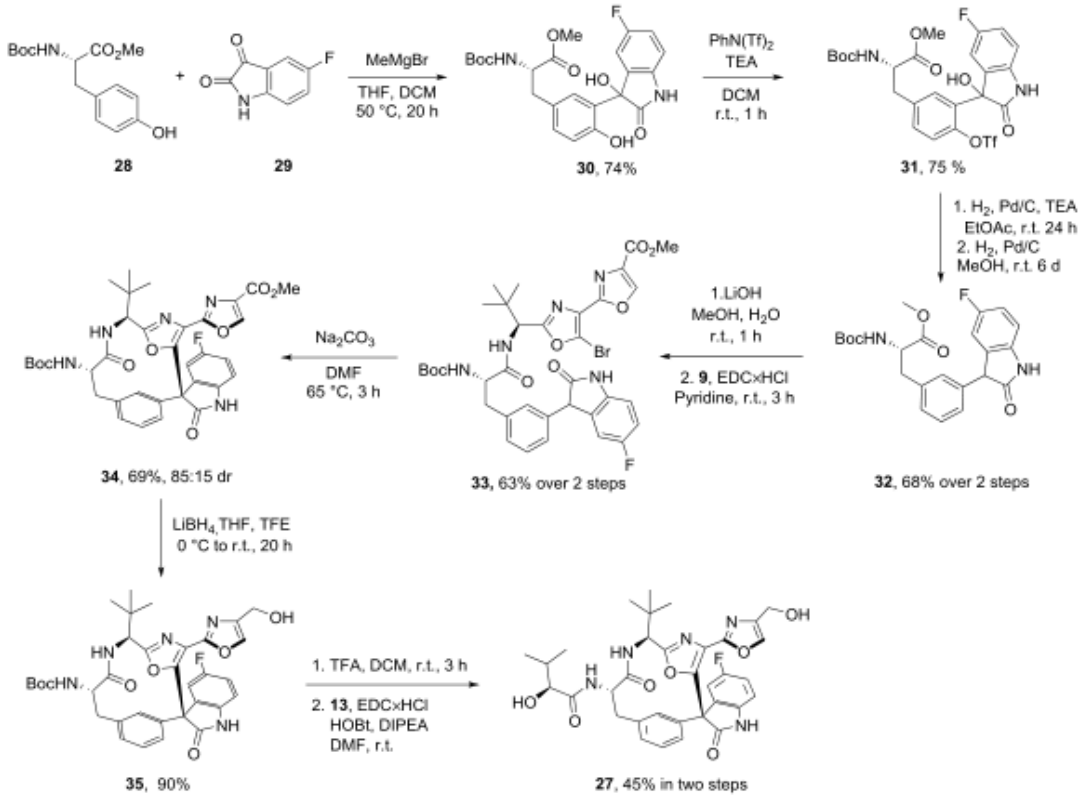

(prepared from **28** and MeMgBr) was added to unprotected isatin **29** to furnish adduct **30** in 74% yield (1:1 dr). Subsequent conversion of phenol **30** into triflate **31** by *N*-phenyl-bis(trifluoromethanesulfonimide (75% yield) was followed by Pd-catalyzed reductive cleavage of triflate (H_2, Pd/C, TEA, EtOAc) and hydrogenolysis of the resulting tertiary alcohol (H_2, Pd/C, MeOH) to deliver ester **32** (68%, 1:1 dr). Saponification with LiOH and coupling with bromo-bioxazole **9** provided macrocyclization precursor **33** (63% over two steps). Gratifyingly, the macrocyclization under Sammakia's conditions (Na_2CO_3 as a base in DMF) afforded the desired 12-membered macrocycle **34** as an 85:15 mixture of diastereomers (69% yield). Major diastereomer was obtained after chromatography, and absolute configuration at the quaternary stereogenic center was assigned *R* by analogy to Sammakia's work. The synthesis end-game involved the reduction of ester moiety in **34** to alcohol **35**, *N*-Boc cleavage and amide bond formation with (*S*)-hydroxyisovaleric acid (**13**).

Biological Evaluation. *In Vitro Antiproliferative Activities.* All synthesized 12-membered macrocycles **14a−k**, **16−26**, and 13-membered homologues **15a,b,i** as well as *epi*-**15i** and macrocycle **27** were evaluated for their *in vitro* antiproliferative activity against four cancer cell lines (epithelial pancreatic carcinoma PANC-1, pancreatic carcinoma MiaPa-Ca-2, estrogen-positive breast adenocarcinoma MCF-7, and estrogen-negative breast adenocarcinoma MDA-MB-231) by the MTT assay with vinorelbine as the positive control (see Table 1). Noticeably, the antiproliferative activity of the tested compounds was influenced substantially by steric properties of substituent at the chiral quaternary stereogenic center. Thus, GI_{50} values in the low micromolar to high nanomolar range

https://doi.org/10.1021/acs.jmedchem.4c00388
J. Med. Chem. 2024, 67, 9227−9259

Table 1. *In Vitro* **Antiproliferative Activity Data**

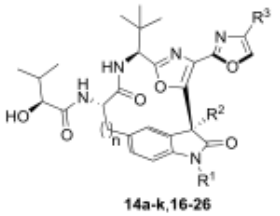

14a-k,16-26

						GI_{50}, μM			
entry	compound	*n*	R^1	R^2	R^3	PANC-1	MiaPaCa-2	MCF-7	MDA-MB-231
1	vinorelbine	-	-	-	-	0.0030 ± 0.0004	0.0008 ± 0.0001	0.0039 ± 0.0004	0.0045 ± 0.0004
2	**14a**	1	H	Ph	CO_2Me	12 ± 2	0.67 ± 0.05	1.2 ± 0.3	8 ± 2
3	**14b**	1	H	Me	CO_2Me	11 ± 2	0.68 ± 0.09	0.53 ± 0.09	1.4 ± 0.3
4	**14c**	1	H	iPr	CO_2Me	>100	39 ± 3	>100	98 ± 11
5	**14d**	1	H	3,5-diMePh	CO_2Me	>100	>100	>100	>100
6	**14e**	1	H	2-Naphth	CO_2Me	36 ± 2	29 ± 5	67 ± 4	28 ± 3
7	**14f**	1	H	H	CO_2Me	>100	>100	89 ± 7	>100
8	**14g**	1	Me	H	CO_2Me	>100	54 ± 2	63 ± 7	>100
9	**14h**	1	Me	Ph	CO_2Me	1.2 ± 0.2	0.42 ± 0.07	0.39 ± 0.08	0.36 ± 0.02
10	**14i**	1	Me	Me	CO_2Me	4.5 ± 1.4	0.55 ± 0.02	0.75 ± 0.07	2.50 ± 0.14
11	**14j**	1	Me	Et	CO_2Me	13 ± 1	3.50 ± 0.62	2.86 ± 0.31	19 ± 4
12	**14k**	1	Me	Bn	CO_2Me	>100	95 ± 5	82 ± 1	54 ± 9
13	**15a**	2	H	Ph	CO_2Me	1.2 ± 0.3	0.46 ± 0.04	7.7 ± 0.3	0.26 ± 0.03
14	**15b**	2	H	Me	CO_2Me	>100	17 ± 2	12 ± 3	21 ± 3
15	**15i**	2	Me	Me	CO_2Me	>100	>100	15 ± 2	4.8 ± 1.3
16	*epi*-**15i**	2	Me	Me	CO_2Me	>100	>100	79 ± 6	75 ± 8
17	**16**	1	H	Ph	CO_2H	>100	38 ± 3	49 ± 1	93 ± 11
18	**17**	1	H	Ph	$CONMe_2$	>100	56 ± 3	74 ± 13	99 ± 1
19	**18**	1	H	Ph	$CONH_2$	>100	>100	98 ± 2	99 ± 1
20	**19**	1	H	Ph	CONHMe	>100	89 ± 13	44 ± 8	88 ± 5
21	**20**	1	H	Me	CO_2i-Pr	2.6 ± 0.1	0.18 ± 0.04	0.24 ± 0.01	21.8 ± 2.3
22	**21**	1	H	Me	CO_2Bn	6.5 ± 1.8	0.081 ± 0.006	0.044 ± 0.015	0.73 ± 0.17
23	**23**	1	H	Ph	CN	23 ± 3	1.9 ± 0.4	2.2 ± 0.1	6.1 ± 0.3
24	**24**	1	H	Ph	CO_2Bn	1.2 ± 0.1	0.15 ± 0.01	0.26 ± 0.1	2.1 ± 0.5
25	**25**	1	H	Ph	CH_2OH	68 ± 6	20 ± 5	16 ± 4	95 ± 11
26	**26**	1	H	Me	CO_2H	-	-	-	67.1 ± 1.1
27	**27**	-	-	-	-	>100	45 ± 9	96 ± 6	>100

were observed for phenyl and methyl group-containing macrocycles **14a** and **14b** (R^2 = Ph and Me; Table 1, entries 2 and 3, respectively). Analogues with sterically more demanding *i*-Pr group (entry 4) and aryl moieties (entries 5 and 6) featured several orders of magnitude weaker potency. On the other hand, tertiary stereogenic center-containing macrocycle **14f** (R^2 = H, entry 7) also was virtually inactive. A similar SAR profile was also observed in *N*-Me indolinone series **14g−k** (entries 8−12, Table 1), where phenyl and methyl-substituted analogues **14h** and **14i** showed superior antiproliferative activities (entries 9 and 10). Notably, an order of magnitude drop in potency was observed when going from methyl- (entry 10) to ethyl-substituted macrocycles (entry 11), and further increase of steric demand (R^2 = Bn, entry 12) led to the reduction of antiproliferative activity by another order of magnitude. Consistent with the SAR in *N*-Me indolinone series (entry 7), macrocycle **14g** (R^2 = H, entry 8) was virtually inactive, pointing to the importance of quaternary stereogenic center for antiproliferative activity.

Next, SAR around the bioxazole substituent R^3 was explored using macrocycle series **14a**, **16−19**, and **23−25** with phenyl substituent at the quaternary stereogenic center (entries 2, 17−20, and 23−25, Table 1). The presence of ester functional group in the bioxazole subunit turned out to be critical for the antiproliferative effect with benzyl ester **24** being more potent than methyl ester **14a** (entries 2 and 24). Carboxylic acid **16** (entry 17), the corresponding amides **17−19** (entries 18−20), as well as hydroxymethyl-substituted macrocycle **25** (entry 25) exerted 2 orders of magnitude weaker antiproliferative effect with GI_{50} values spanning the low to high micromolar range. Likewise, nitrile **23** also showed inferior efficacy (entry 23, Table 1). The superiority of ester substituent at the bioxazole subunit was also observed in macrocycle series **14b**, **20**, **21**, and **26**, having methyl substituent at the quaternary stereogenic center (entries 3, 21, 22, and 26). Thus, benzyl ester **21** (entry 22) possessed the highest antiproliferative activity among all macrocycles tested against MCF-7 and MiaPaCa cancer cell lines. Isopropyl ester **20** (entry 21) featured reduced activity that was comparable to that of methyl ester **14b** (entry 3), whereas carboxylic acid **26** (entry 26) showed virtually no antiproliferative activity against MDA-MB-231 cancer cell line.

Ring enlargement to 13-membered homologue **15a** (R^2 = Ph, entry 13) helped to increase activity against MDA-MB-231

https://doi.org/10.1021/acs.jmedchem.4c00388
J. Med. Chem. 2024, 67, 9227−9259

Table 2. *In Vitro* Antiproliferative Activities of Selected Series against Cancer Cell Lines and Non-cancerous Cells

entry	compound	GI_{50}, μM				
		U937	A2058	HCC-44	Hek293	GM08402
1	vinorelbine	0.0041 ± 0.0005	0.0024 ± 0.0002	0.0053 ± 0.0003	0.05 ± 0.01	>100
2	**14b**	0.084 ± 0.007	0.35 ± 0.01	2.38 ± 0.07	44 ± 8	53 ± 9
3	**14h**	0.043 ± 0.001	0.31 ± 0.03	1.25 ± 0.12	1.2 ± 0.3	>100
4	**14i**	0.098 ± 0.01	0.48 ± 0.01	1.52 ± 0.01	0.19 ± 0.01	>100
5	**15a**	0.0087 ± 0.001	0.049 ± 0.001	0.26 ± 0.02	10 ± 1	17 ± 3
6	**20**	0.031 ± 0.004	0.049 ± 0.005	0.22 ± 0.02	3.05 ± 0.02	>100
7	**21**	0.011 ± 0.001	0.0095 ± 0.0004	0.035 ± 0.002	1.67 ± 0.19	33 ± 3
8	**24**	0.014 ± 0.0004	0.080 ± 0.005	0.18 ± 0.01	n.d.	n.d.
9	**26**	12.3 ± 1.2	26.2 ± 1.3	n.d.	43.4 ± 1.2	n.d.

and PANC-1, while keeping comparable efficacy against MCF-7 and MiaPaCa cancer cell lines as compared to the 12-membered congener **14a** (entry 2). In contrast, considerable drop in the antiproliferative activity against all cell lines was observed when going from 12- to 13-membered macrocycles, possessing methyl group at the quaternary center (**15b** vs **14b**, entry 14 vs entry 3). Hence, the phenyl at quaternary center is superior substituent to the methyl group in the 13-membered macrocycle series.

Finally, antiproliferative activity of macrocycle **27** with differently disconnected tetracyclic subunit was compared to that of structurally related indoline congener **25** (Table 1, entries 25 and 27). Marcocycle **27** turned out to be less potent than **25** against all four cancer cell lines with the largest difference in antiproliferative activity measured for MCF-7 cancer cell line.

The influence of substituent at indolinone nitrogen (R^1 = H or Me) was pronounced only for macrocycles possessing Ph group at quaternary center, where *N*−Me analogue **14h** showed superior antiproliferative activity to that of its *N*−H counterpart **14a** (entries 9 vs entry 2). In contrast, similar levels of potency for *N*−Me/*N*−H pairs were observed in 12-membered macrocycle series (**14b** and **14i**; entries 3 and 10) as well as 13-membered homologues **15b** and **15i** (entries 14 and 15). Finally, the considerably higher antiproliferative effect exerted on MDA-MB-231 cell line by **15i** as opposed to its epimer *epi*-**15i** (entry 15 vs 16, respectively) highlighted the importance of configuration at the quaternary stereogenic center for the activity of macrocycles. Overall, the SAR study has helped to identify benzyl ester as the substituent of choice at bioxazole subunit. However, comparable activity of macrocycle series with Ph and Me substituents at quaternary center as well as those at indolinone nitrogen prompted us to continue SAR studies using additional cancer cell lines.

The antiproliferative efficacy of the best-performing macrocycles **14b**,**h**,**i**, **15a**, **20**, **21**, **24**, and carboxylic acid **26** as the assay negative control (Table 1) was further evaluated in a series of additional cancer cell lines (histiocytic lymphoma U-937, melanoma A-2058, and lung adenocarcinoma HCC-44) by the MTT assay with vinorelbine as the positive control (see Table 2). Gratifyingly, benzyl ester **21** possessing Me group at the quaternary center demonstrated the highest antiproliferative activity with GI_{50} values in the low nanomolar range for all three cell lines (entry 7). Strikingly, phenyl-substituted benzyl ester **24** turned out to be an order of magnitude less potent against A2058 and HCC-44 cancer cell lines, albeit it was equipotent against U937 cell line (entry 8). As anticipated, isopropyl ester **20** (entry 6) as well as 13-membered macrocycle **15a** (entry 5) were slightly inferior to **21**. Methyl esters **14b**,**h**,**i** (entries 2−4, Table 2) also showed a reduced antiproliferative effect. Consistent with the established SAR, carboxylic acid **26** exerted up to 3 orders of magnitude lower antiproliferative activity than the most efficient macrocyclic benzyl ester **21** (entry 9 vs 7).

The selectivity of toxicity for macrocycles **14b**,**h**,**i**, **15a**, **20**, and **21** was also evaluated using noncancerous cell lines such as human embryonic kidney cells (HEK-293) and human dermal fibroblast (GM08402; see Table 2). Surprisingly, *N*-methyl indolinone derivatives **14h**,**i** showed poor selectivity with antiproliferative activity levels in HEK-293 cells comparable to those in cancer cell lines (PANC-1 and HCC-34; see entries 3 and 4, Table 2). In contrast, *N*−H indolinones **14b**, **15a**, **20**, and **21** featured 1 to 3 orders of magnitude lower activity against noncancerous cells as compared to cancer cell lines. Similarly, high selectivity of toxicity was also observed for all macrocycles when human dermal fibroblast cells GM08402 were used.

Further, 12-membered macrocycles **14b** and **21** as well as 13-membered homologue **15a** were submitted to dose−response screening assay against 60 human tumor cell line panel NCI-60 (US National Cancer Institute) at five concentrations (ranging from 0.01 to 100 μM).[20] Macrocycles **15a** and **21** displayed submicromolar average GI_{50} values whereas **14b** exhibited mean inhibitory activity at the micromolar range (Table 3, entries 1−3). Gratifyingly, despite considerable structural simplification, macrocycle **21** appears to be only ca. 10-fold less active than the natural diazonamide

Table 3. NCI-60 Dose−Response Data

entry	compound	NSC number	mean GI_{50}, μM	mean TGI, μM	mean LC_{50}, μM
1	**14b**	NSC #830922	4.1	>100[a]	>100[a]
2	**15a**	NSC #830921	0.38	>100[a]	>100[a]
3	**21**	NSC #831032	0.19	>11[b]	>100[a]
4	vinorelbine[c]	NSC #608210	0.018	4.2	52
5	paclitaxel[c]	NSC #125973	0.025	3.9	75
6	diazonamide **1a**[d]	NSC #700089	0.011	>10[e]	>10[e]

[a]TGI and LC_{50} values exceeded the upper concentration limit (100 μM) for more than half of NCI-60 cell lines. [b]TGI values for 11 out of 59 cell lines exceeded the upper concentration limit of 100 μM. [c]Data from ref26. [d]Data from ref25. [e]TGI values exceeded the upper concentration limit (10 μM) for more than half and LC_{50} for 90% of cell lines in NCI-60 panel.

https://doi.org/10.1021/acs.jmedchem.4c00388
J. Med. Chem. 2024, 67, 9227−9259

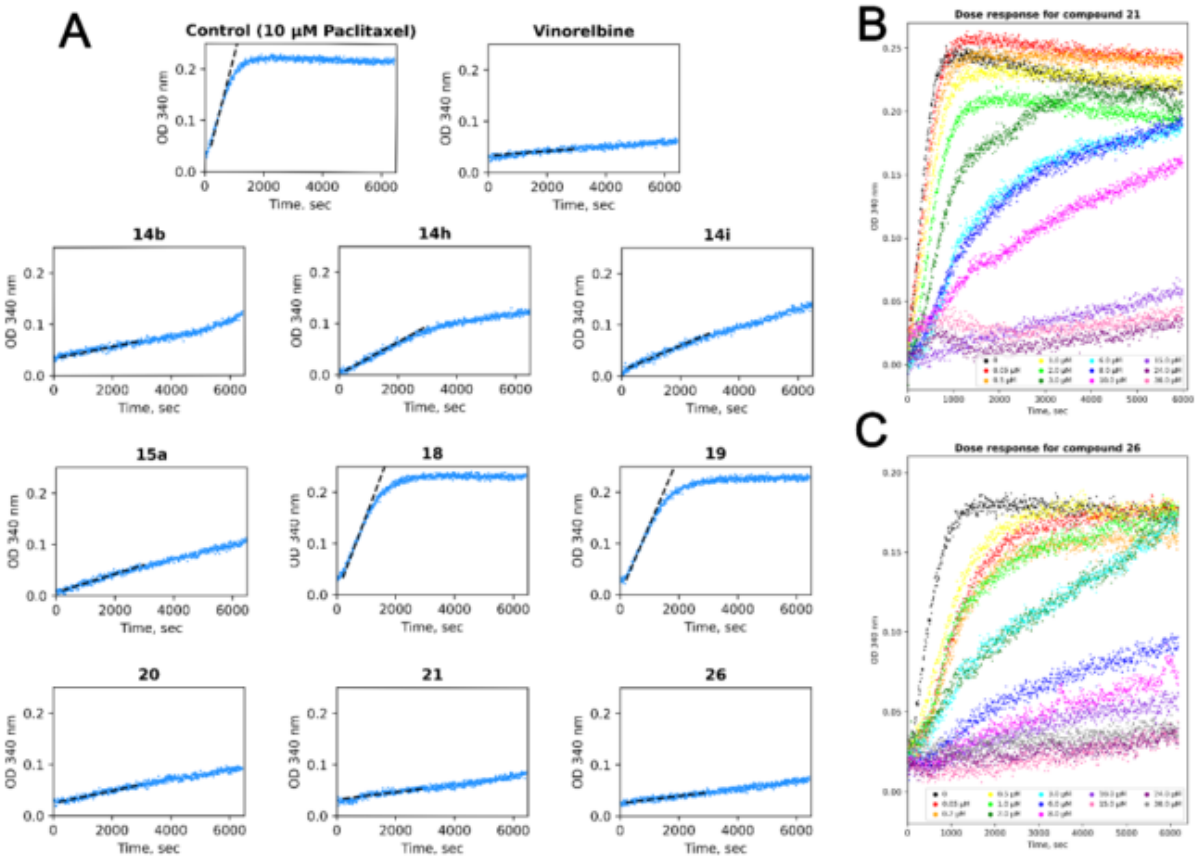

Figure 2. Enhancer control tubulin self-polymerization assay results for macrocycles **14b**,**h**,**i**, **15a**, **18**−**20**, **21**, **26**, and vinorelbine (A); dose-dependent inhibition of tubulin polymerization by benzyl ester **21** (B); dose-dependent inhibition of tubulin polymerization by acid **26** (C).

1a as well as marketed MTA vinorelbine and paclitaxel as evidenced by their mean GI_{50} values in NCI-60 panel (entry 3 vs entries 4−6). Moreover, antiproliferative activity within the same order of magnitude was observed for macrocycle **21** and diazonamide **1a** against 19 out of 60 cell lines in the NCI panel (see Table S1, page S15 for complete NCI data). For example, comparable GI_{50} values have been observed for **21** and **1a** in multiple myeloma cell line RPMI-8226 (31.6 nM vs 10.5 nM, respectively), large cell immunoblastic lymphoma SR (<10.0 nM vs 1.9 nM, respectively), human colon adenocarcinoma COLO 205 (50.1 nM vs 17.4 nM, respectively), human brain (astrocytoma) cell line SNB-75 (26.9 nM vs 40.7 nM, respectively), melanoma cancer cell lines MDA-MB-435 (<10.0 nM vs 2.9 nM, respectively), SK-MEL-2 (25.7 nM vs 11.2 nM, respectively), and UACC-62 (28.2 nM vs 19.1 nM, respectively), as well as ovarian cancer cell line OVCAR-8 (49.0 nM vs 14.5 nM, respectively) and renal carcinoma cell lines RXF-393 (21.4 nM vs 5.50 nM, respectively) and SN12C (38.0 nM vs 10.7 nM, respectively). Overall, the results of dose−response screening assay against NCI-60 panel cell lines (Table 3) are in line with our data (Tables 1 and 2) and point to the high antiproliferative potency of macrocycle **21**.

A difference between toxic concentrations of **21** (mean LC_{50} > 100 μM) and the concentration required for total growth inhibition (mean TGI > 11 μM) suggests that macrocycle **21** possibly possesses cytostatic rather than cytotoxic properties (entry 3, Table 3).[21−23] Similar differences between LC_{50} and TGI concentrations have been determined for marketed tubulin-targeting agents vinorelbine and paclitaxel (entries 4 and 5, Table 3) that are inherently cytostatic because interference with microtubule dynamics leads to proliferation arrest.[24] Hence, NCI-60 data suggest that macrocycle **21** might act in a similar manner. In addition, macrocycle **21** demonstrated a differential cytotoxicity pattern, which was highly similar to that of paclitaxel and vinblastine (correlation coefficients 0.79 and 0.77, respectively as indicated by COMPARE algorithm).[20,25] Overall, the cytotoxicity pattern for macrocycle **21** and marketed MTA paclitaxel and vinblastine suggests that the measured antiproliferative activity of macrocyclic series is associated with their effect on microtubule dynamics.

Tubulin Polymerization Assay. An *in vitro* tubulin polymerization assay was performed to evaluate the effect of macrocycles on microtubule dynamics and stability. In the assay, paclitaxel-induced self-polymerization of soluble α/β-tubulin heterodimer to microtubules under buffered conditions was monitored in the presence or absence of the desired ligands by measuring changes in light scattering at 340 nm.[27,28] A slope was calculated for the linear growth phase of the tubulin polymerization curves to render a comparison vs the positive assembly control containing 10 μM paclitaxel (see Figure 2).[29] Paclitaxel-induced tubulin self-polymerization was

https://doi.org/10.1021/acs.jmedchem.4c00388
J. Med. Chem. 2024, 67, 9227−9259

measured in the presence of the most cytotoxic macrocyclic esters **14b,h,i**, **15a**, **20**, **21**. In addition, poorly cytotoxic macrocycles such as amides **18,19** as well as carboxylic acid **26** were also examined to verify the correlation between antiproliferative activity of the macrocycles and effect they exert on tubulin polymerization dynamics. Finally, vinorelbine was also tested as a positive control of assembly inhibition (see Figure 2).

A good correlation between the inhibition of tubulin polymerization and *in vitro* antiproliferative activity was observed for macrocycles **14b,h,i**, **15a**, **18**−**21** (Table 4).

Table 4. Results of the Tubulin Polymerization Assay

entry	ligand[a]	slope[b]	R^2 fit	time span of R^2 fit, s
1	control	1.000	0.99	290−740
2	vinorelbine	0.023	0.83	110−6420
3	**14b**	0.060	0.95	110−5500
4	**14h**	0.155	0.97	516−3000
5	**14i**	0.120	0.99	316−6420
6	**15a**	0.090	0.98	316−6420
7	**18**	0.750	0.97	470−920
8	**19**	0.700	0.98	470−1835
9	**20**	0.060	0.97	110−6420
10	**21**	0.036	0.94	110−6420
11	**26**	0.035	0.94	110−6420

[a]At 15 μM concentration of ligand (2:1 tubulin:ligand ratio). [b]Slope values are relative to that of control (entry 1).

Thus, the most cytotoxic macrocycle **21** turned out to be the most potent inhibitor of tubulin polymerization across the series (entry 10, Table 4). Structurally related 12-membered macrocyclic esters **14b**, **20**, and 13-membered analogue **15a** also inhibited polymerization, albeit they were less efficient than macrocycle **21** (entries 3, 9, and 6, respectively). A further drop in inhibitory efficiency was observed for macrocycles **14h,i** (entries 4 and 5), and this observation is consistent with their reduced antiproliferative effect (cf. Table 2). Not surprisingly, poorly cytotoxic amides **18**, **19** were measured to be the least potent inhibitors in a series (entries 7 and 8, respectively). In striking contrast, acid **26** showed an inhibitory effect similar to that of the most efficient macrocycle **21** (entry 11 vs entry 10, Table 4) despite acid **26** displaying the lowest *in vitro* antiproliferative activity among all tested macrocycles (cf. Tables 1 and 2). The high inhibitory efficiency of tubulin polymerization observed both for ester **21** and the corresponding acid **26** prompted us to perform a dose-dependent tubulin polymerization assay for both macrocycles (Figure 2B,C). From the assay data, we were able to estimate IC_{50} values for ester **21** (IC_{50} = 2.30 μM) and acid **26** (IC_{50} = 2.74 μM). The similar calculated IC_{50} values confirm that both ester **21** and acid **26** are equally potent inhibitors of tubulin polymerization. The apparent lack of correlation between *in vitro* antiproliferative activity and efficiency in the tubulin polymerization assay for acid **26** led us to hypothesize that poor cell permeability could be responsible for the lack of *in vitro* activity (*vide infra*). Finally, vinorelbine strongly inhibited the polymerization of tubulin (entry 2, Table 4). Overall, the observed inhibition of tubulin polymerization in the presence of macrocycles **14b,h,i**, **15a**, **20**, **21** provides evidence that *in vitro* cytotoxicity effects are to be attributed to binding tubulin and inhibiting the assembly of microtubule networks within cells.

Differential cytotoxicity pattern data (determined from NCI-60 panel by the COMPARE algorithm) and tubulin polymerization assay results provided evidence that the antiproliferative effect for the structurally simplified diazonamide analogue series is exerted through regulation of microtubule dynamics in cells. To determine the binding affinity for tubulin, we employed an ultracentrigation/HPLC assay as described in the Experimental Section. We found that macrocycles **14a,b,h,i** and **15a** bind to tubulin with 20−80 μM affinity, showing a loss of 2 orders of magnitude in binding power in comparison to vinblastine (K_d = 0.54 μM).[30] In order to confirm the binding site of the macrocycles in tubulin, we performed competition experiments of vinblastine with **14a,b,h,i** and **15a** by using the ultracentrifugation/HPLC assay. We found that at equimolar 10 μM concentrations, the macrocycles weakly compete with vinblastine (less than 10% displacement as expected from their 2 orders of magnitude lower binding affinity). This is in agreement with previous reports of biotinylated diazonamide analogue **2**, which binding to tubulin was blocked in a dose−response manner by vinca domain MTA vinorelbine.[12] In addition, in the structural analysis, the apparent overlapping of binding sites for **2** and vinorelbine was confirmed by X-ray crystal structure of **2** bound at vinca domain of the tubulin heterodimer.[12] We also attempted the analysis of the binding site by X-ray crystallography. Unfortunately, very poor diffraction or poorly defined electron density at the tubulin interdimer interface was observed for crystals of T_2R-TTL (two α/β-tubulin dimers in complex with the stathmin-like protein RB3 and tubulin tyrosine ligase) that were soaked for different times with the most efficient macrocycles **21** and **26**. Although the density highlights perturbation at the vinca site, it is poorly defined and does not allow modeling of the correct pose of the compounds. Further work is ongoing at our laboratory to establish the binding site of macrocycles to tubulin/microtubules.

*Effects of Macrocycle **21** on Cell Morphology.* To further investigate the antiproliferative activity of macrocycle **21** and vinorelbine, morphological changes were examined in melanoma A2058 cells. Initially, cells were stained for tubulin (yellow) and DAPI (blue) (Figure 3). When treated with **21** and vinorelbine, the cells detached and became rounded. In the treatment groups, a substantially higher number of cells were stuck in metaphase, which further resulted in apoptosis and degradation (Figures 3 and 5). Thus, **21** and vinorelbine halted cell proliferation, and the cells entering the cell division phase became apoptotic within 4−48 h after the beginning of treatment (see also Figure 4). The remaining cells attached to the plate became substantially larger while polymerized tubulin structure remained intact. Overall, the arrest of the cell cycle and induction of apoptosis were similar in **21**- and vinorelbine-treated cells. Furthermore, the effects of compounds on mitochondria were tested using MitoTracker Deep Red. Both compounds **21** and vinorelbine did not affect the number of mitochondria and their morphology despite substantially increased cell size.

*Evaluation of the Effect of Macrocycle **21** on the Cell Cycle.* To investigate the antiproliferative mechanisms of **21**, the time-dependent effect on cell cycle distribution in melanoma A2058 cells was examined (Figure 4). In the control group, relative cell count at G1, S and G2 phases remained unchanged over 24 h period. The treatment with **21** and vinorelbine caused strong cell cycle arrest in the G2/M phase. The arrest of the cell cycle induced by both compounds

https://doi.org/10.1021/acs.jmedchem.4c00388
J. Med. Chem. 2024, 67, 9227−9259

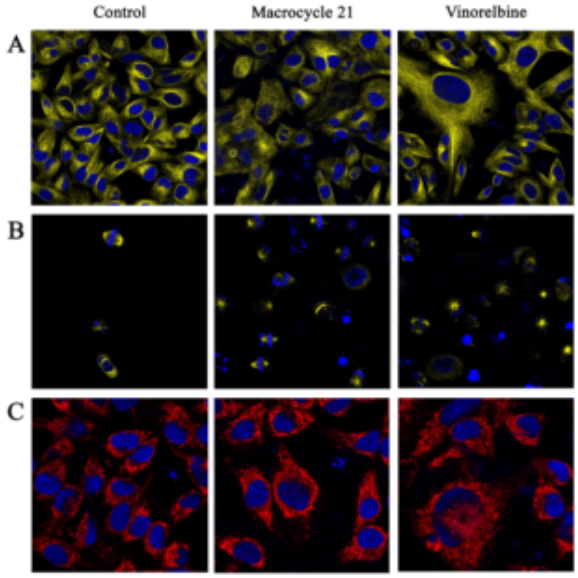

Figure 3. Melanoma A2058 cell morphology analysis after incubation with compound 21 (200 nM) and vinorelbine (10 nM). Cells were stained for tubulin (yellow) and Hoechst 33342 (blue) after 24 h incubation with and without compounds. Confocal images show attached cell (A) and floating cell (B) morphology. In the third panel (C), cells are stained with MitoTracker Deep Red to evaluate changes in the number of mitochondria and their structure.

was also time-dependent. A higher number of G2/M cells were evident already after 4 h treatment with **21** while two times more G2/M cells were counted after 24 h incubation period. Thus, after 24 h incubation in the presence of **21** and vinorelbine, approximately 40−50% of cells were arrested at the G2/M phase. Overall, macrocycle **21** (at 200 nM concentration) and vinorelbine (at 10 nM concentration) induced similar effects on the cell cycle.

Evaluation of the Compound-Induced Effects on Apoptosis. In the MTT assay, we observed a time-dependent loss of cell viability. Here, we evaluated apoptotic and necrotic cell death using PI and annexin staining and FACS counting. In the control cells without treatment, 5% necrotic and 15% apoptotic cells were counted. In the presence of **21** and vinorelbine, necrotic cell count gradually increased reaching 10% after 24 h incubation. This indicated that the antiproliferative effect of **21** was not related to the induction of necrotic cell death. Furthermore, incubation with compounds increased both early and late apoptotic cell count in a time-dependent manner. Thus, at the 24 h time point, apoptotic cells were about 40% (10% early and 30% late) of the total cell number in both treatment groups (Figure 5). These results confirm that similarly to vinorelbine, the antiproliferative effect of **21** occurs due to inhibited cell division and induction of apoptotic cell death due to arrested cell cycle.

*Evaluation of Intracellular Uptake, Metabolism, and Efflux of Ester **21** and Acid **26**.* Intracellular uptake of macrocyclic benzyl ester **21** and the corresponding acid **26** was evaluated to address the observed lack of correlation between *in vitro* antiproliferative activity and efficiency in the tubulin polymerization assay for **26** (Figure 2, Table 4). To this end, melanoma A2058 cells were incubated with ester **21** or acid **26** for up to 16 h. Already during the first 4 h of incubation with ester **21**, acid **26** reached high intracellular levels that decreased gradually over the 16 h incubation period. In sharp contrast, incubation with acid **26** at 5 times higher concentration (1000 nM) resulted in very low intracellular levels. The limited cellular uptake of acid **26** explains its poor antiproliferative effect. However, 2- to 3-fold higher intracellular concentration of the acid **26** as compared to that of the parent benzyl ester **21** at all time points suggests that metabolization of ester **21** to acid **26** occurs *inside* the melanoma A2058 cells that were incubated with ester **21** (Figure 6A). In the meantime, a gradual decrease of intracellular acid **26** concentration points to its slow metabolic degradation. Indeed, a degradation product with an exact mass of 479.18 Da was observed in A2058 cell lysate. The metabolite possibly corresponds to the cleavage of (*S*)-2-hydroxy-3-methylbutanoyl moiety in acid **26**. A small amount of the metabolite was detected already after 4 h of incubation, and the amount increased substantially after 16 h of incubation (see Supporting Information, page S17). In addition, slow efflux of ester **21** and acid **26** from A2058 cells to cell media was also observed (Figure 6B). Importantly, the increase in the concentration of acid **26** in cell media over 4 h is greater than the decrease in ester **21** concentration. This observation rules out the possibility that acid **26** concentration increases only because of ester **21** hydrolysis in cell media. Overall, the metabolism of ester **21** into acid **26** did not reduce the antiproliferative effect of **21** because both **21** and **26** exert a similar effect on tubulin polymerization.

■ CONCLUSIONS

In summary, a series of structurally simplified analogues of highly complex natural product diazonamide A were developed by the replacement of the challenging-to-synthesize tetracyclic subunit and removing the right-hand heteroaromatic macrocycle. The structurally simplified macrocycles are relatively easy to synthesize, and the most potent macrocycle **21** was obtained in 12 steps from readily available indolin-2-one and *tert*-leucine with excellent diastereoselectivity (99:1 dr) in the key macrocyclization step. Despite the considerably reduced structural complexity, macrocyle **21** possesses nanomolar antiproliferative activity against a range of tumor cell lines. In the meantime, **21** featured 1 to 3 orders of magnitude selectivity of toxicity against noncancerous cells such as HEK-293 and GM08402. Macrocycle **21** is a potent inhibitor of tubulin assembly, and it exerts similar effects to the marketed MTA vinorelbine on the cell cycle progression and induction of apoptosis in A2058 cell line. Even though in melanoma A2058 cells, macrocyclic ester **21** metabolizes into the corresponding acid **26**, the latter shows tubulin assembly inhibitory potency similar to that of the parent ester **21**. Taken together, our data provide strong evidence that the antiproliferative effect for the developed structurally simplified diazonamide A analogue series is to be attributed to binding tubulin and inhibiting the assembly of microtubule networks within cells. As such, our work demonstrates that a highly complex natural product can be structurally simplified while retaining the mechanism of action and high antitumor potency. Macrocycle **21** is a promising lead compound that deserves further development as a potential anticancer agent.

https://doi.org/10.1021/acs.jmedchem.4c00388
J. Med. Chem. 2024, 67, 9227−9259

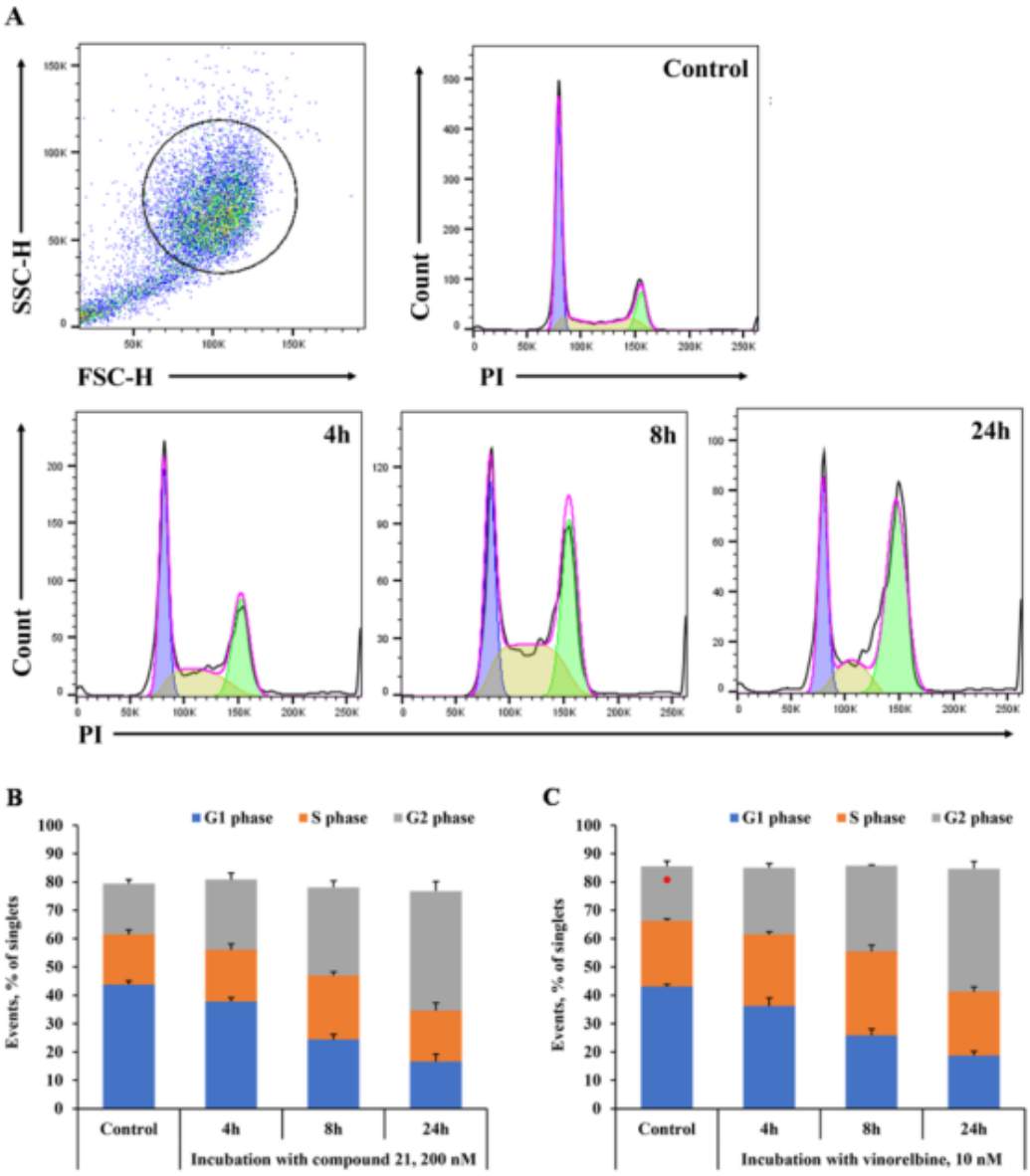

Figure 4. Flow cytometry analysis of cell cycle progression of A2058 cells after incubation with compound **21** (200 nM) for up to 24 h (A). Quantitative results of the effects of compound **21** on cell distribution among phases of the cell cycle (B) in comparison with equitoxic concentration (10 nM) of vinorelbine (C). The data are presented as the mean ± SEM of three independent experiments in triplicate.

■ EXPERIMENTAL SECTION

***In Vitro* Antiproliferative Activity.** MCF-7, PANC-1, MDA-MB-231, MIAPaCa-2, Hek293, A2058, and U937 cell lines were obtained from ATCC (Manassas, VA, USA). GM08402 was obtained from the Coriell Institute for Medical Research (Camden, NJ, USA). HCC44 was obtained from the DSMZ-German Collection, Leibniz institute (Braunschweig, Germany). MCF-7, PANC-1, MDA-MB-231, MIAPaCa-2, and A2058 cells were cultured in DMEM with 10% FBS and 1% penicillin−streptomycin. Hek293 and GM08402 cells were cultured in EMEM with 10% FBS and 1% penicillin−streptomycin. HCC44 and U937 cells were cultured in RPMI-1640 medium with 10% FBS and 1% penicillin−streptomycin. Cells were cultivated in a 37 °C temperature with 5% CO_2, 95% air, and complete humidity. Cells were seeded in a 96-well plate in following concentrations: 5000 cells per well for MCF-7, PANC1, MDA-MB-231, MiaPaCa, Hek293, GM08402; 4000 cells per well for A2058, HCC44; 10000 cells per well for U937. The compounds were added to the cells (n = 6) in a serial dilution fashion. MTT assay was performed after 48 h of incubation.[31] All compounds were tested in two independent experiments for each cell line. The GI_{50} values were calculated using Graph Pad Prism (GraphPad Software, Inc., La Jolla, CA, USA).

NCI-60 Assay. Compounds **14b**, **15a**, and **21** were submitted to NCI-60 human tumor cell line panel at US

https://doi.org/10.1021/acs.jmedchem.4c00388
J. Med. Chem. 2024, 67, 9227−9259

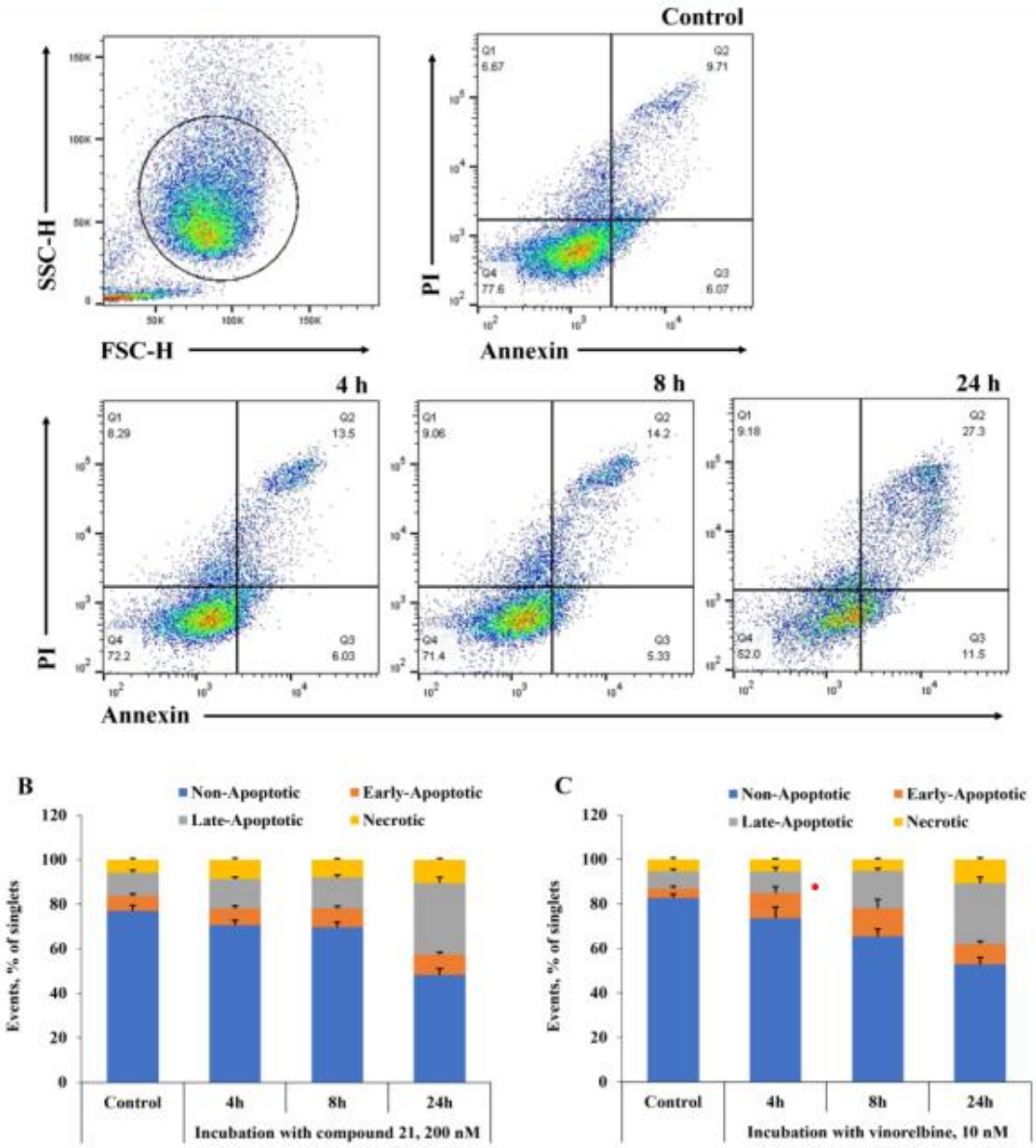

Figure 5. Representative plots from flow cytometry analysis of apoptosis after incubation with compound 21 (200 nM) for time points up to 24 h in A2058 cells (A). Effects of compound 21 on induction of apoptosis (B) in comparison with equitoxic concentration (10 nM) of vinorelbine (C). The data are presented as the mean ± SEM of three independent experiments in triplicate.

National Cancer Institute's Division of Cancer Treatment and Diagnosys (Bethesda, MD, USA). The assay was conducted at five doses (from 0.01 to 100 μM) according to the methodology described in literature.[32]

Tubulin Polymerization Assay. The assay was conducted as described in HTS-Tubulin Polymerization Assay Biochem Kit Cat. #BK004P in the presence of 10 μM Paclitaxel.[28] Commercial lyophilized tubulin (>99% pure tubulin protein, porcine brain, catalog number T240-D; Cytoskeleton, Inc.) was employed in the assay. Test compounds as well as control vinorelbine ditartrate (Sigma-Aldrich) were solubilized in DMSO at 2 mM and stored at 4 °C until used. Reagents and buffers: general tubulin buffer (80 mM PIPES pH 6.9, 2 mM $MgCl_2$, 0.5 mM EGTA), GTP (100 mM), G-PEM buffer (1 mM GTP in general tubulin buffer), cushion Buffer (60% v/v glycerol in general tubulin buffer), G-PEM Buffer plus 5% glycerol, paclitaxel (Acros Organics; was solubilized in DMSO at 2 mM and stored at 4 °C until used), tubulin protein (4 mg/mL – each vial of tubulin protein was reconstituted with 1 mL of ice cold G-PEM buffer plus 5% glycerol). Paclitaxel-induced assembly of tubulin was monitored in the presence of 10 μM of the desired ligand, prior to initiating the assay, the spectrophotometer Hidex Sense was set to 340 nm at 37 °C for performing a kinetic measurement. The plate was read kinetically for 60 min.

https://doi.org/10.1021/acs.jmedchem.4c00388
J. Med. Chem. 2024, 67, 9227−9259

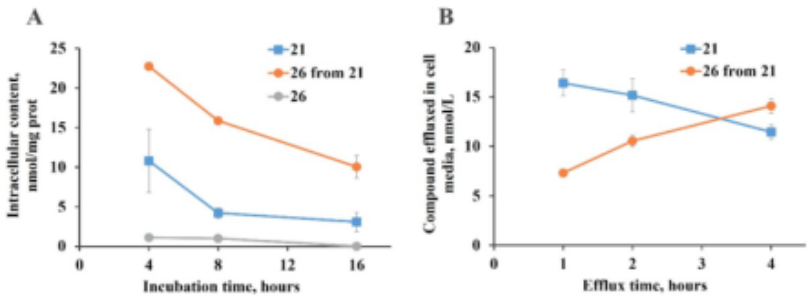

Figure 6. Intracellular uptake of **21** and **26** and the metabolism of **21** (A) as well as efflux from A2058 cells (B). Intracellular uptake of **21** and **26** was measured after incubation with compounds **21** (200 nM) and **26** (1000 nM) for 4−16 h in A2058 cells (A). In the uptake experiment for **21**, metabolism was also evaluated by measuring the concentration of **26** as the main metabolite of **21**. Efflux from A2058 cells was measured in cell media at 1−4 h time points after incubation with ester **21** for 4 h, washing, and addition of fresh cell media (without **21**). The data are presented as the mean ± SEM of three parallels.

Binding of the Compounds to Tubulin. Binding affinity and competition of the compounds for dimeric tubulin were determined using a cosedimentation assay. Briefly, a fixed concentration (10 μM) of the desired compounds was incubated with increasing amounts of dimeric tubulin (up to 100 μM) purified from calf brains as described in the literature[33] and lyophilized for storage. Tubulin was prepared in PEDTA buffer (10 mM NaPi pH 7.0, 1 mM EDTA, 1.5 mM $MgCl_2$, 0.1 mM GTP) and incubated with the compounds for 1/2 h at 25 °C. Samples were centrifuged at 100000 rpm in a TLA-100.2 rotor in an Optima-MAX-XP ultracentrifuge for 2 h at 25 °C. Then, samples were divided into upper (100 μL) and lower (100 μL) parts, and 20 μM noscapine was added to them as internal standard. Samples were subjected three times to an organic extraction using dichloromethane (v:v). Dichloromethane was removed by evaporation, and samples were resuspended in 45% 5 mM NaPi pH 6.0 − 55% acetonitrile. Finally, ligand content was analyzed using an HPLC system (Agilent 1100 Series), and samples were separated using a Zorbax Eclipse XDB C18 column (45% 5 mM NaPi pH 6.0 − 55% acetonitrile isocratic condition; 10 min runs). Competition experiments were performed at fixed concentrations of 10 μM of the desired compounds: 10 μM vinblastine (Sigma-Aldrich) and 10 μM dimeric tubulin.

Data coming out from the HPLC analysis were converted to molar saturation fraction and plotted against the concentration of free tubulin. Then, data were fitted to a one binding site model to obtain the binding constants of the compounds to tubulin.

Cell Morphology Studies. A2058 cells were seeded in ibidi 8-well μ-slides at a density of 1×10^5 cells/mL. The cells were then allowed to rest and adhere to the slides for 5 h. Subsequently, cells were treated with equitoxic concentrations (assessed in the cytotoxicity assay) of vinorelbine and **21** for 24 h. In parallel, cells were stained with SPY555-tubulin live cell probe for fluorescent imaging of microtubules. After incubation and immediately before imaging, cell nuclei were stained with Hoechst 33342 (1 μg/mL final concentration) and MitoTracker Deep Red dye (100 nM final concentration). Live cell imaging was performed with Leica Stellaris 8 confocal microscope.

Cell Cycle Studies. A2058 cells were seeded in 24-well plates at a density of 1×10^5 cells/mL. The cells were then allowed to rest and adhere to the plate for 5 h. Subsequently, cells were treated with equitoxic concentrations of vinorelbine and **21** for 4, 8, and 24 h.

To assess the distribution of cells between cell cycle phases, we performed cell cycle analysis using quantification of DNA content with the commercially available kit (Abcam, ab139418) according to the manufacturer's instructions. In brief, after incubation with the test compounds, cells were harvested using trypsin, washed with PBS, and fixed with 66% ice-cold ethanol. After fixation, cells were washed with PBS and incubated with propidium iodide (PI) (50 μg/mL) and RNase (550 U/mL) solution for 30 min in the dark at 37 °C. After incubation, the cells were transferred to ice and prepared for flow cytometry analysis using the BD FACS Melody Cell Sorter (BD Biosciences, San Jose, CA, USA). Quantitative results are expressed as the mean ± SEM. All experiments were carried out in triplicate with three technical replicates.

Compound-Induced Apoptosis. A2058 cells were seeded in 24-well plates at a density of 1×10^5 cells/mL. The cells were then allowed to rest and adhere to the plate for 5 h. Subsequently, cells were treated with equitoxic concentrations of vinorelbine and **21** for 4, 8, and 24 h.

To detect the mechanisms of A2058 cell death, we performed double staining using Annexin-V and PI.[34] After incubation with the test compounds, cells were harvested using trypsin, washed with PBS, and resuspended in 100 μL of staining buffer with Annexin V conjugated to APC (1:200) and PI (end concentration 2 μg/mL). The samples were incubated for 20 min in the dark at room temperature and then analyzed by flow cytometry. Quantitative results are expressed as the mean ± SEM. All experiments were carried out in triplicate with three technical replicates.

Intracellular Uptake, Metabolism, and Efflux. A2058 cells were seeded in 24-well plates at a density of 1×10^5 cells/mL. The cells were then allowed to rest and adhere to the plate for 5 h. The cells were then treated with **21** (200 nM) and **26** (1000 nM) in a time-dependent manner for 4−16 h. After incubation, the cells were washed with PBS buffer solution and lysed with 0.1 N NaOH solution. To assess the potential efflux of compound **21** and its metabolite **26**, A2058 cells were incubated with **21** for 4 h. After the incubation, cells were washed 2 times with PBS, and fresh media were added. Sampling of the media was performed at time points from 1 up to 4 h. Concentrations of **21** and **26** in cell lysate or cell media samples were measured by liquid chromatography-tandem mass spectrometry (LC/MS/MS) in positive electrospray

https://doi.org/10.1021/acs.jmedchem.4c00388
J. Med. Chem. 2024, 67, 9227−9259

ionization (ESI+) in multiple reaction monitoring (MRM) mode.

All analyses were performed on a Waters Acquity UPLC chromatograph coupled to Waters XEVO TQ-Smicro tandem mass spectrometer. Chromatographic separation was carried out on a Waters Acquity BEH C18 column (2.1 × 50 mm, 1.7 μm). Column temperature was 30 °C, flow rate was 0.4 mL/min. Linear gradient elution was applied, solvent A was 0.1% formic acid solution in water, and solvent B was acetonitrile. The gradient program was: 0 min −5% B; 2.5 min −95% B; 3.5 min −95% B; 3.7 min −5% B; 5 min −5% B. Injection volume was 5 μL.

Mass spectrometry parameters were obtained experimentally by direct infusion of standard solutions of compounds **21** and **26**. The quantification of each analyte was acquired with transitions of the protonated ion at m/z 670.4 → 339.1 (cone voltage 40 V, and collision energy 32 eV) for **21**, and m/z 580.2 → 435.2 (cone voltage 20 V and collision energy 30 eV) for **26**, respectively.

Compounds **21** and **26** were extracted from cell lysate or media by single-step protein precipitation. 500 μL of 3:1 acetonitrile/methanol mixture was added to 100 μL of spiked standard or analytical samples. Samples were vortex mixed for 1 min and centrifuged at 10000*g* for 10 min. Supernatants were collected, diluted 1:1 with 0.1% formic acid solution in water, and injected into the LCMS system. Data acquisition was carried out using the MassLynx 4.1 software (Waters Corp., Milford, MA, USA). Standardization of the uptake measurements was performed according to protein content in the sample, assessed by Lowry method.

■ CHEMISTRY

General. Unless otherwise noted, all chemicals were used as obtained from commercial sources, and all reactions were performed under argon atmosphere in oven-dried (120 °C) glassware. Anhydrous MeOH, pyridine, DMF, DMA, and DMSO were purchased from Acros. Anhydrous PhMe, Et_2O, THF, and DCM were obtained by passing commercially available solvent through activated alumina columns. Reactions were monitored by analytical TLC (precoated silica gel F-254 plates, Merck) or by UPLC-MS assay (Waters Acquity column: Acquity UPLC BEH-C18 (2.1 mm × 50 mm, 1.7 μm (30.0 ± 5.0) °C); gradient, 0.01% TFA in water/CH_3CN 90:10 to 0.01% TFA in water/CH_3CN 5:95; flow rate, 0.5 mL/min; run time, 8 min; detector, PDA (photodiode matrix), 220−320 nm, SQ detector with an electrospray ion source (APCI). Purification by preparative reverse phase chromatography was performed using a Waters Xbridge BEH C18 OBD column (5 μm, 10 × 150 mm) or Waters Atlantis Prep OBD T3 column (30 mm × 100 mm, 5 μm). All NMR spectra were recorded at 600, 400, or 300 MHz for ^{1}H NMR and 151, 101, or 75 MHz for ^{13}C NMR. Chemical shifts are reported in parts per million (ppm) relative to TMS or with the residual solvent peak as an internal reference. High-resolution mass spectra (HRMS) were recorded on a Waters Synapt G2-Si TOF MS instrument using the ESI technique. Specific rotation was recorded on a Kruss P3000 instrument. The purity of all target inhibitors was confirmed to be ≥95% by the reversed-phase ultrahigh-performance liquid chromatography−mass spectrometry (UPLC-MS) assay.

General Procedure A for the Addition of R^2 MgX to Isatin. A suspension of 5-iodoisatin in anhydrous THF was cooled to 0 °C (crushed ice bath) under argon atmosphere. NaH (60% suspension in mineral oil) was added, and the resulting dark red slurry was stirred for 15 min. Solution of R^2 MgX was added dropwise, and the resulting red solution was stirred for 10 min at 0 °C, then warmed to room temperature, and left to stir for 18 h. Upon completion of the reaction, aqueous saturated NH_4Cl and EtOAc were added. Layers were separated, and water phase was extracted with EtOAc. Combined organic extracts were washed with brine, dried (Na_2SO_4), and evaporated to dryness under reduced pressure. Purification by column chromatography afforded 3-hydroxy-5-iodooxindole.

General Procedure B for Dehydratation of Hydroxy-Oxindole. Suspension of 3-hydroxy-5-iodooxindole and anhydrous $SnCl_2$ in glacial AcOH was heated at 100 °C with vigorous stirring. Upon full conversion (typically 16−48 h), the orange solution was cooled to room temperature and evaporated to dryness under the reduced pressure. The residue was dissolved in EtOAc, and aqueous saturated $NaHCO_3$ was added. The resulting biphasic suspension was filtered through a plug of Celite, and the filter cake was washed with additional EtOAc. Combined filtrates were separated, and the EtOAc layer was washed with aqueous saturated $NaHCO_3$, brine, dried (Na_2SO_4), and evaporated to dryness under reduced pressure.

General Procedure C for Negishi Cross-Coupling. Aryl iodide **10a−h**, $Pd_2(dba)_3$, and SPhos were dissolved in anhydrous DMF under argon atmosphere, and freshly prepared alkyl zinc iodide **11** (prepared as described in literature)[16] was added. The yellow solution was stirred at 65 °C until complete conversion (typically 2−48 h). Then, the solution was cooled to room temperature, and aqueous saturated NH_4Cl and EtOAc were added. Layers were separated, and EtOAc solution was washed with water and brine, dried (Na_2SO_4), and evaporated under reduced pressure to dryness. Pure products were obtained by column chromatography.

General Procedure D for the Formation of Amide from Methyl Ester. Methyl ester **7a−h** was dissolved in MeOH, and water mixture and stream of argon was passed through the solution for 20 min. Solid LiOH was added, and the clear solution was stirred at room temperature for 2 h, whereupon aqueous HCl (1 M) was added, and MeOH was evaporated under reduced pressure. The resulting suspension was extracted with EtOAc (three times), combined organic extracts were washed with brine, dried (Na_2SO_4), and concentrated *in vacuo*. To the resulting crude acid was added the corresponding amine, EDC × HCl in anhydrous pyridine. The resulting suspension was stirred at room temperature until complete conversion (typically 1−18 h), and the orange solution was evaporated under reduced pressure to dryness. The residue was dissolved in EtOAc and washed with aqueous HCl (1 M) and brine, dried (Na_2SO_4), and evaporated under reduced pressure. Pure products were obtained by column chromatography.

General Procedure E for Amide Formation from Benzyl Ester. Benzyl ester **8a,b,i** and Pd on carbon were suspended in EtOAc, and a stream of hydrogen gas was passed through the suspension for 3 h at room temperature. Then, the suspension was filtered through a plug of Celite, the filter cake was washed with EtOAc, and combined filtrates were evaporated under reduced pressure to dryness. To the crude acid was added amine **9**, EDC × HCl in anhydrous pyridine, and the resulting suspension was stirred at room temperature

https://doi.org/10.1021/acs.jmedchem.4c00388
J. Med. Chem. 2024, 67, 9227−9259

until complete conversion (typically 4−16 h), whereupon the orange solution was evaporated under reduced pressure to dryness. The residue was dissolved in EtOAc and washed with aqueous HCl (1 M) and brine, dried ($MgSO_4$), and concentrated *in vacuo*. Pure products were obtained by column chromatography.

General Procedure F for Macrocyclization. Compound **5a−h** and an oven-dried base (K_2CO_3 or K_3PO_4) were suspended in anhydrous degassed DMF and a stream of argon was passed through the solution for 10 min. Then the suspension was stirred at 65 °C until complete conversion (typically 1−60 h), whereupon it was cooled to room temperature, quenched with aqueous saturated NH_4Cl and extracted with EtOAc (two times). Combined organic extracts were washed with brine, dried (Na_2SO_4) and evaporated under reduced pressure. Pure products were obtained by column chromatography.

General Procedure G (For Alkylation of Macrocycle). To ice ice-cold solution of macrocycle **3g** in anhydrous degassed DMF was added NaH (60% suspension in mineral oil), and the resulting solution was stirred for 15 min (*caution! gas evolution*), whereupon neat alkylating reagent was added dropwise. The resulting solution was left to stir at room temperature for 1 h and then diluted with aqueous saturated NH_4Cl and EtOAc. Layers were separated, and the organic phase was washed with brine, dried (Na_2SO_4), and evaporated under reduced pressure. Pure products were obtained by column chromatography.

General Procedure H for Boc Cleavage and Introduction of HiVA Side Chain. Neat TFA was added to a solution of intermediate **3a−h** or **4a,b,i** in anhydrous DCM. After stirring at room temperature until complete conversion (typically 1−48 h), the reaction mixture was evaporated under reduced pressure to dryness and redissolved in EtOAc. Layers were separated, and organic phase was washed with aqueous saturated $NaHCO_3$ and brine, dried (Na_2SO_4), and evaporated under reduced pressure to dryness. The yellow oily residue was dissolved in anhydrous DMF and (*S*)-2-hydroxy-3-methylbutanoic acid ((*S*)-2-hydroxy-3-methylbutanoic acid; **13**), EDC × HCl and HOBt were added followed by DIPEA. The solution was stirred at room temperature until complete conversion was achieved (typically 1−18 h) and then diluted with aqueous saturated NH_4Cl and EtOAc. Layers were separated, and the organic phase was washed with water and brine, dried (Na_2SO_4), and evaporated. Pure products were obtained by column chromatography.

*5-Iodo-3-phenyl-2,3-dihydro-1H-indol-2-one (**10a**).* Step 1: 3-hydroxy-5-iodo-3-phenyl-2,3-dihydro-1*H*-indol-2-one was prepared according to general procedure A from 5-iodoisatin (1.46 g; 5.33 mmol), NaH (60% suspension in mineral oil; 256 mg; 6.40 mmol; 1.2 equiv), PhMgBr (1 M solution in THF; 8.00 mL; 8.00 mmol; 1.5 equiv), and THF (30 mL) within 18 h. Purification by column chromatography on silica gel (gradient elution from 100% DCM to 10% MeOH in DCM) afforded 3-hydroxy-5-iodo-3-phenyl-2,3-dihydro-1*H*-indol-2-one (1.22 g, 65%) as a pale yellow amorphous solid. Step 2: compound **10a** was prepared according to general procedure B from 3-hydroxy-5-iodo-3-phenyl-2,3-dihydro-1*H*-indol-2-one (1.22 g; 3.48 mmol), $SnCl_2$ (1.65 g; 3.48 mmol; 2.5 equiv), and AcOH (20 mL) within 16 h. Product **10a** was obtained as a white amorphous solid (792 mg, 68%). ^{1}H NMR (400 MHz, DMSO-d_6): δ 10.65 (s, 1H), 7.56 (ddd, J = 8.1, 1.8, 0.9 Hz, 1H), 7.38−7.26 (m, 4H), 7.17−7.11 (m, 2H), 6.76 (d, J = 8.1 Hz, 1H), 4.79 (s, 1H). ^{13}C NMR (101 MHz, DMSO-d_6): δ 176.6, 142.5, 137.2, 136.6, 133.0, 132.9, 128.8, 128.3, 127.3, 112.0, 84.4, 51.6. HRMS-ESI (m/z) calcd for $C_{14}H_{11}NOI$ [M + H]$^+$ 335.9885; found: 335.9892.

*5-Iodo-3-methyl-2,3-dihydro-1H-indol-2-one (**10b**).* Step 1: 3-hydroxy-5-iodo-3-methyl-2,3-dihydro-1*H*-indol-2-one was prepared according to general procedure A from 5-iodoisatin (5.0 g; 18.3 mmol), NaH (60% suspension in mineral oil; 805 mg; 20.14 mmol; 1.1 equiv), methylmagnesium bromide (3 M in Et_2O; 6.71 mL; 20.14 mmol; 1.1 equiv), and THF (40 mL) within 18 h. Purification by column chromatography on silica gel (gradient elution from 100% DCM to 100% acetone) afforded 3-hydroxy-5-iodo-3-methyl-2,3-dihydro-1*H*-indol-2-one (2.92 g, 55%) as a pale yellow amorphous solid. Step 2: compound **10b** was prepared according to general procedure B from 3-hydroxy-5-iodo-3-methyl-2,3-dihydro-1*H*-indol-2-one (1.39 g; 4.80 mmol), $SnCl_2$ (2.28 g; 12.02 mmol; 2.5 equiv), and AcOH (20 mL) within 12 h. Purification by column chromatography on silica gel (gradient elution from 100% DCM to 60% EtOAc in DCM) afforded **10b** (990 mg, 75%) as a yellow amorphous solid. ^{1}H NMR (400 MHz, $CDCl_3$): δ 8.64 (s, 1H), 7.57−7.48 (m, 2H), 6.69 (d, J = 8.0 Hz, 1H), 3.46 (q, J = 7.7 Hz, 1H), 1.48 (d, J = 7.7 Hz, 3H). ^{13}C NMR (101 MHz, $CDCl_3$): δ 180.5, 141.0, 136.9, 133.8, 132.9, 111.8, 85.0, 41.0, 15.3. HRMS-ESI (m/z) calcd for C_9H_9NOI [M + H]$^+$ 273.9729; found: 273.9733.

*5-Iodo-3-(propan-2-yl)-2,3-dihydro-1H-indol-2-one (**10c**).* Step 1: 3-hydroxy-5-iodo-3-(propan-2-yl)-2,3-dihydro-1*H*-indol-2-one was prepared according to general procedure A from 5-iodoisatin (2.20 g; 8.06 mmol), NaH (60% suspension in mineral oil; 419 mg; 10.48 mmol; 1.3 equiv), isopropylmagnesium chloride (2 M in THF; 6.04 mL; 12.08 mmol; 1.5 equiv), and THF (15 mL) within 18 h. Purification by reverse phase column chromatography (gradient elution from 5% to 95% MeCN in water) afforded 3-hydroxy-5-iodo-3-(propan-2-yl)-2,3-dihydro-1*H*-indol-2-one (900 mg, 35%) as a red amorphous solid. Step 2: compound **10c** was prepared according to general procedure B from 3-hydroxy-5-iodo-3-(propan-2-yl)-2,3-dihydro-1*H*-indol-2-one (900 mg; 2.84 mmol), $SnCl_2$ (2.42 g; 12.77 mmol; 4.5 equiv), and AcOH (15 mL) in 48 h. Purification by reverse phase column chromatography (gradient elution from 5% to 95% MeCN in water) afforded **10c** (465 mg, 54%) as a pale red solid. ^{1}H NMR (400 MHz, DMSO-d_6): δ 10.43 (s, 1H), 7.55−7.49 (m, 2H), 6.66 (d, J = 8.0 Hz, 1H), 3.39 (d, J = 3.5 Hz, 1H), 2.32 (sept d, J = 6.9, 3.5 Hz, 1H), 0.93 (d, J = 6.9 Hz, 3H), 0.87 (d, J = 6.9 Hz, 3H). ^{13}C NMR (101 MHz, DMSO-d_6): δ 177.5, 142.9, 136.1, 132.5, 131.4, 111.4, 84.0, 50.9, 29.9, 18.9, 18.3. HRMS-ESI (m/z) calcd for $C_{11}H_{13}NOI$ [M + H]$^+$ 302.0042; found: 302.0043.

*3-(3,5-Dimethylphenyl)-5-iodo-2,3-dihydro-1H-indol-2-one (**10d**).* Step 1: 3-(3,5-dimethylphenyl)-3-hydroxy-5-iodo-2,3-dihydro-1*H*-indol-2-one was prepared according to general procedure A from 5-iodoisatin (1.46 g; 5.33 mmol), NaH (60% suspension in mineral oil; 256 mg; 6.40 mmol; 1.2 equiv), 3,5-dimethylphenylmagnesium bromide (1 M in THF; 8.00 mL; 8.00 mmol; 1.5 equiv), and THF (30 mL) within 18 h. Purification by column chromatography on silica gel (gradient elution from 100% DCM to 10% MeOH in DCM) afforded 3-(3,5-dimethylphenyl)-3-hydroxy-5-iodo-2,3-dihydro-1*H*-indol-2-one (1.38 g, 69%) as a pale yellow amorphous solid. Step 2: compound **10d** was prepared according to general procedure B from 3-(3,5-dimethylphenyl)-3-hydroxy-

https://doi.org/10.1021/acs.jmedchem.4c00388
J. Med. Chem. 2024, 67, 9227−9259

5-iodo-2,3-dihydro-1*H*-indol-2-one (1.35 g; 3.56 mmol), $SnCl_2$ (1.55 g; 8.19 mmol; 2.30 equiv), and AcOH (30 mL) within 17 h. Product **10d** was obtained as a white amorphous solid (1.05 g, 81%). ^{1}H NMR (400 MHz, DMSO-d_6): δ 10.61 (s, 1H), 7.55 (ddd, J = 8.1, 1.8, 0.9 Hz, 1H), 7.26−7.23 (m, 1H), 6.93−6.91 (m, 1H), 6.75 (d, J = 8.1 Hz, 1H), 6.73−6.70 (m, 2H), 4.67 (s, 1H), 2.23 (s, 6H). ^{13}C NMR (101 MHz, DMSO-d_6): δ 176.7, 142.5, 137.8, 137.1, 136.5, 133.3, 132.7, 128.7, 126.0, 111.9, 84.3, 51.6, 20.8. HRMS-ESI (m/z) calcd for $C_{16}H_{13}NOI$ $[M - H]^-$ 362.0042; found: 362.0051.

*5-Iodo-3-(naphthalen-2-yl)-2,3-dihydro-1H-indol-2-one (**10e**).* Step 1: 3-hydroxy-5-iodo-3-(naphthalen-2-yl)-2,3-dihydro-1*H*-indol-2-one was prepared according to general procedure A from 5-iodoisatin (1.46 g; 5.33 mmol), NaH (60% suspension in mineral oil; 256 mg; 6.40 mmol; 1.2 equiv), 2-naphtylmagnesium bromide (1 M in THF; 8.00 mL; 8.00 mmol; 1.5 equiv), and THF (30 mL) within 18 h. Purification by column chromatography on silica gel (gradient elution from 100% DCM to 10% MeOH in DCM) afforded 3-hydroxy-5-iodo-3-(naphthalen-2-yl)-2,3-dihydro-1*H*-indol-2-one (1.90 g, 89%) as a pale yellow amorphous solid. Step 2: compound **10e** was prepared according to general procedure B from 3-hydroxy-5-iodo-3-(naphthalen-2-yl)-2,3-dihydro-1*H*-indol-2-one (1.87 g; 4.66 mmol), $SnCl_2$ (2.03 g; 10.72 mmol; 2.3 equiv), and AcOH (25 mL) within 28 h. Product **10e** was obtained as a white amorphous solid (1.03 g, 57%). ^{1}H NMR (400 MHz, DMSO-d_6): δ 10.73 (s, 1H), 7.93−7.85 (m, 3H), 7.77−7.73 (m, 1H), 7.59 (ddd, J = 8.1, 1.8, 0.9 Hz, 1H), 7.55−7.47 (m, 2H), 7.35−7.31 (m, 1H), 7.19 (dd, J = 8.5, 1.8 Hz, 1H), 6.81 (d, J = 8.1 Hz, 1H), 4.98 (s, 1H). ^{13}C NMR (101 MHz, DMSO-d_6): δ 176.6, 142.6, 136.7, 134.7, 133.04, 132.99, 132.9, 132.1, 128.5, 127.6, 127.5, 127.3, 126.4, 126.2, 126.1, 112.0, 84.5, 51.8. HRMS-ESI (m/z) calcd for $C_{18}H_{13}NOI$ $[M + H]^+$ 386.0042; found: 386.0052.

*5-Iodo-2,3-dihydro-1H-indol-2-one (**10f**).* It was synthesized as described in the literature.[35] Thus, a solution of 2-oxindole (300 mg; 2.25 mmol) and NIS (608 mg; 2.70 mmol; 1.2 equiv) in glacial acetic acid (2.5 mL) was stirred at room temperature for 2 h, whereupon water (10 mL) was added. The formed precipitate was filtered, washed with water, and dried on filter. The red powder was then washed with EtOAc to yield **10f** (275 mg, 47%) as a beige amorphous solid. ^{1}H NMR (300 MHz, DMSO-d_6): δ 10.45 (s, 1H), 7.54−7.46 (m, 2H), 6.65 (d, J = 8.0 Hz, 1H), 3.48 (s, 2H). ^{13}C NMR (101 MHz, DMSO-d_6): δ 175.7, 143.5, 135.9, 132.7, 128.8, 111.5, 83.8, 35.5. HRMS-ESI (m/z) calcd for C_8H_7NOI $[M + H]^+$ 259.9572; found: 259.9573.

*5-Iodo-1-methyl-2,3-dihydro-1H-indol-2-one (**10g**).* It was synthesized as described in the literature.[36] Accordingly, NaH (60% in mineral oil; 879 mg; 22.0 mmol; 1.2 equiv) was added to a precooled (0 °C) solution of 5-iodoisatin (5.0 g; 18.3 mmol) in anhydrous DMF (40 mL). The resulting dark purple solution was stirred 10 min, then MeI (1.37 mL; 3.12 mmol; 1.2 equiv) was added, and the reaction mixture was warmed to room temperature. After stirring for 18 h, water was added. The dark red solid was filtered through a sintered glass filter, washed on filter with water, hexanes, and dried on air. The solid was dissolved in hydrazine hydrate (34.0 mL; 0.70 mol; 40.0 equiv), and the clear green solution was heated at 120 °C for 3 h. The appearance of the solution gradually changed to yellow suspension. After cooling to room temperature, water (100 mL) and EtOAc (100 mL) were added, and layers were separated. Organic layer was washed with aqueous 1 M HCl and brine, dried ($MgSO_4$), and filtered through a sintered glass filter. The clear red filtrate was evaporated to dryness, redissolved in small amount of hot MeOH, and cooled to room temperature. The formed orange amorphous powder was filtered to afford compound **10g** (3.50 g, 69%). ^{1}H NMR (400 MHz, DMSO-d_6): δ 7.62−7.58 (m, 1H), 7.57−7.54 (m, 1H), 6.81 (d, J = 8.2 Hz, 1H), 3.54 (s, 2H), 3.08 (s, 3H). ^{13}C NMR (101 MHz, DMSO-d_6): δ 173.7, 144.8, 135.9, 132.4, 127.6, 110.6, 84.7, 34.8, 25.9. HRMS-ESI (m/z) calcd for C_9H_9NOI $[M + H]^+$ 273.9729; found: 273.9735.

*5-Iodo-1-methyl-3-phenyl-2,3-dihydro-1H-indol-2-one (**10h**).* 3-Hydroxy-5-iodo-3-phenyl-2,3-dihydro-1*H*-indol-2-one (1.0 g, 3.7 mmol) in anhydrous DMF (15 mL) was cooled to 0 °C (crushed ice bath), and NaH (60% dispersion in mineral oil; 285 mg; 7.1 mmol; 2.5 equiv) was added in one portion turning the suspension into red slurry. After stirring the resulting red slurry for 5 min, iodomethane (0.53 mL; 8.5 mmol; 3.0 equiv) was added, and stirring at 0 °C was continued for 30 min. The suspension turned green and then to yellow over time. The resulting suspension was stirred at room temperature for 18 h. After completion, it was poured into aqueous saturated NH_4Cl and extracted with EtOAc (3 × 50 mL). Combined organic layers were washed with water, brine, dried ($MgSO_4$), and concentrated under reduced pressure to give crude 5-iodo-3-methoxy-1-methyl-3-phenyl-2,3-dihydro-1*H*-indol-2-one (1.05 g, 99%), which was used in the next step without further purification. The title compound **10h** was prepared according to general procedure B from crude 5-iodo-3-methoxy-1-methyl-3-phenyl-2,3-dihydro-1*H*-indol-2-one (730 mg; 2.00 mmol), $SnCl_2$ (758 mg; 4.00 mmol; 2.0 equiv), and AcOH (10 mL) within 16 h. Purification by column chromatography on silica gel (gradient elution from 100% DCM to 5% MeOH in DCM) afforded **10h** (500 mg, 72%) as a yellow amorphous solid. ^{1}H NMR (400 MHz, $CDCl_3$): δ 7.65 (ddd, J = 8.2, 1.8, 0.9 Hz, 1H), 7.44 (t, J = 1.5 Hz, 1H), 7.38−7.27 (m, 3H), 7.20−7.14 (m, 2H), 6.68 (d, J = 8.2 Hz, 1H), 4.59 (s, 1H), 3.23 (s, 3H). ^{13}C NMR (101 MHz, $CDCl_3$): δ 175.3, 144.3, 137.4, 136.0, 133.8, 131.4, 129.2, 128.5, 128.0, 110.3, 85.3, 51.9, 26.6. HRMS-ESI (m/z) calcd for $C_{16}H_{13}INO$ $[M + H]^+$ 350.0042; found: 350.0054.

*5-Iodo-1,3-dimethyl-2,3-dihydro-1H-indol-2-one (**10i**).* 3-Hydroxy-5-iodo-3-methyl-2,3-dihydro-1*H*-indol-2-one (150 mg, 0.52 mmol) was dissolved in anhydrous DMF (3 mL) and cooled to 0 °C, whereupon NaH (60% dispersion in mineral oil; 52 mg; 1.3 mmol; 2.5 equiv) was added in one portion. The resulting red slurry was stirred for 5 min, and then iodomethane (100 μL; 1.56 mmol; 3 equiv) was added. After stirring at 0 °C for 30 min, the resulting purple suspension was warmed to room temperature and stirred for 18 h. After completion, it was poured into aqueous saturated NH_4Cl and extracted with EtOAc (3 × 20 mL). Combined organic extracts were washed with water, brine, dried ($MgSO_4$), and concentrated under reduced pressure to give crude 5-iodo-3-methoxy-1,3-dimethyl-2,3-dihydro-1*H*-indol-2-one (160 mg, 97%), which was used in the next step without further purification. The title compound **10i** was prepared according to general procedure B from 5-iodo-3-methoxy-1,3-dimethyl-2,3-dihydro-1*H*-indol-2-one (95 mg; 0.31 mmol), $SnCl_2$ (149 mg; 0.78 mmol; 2.5 equiv), and AcOH (4 mL) within 48 h. Purification by column chromatography on silica gel (gradient elution from 100% hexanes to 80% EtOAc in hexanes) afforded **10i** (51 mg, 57%) as a yellow amorphous solid. ^{1}H NMR (400 MHz, $CDCl_3$): δ 7.58 (ddd, J = 8.1, 1.8,

https://doi.org/10.1021/acs.jmedchem.4c00388
J. Med. Chem. 2024, 67, 9227−9259

0.8 Hz, 1H), 7.52−7.50 (m, 1H), 6.60 (d, J = 8.1 Hz, 1H), 3.41 (q, J = 7.6 Hz, 1H), 3.17 (s, 3H), 1.45 (d, J = 7.6 Hz, 3H). ^{13}C NMR (101 MHz, $CDCl_3$): δ 177.9, 143.8, 136.8, 133.1, 132.5, 110.1, 85.0, 40.5, 26.3, 15.4. HRMS-ESI (m/z) calcd for $C_{10}H_{11}INO$ $[M + H]^+$ 287.9885; found: 287.9890.

*Methyl (2S)-2-{[(tert-Butoxy)carbonyl]amino}-3-(2-oxo-3-phenyl-2,3-dihydro-1H-indol-5-yl)propanoate (**7a**).* The title compound was prepared according to general procedure C from oxindole **10a** (800 mg; 2.39 mmol), alkyl zincate **11** (0.5 M in DMF; 5.25 mL; 2.63 mmol; 1.1 equiv), $Pd_2(dba)_3$ (22 mg; 0.024 mmol; 0.01 equiv), SPhos (39 mg; 0.096 mmol; 0.04 equiv), and DMF (6 mL) in 3 h. Purification by column chromatography on silica gel (gradient elution for 20% to 50% EtOAc in hexanes) afforded **7a** (800 mg, 82%; dr 3:2) as a yellow amorphous solid. ^{1}H NMR (400 MHz, $CDCl_3$): δ 8.51 (s, 1H), 7.39−7.27 (m, 3H), 7.22−7.16 (m, 2H), 7.04−6.96 (m, 1H), 6.90−6.82 (m, 2H), 5.03−4.92 (m, 1H), 4.60 (s, 0.6 H), 4.59 (s, 0.4 H) 4.57−4.45 (m, 1H), 3.64 (s, 1H), 3.53 (s, 2H), 3.09−2.92 (m, 2H), 1.41 (s, 5H), 1.37 (s, 4H). ^{13}C NMR (101 MHz, $CDCl_3$): δ 178.81, 178.79, 172.5, 172.2, 155.2, 155.1, 140.8, 136.54, 136.52, 130.6, 130.5, 130.2, 129.5, 129.4, 129.12, 129.09, 128.62, 128.59, 127.8, 126.2, 110.1, 110.0, 80.1, 54.8, 54.7, 52.82, 52.80, 52.3, 52.2, 38.3, 38.0, 28.4. HRMS-ESI (m/z) calcd for $C_{23}H_{26}N_2O_5Na$ $[M + Na]^+$ 433.1739; found 433.1735.

*Methyl (2S)-2-{[(tert-Butoxy)carbonyl]amino}-3-(3-methyl-2-oxo-2,3-dihydro-1H-indol-5-yl)propanoate (**7b**).* The title compound was prepared according to general procedure C from oxindole **10b** (415 mg; 1.52 mmol), alkyl zincate **11** (0.5 M in DMF; 8.05 mL; 4.03 mmol; 2.7 equiv), $Pd_2(dba)_3$ (28 mg; 0.030 mmol; 0.02 equiv), SPhos (31 mg; 0.076 mmol; 0.05 equiv), and DMF (6 mL) in 2 h. Purification by column chromatography on silica gel (gradient elution from 20% to 70% EtOAc in hexanes) was followed by reverse phase column chromatography (gradient elution from 15% to 70% MeCN in water) afforded **7b** (410 mg, 77%; dr 1:1) as beige amorphous solid. ^{1}H NMR (400 MHz, $CDCl_3$): δ 8.88 (s, 0.5H), 8.79 (s, 0.5H), 7.00−6.91 (m, 2H), 6.82 (s, 0.5H), 6.80 (s, 0.5H), 5.11−4.96 (m, 1H), 4.64−4.48 (m, 1H), 3.71 (s, 3H), 3.48−3.35 (m, 1H), 3.17−2.92 (m, 2H), 1.47 (d, J = 3.6 Hz, 1.5H), 1.46 (d, J = 3.6 Hz, 1.5H), 1.41 (s, 9H). ^{13}C NMR (101 MHz, $CDCl_3$): δ 181.32, 181.26, 172.5, 172.4, 155.13, 155.05, 140.2, 131.6, 131.6, 130.11, 130.07, 128.8, 128.7, 124.8, 109.7, 80.0, 54.7, 52.3, 52.2, 41.0, 38.13, 38.06, 28.3, 15.2. HRMS-ESI (m/z) calcd for $C_{18}H_{23}N_2O_5$ $[M - H]^-$: 347.1607; found 347.1606.

*Methyl (2S)-2-{[(tert-Butoxy)carbonyl]amino}-3-[2-oxo-3-(propan-2-yl)-2,3-dihydro-1H-indol-5-yl]propanoate (**7c**).* The title compound was prepared according to general procedure C from oxindole **10c** (380 mg; 1.26 mmol), alkyl zincate **11** (0.5 M in DMF; 3.79 mL; 1.89 mmol; 1.5 equiv), $Pd_2(dba)_3$ (12 mg; 0.013 mmol; 0.01 equiv), SPhos (21 mg; 0.051 mmol; 0.04 equiv), and DMF (6 mL) in 2 h. Purification by reverse phase column chromatography (gradient elution from 5% to 95% MeCN in water) afforded **7c** (256 mg, 54%; dr 1:1) as yellow oil. ^{1}H NMR (400 MHz, $CDCl_3$): δ 8.77 (s, 1H), 7.01 (s, 1H), 6.95 (d, J = 7.9 Hz, 1H), 6.80 (d, J = 7.9 Hz, 1H), 5.09−4.97 (m, 1H), 4.61−4.50 (m, 1H), 3.702 (s, 1.5H), 3.699 (s, 1.5H), 3.35 (t, J = 3.7 Hz, 1H), 3.14−2.95 (m, 2H), 2.47 (sept d, J = 7.0, 3.4 Hz, 1H), 1.41 (s, 4.5H), 1.40 (s, 4.5H), 1.14−1.08 (m, 3H), 0.89 (d, J = 7.0, 3H). ^{13}C NMR (101 MHz, $CDCl_3$): δ 180.0, 172.5, 155.2, 155.1, 141.2, 129.7, 128.8, 128.8, 128.7, 125.8, 125.8, 109.63, 109.60, 80.1, 54.8, 54.7, 52.4, 52.2, 38.3, 38.1, 30.9, 28.4, 20.2, 20.1, 18.0. HRMS-ESI (m/z) calcd for $C_{20}H_{29}N_2O_5$ $[M + H]^+$ 377.2076; found 377.2069.

*Methyl (2S)-2-{[(tert-Butoxy)carbonyl]amino}-3-[3-(3,5-dimethylphenyl)-2-oxo-2,3-dihydro-1H-indol-5-yl]propanoate (**7d**).* The title compound was prepared according to general procedure C from **10d** (1.00 g; 2.75 mmol), alkyl zincate **11** (0.5 M in DMF; 6.61 mL; 3.30 mmol; 1.2 equiv), $Pd_2(dba)_3$ (25 mg; 0.028 mmol; 0.01 equiv), SPhos (57 mg; 0.14 mmol; 0.05 equiv), and DMF (6 mL) in 48 h. Purification by column chromatography on silica gel (gradient elution from 10% to 40% EtOAc in hexanes) afforded **7d** (900 mg, 75%; dr 1:1) as yellow amorphous solid. ^{1}H NMR (300 MHz, $CDCl_3$): δ 8.24 (s, 1H), 7.05−6.95 (m, 1H), 6.91 (s, 1H), 6.88−6.82 (m, 2H), 6.78 (s, 2H), 5.05−4.88 (m, 1H), 4.57−4.43 (m, 2H), 3.63 (s, 1.5 H), 3.53 (s, 1.5 H), 3.10−2.93 (m, 2H), 2.28 (s, 6H), 1.42 (s, 4.5 H), 1.37 (s, 4.5H). ^{13}C NMR (101 MHz, $CDCl_3$): δ 178.9, 178.8, 172.5, 172.2, 155.2, 155.1, 140.7, 138.7, 136.4, 136.3, 130.62, 130.60, 130.5, 130.4, 129.64, 129.59, 129.4, 129.3, 126.41, 126.38, 126.3, 109.93, 109.87, 80.1, 54.9, 54.7, 52.82, 52.77, 52.3, 52.1, 38.4, 38.1, 28.5, 28.4, 21.42, 21.39. HRMS-ESI (m/z) calcd for $C_{25}H_{30}N_2O_5Na$ $[M + Na]^+$ 461.2052; found 461.2053.

*Methyl (2S)-2-{[(tert-Butoxy)carbonyl]amino}-3-[3-(naphthalen-2-yl)-2-oxo-2,3-dihydro-1H-indol-5-yl]propanoate (**7e**).* The title compound was prepared according to general procedure C from oxindole **10e** (600 mg; 1.56 mmol), alkyl zincate **11** (0.5 M in DMF; 3.43 mL; 1.71 mmol; 1.1 equiv), $Pd_2(dba)_3$ (43 mg; 0.047 mmol; 0.03 equiv), SPhos (51 mg; 0.12 mmol; 0.08 equiv), and DMF (16 mL) in 18 h. Purification by column chromatography on silica gel (gradient elution from 20% to 50% EtOAc in hexanes) followed by reverse phase column chromatography (gradient elution from 30% to 70% MeCN in water) afforded **7e** (319 mg, 45%; dr ∼1:1) as white amorphous solid. ^{1}H NMR (400 MHz, $CDCl_3$): δ 8.66 (s, 0.5H), 8.61 (s, 0.5H), 7.87−7.78 (m, 3H), 7.74−7.71 (m, 0.5H), 7.71−7.67 (m, 0.5H), 7.52−7.43 (m, 2H), 7.29−7.23 (m, 1H, overlaps with $CDCl_3$) 7.04−6.97 (m, 1H), 6.91−6.83 (m, 2H), 5.05−4.92 (m, 1H), 4.77 (s, 0.5H), 4.75 (s, 0.5H), 4.57−4.45 (m, 1H), 3.62 (s, 1.5H), 3.46 (s, 1.5H), 3.10−2.90 (m, 2H), 1.40 (s, 5H), 1.29 (s, 4H). ^{13}C NMR (101 MHz, $CDCl_3$): δ 178.4, 178.3, 172.3, 172.1, 155.1, 154.9, 140.7, 140.6, 133.8, 133.7, 133.6, 133.5, 132.9, 132.8, 130.6, 130.5, 129.94, 129.90, 129.5, 129.4, 128.91, 128.87, 127.9, 127.66, 127.65, 127.6, 126.4, 126.3, 126.11, 126.09, 126.0, 109.92, 109.89, 80.0, 79.9, 54.7, 54.5, 52.8, 52.7, 52.2, 52.1, 38.2, 37.9, 28.3, 28.2. HRMS-ESI (m/z) calcd for $C_{27}H_{28}N_2O_5Na$ $[M + Na]^+$ 483.1896; found 483.1883.

*Methyl (2S)-2-{[(tert-Butoxy)carbonyl]amino}-3-(2-oxo-2,3-dihydro-1H-indol-5-yl)propanoate (**7f**).* The title compound was prepared according to general procedure C from 5-iodo-2-oxindole **10f** (100 mg; 0.39 mmol), alkyl zincate **11** (0.5 M in DMF; 1.16 mL; 0.58 mmol; 1.5 equiv), $Pd_2(dba)_3$ (7 mg; 0.008 mmol; 0.02 equiv), SPhos (8 mg; 0.02 mmol; 0.05 equiv), and DMF (2 mL) in 42 h. Purification by column chromatography on silica gel (gradient elution from 0% to 100% EtOAc in hexanes) afforded **7f** (64 mg, 50%) as orange solid. ^{1}H NMR (300 MHz, $CDCl_3$): δ 8.05 (s, 1H), 7.04−6.90 (m, 2H), 6.78 (d, J = 7.9 Hz, 1H), 5.00 (d, J = 8.3 Hz, 1H), 4.59−4.48 (m, 1H), 3.72 (s, 3H), 3.50 (s, 2H), 3.09 (dd, J = 13.9, 5.9 Hz, 1H), 2.98 (dd, J = 13.9, 5.9 Hz, 1H), 1.41 (s, 9H). ^{13}C NMR (101 MHz, $CDCl_3$): δ 177.5, 172.5, 155.2, 141.6, 130.2, 128.9, 125.7, 109.7, 80.2, 54.8, 52.4, 38.2, 36.3,

https://doi.org/10.1021/acs.jmedchem.4c00388
J. Med. Chem. 2024, 67, 9227−9259

28.4. HRMS-ESI (m/z) calcd for $C_{17}H_{22}N_2O_5Na$ $[M + Na]^+$ 357.1426; found 357.1423. $[\alpha]_D^{20}$ 77.0 (c 1.0, $CHCl_3$).

*Methyl (2S)-2-{[(tert-Butoxy)carbonyl]amino}-3-(1-methyl-2-oxo-2,3-dihydro-1H-indol-5-yl)propanoate (**7g**).* The title compound was prepared according to general procedure C from oxindole **10g** (4.00 g; 12.82 mmol), alkyl zincate **11** (0.5 M in DMF; 30.00 mL; 15.00 mmol; 1.2 equiv), $Pd_2(dba)_3$ (117 mg; 0.13 mmol; 0.01 equiv), SPhos (132 mg; 0.32 mmol; 0.03 equiv), and DMF (50 mL) in 2 h. Purification by column chromatography on silica gel (gradient elution from 0% to 100% EtOAc in hexanes) afforded **7g** (3.86 g, 86%) as yellow amorphous solid. ^{1}H NMR (400 MHz, $CDCl_3$): δ 7.04−6.99 (m, 2H), 6.72 (d, J = 8.0 Hz, 1H), 5.00 (d, J = 8.3 Hz, 1H), 4.57−4.49 (m, 1H), 3.71 (s, 3H), 3.47 (s, 2H), 3.17 (s, 3H), 3.08 (dd, J = 13.9, 5.7 Hz, 1H), 2.99 (dd, J = 13.9, 6.0 Hz, 1H), 1.40 (s, 9H). ^{13}C NMR (101 MHz, $CDCl_3$): δ 175.0, 172.4, 155.2, 144.3, 130.2, 128.8, 125.4, 124.9, 108.1, 80.1, 54.7, 52.4, 38.2, 35.8, 28.4, 26.3. HRMS-ESI (m/z) calcd for $C_{18}H_{25}N_2O_5$ $[M + H]^+$ 349.1763; found 349.1771. $[\alpha]_D^{20}$ 7.7 (c 1.0, MeOH).

*Methyl (2S)-2-{[(tert-Butoxy)carbonyl]amino}-3-(1-methyl-2-oxo-3-phenyl-2,3-dihydro-1H-indol-5-yl)propanoate (**7h**).* The title compound was prepared according to general procedure C from **10h** (490 mg; 1.40 mmol), alkyl zincate **11** (0.5 M in DMF; 3.65 mL; 1.82 mmol; 1.3 equiv), $Pd_2(dba)_3$ (19 mg; 0.021 mmol; 0.02 equiv), SPhos (23 mg; 0.056 mmol; 0.04 equiv), and DMF (5 mL) in 2 h. Purification by column chromatography on silica gel (gradient elution from 35% to 65% EtOAc in hexanes) afforded **7h** (550 mg, 92%; dr 1:1) as off-white amorphous solid. ^{1}H NMR (400 MHz, $CDCl_3$): δ 7.36−7.30 (m, 2H), 7.30−7.25 (m, 1H), 7.21−7.15 (m, 2H), 7.12−7.05 (m, 1H), 6.92−6.88 (m, 1H), 6.82 (d, J = 7.9, 1H), 5.01−4.97 (m, 1H), 4.58 (s, 0.5H), 4.56 (s, 0.5H), 4.56−4.46 (m, 1H), 3.64 (s, 1.5H), 3.53 (s, 1.5H), 3.23 (s, 3H), 3.14−2.94 (m, 2H), 1.42 (s, 4.5H), 1.38 (s, 4.5H). ^{13}C NMR (101 MHz, $CDCl_3$): δ 176.0, 172.4, 172.2, 155.2, 155.1, 143.6, 136.69, 136.67, 130.7, 130.5, 129.5, 129.4, 129.3, 129.1, 129.0, 128.6, 128.5, 127.7, 126.2, 126.1, 108.3, 108.2, 80.11, 80.06, 54.9, 54.7, 52.3, 52.24, 52.18, 52.16, 38.4, 38.0, 28.5, 28.4, 26.7. HRMS-ESI (m/z) calcd for $C_{24}H_{29}N_2O_5$ $[M + H]^+$ 425.2076; found 425.2076.

*1-Benzyl 1,3-Dioxo-2,3-dihydro-1H-isoindol-2-yl (2S)-2-{[(tert-butoxy)carbonyl]amino}pentanedioate (**12**).* *N*-Boc-*L*-Glu-OBn (2.00 g; 5.93 mmol), *N*-hydroxyphthalimide (967 mg; 5.93 mmol; 1.0 equiv), and DMAP (72 mg, 0.59 mmol; 0.1 equiv) were suspended in anhydrous DCM (35 mL) under argon atmosphere. *N,N′*-diisopropylcarbodiimide (1.02 mL; 6.52 mmol, 1.10 equiv) was added, and the light yellow suspension was left to stir for 12 h at room temperature, whereupon the bright yellow heterogeneous mixture was filtered through a plug of Celite. Filter cake was washed with DCM, and combined filtrates were concentrated under reduced pressure. The crude product was purified by column chromatography on silica gel (gradient elution from 100% to 40% Et_2O in DCM) to yield **12** (2.32 g, 81%) as a colorless thick oil that solidified upon standing. ^{1}H NMR (400 MHz, $CDCl_3$) δ 7.92−7.85 (m, 2H), 7.82−7.76 (m, 2H), 7.40−7.30 (m, 5H), 5.28−5.15 (m, 3H), 4.52−4.38 (m, 1H), 2.74 (qdd, J = 17.0, 9.3, 6.1 Hz, 2H), 2.43−2.29 (m, 1H), 2.18−2.06 (m, 1H), 1.44 (s, 9H). ^{13}C NMR (101 MHz, $CDCl_3$) δ 171.7, 169.0, 161.9, 155.5, 135.2, 134.9, 129.0, 128.8, 128.7, 128.5, 124.1, 80.4, 67.6, 52.8, 28.4, 27.8, 27.5. HRMS-ESI (m/z) calcd for $C_{25}H_{26}N_2O_8Na$ $[M + Na]^+$ 505.1587; found 505.1591. $[\alpha]_D^{20}$ +7 (c 2.0, $CHCl_3$).

*Benzyl (2S)-2-{[(tert-Butoxy)carbonyl]amino}-4-(2-oxo-3-phenyl-2,3-dihydro-1H-indol-5-yl)butanoate (**8a**).* Aryl iodide **10a** (300 mg; 0.90 mmol), redox-active ester **12** (648 mg; 1.34 mmol; 1.5 equiv), and zinc dust (117 mg; 1.79 mmol; 2 equiv) were suspended in anhydrous DMA (4.5 mL) under argon atmosphere. In a separate vessel, $NiCl_2 \times$ glyme (20 mg; 0.090 mmol; 0.1 equiv) and dtbbpy (24 mg; 0.090 mmol; 0.1 equiv) were dissolved in anhydrous DMA (0.5 mL) under argon atmosphere and stirred at room temperature for 15 min. Then, the blue-green catalyst solution was added to the reaction mixture, and the resulting green suspension was stirred at room temperature for 18 h, whereupon aqueous saturated NH_4Cl and EtOAc were added. Layers were separated, and aqueous layer was extracted with EtOAc. Combined organic extracts were washed with saturated NH_4Cl and brine, dried ($MgSO_4$), and evaporated under the reduced pressure. The residue was purified by reverse phase column chromatography (gradient elution from 10% to 100% MeCN in water). Fractions containing product were combined and additionally purified by column chromatography on silica gel (gradient elution from 100% to 20% Et_2O in DCM) to afford **8a** (103 mg, 23%, 1:1 d.r.) as white foam. ^{1}H NMR (400 MHz, $CDCl_3$): δ 8.30 (s, 1H), 7.40−7.27 (m, 8H), 7.23−7.15 (m, 2H), 7.02−6.93 (m, 1H), 6.87−6.82 (m, 1H), 6.81 (d, J = 8.0 Hz, 1H), 5.24−5.02 (m, 3H), 4.56 (d, J = 4.6 Hz, 1H), 4.40−4.31 (m, 1H), 2.63−2.43 (m, 2H), 2.13−2.00 (m, 1H), 1.94−1.79 (m, 1H), 1.43 (s, 9H). ^{13}C NMR (101 MHz, $CDCl_3$): δ 178.4, 172.6, 155.4, 139.8, 136.6, 135.47, 135.46, 135.4, 130.0, 129.11, 129.10, 128.7, 128.64, 128.60, 128.55, 128.51, 128.45, 127.8, 125.6, 125.5, 109.8, 80.1, 67.21, 67.18, 53.3, 52.8, 34.9, 34.8, 31.33, 28.4. HRMS-ESI (m/z) calcd for $C_{30}H_{32}N_2O_5Na$ $[M + Na]^+$ 523.2209; found 523.2222.

*Benzyl (2S)-2-{[(tert-Butoxy)carbonyl]amino}-4-(3-methyl-2-oxo-2,3-dihydro-1H-indol-5-yl)butanoate (**8b**).* $NiCl_2 \times$ glyme (40 mg; 0.18 mmol; 0.1 equiv) and dtbbpy (49 mg; 0.18 mmol; 0.1 equiv) were dissolved in anhydrous DMA (2.5 mL) under argon atmosphere, and the resulting blue-colored solution was stirred at room temperature for 20 min. In a separate flask, zinc dust (300 mg; 4.58 mmol; 2.5 equiv) was heated by a heat gun for 2 min and then cooled under argon atmosphere to room temperature. The heating/cooling sequence was repeated twice, whereupon anhydrous DMA (2.5 mL) was added via septa, followed by iodine (47 mg; 0.18 mmol; 0.1 equiv), and the resulting brown suspension was stirred at room temperature until the color faded (approximately 20 min). To the suspension was then added solid aryl iodide **10b** (500 mg; 1.83 mmol), followed by the previously prepared blue-colored catalyst solution. Then, to the yellow suspension was portionwise added redox-active ester **12** (1.06 g; 2.20 mmol; 1.2 equiv) in anhydrous DMA (1.5 mL) within a course of 10 h. After the addition was completed, the moss-green solution was stirred 8 h at room temperature and quenched by aqueous saturated NH_4Cl and EtOAc. Layers were separated, and the water layer was extracted with EtOAc. Combined organic extracts were washed with saturated $NaHCO_3$ and brine, dried ($MgSO_4$), and evaporated under reduced pressure. Purification by reverse phase column chromatography (gradient elution from 10% MeCN in water to 100% MeCN) afford **8b** (283 mg, 35%, dr 1:1) as a yellow amorphous solid. ^{1}H NMR (400 MHz, $CDCl_3$): δ 8.16 (s, 1H), 7.40−7.30 (m, 5H), 6.97−6.91 (m, 2H), 6.77 (d, J = 7.8

https://doi.org/10.1021/acs.jmedchem.4c00388
J. Med. Chem. 2024, 67, 9227−9259

Hz, 1H), 5.26−5.06 (m, 3H), 4.43−4.34 (m, 1H), 3.39 (q, J = 7.4 Hz, 1H), 2.67−2.50 (m, 2H), 2.17−2.07 (m, 1H), 1.97−1.86 (m, 1H), 1.51−1.38 (m, 12H). ^{13}C NMR (101 MHz, $CDCl_3$): δ 181.3, 173.0, 155.8, 139.7, 135.8, 135.3, 131.9, 129.1, 129.0, 128.8, 128.2, 124.5, 109.9, 80.5, 67.5, 53.7, 41.4, 35.2, 31.7, 28.8, 15.7. HRMS-ESI (m/z) calcd for $C_{25}H_{30}N_2O_5Na$ [M + Na]$^+$ 461.2052; found 461.2053.

*Benzyl (2S)-2-{[(tert-Butoxy)carbonyl]amino}-4-(1,3-dimethyl-2-oxo-2,3-dihydro-1H-indol-5-yl)butanoate (**8i**).* $NiCl_2$ × glyme (40 mg; 0.18 mmol; 0.1 equiv) and dtbbpy (49 mg; 0.18 mmol; 0.1 equiv) were dissolved in anhydrous DMA (2.5 mL) under argon atmosphere, and the resulting blue-colored solution was stirred at room temperature for 20 min. In a separate flask, zinc dust (300 mg; 4.58 mmol; 2.5 equiv) under vacuum was heated by a heat gun for 2 min and then cooled under argon atmosphere to room temperature. The heating/cooling sequence was repeated twice, whereupon anhydrous DMA (2.5 mL) was added via septa followed by iodine (47 mg; 0.18 mmol; 0.1 equiv), and the resulting brown suspension was stirred at room temperature until the color faded (approximately 20 min). To the suspension was then added solid aryl iodide **10i** (500 mg; 1.83 mmol) followed by the previously prepared blue-colored catalyst solution. Then, to the yellow suspension was portionwise added the redox-active ester **12** (1.06 g; 2.20 mmol; 1.2 equiv) in anhydrous DMA (1.5 mL) within a course of 10 h. After the addition was completed, the moss-green solution was stirred 8 h at room temperature and quenched by aqueous saturated NH_4Cl and EtOAC. Layers were separated, and the water layer was extracted with EtOAc. Combined organic extracts were washed with saturated $NaHCO_3$ and brine, dried ($MgSO_4$), and evaporated under reduced pressure. Purification by reverse phase column chromatography (gradient elution from 10% MeCN in water to 100% MeCN) afforded **8i** (430 mg, 52%; dr 1:1) as a yellow amorphous solid. ^{1}H NMR (400 MHz, $CDCl_3$): δ 7.40−7.31 (m, 5H), 7.04−6.97 (m, 1H), 6.99−6.94 (m, 1H), 6.71 (d, J = 7.9 Hz, 1H), 5.26−5.04 (m, 3H), 4.43−4.34 (m, 1H), 3.37 (q, J = 7.4 Hz, 1H), 3.18 (s, 3H), 2.70−2.51 (m, 2H), 2.16−2.06 (m, 1H), 1.99−1.84 (m, 1H), 1.48−1.40 (m, 12H). ^{13}C NMR (101 MHz, $CDCl_3$): δ 179.0, 173.0, 171.6, 155.8, 142.7, 135.8, 135.4, 131.4, 129.1, 129.0, 128.8, 128.1, 124.2, 108.3, 80.5, 67.5, 53.6, 41.0, 35.3, 31.7, 28.8, 26.7, 15.8. HRMS-ESI (m/z) calcd for $C_{26}H_{32}N_2O_5Na$ [M + Na]$^+$ 475.2209; found 475.2206.

*Methyl 2-{5-Bromo-2-[(1S)-1-[(2S)-2-{[(tert-butoxy)-carbonyl]amino}-3-(2-oxo-3-phenyl-2,3-dihydro-1H-indol-5-yl)propanamido]-2,2-dimethylpropyl]-1,3-oxazol-4-yl}-1,3-oxazole-4-carboxylate (**5a**).* The title compound was prepared according to general procedure D from ester **7a** (520 mg; 1.27 mmol), LiOH (152 mg; 6.33 mmol; 5 equiv) in MeOH/water (3:1 v/v; 8 mL), amine **9** (452 mg; 1.26 mmol; 1 equiv), and EDC × HCl (363 mg; 1.89 mmol; 1.5 equiv) in pyridine (5 mL) in 18 h. Purification by column chromatography on silica gel (gradient elution from 30% to 60% EtOAc in hexanes) afforded **5a** (465 mg, 50%, 1:1 d.r.) as a yellow oil. ^{1}H NMR (400 MHz, $CDCl_3$): δ 8.74−8.63 (m, 1H), 8.28 (s, 0.5H), 8.23 (s, 0.5H), 7.37−7.26 (m, 3H), 7.20−7.10 (m, 2H) 7.08−6.88 (m, 2H), 6.84−6.62 (m, 1.5H), 6.54 (d, J = 9.4 Hz, 0.5H), 5.15 (t, J = 8.8 Hz, 1H), 5.03 (d, J = 2.0 Hz, 0.5H), 5.01 (d, J = 2.1 Hz, 0.5H), 4.56 (s, 0.5H), 4.46 (s, 0.5H), 4.30−4.17 (m, 1H), 3.93 (s, 1.5H), 3.90 (s, 1.5H), 3.01−2.86 (m, 2H), 1.40 (s, 9H), 0.92 (s, 9H). ^{13}C NMR (101 MHz, $CDCl_3$): δ 178.3, 178.2, 171.2, 171.1, 164.8, 164.7, 161.42, 161.38, 155.6, 155.5, 154.7, 154.6, 144.21, 144.19, 140.8, 140.7, 136.52, 136.47, 134.64, 134.60, 130.9, 130.8, 130.3, 130.2, 129.4, 129.3, 129.1, 129.0, 128.63, 128.59, 128.5, 128.04, 127.99, 127.8, 127.7, 126.1, 123.1, 123.0, 110.1, 109.9, 80.4, 56.5, 55.7, 55.6, 52.6, 52.5, 52.4, 37.9, 36.1, 35.9, 28.4, 26.2. HRMS-ESI (m/z) calcd for $C_{35}H_{38}BrN_5O_8Na$ [M + Na]$^+$ 758.1801; found 758.1810.

*Methyl 2-{5-Bromo-2-[(1S)-1-[(2S)-2-{[(tert-butoxy)-carbonyl]amino}-3-(3-methyl-2-oxo-2,3-dihydro-1H-indol-5-yl)propanamido]-2,2-dimethylpropyl]-1,3-oxazol-4-yl}-1,3-oxazole-4-carboxylate (**5b**).* The title compound was prepared according to general procedure D from ester **7b** (410 mg; 1.18 mmol), LiOH (141 mg; 5.88 mmol; 5 equiv) in MeOH/water (5:2 v/v; 7 mL), amine **9** (421 mg; 1.18 mmol; 1 equiv), and EDC × HCl (338 mg; 1.76 mmol; 1.5 equiv) in pyridine (10 mL) in 2 h. Purification by column chromatography on silica gel (gradient elution from 50% to 100% EtOAc in hexanes) afforded **5b** (435 mg, 55%; dr 1:1) as a yellow oil. ^{1}H NMR (400 MHz, MeOH-d_4): δ 8.64 (s, 1H), 7.09 (s, 0.5H), 7.01−6.96 (m, 1H), 6.88 (d, J = 7.9 Hz, 0.5H), 6.63 (d, J = 8.0 Hz, 0.5H), 6.53 (d, J = 7.9 Hz, 0.5H), 4.98 (s, 0.5H), 4.94 (s, 0.5H), 4.43−4.31 (m, 1H), 3.93 (s, 1.5H), 3.92 (s, 1.5H), 3.35 (s, 1H), 2.89−2.81 (m, 2H), 1.42 (s, 9H), 1.33 (d, J = 1.8 Hz, 1.5H), 1.31 (d, J = 1.8 Hz, 1.5H), 0.97 (s, 9H). ^{13}C NMR (101 MHz, MeOH-d_4): δ 183.0, 182.8, 174.2, 165.9, 165.8, 162.7, 162.6, 157.52, 157.49, 156.1, 156.0, 146.34, 146.31, 141.6, 135.3, 132.9, 132.7, 131.84, 131.76, 129.8, 129.7, 128.8, 128.7, 126.0, 125.9, 124.7, 124.5, 110.3, 109.9, 80.53, 80.51, 57.6, 57.5, 56.9, 56.7, 52.6, 42.2, 42.1, 39.0, 36.79, 36.76, 28.7, 26.6, 26.5, 15.5, 15.3. HRMS-ESI (m/z) calcd for $C_{30}H_{36}N_5O_8BrNa$ [M + Na]$^+$ 696.1645; found 696.1661.

*Methyl 2-{5-Bromo-2-[(1S)-1-[(2S)-2-{[(tert-butoxy)-carbonyl]amino}-3-[2-oxo-3-(propan-2-yl)-2,3-dihydro-1H-indol-5-yl]propanamido]-2,2-dimethylpropyl]-1,3-oxazol-4-yl}-1,3-oxazole-4-carboxylate (**5c**).* The title compound was prepared according to general procedure D from ester **7c** (110 mg; 0.29 mmol), LiOH (21 mg; 0.88 mmol; 3 equiv) in MeOH/water (4:1 v/v; 2.5 mL), amine **9** (105 mg; 0.29 mmol; 1 equiv), and EDC × HCl (67 mg; 0.35 mmol; 1.2 equiv) in pyridine (5 mL) in 3 h. Purification by reverse phase column chromatography (gradient elution from 5% to 95% MeCN in water) afforded **5c** (110 mg, 54%; dr 1:1) as a yellow oil. ^{1}H NMR (400 MHz, $CDCl_3$): δ 8.39 (s, 0.5H), 8.33 (s, 0.5H), 8.314 (s, 0.5H), 8.306 (s, 0.5H), 7.10 (s, 0.5H), 7.06 (s, 0.5H), 6.99 (d, J = 8.0 Hz, 0.5H), 6.91 (d, J = 8.0 Hz, 0.5H), 6.83 (d, J = 8.0 Hz, 0.5H), 6.77 (d, J = 8.0 Hz, 0.5H), 6.73 (d, J = 8.0 Hz, 0.5H), 6.67 (d, J = 8.0 Hz, 0.5H), 5.21−5.13 (m, 1H), 5.07 (d, J = 9.4 Hz, 0.5H), 5.06 (d, J = 9.4 Hz, 0.5H), 4.36−4.24 (m, 1H), 3.94 (s, 1.5H), 3.93 (s, 1.5H), 3.29 (d, J = 3.4 Hz, 0.5H), 3.24 (d, J = 3.4 Hz, 0.5H), 3.05−2.93 (m, 2H), 2.41 (sept d, J = 6.9, 3.4 Hz, 1H), 1.42 (s, 4.5H), 1.41 (s, 4.5H), 1.05 (d, J = 1.3 Hz, 3H), 0.95 (s, 9H), 0.88 (d, J = 6.9 Hz, 1.5H), 0.82 (d, J = 6.9 Hz, 1.5H). ^{13}C NMR (101 MHz, $CDCl_3$): δ 179.43, 179.39, 164.9, 164.8, 161.41, 161.38, 155.6, 154.7, 154.7, 144.2, 144.1, 141.0, 134.67, 134.65, 130.3, 130.1, 128.9, 128.8, 128.7, 128.1, 128.0, 125.5, 123.1, 123.0, 109.7, 109.5, 80.4, 56.5, 55.7, 55.6, 52.48, 52.45, 52.1, 52.0, 37.7, 36.1, 36.0, 30.84, 30.79, 28.4, 26.3, 20.0, 19.9, 18.3, 18.1. HRMS-ESI (m/z) calcd for $C_{32}H_{40}N_5O_8BrNa$ [M + Na]$^+$ 724.1958; found 724.1967.

Methyl 2-{5-Bromo-2-[(1S)-1-[(2S)-2-{[(tert-butoxy)-carbonyl]amino}-3-[3-(3,5-dimethylphenyl)-2-oxo-2,3-dihydro-1H-indol-5-yl]propanamido]-2,2-dimethylpropyl]-1,3-

https://doi.org/10.1021/acs.jmedchem.4c00388
J. Med. Chem. 2024, 67, 9227−9259

*oxazol-4-yl)-1,3-oxazole-4-carboxylate (**5d**).* The title compound was prepared according to general procedure D from ester **7d** (600 mg; 1.37 mmol), LiOH (164 mg; 6.84 mmol; 5 equiv) in MeOH/water (4:1 v/v; 6 mL), amine **9** (500 mg; 1.40 mmol; 1 equiv), and EDC × HCl (401 mg; 2.09 mmol; 1.5 equiv) in pyridine (5 mL) in 18 h. Purification by column chromatography on silica gel (gradient elution from 30% to 60% EtOAc in hexanes) afforded **5d** (700 mg, 66%; dr 1:1) as a yellow oil. ^{1}H NMR (400 MHz, $CDCl_3$): δ 8.78 (s, 0.5H), 8.73 (s, 0.5H), 8.28 (s, 0.5H), 8.23 (s, 0.5H), 7.04−6.99 (m, 0.5H), 6.96 (s, 0.5), 6.91−6.87 (m, 2H), 6.77 (d, J = 7.9 Hz, 0.5H), 6.75−6.71 (m, 2H), 6.69 (d, J = 7.9 Hz, 0.5 H), 6.63 (d, J = 9.4 Hz, 0.5 H), 6.54 (d, J = 9.4 Hz, 0.5 H), 5.15 (t, J = 7.9 Hz, 1H), 5.03 (d, J = 2.7 Hz, 0.5H), 5.01 (d, J = 2.8 Hz, 0.5H), 4.47 (s, 0.5H), 4.35 (s, 0.5H), 4.27−4.17 (m, 1H), 3.93 (s, 1.5H), 3.90 (s, 1.5H), 3.00−2.89 (m, 2H), 2.26 (s, 3H), 2.25 (s, 3H), 1.39 (d, J = 1.9 Hz, 9H), 0.93 (s, 9H). ^{13}C NMR (101 MHz, $CDCl_3$): δ 178.8, 178.7, 171.2, 171.1, 164.8, 164.7, 161.42, 161.37, 155.6, 155.5, 154.7, 154.6, 144.2, 140.7, 140.6, 138.5, 136.3, 134.63, 134.60, 130.84, 130.82, 130.7, 129.6, 129.5, 129.21, 129.19, 128.02, 127.96, 126.40, 126.35, 126.1, 126.0, 123.1, 123.0, 110.0, 109.8, 80.4, 56.5, 55.7, 55.6, 52.74, 52.71, 52.5, 52.4, 41.0, 37.9, 36.0, 35.9, 28.4, 26.2, 21.4. HRMS-ESI (m/z) calcd for $C_{37}H_{42}BrN_5O_8Na$ [M + Na]$^+$ 786.2114; found 786.2114.

*Methyl 2-{5-Bromo-2-[(1S)-1-[(2S)-2-{[(tert-butoxy)-carbonyl]amino}-3-[3-(naphthalen-2-yl)-2-oxo-2,3-dihydro-1H-indol-5-yl]propanamido]-2,2-dimethylpropyl]-1,3-oxazol-4-yl}-1,3-oxazole-4-carboxylate (**5e**).* The title compound was prepared according to general procedure D from ester **7e** (300 mg; 0.65 mmol), LiOH (78 mg; 3.26 mmol; 5 equiv) in MeOH/water (3:1 v/v; 4 mL), amine **9** (233 mg; 0.65 mmol; 1 equiv), and EDC × HCl (187 mg; 0.98 mmol; 1.5 equiv) in pyridine (10 mL) in 18 h. Purification by column chromatography on silica gel (gradient elution from 10% to 75% EtOAc in hexanes) was followed by reverse phase column chromatography (gradient elution from 40% to 90% MeCN in water) and afforded **5e** (130 mg, 25%; dr 1:1) as a yellow oil. ^{1}H NMR (400 MHz, $CDCl_3$): δ 8.36−8.29 (m, 1H), 8.27 (s, 0.5H), 8.21 (s, 0.5H), 7.85−7.74 (m, 3H), 7.67 (s, 1H), 7.51−7.42 (m, 2H), 7.22 (dd, J = 8.4, 1.8 Hz, 0.5H), 7.18 (dd, J = 8.5, 1.8 Hz, 0.5H), 7.05−6.98 (m, 1H), 6.98−6.92 (m, 1H), 6.80 (d, J = 8.0 Hz, 0.5H), 6.73 (d, J = 7.9 Hz, 0.5H), 6.57 (d, J = 9.4 Hz, 0.5H), 6.44 (d, J = 9.4 Hz, 0.5H), 5.15−5.06 (m, 1H), 5.03 (d, J = 9.4 Hz, 0.5H), 5.00 (d, J = 9.4 Hz, 0.5H), 4.74 (s, 0.5H), 4.62 (s, 0.5H), 4.26−4.18 (m, 1H), 3.95 (s, 1.5H), 3.90 (s, 1.5H), 3.01−2.88 (m, 2H), 1.38 (s, 4.5H), 1.37 (s, 4.5H), 0.93 (s, 4.5H), 0.90 (s, 4.5H). ^{13}C NMR (101 MHz, $CDCl_3$): δ 177.9, 177.8, 171.0, 170.8, 164.7, 164.6, 161.28, 161.26, 155.41, 155.37, 154.6, 154.5, 144.0, 140.6, 140.5, 134.51, 134.49, 133.8, 133.7, 133.51, 133.50, 132.82, 132.80, 130.82, 130.79, 130.19, 130.15, 129.34, 129.30, 128.84, 128.81, 127.92, 127.90, 127.86, 127.74, 127.66, 126.24, 126.21, 126.14, 126.12, 126.03, 125.99, 125.96, 123.0, 122.9, 110.0, 109.8, 80.3, 56.4, 55.49, 55.46, 52.6, 52.4, 52.3, 37.9, 37.8, 35.9, 35.8, 28.2, 26.13, 26.09. HRMS-ESI (m/z) calcd for $C_{39}H_{40}BrN_5O_8Na$ [M + Na]$^+$ 808.1958; found 808.1940.

*Methyl 2-{5-Bromo-2-[(1S)-1-[(2S)-2-{[(tert-butoxy)-carbonyl]amino}-3-(2-oxo-2,3-dihydro-1H-indol-5-yl)-propanamido]-2,2-dimethylpropyl]-1,3-oxazol-4-yl}-1,3-oxazole-4-carboxylate (**5f**).* The title compound was prepared according to general procedure D from ester **7f** (220 mg; 0.66 mmol), LiOH (47 mg; 1.97 mmol; 3 equiv) in MeOH/water (4:1 v/v; 3.5 mL), amine **9** (237 mg; 0.66 mmol; 1 equiv), and EDC × HCl (165 mg; 0.86 mmol; 1.3 equiv) in pyridine (3 mL) in 18 h. Purification by column chromatography on silica gel (gradient elution from 40% to 70% EtOAc in hexanes) afforded **5f** (135 mg, 31%) as a yellow oil. ^{1}H NMR (400 MHz, $CDCl_3$): δ 8.54 (s, 1H), 8.31 (s, 1H), 7.05 (s, 1H), 6.94 (dd, J = 8.0, 1.7 Hz, 1H), 6.81 (d, J = 9.3 Hz, 1H), 6.67 (d, J = 8.0 Hz, 1H), 5.28 (d, J = 8.2 Hz, 1H), 5.04 (d, J = 9.3 Hz, 1H), 4.34−4.24 (m, 1H), 3.93 (s, 3H), 3.46−3.28 (m, 2H), 2.99 (dd, J = 13.8, 6.8 Hz, 1H), 2.94 (dd, J = 13.8, 8.0 Hz, 1H), 1.43 (s, 9H), 0.94 (s, 9H). ^{13}C NMR (101 MHz, CDCl3) δ 177.4, 171.3, 164.9, 161.4, 155.6, 154.7, 144.2, 141.4, 134.6, 130.6, 128.8, 128.0, 125.8, 125.6, 123.0, 109.8, 80.4, 56.6, 55.7, 52.5, 38.0, 36.2, 36.0, 28.4, 26.3. HRMS-ESI (m/z) calcd for $C_{29}H_{34}BrN_5O_8Na$ [M + Na]$^+$ 682.1488; found 682.1494 $[\alpha]_D^{20}$ +6 (c 0.9, $CHCl_3$).

*Methyl 2-{5-Bromo-2-[(1S)-1-[(2S)-2-{[(tert-butoxy)-carbonyl]amino}-3-(1-methyl-2-oxo-2,3-dihydro-1H-indol-5-yl)propanamido]-2,2-dimethylpropyl]-1,3-oxazol-4-yl}-1,3-oxazole-4-carboxylate (**5g**).* The title compound was prepared according to general procedure D from ester **7g** (2.15 g; 6.17 mmol), LiOH (443 mg; 18.51 mmol; 3 equiv) in MeOH/water (3:2 v/v; 25 mL), amine **9** (2.21 g; 6.17 mmol; 1 equiv), and EDC × HCl (1.42 g; 7.40 mmol; 1.2 equiv) in pyridine (20 mL) in 1 h. Purification by reverse phase column chromatography (gradient elution from 95% to 50% water in MeCN) afforded **5g** (1.80 g, 43%) as a yellow oil. ^{1}H NMR (400 MHz, $CDCl_3$): δ 8.31 (s, 1H), 7.08 (s, 1H), 7.04 (d, J = 8.0 Hz, 1H), 6.60 (d, J = 8.0 Hz, 2H), 5.10−5.05 (m, 1H), 5.03 (d, J = 9.4 Hz, 1H), 4.25 (dd, J = 14.6, 7.2 Hz, 1H), 3.94 (s, 3H), 3.46 (d, J = 22.1 Hz, 1H), 3.38 (d, J = 22.1 Hz, 1H), 3.07 (s, 3H), 3.05−2.94 (m, 2H), 1.42 (s, 9H), 0.94 (s, 9H). ^{13}C NMR (101 MHz, $CDCl_3$): δ 175.0, 171.1, 164.8, 161.3, 155.6, 154.6, 144.2, 144.1, 134.8, 130.5, 128.8, 128.0, 125.5, 125.1, 122.9, 107.9, 80.5, 56.5, 55.7, 52.4, 37.7, 36.01, 35.8, 28.4, 26.3, 26.2. HRMS-ESI (m/z) calcd for $C_{30}H_{37}N_5O_8Br$ [M + H]$^+$ 674.1826; found 674.1823. $[\alpha]_D^{20}$ −18 (c 1.0, MeOH).

*Methyl 2-{5-Bromo-2-[(1S)-1-[(2S)-2-{[(tert-butoxy)-carbonyl]amino}-3-(1-methyl-2-oxo-3-phenyl-2,3-dihydro-1H-indol-5-yl)propanamido]-2,2-dimethylpropyl]-1,3-oxazol-4-yl}-1,3-oxazole-4-carboxylate (**5h**).* The title compound was prepared according to general procedure D from ester **7h** (500 mg; 1.18 mmol), LiOH (141 mg; 5.89 mmol; 5 equiv) in MeOH/water (5:1 v/v; 12 mL), amine **9** (419 mg; 1.17 mmol; 1 equiv), and EDC × HCl (336 mg; 1.75 mmol; 1.5 equiv) in pyridine (10 mL) in 18 h. Purification by column chromatography on silica gel (gradient elution from 40% to 60% EtOAc in hexanes) afforded **5h** (600 mg, 68%; dr 1:1) as a yellow oil. ^{1}H NMR (400 MHz, $CDCl_3$): δ 8.30 (s, 0.5H), 8.23 (s, 0.5H), 7.33−7.21 (m, 3H), 7.17−7.09 (m, 2.5H), 7.05−6.97 (m, 1.5H), 6.71 (d, J = 7.9 Hz, 0.5H) 6.69−6.53 (m, 1.5H), 5.10−4.97 (m, 2H), 4.57 (s, 0.5H), 4.48 (s, 0.5H), 4.27−4.18 (m, 1H), 3.94 (s, 1.5H), 3.92 (s, 1.5H), 3.12 (s, 1.5H), 3.10 (s, 1.5H), 2.01−2.95 (m, 2H), 1.39 (s, 9H), 0.94 (s, 9H). ^{13}C NMR (101 MHz, $CDCl_3$): δ 175.93, 175.86, 171.03, 170.96, 164.8, 164.7, 161.30, 161.25, 155.6, 155.5, 154.6, 144.14, 144.09, 143.5, 143.4, 136.5, 134.8, 134.7, 131.0, 130.9, 129.6, 129.4, 129.3, 129.0, 128.54, 128.51, 128.02, 127.98, 127.7, 127.6, 126.1, 126.0, 123.0, 122.8, 108.1, 107.8, 80.5, 56.4, 55.7, 55.6, 52.42, 52.39, 52.1, 37.6, 37.5, 36.1, 36.0,

https://doi.org/10.1021/acs.jmedchem.4c00388
J. Med. Chem. 2024, 67, 9227−9259

28.4, 26.54, 26.48, 26.3. HRMS-ESI (m/z) calcd for $C_{36}H_{41}BrN_5O_8$ $[M + H]^+$ 750.2161; found 750.2139.

*Methyl 2-{5-Bromo-2-[(1S)-1-[(2S)-2-{[(tert-butoxy)carbonyl]amino}-4-(2-oxo-3-phenyl-2,3-dihydro-1H-indol-5-yl)butanamido]-2,2-dimethylpropyl]-1,3-oxazol-4-yl}-1,3-oxazole-4-carboxylate (**6a**).* The title compound was prepared according to general procedure E from ester **8a** (115 mg; 0.23 mmol), 5% Pd on carbon (49 mg; 0.023 mmol; 0.1 equiv) in EtOAc (5 mL), amine **9** (94 mg; 0.26 mmol; 1.2 equiv), and EDC × HCl (57 mg; 0.30 mmol; 1.3 equiv) in pyridine (2 mL) in 16 h. Purification by column chromatography on silica gel (gradient elution from 100% DCM to 75% Et_2O in DCM) afforded **6a** (114 mg, 66%, dr 1:1) as a white amorphous solid. ^{1}H NMR (400 MHz, $CDCl_3$): δ 8.88 (s, 0.5H), 8.52 (s, 0.5H), 8.29 (s, 0.5H), 8.27 (s, 0.5H), 7.57 (s, 0.5H), 7.35−7.24 (m, 2.5H), 7.28−7.21 (m, 1H), 7.22−7.12 (m, 2H), 7.04−6.95 (m, 1.5H), 6.95−6.88 (m, 1H), 6.78 (d, J = 7.9 Hz, 0.5H), 5.16 (d, J = 7.2 Hz, 1H), 5.11−5.02 (m, 1H), 4.99 (d, J = 8.7 Hz, 0.5H), 4.56 (s, 0.5H), 4.51 (s, 0.5H), 4.17−4.01 (m, 1H), 3.94 (s, 3H), 2.69−2.54 (m, 2H), 2.13−2.02 (m, 1H), 1.93−1.81 (m, 1H), 1.46 (s, 4.5H), 1.43 (s, 4.5H), 0.95 (s, 4.5H), 0.88 (s, 4.5H). ^{13}C NMR (101 MHz, CDCl3): δ 178.2, 178.1, 172.4, 171.9, 165.2, 165.1, 161.43, 161.41, 156.0, 154.92, 154.89, 144.1, 140.4, 140.1, 136.74, 136.66, 135.0, 134.7, 134.6, 130.0, 129.9, 129.2, 129.0, 128.9, 128.7, 128.61, 128.57, 128.1, 128.0, 127.7, 127.6, 125.5, 125.4, 123.14, 123.10, 110.1, 109.6, 80.5, 80.4, 56.3, 56.0, 53.4, 53.0, 52.8, 52.7, 52.5, 35.8, 35.5, 33.1, 32.9, 31.5, 31.3, 28.4, 26.3. HRMS-ESI (m/z) calcd for $C_{36}H_{40}N_5O_8BrNa$ $[M + Na]^+$ 772.1958; found 772.1967.

*Methyl 2-{5-Bromo-2-[(1S)-1-[(2S)-2-{[(tert-butoxy)carbonyl]amino}-4-(3-methyl-2-oxo-2,3-dihydro-1H-indol-5-yl)butanamido]-2,2-dimethylpropyl]-1,3-oxazol-4-yl}-1,3-oxazole-4-carboxylate (**6b**).* The title compound was prepared according to general procedure E from ester **8b** (325 mg; 0.74 mmol), 10% Pd on carbon (79 mg; 0.074 mmol; 0.1 equiv) in EtOAc (15 mL), amine **9** (283 mg; 0.79 mmol; 1.1 equiv), and EDC × HCl (179 mg; 0.93 mmol; 1.3 equiv) in pyridine (5 mL) in 4 h. Product **6b** was purified by column chromatography on silica gel (gradient elution from 100% hexanes to 100% EtOAc) to afford 308 mg (62%; dr 1:1) as a white amorphous solid. ^{1}H NMR (400 MHz, MeOH-d_4): δ 8.62 (s, 0.5H), 8.62 (s, 0.5H), 7.05 (d, J = 10.3 Hz, 1H), 6.99 (d, J = 8.0 Hz, 1H), 6.75 (d, J = 8.0 Hz, 1H), 5.03 (s, 0.5H), 5.02 (s, 0.5H), 4.16−4.10 (m, 1H), 3.91 (s, 1.5H), 3.91 (s, 1.5H), 3.42−3.36 (m, 1H), 2.69−2.53 (m, 2H), 2.04−1.93 (m, 1H), 1.92−1.81 (m, 1H), 1.45 (s, 9H), 1.38 (d, J = 4.5 Hz, 1.5H), 1.37 (d, J = 4.5 Hz, 1.5H), 1.06 (s, 9H). ^{13}C NMR (101 MHz, MeOH-d_4): δ 183.3, 175.1, 166.4, 162.6, 157.9, 156.2, 146.2, 141.2, 136.5, 135.3, 133.1, 129.0, 128.9, 125.0, 124.8, 110.6, 80.7, 57.4, 55.3, 52.6, 42.4, 36.4, 35.0, 32.7, 28.7, 26.7, 15.7, 15.6. HRMS-ESI (m/z) calcd for $C_{31}H_{38}N_5O_8BrNa$ $[M + Na]^+$ 710.1801; found 710.1805.

*Methyl 2-{5-Bromo-2-[(1S)-1-[(2S)-2-{[(tert-butoxy)carbonyl]amino}-4-(1,3-dimethyl-2-oxo-2,3-dihydro-1H-indol-5-yl)butanamido]-2,2-dimethylpropyl]-1,3-oxazol-4-yl}-1,3-oxazole-4-carboxylate (**6i**).* The title compound was prepared according to general procedure E from ester **8i** (363 mg; 0.80 mmol), 10% Pd on carbon (85 mg; 0.080 mmol; 0.1 equiv) in EtOAc (16 mL), amine **9** (304 mg; 0.85 mmol; 1.1 equiv), and EDC × HCl (193 mg; 1.00 mmol; 1.3 equiv) in pyridine (5 mL) in 4 h. Purification by column chromatography on silica gel (gradient elution from 100% hexanes to 100% EtOAc) afforded **6i** (396 mg, 73%; dr 1:1) as a white amorphous solid. ^{1}H NMR (400 MHz, MeOH-d_4): δ 8.62 (s, 1H), 7.14−7.04 (m, 2H), 6.82 (d, J = 8.3 Hz, 1H), 5.03 (s, 0.5H), 5.03 (s, 0.5H), 4.15 (d, J = 8.4 Hz, 0.5H), 4.13 (d, J = 8.4 Hz, 0.5H), 3.91 (s, 1.5H), 3.90 (s, 1.5H), 3.45−3.36 (m, 1H), 3.16 (s, 3H), 2.70−2.56 (m, 2H), 2.05−1.95 (m, 1H), 1.93−1.82 (m, 1H), 1.45 (s, 9H), 1.38 (d, J = 4.1 Hz, 1.5H), 1.36 (d, J = 4.1 Hz, 1.5H), 1.06 (s, 9H). ^{13}C NMR (101 MHz, MeOH-d_4): δ 180.9, 175.0, 166.5, 162.6, 157.9, 156.2, 146.2, 143.1, 137.1, 135.3, 132.2, 132.1, 129.02, 128.96, 124.8, 109.4, 80.7, 57.4, 55.2, 52.6, 41.9, 36.4, 35.0, 32.6, 28.7, 26.7, 26.5. HRMS-ESI (m/z) calcd for $C_{32}H_{40}N_5O_8BrNa$ $[M + Na]^+$ 724.1958; found 724.1948.

*Methyl 2-[(1S,6S,9S)-9-{[(tert-Butoxy)carbonyl]amino}-6-tert-butyl-8,16-dioxo-1-phenyl-19-oxa-4,7,15-triazatetracyclo[9.5.2.1^{2,5}.0^{14,17}]nonadeca-2,4,11,13,17-pentaen-3-yl]-1,3-oxazole-4-carboxylate (**3a**).* The title compound was prepared according to general procedure F from amide **5a** (400 mg; 0.54 mmol) and Na_2CO_3 (173 mg; 1.63 mmol; 3 equiv) in DMF (40 mL) in 4 h. Purification by column chromatography on silica gel (gradient elution from 20% to 50% EtOAc in hexanes) afforded **3a** (230 mg, 65%, dr 99:1) as a white amorphous solid. ^{1}H NMR (400 MHz, $CDCl_3$): δ 9.15 (s, 1H), 7.89 (s, 1H), 7.47−7.37 (m, 2H), 7.32−7.26 (m, 3H), 7.21 (s, 1H), 7.07 (dd, J = 8.0, 1.8 Hz, 1H), 6.77 (d, J = 8.0 Hz, 1H), 6.31 (d, J = 8.6 Hz, 1H), 5.38 (d, J = 9.1 Hz, 1H), 4.94 (d, J = 8.6 Hz, 1H), 3.99 (ddd, J = 12.3, 9.2, 3.5 Hz, 1H), 3.90 (s, 3H), 3.16 (dd, J = 12.3, 12.3 Hz, 1H), 2.80 (dd, J = 12.3, 3.5 Hz, 1H), 1.43 (s, 9H), 1.03 (s, 9H). ^{13}C NMR (101 MHz, $CDCl_3$): δ 175.2, 172.2, 162.7, 161.6, 155.3, 155.2, 150.5, 144.5, 139.6, 135.4, 134.2, 132.5, 131.5, 129.9, 129.7, 129.0, 128.5, 127.6, 127.3, 111.2, 80.4, 59.1, 58.2, 57.3, 52.4, 38.2, 33.3, 28.4, 26.5. HRMS-ESI (m/z) calcd for $C_{35}H_{38}N_5O_8$ $[M + H]^+$ 656.2720; found 656.2740. $[\alpha]_D^{20}$ −203 (c 1.0, $CHCl_3$).

*Methyl 2-[(1S,6S,9S)-9-{[(tert-Butoxy)carbonyl]amino}-6-tert-butyl-1-methyl-8,16-dioxo-19-oxa-4,7,15-triazatetracyclo[9.5.2.1^{2,5}.0^{14,17}]nonadeca-2,4,11,13,17-pentaen-3-yl]-1,3-oxazole-4-carboxylate (**3b**).* The title compound was prepared according to general procedure F from amide **5b** (810 mg; 1.20 mmol) and Na_2CO_3 (636 mg; 6.00 mmol; 5 equiv) in DMF (25 mL) in 3 h. Purification by reverse phase column chromatography (gradient elution from 10% to 50% MeCN in water) afforded **3b** (540 mg, 76%) of a single diastereomer as a white amorphous solid. ^{1}H NMR (400 MHz, $CDCl_3$): δ 9.02 (s, 1H), 8.33 (s, 1H), 7.08 (dd, J = 8.0, 1.7 Hz, 1H), 6.81 (d, J = 8.0 Hz, 1H), 6.77 (s, 1H), 6.11 (d, J = 7.4 Hz, 1H), 5.45 (d, J = 9.2 Hz, 1H), 4.64 (d, J = 7.3 Hz, 1H), 4.08−3.98 (m, 1H), 3.94 (s, 3H), 3.04 (dd, J = 12.3, 12.3 Hz, 1H), 2.85 (dd, J = 12.3, 3.8 Hz, 1H), 1.97 (s, 3H), 1.44 (s, 9H), 0.93 (s, 9H). ^{13}C NMR (101 MHz, $CDCl_3$): δ 177.1, 171.8, 161.5, 161.5, 155.6, 155.3, 150.9, 144.2, 139.8, 134.8, 134.6, 131.2, 129.3, 128.6, 127.9, 111.1, 80.3, 58.3, 58.2, 52.3, 50.6, 38.2, 33.3, 28.3, 26.4, 20.0. HRMS-ESI (m/z) calcd for $C_{30}H_{35}N_5O_8Na$ $[M + Na]^+$ 616.2383; found 616.2386. $[\alpha]_D^{20}$ −230 (c 1.5, MeOH).

*Methyl 2-[(1S,6S,9S)-9-{[(tert-Butoxy)carbonyl]amino}-6-tert-butyl-8,16-dioxo-1-(propan-2-yl)-19-oxa-4,7,15-triazatetracyclo[9.5.2.1^{2,5}.0^{14,17}]nonadeca-2,4,11,13,17-pentaen-3-yl]-1,3-oxazole-4-carboxylate (**3c**).* The title compound was prepared according to general procedure F from amide **5c** (110 mg; 0.16 mmol) and K_3PO_4 (166 mg; 0.78

https://doi.org/10.1021/acs.jmedchem.4c00388
J. Med. Chem. 2024, 67, 9227−9259

mmol; 5 equiv) in DMF (5 mL) in 60 h. Purification by reverse phase column chromatography (gradient elution from 5% to 95% MeCN in water) afforded **3c** (80 mg, 82%) of a single diastereomer as a white amorphous solid. ^{1}H NMR (400 MHz, $CDCl_3$): δ 8.32 (s, 1H), 8.07 (s, 1H), 7.13 (dd, J = 8.0, 1.7 Hz, 1H), 7.04 (d, J = 1.7 Hz, 1H), 6.80 (d, J = 8.0 Hz, 1H), 5.86 (d, J = 8.0 Hz, 1H), 5.22 (d, J = 9.3 Hz, 1H), 4.80 (d, J = 8.0 Hz, 1H), 3.98−3.89 (m, 1H), 3.94 (s, 3H), 3.34 (sept, J = 6.7 Hz, 1H), 3.13 (dd, J = 12.1, 12.1 Hz, 1H), 2.85 (dd, J = 12.1, 3.6 Hz, 1H), 1.44 (s, 9H), 1.07−0.95 (m, 6H), 1.00 (s, 9H). ^{13}C NMR (101 MHz, $CDCl_3$): δ 176.1, 171.7, 161.5, 161.0, 155.6, 155.2, 149.3, 144.3, 140.5, 134.5, 131.1, 130.7, 130.0, 129.3, 127.1, 110.6, 80.4, 59.6, 58.4, 57.5, 52.2, 38.2, 33.4, 31.6, 28.3, 26.4, 18.0, 17.5. HRMS-ESI (m/z) calcd for $C_{32}H_{40}N_5O_8$ $[M + H]^+$ 622.2877; found 622.2886. $[\alpha]_D^{20}$ −18 (c 0.6, $CHCl_3$).

*Methyl 2-[(1S,6S,9S)-9-{[(tert-Butoxy)carbonyl]amino}-6-tert-butyl-1-(3,5-dimethylphenyl)-8,16-dioxo-19-oxa-4,7,15-triazatetracyclo[9.5.2.1^{2,5}.0^{14,17}]nonadeca-2,4,11,13,17-pentaen-3-yl]-1,3-oxazole-4-carboxylate (**3d**).* The title compound was prepared according to general procedure F from amide **5d** (600 mg; 0.78 mmol) and Na_2CO_3 (249 mg; 2.35 mmol; 3 equiv) in DMF (30 mL) in 18 h. Purification by column chromatography on silica gel (gradient elution from 20% to 50% EtOAc in hexanes) afforded **3d** (322 mg, 60%) of a single distereomer as a white amorphous solid. ^{1}H NMR (400 MHz, $CDCl_3$): δ 9.11 (s, 1H), 7.95 (s, 1H), 7.24−7.18 (m, 1H), 7.07 (dd, J = 8.0, 1.7 Hz, 1H), 6.97 (s, 2H), 6.90 (s, 1H), 6.77 (d, J = 8.0 Hz, 1H), 6.33 (d, J = 8.9 Hz, 1H), 5.35 (d, J = 9.2 Hz, 1H), 5.00 (d, J = 8.9 Hz, 1H), 3.98 (ddd, J = 12.3, 9.2, 3.4 Hz, 1H), 3.91 (s, 3H), 3.18 (dd, J = 12.3, 12.3 Hz, 1H), 2.80 (dd, J = 12.3, 3.4 Hz, 1H), 2.23 (s, 6H), 1.44 (s, 9H), 1.05 (s, 9H). ^{13}C NMR (101 MHz, $CDCl_3$): δ 175.6, 172.3, 162.8, 161.6, 155.33, 155.30, 150.6, 144.6, 139.5, 138.7, 135.0, 134.0, 132.7, 131.4, 130.3, 129.8, 129.7, 127.0, 125.2, 111.2, 80.5, 59.2, 58.2, 57.2, 52.5, 38.3, 33.3, 28.4, 26.5, 21.5. HRMS-ESI (m/z) calcd for $C_{37}H_{42}N_5O_8$ $[M + H]^+$ 684.3033; found 684.3025. $[\alpha]_D^{20}$ −224 (c 1.0, $CHCl_3$).

*Methyl 2-[(1S,6S,9S)-9-{[(tert-Butoxy)carbonyl]amino}-6-tert-butyl-1-(naphthalen-2-yl)-8,16-dioxo-19-oxa-4,7,15-triazatetracyclo[9.5.2.1^{2,5}.0^{14,17}]nonadeca-2,4,11,13,17-pentaen-3-yl]-1,3-oxazole-4-carboxylate (**3e**).* The title compound was prepared according to general procedure F from amide **5e** (100 mg; 0.13 mmol) and K_3PO_4 (108 mg; 0.51 mmol; 4 equiv) in DMF (10 mL) in 48 h. Purification by column chromatography on silica gel (gradient elution from 30% to 70% EtOAc in hexanes) afforded **3e** (55 mg, 61%) of a single diastereomer as a light yellow amorphous solid. ^{1}H NMR (400 MHz, $CDCl_3$): δ 9.17 (d, J = 5.9 Hz, 1H), 7.94 (s, 1H), 7.81−7.71 (m, 4H), 7.50−7.43 (m, 3H), 7.28 (s, 1H), 7.08 (dd, J = 8.1, 1.7 Hz, 1H), 6.80 (d, J = 8.0 Hz, 1H), 6.33 (d, J = 7.2 Hz, 1H), 5.36 (d, J = 9.2 Hz, 1H), 4.97 (d, J = 8.7 Hz, 1H), 4.01 (ddd, J = 12.3, 9.2, 3.5 Hz, 1H), 3.84 (s, 3H), 3.18 (dd, J = 12.3, 12.3 Hz, 1H), 2.81 (dd, J = 12.3, 3.5 Hz, 1H), 1.44 (s, 9H), 1.05 (s, 9H). ^{13}C NMR (101 MHz, $CDCl_3$): δ 175.1, 172.1, 162.7, 161.4, 155.2, 154.9, 150.3, 144.3, 139.5, 134.0, 133.1, 132.9, 132.4, 131.4, 129.9, 129.7, 128.8, 128.2, 127.5, 127.4, 126.9, 126.6, 126.5, 124.7, 111.2, 80.3, 59.1, 58.1, 57.2, 52.3, 38.1, 33.2, 28.3, 26.4. HRMS-ESI (m/z) calcd for $C_{39}H_{40}N_5O_8$ $[M + H]^+$ 706.2877; found 706.2896. $[\alpha]_D^{20}$ −242 (c 0.4, $CHCl_3$).

*Methyl 2-[(1S,6S,9S)-9-{[(tert-Butoxy)carbonyl]amino}-6-tert-butyl-8,16-dioxo-19-oxa-4,7,15-triazatetracyclo[9.5.2.1^{2,5}.0^{14,17}]nonadeca-2,4,11,13,17-pentaen-3-yl]-1,3-oxazole-4-carboxylate (**3f**).* The title compound was prepared according to general procedure F, from amide **5f** (85 mg; 0.13 mmol) and Na_2CO_3 (41 mg; 0.39 mmol; 3 equiv) in DMF (8 mL) in 60 h. Purification by column chromatography on silica gel (gradient elution from 30% to 60% EtOAc in hexanes) afforded **3f** (40 mg, 54%) of a single diastereomer as a white amorphous solid. ^{1}H NMR (400 MHz, $CDCl_3$): δ 8.76 (s, 1H), 8.32 (s, 1H), 7.12−7.06 (m, 1H), 6.83 (d, J = 8.0 Hz, 1H), 6.58 (s, 1H), 6.06 (d, J = 6.8 Hz, 1H), 5.60 (s, 1H), 5.30 (d, J = 9.3 Hz, 1H), 4.62 (d, J = 6.8 Hz, 1H), 3.97−3.89 (m, 4H), 3.02 (dd, J = 12.2, 12.2 Hz, 1H), 2.76 (dd, J = 12.2, 3.6 Hz, 1H), 1.43 (s, 9H), 0.94 (s, 9H). ^{13}C NMR (101 MHz, $CDCl_3$): δ 174.4, 171.8, 163.6, 161.6, 155.9, 155.4, 148.0, 143.9, 141.7, 134.6, 131.7, 129.7, 129.6, 129.5, 129.4, 111.3, 80.6, 59.2, 58.2, 52.4, 45.9, 37.8, 33.3, 28.4, 26.6. HRMS-ESI (m/z) calcd for $C_{29}H_{34}N_5O_8$ $[M + H]^+$ 580.2407; found 580.2420. $[\alpha]_D^{20}$ −77 (c 0.7, $CHCl_3$).

*Methyl 2-[(1S,6S,9S)-9-{[(tert-Butoxy)carbonyl]amino}-6-tert-butyl-15-methyl-8,16-dioxo-19-oxa-4,7,15-triazatetracyclo[9.5.2.1^{2,5}.0^{14,17}]nonadeca-2,4,11,13,17-pentaen-3-yl]-1,3-oxazole-4-carboxylate (**3g**).* The title compound was prepared according to general procedure F from amide **5g** (800 mg; 1.19 mmol) and K_3PO_4 (755 mg; 3.56 mmol; 3 equiv) in DMF (20 mL) in 1 h. Purification by reverse phase column chromatography (gradient elution from 5% to 95% MeCN in water) afforded **3g** (570 mg, 81%) of a single diastereomer as a white amorphous solid. ^{1}H NMR (300 MHz, $CDCl_3$): δ 8.33 (s, 1H), 7.24 (d, J = 8.0 Hz, 1H), 6.85 (d, J = 8.0 Hz, 1H), 6.63 (s, 1H), 5.75 (d, J = 7.0 Hz, 1H), 5.65 (s, 1H), 5.12 (d, J = 9.3 Hz, 1H), 4.63 (d, J = 7.0 Hz, 1H), 3.93 (s, 3H), δ 3.85 (ddd, J = 12.2, 9.3, 3.4 Hz, 1H), 3.26 (s, 3H), 3.08 (dd, J = 12.2, 12.2 Hz, 1H), 2.80 (dd, J = 12.2, 3.4 Hz, 1H), 1.43 (s, 9H), 0.95 (s, 9H). ^{13}C NMR (101 MHz, $CDCl_3$): δ 172.4, 171.6, 163.5, 161.6, 155.9, 155.3, 148.1, 144.3, 143.9, 134.7, 132.0, 129.7, 129.6, 129.5, 128.8, 109.5, 80.5, 59.2, 58.5, 52.3, 45.6, 37.7, 33.3, 28.4, 27.0, 26.6. HRMS-ESI (m/z) calcd for $C_{30}H_{36}N_5O_8$ $[M + H]^+$ 594.2564; found 594.2560. $[\alpha]_D^{20}$ −50 (c 1.0, $CHCl_3$).

*Methyl 2-[(1S,6S,9S)-9-{[(tert-Butoxy)carbonyl]amino}-6-tert-butyl-15-methyl-8,16-dioxo-1-phenyl-19-oxa-4,7,15-triazatetracyclo[9.5.2.1^{2,5}.0^{14,17}]nonadeca-2,4,11,13,17-pentaen-3-yl]-1,3-oxazole-4-carboxylate (**3h**).* The title compound was prepared according to general procedure F from amide **5h** (600 mg; 0.80 mmol) and Na_2CO_3 (245 mg; 2.40 mmol; 3 equiv) in DMF (40 mL) in 3 h. Product **3h** was purified by column chromatography on silica gel (gradient elution from 20% to 50% EtOAc in hexanes) to afford 400 mg (75%) of a single diastereomer as a white amorphous solid. ^{1}H NMR (400 MHz, $CDCl_3$): δ 8.12 (s, 1H), 7.43−7.36 (m, 3H), 7.34−7.27 (m, 3H), 7.21 (dd, J = 8.0, 1.7 Hz, 1H), 6.79 (d, J = 8.0 Hz, 1H), 5.65 (d, J = 9.1 Hz, 1H), 5.17 (d, J = 9.1 Hz, 1H), 5.02 (d, J = 9.1 Hz, 1H), 3.89 (s, 3H), 3.79 (ddd, J = 12.3, 9.1, 3.5 Hz, 1H), 3.22 (dd, J = 12.3, 12.3 Hz, 1H), 3.19 (s, 3H), 2.80 (dd, J = 12.3, 3.5 Hz, 1H), 1.43 (s, 9H), 1.06 (s, 9H). ^{13}C NMR (101 MHz, $CDCl_3$): δ 172.4, 171.9, 162.8, 161.5, 155.2, 154.9, 150.8, 144.6, 142.4, 135.6, 134.1, 131.4, 131.1, 129.8, 129.5, 129.0, 128.4, 127.8, 126.5, 109.3, 80.4, 58.6, 58.5, 56.6, 52.2, 38.0, 33.1, 28.4, 27.0, 26.4. HRMS-ESI (m/z) calcd for

https://doi.org/10.1021/acs.jmedchem.4c00388
J. Med. Chem. 2024, 67, 9227−9259

$C_{36}H_{40}N_5O_8$ $[M + H]^+$ 670.2877; found 670.2883. $[\alpha]_D^{20}$ −247 (c 1.0, $CHCl_3$).

*Methyl 2-[(1S,6S,9S)-9-{[(tert-Butoxy)carbonyl]amino}-6-tert-butyl-1,15-dimethyl-8,16-dioxo-19-oxa-4,7,15-triazatetracyclo[9.5.2.1^{2,5}.0^{14,17}]nonadeca-2,4,11,13,17-pentaen-3-yl]-1,3-oxazole-4-carboxylate (**3i**).* The title compound was prepared according to general procedure G from macrocycle **3g** (96 mg; 0.16 mmol), NaH (60% suspension in mineral oil; 6.5 mg; 0.16 mmol; 1 equiv), and methyl iodide (30 μL; 0.48 mmol; 3 equiv) in DMF (2 mL). Product **3i** was formed as a mixture of diastereomers (dr 86:14). Purification by column chromatography on silica gel (gradient elution from 30% EtOAc in DCM) afforded the major diastereomer (*S,S,S*)-**3i** (68 mg, 69%, dr 99:1) as a white amorphous solid. ^{1}H NMR (400 MHz, $CDCl_3$): δ 8.36 (s, 1H), 7.24 (d, *J* = 8.0 Hz, 1H), 6.91 (s, 1H), 6.84 (d, *J* = 8.0 Hz, 1H), 5.57 (d, *J* = 7.6 Hz, 1H), 5.17 (d, *J* = 9.3 Hz, 1H), 4.71 (d, *J* = 7.6 Hz, 1H), 3.93 (s, 3H), δ 3.87 (ddd, *J* = 12.0, 9.3, 3.7 Hz, 1H), 3.22 (s, 3H), 3.10 (dd, *J* = 12.0, 12.0 Hz, 1H), 2.88 (dd, *J* = 12.0, 3.7 Hz, 1H), 1.98 (s, 3H), 1.43 (s, 9H), 0.95 (s, 9H). ^{13}C NMR (101 MHz, $CDCl_3$): δ 175.0, 171.6, 161.6, 161.3, 155.6, 155.3, 151.0, 144.4, 142.4, 134.7, 133.8, 131.5, 129.4, 128.6, 127.7, 109.2, 80.5, 58.7, 58.1, 52.3, 50.2, 38.2, 33.4, 28.4, 26.9, 26.5, 20.4. HRMS-ESI (*m*/*z*) calcd for $C_{31}H_{38}N_5O_8$ $[M + H]^+$ 608.2720; found 608.2722. $[\alpha]_D^{20}$ −42 (c 1.0, $CHCl_3$).

*Methyl 2-[(1S,6S,9S)-9-{[(tert-Butoxy)carbonyl]amino}-6-tert-butyl-1-ethyl-15-methyl-8,16-dioxo-19-oxa-4,7,15-triazatetracyclo[9.5.2.1^{2,5}.0^{14,17}]nonadeca-2,4,11,13,17-pentaen-3-yl]-1,3-oxazole-4-carboxylate (**3j**).* The title compound was prepared according to general procedure G from macrocycle **3g** (100 mg; 0.17 mmol), NaH (60% suspension in mineral oil; 6.7 mg; 0.17 mmol; 1 equiv), and ethyl iodide (40 μL; 0.51 mmol; 3 equiv) in DMF (2 mL). Product **3j** formed as mixture of diastereomers (dr 89:11) and was purified by column chromatography on silica gel (gradient elution from 20% EtOAc in DCM) to afford of the major diastereomer (*S,S,S*)-**3j** (65 mg, 62%; dr 99:1) as a white amorphous solid. ^{1}H NMR (400 MHz, $CDCl_3$): δ 8.36 (s, 1H), 7.24 (dd, *J* = 7.9, 1.4 Hz, 1H), 6.96 (d, *J* = 1.4 Hz, 1H), 6.83 (d, *J* = 7.9 Hz, 1H), 5.65 (d, *J* = 7.9 Hz, 1H), 5.20 (d, *J* = 9.2 Hz, 1H), 4.75 (d, *J* = 7.9 Hz, 1H), 3.93 (s, 3H), 3.92−3.83 (m, 1H), 3.20 (s, 3H), 3.13 (dd, *J* = 12.1, 12.1 Hz, 1H), 2.87 (dd, *J* = 12.1, 3.5 Hz, 1H), 2.75 (dq, *J* = 14.5, 7.3 Hz, 1H), 2.31 (dq, *J* = 14.5, 7.3 Hz, 1H), 1.43 (s, 9H), 0.97 (s, 9H), 0.82 (t, *J* = 7.3 Hz, 3H). ^{13}C NMR (101 MHz, $CDCl_3$): δ 174.2, 171.6, 161.5, 161.1, 155.5, 155.2, 150.2, 144.3, 143.1, 134.5, 131.2, 131.1, 129.3, 129.1, 127.2, 109.0, 80.4, 58.5, 57.7, 55.3, 52.2, 38.1, 33.3, 28.3, 26.7, 26.5, 26.4, 8.9. HRMS-ESI (*m*/*z*) calcd for $C_{32}H_{40}N_5O_8$ $[M + H]^+$ 622.2877; found 622.2878. $[\alpha]_D^{20}$ −40 (c 1.0, $CHCl_3$).

*Methyl 2-[(1S,6S,9S)-1-Benzyl-9-{[(tert-butoxy)carbonyl]-amino}-6-tert-butyl-15-methyl-8,16-dioxo-19-oxa-4,7,15-triazatetracyclo[9.5.2.1^{2,5}.0^{14,17}]nonadeca-2,4,11,13,17-pentaen-3-yl]-1,3-oxazole-4-carboxylate (**3k**).* The title compound was prepared according to general procedure G from macrocycle **3g** (55 mg; 0.093 mmol), NaH (60% suspension in mineral oil; 3.7 mg; 0.093 mmol; 1 equiv), and benzyl bromide (33 μL; 0.28 mmol; 3 equiv) in DMF (2 mL). Product **3k** formed as mixture of diastereomers (dr 92:8) and was purified by column chromatography on silica gel (gradient elution from 30% EtOAc in DCM) to afford (*S,S,S*)-**3k** (45 mg, 71%; dr 99:1) as a white amorphous solid. ^{1}H NMR (400 MHz, $CDCl_3$): δ 8.40 (s, 1H), 7.14 (dd, *J* = 8.0, 1.4 Hz, 1H), 7.11−7.04 (m, 3H), 7.04−6.99 (m, 3H), 6.58 (d, *J* = 8.0 Hz, 1H), 5.58 (d, *J* = 8.0 Hz, 1H), 5.18 (d, *J* = 9.2 Hz, 1H), 4.77 (d, *J* = 8.0 Hz, 1H), 4.36 (d, *J* = 13.0 Hz, 1H), 3.93 (s, 3H), 3.89−3.80 (m, 1H), 3.37 (d, *J* = 13.0 Hz, 1H), 3.16 (dd, *J* = 12.1, 12.1 Hz, 1H), 2.94 (s, 3H), 2.86 (dd, *J* = 12.1, 3.6 Hz, 1H), 1.43 (s, 9H), 0.98 (s, 9H). ^{13}C NMR (101 MHz, $CDCl_3$): δ 173.6, 171.8, 161.6, 161.2, 155.6, 155.3, 150.1, 144.4, 142.8, 134.7, 131.0, 130.8, 130.6, 130.5, 129.4, 129.3, 127.9, 127.7, 127.1, 109.0, 80.5, 58.7, 57.9, 56.2, 52.3, 39.4, 38.2, 33.5, 28.4, 26.6, 26.5. HRMS-ESI (*m*/*z*) calcd for $C_{37}H_{42}N_5O_8$ $[M + H]^+$ 684.3033; found 684.3050. $[\alpha]_D^{20}$ −61 (c 1.0, $CHCl_3$).

*Methyl 2-[(1S,6S,9S)-6-tert-Butyl-9-[(2S)-2-hydroxy-3-methylbutanamido]-8,16-dioxo-1-phenyl-19-oxa-4,7,15-triazatetracyclo[9.5.2.1^{2,5}.0^{14,17}]nonadeca-2,4,11,13,17-pentaen-3-yl]-1,3-oxazole-4-carboxylate (**14a**).* The title compound was prepared according to general procedure H from macrocycle **3a** (50 mg; 0.076 mmol) and TFA (117 μL; 1.53 mmol; 20 equiv) in DCM (0.9 mL) within 1 h, followed by treatment with (*S*)-2-hydroxy-3-methylbutanoic acid (13 mg; 0.11 mmol; 1.5 equiv), EDC × HCl (26 mg; 0.14 mmol; 1.8 equiv), HOBt (31 mg; 0.23 mmol; 3 equiv), and DIPEA (65 μL; 0.38 mmol; 5 equiv) in DMF (1 mL) for 1 h. Purification by reverse phase column chromatography (gradient elution from 10% to 95% MeCN in water) afforded (*S,S,S*)−**14a** (35 mg, 71%, dr 99:1) as a white amorphous solid. ^{1}H NMR (400 MHz, $CDCl_3$): δ 9.50 (s, 1H), 7.82 (s, 1H), 7.65 (d, *J* = 8.9 Hz, 1H), 7.45−7.35 (m, 2H), 7.26−7.21 (m, 2H), 7.13 (s, 1H), 7.03 (d, *J* = 8.1, 1H), 6.84 (d, *J* = 7.9 Hz, 1H), 6.75 (d, *J* = 7.8 Hz, 1H), 4.82 (d, *J* = 7.8 Hz, 1H), 4.56−4.46 (m, 1H), 4.26 (s, 1H), 4.08 (d, *J* = 2.7, 1H), 3.89 (s, 3H), 3.25 (dd, *J* = 12.2, 12.2 Hz, 1H), 2.85−2.71 (m, 1H), 2.25−2.15 (m, 1H), 1.04 (d, *J* = 6.8 Hz, 3H), 1.00 (s, 9H), 0.87 (d, *J* = 6.8 Hz, 3H). ^{13}C NMR (101 MHz, $CDCl_3$): δ 175.2, 173.4, 172.2, 162.2, 161.6, 155.2, 150.7, 144.4, 139.9, 135.4, 134.1, 133.0, 130.9, 129.8, 129.7, 129.0, 128.4, 127.7, 127.3, 111.5, 76.1, 59.0, 58.1, 56.1, 52.5, 38.4, 33.4, 32.0, 26.6, 19.3, 15.6. HRMS-ESI (*m*/*z*) calcd for $C_{35}H_{38}N_5O_8$ $[M + H]^+$ 656.2720; found 656.2737. $[\alpha]_D^{20}$ −260 (c 1.0, MeOH).

*Methyl 2-[(1S,6S,9S)-6-tert-Butyl-9-[(2S)-2-hydroxy-3-methylbutanamido]-1-methyl-8,16-dioxo-19-oxa-4,7,15-triazatetracyclo[9.5.2.1^{2,5}.0^{14,17}]nonadeca-2,4,11,13,17-pentaen-3-yl]-1,3-oxazole-4-carboxylate (**14b**).* The title compound was prepared according to general procedure H, from macrocycle **3b** (110 mg; 0.185 mmol), TFA (427 μL; 5.56 mmol; 30 equiv) in DCM (2 mL) within 2 h, followed by treatment with (*S*)-2-hydroxy-3-methylbutanoic acid (24 mg; 0.20 mmol; 1.1 equiv), EDC × HCl (57 mg; 0.30 mmol; 1.6 equiv), HOBt (85 mg; 0.56 mmol; 3 equiv), and DIPEA (128 μL; 0.74 mmol; 4 equiv) in DMF (5 mL) for 18 h. Purification by reverse phase column chromatography (gradient elution from 20% to 100% MeCN in water) afforded (*S,S,S*)−**14b** (71 mg, 65%; dr 99:1) as a white amorphous solid. ^{1}H NMR (400 MHz, MeOH-d_4): δ 8.72 (s, 1H), 7.29 (dd, *J* = 8.0, 1.8 Hz, 1H), 6.96 (d, *J* = 8.0 Hz, 1H), 6.81 (d, *J* = 1.6 Hz, 1H), 4.63 (s, 1H), 4.54 (dd, *J* = 11.6, 4.2 Hz, 1H), 3.94 (s, 3H), 3.88 (d, *J* = 3.7 Hz, 1H), 3.05 (dd, *J* = 12.0, 12.0 Hz, 1H), 2.89 (dd, *J* = 12.5, 4.2 Hz, 1H), 2.15−2.05 (m, 1H), 1.98 (s, 3H), 1.02 (d, *J* = 7.0 Hz, 3H), 0.98 (s, 9H), 0.91 (d, *J* = 6.8 Hz, 3H). ^{13}C NMR (101 MHz, MeOH-d_4): δ 178.9, 175.8, 173.7, 163.7, 162.8, 156.9, 152.8, 146.5, 141.7, 136.2, 135.3, 132.2, 131.0, 129.4, 128.2, 112.2, 76.8, 60.0, 56.6, 52.6, 52.1, 39.3, 34.2, 33.1,

https://doi.org/10.1021/acs.jmedchem.4c00388
J. Med. Chem. 2024, 67, 9227−9259

26.7, 20.5, 19.5, 16.3. HRMS-ESI (m/z) calcd for $C_{30}H_{36}N_5O_8$ $[M + H]^+$ 594.2564; found 594.2576. $[\alpha]_D^{20}$ −121 (c 1.1, MeOH).

*Methyl 2-[(1S,6S,9S)-6-tert-Butyl-9-[(2S)-2-hydroxy-3-methylbutanamido]-8,16-dioxo-1-(propan-2-yl)-19-oxa-4,7,15-triazatetracyclo[9.5.2.1^{2,5}.0^{14,17}]nonadeca-2,4,11,13,17-pentaen-3-yl]-1,3-oxazole-4-carboxylate (**14c**).* The title compound was prepared according to general procedure H from macrocycle **3c** (80 mg; 0.13 mmol), TFA (99 μL; 1.29 mmol; 10 equiv) in DCM (2 mL) in 3 h and (*S*)-2-hydroxy-3-methylbutanoic acid (23 mg; 0.19 mmol; 1.5 equiv), EDC × HCl (44 mg; 0.23 mmol; 1.8 equiv), HOBt (52 mg; 0.38 mmol; 3 equiv), and DIPEA (111 μL; 0.64 mmol; 5 equiv) in DMF (2 mL) in 2 h. Purification by reverse phase column chromatography (gradient elution from 5% to 95% MeCN in water) afforded **14c** (28 mg, 35%; dr 99:1) as a white amorphous solid. ^{1}H NMR (400 MHz, MeOH-d_4): δ 8.67 (s, 1H), 7.27 (dd, J = 8.1, 1.8 Hz, 1H), 7.11 (d, J = 1.8 Hz, 1H), 6.90 (d, J = 8.1 Hz, 1H), 4.79 (s, 1H), 4.49 (dd, J = 11.7, 3.9 Hz, 1H), 3.92 (s, 3H), 3.86 (d, J = 3.9 Hz, 1H), 3.34−3.25 (m, 1H, overlapping with MeOH-d_4), 3.15 (dd, J = 12.2, 12.2 Hz, 1H), 2.86 (dd, J = 12.2, 3.9 Hz, 1H), 2.09 (sept d, J = 6.8, 3.1 Hz, 1H), 1.06−0.97 (m, 9H), 1.02 (s, 9H), 0.89 (d, J = 6.8 Hz, 3H). ^{13}C NMR (101 MHz, MeOH-d_4): δ 178.0, 175.8, 173.9, 163.0, 162.8, 157.1, 151.3, 146.5, 143.0, 135.2, 131.8, 131.6, 131.1, 131.0, 127.5, 111.9, 76.8, 61.0, 59.0, 56.8, 52.6, 39.4, 34.3, 33.2, 33.1, 26.7, 19.6, 18.3, 17.8, 16.3. HRMS-ESI (m/z) calcd for $C_{32}H_{40}N_5O_8$ $[M + H]^+$ 622.2877; found 622.2875. $[\alpha]_D^{20}$ −114 (c 1.0, MeOH).

*Methyl 2-[(1S,6S,9S)-6-tert-Butyl-1-(3,5-dimethylphenyl)-9-[(2S)-2-hydroxy-3-methylbutanamido]-8,16-dioxo-19-oxa-4,7,15-triazatetracyclo[9.5.2.1^{2,5}.0^{14,17}]nonadeca-2,4,11,13,17-pentaen-3-yl]-1,3-oxazole-4-carboxylate (**14d**).* The title compound was prepared according to general procedure H, from macrocycle **3d** (80 mg; 0.12 mmol), TFA (90 μL; 1.17 mmol; 10 equiv) in DCM (1 mL) in 1 h and (*S*)-2-hydroxy-3-methylbutanoic acid (21 mg; 0.17 mmol; 1.5 equiv), EDC × HCl (40 mg; 0.21 mmol; 1.8 equiv), HOBt (47 mg; 0.35 mmol; 3 equiv), and DIPEA (101 μL; 0.58 mmol; 5 equiv) in DMF (1 mL) in 18 h. Purification by reverse phase column chromatography (gradient elution from 10% to 95% MeCN in water) afforded **14d** (65 mg, 81%; dr 99:1) as a white amorphous solid. ^{1}H NMR (400 MHz, MeOH-d_4): δ 8.49 (d, J = 8.6 Hz, 1H), 8.41 (s, 1H), 7.97 (d, J = 8.2, Hz, 1H), 7.26 (dd, J = 8.0, 1.8 Hz, 1H), 7.22 (d, J = 1.8 Hz, 1H), 6.99 (s, 2H), 6.95 (s, 1H), 6.91 (d, J = 8.0 Hz, 1H), 4.96 (d, J = 8.6 Hz, 1H), 4.50−4.40 (m, 1H), 3.89 (s, 3H), 3.86 (d, J = 3.8 Hz, 1H), 3.18 (t, J = 12.4 Hz, 1H), 2.81 (dd, J = 12.4, 3.8 Hz, 1H), 2.25 (s, 6H), 2.08 (sept d, J = 6.9, 3.9 Hz, 1H), 1.06 (s, 9H), 1.00 (d, J = 6.9 Hz, 3H), 0.89 (d, J = 6.9 Hz, 3H). ^{13}C NMR (101 MHz, MeOH-d_4): δ 176.4, 175.9, 175.8, 174.1, 174.1, 164.6, 162.6, 156.5, 152.6, 146.6, 141.7, 139.8, 136.8, 134.8, 133.8, 132.2, 131.3, 130.8, 130.5, 127.3, 126.4, 112.0, 76.8, 60.4, 58.5, 56.7, 52.6, 39.3, 34.1, 33.1, 26.7, 21.3, 19.5, 16.3. HRMS-ESI (m/z) calcd for $C_{37}H_{42}N_5O_8$ $[M + H]^+$ 684.3033; found 684.3031. $[\alpha]_D^{20}$ −218 (c 1.0, $CHCl_3$).

*Methyl 2-[(1S,6S,9S)-6-tert-Butyl-9-[(2S)-2-hydroxy-3-methylbutanamido]-1-(naphthalen-2-yl)-8,16-dioxo-19-oxa-4,7,15-triazatetracyclo[9.5.2.1^{2,5}.0^{14,17}]nonadeca-2,4,11,13,17-pentaen-3-yl]-1,3-oxazole-4-carboxylate (**14e**).* The title compound was prepared according to general procedure H, from a macrocycle **3e** (60 mg; 0.085 mmol), TFA (196 μL; 2.55 mmol; 30 equiv) in DCM (2 mL) in 2 h and (*S*)-2-hydroxy-3-methylbutanoic acid (11 mg; 0.94 mmol; 1.1 equiv), EDC × HCl (26 mg; 0.14 mmol; 1.6 equiv), HOBt (39 mg; 0.26 mmol; 3 equiv), and DIPEA (59 μL; 0.34 mmol; 4 equiv) in DMF (2 mL) in 18 h. Purification by column chromatography on silica gel (gradient elution from 20% to 80% EtOAc in hexanes) was followed by reverse phase column chromatography (gradient elution from 40% to 80% MeCN in water) and afforded **14e** (32 mg, 53%; dr 99:1) as a white amorphous solid. ^{1}H NMR (400 MHz, $CDCl_3$): δ 9.37 (m, 1H), 7.95 (s, 1H), 7.84−7.65 (m, 4H), 7.60−7.40 (m, 4H), 7.22 (s, 1H), 7.07 (d, J = 7.7 Hz, 1H), 6.87 (d, J = 7.9 Hz, 1H), 6.69−6.54 (m, 1H), 4.94−4.82 (m, 1H), 4.51−4.37 (m, 1H), 4.05 (s, 1H), 3.84 (s, 3H), 3.26 (dd, J = 12.2, 12.2 Hz, 1H), 2.79 (dd, J = 12.3, 3.4 Hz, 1H), 2.24−2.17 (m, 1H), 1.09−0.94 (m, 12H), 0.87 (d, J = 6.8 Hz, 3H). ^{13}C NMR (101 MHz, $CDCl_3$): δ 175.0, 173.2, 171.8, 162.4, 161.3, 155.0, 150.5, 144.2, 139.8, 133.9, 133.1, 132.8, 132.8, 132.3, 130.9, 129.8, 129.7, 128.7, 128.2, 127.6, 127.5, 126.8, 126.6, 126.5, 124.6, 111.4, 76.0, 59.0, 57.7, 56.1, 52.2, 38.2, 33.3, 31.9, 26.4, 19.2, 15.5. HRMS-ESI (m/z) calcd for $C_{39}H_{40}N_5O_8$ $[M + H]^+$ 706.2877; found 706.2891. $[\alpha]_D^{20}$ −295 (c 0.5, $CHCl_3$).

*Methyl 2-[(1S,6S,9S)-6-tert-Butyl-9-[(2S)-2-hydroxy-3-methylbutanamido]-8,16-dioxo-19-oxa-4,7,15-triazatetracyclo[9.5.2.1^{2,5}.0^{14,17}]nonadeca-2,4,11,13,17-pentaen-3-yl]-1,3-oxazole-4-carboxylate (**14f**).* The title compound was prepared according to general procedure H from macrocycle **3f** (40 mg; 0.069 mmol), TFA (106 μL; 1.38 mmol; 20 equiv) in DCM (1 mL) in 2 h and (*S*)-2-hydroxy-3-methylbutanoic acid (12 mg; 0.10 mmol; 1.5 equiv), EDC × HCl (24 mg; 0.12 mmol; 1.8 equiv), HOBt (30 mg; 0.21 mmol; 3 equiv), and DIPEA (60 μL; 0.34 mmol; 5 equiv) in DMF (1 mL) in 1 h. Purification by reverse phase column chromatography (gradient elution from 10% to 95% MeCN in water) afforded **14f** (26 mg, 65%; dr 92:8) as a white amorphous solid. ^{1}H NMR (400 MHz, MeOH-d_4): δ 8.68 (s, 1H), 7.28 (dd, J = 8.1, 1.8 Hz, 1H), 6.95 (d, J = 8.1 Hz, 1H), 6.52 (d, J = 1.8 Hz, 1H), 4.55 (s, 1H), 4.51 (dd, J = 12.0, 4.1 Hz, 1H), 3.93 (s, 3H), 3.85 (d, J = 3.6 Hz, 1H), 2.99 (dd, J = 12.0, 12.0 Hz, 1H), 2.80 (dd, J = 12.0, 4.1 Hz, 1H), 2.07 (sept d, J = 6.9, 3.6 Hz, 1H), 0.99 (d, J = 6.9 Hz, 3H), 0.97 (s, 9H), 0.88 (d, J = 6.9 Hz, 3H). ^{13}C NMR (101 MHz, MeOH-d_4): δ 176.5, 175.8, 173.7, 165.7, 162.9, 157.2, 150.2, 146.1, 143.9, 135.3, 132.6, 131.3, 131.1, 130.3, 129.9, 112.4, 76.8, 61.0, 56.5, 52.6, 39.0, 34.1, 33.1, 26.8, 19.5, 16.3. HRMS-ESI (m/z) calcd for $C_{29}H_{34}N_5O_8$ $[M + H]^+$ 580.2407; found 580.2411. $[\alpha]_D^{20}$ −96 (c 1.0, MeOH).

*Methyl 2-[(1S,6S,9S)-6-tert-Butyl-9-[(2S)-2-Hydroxy-3-methylbutanamido]-15-methyl-8,16-dioxo-19-oxa-4,7,15-triazatetracyclo[9.5.2.1^{2,5}.0^{14,17}]nonadeca-2,4,11,13,17-pentaen-3-yl]-1,3-oxazole-4-carboxylate (**14g**).* The title compound was prepared according to general procedure H from macrocycle **3g** (100 mg; 0.17 mmol), TFA (129 μL; 1.68 mmol; 10 equiv) in DCM (3 mL) in 3 h and (*S*)-2-hydroxy-3-methylbutanoic acid (30 mg; 0.25 mmol; 1.5 equiv), EDC × HCl (58 mg; 0.30 mmol; 1.8 equiv), HOBt (68 mg; 0.50 mmol; 3 equiv), and DIPEA (146 μL; 0.84 mmol; 5 equiv) in DMF (3 mL) in 2 h. Purification by reverse phase column chromatography (gradient elution from 5% to 50% MeCN in water) afforded **14g** (44 mg, 44%; dr 94:6) as a white amorphous solid. ^{1}H NMR (400 MHz, $CDCl_3$): δ 8.33 (s, 1H), 7.32 (d, J = 8.6 Hz, 1H), 7.25 (d, J = 7.7 Hz, 1H), 6.87

https://doi.org/10.1021/acs.jmedchem.4c00388
J. Med. Chem. 2024, 67, 9227−9259

(d, J = 7.7 Hz, 1H), 6.61 (s, 1H), 6.04 (d, J = 6.7 Hz, 1H), 5.64 (s, 1H), 4.58 (d, J = 6.7 Hz, 1H), 4.33−4.24 (m, 1H), 4.00 (d, J = 2.8 Hz, 1H), 3.93 (s, 3H), 3.25 (s, 3H), 3.18 (dd, J = 12.0, 12.0 Hz, 1H), 2.77 (dd, J = 12.6, 3.2 Hz, 1H), 2.51 (br s, 1H), 2.17 (sept d, J = 7.0, 2.7 Hz, 1H), 1.00 (d, J = 7.0 Hz, 3H), 0.92 (s, 9H), 0.86 (d, J = 7.0 Hz, 3H). ^{13}C NMR (101 MHz, $CDCl_3$): δ 173.2, 172.4, 171.5, 163.4, 161.6, 155.8, 148.2, 144.5, 144.0, 134.7, 131.5, 129.8, 129.5, 129.4, 128.9, 109.6, 76.2, 59.4, 56.3, 52.4, 45.6, 37.9, 33.3, 32.0, 27.0, 26.7, 19.3, 15.5. HRMS-ESI (m/z) calcd for $C_{30}H_{36}N_5O_8$ $[M + H]^+$ 594.2564; found 594.2561. $[\alpha]_D^{20}$ −90 (c 1.0, $CHCl_3$).

*Methyl 2-[(1S,6S,9S)-6-tert-Butyl-9-[(2S)-2-hydroxy-3-methylbutanamido]-15-methyl-8,16-dioxo-1-phenyl-19-oxa-4,7,15-triazatetracyclo[9.5.2.1^{2,5}.0^{14,17}]nonadeca-2,4,11,13,17-pentaen-3-yl]-1,3-oxazole-4-carboxylate (**14h**).* The title compound was prepared according to general procedure H from macrocycle **3h** (100 mg; 0.15 mmol), TFA (172 μL; 2.24 mmol; 15 equiv) in DCM (1 mL) in 1 h and (*S*)-2-hydroxy-3-methylbutanoic acid (26 mg; 0.22 mmol; 1.5 equiv), EDC × HCl (51 mg; 0.27 mmol; 1.8 equiv), HOBt (60 mg; 0.45 mmol; 3 equiv), and DIPEA (129 μL; 0.75 mmol; 5 equiv) in DMF (1 mL) in 3 h. Purification by reverse phase column chromatography (gradient elution from 10% to 95% MeCN in water) afforded **14h** (43 mg, 43%; dr 99:1) as a white amorphous solid. ^{1}H NMR (400 MHz, CD_3CN): δ 8.38 (s, 1H), 7.42−7.26 (m, 7H), 7.17 (d, J = 8.3 Hz, 1H), 6.98−6.90 (m, 2H), 5.06−5.02 (m, 1H), 4.28−4.20 (m, 1H), 3.85 (s, 3H), 3.81 (d, J = 3.4 Hz, 1H), 3.60 (s, 1H), 3.19−3.11 (m, 4H), 2.76 (dd, J = 12.6, 3.6 Hz, 1H), 2.05−1.97 (m, 1H), 1.02 (s, 9H), 0.94 (d, J = 6.9 Hz, 3H), 0.80 (d, J = 6.9 Hz, 3H). ^{13}C NMR (101 MHz, CD_3CN): δ 173.5, 172.9, 172.9, 165.0, 162.1, 155.4, 151.9, 146.2, 143.4, 137.0, 134.6, 132.5, 131.5, 131.1, 129.9, 129.4, 129.3, 128.9, 126.0, 110.1, 76.2, 59.4, 56.6, 56.4, 52.6, 38.8, 33.7, 32.8, 27.5, 26.5, 19.4, 16.0. HRMS-ESI (m/z) calcd for $C_{36}H_{40}N_5O_8$ $[M + H]^+$ 670.2877; found 670.2874. $[\alpha]_D^{20}$ −347 (c 1.0, MeOH).

*Methyl 2-[(1S,6S,9S)-6-tert-Butyl-9-[(2S)-2-hydroxy-3-methylbutanamido]-1,15-dimethyl-8,16-dioxo-19-oxa-4,7,15-triazatetracyclo[9.5.2.1^{2,5}.0^{14,17}]nonadeca-2,4,11,13,17-pentaen-3-yl]-1,3-oxazole-4-carboxylate (**14i**).* The title compound was prepared according to general procedure H from macrocycle **3i** (55 mg; 0.09 mmol)), TFA (70 μL; 0.91 mmol; 10 equiv) in DCM (2 mL) in 3 h and (*S*)-2-hydroxy-3-methylbutanoic acid (16 mg; 0.14 mmol; 1.5 equiv), EDC × HCl (39 mg; 0.20 mmol; 2.2 equiv), HOBt (46 mg; 0.34 mmol; 3.7 equiv), and DIPEA (97 μL; 0.56 mmol; 6.2 equiv) in DMF (2 mL) in 2 h. Purification by reverse phase column chromatography (gradient elution from 5% to 50% MeCN in water) afforded **14i** (22 mg, 40%; dr 99:1) as a white amorphous solid. ^{1}H NMR (400 MHz, MeOH-d_4): δ 8.70 (s, 1H), 8.22 (d, J = 7.4 Hz, 1H), 7.35 (dd, J = 8.1, 1.8 Hz, 1H), 7.04 (d, J = 8.1 Hz, 1H), 6.94 (d, J = 1.8 Hz, 1H), 4.73−4.64 (m, 1H), 4.50 (dd, J = 11.7, 3.9 Hz, 1H), 3.93 (s, 3H), 3.86 (d, J = 3.9 Hz, 1H), 3.23 (s, 3H), 3.09 (dd, J = 12.1, 12.1 Hz, 1H), 2.88 (dd, J = 12.1, 3.9 Hz, 1H), 2.08 (sept d, J = 6.9, 3.9 Hz, 1H), 1.95 (s, 3H), 1.00 (d, J = 6.9 Hz, 3H), 0.97 (s, 9H), 0.89 (d, J = 6.9 Hz, 3H). ^{13}C NMR (101 MHz, MeOH-d_4): δ 176.7, 175.8, 173.8, 163.9, 162.8, 156.7, 152.7, 146.6, 143.5, 135.2, 134.9, 132.8, 131.1, 129.0, 127.7, 110.8, 76.8, 59.6, 56.6, 52.6, 51.6, 39.2, 34.2, 33.1, 27.1, 26.7, 20.3, 19.5, 16.3. HRMS-ESI (m/z) calcd for $C_{31}H_{38}N_5O_8$ $[M + H]^+$ 608.2720; found 608.2720. $[\alpha]_D^{20}$ −94 (c 1.0, MeOH).

*Methyl 2-[(1S,6S,9S)-6-tert-Butyl-1-ethyl-9-[(2S)-2-hydroxy-3-methylbutanamido]-15-methyl-8,16-dioxo-19-oxa-4,7,15-triazatetracyclo[9.5.2.1^{2,5}.0^{14,17}]nonadeca-2,4,11,13,17-pentaen-3-yl]-1,3-oxazole-4-carboxylate (**14j**).* The title compound was prepared according to general procedure H from macrocycle **3j** (50 mg; 0.13 mmol), TFA (62 μL; 0.80 mmol; 10 equiv) in DCM (2 mL) in 3 h and (*S*)-2-hydroxy-3-methylbutanoic acid (14 mg; 0.12 mmol; 1.5 equiv), EDC × HCl (28 mg; 0.15 mmol; 1.8 equiv), HOBt (33 mg; 0.24 mmol; 3 equiv), and DIPEA (70 μL; 0.40 mmol; 5 equiv) in DMF (2 mL) in 2 h. Purification by reverse phase column chromatography (gradient elution from 5% to 50% MeCN in water) afforded **14j** (33 mg, 66%; dr 99:1) as a white amorphous solid. ^{1}H NMR (400 MHz, MeOH-d_4): δ 8.69 (s, 1H), 7.36 (dd, J = 8.1, 1.6 Hz, 1H), 7.05−7.01 (m, 2H), 4.76 (s, 1H), 4.50 (dd, J = 11.8, 4.0 Hz, 1H), 3.93 (s, 3H), 3.87 (d, J = 4.0 Hz, 1H), 3.21 (s, 3H), 3.14 (t, J = 12.2 Hz, 1H), 2.88 (dd, J = 12.2, 4.0 Hz, 1H), 2.69 (dq, J = 7.0, 7.0 Hz, 1H), 2.38 (dq, J = 7.0, 7.0 Hz, 1H), 2.09 (sept d, J = 7.0, 4.0 Hz, 1H), 1.01 (d, J = 7.0 Hz, 3H), 1.00 (s, 9H), 0.89 (d, J = 7.0 Hz, 3H), 0.83 (t, J = 7.0 Hz, 3H). ^{13}C NMR (101 MHz, MeOH-d_4): δ 175.9, 175.8, 173.8, 163.8, 162.7, 156.7, 152.0, 146.6, 144.3, 135.2, 132.7, 132.1, 131.16, 129.6, 127.3, 110.7, 76.8, 59.2, 56.8, 56.7, 52.6, 39.2, 34.2, 33.1, 27.4, 27.0, 26.7, 19.6, 16.3, 9.1. HRMS-ESI (m/z) calcd for $C_{32}H_{40}N_5O_8$ $[M + H]^+$ 622.2877; found 622.2880. $[\alpha]_D^{20}$ −118 (c 1.0, MeOH).

*Methyl 2-[(1S,6S,9S)-1-Benzyl-6-tert-butyl-9-[(2S)-2-hydroxy-3-methylbutanamido]-15-methyl-8,16-dioxo-19-oxa-4,7,15-triazatetracyclo[9.5.2.1^{2,5}.0^{14,17}]nonadeca-2,4,11,13,17-pentaen-3-yl]-1,3-oxazole-4-carboxylate (**14k**).* The title compound was prepared according to general procedure H from macrocycle **3k** (45 mg; 0.07 mmol), TFA (51 μL; 0.66 mmol; 10 equiv) in DCM (5 mL) in 3 h and (S)-2-hydroxy-3-methylbutanoic acid (12 mg; 0.10 mmol; 1.5 equiv), EDC × HCl (22 mg; 0.12 mmol; 1.8 equiv), HOBt (27 mg; 0.20 mmol; 3 equiv), and DIPEA (56 μL; 0.33 mmol; 5 equiv) in DMF (2 mL) in 2 h. Purification by reverse phase column chromatography (gradient elution from 5% to 50% MeCN in water) afforded **14k** (23 mg, 52%; dr 99:1) as a white amorphous solid. ^{1}H NMR (400 MHz, MeOH-d_4): δ 8.74 (s, 1H), 7.25 (dd, J = 8.1, 1.7 Hz, 1H), 7.10−7.00 (m, 6H), 6.78 (d, J = 8.1 Hz, 1H), 4.76 (s, 1H), 4.48 (dd, J = 12.1, 4.0 Hz, 1H), 4.26 (d, J = 13.1 Hz, 1H), 3.92 (d, J = 5.4 Hz, 3H), 3.87 (d, J = 4.0 Hz, 1H), 3.49 (d, J = 13.1 Hz, 1H), 3.16 (dd, J = 12.1, 12.1 Hz, 1H), 2.95 (s, 3H), 2.86 (dd, J = 12.1, 4.0 Hz, 1H), 2.09 (sept d, J = 7.0, 4.0 Hz, 1H), 1.01 (d, J = 7.0 Hz, 3H), 1.00 (s, 9H), 0.91 (d, J = 7.0 Hz, 3H). ^{13}C NMR (101 MHz, MeOH-d_4): δ 175.8, 175.4, 173.9, 163.7, 162.8, 156.8, 151.7, 146.7, 143.9, 136.1, 135.2, 132.5, 132.0, 131.4, 131.1, 130.1, 128.8, 128.1, 127.8, 110.5, 76.8, 59.4, 57.6, 56.7, 52.6, 40.0, 39.3, 34.2, 33.1, 26.7, 19.6, 16.3. HRMS-ESI (m/z) calcd for $C_{37}H_{42}N_5O_8$ $[M + H]^+$ 684.3033; found 684.3035. $[\alpha]_D^{20}$ −156 (c 1.0, MeOH).

*Methyl 2-[(1S,6S,9S)-6-tert-Butyl-9-[(2S)-2-hydroxy-3-methylbutanamido]-8,17-dioxo-1-phenyl-20-oxa-4,7,16-triazatetracyclo[10.5.2.1^{2,5}.0^{15,18}]icosa-2,4,12,14,18-pentaen-3-yl]-1,3-oxazole-4-carboxylate (**15a**).* A stream of argon was passed for 10 min through light yellow suspension of **6a** (60 mg; 0.080 mmol) and oven-dried K_3PO_4 (51 mg; 0.24 mmol; 3 equiv) in anhydrous degassed DMSO (3.6 mL). Subsequently, the suspension was left to stir at 65 °C for 6 h, cooled to room temperature, quenched with aqueous saturated

https://doi.org/10.1021/acs.jmedchem.4c00388
J. Med. Chem. 2024, 67, 9227−9259

NH_4Cl, and extracted with EtOAc (two times). Combined organic extracts were washed with brine, dried ($MgSO_4$), and evaporated under the reduced pressure to afford macrocycle **4a** as 62:38 mixture of diastereomers. Purification by reverse phase column chromatography (gradient elution from 10% to 100% MeCN in water) yielded macrocycle **4a** (17 mg, 32%, dr 76:24.) as white amorphous solid.

The cleavage of *N*-Boc protection in macrocycle **4a** and amide bond formation was accomplished as described in general procedure H using TFA (21 μL; 0.27 mmol; 10 equiv) in DCM (1 mL) within 16 h, followed by treatment with (*S*)-2-hydroxy-3-methylbutanoic acid (3.7 mg; 0.0.32 mmol; 1.5 equiv), EDC × HCl (8.1 mg; 0.042 mmol; 2 equiv), HOBt (5.7 mg; 0.042 mmol; 2 equiv), and DIPEA (11 μL; 0.64 mmol; 3 equiv) in DMF (0.5 mL) for 3 h. Purification by reverse phase preparative HPLC (gradient elution from 10% to 95% MeCN in 0.1% aqueous AcOH) yielded (*S,S,S*)−**15a** (3.0 mg, 21%; dr 99:1) as a white amorphous solid. Absolute configuration of the newly formed quaternary center for the major product was assigned as *S* in analogy to compound **15i** (see Supporting Information, page S19). ^{1}H NMR (400 MHz, MeOH-d_4): δ 8.23 (s, 1H), 7.40−7.35 (m, 2H), 7.33−7.24 (m, 3H), 7.17 (dd, J = 8.0, 1.8 Hz, 1H), 7.14−7.11 (m, 1H), 6.92 (d, J = 8.0 Hz, 1H), 4.75 (s, 1H), 4.08 (dd, J = 6.4, 3.3 Hz, 1H), 3.87 (s, 3H), 3.84 (d, J = 4.0 Hz, 1H), 3.01−2.92 (m, 1H), 2.82−2.69 (m, 2H), 2.11−2.04 (m, 1H), 1.86−1.75 (m, 1H), 1.03 (s, 9H), 0.99 (d, J = 6.9 Hz, 3H), 0.87 (d, J = 6.9 Hz, 3H). ^{13}C NMR (101 MHz, MeOH-d_4): δ 176.9, 176.6, 173.9, 163.7, 162.6, 156.8, 151.8, 146.3, 140.4, 138.6, 136.2, 134.8, 133.5, 131.2, 129.9, 129.1, 128.2, 127.8, 127.6, 111.6, 77.0, 59.9, 58.9, 52.7, 52.5, 34.6, 33.1, 32.4, 31.4, 26.7, 19.5, 16.4. HRMS-ESI (m/z) calcd for $C_{36}H_{40}N_5O_8$ $[M + H]^+$ 670.2877; found 670.2884. $[\alpha]_D^{20}$ −96 (c 0.4, MeOH).

*Methyl 2-[(1S,6S,9S)-6-tert-Butyl-9-[(2S)-2-hydroxy-3-methylbutanamido]-1-methyl-8,17-dioxo-20-oxa-4,7,16-triazatetracyclo[10.5.2.1^{2,5}.0^{15,18}]icosa-2,4,12,14,18-pentaen-3-yl]-1,3-oxazole-4-carboxylate (**15b**).* Compound **6b** (278 mg; 0.40 mmol) and oven-dried K_3PO_4 (257 mg; 1.21 mmol; 3 equiv) were suspended in anhydrous degassed DMSO (20 mL), and stream of argon was passed through the mixture for 10 min. The light yellow suspension was stirred at 65 °C for 6 h. Compound **4b** was formed as a mixture of diastereomers with ratio 79:21. Vial was cooled to r.t., and reaction was quenched with aqueous saturated NH_4Cl and extracted with EtOAc. Combined organic layers were washed with brine, dried ($MgSO_4$), and evaporated. The macrocyclic compound **4b** was purified by reverse phase column chromatography (10% to 100% MeCN in water) to yield 120 mg (49%) of mixture of diastereomers (dr 81:19) as white amorphous solid. The obtained mixture (110 mg; 0.18 mmol) was subjected to general procedure H using TFA (139 μL; 1.81 mmol; 10 equiv) in DCM (3 mL) in 48 h and (*S*)-2-hydroxy-3-methylbutanoic acid (21 mg; 0.18 mmol; 1.5 equiv), EDC × HCl (45 mg; 0.24 mmol; 2 equiv), HOBt (32 mg; 0.24 mmol; 2 equiv), and DIPEA (61 μL; 0.35 mmol; 3 equiv) in DMF (2 mL) in 2 h. Purification by reverse phase column chromatography (gradient elution from 10% to 100% MeCN in water) afforded **15b** (44 mg, 44%; dr 98:2) of white amorphous solid. Absolute configuration of the newly formed quaternary center for the major product was assigned as *S* in analogy to compound **15i** (see Supporting Information, page S19). ^{1}H NMR (400 MHz, MeOH-d_4): δ 8.70 (s, 1H), 7.16 (dd, J = 7.9, 1.7 Hz, 1H), 6.95−6.88 (m, 2H), 4.54 (s, 1H), 4.03 (dd, J = 6.2, 3.3 Hz, 1H), 3.92 (s, 3H), 3.82 (d, J = 4.1 Hz, 1H), 3.04−2.92 (m, 1H), 2.83−2.67 (m, 2H), 2.08−2.00 (m, 1H), 1.98 (s, 3H), 1.85−1.78 (m, 1H), 0.97 (d, J = 6.9 Hz, 3H), 0.95 (s, 9H), 0.87 (d, J = 6.9 Hz, 3H). ^{13}C NMR (101 MHz, MeOH-d_4): δ 179.3, 176.6, 173.9, 163.1, 162.8, 157.1, 152.0, 146.4, 140.4, 135.7, 135.3, 135.2, 131.2, 127.6, 126.4, 111.4, 76.9, 59.6, 52.6, 52.4, 51.5, 34.6, 33.1, 32.9, 31.1, 26.7, 22.0, 19.5, 16.5. HRMS-ESI (m/z) calcd for $C_{31}H_{38}N_5O_8$ $[M + H]^+$ 608.2720; found 608.2719. $[\alpha]_D^{20}$ −82 (c 1.4, MeOH).

*Methyl 2-[(1S,6S,9S)-6-tert-Butyl-9-[(2S)-2-hydroxy-3-methylbutanamido]-1,16-dimethyl-8,17-dioxo-20-oxa-4,7,16-triazatetracyclo[10.5.2.1^{2,5}.0^{15,18}]icosa-2,4,12,14,18-pentaen-3-yl]-1,3-oxazole-4-carboxylate (**15i**) and Methyl 2-[(1R,6S,9S)-6-tert-Butyl-9-[(2S)-2-hydroxy-3-methylbutanamido]-1,16-dimethyl-8,17-dioxo-20-oxa-4,7,16-triazatetracyclo[10.5.2.1^{2,5}.0^{15,18}]icosa-2,4,12,14,18-pentaen-3-yl]-1,3-oxazole-4-carboxylate (**epi-15i**).* Compound **6i** (366 mg; 0.52 mmol) and oven-dried K_3PO_4 (332 mg; 1.56 mmol; 3 equiv) were suspended in anhydrous degassed DMSO (25 mL), and stream of argon was passed through the mixture for 10 min. The light yellow suspension was stirred at 65 °C for 6 h. Compound **4i** was formed as a mixture of diastereomers with ratio 85:15. Vial was cooled to r.t., and reaction was quenched with aqueous saturated NH_4Cl and extracted with EtOAc. Combined organic layers were washed with brine, dried ($MgSO_4$), and evaporated. Compound **4i** was purified by reverse phase column chromatography (10% to 100% MeCN in water) to yield 192 mg (59%) of mixture of diastereomers (dr 87:13) as white amorphous solid. The obtained mixture (175 mg; 0.28 mmol) was subjected to general procedure H using TFA (216 μL; 2.81 mmol; 10 equiv) in DCM (3 mL) in 48 h and (*S*)-2-hydroxy-3-methylbutanoic acid (54 mg; 0.46 mmol; 1.5 equiv), EDC × HCl (118 mg; 0.61 mmol; 2 equiv), HOBt (83 mg; 0.61 mmol; 2 equiv), and DIPEA (159 μL; 0.92 mmol; 3 equiv) in DMF (3 mL) in 3 h. Compounds **15i** and *epi*-**15i** were separated and purified by reverse phase column chromatography (gradient elution from 10% to 100% MeCN in water) to afford 97 mg (51%; dr 94:6) of **15i** and 6.9 mg (4%; dr 99:1) of *epi*-**15i** as white amorphous solids. Absolute configuration of the newly formed quaternary centers was determined comparing experimental and calculated CD spectra for both diastereomeric compounds (see Supporting Information, page S19). It was assigned to be *S* for **15i** and *R* for *epi*-**15i**. Data for compound **15i**: ^{1}H NMR (400 MHz, MeOH-d_4): δ 8.69 (s, 1H), 8.20 (d, J = 7.9 Hz, 1H), 7.73 (d, J = 7.3 Hz, 1H), 7.25 (dd, J = 8.0, 1.7 Hz, 1H), 7.04 (d, J = 1.7 Hz, 1H), 7.01 (d, J = 8.0 Hz, 1H), 4.63 (d, J = 7.3 Hz, 1H), 4.06−4.02 (m, 1H), 3.92 (s, 3H), 3.83 (d, J = 4.0 Hz, 1H), 3.23 (s, 3H), 3.05−2.98 (m, 1H), 2.84−2.69 (m, 2H), 2.08−2.01 (m, 1H), 1.97 (s, 3H), 1.83−1.75 (m, 1H), 1.00−0.95 (m, 12H), 0.87 (d, J = 6.9 Hz, 3H). ^{13}C NMR (101 MHz, MeOH-d_4): δ 177.1, 176.5, 173.9, 163.3, 162.8, 157.0, 151.8, 146.5, 142.2, 136.6, 135.2, 134.0, 131.1, 127.2, 126.1, 110.2, 76.9, 59.2, 52.6, 52.5, 50.9, 34.6, 33.1, 32.6, 31.4, 27.1, 26.7, 21.9, 19.5, 16.4. HRMS-ESI (m/z) calcd for $C_{32}H_{39}N_5O_8$ $[M + H]^+$ 622.2877; found 622.2875. $[\alpha]_D^{20}$ −121 (c 0.8, MeOH). Data for compound *epi*-**15i**: ^{1}H NMR (400 MHz, MeOH-d_4): 8.65 (s, 1H), 8.27 (d, J = 6.2 Hz, 1H), 8.03 (d, J = 8.0 Hz, 1H), 7.25 (d, J = 1.6 Hz, 1H), 7.14 (dd, J = 8.0, 1.6 Hz, 1H), 6.93 (d, J = 8.0 Hz, 1H), 4.80−4.71 (m, 1H), 4.44 (d, J = 6.2 Hz, 1H), 3.92 (s, 3H), 3.84 (d, J = 3.9 Hz, 1H), 3.25 (s, 3H), 2.93−2.75 (m, 2H),

https://doi.org/10.1021/acs.jmedchem.4c00388
J. Med. Chem. 2024, 67, 9227−9259

2.50−2.35 (m, 1H), 2.11 (dp, J = 6.8, 3.9 Hz, 1H), 2.05−1.93 (m, 1H), 1.89 (s, 3H), 1.16 (s, 9H), 1.01 (d, J = 6.8 Hz, 3H), 0.91 (d, J = 6.8 Hz, 3H). ^{13}C NMR (101 MHz, MeOH-d_4): 176.4, 175.9, 173.1, 163.9, 162.7, 156.5, 152.3, 146.6, 142.0, 137.7, 134.9, 132.4, 130.5, 125.6, 124.3, 110.4, 76.9, 59.5, 54.5, 52.5, 50.4, 34.4, 34.1, 33.3, 33.0, 27.2, 26.9, 21.0, 19.6, 16.5. HRMS-ESI (m/z) calcd for $C_{32}H_{39}N_5O_8$ [M + H]$^+$ 622.2877; found 622.2853. $[\alpha]_D^{20}$ −135 (c 0.3, MeOH).

*2-[(1S,6S,9S)-6-tert-Butyl-9-[(2S)-2-hydroxy-3-methylbutanamido]-8,16-dioxo-1-phenyl-19-oxa-4,7,15-triazatetracyclo[9.5.2.1^{2,5}.0^{14,17}]nonadeca-2,4,11,13,17-pentaen-3-yl]-1,3-oxazole-4-carboxylic acid (**16**).* To a solution of methyl ester **14a** (130 mg, 0.20 mmol) in MeOH (2 mL) and water (1 mL) was added LiOH × H_2O (25 mg, 0.60 mmol, 3.0 equiv), and the resulting suspension was stirred at room temperature for 30 min. Then, the solution was acidified with aqueous 1 M HCl to pH 2, and the resulting suspension was extracted with EtOAc (three times). Combined organic extracts were washed with brine, dried (Na_2SO_4) and evaporated under reduced pressure. Purification by reverse phase column chromatography (gradient elution from 10% to 50% MeCN in 0.01% aqueous TFA) provided carboxylic acid **16** (100 mg, 80%) as a white amorphous solid. ^{1}H NMR (400 MHz, MeOH-d_4): δ 8.37 (s, 1H), 7.45−7.39 (m, 2H), 7.38−7.30 (m, 3H), 7.29−7.25 (m, 2H), 6.92 (d, J = 8.4 Hz, 1H), 4.96 (s, 1H), 4.45 (dd, J = 11.8, 3.8 Hz, 1H), 3.86 (d, J = 3.8 Hz, 1H), 3.18 (dd, J = 12.2, 12.2 Hz, 1H), 2.82 (dd, J = 12.7, 3.8 Hz, 1H), 2.07 (sept d, J = 6.9, 3.8 Hz, 1H), 1.06 (s, 9H), 1.00 (d, J = 6.9 Hz, 3H), 0.89 (d, J = 6.9 Hz, 3H).^{13}C NMR (101 MHz, MeOH-d_4): δ 176.2, 175.8, 174.0, 164.5, 163.5, 156.3, 152.2, 146.5, 141.8, 137.2, 135.5, 133.5, 132.2, 131.4, 130.5, 130.0, 129.4, 128.7, 127.5, 112.0, 76.8, 60.5, 58.3, 56.7, 39.3, 34.1, 33.1, 26.7, 19.5, 16.3. HRMS-ESI (m/z) calcd for $C_{34}H_{36}N_5O_8$ [M + H]$^+$ 642.2564; found: 642.2571. $[\alpha]_D^{20}$ −226 (c 1.0, MeOH).

*2-[(1S,6S,9S)-6-tert-Butyl-9-[(2S)-2-hydroxy-3-methylbutanamido]-8,16-dioxo-1-phenyl-19-oxa-4,7,15-triazatetracyclo[9.5.2.1^{2,5}.0^{14,17}]nonadeca-2,4,11,13,17-pentaen-3-yl]-N,N-dimethyl-1,3-oxazole-4-carboxamide (**17**).* EDC × HCl (36 mg, 0.19 mmol, 2.0 equiv), HOBt (38 mg, 0.28 mmol, 3.0 equiv), $NHMe_2$ × HCl (38 mg, 0.47 mmol, 5 equiv), and DIPEA (80 μL, 0.47 mmol, 5.0 equiv) were sequentially added to a solution of carboxylic acid **16** (60 mg, 0.094 mmol) in anhydrous DMF (0.5 mL) at room temperature. After stirring for 2 h, the resulting yellow solution was diluted with aqueous saturated NH_4Cl and EtOAc. The layers were separated, and the organic phase was washed with water, brine, dried (Na_2SO_4), and evaporated under reduced pressure. Purification by reverse phase column chromatography (gradient elution from 10% to 50% MeCN in 0.01% aqueous TFA) provided amide **17** (39 mg, 62%) as a white amorphous solid. ^{1}H NMR (400 MHz, MeOH-d_4): δ 8.23 (s, 1H), 7.45−7.40 (m, 2H), 7.37−7.29 (m, 3H), 7.27 (dd, J = 8.0, 1.8 Hz, 1H), 7.22 (d, J = 1.8 Hz, 1H), 6.92 (d, J = 8.0 Hz, 1H), 4.91 (s, 1H), 4.47 (dd, J = 11.7, 3.8 Hz, 1H), 3.86 (d, J = 3.8 Hz, 1H), 3.28 (s, 3H), 3.16 (dd, J = 12.1, 12.1 Hz, 1H), 3.05 (s, 3H), 2.82 (dd, J = 12.6, 3.8 Hz, 1H), 2.08 (sept d, J = 6.9, 3.8 Hz, 1H), 1.06 (s, 9H), 1.00 (d, J = 6.9 Hz, 3H), 0.89 (d, J = 6.9 Hz, 3H). ^{13}C NMR (101 MHz, MeOH-d_4): δ 176.2, 175.8, 174.0, 164.3, 151.9, 144.7, 141.7, 137.4, 133.9, 132.2, 131.3, 130.6, 129.9, 129.3, 128.6, 128.1, 112.0, 76.8, 60.5, 58.6, 56.7, 39.2, 36.6, 34.2, 33.2, 26.7, 19.5, 16.3. HRMS-ESI (m/z) calcd for $C_{36}H_{41}N_6O_7$ [M + H]$^+$ 669.3037; found: 669.3029. $[\alpha]_D^{20}$ −229 (c 1.0, MeOH).

*2-[(1S,6S,9S)-6-tert-Butyl-9-[(2S)-2-hydroxy-3-methylbutanamido]-8,16-dioxo-1-phenyl-19-oxa-4,7,15-triazatetracyclo[9.5.2.1^{2,5}.0^{14,17}]nonadeca-2,4,11,13,17-pentaen-3-yl]-1,3-oxazole-4-carboxamide (**18**).* A clear solution of methyl ester **14a** (22 mg, 0.034 mmol) in anhydrous ammonia (7 N solution in MeOH, 0.24 mL, 1.68 mmol, 50 equiv) was stirred at room temperature for 20 h and evaporated to dryness under the reduced pressure. The residue was purified by reverse phase column chromatography (gradient elution from 10% to 50% MeCN in 0.01% aqueous TFA) to provide amide **18** (18 mg, 84%) as a white amorphous solid. ^{1}H NMR (400 MHz, MeOH-d_4): δ 8.21 (s, 1H), 7.49−7.41 (m, 2H), 7.37−7.29 (m, 3H), 7.28 (dd, J = 8.0, 1.7 Hz, 1H), 7.18 (d, J = 1.7 Hz, 1H), 6.93 (d, J = 8.0 Hz, 1H), 4.86 (s, 1H), 4.50 (dd, J = 11.7, 4.0 Hz, 1H), 3.86 (d, J = 3.8 Hz, 1H), 3.14 (dd, J = 12.1, 12.1 Hz, 1H), 2.83 (dd, J = 12.6, 4.0 Hz, 1H), 2.09 (sept d, J = 6.9, 3.8 Hz, 1H), 1.05 (s, 9H), 1.00 (d, J = 6.9 Hz, 3H), 0.89 (d, J = 6.9 Hz, 3H). ^{13}C NMR (101 MHz, MeOH-d_4): δ 176.5, 175.8, 174.0, 164.8, 164.4, 155.4, 152.2, 143.7, 141.6, 138.0, 137.3, 134.4, 132.3, 131.3, 130.5, 129.9, 129.3, 128.6, 128.3, 112.1, 76.8, 60.6, 59.0, 56.6, 39.2, 34.2, 33.2, 26.7, 19.5, 16.3. HRMS-ESI (m/z) calcd for $C_{34}H_{37}N_6O_7$ [M + H]$^+$ 641.2724; found: 641.2726. $[\alpha]_D^{20}$ −192 (c 1.0, MeOH).

*2-[(1S,6S,9S)-6-tert-Butyl-9-[(2S)-2-hydroxy-3-methylbutanamido]-8,16-dioxo-1-phenyl-19-oxa-4,7,15-triazatetracyclo[9.5.2.1^{2,5}.0^{14,17}]nonadeca-2,4,11,13,17-pentaen-3-yl]-N-methyl-1,3-oxazole-4-carboxamide (**19**).* A clear solution of methyl ester **14a** (35 mg, 0.053 mmol) in anhydrous $MeNH_2$ (33% solution in EtOH, 0.56 mL, 5.34 mmol, 100 equiv) was stirred at room temperature for 20 h and evaporated to dryness under reduced pressure. The residue was purified by reverse phase column chromatography (gradient elution from 10% to 50% MeCN in water) to provide amide **19** (31 mg, 89%) as a white amorphous solid. ^{1}H NMR (400 MHz, MeOH-d_4): δ 8.18 (s, 1H), 7.44−7.40 (m, 2H), 7.36−7.26 (m, 4H), 7.17 (d, J = 1.7 Hz, 1H), 6.93 (d, J = 8.0 Hz, 1H), 4.85 (s, 1H), 4.49 (dd, J = 11.7, 4.0 Hz, 1H), 3.86 (d, J = 3.8 Hz, 1H), 3.14 (dd, J = 12.2, 12.2 Hz, 1H), 2.88 (s, 3H), 2.84 (dd, J = 12.6, 4.0 Hz, 1H), 2.09 (sept d, J = 6.9, 3.8 Hz, 1H), 1.04 (s, 9H), 1.00 (d, J = 6.9 Hz, 3H), 0.89 (d, J = 6.9 Hz, 3H). ^{13}C NMR (101 MHz, MeOH-d_4): δ 176.6, 175.8, 174.0, 164.4, 163.1, 155.3, 152.1, 142.9, 141.6, 138.1, 137.3, 134.4, 132.3, 131.3, 130.5, 129.9, 129.2, 128.6, 128.4, 112.1, 76.8, 60.7, 59.0, 56.6, 39.2, 34.2, 33.2, 26.7, 25.9, 19.5, 16.3. HRMS-ESI (m/z) calcd for $C_{35}H_{39}N_6O_7$ [M + H]$^+$ 655.2880; found: 655.2877. $[\alpha]_D^{20}$ −176 (c 1.0, MeOH).

*Propan-2-yl 2-[(1S,6S,9S)-6-tert-butyl-9-[(2S)-2-hydroxy-3-methylbutanamido]-1-methyl-8,16-dioxo-19-oxa-4,7,15-triazatetracyclo[9.5.2.1^{2,5}.0^{14,17}]nonadeca-2,4,11,13,17-pentaen-3-yl]-1,3-oxazole-4-carboxylate (**20**).* To a solution of methyl ester **14b** (50 mg, 0.084 mmol) in anhydrous toluene (0.5 mL) was added iPrOH (258 μL, 3.37 mmol, 40 equiv), followed by dropwise addition of neat Ti(OiPr)$_4$ (25 μL, 0.084 mmol, 1.0 equiv). After addition was completed, the vial was placed in preheated oil bath and stirred at 100 °C for 20 h. After cooling to room temperature, the reaction mixture was quenched with aqueous 1 M HCl and extracted with EtOAc (two times). Combined organic extracts were washed with brine, dried (Na_2SO_4), and evaporated under reduced

https://doi.org/10.1021/acs.jmedchem.4c00388
J. Med. Chem. 2024, 67, 9227−9259

pressure. The resulting yellow oily residue was purified by reverse phase column chromatography (gradient elution from 10% to 50% MeCN in water) to give ester **20** (45 mg, 86%) as a white amorphous solid. ^{1}H NMR (400 MHz, MeOH-d_4): δ 8.66 (s, 1H), 7.27 (dd, J = 8.0, 1.7 Hz, 1H), 6.94 (d, J = 8.0 Hz, 1H), 6.80 (d, J = 1.7 Hz, 1H), 5.25 (hept, J = 6.3 Hz, 1H), 4.61 (s, 1H), 4.52 (dd, J = 11.6, 4.2 Hz, 1H), 3.86 (d, J = 3.7 Hz, 1H), 3.04 (t, J = 12.0 Hz, 1H), 2.87 (dd, J = 12.5, 4.2 Hz, 1H), 2.08 (sept d, J = 6.9, 3.5 Hz, 1H), 1.96 (s, 3H), 1.38 (d, J = 6.3 Hz, 6H), 1.00 (d, J = 6.9 Hz, 3H), 0.96 (s, 9H), 0.89 (d, J = 6.9 Hz, 3H). ^{13}C NMR (101 MHz, MeOH-d_4): δ 178.9, 175.8, 173.7, 163.6, 161.9, 156.8, 152.8, 146.3, 141.7, 136.2, 135.9, 132.2, 131.0, 129.4, 128.2, 112.1, 76.8, 70.3, 60.0, 56.6, 52.1, 39.3, 34.2, 33.1, 26.7, 22.1, 20.5, 19.5, 16.3. HRMS-ESI (m/z) calcd for $C_{32}H_{40}N_5O_8$ [M + H]$^+$ 622.2877; found: 622.2874. $[\alpha]_D^{20}$ −120 (c 1.0, MeOH).

*Benzyl 2-[(1S,6S,9S)-6-tert-Butyl-9-[(2S)-2-hydroxy-3-methylbutanamido]-1-methyl-8,16-dioxo-19-oxa-4,7,15-triazatetracyclo[9.5.2.1^{2,5}.0^{14,17}]nonadeca-2,4,11,13,17-pentaen-3-yl]-1,3-oxazole-4-carboxylate (**21**).* To a solution of methyl ester **14b** (130 mg, 0.22 mmol) in anhydrous toluene (1 mL), BnOH (0.9 mL, 8.8 mmol, 40 equiv), and neat Ti(OiPr)$_4$ (65 μL, 0.22 mmol, 1.0 equiv) were added dropwise. After addition the vial was placed in preheated oil bath at 100 °C and stirred for 2 h. After cooling to room temperature, reaction was quenched with aqueous HCl (1 M) and extracted with EtOAc. The combined organic layers were washed with brine, dried (Na_2SO_4), and evaporated under reduced pressure. The resulting yellow oil was purified with reverse phase column chromatography (10% to 70% MeCN in water) to give 127 mg (87%) of ester **21** as white amorphous solid. ^{1}H NMR (400 MHz, MeOH-d_4): δ 8.71 (s, 1H), 8.17 (d, J = 7.0 Hz, 1H), 7.51−7.45 (m, 2H), 7.42−7.30 (m, 3H), 7.27 (dd, J = 8.1, 1.7 Hz, 1H), 6.94 (d, J = 8.0 Hz, 1H), 6.79 (d, J = 1.7 Hz, 1H), 5.39 (s, 2H), 4.64−4.57 (m, 1H), 4.52 (dd, J = 11.6, 4.2 Hz, 1H), 3.86 (d, J = 3.7 Hz, 1H), 3.03 (dd, J = 12.0, 12.0 Hz, 1H), 2.86 (dd, J = 12.5, 4.2 Hz, 1H), 2.08 (sept d, J = 6.8, 3.3 Hz, 1H), 1.96 (s, 3H), 1.00 (d, J = 6.9 Hz, 3H), 0.96 (s, 9H), 0.89 (d, J = 6.9 Hz, 3H). ^{13}C NMR (101 MHz, MeOH-d_4): δ 178.9, 175.8, 173.8, 173.7, 163.7, 162.1, 156.9, 152.8, 146.7, 141.7, 137.2, 136.3, 135.4, 132.2, 131.0, 129.6, 129.4, 128.2, 112.2, 76.8, 67.8, 60.1, 56.7, 52.1, 39.3, 34.2, 33.1, 26.7, 20.5, 19.5, 16.3. HRMS-ESI (m/z) calcd for $C_{36}H_{40}N_6O_8$ [M + H]$^+$ 670.2877; found: 670.2885. $[\alpha]_D^{20}$ −99 (c 1.0, MeOH).

*tert-Butyl N-[(1S,6S,9S)-6-tert-Butyl-3-(4-cyano-1,3-oxazol-2-yl)-8,16-dioxo-1-phenyl-19-oxa-4,7,15-triazatetracyclo[9.5.2.1^{2,5}.0^{14,17}]nonadeca-2,4,11,13,17-pentaen-9-yl]carbamate (**22**).* A solution of *N*-Boc-protected ester **3a** (110 mg, 0.17 mmol, 1.0 equiv) in anhydrous ammonia (7 M solution in MeOH, 0.72 mL, 5.0 mmol, 30 equiv) was stirred at room temperature for 20 h and was evaporated to dryness under reduced pressure. The resulting white amorphous solid (50 mg, 0.08 mmol, 1 equiv) was dissolved in anhydrous MeCN (0.5 mL), and anhydrous pyridine (32 μL, 0.23 mmol, 3 equiv) was added. The vial was cooled to 0 °C, and TFAA (22 μL, 0.16 mmol, 2 equiv) was added. The reaction mixture was warmed to room temperature and stirred for 2 h. The reaction mixture was quenched with saturated aqueous $NaHCO_3$ and extracted with EtOAc two times. Organics were combined, washed with brine, dried over Na_2SO_4, and evaporated under reduced pressure. The yellow amorphous solid residue was purified by reverse phase column chromatography (gradient elution from 10% to 50% MeCN in water) to give nitrile **22** (27 mg, 56%) as a white amorphous solid. ^{1}H NMR (400 MHz, MeOH-d_4): δ 8.58 (s, 1H), 7.44−7.39 (m, 2H), 7.38−7.30 (m, 3H), 7.28−7.22 (m, 2H), 6.90 (d, J = 8.0 Hz, 1H), 4.96 (s, 1H), 4.05 (dd, J = 12.3, 3.7 Hz, 1H), 3.12 (dd, J = 12.3, 12.3 Hz, 1H), 2.78 (dd, J = 12.3, 3.7 Hz, 1H), 1.43 (s, 9H), 1.08 (s, 9H). ^{13}C NMR (101 MHz, MeOH-d_4): δ 176.1, 174.9, 164.8, 157.1, 156.9, 152.8, 149.6, 141.6, 137.2, 133.4, 132.8, 131.4, 130.6, 130.0, 129.4, 128.7, 126.7, 116.5, 112.5, 112.0, 80.5, 60.4, 58.5, 58.3, 38.8, 34.1, 28.7, 26.7. HRMS-ESI (m/z) calcd for $C_{34}H_{35}N_6O_6$ [M + H]$^+$ 623.2618; found: 623.2609. $[\alpha]_D^{20}$ −228 (c 1.0, MeOH).

*(2S)-N-[(1S,6S,9S)-6-tert-Butyl-3-(4-cyano-1,3-oxazol-2-yl)-8,16-dioxo-1-phenyl-19-oxa-4,7,15-triazatetracyclo-[9.5.2.1^{2,5}.0^{14,17}]nonadeca-2,4,11,13,17-pentaen-9-yl]-2-hydroxy-3-methylbutanamide (**23**).* The title compound was prepared according to general procedure H from macrocycle **22** (27 mg; 0.043 mmol), TFA (33 μL; 0.43 mmol; 10 equiv) in DCM (0.5 mL) within 3 h, followed by treatment with (*S*)-2-hydroxy-3-methylbutanoic acid (8 mg; 0.065 mmol; 1.5 equiv), EDC × HCl (17 mg; 0.09 mmol; 2.0 equiv), HOBt (17 mg; 0.13 mmol; 3.0 equiv), and DIPEA (37 μL; 0.22 mmol; 5 equiv) in DMF (0.5 mL) for 1 h. Purification by reverse phase column chromatography (gradient elution from 10% to 95% MeCN in 0.1% TFA in water) afforded amide **23** (13 mg, 49%; dr 99:1) as a white amorphous solid. ^{1}H NMR (400 MHz, MeOH-d_4): δ 8.57 (s, 1H), 7.45−7.40 (m, 2H), 7.39−7.32 (m, 3H), 7.28 (dd, J = 8.0, 1.7 Hz, 1H), 7.24 (d, J = 1.7 Hz, 1H), 6.93 (d, J = 8.0 Hz, 1H), 4.93 (s, 1H), 4.46 (dd, J = 11.7, 3.8 Hz, 1H), 3.86 (d, J = 3.8 Hz, 1H), 3.18 (dd, J = 12.2, 12.2 Hz, 1H), 2.82 (dd, J = 12.6, 3.8 Hz, 1H), 2.07 (sept d, J = 6.9, 3.8 Hz, 1H), 1.06 (s, 9H), 1.00 (d, J = 6.9 Hz, 3H), 0.89 (d, J = 6.9 Hz, 3H). ^{13}C NMR (101 MHz, MeOH-d_4): δ 176.1, 175.8, 174.0, 164.6, 156.8, 152.9, 149.6, 141.8, 137.1, 133.6, 132.3, 131.5, 130.6, 130.0, 129.4, 128.7, 126.9, 116.5, 112.5, 112.1, 76.8, 60.4, 58.5, 56.7, 39.2, 34.2, 33.2, 26.7, 19.5, 16.3. HRMS-ESI (m/z) calcd for $C_{34}H_{35}N_6O_6$ [M + H]$^+$ 623.2618; found: 623.2629. $[\alpha]_D^{20}$ −256 (c 1.0, MeOH).

*Benzyl 2-[(1R,6S,9R)-6-tert-Butyl-9-(2-hydroxy-3-methylbutanamido)-8,16-dioxo-1-phenyl-19-oxa-4,7,15-triazatetracyclo[9.5.2.1^{2,5}.0^{14,17}]nonadeca-2,4,11,13,17-pentaen-3-yl]-1,3-oxazole-4-carboxylate (**24**).* To a solution of methyl ester **3a** (133 mg, 0.20 mmol) in anhydrous toluene (2 mL), BnOH (0.83 mL, 8.0 mmol, 40 equiv) and neat Ti(OiPr)$_4$ (60 μL, 0.2 mmol, 1.0 equiv) were added dropwise. After addition the vial was placed in preheated oil bath at 100 °C and stirred for 2 h. After cooling to room temperature reaction was quenched with aqueous HCl (1M) and extracted with EtOAc. The combined organic layers were washed with brine, dried (Na_2SO_4), and evaporated under reduced pressure. The resulting yellow oil was purified with reverse phase column chromatography (10% to 90% MeCN in water) to give 80 mg of benzyl ester as white amorphous solid. The crude benzyl ester was converted into the title compound according to general procedure H, involving *N*-Boc cleavage by TFA (335 μL; 4.37 mmol; 10 equiv) in DCM (2 mL) within 3 h, followed by amide bond formation with (*S*)-2-hydroxy-3-methylbutanoic acid (19 mg; 0.16 mmol; 1.5 equiv) in the presence of EDC × HCl (42 mg; 0.22 mmol; 1.8 equiv), HOBt (44 mg; 0.33 mmol; 3 equiv) and DIPEA (94 μL; 0.55 mmol; 5 equiv) in DMF (3 mL) within 2 h. Purification by

https://doi.org/10.1021/acs.jmedchem.4c00388
J. Med. Chem. 2024, 67, 9227−9259

reverse phase column chromatography (10% to 50% MeCN in water) afforded 48 mg (32%; dr 99:1) of macrocycle **24** as a yellowish amorphous solid. ^{1}H NMR (400 MHz, MeOH-d_4): 8.42 (s, 1H), 7.52−7.21 (m, 12H), 6.90 (d, J = 8.6 Hz, 1H), 5.34 (s, 2H), 5.01−4.93 (m, 1H), 4.44 (dd, J = 11.7, 3.8 Hz, 1H), 3.86 (d, J = 3.8 Hz, 1H), 3.18 (dd, J = 12.2, 12.2 Hz, 1H), 2.81 (dd, J = 12.6, 3.8 Hz, 1H), 2.07 (sept d, J = 6.8, 3.7 Hz, 1H), 1.06 (s, 9H), 1.00 (d, J = 6.8 Hz, 3H), 0.89 (d, J = 6.8 Hz, 3H). 13C NMR (101 MHz, MeOH-d_4) δ 176.1, 175.7, 174.1, 174.0, 164.5, 162.0, 156.4, 152.3, 146.8, 141.7, 137.1, 134.9, 133.4, 132.2, 131.4, 130.6, 129.9, 129.6, 129.5, 129.4, 129.3, 128.7, 127.3, 112.0, 76.8, 67.8, 60.4, 58.3, 56.7, 39.2, 34.1, 33.1, 26.7, 19.5, 16.3. HRMS-ESI (m/z) calcd for $C_{41}H_{42}N_5O_8$ $[M + H]^+$ 732.3028; found: 732.3057. $[\alpha]_D^{20}$ −204 (c 1.0, MeOH)

*(2S)-N-[(1S,6S,9S)-6-tert-Butyl-3-[4-(hydroxymethyl)-1,3-oxazol-2-yl]-8,16-dioxo-1-phenyl-19-oxa-4,7,15-triazatetracyclo[9.5.2.1^{2,5}.0^{14,17}]nonadeca-2,4,11,13,17-pentaen-9-yl]-2-hydroxy-3-methylbutanamide (**25**).* Macrocycle **3a** (53 mg; 0.08 mmol) was dissolved in anhydrous THF (1 mL) and trifluoroethanol (57 μL) was added. The resulting solution was cooled to 0 °C (crushed ice bath), and $LiBH_4$ (9 mg; 0.40 mmol; 5 equiv) was added portionwise. The resulting suspension was warmed to room temperature and stirred for 3 h, whereupon it was poured into aqueous saturated NH_4Cl and extracted with EtOAc (two times). Combined organic extracts were washed with brine, dried (Na_2SO_4), and concentrated under reduced pressure. The yellow oily residue was purified by reverse phase column chromatography (gradient elution from 10% to 50% MeCN in water) to give alcohol (48 mg) as white amorphous solid. The crude alcohol was converted into the title compound **25** according to general procedure H, involving *N*-Boc cleavage by TFA (117 μL; 1.54 mmol; 10 equiv) in DCM (1 mL) within 3 h, followed by amide bond formation with (*S*)-2-hydroxy-3-methylbutanoic acid (13 mg; 0.11 mmol; 1.5 equiv) in the presence of EDC × HCl (26 mg; 0.14 mmol; 1.8 equiv), HOBt (31 mg; 0.23 mmol; 3 equiv), and DIPEA (66 μL; 0.38 mmol; 5 equiv) in DMF (2 mL) within 2 h. Purification by reverse phase column chromatography (10% to 95% MeCN in water) afforded 27 mg (57%; dr 99:1) of compound **25** as a white amorphous solid. ^{1}H NMR (400 MHz, MeOH-d_4): δ 7.64 (s, 1H), 7.45−7.38 (m, 2H), 7.37−7.29 (m, 3H), 7.29−7.20 (m, 2H), 6.91 (dd, J = 8.0, 2.3 Hz, 1H), 4.94−4.91 (m, 1H), 4.54−4.40 (m, 3H), 3.88−3.82 (m, 1H), 3.33−3.11 (m, 1H), 2.86−2.78 (m, 1H), 2.15−2.02 (m, 1H), 1.06 (s, 9H), 1.00 (d, J = 6.9, 3H), 0.89 (d, J = 6.9, 3H). ^{13}C NMR (101 MHz, MeOH-d_4): δ 176.3, 175.8, 174.0, 164.3, 155.8, 151.4, 143.1, 141.7, 137.9, 137.4, 133.9, 132.2, 131.3, 130.5, 129.9, 129.2, 128.7, 128.4, 112.0, 76.8, 60.5, 58.5, 57.1, 56.6, 39.2, 34.2, 33.1, 26.7, 19.5, 16.3. HRMS-ESI (m/z) calcd for $C_{34}H_{38}N_5O_7$ $[M + H]^+$ 628.2771; found 628.2786. $[\alpha]_D^{20}$ −233 (c 1.0, MeOH).

*2-[(1S,6S,9S)-6-tert-Butyl-9-[(2S)-2-hydroxy-3-methylbutanamido]-1-methyl-8,16-dioxo-19-oxa-4,7,15-triazatetracyclo[9.5.2.1^{2,5}.0^{14,17}]nonadeca-2,4,11,13,17-pentaen-3-yl]-1,3-oxazole-4-carboxylic acid (**26**).* To a solution of methyl ester **14b** (150 mg, 0.25 mmol) in MeOH (2 mL) and water (1 mL) was added LiOH × H_2O (32 mg, 0.76 mmol, 3.0 equiv), and the resulting suspension was stirred at room temperature for 30 min. Then, aqueous 1 M HCl was added, and the resulting suspension was extracted with EtOAc (three times) Combined organic layers were washed with brine, dried (Na_2SO_4), and evaporated under reduced pressure. Purification by reverse phase column chromatography (gradient elution from 10% to 50% MeCN in 0.01% aqueous TFA) provided carboxylic acid **26** (130 mg, 89%) as a white amorphous solid. ^{1}H NMR (300 MHz, MeOH-d_4): δ 8.67 (s, 1H), 7.28 (dd, J = 8.1, 1.7 Hz, 1H), 6.95 (d, J = 8.1 Hz, 1H), 6.79 (d, J = 1.7 Hz, 1H), 4.60 (s, 1H), 4.53 (dd, J = 11.6, 4.2 Hz, 1H), 3.86 (d, J = 3.6 Hz, 1H), 3.03 (dd, J = 12.0, 12.0 Hz, 1H), 2.87 (dd, J = 12.4, 4.2 Hz, 1H), 2.09 (sept d, J = 6.9, 3.8 Hz, 1H), 1.96 (s, 3H), 1.00 (d, J = 6.9 Hz, 3H), 0.96 (s, 9H), 0.89 (d, J = 6.9 Hz, 3H). ^{13}C NMR (75 MHz, MeOH-d_4): δ 179.0, 175.9, 173.7, 163.7, 152.7, 146.5, 141.8, 136.2, 132.23 131.0, 129.4, 128.4, 112.2, 76.8, 60.0, 56.6, 52.1, 39.3, 34.2, 33.1, 26.7, 20.4, 19.5, 16.3. HRMS-ESI (m/z) calcd for $C_{29}H_{34}N_5O_8$ $[M + H]^+$ 580.2407; found: 580.2415. $[\alpha]_D^{20}$ −120 (c 1.0, MeOH).

*Methyl (2S)-2-{[(tert-Butoxy)carbonyl]amino}-3-[3-(5-fluoro-3-hydroxy-2-oxo-2,3-dihydro-1H-indol-3-yl)-4-hydroxyphenyl]propanoate (**30**).* The title compound was synthesized according to literature procedure.[14] MeMgBr (3.0 M solution in Et_2O; 4.85 mL; 14.5 mmol, 1.6 equiv) was added dropwise via syringe to an ice cold (0 °C) solution of *N*-Cbz-L-tyrosine methyl ester (**28**, 3.48 g; 11.8 mmol; 1.3 equiv) in anhydrous THF (30 mL) under argon atmosphere. The crushed ice bath was removed, the yellow solution was warmed to room temperature and left to stir for 30 min. Concentration under reduced pressure provided yellow solid magnesium phenoxide to which 5-fluoroisatin (**29**, 1.50 g; 9.1 mmol; 1.0 equiv) was added, followed by anhydrous DCM (60 mL). The resulting heterogeneous dark brown reaction mixture was heated under reflux for 20 h, then cooled to room temperature, and quenched by addition of aqueous 1 M HCl (50 mL). Layers were separated, and the aqueous layer was extracted with EtOAc (3 × 40 mL). Combined organic extracts were washed with brine (50 mL), dried ($MgSO_4$), and concentrated under reduced pressure to provide a yellow foam. Purification by column chromatography on silica gel (gradient elution from 10% to 70% EtOAc in hexanes) afforded **30** (3.07 g; 74%; dr 3:2) as a yellowish foam. ^{1}H NMR (600 MHz, MeOH-d_4): δ 7.51−7.47 (m, 1H), 7.02−6.97 (m, 1H), 6.97−6.92 (m, 1H), 6.88−6.83 (m, 1H), 6.79 (dd, J = 7.7, 2.1 Hz, 0.6H), 6.75 (dd, J = 7.7, 2.1 Hz, 0.4H), 6.66−6.61 (m, 1H), 4.40 (dd, J = 7.9, 5.9 Hz, 0.6H), 4.34 (dd, J = 7.9, 5.9 Hz, 0.4H), 3.71 (s, 2H), 3.70 (s, 1H), 3.09 (dd, J = 13.8, 5.7 Hz, 0.4H), 3.04 (dd, J = 13.8, 5.7 Hz, 0.6H), 2.94 (dd, J = 13.8, 8.4 Hz, 0.4H), 2.87 (dd, J = 13.8, 8.4 Hz, 0.6H), 1.42 (s, 3H), 1.39 (s, 6H). ^{13}C NMR (151 MHz, MeOD) (no ^{13}C−{^{19}F} was possible, signals are listed as they appear) δ 181.83, 181.79, 174.3, 161.3, 159.7, 157.84, 157.77, 154.6, 139.94, 139.88, 135.8, 135.73, 135.68, 131.0, 130.9, 128.9, 128.7, 128.63, 128.58, 127.4, 116.5, 116.3, 116.34, 116.32, 116.19, 116.17, 113.2, 113.03, 112.99, 112.9, 111.53, 111.48, 111.4, 80.70, 80.65, 78.01, 77.96, 56.8, 56.7, 52.6, 38.2, 38.1, 28.7. HRMS-ESI (m/z) calcd for $C_{23}H_{25}N_2O_7F$ $[M + Na]^+$ 483.1543; found: 483.1562.

*Methyl (2S)-2-{[(tert-Butoxy)carbonyl]amino}-3-[3-(5-fluoro-3-hydroxy-2-oxo-2,3-dihydro-1H-indol-3-yl)-4-(trifluoromethanesulfonyloxy)phenyl]propanoate (**31**).* The title compound was synthesized according to literature procedure.[8b] Thus, phenol **30** (1.00 g; 2.20 mmol; 1.0 equiv) and $PhN(Tf)_2$ (970 mg; 2.70 mmol; 1.25 equiv) were dissolved in anhydrous DCM (20 mL) under argon atmosphere. Et_3N (908 μL, 6.50 mmol, 3.0 equiv) was added, and the resulting yellow solution was stirred at room

https://doi.org/10.1021/acs.jmedchem.4c00388
J. Med. Chem. 2024, 67, 9227−9259

temperature for 2 h, whereupon it was concentrated under reduced pressure. Purification of a yellow oily residue by column chromatography on silica gel (gradient elution from 10% to 40% EtOAc in hexanes) provided triflate **31** (970 mg; 75%; dr 2:3) as a colorless oil. ^{1}H NMR (600 MHz, MeOH-d_4): δ 8.07 (s, 0.5H), 8.04 (s, 0.5H), 7.37 (d, J = 8.5 Hz, 0.5H), 7.34 (d, J = 8.5 Hz, 0.5H), 7.31−7.26 (m, 1H), 7.06−6.99 (m, 1H), 6.96−6.92 (m, 1H), 6.85 (d, J = 7.8 Hz, 0.5H), 6.76 (d, J = 7.8 Hz, 0.5H), 4.58 (dd, J = 9.5, 5.2 Hz, 0.5H), 4.45 (dd, J = 8.9, 5.2 Hz, 1H), 3.78 (s, 1.8H), 3.75 (s, 1.2H), 3.35−3.31 (m, 0.5H, overlapping with MeOH-d_4), 3.25 (dd, J = 13.8, 5.4 Hz, 0.5H), 3.12 (dd, J = 13.8, 9.5 Hz, 0.5H), 3.00 (dd, J = 13.8, 9.5 Hz, 0.5H), 1.42 (s, 4H), 1.35 (s, 5H). ^{13}C NMR (151 MHz, MeOH-d_4): (no^{13}C−{^{19}F} was possible, signals are listed as they appear) δ 210.1, 179.7, 173.8, 173.7, 161.43, 161.40, 159.84, 159.81, 157.8, 157.7, 147.2, 139.9, 139.8, 138.8, 138.7, 134.30, 134.25, 134.22, 134.18, 133.0, 132.2, 131.9, 131.4, 131.2, 122.8, 120.7, 120.6, 120.3, 118.6, 117.5, 117.4, 117.3, 117.2, 113.5, 113.3, 113.2, 113.0, 112.93, 112.87, 112.80, 112.75, 80.8, 80.7, 76.7, 56.3, 56.1, 52.83, 52.78, 38.4, 37.9, 30.7, 28.68, 28.65. HRMS-ESI (m/z) calcd for $C_{24}H_{24}F_4N_2O_9S$ [M + Na]$^+$ 615.1046; found: 615.1036.

*Methyl (2S)-2-{[(tert-Butoxy)carbonyl]amino}-3-[3-(5-fluoro-2-oxo-2,3-dihydro-1H-indol-3-yl)phenyl]propanoate (**32**).* The title compound was synthesized according to literature procedure.[8b] Accordingly, 10% Pd on carbon (162 mg; 0.15 mmol; 0.1 equiv) was added to a solution of triflate **31** (900 mg; 1.52 mmol; 1.0 equiv) and Et_3N (740 μL; 5.32 mmol; 3.5 equiv) in MeOH (15 mL). The black suspension was stirred under 5 atm hydrogen pressure at room temperature for 24 h, then filtered through a short pad of Celite, and rinsed with MeOH (50 mL). Combined filtrates were evaporated under reduced pressure to give crude alcohol as a yellow foam (675 mg) that was used in the next step without additional purification. 10% Pd on carbon (323 mg; 0.30 mmol; 0.2 equiv) was added to a solution of tertiary alcohol (675 mg; 1.52 mmol; 1.0 equiv) in MeOH (20 mL). The black suspension was stirred under 10 atm hydrogen pressure at room temperature for 6 days. The heterogeneous mixture was filtered through a short pad of Celite and rinsed with MeOH (50 mL). Purification by column chromatography on silica gel (gradient elution from 0% to 5% MeOH in DCM) provided **32** (440 mg, 68%; dr 1:1) as a white foam. ^{1}H NMR (400 MHz, $CDCl_3$): δ 9.04 (s, 1H), 7.29 (t, J = 7.7 Hz, 1H), 7.13−7.06 (m, 2H), 6.97−6.90 (m, 2H), 6.88−6.83 (m, 2H), 5.04−4.98 (m, 1H), 4.61−4.52 (m, 2H), 3.65 (s, 1.4H), 3.63 (s, 1.6H), 3.18−2.97 (m, 2H), 1.40 (s, 9H). ^{13}C-{^{19}F} NMR (151 MHz, $CDCl_3$): δ 178.5, 172.4, 172.3, 159.3, 155.2, 137.7, 137.6, 137.14, 137.07, 136.22, 136.17, 131.2, 129.41, 129.39, 129.3, 129.1, 129.0, 127.4, 127.3, 122.4, 115.1, 113.3, 113.2, 110.7, 80.1, 54.5, 54.4, 53.0, 52.3, 38.4, 38.2, 28.4. HRMS-ESI (m/z) calcd for $C_{23}H_{25}N_2O_5F$ [M + Na]$^+$ 451.1645; found: 451.1645.

*Methyl 2-{5-Bromo-2-[(1S)-1-[(2S)-2-{[(tert-butoxy)carbonyl]amino}-3-[3-(5-fluoro-2-oxo-2,3-dihydro-1H-indol-3-yl)phenyl]propanamido]-2,2-dimethylpropyl]-1,3-oxazol-4-yl}-1,3-oxazole-4-carboxylate (**33**).* The title compound was synthesized according to literature procedure.[8b] Thus, ester **32** (440 mg; 1.03 mmol; 1.0 equiv) was dissolved in 2:1 THF/water mixture (33 mL) and solid LiOH (74 mg; 3.08 mmol; 3.0 equiv) was added. The clear solution was stirred at room temperature for 1 h, then aqueous 1 M HCl was added until pH 2, and the resulting suspension was extracted with EtOAc (three times). Combined organic extracts were washed with brine, dried (Na_2SO_4), and evaporated under reduced pressure. To the resulting crude acid (yellow oil; 426 mg) were added bioxazole **9** (368 mg; 1.03 mmol; 1.0 equiv), EDC × HCl (394 mg; 2.00 mmol; 2.0 equiv), and anhydrous pyridine (15 mL). The resulting suspension was stirred at room temperature for 2 h, and then the orange solution was evaporated to dryness under reduced pressure. The residue was dissolved in EtOAc, washed with aqueous 1 M HCl, brine, dried (Na_2SO_4), and evaporated under reduced pressure. Purification by reverse phase column chromatography (gradient elution from 0% to 70% MeCN in 0.1% TFA in water) provided **33** (490 mg, 63%; dr 1:1) as a yellow foam. ^{1}H NMR (400 MHz, $CDCl_3$): δ 8.71(s, 0.5H), 8.59(s, 0.5H), 8.30 (s, 0.5H), 8.29 (s, 0.5H), 7.21−7.05 (m, 3H), 7.02−6.79 (m, 5H), 5.19−5.11 (m, 1H), 5.05 (dd, J = 9.3, 8.5 Hz, 1H), 4.56 (s, 0.5H), 4.52 (s, 0.5H), 4.41−4.29 (m, 1H), 3.92 (s, 3H), 3.10−2.95 (m, 2H), 1.40 (s, 9H), 0.94 (s, 9H). ^{13}C−{^{19}F} NMR (151 MHz, $CDCl_3$): δ 178.10, 178.05, 171.2, 164.9, 164.8, 161.4, 159.3, 159.2, 155.7, 154.9, 154.8, 144.1, 137.73, 137.65, 136.3, 134.64, 134.61, 131.1, 129.6, 129.4, 129.3, 129.2, 128.9, 128.0, 127.0, 126.8, 123.2, 123.1, 115.0, 115.0, 113.3, 113.2, 110.68, 110.65, 80.52, 80.46, 55.8, 55.7, 52.9, 52.4, 37.7, 37.4, 35.89, 35.85, 28.4, 26.30, 26.28. HRMS-ESI (m/z) calcd for $C_{35}H_{37}N_5O_8BrF$ [M + Na]$^+$ 776.1721; found: 776.1707.

*Methyl 2-[(3R,7′S,10′S)-10′-{[(tert-Butoxy)carbonyl]amino}-7′-tert-butyl-5-fluoro-2,9′-dioxo-1,2-dihydro-17′-oxa-5′,8′-diazaspiro[indole-3,2′-tricyclo[10.3.1.1^{3,6}]heptadecane]-1′(16′),3′,5′,12′,14′-pentaen-4′-yl]-1,3-oxazole-4-carboxylate (**34**).* The title compound was synthesized according to literature procedure.[8b] A suspension of amide **33** (490 mg; 0.65 mmol; 1.0 equiv) and anhydrous Na_2CO_3 (206 mg; 1.95 mmol; 3.0 equiv) in anhydrous DMF (25 mL) was stirred at 65 °C for 3 h under argon atmosphere. After cooling to room temperature, saturated aqueous NH_4Cl solution (50 mL) and EtOAc (100 mL) were added, and layers were separated. The aqueous layer was extracted with EtOAc (3 × 50 mL), and combined organic extracts were washed with brine (50 mL), dried (Na_2SO_4), and concentrated under reduced pressure to provide a yellow oil. Purification by reverse phase column chromatography (gradient elution from 0% to 70% MeCN in 0.1% TFA in water) provided macrocycle **34** (300 mg, 69%; dr 99:1) as a white amorphous solid. ^{1}H NMR (400 MHz, $CDCl_3$): δ 9.32 (s, 1H), 7.98 (s, 1H), 7.28−7.19 (m, 2H), 7.13 (d, J = 7.8 Hz, 1H), 6.95 (dd, J = 8.7, 4.2 Hz, 1H), 6.89 (s, 1H), 6.83 (td, J = 8.7, 2.6 Hz, 1H), 6.73 (dd, J = 7.8, 2.6 Hz, 1H), 6.65 (d, J = 7.0 Hz, 1H), 5.40 (d, J = 9.2 Hz, 1H), 4.75 (d, J = 7.0 Hz, 1H), 4.26−4.18 (m, 1H), 3.83 (s, 3H), 3.25 (t, J = 11.9 Hz, 1H), 2.85 (dd, J = 12.6, 3.2 Hz, 1H), 1.47 (s, 9H), 0.95 (s, 9H). ^{13}C NMR (101 MHz, $CDCl_3$): δ 175.0, 172.4, 163.3, 161.1, 159.1 (J_{CF} = 241.5 Hz), 155.4, 154.8, 150.5, 143.9, 139.4, 137.9 (J_{CF} = 2.0 Hz), 136.5, 134.1, 132.0, 131.2 (J_{CF} = 8.0 Hz), 129.2, 128.7, 127.1, 124.7, 115.6 (J_{CF} = 23.0 Hz), 111.8 (J_{CF} = 25.2 Hz), 111.3 (J_{CF} = 7.8 Hz), 80.6, 59.1, 58.5, 57.2, 52.1, 38.6, 33.4, 28.5, 26.6. HRMS-ESI (m/z) calcd for $C_{35}H_{36}N_5O_8F$ [M + Na]$^+$ 696.2438; found: 696.2446. $[\alpha]_D^{20}$ −354 (c 1.0, $CHCl_3$).

(2S)-N-[(3R,7′S,10′S)-7′-tert-Butyl-5-fluoro-4′-[4-(hydroxymethyl)-1,3-oxazol-2-yl]-2,9′-dioxo-1,2-dihydro-17′-oxa-5′,8′-diazaspiro[indole-3,2′-tricyclo[10.3.1.1^{3,6}]heptadecane]-1′(16′),3′,5′,12′,14′-pentaen-10′-yl]-2-hy-

https://doi.org/10.1021/acs.jmedchem.4c00388
J. Med. Chem. 2024, 67, 9227−9259

droxy-3-methylbutanamide (27). Macrocycle **34** (290 mg; 0.43 mmol) was dissolved in anhydrous THF (3 mL) under argon atmosphere and cooled to 0 °C (crushed ice bath). Then, TFE (310 μL, 4.31 mmol, 10 equiv) was added dropwise, followed by solid $LiBH_4$ (47 mg, 2.16 mmol, 5.0 equiv). The resulting suspension was warmed to room temperature and stirred for 18 h. Saturated aqueous NH_4Cl solution (20 mL) was then added, and after stirring for 10 min, the white suspension was poured into aqueous 1 M HCl (30 mL) and extracted with EtOAc (3 × 50 mL). Combined organic extracts were washed with brine (50 mL), dried (Na_2SO_4), and concentrated under reduced pressure to provide alcohol **35** (250 mg; 90%) as a white amorphous solid, which was used in the next step without additional purification. The primary alcohol **35** (100 mg; 0.16 mmol) was dissolved in anhydrous DCM (2 mL), and TFA (120 μL; 1.55 mmol; 10 equiv) was added. The solution was stirred at room temperature for 3 h, then evaporated to dryness under reduced pressure, and redissolved in EtOAc. Organic layer was washed with aqueous saturated $NaHCO_3$ and brine, dried (Na_2SO_4), and evaporated to dryness under reduced pressure to give amine (84 mg; 0.15 mmol) as a yellow oil that was dissolved in anhydrous DCM (2 mL). (*S*)-2-Hydroxy-3-methylbutanoic acid (**13**, 22 mg; 0.19 mmol; 1.2 equiv), EDC × HCl (59 mg; 0.31 mmol; 2.0 equiv), and HOBt (62 mg; 0.46 mmol; 3.0 equiv) were added to the solution, followed by DIPEA (160 μL; 0.92 mmol; 6.0 equiv). The resulting mixture was stirred at room temperature for 3 h, whereupon the yellow solution was diluted with aqueous saturated NH_4Cl and EtOAc. Layers were separated, and the organic phase was washed with water, brine, dried (Na_2SO_4), and evaporated under reduced pressure. Purification by reverse phase column chromatography (gradient elution from 10% to 95% MeCN in 0.1% TFA in water) provided **27** (40 mg; 40%; dr 99:1) as a white solid. ^{1}H NMR (400 MHz, MeOH-d_4): δ 7.52 (t, J = 1.0 Hz, 1H), 7.32−7.30 (m, 1H), 7.29 (d, J = 1.0 Hz, 1H), 7.14−7.09 (m, 1H), 7.00−6.89 (m, 2H), 6.87 (s, 1H), 6.82 (dd, J = 8.2, 2.4 Hz, 1H), 4.72 (dd, J = 11.4, 3.5 Hz, 1H), 4.67 (s, 1H), 4.32 (d, J = 1.0 Hz, 2H), 3.89 (d, J = 3.5 Hz, 1H), 3.21 (t, J = 12.0 Hz, 1H), 2.83 (dd, J = 12.6, 3.5 Hz, 1H), 2.12 (sept d, J = 6.9, 3.8 Hz, 1H), 1.06−1.00 (m, 12H), 0.91 (d, J = 6.9 Hz, 3H). ^{13}C NMR (101 MHz, MeOH-d_4): δ 177.1, 175.8, 174.4, 165.1, 160.5 (J_{CF} = 239.6 Hz), 155.4, 151.1, 143.6, 141.5, 139.7 (J_{CF} = 2.4 Hz), 137.7, 137.3, 133.4 (J_{CF} = 8.4 Hz), 133.1, 129.93, 129.90, 128.7, 125.3, 116.4 (J_{CF} = 23.8 Hz), 112.4 (J_{CF} = 26.1 Hz), 112.2 (J_{CF} = 8.3 Hz), 76.9, 60.9, 60.0, 57.3, 55.7, 39.6, 34.3, 33.2, 26.9, 19.6, 16.3. HRMS-ESI (m/z) calcd for $C_{34}H_{36}N_5O_7F$ $[M + H]^+$ 646.2680; found: 646.2677. $[\alpha]_D^{20}$ −354 (c 1.0, MeOH).

■ ASSOCIATED CONTENT

Supporting Information

The Supporting Information is available free of charge at https://pubs.acs.org/doi/10.1021/acs.jmedchem.4c00388

NCI-60 assay results for macrocycles **14b**, **15a**, and **21**; acid **26** metabolite identification in A2058 cell lysate; ECD spectra for macrocycle **15i**; crystal data and structure refinement for macrocycle **14d**; geometries and energies of the DFT calculated stationary points; HPLC traces of macrocycles **14a-k**, **15a,b,i**, **16−21**, **23−27**; copies of NMR spectra (PDF)

Crystallographic data for **14d** deposited at the Cambridge Crystallographic Data Centre as Supplementary Publication Number CCDC 2295669 (CSV)

■ AUTHOR INFORMATION

Corresponding Authors

Edgars Liepinsh − *Latvian Institute of Organic Synthesis, Riga LV-1006, Latvia;* orcid.org/0000-0003-2213-8337; Email: ledgars@farm.osi.lv

Edgars Suna − *Latvian Institute of Organic Synthesis, Riga LV-1006, Latvia;* orcid.org/0000-0002-3078-0576; Email: edgars@osi.lv

Authors

Toms Kalnins − *Latvian Institute of Organic Synthesis, Riga LV-1006, Latvia*

Viktorija Vitkovska − *Latvian Institute of Organic Synthesis, Riga LV-1006, Latvia*

Mihail Kazak − *Latvian Institute of Organic Synthesis, Riga LV-1006, Latvia*

Diana Zelencova-Gopejenko − *Latvian Institute of Organic Synthesis, Riga LV-1006, Latvia;* orcid.org/0000-0002-6931-2294

Melita Ozola − *Latvian Institute of Organic Synthesis, Riga LV-1006, Latvia;* orcid.org/0000-0002-3453-0099

Nauris Narvaiss − *Latvian Institute of Organic Synthesis, Riga LV-1006, Latvia*

Marina Makrecka-Kuka − *Latvian Institute of Organic Synthesis, Riga LV-1006, Latvia*

Ilona Domračeva − *Latvian Institute of Organic Synthesis, Riga LV-1006, Latvia*

Artis Kinens − *Latvian Institute of Organic Synthesis, Riga LV-1006, Latvia;* orcid.org/0000-0003-1992-525X

Baiba Gukalova − *Latvian Institute of Organic Synthesis, Riga LV-1006, Latvia*

Nele Konrad − *Department of Chemistry and Biotechnology, Tallinn University of Technology, Tallinn, Harju Maakon 12618, Estonia*

Riina Aav − *Department of Chemistry and Biotechnology, Tallinn University of Technology, Tallinn, Harju Maakon 12618, Estonia;* orcid.org/0000-0001-6571-7596

Francesca Bonato − *Unidad BICS, Centro de Investigaciones Biologicas Margarita Salas, Consejo Superior de Investigaciones Cientificas, Madrid 28040, Spain*

Daniel Lucena-Agell − *Unidad BICS, Centro de Investigaciones Biologicas Margarita Salas, Consejo Superior de Investigaciones Cientificas, Madrid 28040, Spain*

J. Fernando Díaz − *Unidad BICS, Centro de Investigaciones Biologicas Margarita Salas, Consejo Superior de Investigaciones Cientificas, Madrid 28040, Spain;* orcid.org/0000-0003-2743-3319

Complete contact information is available at: https://pubs.acs.org/10.1021/acs.jmedchem.4c00388

Author Contributions

All authors have given approval to the final version of the manuscript.

Notes

The authors declare no competing financial interest.

■ ACKNOWLEDGMENTS

This work was supported by ERDF (Grants 1.1.1.1/16/A/281 and KC-PI-2020/16). V.V. is grateful to MikroTik Ltd. and the University of Latvia Foundation for doctoral scholarship. R.A. and N.K. thank the support from Estonian Reaserch Council (Grant PRG399) and J.F.D. acknowledges the support from Ministerio de Ciencia e Innovación (Grant PID2022-136765OB-I00). The authors thank Prof. M. O. Steinmetz and Dr. A. Prota (Paul Scherrer Institut) for analysis of the macrocycle binding site by X-ray crystallography, Dr. S. Belyakov (Latvian Institute of Organic Synthesis) for X-ray crystallographic analysis of macrocyclic inhibitor, and Ganadería Fernando Díaz for calf brains supply.

■ REFERENCES

(1) Sung, H.; Ferlay, J.; Siegel, R. L.; Laversanne, M.; Soerjomataram, I.; Jemal, A.; Bray, F. Global Cancer Statistics 2020: GLOBOCAN Estimates of Incidence and Mortality Worldwide for 36 Cancers in 185 Countries. *Ca-Cancer J. Clin.* **2021**, *71*, 209−249.

(2) (a) Vaidya, F. U.; Sufiyan Chhipa, A.; Mishra, V.; Gupta, V. K.; Rawat, S. G.; Kumar, A.; Pathak, C. Molecular and Cellular Paradigms of Multidrug Resistance in Cancer. *Cancer Rep.* 2022, *5*. . (b) Cree, I. A.; Charlton, P. Molecular Chess? Hallmarks of Anti-Cancer Drug Resistance. *BMC Cancer* **2017**, *17* (1), 10.

(3) Newman, D. J.; Cragg, G. M. Natural Products as Sources of New Drugs over the Nearly Four Decades from 01/1981 to 09/2019. *J. Nat. Prod.* **2020**, *83*, 770−803.

(4) Huang, M.; Lu, J.-J.; Ding, J. Natural Products in Cancer Therapy: Past, Present and Future. *Nat. Prod. Bioprospect.* **2021**, *11*, 5−13.

(5) Wang, S.; Dong, G.; Sheng, C. Structural Simplification: An Efficient Strategy in Lead Optimization. *Acta Pharm. Sin. B* **2019**, *9*, 880−901.

(6) Lindquist, N.; Fenical, W.; Van Duyne, G. D.; Clardy, J. Isolation and Structure Determination of Diazonamides A and B, Unusual Cytotoxic Metabolites from the Marine Ascidian Diazona Chinensis. *J. Am. Chem. Soc.* **1991**, *113*, 2303−2304.

(7) (a) Burgett, A. W. G.; Li, Q.; Wei, Q.; Harran, P. G. A Concise and Flexible Total Synthesis of (−)-Diazonamide A. *Angew. Chem., Int. Ed.* **2003**, *42*, 4961−4966. (b) Nicolaou, K. C.; Bella, M.; Chen, D. Y.-K.; Huang, X.; Ling, T.; Snyder, S. A. Total Synthesis of Diazonamide A. *Angew. Chem., Int. Ed.* **2002**, *41*, 3495−3499. (c) Nicolaou, K. C.; Chen, D. Y.-K.; Huang, X.; Ling, T.; Bella, M.; Snyder, S. A. Chemistry and Biology of Diazonamide A: First Total Synthesis and Confirmation of the True Structure. *J. Am. Chem. Soc.* **2004**, *126*, 12888−12896. (d) Nicolaou, K. C.; Chen, D. Y.-K.; Huang, X.; Ling, T.; Bella, M.; Snyder, S. A. The Second Total Synthesis of Diazonamide A. *Angew. Chem., Int. Ed.* **2003**, *42*, 1753−1758. (e) Nicolaou, K. C.; Chen, D. Y.-K.; Huang, X.; Ling, T.; Bella, M.; Snyder, S. A. Chemistry and Biology of Diazonamide A: Second Total Synthesis and Biological Investigations. *J. Am. Chem. Soc.* **2004**, *126*, 12897−12906. (f) Knowles, R. R.; Carpenter, J.; Blakey, S. B.; Kayano, A.; Mangion, I. K.; Sinz, C. J.; MacMillan, D. W. C. Total Synthesis of Diazonamide A. *Chem. Sci.* **2011**, *2*, 308−311.

(8) (a) Cheung, C.-M.; Goldberg, F. W.; Magnus, P.; Russell, C. J.; Turnbull, R.; Lynch, V. An Expedient Formal Total Synthesis of (−)-Diazonamide A via a Powerful, Stereoselective O-Aryl to C-Aryl Migration To Form the C10 Quaternary Center. *J. Am. Chem. Soc.* **2007**, *129*, 12320−12327. (b) Mai, C.-K.; Sammons, M. F.; Sammakia, T. A Concise Formal Synthesis of Diazonamide A by the Stereoselective Construction of the C10 Quaternary Center. *Angew. Chem., Int. Ed.* **2010**, *49*, 2397−2400.

(9) (a) Cruz-Monserrate, Z.; Vervoort, H. C.; Bai, R.; Newman, D. J.; Howell, S. B.; Los, G.; Mullaney, J. T.; Williams, M. D.; Pettit, G. R.; Fenical, W.; Hamel, E. Diazonamide A and a Synthetic Structural Analog: Disruptive Effects on Mitosis and Cellular Microtubules and Analysis of Their Interactions with Tubulin. *Mol. Pharmacol.* **2003**, *63*, 1273−1280. (b) Bai, R.; Cruz-Monserrate, Z.; Fenical, W.; Pettit, G. R.; Hamel, E. Interaction of Diazonamide A with Tubulin. *Arch. Biochem. Biophys.* **2020**, *680*, 108217.

(10) Wang, G.; Shang, L.; Burgett, A. W. G.; Harran, P. G.; Wang, X. Diazonamide Toxins Reveal an Unexpected Function for Ornithine δ-Amino Transferase in Mitotic Cell Division. *Proc. Natl. Acad. Sci. U. S. A.* **2007**, *104*, 2068−2073.

(11) Ding, H.; DeRoy, P. L.; Perreault, C.; Larivée, A.; Siddiqui, A.; Caldwell, C. G.; Harran, S.; Harran, P. G. Electrolytic Macrocyclizations: Scalable Synthesis of a Diazonamide-Based Drug Development Candidate. *Angew. Chem., Int. Ed.* **2015**, *54*, 4818−4822.

(12) Wieczorek, M.; Tcherkezian, J.; Bernier, C.; Prota, A. E.; Chaaban, S.; Rolland, Y.; Godbout, C.; Hancock, M. A.; Arezzo, J. C.; Ocal, O.; et al. The Synthetic Diazonamide DZ-2384 has Distinct Effects on Microtubule Curvature and Dynamics without Neurotoxicity. *Sci. Transl. Med.* **2016**, *8* (365), ra365159.

(13) Williams, N. S.; Burgett, A. W. G.; Atkins, A. S.; Wang, X.; Harran, P. G.; McKnight, S. L. Therapeutic Anticancer Efficacy of a Synthetic Diazonamide Analog in the Absence of Overt Toxicity. *Proc. Natl. Acad. Sci. U. S. A.* **2007**, *104*, 2074−2079.

(14) (a) Stereoselective construction of chiral, non-racemic quaternary center has been a challenge in the total synthesis of diazonamide A (**1a**): Lachia, M.; Moody, C. J. The Synthetic Challenge of Diazonamide A, a Macrocyclic Indole Bis-Oxazole Marine Natural Product. *Nat. Prod. Rep.* **2008**, *25*, 227−253. (b) Peris, G.; Vedejs, E. Enantiocontrolled Synthesis of a Tetracyclic Aminal Corresponding to the Core Subunit of Diazonamide A. *J. Org. Chem.* **2015**, *80*, 3050−3057. (c) Mutule, I.; Kalnins, T.; Vedejs, E.; Suna, E. Diazonamide Synthetic Studies. Reactivity of N-Unsubstituted Benzofuro[2,3-b]Indolines. *Chem. Heterocycl. Compd.* **2015**, *51*, 613−620.

(15) Kazak, M.; Vasilevska, A.; Suna, E. Preparative Scale Synthesis of Functionalized Bioxazole. *Chem. Heterocycl. Compd.* **2020**, *56*, 355−364.

(16) Ross, A. J.; Lang, H. L.; Jackson, R. F. W. Much Improved Conditions for the Negishi Cross-Coupling of Iodoalanine Derived Zinc Reagents with Aryl Halides. *J. Org. Chem.* **2010**, *75*, 245−248.

(17) Huihui, K. M. M.; Caputo, J. A.; Melchor, Z.; Olivares, A. M.; Spiewak, A. M.; Johnson, K. A.; DiBenedetto, T. A.; Kim, S.; Ackerman, L. K. G.; Weix, D. J. Decarboxylative Cross-Electrophile Coupling of *N* -Hydroxyphthalimide Esters with Aryl Iodides. *J. Am. Chem. Soc.* **2016**, *138*, 5016−5019.

(18) Toriyama, F.; Cornella, J.; Wimmer, L.; Chen, T.-G.; Dixon, D. D.; Creech, G.; Baran, P. S. Redox-Active Esters in Fe-Catalyzed C−C Coupling. *J. Am. Chem. Soc.* **2016**, *138*, 11132−11135.

(19) Even though the configuration at quaternary center could be established, the correct analysis of the bond lengths and valence angles was not possible due to small sizes of the single crystals of **14d**. For further details, see Supporting Information, page S27 and crystallographic data for **14d** deposited at the Cambridge Crystallographic Data Centre as Supplementary Publication Number CCDC 2295669.

(20) Shoemaker, R. H. The NCI60 Human Tumour Cell Line Anticancer Drug Screen. *Nat. Rev. Cancer* **2006**, *6*, 813−823.

(21) Sisco, E.; Barnes, K. L. Design, Synthesis, and Biological Evaluation of Novel 1,3-Oxazole Sulfonamides as Tubulin Polymerization Inhibitors. *ACS Med. Chem. Lett.* **2021**, *12*, 1030−1037.

(22) An additional cell proliferation rate experiment was performed to investigate cytostatic vs. cytotoxic properties of macrocyclic ester **21**. Melanoma A2058 cells treated with **21** exhibited an approximately two-fold decrease in proliferation rate as compared to untreated control cells suggesting that the effects of compound **21** should be considered as cytostatic rather than cytotoxic (see SI, Figure S1, page S18).

(23) (a) It has been proposed that cytostatic (antiproliferative) anticancer agents are prone to fewer resistance mechanisms than are cytotoxic agents: ref. 2b. (b) Krause, W. Resistance to Anti-Tubulin

Agents: From Vinca Alkaloids to Epothilones. *Cancer Drug Resist.* **2019**, *2* (1), 82−106. (c) Cortes, J.; Vidal, M. Beyond Taxanes: The next Generation of Microtubule-Targeting Agents. *Breast Cancer Res. Treat* **2012**, *133* (3), 821−830.
(24) Rixe, O.; Fojo, T. Is Cell Death a Critical End Point for Anticancer Therapies or Is Cytostasis Sufficient? *Clin. Cancer Res.* **2007**, *13*, 7280−7287.
(25) National Cancer Institute; *Publicly accessible database of NCI-60 panel screening results and COMPARE analysis*, 2021, https://dtp.cancer.gov/public_compare/.
(26) Holbeck, S. L.; Collins, J. M.; Doroshow, J. H. Analysis of Food and Drug Administration−Approved Anticancer Agents in the NCI60 Panel of Human Tumor Cell Lines. *Mol. Cancer Ther.* **2010**, *9*, 1451−1460.
(27) Gaskin, F.; Cantor, C. R.; Shelanski, M. L. Turbidimetric Studies of the in Vitro Assembly and Disassembly of Porcine Neurotubules. *J. Mol. Biol.* **1974**, *89*, 737−755.
(28) *The assay was conducted following Enhancer Control Polymerization Assay Method described in Tubulin Polymerization Assay Kit manual by Cytoskeleton*, Cytoskeleton Inc, https://www.cytoskeleton.com/pdf-storage/datasheets/bk004p.pdf.
(29) (a) The slope values derived from the tubulin polymerization assay have been used in quantification of functional activity and comparison across analog series: ref. 21. (b) Argirova, M.; Guncheva, M.; Momekov, G.; Cherneva, E.; Mihaylova, R.; Rangelov, M.; Todorova, N.; Denev, P.; Anichina, K.; Mavrova, A.; Yancheva, D. Modulation Effect on Tubulin Polymerization, Cytotoxicity and Antioxidant Activity of 1H-Benzimidazole-2-Yl Hydrazones. *Molecules* **2023**, *28* (1), 291.
(30) Safa, A. R.; Hamel, E.; Felsted, R. L. Photoaffinity Labeling of Tubulin Subunits with a Photoactive Analog of Vinblastine. *Biochemistry* **1987**, *26*, 97−102.
(31) Mosmann, T. Rapid Colorimetric Assay for Cellular Growth and Survival: Application to Proliferation and Cytotoxicity Assays. *J. Immunol. Methods* **1983**, *65*, 55−63.
(32) *NCI-60 Screening Methodology | NCI-60 Human Tumor Cell Lines Screen | Discovery & Development Services | Developmental Therapeutics Program (DTP)*, https://dtp.cancer.gov/discovery_development/nci-60/methodology.htm. (accessed 2023−06−13).
(33) Andreu, J. M. Large Scale Purification of Brain Tubulin With the Modified Weisenberg Procedure. *Methods Mol. Med.* **2007**, 17−28.
(34) Cornelissen, M.; Philippé, J.; De Sitter, S.; De Ridder, L. Annexin V Expression in Apoptotic Peripheral Blood Lymphocytes: An Electron Microscopic Evaluation. *Apoptosis* **2002**, *7* (1), 41−47.
(35) Alanine, A.; Buettelmann, B.; Heitz, N. M.-P.; Jaeschke, G.; Pinard, E.; Wyler, R.; *Pyrrolidine and Piperidine Derivatives and Their Use for the Treament of Neurodegenerative Disorders*, 2001, WO 0,181,303 A1.
(36) Zhang, J.-Q.; Li, S.-M.; Wu, C.-F.; Wang, X.-L.; Wu, T.-T.; Du, Y.; Yang, Y.-Y.; Fan, L.-L.; Dong, Y.-X.; Wang, J.-T.; Tang, L. The Synthesis of Symmetrical 3,3-Disubstituted Oxindoles by Phosphine-Catalyzed γ/γ-Addition of Oxindoles with Allenoates. *Catal. Commun.* **2020**, *138*, 105838.

https://doi.org/10.1021/acs.jmedchem.4c00388
J. Med. Chem. 2024, 67, 9227−9259

Appendix V – Publications of conference abstracts

Mutule, I.; Medne, Z.; **Kalniņš, T.**; Vedejs, E.; Suna, E. Stereoselective synthesis of the Diazonamide A macrocyclic core. Organometallic Chemistry Directed Towards Organic Synthesis OMCOS18, 2015, Sitges, Spain. Program and abstract book, P-577.

Mutule, I.; Medne, Z.; **Kalniņš, T.** Stereoselective synthesis of the Diazonamide A macrocyclic core. 9th Paul Walden Symposium on Organic Chemistry, Riga, Latvia, May 21 – 22, 2015. Abstract published in Material Science and Applied Chemistry, 2015, vol. 31, p. 66.

Kalniņš, T., Suna, E. Studies towards the synthesis of novel anticancer agents based on Diazonamide A. 11th Paul Walden Symposium on Organic Chemistry 2019, Riga, Latvia, September 19 – 20. Program and abstract book, D-6.

P-577

STEREOSELECTIVE SYNTHESIS OF THE DIAZONAMIDE A MACROCYCLIC CORE

Mr Toms Kalnins[1], Ms Ilga Mutule[1], Ms Zane Medne[1], Prof Edwin Vedejs[1,2], Prof Edgars Suna[1]
[1]Latvian Institute of Organic Synthesis, Riga, Latvia, [2]University of Michigan, Ann Arbor, USA

Poster Session 2

Diazonamide A (1) is a marine natural product, which possesses unique anti-cancer activity in terms of efficiency, specificity and mechanism of action. Herein we report the stereoselective construction of the right-hand heteroaromatic macrocycle 2 en route to the total synthesis of compound 1.

The macrocycle 2 was assembled in a palladium-dioxygen complex-catalyzed Suzuki-Miyaura cross-coupling between tetracycle 5 and boronate 4 followed by atropodiastereoselective Dieckmann-type macrocyclization of biaryl 3 [1].

Authors are thankful to European Social Fund (1DP/1.1.1.2.0/13/APIA/VIAA/006) for financial support of the research and InnovaBalt project (REGPOT-CT-2013-316149) for travel grant for dissemination of the results.

References:

[1] Mutule, I.; Joo, B.; Medne, Z.; Kalnins, T.; Vedejs, E.; Suna, E. J. Org. Chem. 2015, 80, 3058

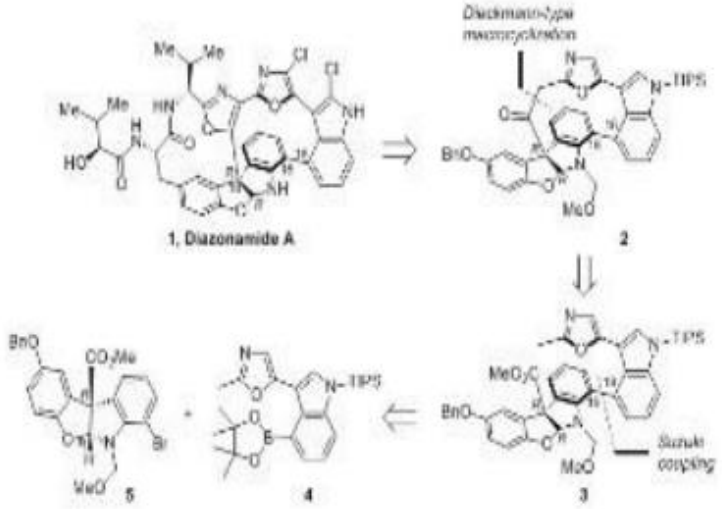

D3

Stereoselective Synthesis of the Diazonamide A Macrocyclic Core

Zane Medne, Toms Kalnins,
Latvian Institute of Organic Synthesis, Aizkraukles 21, Riga, LV-1006, Latvia
E-mail: toms@osi.lv

Introduction

Diazonamide A **1** is a marine natural product, which possesses unique anti-cancer activity in terms of efficiency, selectivity and mechanism of action. Herein we report the stereoselective construction of the right-hand heteroaromatic macrocycle **2** *en route* to the total synthesis of compound **1**.

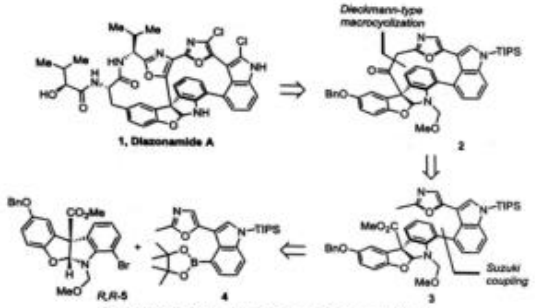

Scheme 1. Retrosynthesis of diazonamide **1**.

Results and Discussions

Our approach towards the heteroaromatic macrocycle **2** is based on Suzuki cross-coupling of enantiomerically pure hemiaminal bromide (*R,R*)-**5** with indolyl boronate **4**, followed by atropodiastereoselective Dieckmann-type macrocyclization of biaryl **3** (Scheme 1), [1].

The major challenge in synthesis proved to be the Suzuki cross-coupling between compounds **4** and **5**, which did not work well with the most frequently used palladium sources and ligands. After considerable work palladium dioxygen complex $(Cy_3P)_2Pd(\eta^2\text{-}O_2)$ (**6**) (Scheme 2) was found to be the best catalyst, which allowed the reaction to proceed with 82 % yield. Noteworthy, Pd-dioxygen complex **6** has never been reported as a catalyst for the Suzuki-Miyaura cross-coupling.

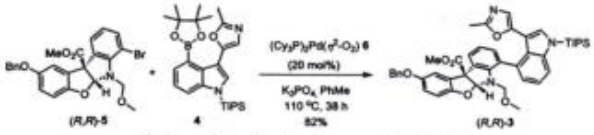

Scheme 2. Synthesis of compound (*R,R*)-**3**.

Fig. 1. X-ray of comlex **6**

It was found that compound (*P,R,R*)-**3** exists as a mixture of two atropisomers in a 3:2 ratio. Unfortunately, only the major isomer underwent Dieckmann-type cyclization at –78 °C to produce the macrocycle **2** with 43 % yield (Scheme 3). The other isomer was unreactive and it could be recovered after workup as a 3:2 mixture of atropisomers.

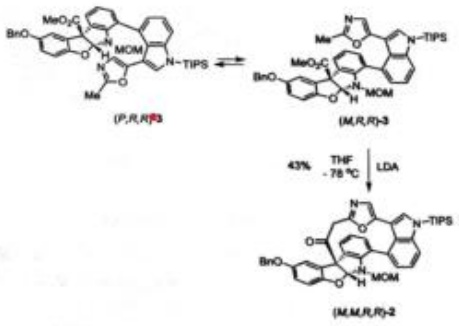

Scheme 3. Synthesis of macrocycle **2**.

Atropodiastereoselective Dieckman-type cyclization provides an access to the macrocyclic core of diazonamide A in enantiomerically pure form. The biaryl (*R,R*)-**3** was prepared in the Suzuki-Miyaura cross-coupling between the chiral, non-racemic tetracyclic hemiaminal bromide and indolyl boronate. Unexpectedly, palladium dioxygen complex $(PCy_3)_2Pd(\eta^2\text{-}O_2)$ **6** was found to be the most efficient catalyst in the Suzuki-Miyaura reaction.

Supervisors: Prof. E. Suna,
Prof. E. Vedejs,
Dr. chem. I. Mutule

Acknowledgement

Authors are grateful to European Social Fund (project Nr. 1DP/1.1.1.2.0/13/APIA/VIAA/006) for the financial support.

References

[1] Mutule, I.; Joo, B.; Medne, Z.; Kalnins, T.; Vedejs, E.; Suna, E. *J. Org. Chem.* 2015, *80*, 3058

D-6

Studies towards the synthesis of novel anticancer agents based on Diazonamide A

Toms Kalnins

Latvian Institute of Organic Synthesis
E-mail: toms@osi.lv

Diazonamides are a structurally unique class of secondary metabolites first isolated in 1991 from the colonial marine ascidian *Diazona angulata*.[1] Diazonamide A (**1**) was found to be highly efficient against various cancer cell lines with IC_{50} up to 57 nM.[1,2] Studies conducted by Harran[3] revealed that DZ-2384 (**2**), a structurally simplified analog of **1**, was more potent (IC_{50} = 0,47 nM) and longer survived in the bloodstream. Compound **2** is currently undergoing preclinical studies.

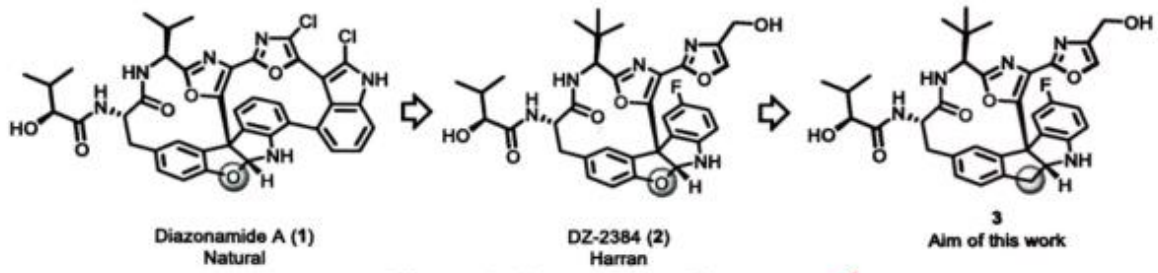

Figure 1. Compounds of interest.

Herein we report the results of studies directed towards synthesis of compound **3**, which is a close analogue of DZ-2384 (2). Synthesis and subsequent evaluation of biological activity of compound **3** would give access to structurally novel class of anticancer agents and allow to establish a deeper understanding of SAR in Diazonamide series.

Supervisor: Dr. chem. E. Suna

Acknowledgements
We thank *MSc. chem.* Diana Zelencova for performing of ITC experiments and *Dr. chem.* Ilona Domraceva for *in vitro* tests.

References

1. Lindquist, N.; Fenical, W.; Van Duyne, G. D.; Clardy, J. *J. Am. Chem. Soc.* **1991**, *113*, 2303.
2. Cardwell, C.; Wei, Q.; Zhou, M.; Hanson, G. J. Diazonamide Analogs. U.S Patent 8153619; Apr. 10, 2012.
3. Wei, Q.; Zhou, M.; Xu, X.; Caldwell, C.; Harran, S.; Wang, L. Diazonamide Analogs. U.S. Patent 8846734; Sep. 30, 2014.